

4th Hull Performance & Insight Conference

HullPIC'19

Gubbio, 6-8 May 2019

Edited by Volker Bertram

Sponsored by



www.jotun.com



DNV-GL

www.dnvgl.com



www.insatech.com



www.napa.fi



www.vaf.nl



www.ppgpmc.com



www.miros.no



www.hempel.com



www.selektope.com



www.hoppe-marine.com



www.stratumfive.com



www.kyma.no



www.hullwiper.co



www.akzonobel.com



www.foreship.com



www.veinland.net



www.c-leanship.com



www.enamor.pl



www.silverstream-tech.com



www.vpsolutions.dk



www.bmt.org



www.idealship.de

Index

Johnny Eliasson <i>Discussion on Ecological Risks of Bio-Fouling: Harmonizing and Vetting Related Approaches</i>	4
Volker Bertram <i>Some Fairy Tales in Performance Monitoring Revisited</i>	9
Inno Gatin, Vuko Vukčević, Hrvoje Jasak <i>Fully Automated CFD Analysis for Full-Scale Ship Hydrodynamics</i>	13
Naoto Sogihara, Takashi Yonezawa, Tsuyoshi Ishiguro, Yoshihiko Sugimoto, Shinta Masuyama, Hirohisa Mieno, Mamoru Shimada, Yoshiro Matsubara <i>Introduction of OCTARVIA Project: Project for Ship Performance in Actual Seas</i>	21
Matthew Patey <i>Performance Monitoring Information Feedback to Design</i>	31
Tetsuro Ashida, Naoki Mizutani, Pekka Pakkanen, Arttu Väisänen, Teemu Manderbacka <i>Performance Monitoring Insight at MOL</i>	38
Erik van Ballegooijen, Torben Helsloot <i>An Approach to Monitor the Propeller Separately from the Hull</i>	50
Nikos Themelis, Christos Spandonidis, Christos Giordamlis <i>Evaluating the Efficiency of an Energy-Saving Device by Performance Monitoring</i>	56
Florian Kluwe, Lars-Uve Schrader, Herbert Bretschneider <i>From Bow to Stern: Hydrodynamic Measures for Increased Hull Performance</i>	65
Paolo Becchi <i>ISO 19030: Onboard Monitoring System for Real-time Performance Feedback, Prediction and Optimization</i>	76
Miyeon Jeon, Yoojeong Noh, Kyung Hwan Jeon, Sang Bong Lee, Inwon Lee <i>Real Ship Maritime Big Data Analysis for Prediction of Fuel Consumption</i>	86
Simon Doran <i>A Short History of Hull Cleaning and Where Do We Go Now</i>	97
Serena Lim, Roger Teo, Teck Chong Sia <i>A Digital Business Model for Vessel Performance Monitoring</i>	103
Gunnar Prytz, Rune Gangeskar, Vemund Svanes Bertelsen <i>Distributing Real-Time Measurements of Speed Through Water from Ship to Shore</i>	114
Jean-Marc Bonello, Tristan Smith <i>Exploring the Effect of Vessel Performance Information Barriers on Decision-Making Practice: A Time Charter Application</i>	128
Carlos Gonzalez, David Lara Arango <i>Techniques for the Automated Detection of Anomalies and Assessment of Quality in High-Frequency Data Collection Systems</i>	143
Anders Östman, Kouros Koushan, Luca Savio <i>Study on Additional Ship Resistance due to Roughness using CFD</i>	153
Daniel Schmode, Ole Hympehdahl, Francesco Bellusci <i>Influence of Data Sources on Hull Performance Prediction</i>	162
Tomoki Wakabayashi, Yasuhiko Inukai, Takeshi Yonezawa, Norihide Igarashi, Masahiko Mushiake, Satoshi Kawanami <i>Full-Scale Measurement of a Flow Field at Stern using Multi-Layered Doppler Sonar (MLDS)</i>	172

Iason Stefanatos, André Kauffeldt, Eirinaios Petoumenos <i>Case Study on Performance Improvement using Advanced Hull Performance Analysis Methodologies</i>	179
Beom Jin Park, Myung-Soo Shin, Gyeong Joong Lee, Min Suk Ki <i>Application of an ISO15016:2015 based Method in Analysing Ship's Performance</i>	193
Luke De Freitas, Noah Silberschmidt, Takis Pappas, David Connolly <i>Full-Scale Performance Measurement and Analysis of the Silverstream Air Lubrication System</i>	201
Najmeh Montazeri, Jakob Buus Petersen, Søren Vinther Hansen <i>Autolog Data Processing for Vessel Performance Application</i>	211
Ditte Gundermann, Danny McLaughlin <i>When ISO19030 Fails: Utilizing Basic Machine Learning/Data Fitting Methods for Performance Analysis without Reference Data</i>	220
Angelos Ikonomakis, Jesper Dietz, Klaus Kähler Holst, Roberto Galeazzi, Ulrik Dam Nielsen <i>Application of Sensor Fusion to Drive Vessel Performance</i>	229
Abel Vargas, Hua Shan, Eric Holm <i>Using CFD to Predict Ship Resistance due to Biofouling and Plan Hull Maintenance</i>	242
Bastian Marquardt, Alessandro Castagna, Amirhossein Rahimi, Aaqib Gulzar Khan, Johanna Marie Daniel, Christian Voosen, Nikhil Mathew <i>Reducing the Resistance of Container Ships with a FLUME® Roll Damping Tank</i>	254
Sergiu Paereli, Manolis Levantis <i>ISO 19030 2.0: How to Improve</i>	261
Kevin Murrant, Allison Kennedy, Rob Pallard, Marcel Montrose <i>Effects of Hull and Propeller Cleaning on Propulsion Efficiency of an Offshore Patrol Vessel</i>	272
Wojciech Gorski <i>Information Sharing Concept in Ship Performance Management Systems</i>	292
Philip Chaabane, Catherine Austin, Dan Isaksson, Oliver Weigenand, Cecilia Ohlauson <i>Application of Biotechnology in Antifouling Solutions for Hard Fouling Prevention</i>	301
Index of authors	312
Call for Papers for next HullPIC	

Discussion on Ecological Risks of Bio-Fouling: Harmonizing and Vetting Related Approaches

Johnny Eliasson, Chevron Shipping LCC, San Ramon/USA, Johnny.Eliasson@chevron.com

Abstract

This paper highlights some of the issues of decreasing the environmental footprint of shipping we are faced with and the complex environment under which new guidelines, and possibly future regulations are developed. To serve the marine industry NACE International has started working group to discuss the environmental concerns of biofouling on ships. This working group is not tasked to write guidelines or standards. It is simply tasked with discussing the subject. The group has, however been asked to act as a review group for other organizations that are developing guidelines. This can help with harmonization and vetting of such developments. The NACE TEG532X is open to all, and participation is encouraged particularly by ship operators.

1. Introduction

The part of the United Nations tasked with governing worldwide shipping is the International Maritime Organization (IMO). Shipping is in effect governed by international law. IMO develop mandatory regulations that the Nation States enact into law and enforce. The regulations are adopted by consensus by all member states. Each member state may impose stricter local regulations above and beyond the minimum required by IMO regulations. This is however generally discouraged. To have uniform and global rules facilitate smooth transport an essential part of global trade.

With the increased concern about human influenced global warming trends IMO must take action to reduce the footprint from shipping. There are also other environmental related issues IMO has been addressing in recent decades, such as the emission of acid exhaust gases. This paper will focus on the effect of ship biofouling and highlight some of the activities under way at IMO and outside of IMO.

Biofouling present primarily two risks to the marine environment;

1. It increase the ships' hull resistance
2. It presents a risk of spreading invasive aquatic species

The increase in hull resistance directly influence fuel usage and as such greenhouse gas emissions. Introduction of invasive aquatic organisms into a new marine environment not only affects biodiversity and the health of eco systems but can also have detrimental impacts on a number of economic sectors such as fisheries, aquaculture and ocean energy.

2. IMO and the environment

IMO adopted the Ship Energy Efficiency Management Plan (MEPC.282(70) and the Guidelines for the control and management of ship's biofouling to minimize the transfer of invasive aquatic species, Resolution MEPC.207(62), in July of 2011. The latter sets out the format and recommendations for a vessel specific Biofouling Management Plan and Biofouling Record Book. United States Coast Guard (USCG) required vessels to have such a plan effective June 21, 2012 (CFR 151 2000). California imposed the same as of 1/1/2018. Add to this New Zealand, Australia and other. These documents are subject to Port State Control vetting.

The IMO has launched a new international effort to combat the negative environmental impacts of biofouling - The GloFouling Partnership. The official launch was in London on October 25th, 2018, in conjunction with the IMO Marine Environmental Protection Committee (MEPC) 73, and the first GloFouling event was organized in London, in February 2019.

GloFouling is a collaborative project involving the Global Environment Facility (GEF) and the United Nations Development Programme (UNDP) and the IMO tasked it with pushing for the implementation of IMO Guidelines for the control and management of ships' biofouling, via development of best practices and standards.

Although the core group behind this effort involves 12 nations, a mix of developing nations and small island states, it has received endorsement from over 40 major stakeholders, representing academia, industry associations, technology developers and private sector companies in the marine field.

IMO will focus on shipping while the Intergovernmental Oceanographic Commission of UNESCO (IOC) will join to lead the approach to other marine sectors.

Hiroyuki Yamada, director of the Maritime Environmental Division at IMO, stated "This joint effort to implement the IMO Biofouling Guidelines and best practices for other marine industries will help nations to deliver essential contributions to the 2030 Agenda for Sustainable Development Goals." He also highlighted the additional contribution of biofouling management to the reduction of greenhouse gas (GHG) emissions from shipping through energy-efficiency gains resulting from clean hulls.

3. Other active organizations

International Paint & Printing Ink Council (IPPIC) lead a GloFouling session at the Sustainable Ocean Summit (SOS) in Hong Kong, 14 November 2018, with members from NACE TEG532X, IPPIC presenting among others. Some highlights included improvements in performance monitoring, optimum antifouling selection, data to evaluate fouling risk via diver inspections, the balance of risk AIS vs biocide usage, the activities at NACE TEG532X, NACE's involvement at IMO and at other related venues, BIMCO's hull cleaning standard development, etc.

IPPIC highlights that "the development of innovative coatings that control biofouling on ships, offshore structures, and other key infrastructures involves not only technical research hurdles, but also a host of regulatory challenges producers must face bringing these products to markets. Coatings researchers must balance the requirement for products that not only control biofouling effectively, but which do so in a way that is cognizant of the need to minimize ancilliary environmental damage, including harm to other (non-target) species that are not implicated in (ship) fouling." (Allen Irish, airish@paint.org)

Shipping conference / workshop Shiptec in China is very focused on the environment with high goals to exercise control. The efforts are presently apparently mainly focused on greenhouse gas (GHG), Sulfur and Nitrous oxide gas reductions.

Active Shipbuilding Experts Federation (ASEF) is actively involved in the GloFouling project and keep a close relationship to NACE. Members of ASEF are also contributing to the NACE TEG532X working group. At the Tripartite (owner and ship builder organization's annual) meeting in November of 2017 discussions was held on what the shipbuilder industry can contribute to Biofouling Management.

Baltic and International Maritime Council (BIMCO) is developing a hull cleaning standard or best practice guideline. This work started in 2018. This attempt to standardize terms and tools for hull grooming and cleaning will facilitate use of these important tools. NACE TEG532X is acting as a review group in support of that important effort. Hull grooming or cleaning is an important part of ensuring maximum performance of ships' hulls and as such should be considered a part of an overall hull performance plan. BIMCO also launched a membership survey to gain better insight into how shipowners are dealing with the biofouling issues.

Institute of Marine Engineering (ImarEst) in cooperation with IPPIC launched a template Biofouling Management Plan on August 2017 (Allen Irish, airish@paint.org). Such plans are mandatory to have

onboard ships delivered on or after 1 January 2018 and to other ships on completion of their first regularly scheduled out-of-water maintenance (i.e. drydocking) on or after that date by mandate in California. An IMarEst TV recording of the 22 February 2018 presented a technical lecture to the Victoria Branch in Melbourne on “Biofouling of Ships – Operational and Environmental impacts and the efficacy of Management Measures.” IMarEST Biofouling Expert Group was formed following the inaugural Australia /New Zealand /Pacific (ANZPAC) Workshop on Biofouling Management for Sustainable Shipping, held in Melbourne, Australia, in May 2013. The aim of the group was to assist and promote further discussions and international consultation on the development and implementation of practical, effective and globally consistent biofouling management measures for shipping. The key issues identified were:

1. Effective & practical biofouling management measures
2. Biofouling management guidelines, requirements & regulations: present & future
3. In-water cleaning of ship hulls: costs, benefits, impacts & regulation
4. Regulation & scrutiny of new and existing fouling control coatings and antifouling biocides
5. Costs & impacts of biofouling: ship energy efficiency & harmful aquatic species transfer
6. Ship biofouling management: best practice guidance

New Zealand will require all vessels that arrive in its waters to have “clean hulls”, with varying levels of allowable biofouling depending on the vessels itinerary. The State of California tightened up its regulations on biofouling as of 1 January 2018, to include the mandatory management of biofouling on the vessels’ wetted hulls. Australia issued a Marine Notice in September 2017 advising about revisions of the 2015 Antifouling and In-water Cleaning Guidelines for Australia.

International Association of Classification Societies (IACS) holds the view that biofouling regulations are likely to grow in scope and geographical reach.

Niche areas (sea chests, bow thrusters etc.) generally have restricted access meaning the application of antifouling control products can be challenging. When in service, changes in water flow in these areas can also lead to increased fouling challenge compared to the main hull areas. Biofouling control in sea chests are often assisted by the use of Marine Growth Prevention Systems (MGPS). The IMO guidelines give advice on design and construction to minimize small niche areas. However, effective fouling control can only be achieved via correct use of antifouling paints and operation of the MGPS in conjunction with regular in-service inspections.

4. NACE TEG532X

The TEG532X working group at NACE International is tasked with Discussion on Ecological Risks of BioFouling. The group is not tasked with producing standards or other specific documents. It is tasked simply with discussing the subject. It is a very large and international group with members that are also members of many of the other groups, some mentioned herein, working on various related solutions, best practices and standards. This does not mean that other NACE working groups cannot evolve as a spin-off of these discussions. One example is a new NACE working group that was formed around developing a best practice standard on hull treatment of ships in a dry dock.

5. Chevron experience

There are already known best practices that might not be utilized at present to the fullest. A project started at Chevron Shipping in 2014 with the aggressive target of reducing the fuel used per miles travelled by 20%. The result after 4 years is a reduction of 29% well above the original target. It should also be mentioned that the performance data used, noon reports in combination with publicly available data, is not granular enough, and the result might best be described as a range between 25% and 35%. The analysis used ISO19030 with some necessary modifications.

This is the result of many contributing factors:

1. Strict adherence to our propeller polishing policy
2. Structured monitoring of the fouling degree / evolution by divers
3. Early hull grooming rather than late hull cleaning
4. Optimizing hull treatment in dry dock; squaring preferred over spot blasting
5. Optimizing antifouling selection based on the ships' actual operative profile
6. Monitoring of hull performance
7. Power trail improvements
8. Raised awareness onboard

In other words, it is important to employ all cost-effective solutions we have at our disposal to yield the most promising result.

6. Mapping the various biofouling activities

There are many organizations worldwide developing best practices and other solutions with the aim of reducing biofouling on ships. Fig.1 shows many of these organizations and how they interact. Harmonization of efforts is imperative that the outcome is practical and effective.

References

IMO MEPC.282(70) - *The Ship Energy Efficiency Management Plan*

IMO MEPC.207(62) - *The Guidelines for the control and management of ship's biofouling to minimize the transfer of invasive aquatic species*

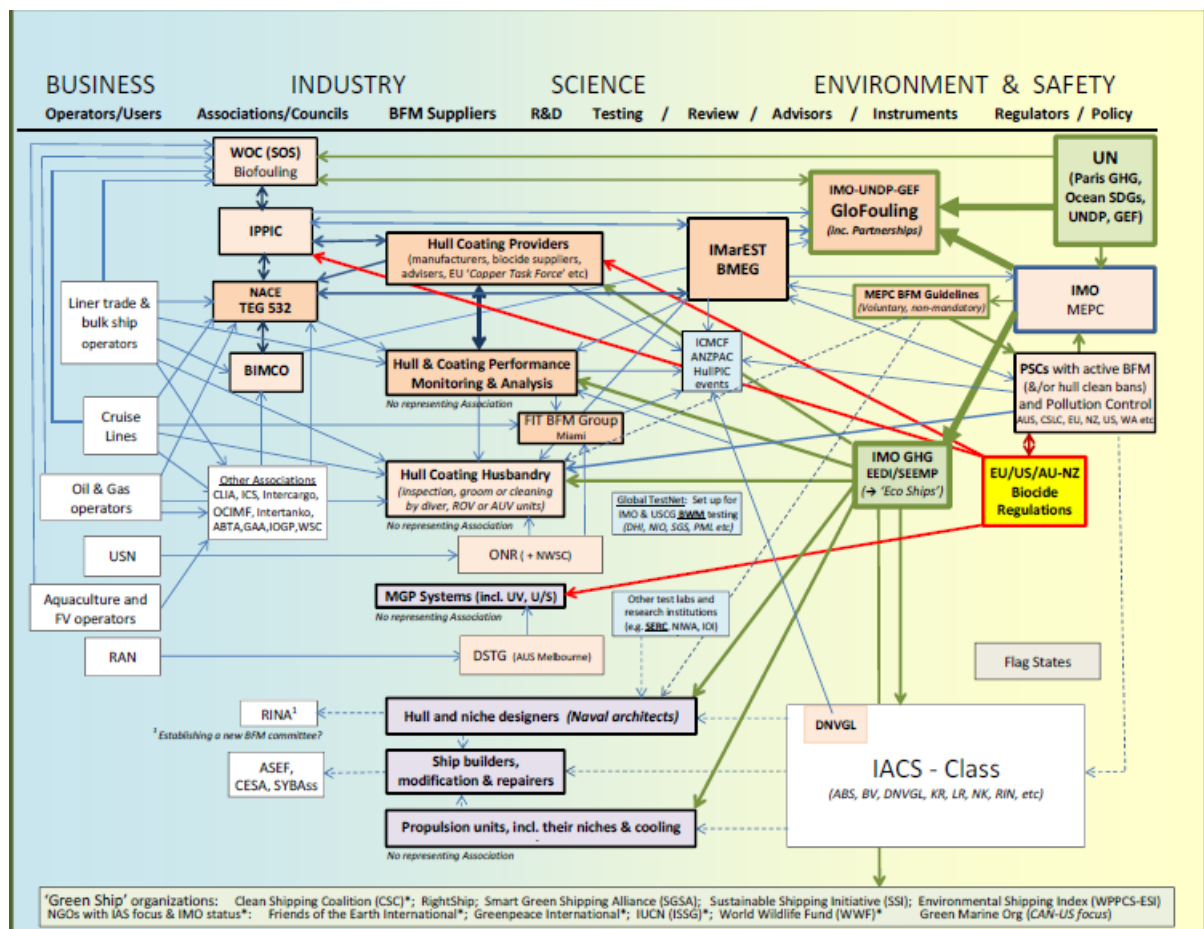
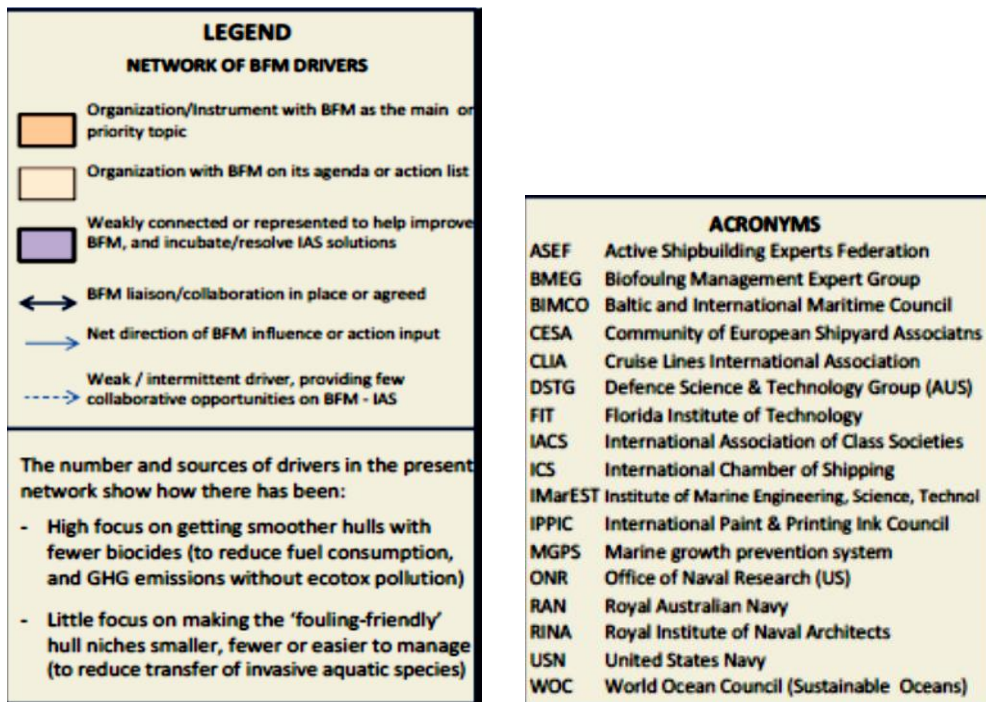


Fig.1: Organizations developing best practices and other solutions to reduce biofouling on ships, see Fig.2 for abbreviations



Produced for NACE TEG532 [Ecological Risks of Biofouling] by Intermarine Consulting Pty Ltd

Updated October 1, 2018

Fig.2: Abbreviations used in Fig.1

Some Fairy Tales in Performance Monitoring Revisited

Volker Bertram, DNV GL, Hamburg/Germany, volker.bertram@dnvgl.com

Abstract

This paper looks critically at some assumptions and allegations floating around in performance monitoring: data frequency as a cure-all; capability to separate hull degradation and propeller degradation; capability to correct for sea state 4 and above. Lack of error analyses is pointed out as a frequent root cause for questionable confidence and assertions.

1. Introduction

The HullPIC conference has promoted our collective insight into hull and propeller performance monitoring. And, by and large, the performance monitoring solutions employed now are much better than what was on the market when the Working Group for ISO 19030 started its work.

We have moved from the dark middle ages to a period of (early) enlightenment. However, some old wives' tales and half-truths are hard to eradicate, especially if they make for convenient short-cuts in performance monitoring models. Most old wives' tales contain some truth or are sometimes true, and therefore sound so convincing. And covered in a cloak of a nice-sounding "law" or Big Data new-age mumbo-jumbo, the middle-age beliefs keep coming back. Maybe this paper can contribute to more transparency and enlightenment on some of the most popular half-truths (a.k.a. fairy tales, old wives' tales, urban myths, or marketing).

2. Urban myths concerning data quantity

2.1. More data sets = better results, always

"The higher the frequency in data logging, the better the results." There is a widespread belief that ever-higher sampling frequency will improve insight. ISO 19030 uses 0.07 Hz (1 data set every 15 s) as minimum requirement for the default method, but some in the industry boast sampling rates of 1 Hz and above. But how useful is higher data sampling frequency really?

We could copy and paste the same data set 1000000 times. Obviously, that would not give any more insight. More data sets are no good if they are exactly the same, and little good if they are almost the same. We need independent data sets with sufficient variation in (steady) variables to derive useful insight. If the sampling frequency is higher than the frequency of ship motions (encounter frequency), there will be spurious changes in key variables. While added resistance in waves is negligible for most ships up to sea state 3, the periodic surge motion in longitudinal direction induces non-negligible changes in speed, propeller rpm and torque. These make averaging a necessity. The recommendations of ISO 19030 make sense here. With 10-minutes averaging, the fluctuations due to ship motions will average out for most cases. Only in following seas, very low encounter frequencies may occur.

There is no harm (and little gain) in higher data sampling frequency. The average values over 10 minutes are probably quite constant if data frequency is increased. Perhaps someone with access to high-frequency data could verify this assumption. The advantage of high-frequency data is that both average value and standard deviation (or another measure of variation) can be derived. This can help in filtering data sets where above-average variation indicates atypical conditions during the sampling interval, e.g. maneuvering.

In any case, averaging intervals should be short enough to ensure that the statistical characteristics of the seaway (significant height and period, direction) and ship speed are constant. Again, the ISO 19030 default recommendations of 10 minutes fulfills this requirement.

2.2. Everything will average out for the best

“Everything will average out for the best.” This is another hopeful adage in performance monitoring, particularly if correction methods are weak. But this assumes that there are no long-term operational changes (e.g. different routes due to different demand), no large-scale ambient changes such as fluctuations in the Gulf stream or sea state climates.

For ferries on a fixed route, with little variability in draft, trim, speed, etc., “everything will [indeed] work out for the best”. For chartered multi-purpose vessel, most likely by the time averaging has taken care of your errors, any useful insight comes too late.

3. Hull and propeller lived separately ever after

“We can separate propeller and hull performance without thrust meter.” And we can make it look scientific or we can make it simple and appealing to the common sense. We have three (virtually) independent variables: speed, propeller rpm and torque. If, compared to the clean reference condition at same propeller rpm, we have

- a) Lower speed, then the resistance has increased and we blame hull fouling
- b) Higher torque, then we blame propeller fouling/degradation

In reality, for same rpm, we will typically see both speed loss and torque increase. The hull fouling will change the inflow to the propeller and thus also propeller efficiency. But let’s say these interaction effects are small; then we could use as a rule of thumb the percentage loss in speed and the percentage torque increase and split the total degradation accordingly. But this is very coarse and the insight is mostly that you should clean both propeller and hull.

One can try to estimate the contributions from propeller and from hull by using more elaborate theories. Maybe I should be pleased that many such attempts give reference to my book, *Bertram (2012)*. But should I be pleased when the formulas are used without the hydrodynamic understanding that I had hoped the book would bring? Maybe they don’t see it, maybe they try to blind us with science. The formulas use assorted efficiencies η and/or wake fraction w and thrust deduction t . If you only look at the design condition (design draft, zero trim, design speed, no wind, no sea state), these variables are constants as the single symbol suggests. But for performance monitoring, they are functions of many parameters. For example, we should write $w(V, T, \theta, \dots)$ instead of w ; and any approach should document how each function is modelled. For example: “ w will change with draft, but we don’t know how and therefore always take the value at design draft. w will change with trim, but we don’t know how and therefore always take the value for zero trim. w will change with...” You get the idea.

The quantities depend also on scale, i.e. they differ between model tests and full-scale ship. This should be kept in mind, as many approaches take them from model basin reports where “experience-based” extrapolation leads to significant variations (10% have been reported in oral communication by Maersk) between different model basins. If such approximate full-scale extrapolation for a specific ship are not available from model-basin reports, some people use an approximation of the approximation: design formulas (for design conditions and typically based on ships tested in the 1960s) as found in *Bertram (2012)*.

“All models are wrong, but some are [still] useful,” said George Box. More precisely, all models are approximations. Some may be very good approximations, some may just get the order of magnitude right. ISO 19030 quantified the uncertainty for the performance indicator for the default method described in Part II of the standard, using random variations within the range of uncertainties of the input variables to see how this would affect the final results. A corresponding approach would be needed in the assorted hydrodynamic models trying to separate propeller and hull performance. We need to estimate uncertainty (or accuracy) of variables and functions and see how the errors propagate

to the end result. Maybe some very rough estimates are OK, maybe some simplifications lead to 50% variation in the final numbers. Assuming uncertainties and seeing how they propagate is a task any developer can do and we should ask for this at least in scientific publications.

Quantifying the effect of speed, draft, trim, possibly induced motions by ambient waves on e.g. the wake number at full scale would be a nice research project for the CFD (computational fluid dynamics) community.

4. My formula / machine learning can correct for sea state 4 and above

“We can correct for sea state 4 and above.” This may come in disguise with filters set at higher sea states. We can apply formulas and software, but the errors will be high, easily 50%, possibly 100%. Among experts, we may argue whether correcting for sea state 4 is possible with acceptable errors. For sea states up to 3, you can use any correction or none at all (as in the default method of ISO 19030). If your wave heights are derived from sea state estimates from the crew, you may as well omit any correction. See *Bertram (2016)* for a detailed discussion.

If we have good measurements of the actual near-field of waves around the ship and good three-dimensional methods to compute the added power in oblique waves, we may correct for higher sea states. But probably the best approach would be to compute the speed loss or added power and filter based on percentage of the calm-water power for that case, as promoted in *Schmode et al. (2018)*. Vendors of wave measurement equipment and services should publish comparisons with wave buoy measurements to get realistic estimates for errors in wave measurements. Then error propagation analyses should give insight into the effect on performance indicators.

Machine learning is just another (and more obscure) way of approximating a relation between waves and added power or speed loss. It does not change the fundamental dilemma.

5. Conclusion

Data frequency is not a cure-all. Averaging over sampling intervals is necessary to remove fluctuations from ship motions in waves. When averages and standard deviations no longer significantly change with higher frequency, further increase in frequency becomes pointless.

Nobody can correct reasonably for higher sea states, because the initial information on waves becomes too uncertain and the correction methods have large errors in real seaways. Filtering at sea state 3 is fine, filtering at sea state 4 often an uncomfortable necessity; beyond that, the data sets cause more harm than good.

We should collectively work more on error estimates, particularly on error propagation in the performance monitoring models.

Acknowledgement

I am grateful to Prof. Heinrich Söding, who helped sharpening my views on the finer points of (practical) ship hydrodynamics as required for this paper.

References

BERTRAM, V. (2012), *Practical Ship Hydrodynamics*, Butterworth & Heinemann, Oxford

BERTRAM, V. (2016), *Added power in waves – Time to stop lying (to ourselves)*, 1st HullPIC Conf., Pavone, pp.5-13, <http://data.hullpic.info/HullPIC2016.pdf>

BERTRAM, V. (2017), *Some heretic thoughts on ISO 19030*, 2nd HullPIC Conf., Ulrichshusen, pp.4-

11, http://data.hullpic.info/hullpic2017_ulrichshusen.pdf

SCHMODE, P.; HYMPENDAHL, O.; GUNDERMANN, D. (2018), *Hull performance prediction beyond ISO 19030*, 3rd HullPIC Conf., Redworth, pp.135-140, http://data.hullpic.info/hullpic2018_redworth.pdf

Fully Automated CFD Analysis for Full-Scale Ship Hydrodynamics

Inno Gatin, Wikki Ltd, London/UK, i.gatin@wikki.co.uk
Vuko Vukčević, Wikki Ltd, London/UK, v.vukcevic@wikki.co.uk
Hrvoje Jasak, Wikki Ltd, London/UK, h.jasak@wikki.co.uk

Abstract

A Computational Fluid Dynamics (CFD) software environment for establishing full-scale ship hydrodynamic characteristics with low cost and time to delivery is presented in this paper. The framework features fully automated process of CFD analysis from geometry input to report generation. Two applications are supported: prediction of resistance curve and power curve. The automated power curve prediction enables trim optimisation knowledge database calculation for low cost. The software requires minimal user interaction by using pre-set numerical settings that are tailored for steady resistance in calm water and self-propulsion, providing accurate CFD simulations. The framework is based on an open-source software eliminating licence-related fees, enabling low overall cost.

1. CFD in the marine industry

Many speak of Computational Fluid Dynamics (CFD) as the great new technology that can solve all problems in designing ships of all kinds. Yet, we do not seem to see this in everyday life of ship design offices. CFD is getting more accurate, fast and reliable but still it did not spread in the marine industry like many have anticipated. Sure, there is a plethora of research groups and R&D departments in big companies doing CFD but this is still not the market-wide application that can really transform the industry. Small design offices seldom rely on CFD, and only a fraction of the world's fleet uses CFD-generated trim optimisation data-bases to save fuel in daily operation (Reichel, Minchev, & Larsen, 2014).

So where's the problem? It is no secret that CFD is computationally expensive, but is this really the number one reason why it is not spreading through small design offices and ships in service like wild fire? Not really. The cost of High Performance Computing (HPC) has reduced so much that almost any CFD software can calculate ship steady resistance at five speeds for less than 200 EUR of CPU-related costs. Cloud-based HPC services are widely available and easy to use. The problem seems to lie on the other side of the computer screen – the human effort and expertise that are necessary to prepare and interpret the simulations. A man-hour of a highly skilled expert is far more expensive than computer resources, and this is a two-fold obstacle for everyday application of CFD. First, the highly skilled expert can usually do only the one thing – CFD calculations, and second, he is very expensive! This prevents many small to medium ship design offices and ship owners to use CFD: their intermittent needs for CFD do not justify employing an expensive expert to sit around most of the year. Even if they do, it does not guarantee a successful application of the technology.

In order for CFD to really contribute to the shipping industry on a larger scale, these problems need to be addressed. The amount of human effort needs to be minimised to reduce the man-hour cost, while at the same time the number of input parameters needs to be brought down to ship particulars and load condition details, leaving CFD-specific parameters away from the user. This can be done by automating the entire process, which also solves the second problem: the need for a highly skilled CFD engineer. There is a big “however” here, and that is that it is very difficult to automate the complete CFD calculation process, from pre-processing to post-processing. Generating the computational grid is the most time-consuming part of the process, and requires heavy user-interaction in an iterative process. Running the simulation, i.e. processing, requires specific knowledge of CFD in order to properly set-up numerical parameters, often entailing considerable uncertainty of the user with respect to different parameters leading to human error and poor results. The post-processing step is straight forward and does not differ from other similar engineering

activities, where a comprehensive document containing relevant results and graphs should be produced. Still, it consumes a significant amount of precious man-hours.

Despite the difficulties, fully automating the CFD process is possible, but only for narrowly specialised applications. Luckily, calm water ship resistance and self-propulsion are specific enough to allow automation. This paper presents a fully automated numerical framework for these two specific applications that is a result of years of experience in performing such calculations, which yielded a set of numerical settings that are broadly applicable for different vessel types. A parametrised grid generation methodology is developed that is fully autonomous, requiring only basic ship information. The automatic self-propulsion calculation capability is applicable to generating low-cost knowledge data-bases needed for trim optimisation, where the delivered propeller power is calculated depending on the draught, trim and vessel speed. The numerical framework is based on in-house CFD software specialised for naval hydrodynamics called the Naval Hydro Pack.

2. About the software

The Naval Hydro Pack is a CFD software based on collocated Finite Volume method. In this work, we rely on Level Set for interface capturing. Special discretisation techniques are employed based on the Ghost Fluid Method to guarantee high accuracy of the two-phase flow model (*Vukčević, Jasak & Gatin 2017*). The ship propellers are modelled using the actuator disc model where a pressure jump is prescribed on a circular surface representing the propeller. The key feature of the algorithm is the ability to assess the undisturbed propeller inflow velocity without the need to perform a separate open water calculation (*Jasak, Vukčević, Gatin, & Lalović, 2019*).

3. Calm water resistance

The developed automated framework enables various vessel types to be considered, i.e. no assumptions are made on the ratios of L, B and T, number of hulls, or on the Froude numbers. Fig.1 shows a few examples of different vessels during a calm water resistance simulation produced with the fully-automated procedure. Calculation of ship resistance in calm water conditions is very important and therefore deserves to be verified and validated in detailed. The Naval Hydro Pack has shown to be sufficiently accurate and precise in the past (see e.g. *Gatin, Jasak, & Vukčević, 2015*); however, some recent results from *Gatin, Vukčević, Škurić, & Jasak, 2018* will be shown here.

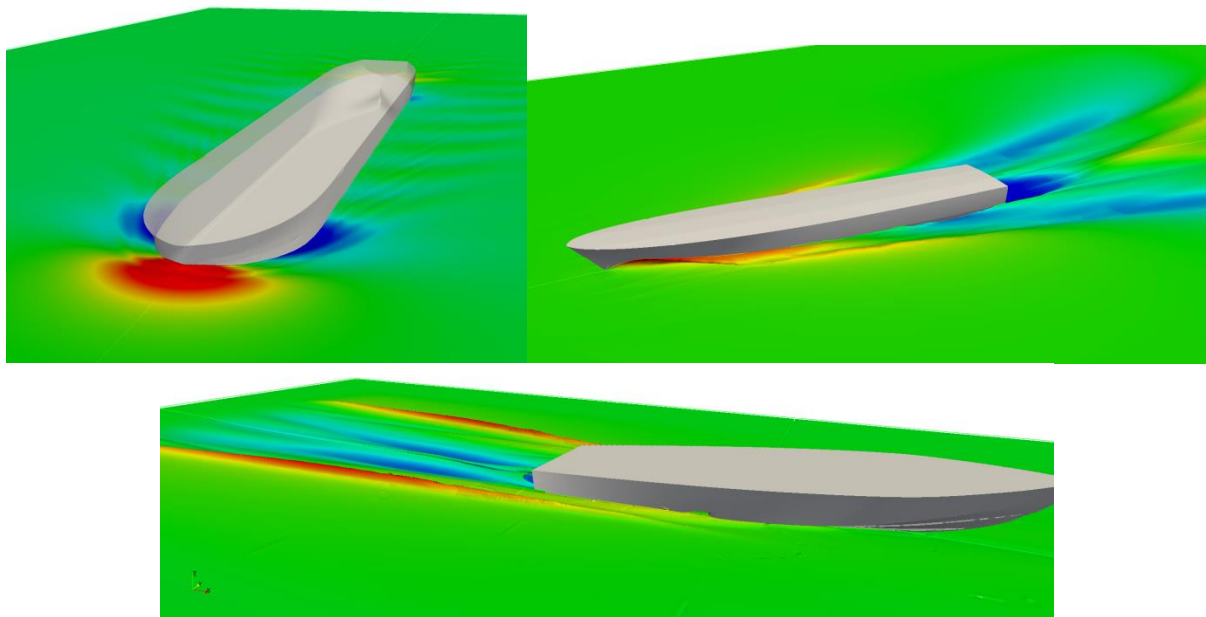


Fig.1: Various hull forms sailing in calm water

To test the automated procedure, three different, publicly available hull forms are selected and simulated. Namely the KCS, JBC and DTMB 5512 hull forms are used, <http://www.t2015.nmri.go.jp/>, <http://www.iuhr.uiowa.edu/shiphydro/efd-data/5512-steady/>, both due to the availability of the geometries and experimental results. Accuracy is reported in this section, while man-hour and computational costs are presented in Section 5.

Table 1 shows the main particulars of the three vessels. Here, λ denotes the scale of the model. Note that the simulations are performed in model scale to allow direct comparison against experimental results; however the numerical framework makes no assumptions on the scale of the ship. Table 2 shows the characteristics of computational grids generated by the automatic framework. Fig.2 shows the side-view of the generated grids for the three hull forms.

Item	KCS	JBC	DTMB
L_{PP} , m	230	280	142
∇ , m ³	52 030.0	178 369.9	8 702.7
V , kt	24	14.5	14.6
F_r	0.26	0.142	0.201
λ	31.6	40.0	46.6

Table 2: Characteristics of computational grids automatically generated for the three test hull forms

	KCS	JBC	DTMB
No. Cells	1 609 281	1 733 267	2 219 751
No. Hexahedra	1 526 009	1 699 753	2 183 431

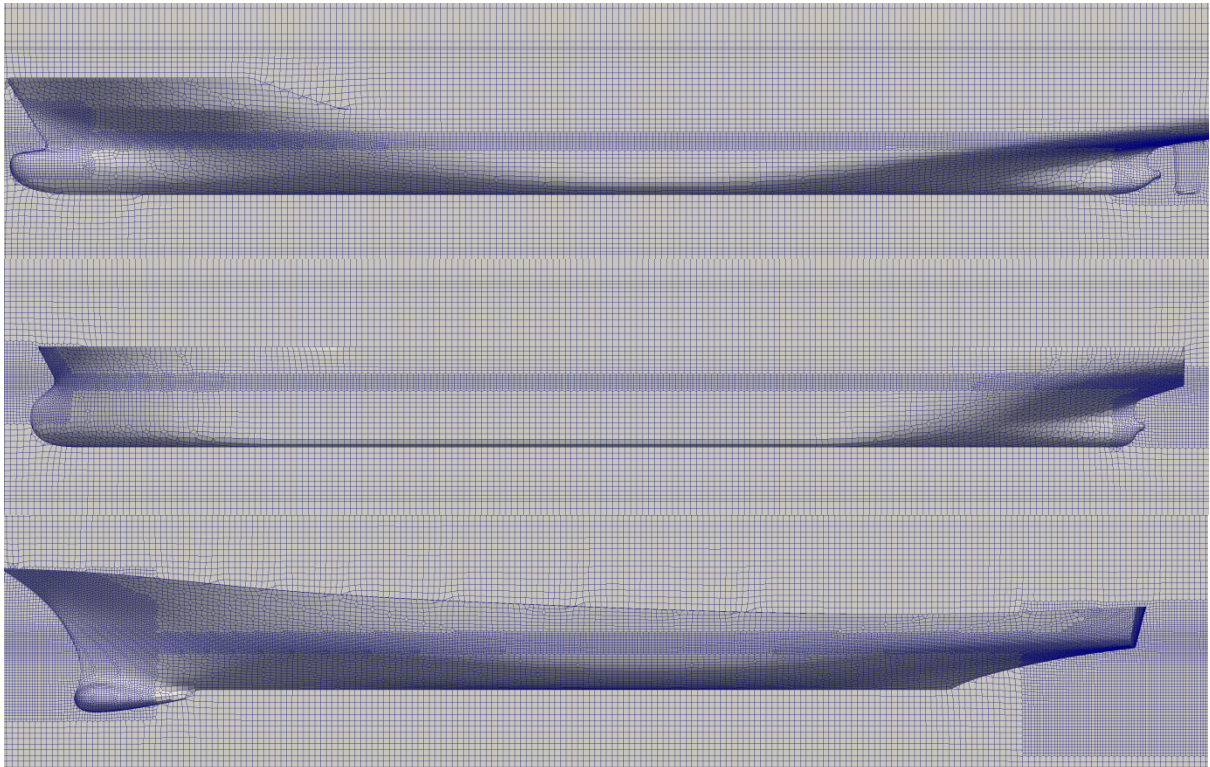


Fig.2: Side-view of the generated computational grids for KCS, JBC and DTMB hulls, in that order from top to bottom

Table 3 shows the results of the steady resistance simulations for KCS, JBC and DTMB hull together with corresponding experimental data. In the table σ denotes the dynamic sinkage, τ stands for dynamic trim angle, while E_{rr} stands for relative error calculated as $E_{rr} = (EFD - CFD)$, where EFD denotes the experimental result and CFD the simulation result. The differences are within 4% for resistance and within small range for sinkage and trim as well. Note that the results are obtained from the first try using the automated framework, and no simulations were repeated in order to get better agreement.

Table 3: Results of ship resistance in calm water for KCS, JBC and DTMB compared to EFD

Item	KCS	JBC	DTMB
$C_T * 10^3$	3.64	4.13	4.54
$C_{T,EFD} * 10^3$	3.71	4.29	4.50
$E_{rr,Ct}, \%$	1.9	3.7	-0.9
σ , m	-0.441	-0.31	-0.08
σ_{EFD} , m	-0.445	-0.24	N/A
$E_{rr,\sigma}$, m	0.004	0.07	N/A
τ , °	0.182	0.104	0.21
τ_{EFD} , °	0.169	0.103	N/A
$E_{rr,\tau}$, °	-0.013	-0.001	N/A

4. Self-propulsion

In order to resolve the complex interaction between the ship's hull and the propeller, a self-propulsion simulation needs to be performed where the resistance of the hull is balanced by the thrust force of the propeller. An actuator disk model is applied in the present numerical model, which is fed with the open-water curves of the actual propeller. A proportional-integral controller is applied in order to adjust the rotation rate of the propeller until the resistance of the hull is balanced by the thrust. The result is the power needed to be delivered to the propeller and rotation rate.

To gain confidence in the current approach the code was tested on three different cases:

1. Self-propelled model-scale JBC test case with experimental comparison published in *Bakica, Gatin, Vukčević, Jasak, & Vladimir, 2019*. It was shown that the resistance force acting on the hull in the self-propelled condition agreed with experimental measurements within 0.3%, while the thrust and torque coefficients were assessed with accuracy of around 8%.
2. Full-scale case of a car-carrier produced by the Uljanik shipyard in Croatia, where the measured mile results were compared to CFD simulations (*Jasak, Vukčević, Gatin, & Lalović, 2019*). Here, instead of fixing the ship speed, the power delivered to the propeller was fixed, while the result was the ship speed on the measured mile and propeller rotation rate. The calculated ship speed was within 0.1% of the measured speed on the fine grid, while the calculated 126.27 RPM gave a difference of 0.24%. Fig.3 shows the forward speed calculated on three different computational grids compared to the value measured at the measured mile on sea-trials. Fig.4 shows the perspective view of the ship in the simulation, where the actuator disc model can be observed.

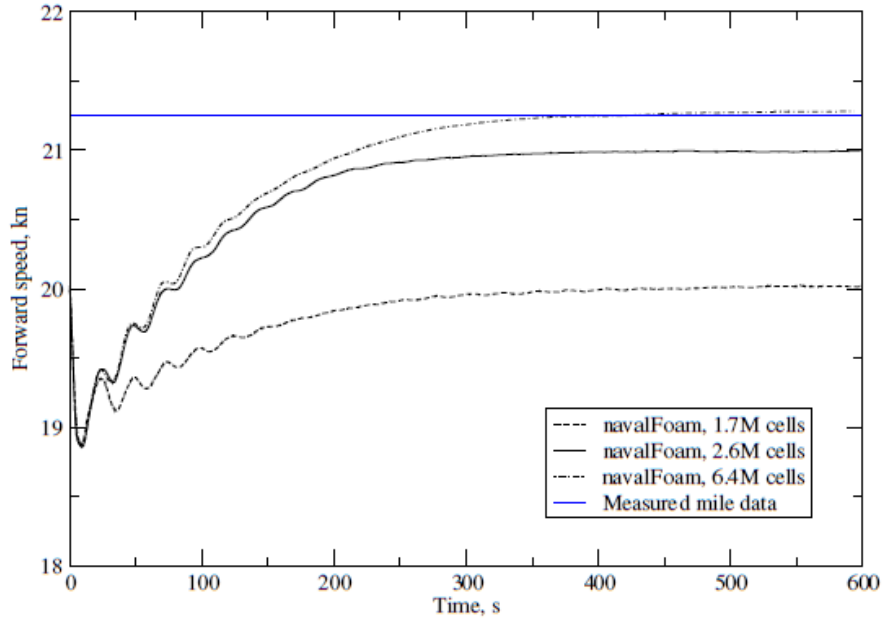


Fig.3: Forward speed of the full-scale, self-propelled car-carrier: CFD results and measured mile data (Jasak, Vukčević, Gatin, & Lalović, 2019).

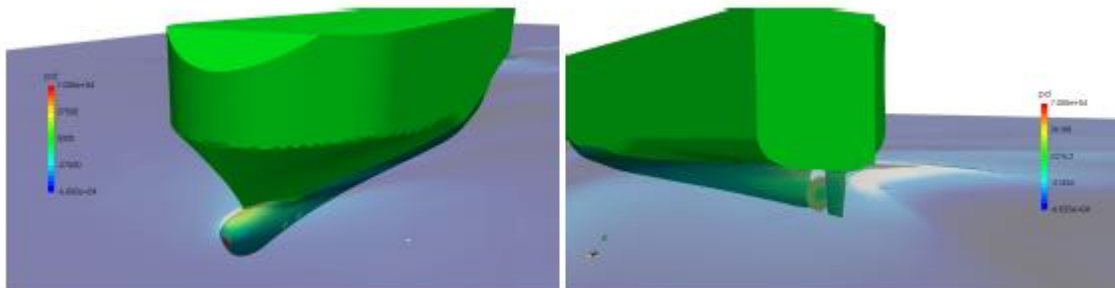


Fig.4: Car-carrier in the self-propulsion simulation

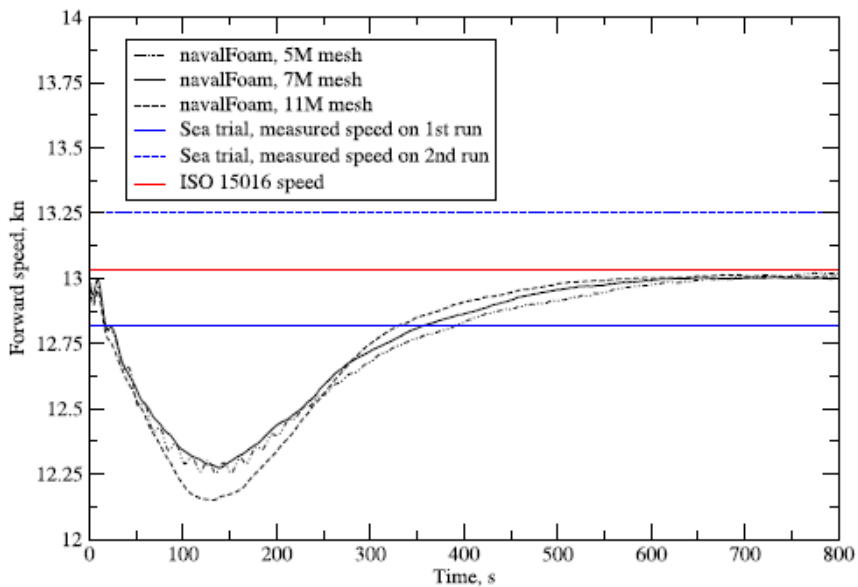


Fig.5: Forward speed of the general cargo carrier Regal, as measured on the sea trial and calculated using CFD (Jasak, Vukčević, Gatin, & Lalović, 2019)

- Full-scale case featured on the Lloyd’s Workshop on Ship Scale Hydrodynamic Computer Simulations, Ponkratov (2017), <http://www.lr.org/en/projects/findings-of-lrs-full-scale-numerical-modelling-workshop.aspx>, where sea trials were conducted to serve as benchmark data. The ship in question is a general cargo carrier Regal. In this case, a fixed propeller rotation rate is applied and the final ship speed is reported. Fig.5 shows the forward speed convergence compared to measured values during the sea trial. It can be observed that CFD converges towards the mean of the two measured values (measured mile in one direction and the opposite, denoted with blue lines). The calculated ship speed falls within 0.2% of the ISO 15016 speed.

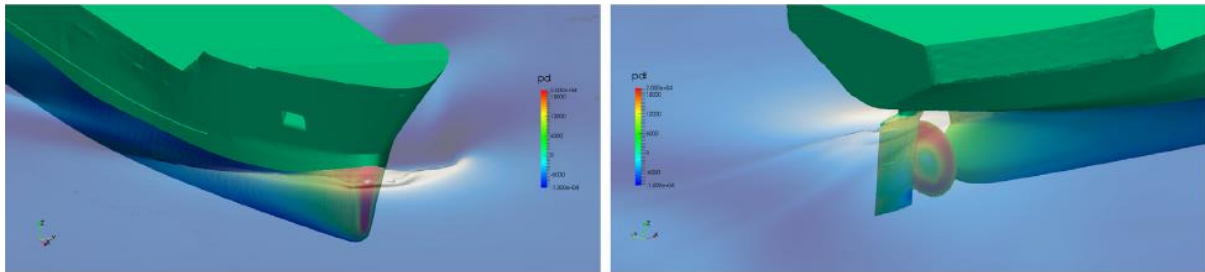


Fig.6: General cargo ship regal during the self-propulsion simulation

5. Automatic framework

The automated procedure starts with user input, where data such as main ship particulars, loading condition particulars (draft and displacement), speed range and similar are supplied to the software. A Python based environment takes over from there, first generating the computational grid and then setting up all the necessary simulations. The simulations are then ready to be executed using the Naval Hydro Pack software. When the simulations are finished, a document is automatically generated comprising results for all load conditions and speeds. Graphs are included where relevant items are plotted against speed, such as resistance, power or RPM. Additionally, for the calm-water resistance simulations polar graphs of inflow velocity distribution in the propeller plane are automatically produced, as shown in Fig.7.

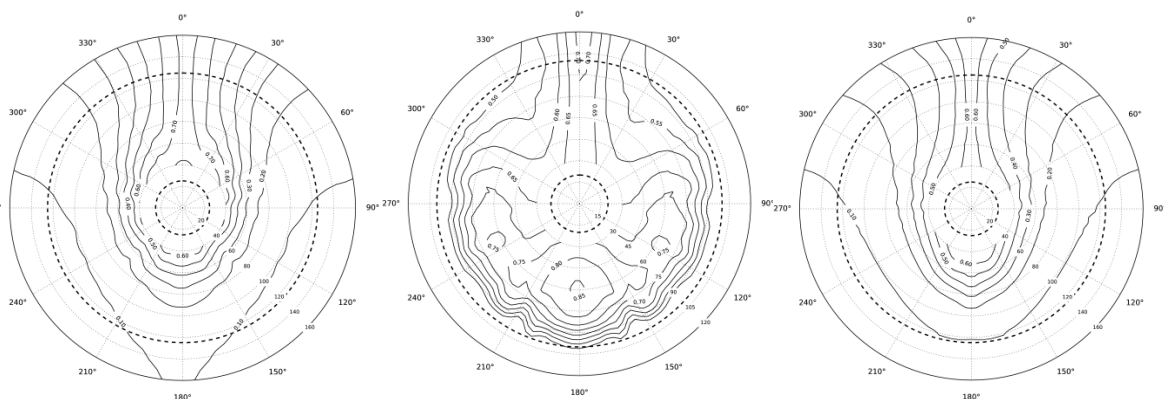


Fig.7: Automatically generated wake field plots for KCS, JBC and DTMB, from left to right

6. Cost analysis

For the three calm water resistance simulations performed in Section 3, an analysis of invested man-hours and computational time is conducted. Note that running the self-propulsion simulations using the automated framework exerts essentially the same amount of human effort; hence the data presented below can be applied to self-propulsion analysis as well. All simulations are conducted on 64 cores of Intel Xeon Processors, E5-2637 v3, 15M Cache, 3.50 GHz.

Table 4 shows the amount of man-hours, computational time and cost required for individual hull

forms. A cost of 0.1 EUR per core-hour is assumed in the computational cost assessment. In average, it takes around 40 minutes of human effort for a single hull form. Note that this number would not change even if more simulations for individual ships were performed, e.g. at five different ship speeds or different static trim angles. Thus, 40 minutes represents an average amount of human effort per ship, irrespective of the total number of simulations conducted for that ship. The computational time scales linearly with the number of simulations, and on average it costs 8.7 EUR to perform a single simulation. Note that self-propulsion simulations can exert more computational resources; hence the price of computations can go upward.

Given the computational cost of individual simulations, it is obvious that the cost of man-hour is indeed dominant. Reducing the man-hour cost to less than one hour per ship is an essential key to bring CFD analyses of this type to widespread industrial application.

Table 4: Man-hour cost and CPU time needed for individual calm water resistance simulations

	KCS	JBC	DTMB	Average
Man-hours per ship, h	0:25	0:46	0:48	0:39
CPU wall-clock time per simulation, h	1:06	1:01	1:58	1:22
Total core-hours per simulation, h	70.4	64.0	126.9	87.1
CPU cost per simulation, EUR	7.0	6.4	12.7	8.7

6. Conclusion

The main reason why CFD is not being applied widely in the marine industry is the cost of conducting accurate and reliable calculations, which is a consequence of high complexity of the method. In an effort to address this issue, and to make a step forward towards CFD application in every-day marine industry activities, a fully automated computational framework is developed and presented in this paper. The framework is based on a CFD software called the Naval Hydro Pack, specialised for problems encountered in marine and offshore hydrodynamics.

The automated framework reduces the required man-hours to 40 minutes per ship, which is an order of magnitude reduction with respect to current practice. This applies to calm water resistance and self-propulsion simulations, which are essential in ship design and for generating knowledge data-bases for trim optimisation onboard ships in service, respectively. As an example, the prediction of calm water resistance for ten different vessel speeds would take 40 minutes of human effort, and around 90 EUR of computational resources.

References

- BAKICA, A.; GATIN, I.; VUKČEVIĆ, V.; JASAK, H.; VLADIMIR, N. (2019), *Accurate assessment of ship-propulsion characteristics using CFD*, Ocean Engineering, pp.149-162
- GATIN, I.; JASAK, H.; VUKČEVIĆ, V. (2015), *Validation and Verification of Steady Resistace KCS Simulations with Sinkage and Trim using Embedded Free Surface Method*, Tokyo 2015: A workshop on CFD in Ship Hydrodynamics
- GATIN, I.; VUKČEVIĆ, V.; JASAK, H.; RUSCHE, H. (2017), *Enhanced coupling of solid body motion and fluid flow in finite volume*, Ocean Engineering, pp.295-304
- GATIN, I.; VUKČEVIĆ, V.; ŠKURIĆ, V.; JASAK, H. (2018), *Fully Automated Ship Resistance Prediction using the Naval Hydro Pack*, Technology and Science for the Ships of the Future, Trieste, pp.256-263
- JASAK, H.; VUKČEVIĆ, V.; GATIN, I.; LALOVIĆ, I. (2019), *CFD validation and grid sensitivity studies of full scale ship self propulsion*, Int. J. Naval Architecture and Ocean Engineering, pp.33-43

PONKRATOV, D. (2017), *2016 Workshop on Ship Scale Hydrodynamic Computer Simulations*, Lloyd's Register, Southampton

PONKRATOV, D.; ZEGOS, C. (2015), *Validation of Ship Scale CFD Self-Propulsion Simulation by the Direct Comparison with Sea Trial Results*, 4th Int. Symp. Marine Propulsors

REICHEL, M.; MINCHEV, A.; LARSEN, N.L. (2014), *Trim Optimisation - Theory and Practice*, Int. J. Marine Navigation and Safety of Sea Transport, pp.387-392

VUKČEVIĆ, J.; JASAK, H. (2015), *Seakeeping Validation and Verification using Decomposition Model based on Embedded Free Surface Method*. Tokyo 2015: A workshop on CFD in Ship Hydrodynamics

VUKČEVIĆ, J.; JASAK, H. (2015), *Validation and Verification of Decomposition Model based on Embedded Free Surface Method for Oblique Wave Seakeeping Simulations*, Tokyo 2015: A workshop on CFD in Ship Hydrodynamics

VUKČEVIĆ, V.; JASAK, H.; GATIN, I. (2017), *Implementation of the Ghost Fluid Method for the Free Surface Flows in Polyhedral Finite Volume Framework*, Computers and Fluids 153, pp.1-19

Introduction of OCTARVIA Project: Project for Ship Performance in Actual Seas

Naoto Sogihara, National Maritime Research Institute, Tokyo/Japan, sogihara@nmri.go.jp

Takashi Yonezawa, Monohakobi Technology Institute, Tokyo/Japan,
takashi_yonezawa@monohakobi.com

Tsuyoshi Ishiguro, Japan Marine United Corporation, Tokyo/Japan, ishiguro-tsuyoshi@jmuc.co.jp

Yoshihiko Sugimoto, Mitsui O.S.K. Lines, Tokyo/Japan, yoshihiko.sugimoto@molgroup.com

Shinta Masuyama, Kawasaki Kisen Kaisha, Tokyo/Japan, masuyama.shinta@jp.kline.com

Hirohisa Mieno, Chugoku Marine Paints, Hiroshima/Japan, hirohisa_mieno@cmp.co.jp

Mamoru Shimada, Nippon Paint Marine Coatings, Tokyo/Japan, Mamoru.Shimada@nippe-marine.co.jp

Yoshiro Matsubara, Kansai Paint Marine, Hyogo/Japan, yoshi.matsubara@kp-marine.co.jp

Abstract

This paper describes the OCTARVIA project, a Japan Maritime Cluster Collaborative Research by 25 stakeholders (including ship operators, shipyards, paint makers, machinery and equipment makers, classification society, research institute, and weather consultants) to establish a “Scale” which can objectively evaluate and compare the ship performance. Three main topics are addressed: evaluating ship performance in operation; predicting ship performance in design; presenting ship performance in operation to owners and operators. The first proposal is validated through the monitoring data of various ship types.

1. Introduction

The Greenhouse Gas (GHG) reduction strategies are decided at International Maritime Organization (IMO), which results in the start of Data Collection System on fuel consumption from January 2019. The evaluation on the performance of ships in service is becoming a trend. The fair implementation of the evaluation strongly requires the accurate measurement of the ship performance in actual seas for each ship. Making the ship performance in actual seas visible under certain indices contributes to realization of more efficient maritime transport and GHG reduction .

A project for the evaluation of ship performance in actual seas called ‘OCTARVIA’, in which 25 companies of a Japanese maritime cluster collaborate, has been launched as a three-years project aiming to establish a “Scale” which can objectively evaluate the ship performance in actual seas. Participants of OCTARVIA project are composed of eight sectors:

- Ship **O**wners
- **C**lassification society
- Pain**T** makers
- Ship**yA**rds
- **P**Ropeller & **R**udder makers
- Go**V**ernor maker
- Research **I**nstitute
- We**A**ther consulting company

The project organizes three working groups for the sub-themes as following;

S1-WG : Working Group for establishment of ship performance monitoring method in actual seas

S2-WG : Working Group for establishment of estimation method of ship performance in actual seas

S3-WG : Working Group for establishment of evaluation of ship performance in actual seas

This paper describes the outlines of OCTARVIA project and introduces the activities of S1-WG which is closely related to the topics of HullPIC.

2. The outlines of OCTARVIA project

OCTARVIA project has discussed the technical issues on the evaluation of ship performance in actual seas as shown in Table 1. To address these issues, OCTARVIA has set up three sub-themes shown in Fig.1. S1-WG treats the performance evaluation at the operation phase, and S2-WG treats the performance evaluation at the design stage. S3-WG treats how to present the ship performance in actual seas to ship owners and operators based on the evaluation method developed by S1-WG and S2-WG.

Table 1: Technical issues on ship performance discussed in OCTARVIA

Phase	Ship performance in calm seas	Ship performance in winds and waves
Design	The validation is enough carried out by tank tests and sea trials.	<ul style="list-style-type: none"> ● The procedure for model tests and prediction is not established. ● The correlation between prediction and full-scale is not validated. ● The performance cannot be compared objectively among ships.
Operation	<ul style="list-style-type: none"> ● The evaluation method of the performance in service is not established because the draft condition in speed trials is limited. ● The current monitoring cannot evaluate the performance enough to assess fouling and aging effect. 	<ul style="list-style-type: none"> ● The procedure for measurement, analysis, and evaluation based on monitoring data is not established. ● The accuracy of monitoring data is not sufficiently ensured. ● The performance resulted from monitoring cannot be compared among ships.

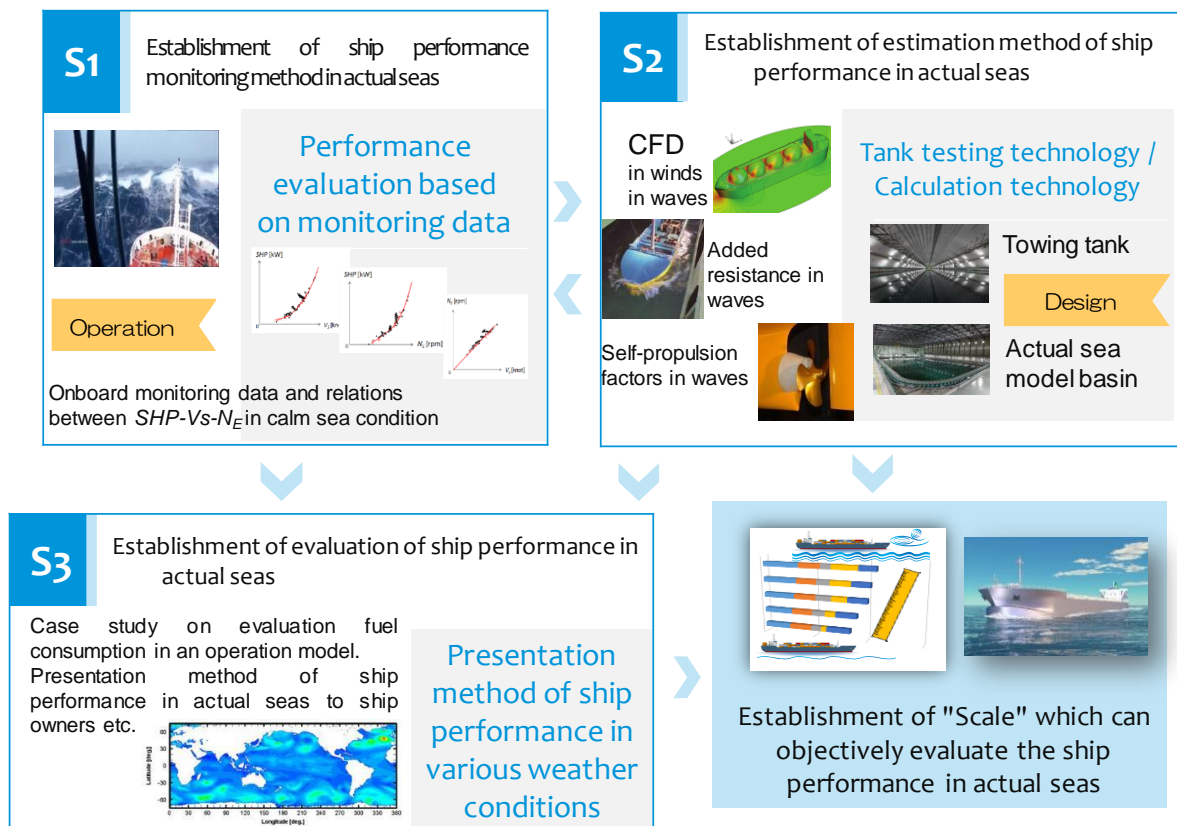


Fig.1: Outlines of OCTARVIA project

OCTARVIA focuses on the development of a ‘Scale’ which can objectively evaluate the ship performance in actual seas. The participants of OCTARVIA are able to apply the outcomes of the project for their own research and development.

2.1 Working Group for establishment of ship performance monitoring method in actual seas (S1-WG)

S1-WG is aiming to establish a performance monitoring method of ships in actual seas and the activity is outlined in section 3. The performance monitoring method has been globally spread and *ISO19030 (2016)* has been developed as an international standard for measurement of changes in hull and propeller performance. However, ISO19030 has noted that the wave correction would be considered in the future revisions of the standard. There is no international standard for evaluation of ship performance in actual seas by analyzing monitored data.

The ship performance in actual seas is derived from the combination of the ship performance in calm seas and the effect of external forces acting on a ship such as winds and waves. In other words, the ship performance in calm seas should be evaluated first. In this regard, shipyards have a lot of experiences and knowledge through sea trials because conventionally they conduct weather corrections of sea trial data. *ISO15016 (2015)* is recognized as an international standard for the assessment of ship performance by an analysis of sea trial data.

One of the objectives of S1-WG is the establishment of the method of a displacement correction. It is well-known that in each voyage a ship varies the displacement resulted from the change in cargo. The Admiralty coefficient can be one solution for the displacement correction, however, its application is limited within small displacement range. The method for a displacement correction applicable to wide displacement range is expected to be developed.

Furthermore, the performance monitoring system involves various kinds of instruments. The accurate evaluation of the ship performance in actual seas requires incorporation of sufficiently accurate instruments. In order to accomplish this, S1-WG discusses the required accuracy of each instrument based on the estimation on the effect of instruments’ accuracy on the ship performance in actual seas.

2.2 Working Group for establishment of estimation method of ship performance in actual seas (S2-WG)

Although a ship performance in actual seas has been evaluated at the design stage based on model tests or theoretical estimation, the method should be further validated through model-scale data and full-scale data. Making an objective and visible evaluation on the ship performance in actual seas requires to improve accuracy of the estimation method. S2-WG addresses the issue above and aims to establish the estimation method of ship performance in actual seas and discusses the following topics.

- 1) Evaluation on the ship performance in waves
- 2) Model test procedures for measurement of ship performance in waves
- 3) Prediction of wind forces and moment
- 4) Model test procedures in wind tunnel

2.2.1 Evaluation on the ship performance in waves

S2-WG incorporates VESTA, *Tsujimoto et al. (2015)*, developed by National Maritime Research Institute (NMRI) as the base program for the evaluation on the ship performance in actual seas. VESTA can predict added resistance in waves by involving the test data obtained in short waves, *Tsujimoto et al. (2008)*, and estimate added resistance in winds by the empirical formula, *Fujiwara et al. (2005)*. VESTA also can calculate self-propulsion factors in waves based on the algorithm of load variation test.

S2-WG addresses the improvement on the estimation on added resistance in ‘beam to following’ waves and self-propulsion factors in waves. Accomplishment of the improvement requires model test data with high accuracy for the validation of the estimation method. The model tests are carried out at the towing tank and the actual sea model basin, Fig.2.



Fig.2: Test in waves of a bulk carrier model at a towing tank

2.2.2 Model test procedure for measurement of ship performance in waves

S2-WG is aiming to establish a model test procedure for the measurement of ship performance in waves. The procedure targets measurement of added resistance and self-propulsion factors in waves with practicality and high accuracy.

The model tests can provide the benchmark data for the validation of the estimation method of added resistance and self-propulsion factors in waves. The model tests in waves also provide the data for the validation of Computational Fluid Dynamics (CFD) simulation. For example, both of the tank test and the numerical simulation are carried out with the models which have different shapes of bow.

2.2.3 Prediction of wind forces and moment

Many studies have been conducted on the prediction of wind forces and moment. They proposed empirical formulae for the prediction of wind forces and moment based on wind tunnel tests. In a few decades CFD technology has been evolutionally advanced and is applied to various fields of industry.

S2-WG aims to develop a comprehensive guideline for the prediction of wind forces and moment by means of CFD. NMRI in-house code "NAGISA", *Ohashi et al. (2018)*, has been utilized in the present study. The following items are mainly discussed with comparing the computed results to the measured data in a wind tunnel.

- ✓ Effect of ship type
- ✓ Effect of wind velocity and direction
- ✓ Effect of wind velocity profile

2.2.4 Model test procedure in wind tunnel

The International Towing Tank Conference (ITTC) introduces wind tunnel tests in its Recommended Procedures and Guidelines as one of means to estimate wind force on speed and power trials, *ITTC (2017)*. In wind tunnel tests, a model fixed to a load cell is set in winds for a measurement of wind forces and moment. Measured forces and moment are transformed into non-dimensional parameters by a representative wind velocity, an air density, a model length, and a projected area of a model.

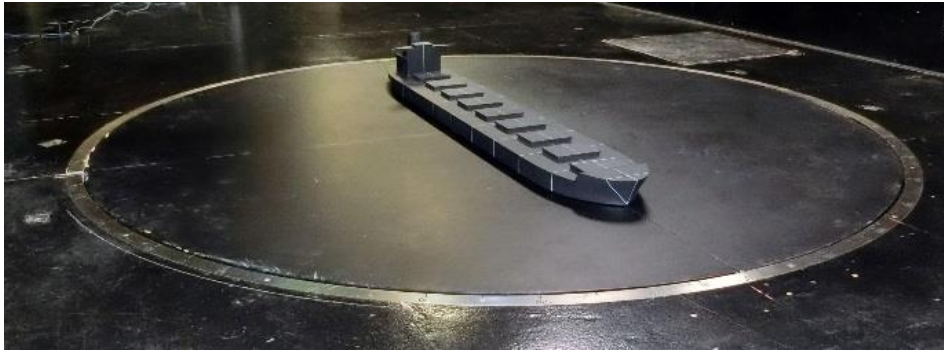


Fig.3: Wind tunnel test with a bulk carrier model

The key parameter of the wind tunnel tests is the representative wind velocity. While the representative wind velocity can be identified in uniform flow, generally the wind velocity profile shows boundary layer generated on the bottom of wind tunnel. The boundary layer is caused by specific phenomena for wind tunnels and some wind tunnels apply exponential wind velocity profile. Therefore, S2-WG discusses carefully the definition of the representative wind velocity and the wind velocity profile to be used for the wind resistance test.

Throughout the discussion including the treatment on the representative wind velocity, S2-WG aims to establish a reliable test procedure in wind tunnels. For the confirmation of the effectiveness of the test procedure, many wind tunnel tests are conducted which provide benchmark data for the CFD guidelines for the prediction of wind forces and moment.

2.3 Working Group for establishment of evaluation of ship performance in actual seas (S3-WG)

S1-WG and S2-WG address the establishment of the estimation method of ship performance in actual seas by means of the ship performance monitoring and the ship performance simulation, respectively. In order to make the best use of the outputs from S1-WG and S2-WG, an index based on the outputs which is easily understood to ship owners and operators is necessary to be developed. S3-WG aims to develop the index of the ship performance in actual seas in order to establish the evaluation method of the ship performance.

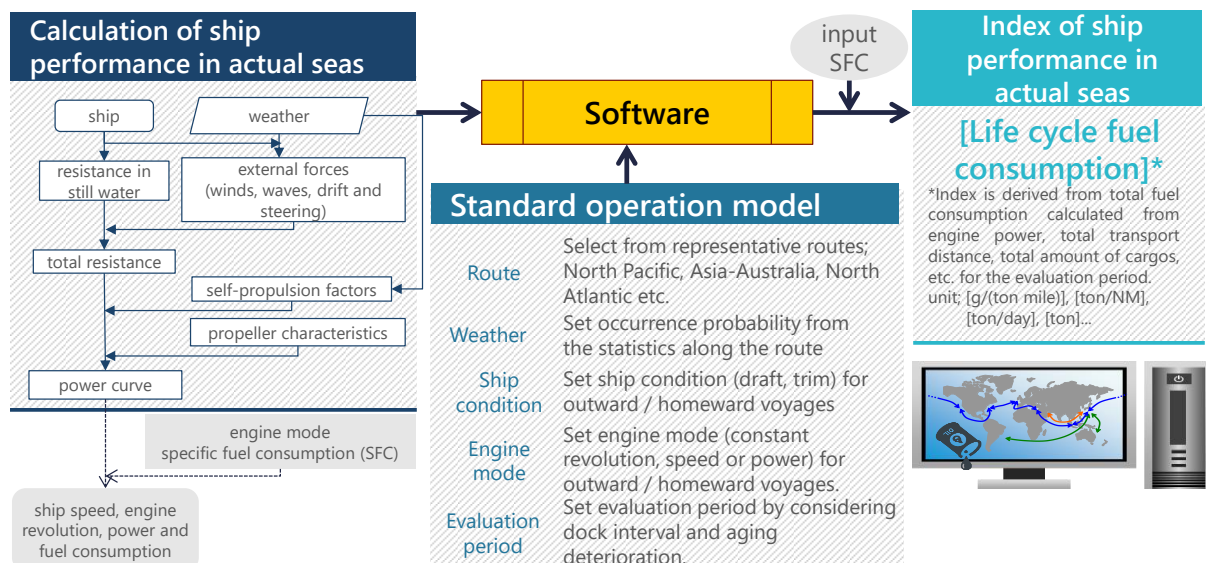


Fig.4 Concept of Life Cycle Fuel Consumption

S3-WG discusses a concept of the index and adopts 'Life-cycle Fuel Consumption (LFC)' derived from the long-term prediction of fuel consumptions in actual seas. The concept of LFC is shown in Fig.4.

LFC is calculated based on the estimation method of ship performance in actual seas developed by S2-WG. LFC is provided by a main engine output derived from the long-term prediction in a standard operation model and a separately prepared specific fuel consumption (SFC). A standard operation model prescribes the conditions for the calculation of the index, such as weather conditions and draft conditions. The calculation of LFC illustrated in Fig.5 includes the effect of fouling and aging deterioration on ship performance in actual seas as well as the occurrence probability of the weather condition.

S3-WG also discusses the target accuracy of OCTARVIA project, which results in 5% accuracy of added resistance and self-propulsion factors in waves required in the evaluation of the ship performance in actual seas. Taking into account that LFC is calculated on the basis of simulated fuel consumption, S3-WG set the target accuracy 2% of fuel consumption in actual seas.

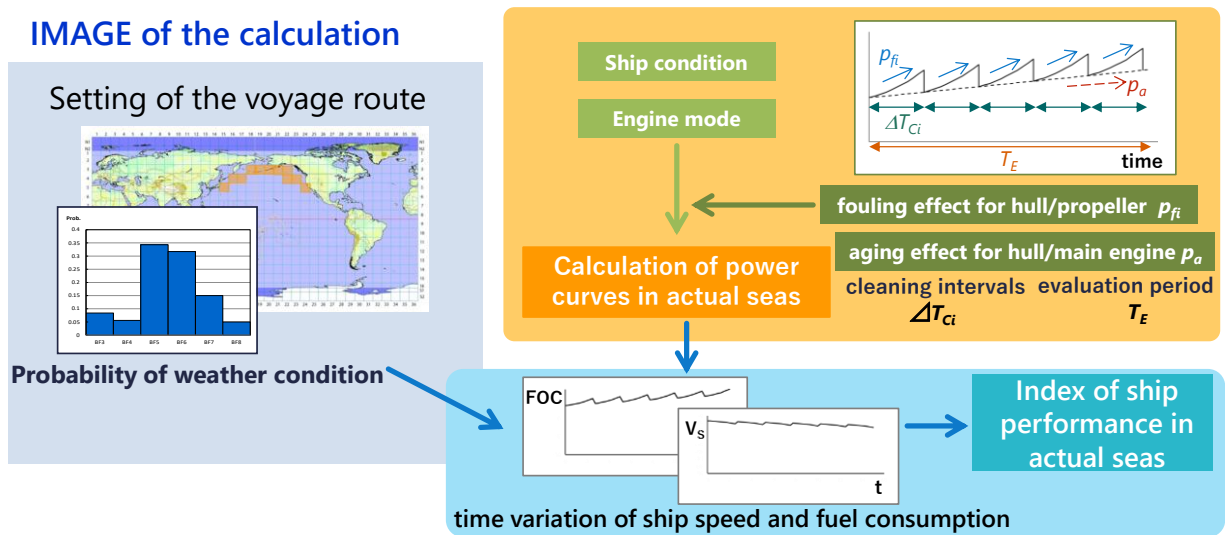


Fig.5: Illustration of calculation of Life-cycle Fuel Consumption

3. The activities of SI-WG: Analysis of ship monitoring data

3.1 Approaches for the analysis of ship monitoring data

S1-WG discusses two approaches for the analysis of ship monitoring data. One approach is ‘Simplified Analysis’ which incorporates the hull form and performance data derived from simplified formulae and does not use the detailed hull form data and tank test data which are usually confidential data for shipyards. Simplified Analysis is a helpful approach for the companies such as ship owners and operators who cannot easily access the detailed hull form data and performance data based on model tests or CFD.

Table 2: Data arrangement for analysis of ship monitoring data

	Propeller open characteristics	Resistance and self-prop. data	Hull form data	Superstructure parameter
Simplified Analysis	Simplified method	Empirical formula and ship monitoring data	Simplified method	Simplified method or GA
Detailed Analysis	Model tests or CFD		Detailed data	GA
Objective	Performance in calm seas		Added resistance in waves	Added resistance in winds

The other approach is ‘Detailed Analysis’ which can incorporate the detailed data mentioned above and can carry out more realistic analysis than Simplified Analysis. Shipyards can perform Detailed Analysis because they can access the detailed data. Table 2 shows data arrangement for the analysis of ship

monitoring data by Simplified Analysis and Detailed Analysis. ‘Simplified method’ or ‘Empirical formula’ in Table 2 requires only limited information such as a ship type and ship principal particulars. Therefore, it is not hard for the companies other than shipyards to analyze ship monitoring data. The effectiveness of Simplified Analysis is verified based on the discussion in the teams for Detailed Analysis in which both Simplified Analysis and Detailed Analysis are performed.

S1-WG has selected 10 ships shown in Table 3 for discussion on the analysis of ship monitoring data, bearing in mind that typical ship types are chosen, and organizes teams for performing analysis of ship monitoring data for every objected ship. While the team for Simplified Analysis performs only Simplified Analysis, the team for Detailed Analysis performs both Simplified Analysis and Detailed Analysis which enables a verification of Simplified Analysis.

Table 3: Ships and approaches for analysis

Ship type	Approach for analysis
Container ship (medium size)	Simplified Analysis
Tanker (MR)	
Container ship-A (large size)	Detailed Analysis
Container ship-B (large size)	
Ocean going PCC-A	
Ocean going PCC-B	
Cape size bulk carrier-A	
Cape size bulk carrier-B	
Very Large Ore Carrier	
Tanker (VLCC)	

3.2 Expression of a mathematical model on performance in calm seas

As shown in Table 2, Simplified Analysis estimates a ship performance in calm seas based on empirical formulae and ship monitoring data. In Simplified Analysis, the data deemed in a calm condition are extracted and expressed as Eqs.(1) and (2) where V_S is the ship speed in knot, N_E is the engine revolution in rpm, and P is the engine output in kW.

$$P = a_n \cdot N_E^{b_n} + c_n \quad (1)$$

$$N_E = d_{nv} \cdot V_S \quad (2)$$

Eqs.(1) and (2) give discretized performance data: the relationship among ship speed, engine revolution, and engine output. The inverse analysis of a power estimation based on the discretized performance data can provide a resistance curve and an effective wake coefficient in full-scale, by involving propeller open characteristics by optimized-design, a thrust deduction factor, and a propeller rotative efficient estimated by empirical formulae. The obtained resistance curve and the effective wake coefficient in full-scale are treated as input data to estimate the ship performance speed drop and fuel oil consumption in actual seas by VESTA.

3.3 Analysis interval of monitoring data

The use of automatic monitoring systems for ship performance evaluation in service is rising. Time histories of ship performance or weather are recorded with high frequency (e.g. 1 s). Some monitoring systems can calculate statistical values such as a mean value and a standard variation onboard and transmit them to land. S1-WG discusses the analysis interval with which statistical values are calculated including the sampling interval. While it is preferable to be provided with statistical values to the analysis, some monitoring systems can transmit only instantaneous values. Therefore, S1-WG also discusses a proper interval which is effective for an instantaneous value instead of statistical value.

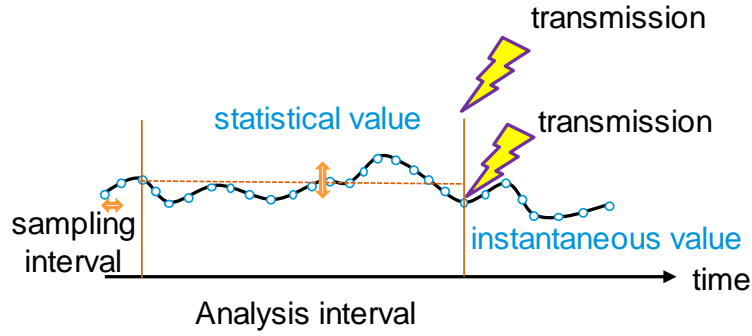


Fig.6: Discussion on analysis interval

3.4 Data filtering conditions

In estimating a ship performance in calm seas by ship performance monitoring, the data in calm seas condition should be appropriately extracted. On this regard, ISO19030 recommends that the data for evaluation on performance in calm seas should be extracted under the condition in which the wind speed is less than 7.9m/s. However, S1-WG considers that it is not preferable to apply such condition to all ships uniformly since the effect of weather on ship performance depends on the size of a ship.

S1-WG focuses on the rate of resistance increase due to winds and waves as a candidate parameter for filtering. The rate of resistance increase is expected to be applied irrespective of ship size since it is relative parameter representing the extent of weather effect. The rate of resistance increase is estimated in accordance with ISO15016, which requires not only wind data but also wave data for the better estimation. Although ISO19030 postpones wave correction, S1-WG incorporates the accurate wave data provided by Japan Weather Association and investigates the effect of waves.

3.5 Example of Simplified Analysis

The example of Simplified Analysis for container ship (medium size) and tanker (MR) shown in Table 3 is demonstrated in this chapter. The principal particulars of the container ship and the tanker are shown in Table 4.

Table 4: Principal particulars of the container ship and the tanker

	Container ship (medium size)	Tanker (MR)
Length between perpendiculars (L_{PP})	270.0 m	185.0 m
Breadth (B)	35.0 m	32.2 m
Draft at desin full condition (d)	12.0 m	13.0 m

Simplified Analysis was performed twice. Simplified Analysis starts with data fitting in calm condition by the mathematical model expressed as Eqs.(1) and (2), which requires the filtering condition for extracting the data in calm seas. Though the discussion on the filtering condition is continued in parallel, the tentative filtering condition is set as shown in Table 5.

Table 5: Tentative filtering condition for extracting the data in calm seas in Simplified Analysis

	Wind speed	Significant wave height
1 st Simplified Analysis	less than 7.9 m/s	none
2 nd Simplified Analysis		less than $1.35\sqrt{\frac{L_{PP}}{100}}$ [m]

20 voyages for the container ship and 18 voyages for the tanker are analyzed. For each the voyage, data fitting by the mathematical model expressed as Eqs.(1) and (2) is conducted, which provides with performance data (i.e. resistance curve and effective wake coefficient in full-scale). Such performance data are input data of the simulation by VESTA of the time history for predicting the ship speed, the engine output, and the fuel oil consumption in actual seas.

The comparison on the total fuel oil consumption in each the voyage between monitoring data and the simulation by VESTA can confirm the accuracy of ship performance in calm seas obtained from the monitoring data. The ship performance in calm seas is essential for the evaluation on that in actual seas. Difference of total fuel oil consumption between monitoring data and the simulation by VESTA is defined as expressed in Eq.(3) where FOC_{VESTA} is the total fuel oil consumption by VESTA simulation and FOC_{MEAS} is that based on monitoring data.

$$\delta FOC = \frac{FOC_{VESTA} - FOC_{MEAS}}{FOC_{MEAS}} \quad (3)$$

The histogram of δFOC for the container ship and that for the tanker are shown in Figs.7 and 8, respectively. The figures confirm that the inclusion of wave height to the filtering condition improves mean and standard deviation of δFOC . On the total fuel oil consumption, VESTA overestimates abt. 3% for the container ship and abt. 5% for the tanker.

The ship performance in calm seas input to VESTA includes the effect of winds and waves, which results in an overestimation of total fuel oil consumption. In other words, the application of the mathematical model to the weather corrected data can give more accurate simulation.

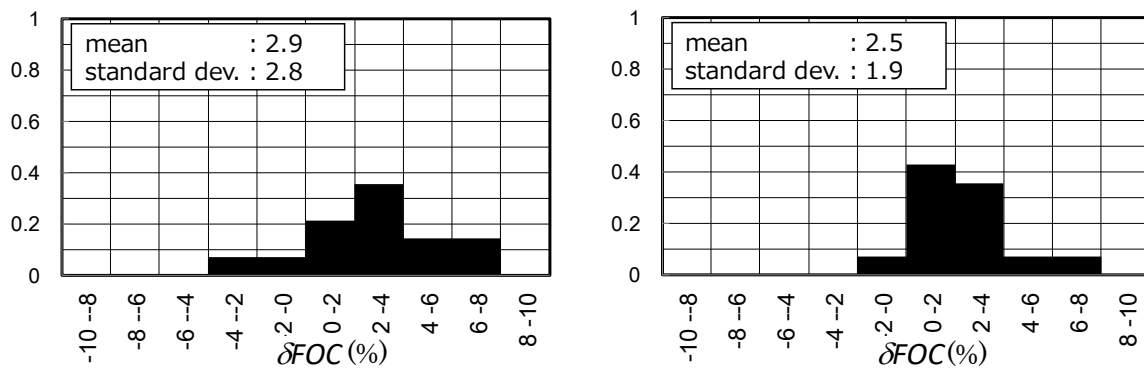


Fig.7 The histogram of δFOC for the container ship
(left: 1st Simplified Analysis, right: 2nd Simplified Analysis)

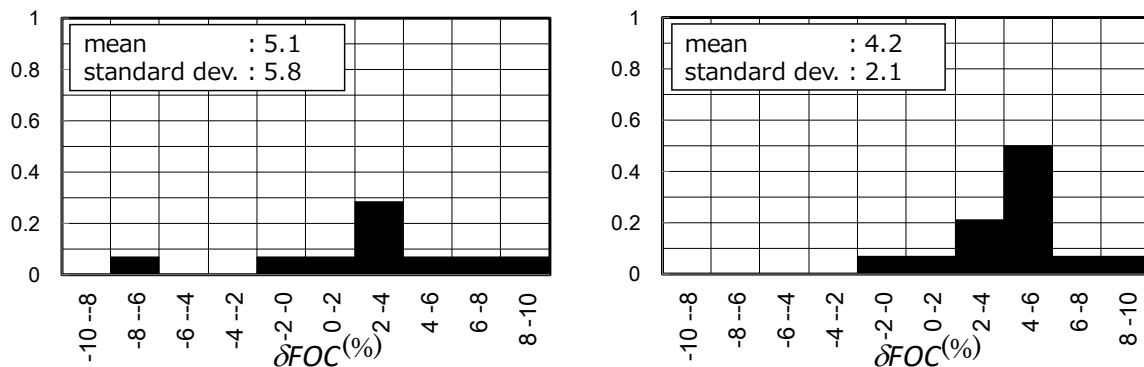


Fig.8 The histogram of δFOC for the tanker
(left: 1st Simplified Analysis, right: 2nd Simplified Analysis)

4. Concluding remarks

This paper outlines the activities of OCTARVIA project and introduces the working groups for its sub-theme. S1-WG addresses establishment of ship performance monitoring method in actual seas, S2-WG addresses establishment of estimation method of ship performance in actual seas at the design stage, and S3-WG addresses establishment of evaluation of ship performance in actual seas. These working groups work together in close cooperation to produce the maximum output in the project.

OCTARVIA project addresses not only technical issues discussed in S1-WG and S2-WG but also the application of the indices on ship performance in actual seas in S3-WG, which contributes to the establishment of a practical and accurate ‘Scale’ for the evaluation of the ship performance. The global implementation of such ‘Scale’ leads to the promotion of building eco-friendly ships and the low-emission operation of GHG. These can contribute to realization of more efficient maritime transport and GHG reduction, which is the goal that OCTARVIA is aiming to achieve.

References

FUJIWARA, T.; UENO, M.; IKEDA, Y. (2006), *Cruising performance of a large passenger ship in heavy sea*, ISOPE2006, San Francisco

ISO 19030 (2016), *Ship and marine technology -Measurement of changes in hull and propeller performance*, ISO, London

ISO 15016 (2016), *Ship and marine technology -Guidelines for the assessment of speed and power performance by analysis of speed trial data*, ISO, London

ITTC (2017), *Preparation, Conduct, and Analysis of Speed/Power Trials (7.5-04-01-01.1)*, International Towing Tank Conference
<https://www.ittc.info/media/8370/75-04-01-011.pdf>

OHASHI, K.; HINO, T.; KOBAYASHI, H.; ONODERA, N.; SAKAMOTO, N. (2018), *Development of a structured overset Navier–Stokes solver with a moving grid and full multigrid method*, JMST, <https://doi.org/10.1007/s00773-018-0594-7>

TSUJIMOTO, M.; SHIBATA, K.; KURODA, M.; TAKAGI, K. (2008), *A Practical Correction Method for Added Resistance in Waves*, J. Japan Society of Naval Architects and Ocean Eng. 8

TSUJIMOTO, M.; SOGIHARA, N.; KURODA, M.; SAKURADA, A. (2015), *Development of a ship performance simulator in actual seas*, OMAE2015, Newfoundland

Performance Monitoring Information Feedback to Design

Matthew Patey, Foreship Ltd., Helsinki/Finland, matthew.patey@foreship.com

Abstract

Performance monitoring solutions and services are primarily intended for ship owners to manage and improve the performance of vessels in operation. The data that is collected can also be useful in the design of new vessels as well as in conversion and retrofit projects. This paper presents some ideas how this can be done as well as an example of the application of collected performance monitoring data in design studies.

1. Eco-efficiency Issues in Ship Design and Conversion Projects

Improving the energy efficiency and environmental impact of shipping operations has continued to be a significant factor in new ship design, as well as a motivating factor for many conversion projects. The decision to make these improvements may be due to legislation, as is the case with some environmental measures like ballast water management systems or exhaust gas scrubbers, or they may be due to other business decisions by the shipowner e.g. to reduce fuel expenses or improve brand appeal. The drive for improvements in performance is always limited by the available resources for the development and implementation of new technologies or procedures. The assessment of new technologies or procedures should therefore be done as realistically as possible, not just to judge the technical effectiveness of a new technology, but also to answer the question does it make practical business sense to implement it.

It is with this practical issue in mind that this paper attempts to present the benefit of using performance monitoring data in the design stage. The issue is not just whether a new technology will “pay off” but also whether or not normal design decisions are actually going to work in practice, given what the owner knows about the performance of the ships in operation compared to the traditional assumptions employed in standardized design procedures.

2. Uncertainty and Complexity in Ship Performance Design

Whenever possible, ship design projects normally work on the basis of experience, for example, through the use of standard procedures to assess the design or by implementation of proven technologies. In a lot of cases the designer has no choice but to follow procedure e.g. because the administration and class society rules dictate how the design assessment is to be carried out. It is true that often there are clauses in rules which state something to the effect that “alternative procedures may be used if it can be shown that they provide an equivalent level of safety”, but the effort involved in proving something “non-standard” to the authorities is something the designer avoids unless they are forced to use an alternative procedure.

But in a lot of other cases the designer has the freedom to do what they like. This can obviously be a problem if experience does not exist in-house or if “standard” procedures to carry out the design have not yet been established. Even in cases when standard procedures do exist and there is time to carry them out, there can be uncertainty in the validity and usefulness of the results.

One familiar example of this is the estimation of required propulsion power. It is standard procedure to evaluate the performance of the hull using RANS CFD methods at an early stage of the design together with some typical propulsion efficiencies and then later by assessing a final version of the hull with self-propulsion tests in a model basin. Two uncertain issues related to this include whether or not the model test procedures sufficiently represent the real full-scale ship and whether or not the CFD procedures model the flow with sufficient detail. While these methods may be sufficient to say “this hull is better than that one”, there is uncertainty in how much better. The same sort of uncer-

tainty exists with the wind resistance. When it comes to additional power required due to the ship operating in waves, there is even more uncertainty in the measurements and calculations.

In the end we get some estimate of required propulsion power based on “standard” model test procedures (which vary in the details from one test basin to another) at constant speed in calm water plus 15% “sea margin” to account for the weather, plus some guess as to the wind resistance. At the design stage this is considered to be the most trustworthy estimate of the required propulsion power. The hydrodynamicist then has to balance this propulsion power estimate with the commercial pressure to try to use as little engine power as possible. At some point, however, there must be a decision about the propulsion solution to implement, the engine arrangement and all their related systems. Uncertainty in the propulsion power means uncertainty in the fuel consumption, uncertainty in the optimal engine arrangement and uncertainty in e.g. the size of the fuel tanks.

But let’s be a little more realistic by adding a few more variables to the problem of the energy consumption on the vessel and the required installed power. For example:

- How is marine growth accounted for in the propulsion power estimate?
- The hotel load on a large cruise ship can be 50% of the total required power for some cruising speeds. How is this estimated in the total power requirement?
- We are considering exhaust gas steam turbine generators, fuel cells, air lubrication system, Flettner rotors, solar panels, etc. but they only work well in certain conditions. So how much less power do we need if we implement this technology and will it cover the cost of implementation?
- We know from experience the engine test bed SFOC curve is never how much fuel the engine burns in practice. How do you account for that when sizing the fuel tanks?
- We are going to use LNG. What is the experience with the fuel consumption for this type of engine?

All of these issues make the challenge of assessing what power plant is the best highly uncertain and difficult to evaluate. Ultimately the energy efficiency and commercial effectiveness of the vessel could be compromised due to conservative decisions made in order to alleviate the risk due to these uncertainties.

Looking at the bullet list above, it can be seen that these examples all have a lot to do with the operation of the vessel. This implies that in order to assess the contribution of these items to the energy balance on the vessel we need to know how the vessel is operated and where it is operating. So we come to the problem of defining the “operational profile” of the vessel.

The operational profile of the vessel includes the distribution of vessel speed, and the distribution of time spent in certain operations (manoeuvring, in transit, at anchor, in port, etc.) but this is only part of the information needed. When speaking of the operational profile we need to know not just the speed profile, but the actual route and time of year the vessel is operating on these routes. This would help us extract the expected environmental conditions, if we actually can get the environmental data from some source. Putting this information together in a useful form to assess e.g. electrical power demand for a diesel electric powered cruise ship is not a simple task, but it is something that is always desired.

3. Use of Performance Data and Voyage Simulations in Design Decisions

Performance data collected onboard an existing ship can help provide some of the data which comprises a new vessel’s operational profile, e.g. speed profile, propulsion power profile, engine mode profile, service load, etc. The post-processing of this data can provide insight into the real expected behaviour of the ship. The quality of the collected data is of course a concern, as is the way in which the raw measured data is post-processed before being made available to the shipowner and the

designer. Even if the data can be trusted, there still is the problem of applying this data to a new design, which may be intended to operate on routes for which very little or even no operational data exists.

There is also the issue of putting all of the measured data together with other data used in the design. This is usually a bit of a mess, with the design team dealing with many sources of data in many different forms from several different design disciplines. Consistency between data sets can be difficult to maintain, especially as the design progresses in different departments in the design organization. It should be more convenient if all of the questions related to the energy balance on the ship could be handled in a more consistent, realistic manner with one approach while reducing the amount of uncertainty in the evaluation of each contributor to the energy consumption onboard.

One way to address this issue is through the use of voyage simulations, Fig.1. In a voyage simulation a mathematical performance model of the vessel is used to calculate the performance of the ship on a given route. “Performance” typically means fuel consumption, but it can also include the seakeeping behaviour, as well as the effectiveness of any equipment contributing to the energy consumption and production. Departure and arrival dates and times at given ports are set and the voyage proceeds according to a series of discrete steps in time or distance. Environmental conditions, typically from a hindcast weather database, are varied during the voyage according to the vessel position, date and time. By varying the date and time of departure, many years of simulations can be conducted, giving many years’ worth of data about fuel consumption, propulsion power, etc. The complexity of the model and the simulation is limited by the software tool employed to conduct the simulations, but it should be apparent that the tool must be capable of modelling the systems which are involved in the energy balance to the level of detail which provides confidence in the related design decision.

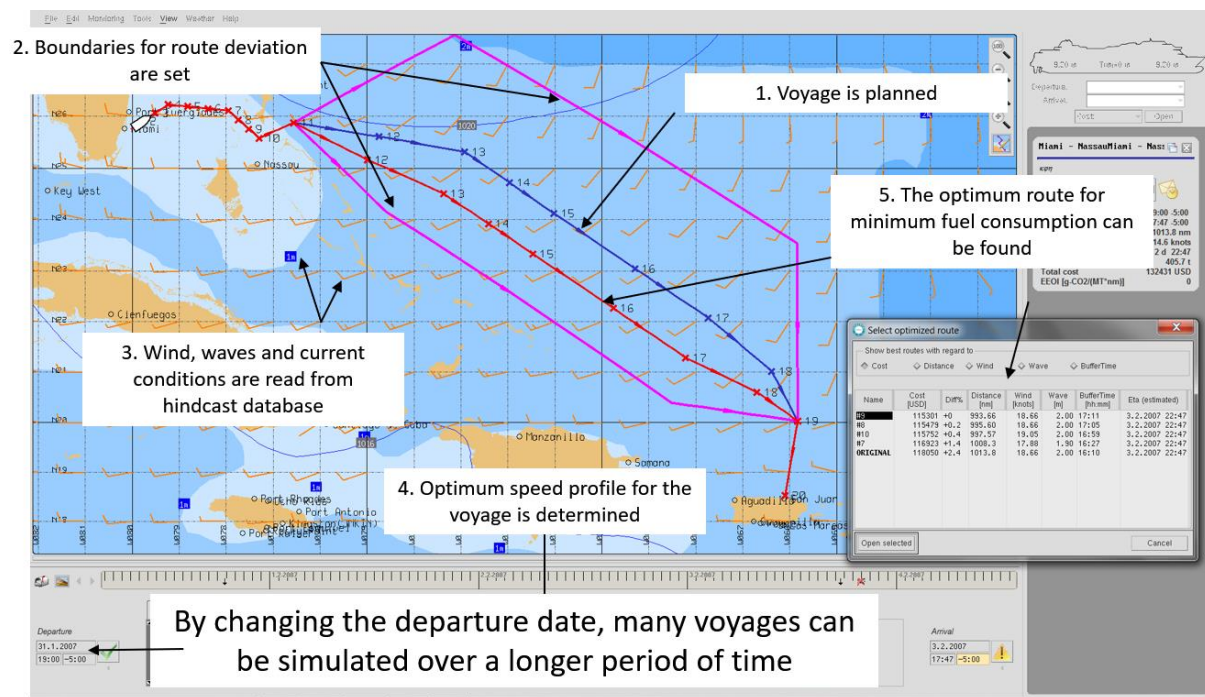


Fig.1: The voyage simulation process, illustrated using a sample voyage in an older version of the NAPA Voyage Optimization software used onboard some ships for voyage planning.

The benefits of using voyage simulations include:

- it is easier to manage many aspects of the energy efficiency analysis of the vessel than with a dozen different spreadsheets and separate analysis programs used by different design departments and disciplines

- simulations can realistically represent the operation and performance of the vessel along the actual planned routes using hindcast weather databases, easing concerns about the realism of the information used in the assessment
- it is easy to modify the vessel design and the performance model to conduct design studies related to energy efficiency
- real operational data can be taken into account, as explained below
- you don't need the operational profile because the operational profile is actually a result of the simulations

Realistic simulations depend very much on the nature and quality of the performance model used in the simulations. Ultimately performance model predictions are based on analytical or statistical formulations, which in turn have been verified and validated by experience. So we get back to the same problem that old experience should be corrected by new observations.

This is where the measured performance data can be used to calibrate the performance model. This is what is normally done in voyage planning software systems used onboard ships – the initial installation of the system contains a baseline performance model used to make recommendations about planned speed and weather routing. The base model is adjusted over time using the measured data from the performance monitoring system. The same approach can be used in simulating voyages using a hindcast weather database and performance data from an existing ship. The measured performance data, e.g. fuel consumption, can be compared to that predicted by simulating the exact same voyage for the ship to derive correction factors and correction methods to apply to the analytical models used.

To apply this data to a new design is the next problem. The same analytical models would be used for the new design, but the predictions should incorporate the calibration factors from an existing reference vessel for which performance data is available. In order to reduce the risk in applying this approach the reference vessel should be as similar as possible to the new design.

Using a reference vessel may seem like a risk if the ships are somewhat dissimilar, or call into question the need to conduct such comprehensive analysis, i.e. why not just use the reference vessel data if it's so close to the new ship? But let's step back from all these details and ask ourselves the really fundamental question:

What information do you trust?

The engineer has to make decisions, and there is always uncertainty. In the current author's experience, it is easier to convince people of the trustworthiness of measured operational data than it is to convince them of model test results, CFD or some empirical formula, as long as common sense and experience agree with the observations. If real operational data is available, it should be used. In a new design this is not available, but neither are the model test or CFD results early in the design process and the empirical formulas are not necessarily reliable. We *always* have to rely on reference ships and reference data at some point. It would seem from a common-sense point of view to be better to rely on measured operational data from a reference vessel than model tests from the reference vessel. Later in the new vessel design the empirical models get replaced by CFD or model test results for the new vessel, but these too should be corrected taking into account the real operational data from the reference vessel. How to make these corrections is a completely new issue and will not be addressed here other than to say that a good deal of "engineering judgement" is required. But the basic principle we try to follow always is use the best data available.

4. An Example from Recent Experience

At Foreship we have been conducting voyage simulations as part of some newbuilding consultancy projects for about 3 years now, primarily focussing on comfort analysis onboard cruise ships and

prediction of fuel consumption on sample voyages, taking into account the weather conditions encountered. The results have been used in making decisions about operational feasibility of particular routes and aspects of the general arrangement design, amongst other things.

We had the opportunity to take advantage of full-scale operational data recently in one of these studies. We approached one owner saying we had a great new way to calculate fuel consumption for their newbuilding project. They were sceptical about the approach in general and they were also questioning the accuracy of the analytical models used in the simulations. There were also several aspects from operational experience that they needed to take into account in any energy efficiency analysis. These included:

- Marine growth effect on powering had to be taken into account, considering also the normal drydocking schedule and cleaning of the hull.
- Engine availability due to planned and unplanned maintenance had to be considered.
- Energy saving technologies were to be employed, namely exhaust gas steam turbine generators, absorption chillers and hull air lubrication systems (ALS).
- The service load should be taken into account as accurately as possible.

To address these concerns, we suggested that we try to use the full-scale performance data they had for their ships, first by calibrating the fuel consumption and propulsion power models with the measurements on specific voyages for their reference vessel and then applying the correction factors to the new design.

4.1 Use of Performance Monitoring Data in the Voyage Simulations

The first thing was to develop the correction factors for the performance model for the reference vessel. The performance model in the simulations consists of, among other things:

- total propulsion power as a function of speed
- propulsion efficiencies
- engine powers, modes and SFOC curves
- service load profile i.e. service load as a function of time of day

We were primarily interested in the required propulsion power and fuel consumption. For this we asked for whatever performance data the owner had which could be used for this, preferably in the raw data format, for as many voyages as possible. We got a flood of data from a 6 month period in a series of text files dumped out of the performance monitoring system using 5 minute or 15 minute averages. From this data we could figure out the actual measured fuel consumption, develop a daily average power profile for the service load and figure out the actual average propulsion power used for any specific section of a voyage.

The calibration process consisted of simulating a section of the measured voyages over which the speed was more or less constant using hindcast weather data for the same dates and times of these voyages. Sections of 36 individual port-to-port voyages were simulated from a single itinerary which was repeated several times over the six month period. The SFOC curves were corrected by a factor provided by the owner based on their experience. The service load profile was developed from the measured service load data. Overall propulsion efficiencies were provided by the owner as standard reference values they wished to use. Performance of the exhaust gas steam turbine generator was taken as an average power from the measured data for each voyage. Based on this a simple estimate of the reduction in the average service load demand as a function of speed could be developed. Finally the performance of the air lubrication system (ALS) was taken into account as a further reduction in propulsion power demand. This was based on an earlier analysis of measured data of propulsion power with the ALS on and off, carried out by the supplier of the performance monitoring system.

Other factors which were tuned in the model were the propulsion power curve and the auxiliary power demand from the activation of an engine. The fit of the performance model was judged by comparing the total fuel consumption and average propulsion power on each voyage according to the simulation to that of the actual measured data. In the beginning, we tried to be clever and employ a genetic algorithm to minimize the discrepancy between the predicted and measured fuel consumption and the predicted and measured propulsion power. This turned out not to be so useful, and in the end the propulsion power curve was easier to adjust manually in 2 or 3 iterations to get already a quite good correlation between predicted and measured average propulsion power. With this manual tweaking of the power curve, the achieved correlation between predicted and measured total fuel consumption was 98% and between predicted and measured average propulsion power 96%. This was considered “close enough” for our purposes. The tweaked “operational” speed-power curve was then compared to the most recent “design” speed-power curve for the reference vessel to develop a set of correction factors to apply to the new vessel.

Statistics of the marine growth effect on propulsion power were provided by the owner and used to adjust the corrected propulsion curve as the simulation progressed. At the beginning of the simulation this effect was set to zero and increased until the next scheduled drydocking, when it was assumed the hull cleaning was so good that the marine growth effect was again zero.

The final step in setting up the problem was using the owner’s statistics regarding engine availability to remove engines from the set of available engines. Planned maintenance was handled by removing one engine on a regular basis for a single port-to-port voyage. Unplanned maintenance i.e. engine failure, was simulated using a random number generator and given probability of failure to remove an engine for a single port-to-port voyage.

In summary, the performance models of both the reference vessel and the new design used data from performance monitoring systems for the following items:

- propulsion power and efficiencies
- fuel consumption
- marine growth
- engine availability
- service load
- ALS net power saving

4.2 Results of the Study

The two vessels (reference vessel currently in operation and the new design) were then run through a series of voyage simulations. Four round-trip itineraries in four different sea areas were simulated, with each itinerary consisting of several port-to-port voyages. The departure and arrival times at each port were fixed. Simulations were run for each itinerary for a 25 year period from 1993 to 2017, with the ship leaving the departure port the next day after it arrived from the previous round trip. During a particular voyage the speed was optimized for minimum fuel consumption over several legs of the voyage and, where applicable, weather routing was used. A lot of information was generated as a result of the simulations, including:

- speed, engine mode and power profiles
- voyage buffer times and late arrival times
- fuel consumption, energy consumption, CO₂ emissions and EEOI
- experienced levels of passenger comfort and seasickness
- experienced weather conditions
- wind, wave and current contributions to the ship powering problem

One of the main conclusions from the simulation process was that the current selection of engines for

the new vessel appeared to be insufficient when it came to the total installed power. Several late arrivals on one of the itineraries were observed in the simulations for the new vessel (but not for the reference vessel). These occurred when there was a high level of marine growth or when one or more engines were out of service in combination with moderate or high marine growth. The installed power of the engines was, however, well in excess of the required power according to the “design” speed-power curve, the expected service load and the traditional 15% sea margin. In addition the selection of engines appeared to offer less possibility for optimizing fuel consumption than in the reference vessel. This was because all the engines were the same in the new ship while the reference vessel had engines of two different sizes, allowing many more combinations of engines and more flexibility to adapt to the variations in power demand encountered. These conclusions helped support the decision to increase the installed power and change the size and configuration of the engines used.

The most interesting part of the simulations from our point of view, however, was that these conclusions were only reached because the measured propulsion power, marine growth effect and engine availability statistics were included in the analysis.

5. Conclusions

The use of voyage simulations coupled with data from performance monitoring systems has for us proven to be a valuable tool in assessing the expected performance of a new vessel design. Voyage simulations allow the study of the energy efficiency of the vessels to be treated in a more comprehensive and realistic manner than what is traditionally done in the ship design process. They also help to remove doubt about the assumptions used in the analysis because they essentially mimic the way the vessel will be operated. Finally, they can bring together all of the essential data needed in studying the performance of the vessel and eliminate a lot of work and guessing in managing and connecting different sources of information.

The key to an accurate assessment of a new vessel’s performance is a realistic performance model. Operational data collected by performance monitoring systems is the best information which can be used to develop these models. This information should be used as much as possible in the design stage, preferably in conjunction with voyage simulations, to really understand how new ship designs will perform in operation.

Performance Monitoring Insight at MOL

Tetsuro Ashida, Mitsui O.S.K. Line, Tokyo/Japan, tetsuro.ashida@molgroup.com

Naoki Mizutani, NAPA, Kobe/Japan, naoki.mizutani@napa.fi

Pekka Pakkanen, NAPA, Helsinki/Finland, pekka.pakkanen@napa.fi

Arttu Väisänen, NAPA, Helsinki/Finland, arttu.vaisanen@napa.fi

Teemu Manderbacka, NAPA, Helsinki/Finland, teemu.manderbacka@napa.fi

Abstract

This paper describes a process for analyzing deviations and trends of ship performance by combining open data-based analytics to customer's proprietary data. Mitsui O.S.K. Line (MOL), as all commercial operators, has collected departure, noon and arrival reports from all the ships in their fleet. There is a massive volume of data. But it also requires lots of effort to make use of these data, for further ship, fleet performance analysis. NAPA has introduced a system where algorithms automatically, and constantly, estimates the fuel consumption of each day for all vessels in the world, and compares the noon-reports with the estimations. The solution helps to improve the fleet's compliance, technical performance and operational performance by identifying which vessels are underperforming compared to benchmark and which vessels could use maintenance, and how effectively past voyages were operated.

1. Introduction

In recent years due to increase in regulations and high prices of crude oil, have many companies started developing fuel and performance monitoring systems for cost saving. Most of these developed systems are onboard systems that require a costly hardware installation that can be a problem for some charters due to the charter party contracts.

Freighting business consists usually of three different types of charter party contract models. Models are voyage-, time- and bareboat charters. These models differ from each other in how the costs are distributed. Costs of a ship consist of capital investment made when ship is ordered and built, operating costs which include supplies, maintenance, crew salaries, insurances etc. and voyage costs that consists of fuel, port and canal fees. In voyage chartering ship owner pays all the above costs. In time chartering ship owner pays capital cost and operating costs and charterer pays voyage costs and hire rate to the ship owner. In bareboat chartering, the ship owner pays the capital cost of the ship and rents the ship to charterer who pays all other costs, *Stopford (2009)*.

On voyage and relatively short time charter cases charterers might hesitate to install costly system to their vessels. Also, contract might prohibit it. This creates a need for flexible systems that can provide estimates of performance without costly installations and hardware.

MOL operates around two hundred bulk carriers of which more than half are chartered in. Monitoring and predicting the changes in the technical performance is relevant from charter party point of view and as it has a large effect on whether the operated spot voyages are profitable or not. However, as these vessels are typically chartered for 1-2 years and consume approximately 15-40 tons of fuel per day, it does not make commercially sense to install torque or fuel flow sensors with high frequency data collection.

So far MOL has been using their internal engineering department for analyzing the data from the fleet's noon reports, but there have been some downsides in the approach. For example, the only data source has been the noon reports and therefore it has taken a long time to form a baseline consumption for a vessel. Sometimes the baseline can also be false or inaccurate due to false input data, either by human accident or on purpose, *Aldous et al. (2013)*, *Safaei et al. (2018)*. In addition, the data frequency in noon report is only one data point per day, which makes any wind, wave, sea current corrections difficult or

in many cases even meaningless, *Aldous et al. (2015), Mannheim (2017)*. Attempts to overcome the challenges of relying purely on noon-report data are made by improving the filtering techniques or introducing alternative methods for the analysis, *Bal Beşikçi et al. (2016, Davies and Bevan (2017))*.

In this article we will present how a reference value for the daily fuel consumption is calculated in a service called NAPA Fleet Intelligence. Calculation is based on high frequency location data from Automatic Identification System (AIS), weather nowcasts and vessel performance models, and the article describes what type of benefits can be achieved with comparing the reported values to the results of the simulations.

2. Challenges of noon-report data

Noon-report is once a day crew made report. It contains a snapshot of the ships daily performance and it contains information on: consumption, location, course, speed, shaft rotational speed (RPM), wind speed, loading conditions (laden or ballast) and timestamp.

The challenge of applying noon-report data lies in the sparse resolution (once per day) and on possible inaccuracies or even human errors since the data is collected using various methods and typed in manually by the crew members. The available sensor readings are dependent on the level of instrumentation on board, which generally varies between the ship types. More expensive ships, such as cruise vessels, ropax or even container and LNG ships can be equipped with fuel flow meters and fixed tank level sensors connected with onboard systems providing better accuracy of consumption monitoring. Whereas tankers and dry bulk vessels might not have such sophisticated installations. In these cases, the crew must take the reading of fuel remaining on board applying a manual level sensor. The manual readings are affected by sea state, causing motions and thus disturbing the accurate reading. Moreover, the trim and possible heel might not be taken properly into account when calculating the amount of the fluid from the level reading. More on the challenges of measuring quantities of fuel on board can be found e.g. in *Pecci (2007)* related to liquid bulk cargo measurements.

Consumption is a key variable and if we look closer to it we can see that, the available data on the consumption depends on the ship type and the quality and the extent of the systems the ship is equipped with. Some ships have level sensors installed in all fuel tanks and the readings are connected to systems like NAPA Loading Computer, which gives the exact quantity of fluid in the fuel tank based on the level sensor reading and geometry of the fuel tank.

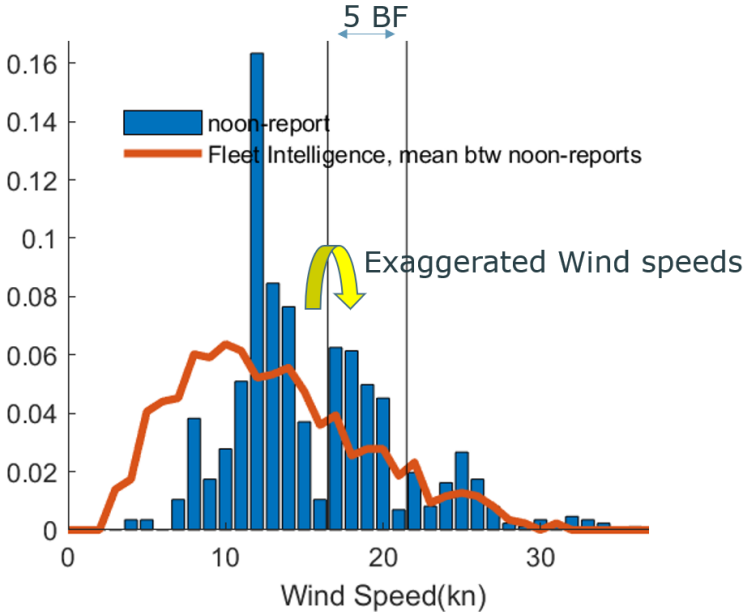


Fig.1: Wind speed distribution of case vessel

Also other reported variables suffer from varying quality. Sometimes this is caused by unclear instructions on what to report, sometimes human mistakes, sometimes the unconscious habit of reporting towards what is expected rather than what is happening. Below example of a Fig.1 shows a case where wind speed close to 5 Beaufort are commonly reported as 5 Beaufort.

In addition to being affected by human error, the sparseness of the reported average values causes significant error if utilized solely. For example, only one value for the wind speed is reported as e.g. 14kn / 335° or sometimes even just 4 BF. However, there are commonly significant variations the environmental conditions (force, direction) during a day and wave height is either not reported at all or is based on visual observations and thus prone to bias based on observer. Approximately on 30% of operational days the wind speed changes over 5 m/s or wind wave height more than 1 m.

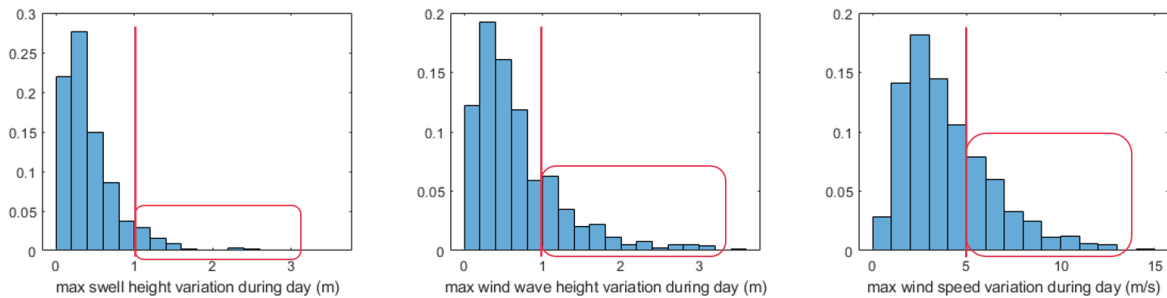


Fig.2 Variation in weather during a day

The impacts of weather and wave conditions are not linear, thus using the average value, even if it could be 100% correct, would be problematic. As seen on Fig.3, variations in only wind direction on 4BF conditions can decrease vessel speed by 15%, or if maintaining a fixed speed, to increase consumption by 50%. Thus, using only one average speed and average weather conditions value for the 24h period is clearly inadequate.

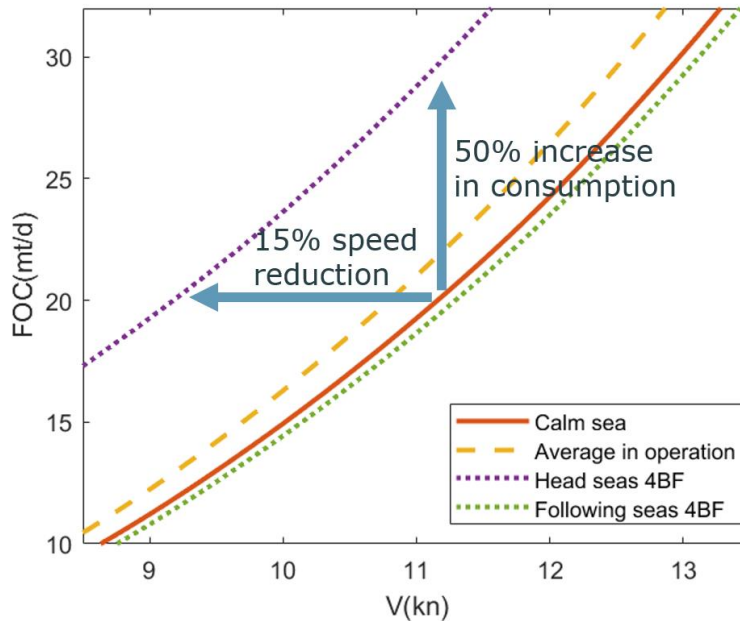


Fig.3 Variations in performance in 4 BF conditions

3. Methodology in this study

The estimation of fouling is based on comparison between the reported consumption and calculated

reference consumption. The reference consumption is calculated for all the days where the noon-reports are obtained. The reference consumption calculation is based on the full hydrodynamic model of the ship including propulsion and engine arrangement. The calculation of reference consumption accounts for the actual weather the ship encountered from noon to noon, including the weather variations. Since the noon-reports obtained from the ships contain manual input, they are filtered, and data is prepared for analysis of level of fouling. The calculation of reference consumption, the preparation of noon-report data, and the estimation of fouling is described in detail in the following subchapters.

3.1. Calculation of reference consumption in NAPA Fleet Intelligence

High frequency ship location data is used to calculate reference consumption. Ship location, speed and heading are obtained from the AIS messages, which are collected in few minute intervals. Besides the location and other information, the AIS message contains information on the draft of the ship. AIS location is based on the Global Navigation Satellite System (GNSS), which usually is Global Positioning System (GPS), these signals can be considered reliable. The draft is included in the AIS message as voyage-related information and is manually entered by the crew and may be inaccurate, *Adland et al. (2017)*.

Global ocean weather now-cast data from independent weather forecast provider is used to obtain the weather at the ship location, including; wave, wind and sea currents. The weather now-casts are provided at spatial resolution of 1.25° , which corresponds to a grid size of approximately 100 km. The weather is updated every 180 minutes. To accurately match the vessel timestamp and position, the now-casts are interpolated to the ship position at each time instant the position is obtained. This is done by trilinear spatio-temporal interpolation, which is described in *Haranen et al. (2017)*. Wave conditions are given as two main wave directions, namely swell and wind waves. For each of these the significant wave height, zero crossing period and direction is given. Wave conditions are based on the data from WAVEWATCH III (WW3) model, which is developed by National Centers for Environmental Prediction (NCEP). Also, the wind the speed with direction, as well as speed and direction of sea current including the effect of tide are given.

The performance of the ship is estimated with first principle hydrodynamics calculation methods based on the ship location, weather data and generic ship specific performance model. The performance model constitutes of; a generic model of ship hull (i.e. lines drawing), which is formed based on the available information of the main characteristics of the ship, a model of ship propulsion and maneuvering arrangement, and a model of the ship powering i.e. installed engine model. Essentially, a digital twin of the ship is produced, as accurately as possible, with the available ship data. The level of the data availability depends on the use of the model, for public use of calculation results, publicly available data is applied. Whereas more accurate data of the ship provided e.g. by the ship-owner, can be applied for the calculations reserved for the ship-owner's use.

Calculation of consumption based on the publicly available data is done by calculating the resistance of the ship in the given operational conditions: speed, loading condition, water depth, wave and wind conditions. All the forces acting on the ship are calculated with hydrodynamics models. Quartering waves and wind cause drifting angle to ship's propagation, which need to be balanced by the rudder. The rudder forces are also included into the model together with the hydrodynamic coefficients accounting for the additional resistance due to the drift angle. Factoring in all the above-mentioned forces, the required thrust to propel the ship at given speed is calculated by solving the force balance. The thrust is calculated considering the propulsion arrangement; propeller diameter, pitch ratio, thrust deduction, and wake factor. Then the required propeller revolutions per minute (rpm) and corresponding required power from the main engine are calculated, and finally, based on these, the consumption is calculated. The calculated consumption will be used as reference consumption to compare with the reported consumption.

Similar approaches have been taken by *Jalkanen et al. (2012)* for estimating the Green House Gas emissions from ships. These studies have taken the effect of weather conditions as average sea margin,

which is a common way in the ship design, however that type of approach can only approximate long-time average consumption and is not suitable for our purpose. The approach taken here calculates the actual consumption in the actual weather conditions and can be deemed as the most advanced one.

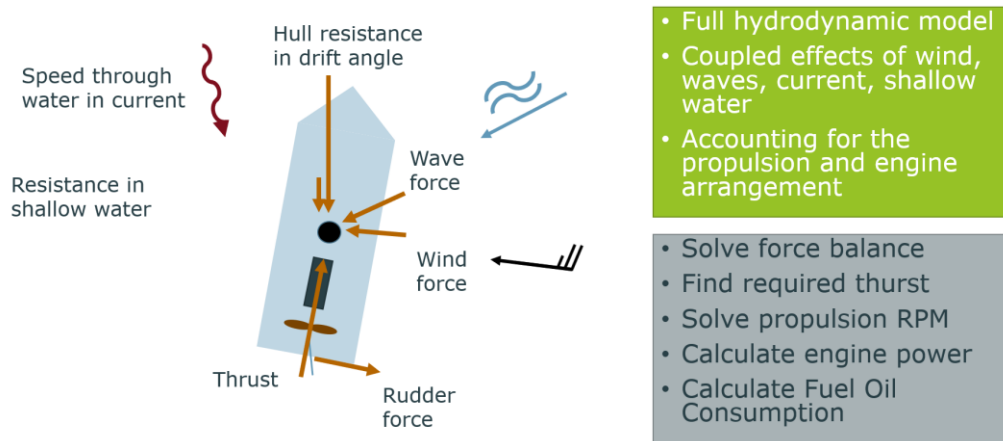


Fig.4 Calculation of required propulsion power for each timestamp

3.2. Noon-report consumption

In this research we used noon-report data provided by MOL. Ships were bulk carriers of size range 30 000-230 000 dead weight tonnage (DWT). Data collection period was approximately 3 years for all ships and altogether there were several thousand points of operational data.

Data filtering and preparation were carried out for both datasets, NAPA Fleet Intelligence data and Noon-report data. NAPA Fleet intelligence data sampling frequency depends on the availability of AIS data and is typically once per hour while at sea. NAPA Fleet Intelligence data was averaged to once per day sample. For Noon-report data a time correction was applied for days that was 23 or 25 hours long. After this were the obvious outliers filtered out of the data.

From the relation of noon-reports load and rpm a variation in rpm can be observed with constant load values. This variation can be assumed as pseudo weather impact to the ship. This can be justified because power is rpm times torque and load is power divided by the maximum continues rating. By combining these two we get equation represented below.

$$\begin{aligned}
 P &= nQ & (1) \\
 Load(\%) &= \frac{P}{P_{MCR}} \\
 &= \frac{nQ}{P_{MCR}}
 \end{aligned}$$

From this we can see that if load is constant and rpm changes the torque needs to change also. Relation of noon-report's load and rpm is presented in Fig.5 and from this we can see that rpm varies so we can assume that this is due to weather.

Because of this variation a new continuous variable that represents weather can be created. A fit was created between noon-report rpm and engine load. With this fit we calculated the residual of measured and predicted rpm. This residual was used to make the continuous variable representing weather condition. Weather variable was named pseudo weather. With new pseudo weather, rpm, consumption and loading condition a model was made to predict consumption. Model is presented in Fig.6.

This model is used for filtering out abnormal data points from noon-report data. This is done so that a consumption prediction is made of noon-report data and the residual is calculated from this prediction and the measured consumption. After all residuals have been calculated 5% of all smallest and largest

points are filtered out.

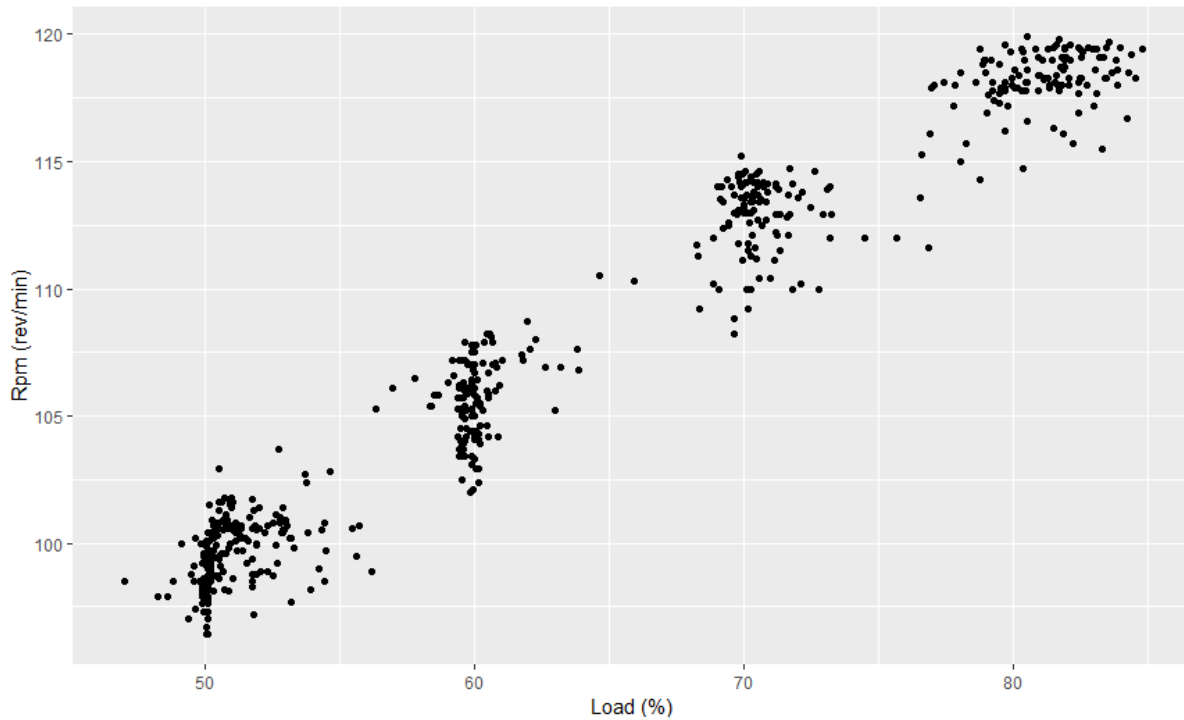


Fig.5: Noon-reports Rpm vs Load

```

call:
lm(formula = corrected_consumption ~ rpm + I(rpm^2) + I(rpm^3) +
    loading_condition + pseudo_weather, data = noon_data)

Residuals:
    Min       1Q   Median       3Q      Max
-4.1003 -0.7281  0.0306  0.8580  5.6141

Coefficients:
                Estimate Std. Error t value Pr(>|t|)
(Intercept)      9.071e+03  7.855e+02  11.547 < 2e-16 ***
rpm              -4.477e+02  3.855e+01 -11.615 < 2e-16 ***
I(rpm^2)         7.350e+00  6.303e-01  11.662 < 2e-16 ***
I(rpm^3)        -3.989e-02  3.434e-03 -11.614 < 2e-16 ***
loading_conditionLaden  5.733e-01  1.194e-01  4.803 1.94e-06 ***
pseudo_weather   -1.448e+00  5.773e-02 -25.081 < 2e-16 ***
---
Signif. codes:  0 '***' 0.001 '**' 0.01 '*' 0.05 '.' 0.1 ' ' 1

Residual standard error: 1.399 on 652 degrees of freedom
Multiple R-squared:  0.946,    Adjusted R-squared:  0.9456
F-statistic: 2285 on 5 and 652 DF,  p-value: < 2.2e-16

```

Fig.6: Model

3.3. Fouling estimation

The reported vessel speed is normally an average speed, and similarly for the wave height, if reported, and for wind speed. However, the consumption, or in this case the speed reduction has non-linear dependency on the wave height and wind speed. For this reason, the average values cannot be used to represent the daily speed-power-or-consumption figure to estimate the level of fouling.

Usually, noon reports with harsh weather conditions are filtered out and not used, or these effects are

intended to be factored out, by calculating separately the added resistance of waves and wind etc. However, the challenge is that these effects do not superpose, instead they affect altogether to the resistance and consumption. For instance, side wind causes drift, which introduces additional resistance through counter maneuvering of the rudder and changes the propeller efficiency and so on. Thus, we will use the performance model described earlier and calculate the performance in each available timestamp.

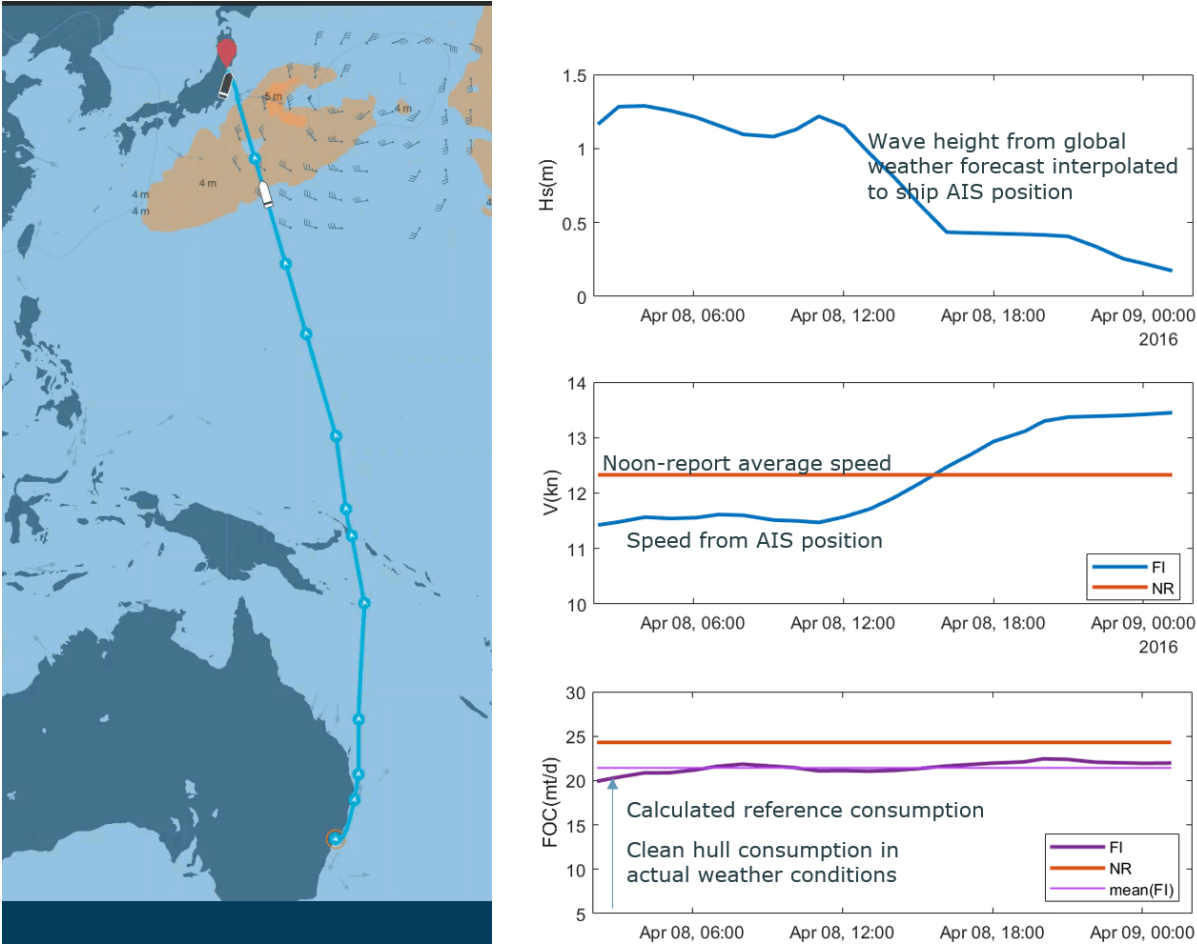


Fig.7: A day of a bulker on voyage from Australia to Japan

In above example we can see how during one day the significant wave height decreased from 1.3 m and at the same time the vessel speed increased from 11.4 kn to 13.6 kn, while the average speed obtained from noon-report shows only one value, 12.3kn. In the noon report also the daily consumption, 24.7 metric tons, has been reported. NAPA Fleet Intelligence calculates the reference fuel consumption for each moment of the day and we can then calculate the average consumption, 21.5mt. From this difference we can calculate, as an example value, the effect of hull fouling as $24.7\text{mt} - 21.5\text{mt} = 3.2\text{mt}$, shown as a red dot in Fig.8.

Similar calculations are performed on all available data points, and as a result we can get a time series chart of the vessel’s increased consumption due to fouling, which can be used to adjust calm water speed – FOC – power curves of the vessel.

Fouling estimate is done by subtracting the NAPA Fleet Intelligence consumption from noon-report consumption and then fitting a trend to this data. In Fig.9 is presented a simple normal least square fit. Obvious outliers are marked with ovals.

We can deal with these outliers by making a robust fit using iteratively reweighted least squares. This

fit is presented in Fig.10. The smaller the weight the less it affects the fit, *Huber (2009)*.

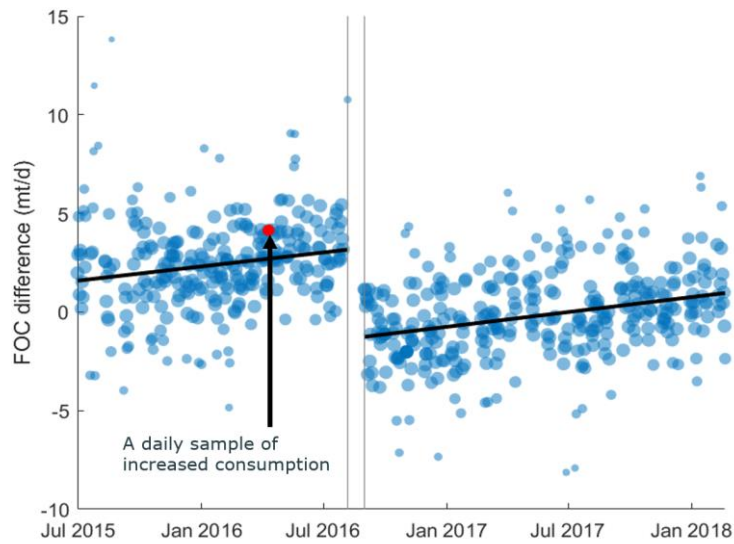


Fig.8: All noon-report and reference calculation based datapoints of increased consumption due to fouling

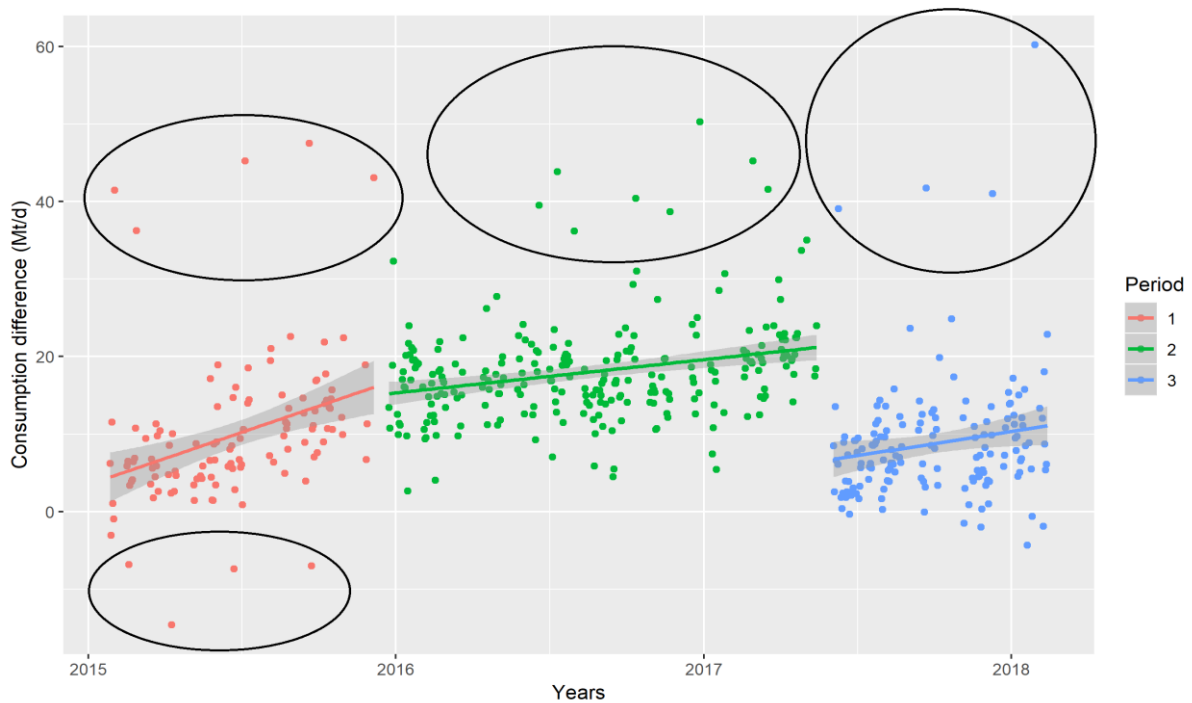


Fig.9: Normal fit

4. Results

The described calculations are implemented in a manner which is easily reproducible for any number or types of vessels. In this study, the main focus is on the methodology and proof of concept using a set of small to medium size bulk carriers operated by MOL.

4.1. Typical changes in the performance

The calculation process allows to easily quantify the decreasing performance of the vessels in the fleet

of interest, which can be then used for decision making regarding for example timing of dry docking or revising the charter party consumption.

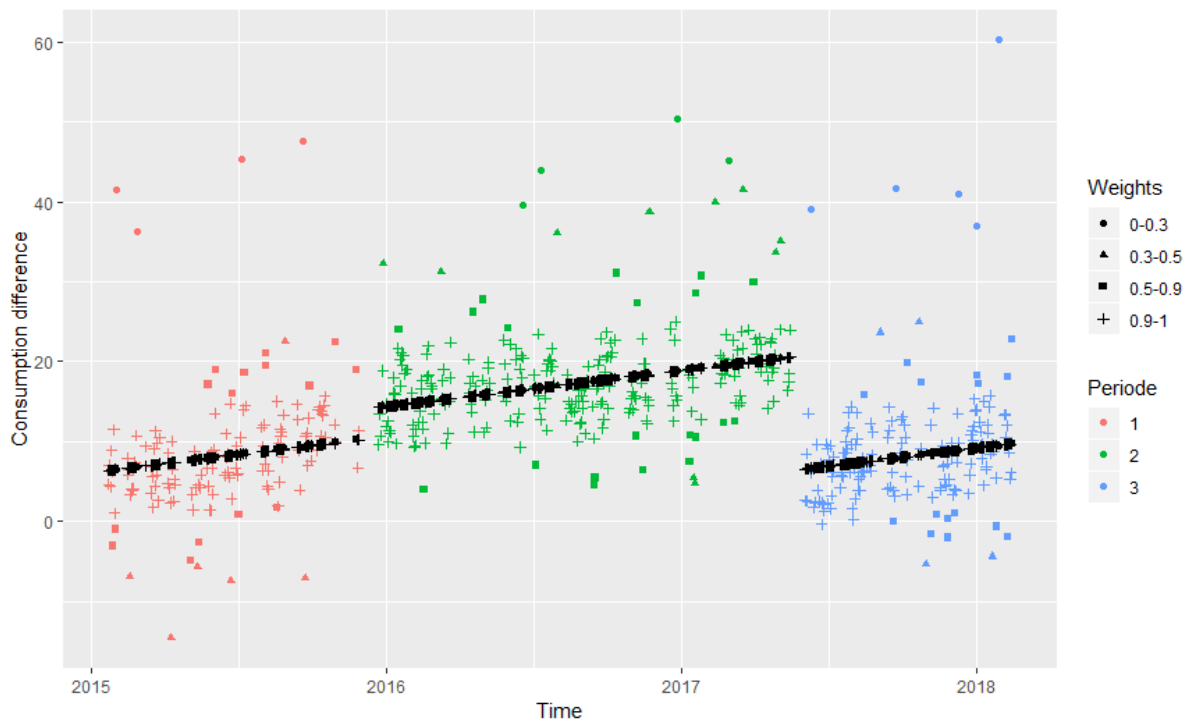


Fig.10: Robust fit

This dataset contained slow steaming bulk carriers. A typical annual increase in consumption on a fixed speed was 7-9%, which is in line with general understanding. However, the variation in performance changes was huge; on some vessels the performance remained stable for the whole monitoring period, on some the performance deviated substantially and the effect of maintenances was very large. This shows that in addition to general understanding of typical scenarios, a constant vessels specific analysis is beneficial.

The maintenance periods of the case fleet varied and there was from zero to two maintenances during this three-year period. The typical benefit of the maintenance was slightly over 10% reduction in fuel consumption.

4.2. Uncertainty of the model prediction

In addition to the performance model inaccuracies, the difference between the reported and predicted values are caused by for example weather forecast inaccuracy, AIS data availability and erroneous input by the crew, either accidental or even purposeful. Thus, as the true value of the consumption is not fully known, we do not talk about error of the model, but rather uncertainty of the prediction. In these comparisons we are not filtering out any harsh conditions, days where half of the time is spent for drifting etc.

In Fig.11, we estimated the uncertainty of the daily hull fouling rate value with an iterative process with certain 95% confidence limits. In other words, with this, we can say that the fouling is at the calculated level and with 95% confidence it is within the confidence limits. For example, after just few weeks of operation after the maintenance on autumn 2016, we could state with 95% confidence that that the vessel daily consumption had improved by 5 ± 1 mt / day. With more data, the limits tend to narrow down and the accuracy improve.

To demonstrate the improvement of uncertainty level, we have calculated the confidence limits after n-days of data collection after the maintenance of the hull for all vessels utilized in this study. Average

value of confidence limits as percentages of average consumption, is shown in Fig.12 as a function of number of days the data is collected.

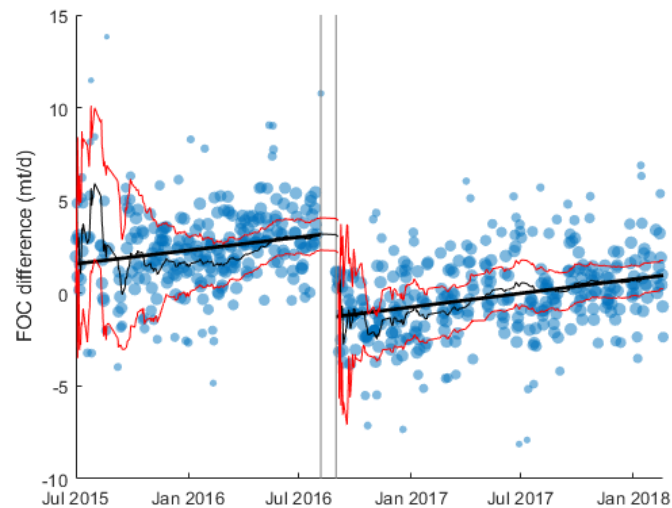


Fig.11: Uncertainty of the hull fouling rate

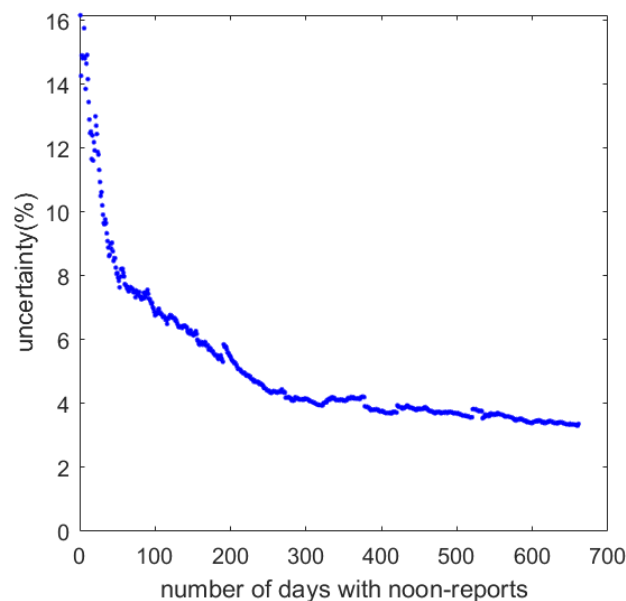


Fig.12: Daily error vs data points curve

The above means that after using all the available data, with 95% confidence the predicted daily fuel consumption values have less than 3% difference to the reported ones. This difference is coming from the typical inaccuracies in the noon report readings, from small inaccuracies in the weather now-cast data and from periodic longer gaps in AIS data.

In this comparison the model uncertainty started quite poor, around 15%, due to large differences in technical performance of bulkers, but rapidly improves. With this method, we have around 5-6% uncertainty after 3-6 months, which is enough for large majority of use cases of ship performance monitoring and analysis. For reference, commonly the model training on purely machine learning based services working with high frequency automation data take from three to six months for bulk carriers.

When comparing longer periods, for example voyages, the uncertainty level would be lower as some of the inaccuracies in for example weather forecasts cancel each other during different days. This is more meaningful comparison for voyage planning purposes and will be estimated on separate studies.

4.3. Estimate stability of the hull fouling trend prediction

To estimate the near future, 3-12 months, performance for a vessel, it is important to be able to estimate the current hull fouling rate of the vessel. The stability of the fouling rate is done by taking two points of data from the start of estimation period and then fitting a line on them. After this the slope is stored in memory and a data point is added and process repeated until whole period is processed. Previous slope data point is subtracted from the following slope data point to get the change size of fits slope. This is done to all periods of all ships to get the slope development vs time curve. In Fig.13 is presented all the data of the periods slope stability relative to the amount of data.

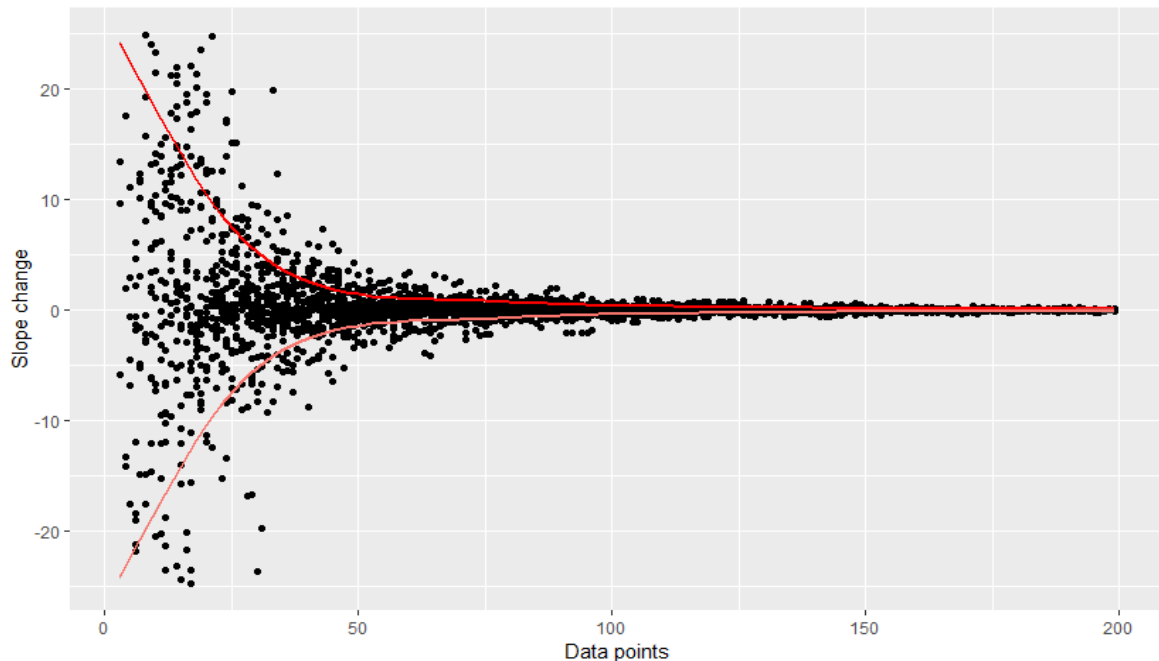


Fig.13: Slope stability vs data points

The above chart tells us that during the first days of operation the variation in the fouling rate prediction is huge. The estimation of the hull fouling trend however stabilizes fast and takes only a few voyages since the data collection start to be able to have some indication of the performance trend. After 50 days there is hardly any variation in the performance trend prediction.

5. Conclusions

In the paper methodology for using noon-reports as a source of information to assess the technical performance was presented. A digital twin of the ship is created based on the naval architecture principles, hydrodynamic models, and experience in ship design. With the proposed methodology; public data, hydrodynamic models and manually reported data are combined into NAPA Performance Model i.e. the digital twin. The methods are implemented in the NAPA Fleet Intelligence system. The challenge of sparse data, one daily data point, obtained from the noon-reports, is overcome with the combination of hydrodynamics and big-data based model. The reference consumption is calculated with these models and compared with the reported one. This enables improvement of the absolute accuracy of the NAPA Fleet Intelligence performance models without onboard installations.

The accuracy of the presented method was studied based on noon-reports over a several years from fleet of dry bulk vessels. The accuracy was shown to improve in good level rapidly with the increasing data.

These models can be used for evaluating or predicting the need for dry docking or other maintenance, for planning of forthcoming schedules and negotiation of contracts, for weather and speed profile

optimization or for several other use cases of which the shipping companies can gain benefit from. Discussed methodology is applicable for small or large fleets without large investments. The service can be started with significantly less interference to ship operations and significantly lower investment than high frequency data collection systems and can enable access to fleet wide analytics in a matter of some weeks or months.

References

ADLAND, R.; JIA, H.; STRANDENES, S.P. (2017), *Are AIS-based trade volume estimates reliable? The case of crude oil exports*, *Maritime Policy and Management* 44 (5), pp.657-665

ALDOUS, L.; SMITH, T.; BUCKNALL, R. (2013), *Noon report data uncertainty*, Low Carbon shipping Conf., London

ALDOUS, L.; SMITH, T.; BUCKNALL, R.; THOMPSON, P. (2015), *Uncertainty analysis in ship performance monitoring*, *Ocean Eng.* 110, pp.29-38,

BAL BEŞİKÇİ, E.; ARSLANA, O.; TURANB, O.; ÖLÇERC, A.I. (2016), *An artificial neural network based decision support system for energy efficient ship operations*, *Computers & Operations Research* 66, pp.393-401

DAVIES, H.; BEVAN, S. (2017), *A Consultative Approach to Charter Party Agreements Based on Virtual on Time Arrival*, *TRANSNAV the Int. J. Marine Navigation and Safety of Sea Transp.* 11(2)

HARANEN, M.; MYÖHÄNEN, S.; CRISTEA, D. S. (2017), *The Role of Accurate Now-Cast Data in Ship Efficiency Analysis*, 2nd Hull Performance & Insight Conference (HullPIC), Ulrichshusen, pp.25-38, http://data.hullpic.info/hullpic2017_ulrichshusen.pdf

HUBER, P.J. (2009), *Robust Statistics*, John Wiley & Sons

JALKANEN, J.P.; JOHANSSON, L.; KUKKONEN, J.; BRINK, A.; KALLI, J.; STIPA, T. (2012), *Extension of an assessment model of ship traffic exhaust emissions for particulate matter and carbon monoxide*, *Atmos. Chem. Phys.* 12, pp.2641-2659

MANNHEIM, D. (2017), *Application of AIS Data in Vessel Performance Analysis*, Master Thesis, DTU and Aalto University, <http://urn.fi/URN:NBN:fi:aalto-201709046891>

PECCI, J. (2007), *Liquid Bulk / Quantity Measurements and other challenges*, SafeWaters UM, http://www.aimuedu.org/aimupapers/Liquid_Bulk_Measurement.pdf

SAFAEI, A.A.; GHASSEMI, H.; GHIASI, M.; (2018), *Correcting and Enriching Vessel's Noon Report Data Using Statistical and Data Mining Methods*, *European Transport \ Trasporti Europei* 67/7

STOPFORD, M. (2009), *Maritime Economics*, Taylor & Francis

An Approach to Monitor the Propeller Separately from the Hull

Erik van Ballegooijen, VAF Instruments, Dordrecht/Netherlands, evballegooijen@vaf.nl

Torben Helsloot, VAF Instruments, Dordrecht/Netherlands, thelsloot@vaf.nl

Abstract

This paper describes an approach to monitor hull performance separately from propeller performance. Use is made of thrust measurements in addition to power, speed and environmental variables. With this data the extra propulsive power required due to fouling and roughness can be ascribed to either the hull, or to the propeller. Without thrust measurements, making such a division would be impossible. Instead of estimating the exact interaction effects, which are difficult to determine in full scale, KPI's are defined that are easy to interpret and make a pragmatic division between efficiency losses related to the hull and losses related to the propeller. By keeping track of these KPI's operators can respond to changes in efficiency and make informed decisions regarding the maintenance of their ships. A case study is presented to demonstrate the usefulness of this approach.

1. Introduction

Ships in service regularly undergo cleanings of both their hulls and their propeller(s). This is done to keep every surface of the ship that is in contact with the water smooth, so that friction decreases and the overall hydrodynamic efficiency increases. Ultimately this saves money, because less fuel needs to be bought to propel a more efficient ship. However, hull cleaning and propeller polishing costs money as well, so there is a tradeoff to be made between maintenance costs and costs incurred by hull and propeller fouling.

Finding the optimal times to schedule a maintenance is impossible without an accurate quantification of the costs of hull fouling and propeller roughness. Poor knowledge of the hydrodynamic performance of a ship is therefore costly, which is why more and more ship owners are investing in tools that will give them the insight that is needed. Sensor data can help provide this insight. With accurate measurements of the power consumption over time the gradual increase in resistance caused by fouling can be detected. Data alone however, does not paint a clear picture. Sensor data of ships in service is extremely complex and noisy, which means a careful analysis is needed to arrive at a performance indicator that can be readily understood and acted upon.

This paper discusses a set of such KPI's that can be used to quantify the costs of propeller roughness and hull fouling. Three KPI's will be presented, one for the total hydrodynamic performance of the ship, one to indicate hull fouling, and one to indicate propeller roughness. To do this, the performance of the hull and the propeller must be separated.

2. Separating hull and propeller

Much has been written about separating the efficiencies of propeller and hull, but the consensus is that thrust measurements are a necessity, see *ISO19030-1*. A promising approach to separate hull and propeller efficiency has been presented by *Paereli et al. (2016)*, *Paereli and Levantis (2017)*. They identify some practical obstacles in obtaining useful performance indicators, such as the immeasurability of the effective power P_E , but are nevertheless able to get some sensible results. In the following paragraphs a method not dissimilar to theirs is presented. Because the effective towing power cannot be determined in full scale an alternative is used. This alternative is named 'hull power':

$$P_H = T * V_S$$

With thrust T and ship speed V_S . In conventional naval architecture terms, P_H relates to the effective towing power and thrust deduction factor t .

$$P_H = \frac{P_E}{(1 - t)}$$

The other quantity that is needed for the analysis in the present paper is the shaft power P_S .

$$P_S = 2\pi * M_S * n_p$$

The main reason for using these quantities is that they are measurable. P_H can be measured with a thrust meter, P_S can be measured with a shaft power meter. With these two powers, we can already make a separation. The intuition behind the separation is the following: some of the power that is available at the shaft is ‘used’ by the hull (P_H), the rest of the power is lost somewhere ‘near’ the propeller. In the form of an equation this reads:

$$P_S = P_H + P_{pr}$$

To understand what the separation precisely means, the characteristics of P_S and P_H must be understood. In equal sailing conditions, P_S changes over time when the overall propulsive efficiency of a ship changes, it is influenced by changes in

- Hull efficiency
- Open water efficiency
- Relative rotative efficiency
- Shaft efficiency

In equal sailing conditions, P_H changes over time either when the resistance of a ship changes or when the thrust deduction factor changes.

When only the resistance increases, both P_H and P_S will increase with the same percentual amount. A five percent increase in resistance leads to five percent increase in P_H and when the rest of the efficiency stays the same a five percent increase in P_S . From this it follows that when the relative increase in P_S is greater than the relative increase in P_H , it must be due to something that is not hull resistance.

The approach that is proposed in this paper to separate hull and propeller effects works with a set of three KPIs. The first KPI is defined in such a way that it tracks the percentual change in total shaft power PS, compared to a certain baseline.

$$KPI_{H+P} = \left(\frac{\text{Measured Shaft Power}}{\text{Baseline Shaft Power}} - 1 \right) * 100\%$$

This KPI is named ‘propulsion power loss’ and tracks the aforementioned changes in:

- Hull efficiency
- Open water efficiency
- Relative rotative efficiency
- Shaft efficiency

The second KPI is defined in such a way that it tracks the percentual change in hull power PH, compared to a certain baseline.

$$KPI_H = \left(\frac{\text{Measured Hull Power}}{\text{Baseline Hull Power}} - 1 \right) * 100\%$$

This KPI is named ‘hull power loss’ and tracks the changes in:

- Hull resistance
- Thrust deduction factor

The third KPI is equal simply to the difference between the other two KPIs. This results in the fact that the third KPI tracks those effects that are included in the first KPI but are not present in the second KPI.

$$KPI_P = KPI_{H+P} - KPI_H$$

This KPI is named ‘propeller power loss’ and tracks the changes in:

- Wake fraction
- Open water efficiency
- Relative rotative efficiency
- Shaft efficiency (not expected to change)

Loosely speaking, KPI_{H+P} tracks the total hydrodynamic performance, KPI_H tracks performance related to the flow around the hull, and KPI_P tracks performance related to the losses in the ship’s wake. The main contributor to KPI_H will be the resistance increase of the hull. The main contributor to KPI_P will be the propeller roughness, but also anything that changes the inflow to the propeller will show up in the propeller power loss. (Changes in propeller inflow will go together with changes in ship resistance. Draught and trim for example, will both change the inflow to the propeller, and resistance. Also energy saving devices such as a wake equalizing duct will have an effect on both resistance and wake.)

Granted, this approach does not perfectly separate the efficiency of the propeller from the efficiency of the hull, which is possible only in theory. However, it does make ‘a’ separation that is both intuitively understandable and ties into conventional naval architecture theory in a clear way.

Another advantage of using the proposed KPIs is that they are all the same thing, so that they can be directly compared to each other. All three of them are expressed as a percentage of baseline power. This percentage may for example be applied to the expected fuel costs to get an estimation of the savings potential in dollars. Or, more accurately, the savings potential can be calculated by multiplying lost power with specific fuel oil consumption and fuel price. The KPIs are thus more closely related to costs than alternatives such as propeller efficiency or speed loss.

3. Case study

The following section describes a case study in which the use of the proposed method is exemplified. The data used in this case study was also used in a previous publication, *Ballegooijen et al. (2018)*, in which a different set of KPIs was used. The case study uses thrust and torque measurements made with the TT-Sense®, shown in Fig.1.

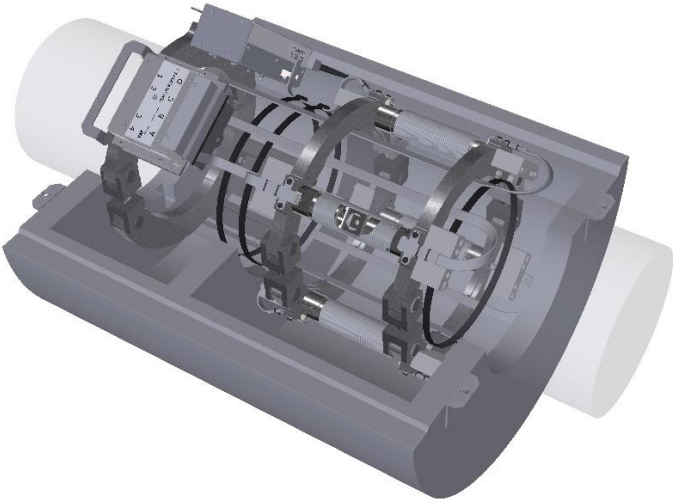


Fig.1: The TT-Sense® thrust and torque meter

3.1 Description of data

The ship under consideration is a large (>50,000GT) passenger vessel that underwent maintenance where both the hull and propeller were cleaned. The data used encompasses 11 months, roughly 5.5 months before and 5.5 months after the maintenance. The data points are chosen to represent quasi-static conditions. Filters are applied for low windspeeds, similar draft and deep water. The goal of the case study is to estimate how effective the maintenance has been.

To account for a noticeable bias in the original speed log a correction method has been applied. The details of this correction method can be found in *Ballegooijen et al. (2018)*.

3.2 Creation of the baseline

In this paper simple baselines are used for the expected thrust and expected power. In practice it would be better to use a more accurate prediction model as a baseline, or use baselines determined from model tests. To demonstrate the proposed KPIs however it suffices to use baselines that are simply a power law fit of the data after the cleanings.

$$\text{Baseline Shaft Power} = a_P * V_{ship}^{b_P}$$

Where a_P and b_P were determined using least squares estimation. Similarly:

$$\text{Baseline Hull Power} = a_T * V_{ship}^{b_T}$$

Where a_T and b_T were again determined using least squares estimation.

3.3 Visualisation of results

Fig.2 shows the set of KPIs computed using the simple power law relations as a baseline. The propulsion KPI shows the percentage of power lost within the total propulsion chain. The Hull KPI shows the percentage of power lost that can primarily be ascribed to effects related to the hull.

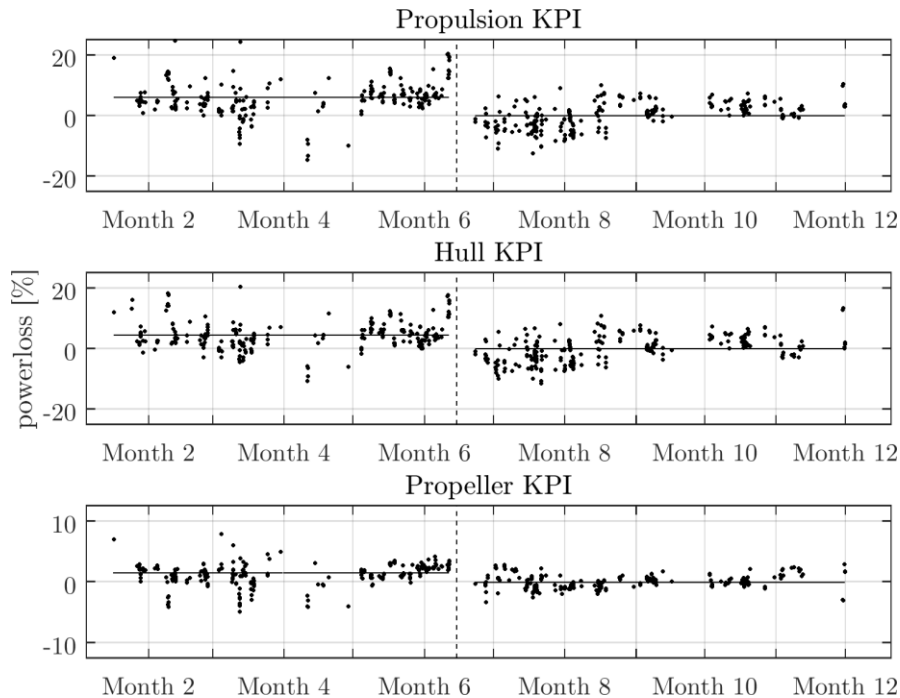


Fig.2: Average performance KPI's before and after maintenance

The Propeller KPI shows the percentage of power lost that can be ascribed to losses in the propeller wake. (Losses in the propeller wake are a result of both the innate (in)efficiency of the propeller and extra losses relating to the quality of the inflow in behind condition.) Please note the y-axis of the bottom subplot is scaled differently.

The data shown can be summarized in two different ways. The first summary is shown in Fig.2 and Table 1, and is based on the average power loss before and after the cleanings. The individual data points show variance due to several reasons. Most causes of variation are expected to average out in the long run. Comparing the averages before and after a maintenance will therefore give a reliable estimate of the maintenance effects. Table 1 displays the average power loss before and after the cleaning event. The estimate says that six percent more power was needed in the period before the cleaning.

Table 1: The effects of the cleaning event on lost power using averages

Mean Power loss	<i>Before Cleaning</i>	<i>After Cleaning</i>	<i>Average Effect</i>
Propulsion losses	6.1%	0.1%	6.0%
Hull losses	4.5%	0.1%	4.4%
Propeller losses	1.6%	0.0%	1.6 %

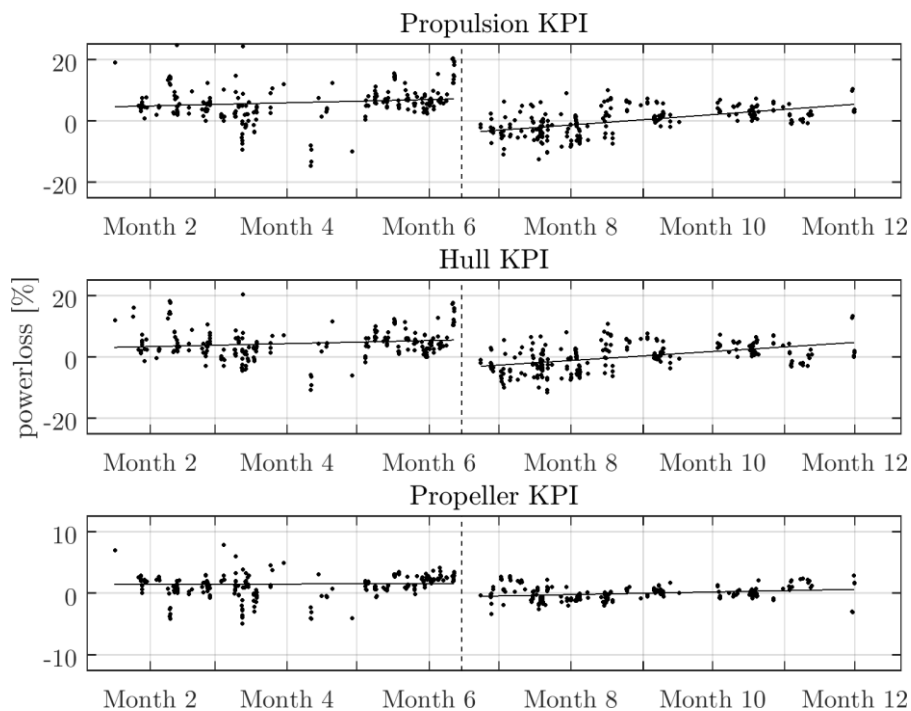


Fig.3: Linear trendlines through KPI's before and after maintenance

Table 2: The effects of the cleaning event on power loss using linear trends

Linear Power loss	<i>Before Cleaning</i>	<i>After Cleaning</i>	<i>Instant Effect</i>
Propulsion losses	4.7% — 7.2%	-3.4% — 5.5%	10.6 %
Hull losses	3.2% — 5.6%	-2.9% — 4.8%	8.5 %
Propeller losses	1.5% — 1.6%	-0.4% — 0.7%	2.0 %

Fig.3 shows the same data as Fig.2, but this time the data summaries are linear trends rather than averages. The linear trendlines reflect the expectation that hull fouling and propeller roughness gradually increase over time. Using the endpoints of the trendlines to estimate the cleaning effect yields larger estimates of the cleaning effect, as shown in Table 2. Whereas the estimate in Table 1 says something about the average effect of the cleaning, Table 2 says something about the instantaneous

decrease in power demand. The difference between them arises because the fouling rates of the two time periods are not the same.

Assuming that the engine's average specific fuel oil consumption (SFOC) of both time periods is approximately equal it follows from the presented analysis that this maintenance has yielded around ten percent instantaneous reduction of fuel consumption, of which roughly eight percent was due to a decrease in resistance and roughly two percent due to improvements of the propeller efficiency and wake. Because the fouling rate was higher in the second period the average reduction of fuel consumption was roughly six percent, of which four-and-a-half percent came from the decrease in hull resistance, and one-and-a-half percent from improvements in propeller efficiency and wake. These numbers can be used to estimate the return on investment of similar cleanings.

Figure 3 also shows that the amount of power loss related to the hull is approaching the value it had before the cleanings, which indicates that it might be a good idea to schedule a new cleaning in the coming months. The power loss related to the propeller has increased somewhat, but is not on the same level as it used to be, which could lead to the decision to not invest in a propeller cleaning yet.

4. Conclusions

Through the use of thrust measurements a pragmatic separation between performance degradation of the hull and the propeller can be made. One way to do this is to use the three KPIs that are introduced in this paper, each of which reflects the percentage of extra power needed to propel a ship with respect to a predefined baseline.

The first KPI, 'propulsion power loss', is affected by changes in the total propulsive efficiency of a ship. Secondly, 'hull power loss' is affected by changes in ship resistance and thrust deduction factor. Lastly, a change in 'propeller power loss' reflects changes in propeller efficiency and wake fraction.

When all other effects are properly accounted for, increasing power loss will reflect increases in propeller roughness and hull fouling. As such, the power loss KPIs can be used to aid scheduling of hull cleaning and propeller polishing. In the presented case study an average and instantaneous effect on the power consumption after a cleaning was determined for both the hull and the propeller. This makes it possible to determine the return on investment of the cleaning.

References

BALLEGOOIJEN, W.; HELSLOOT, T.; TIMMER, M.; (2018), *The propeller as a speedlog: using full scale thrust measurements to quantify propeller efficiency and hull fouling*, RINA Full Scale Ship Performance, London

PAERELI, S.; KRAPP, A.; BERTRAM, V.; (2016), *Splitting propeller performance from hull performance – A challenge*, 1st HullPIC Conf., Pavone

PAERELI S.; LEVANTIS M., *Quantification of Changes in Propeller Performance – Method Validation*, 2nd HullPIC 2017 Conf., Ulrichshusen

ISO 19030-1 (2016), *Ships and marine technology - Measurement of changes in hull and propeller Performance - Part 1: General principles*, ISO, Geneva

Evaluating the Efficiency of an Energy-Saving Device by Performance Monitoring

Nikos Themelis, Prisma Electronics, Greece, nikos.themelis@prismael.com
Christos Spandonidis, Prisma Electronics, Greece, c.spandonidis@prismael.com
Christos Giordamlis, Prisma Electronics, Greece, christos@prismael.com

Abstract

In the current paper, we utilize a performance monitoring system in order to examine the fuel savings for an oil tanker in which an energy saving device (mewis type duct) had installed during dry-dock. Three years of operational data utilizing the LAROS platform for the signal processing, data collection and analysis have been used, covering a period before and after the installation of the duct. The propulsion performance is monitored through several KPIs, whose sensitivity is tested for previous events such as propeller polishing and cleaning. Furthermore, we carried out a comparative study on a sister vessel without such energy saving device, but having similar hull and propeller cleaning history in order to access the long-term performance assessment.

1. Introduction and aim of the study

Nowadays the shipping industry is seeking ways to improve the energy efficiency of ships either for reasons related with cost savings, regulatory compliance or environmental protection. Several design and operational solutions have been proposed. *Bouman et al. (2017)* provides a detailed presentation of studies quantifying the energy reduction potential provided by several technological advances targeting for example optimizations in hull, power and propulsion as well as route planning. For existing ships, an option to increase their energy efficiency is by implementing devices aiming at their propulsion improvement. Such a device can be a mewis type duct mounted in front of a propeller targeting the enhancement of its working conditions and specifically by accelerating and straighten the hull wake into the propeller as well as by producing a net forward thrust. The installation includes also a fin system which provides a pre-swirl to the ship wake which reduces losses in the propeller slipstream and thus resulting in an increase in propeller thrust at a given propulsive power. Model and CFD tests are usually carried out in order to properly design and quantify the benefit from such an installment (see *Schneekluth and Bertram (1998)*). Nevertheless, for several reasons, operators still need to measure and verify the claimed gains during the real operation of a ship when conditions can differ extensively from the design ones.

On the other hand, performance monitoring can be utilized for a variety of reasons, spanning from situational awareness and optimization, triggering maintenance events as well as evaluating the effect of technological interventions such as dry-dock (see e.g. *Themelis et al. (2018)*), while for several case studies see *Bertram (2018)*). Performance assessment of ships is based on the wealth of data produced nowadays and utilizing tools and methods to assess ship' status, while the shipping industry has started to adopt frameworks such as ISO19030, *ISO (2016)*, aiming at standardizing the assessment procedures in a comparable manner.

In the current paper, we utilize a performance monitoring system in order to quantify the fuel savings for an oil tanker fitted with a mewis type duct during dry-dock. Our aim is to examine whether a set of Key Performance Indicators (KPIs) are capable of capturing the effect of the duct in ship performance. Three years of operational data employing the LAROS platform for the data collection and analysis will be utilized, covering a period before and after the installation of the duct. The same set of KPIs will be tested for their sensitivity for changes in performance due to dry-dock and propeller polishing and cleaning. The scope of the analysis is to study whether a practical index could be used before one shall proceed with a more detailed analysis involving methods for the decomposition of hull and propeller performance (see for example *Logan (2011)*, *Grigoropoulos and Theodosiou (2012)*).

2. The Performance monitoring framework

A practical, yet comprehensive approach is to monitor the performance through using specific metrics, the so-called Key Performance Indicators (KPIs). Performance indicators may be characterized by the following aspects:

- The principal components they describe; hull, propeller and /or engine condition
- The ability of the indicator to account for changes in speed, environmental conditions, displacement, etc.
- The physical representation of the indicator; certain parameters are more intuitive and easy to interpret than others
- Ability to identify slow time-varying performance changes, e.g. due to fouling.

A general framework for the calculation of a KPI is shown in Fig.1, where it is pointed out that the required step for data pre-processing.

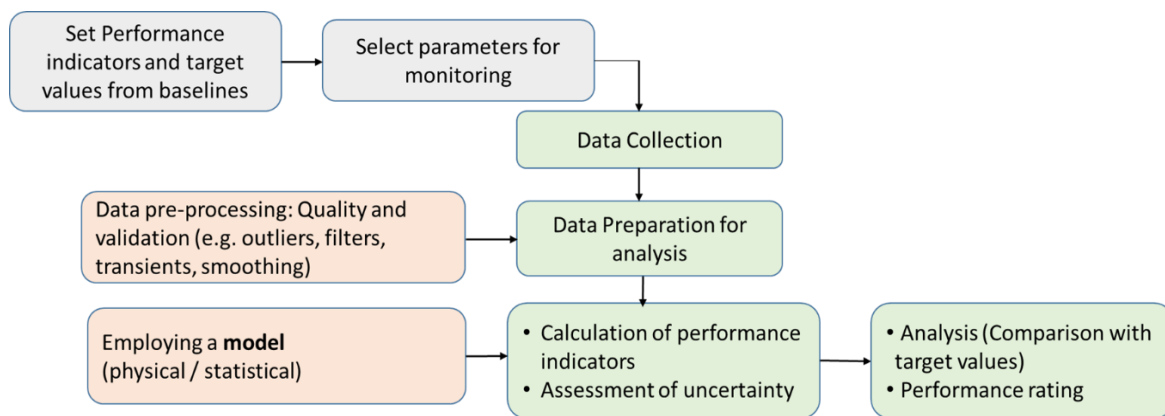


Fig.1: A general framework for KPI calculation.

The set of KPIs to be used in this study is defined as follows:

- KPI_a = % power increase, following the concept of ISO 19030, *ISO (2016)*, and targeting hull and propeller performance
- KPI_b = ME FOC / d, in 1 hr. ME FOC and d are the fuel oil consumed in main engine and the distance travelled respectively. This KPI includes also engine efficiency
- $KPI_c = P / n^3$, where P and n are the shaft power and revolutions respectively. This KPI corresponds to propeller curve coefficient or else power ratio, e.g. *Logan (2011)*

The % power increase KPI is defined as:

$$(\%) (P_m - P_e) / P_e$$

It expresses the % difference between the measured and the expected power for a specific ship's speed V_m . The expected power P_e is read from a speed-power reference curve (e.g. obtained by sea trials) at the measured speed through water (V_m) and at the measured displacement and trim as shown in Fig.2. This KPI follows the filtering requirements as described in Part 2 of ISO 19030 (ISO 2016). Specifically, the next parameters shall be considered for filtering:

- A minimum water depth is defined as $h = \min [3(B * T_m)^{1/2}, 2.75 V_s^2 / g]$, where B, T_m , and V_s are ship's breadth, mean draft and speed respectively.
- rudder angle larger than 5°
- true wind speed values larger than 7.9 m/s

Additionally, we exclude data points that correspond to current speed greater than 1 kn. Furthermore, no extrapolation of speed-power curves is allowed, thus we utilize data only for the speed range of the reference curves. Furthermore, we are not considering measurements that corresponds to values of displacement Δ and trim that deviate more $5\%\Delta$ and $0.5L_{BP}\%$ from the respective values of the reference conditions. A study on the levels of confidence achieved due to uncertainty issues spanning this performance indicator, and mainly due to sampling frequency, has been presented in *Themelis et al. (2018)*.

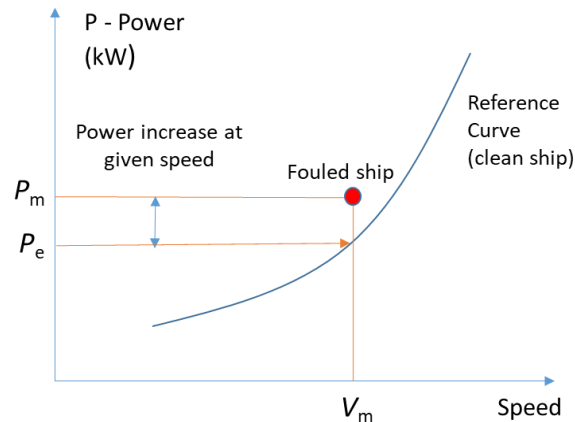


Fig.2: Expected and measured power for a fouled ship.

3. Set up of the case study

The examined ships are two sister Suezmax crude oil tankers with summer deadweight of 158000 mt. High-frequency data with sampling frequency of 1 minute are collected from the ships utilizing the LAROS platform (see Spandonidis et al. 2018). As we will rely on the data collected for the evaluation of the energy saving device, our aim is to consider a time period covering a period before and after the installation of the duct which is placed during dry-dock. Specifically, the available operational data cover a period 3 years. Table 1 shows the key dates for the 2 ships. Due to the fact that the duct was installed during dry-dock, where hull and propeller cleaning were also taken place, the introduction to the analysis of the 2nd sister ship will provide the benchmark for comparison spanning the period after dry-docking. We also have to notice that Ship 1 undergone propeller polishing and cleaning a few months before her scheduled dry dock, while such event did not occur for Ship 2, at least during the monitoring period. Among the whole set of signals monitored using the LAROS platform,

Table 2 presents the required parameters for the study.

Table 1: Key dates (month/year) for performance intervention.

Ship	Mewis Duct installed	Dry-Dock (DD)	Propeller polishing and cleaning (PP)	Start date of monitoring period	End date of monitoring period
Ship 1	1/15	1/15	9/14	6/14	6/17
Ship 2	No	4/15	No	6/14	6/17

Fig.3 to Fig.5 present indicative distributions of operational and weather parameters. Current speed is calculated using speed through water and speed over ground. A pre-processing stage was carried out targeting the filtering of data based on the next criteria as well as the normalization of power values for the loading conditions that correspond to ballast and design drafts (see Table 3) using the Admiralty formula. Correction of power values due to wind resistance was carried out using the method proposed by ISO 19030-Part 2 (ISO 2016).

Table 2: Set of monitoring parameters.

Parameter	Units	Sensor type
Speed over ground	knots	GPS
Speed through water	knots	Speed log
Shaft revolutions	Revolutions per minute	Shaft torque meter
Shaft power	kW	Shaft torque meter
ME fuel oil consumption	Tons/day	Mass flow meter
Drafts	m	Draft indicator
Ship direction	degrees	GPS
Rudder angle	degrees	autopilot
Relative wind speed and direction	m/s, degrees	anemometer
Water depth	m	Echo sounder

Table 3: Characteristics of the reference loading conditions.

Loading condition	Mean draft (m)	Trim (m)
Ballast	7.3	-2.1
Laden @ design draft	15.5	0

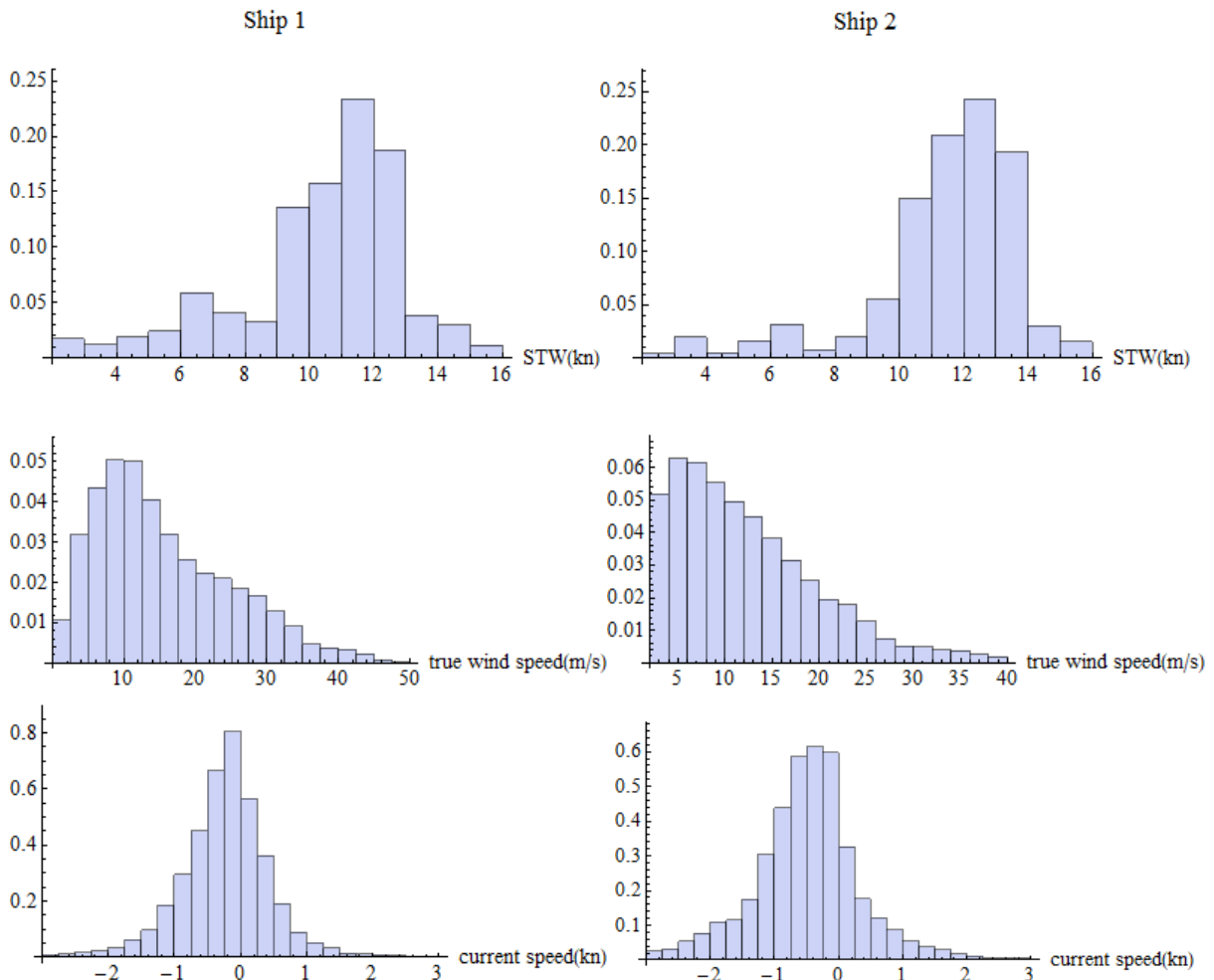


Fig.3: Probability density functions of speed through water, true wind and current speed.

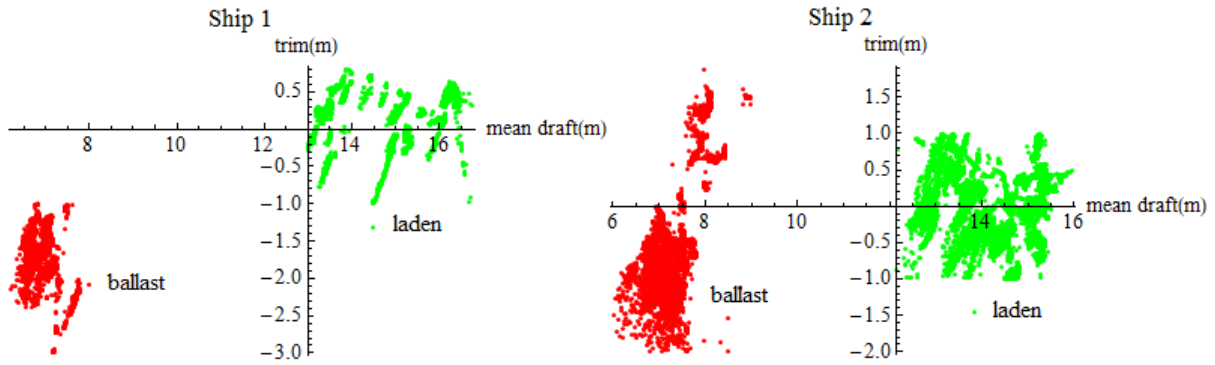


Fig.4: Mean draft versus trim. Positive trim values correspond to trim by the bow.

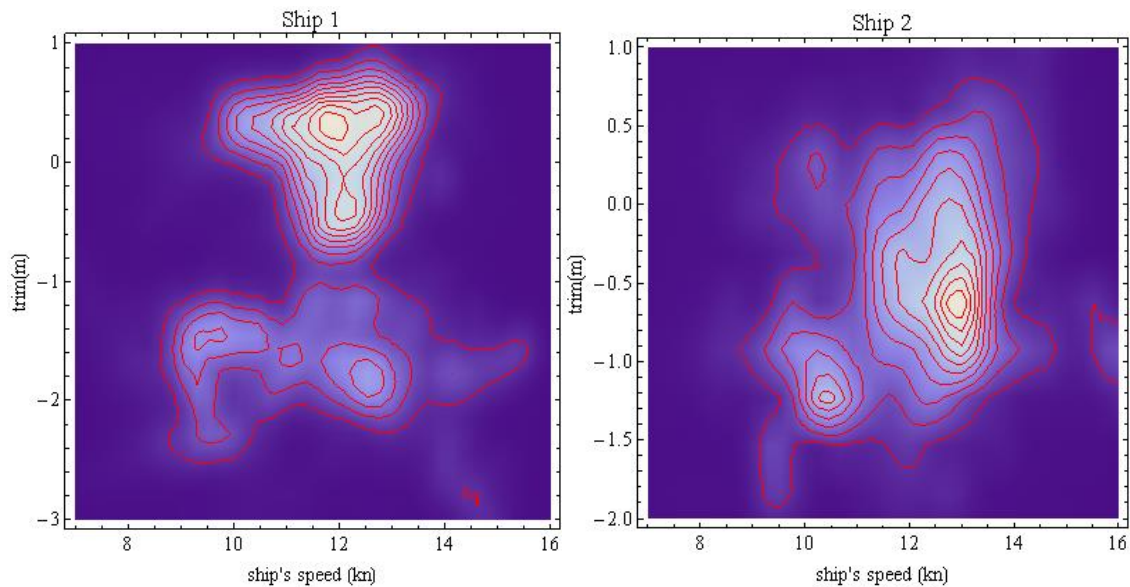


Fig.5: Contours of the joint probability density function of ship's speed and trim. Darker values correspond to the lower values of the pdf.

4. Analysis based on KPIs

Distance travelled is calculated using ship's waypoints, while for the power increase, new baselines for the power - speed curves were obtained by utilising the data of 3 months of operation after the dry-dock and using the form $P = a V^b$. The parameters a and b are calculated by the linear least square method. Fig.6 presents the obtained reference curves for the two loading conditions for Ship 1.

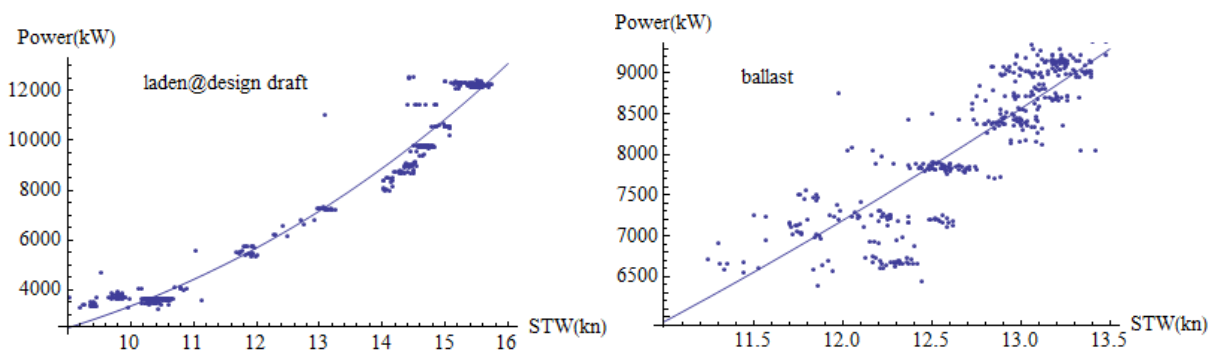


Fig.6: New baselines obtained from operational data for Ship 1. R^2 values are 0.9951 and 0.9949 respectively.

For the calculation of the KPIs, we use the filtered and normalized dataset as obtained by applying the

procedure described in sections 2 and 3. In the first instance, KPIs are derived for the reference loading condition (ballast and laden). Such results are shown in Fig.7, while KPI values, including both loading conditions, are shown in Fig.8 where trend lines have been included for each period.

Both 3 KPIs present significant large values for Ship 1 before her propeller polished and cleaned, revealing inefficient ship operations. After this event there was a significant decrease of the KPIs. Additionally, after dry-docking, the KPIs of Ship 1 were slightly decreased compared with the respective values before dry-docking and after the propeller polishing and cleaning. The KPI's trend line reveal a slight increase for the next 2.5 years of operation following dry-dock, which will be examined later.

On the other hand, the condition of Ship 2 before dry-docking was better than those of Ship 1 and no propeller polishing occurred before dry-docking. However, there was an increasing trend in power deviation and fuel oil consumed per nautical mile of the KPIs. Following dry-dock, KPI values were reduced with an increasing long-term trend.

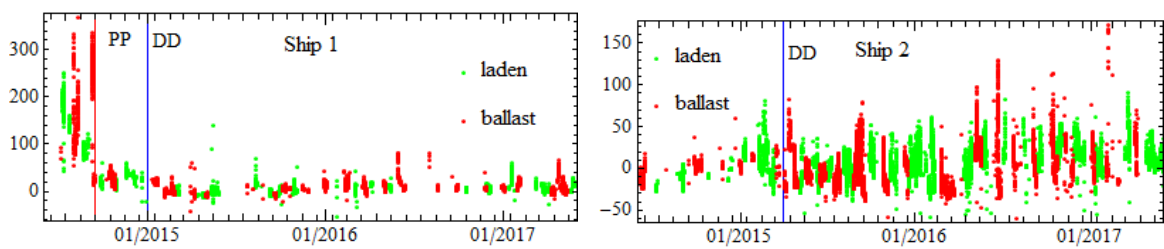


Fig.7: Time history of % power increase (KPI_a). Red and blue dots correspond to ballast and laden condition, respectively. PP and DD stands for propeller polishing/cleaning and dry-docking, respectively.

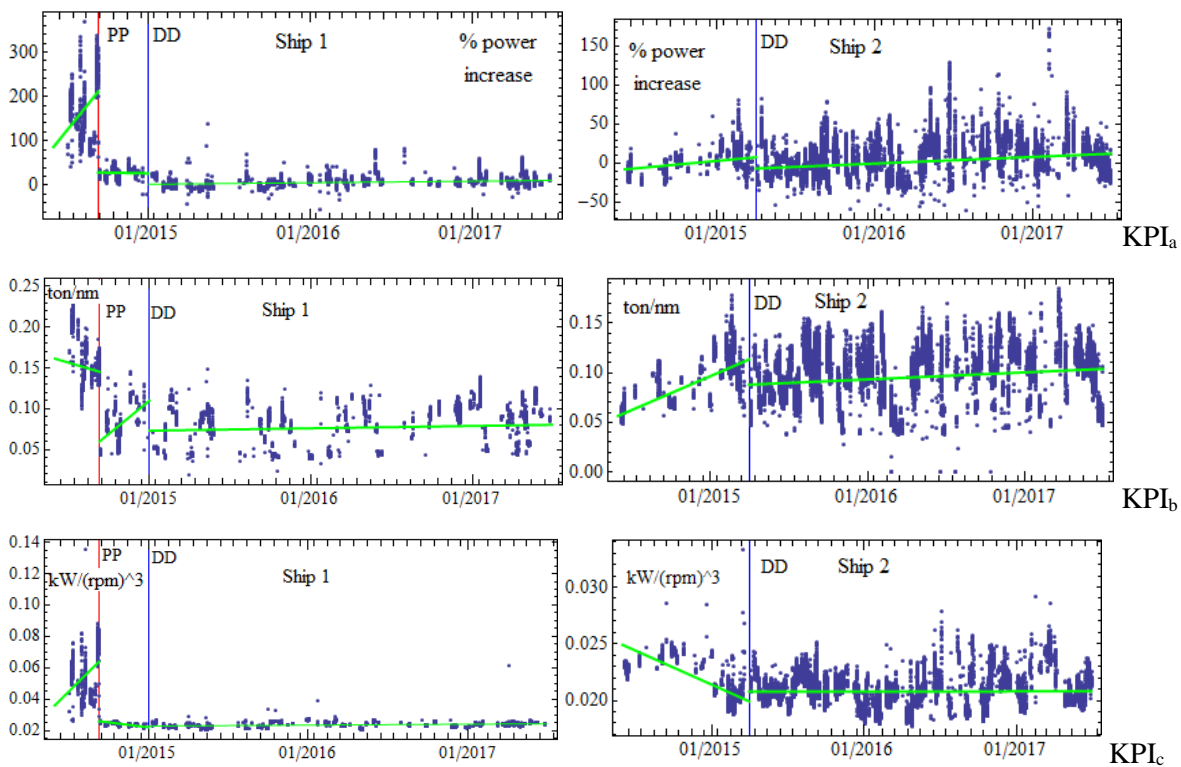


Fig.8: Time histories of KPIs for both ships including trends.

Therefore, as shown in Fig.8, the effects of propeller polishing and cleaning and dry-dock in performance were adequately captured. Nevertheless, the main target is to examine the effect of the

mewis duct provided that it was installed at the same time hull and propeller cleaned in dry-dock. Therefore, as a first step, we need to examine more detailed the long-term behaviour following dry-dock. Fig.9 presents information of the distribution of each KPI, and specifically the mean value, the 25th and 75th percentiles as well as the maximum and minimum values excluding the outliers. Furthermore, these plots have been derived for specific time periods either defined as periods before and among specific events (e.g. propeller polishing or dry-dock) or as yearly intervals following dry-dock aiming at examining ship's performance as gradually departing from dry-dock. Such graphs provide additional information as present the behaviour of the statistical significance zone of the KPI values, except from its average value.

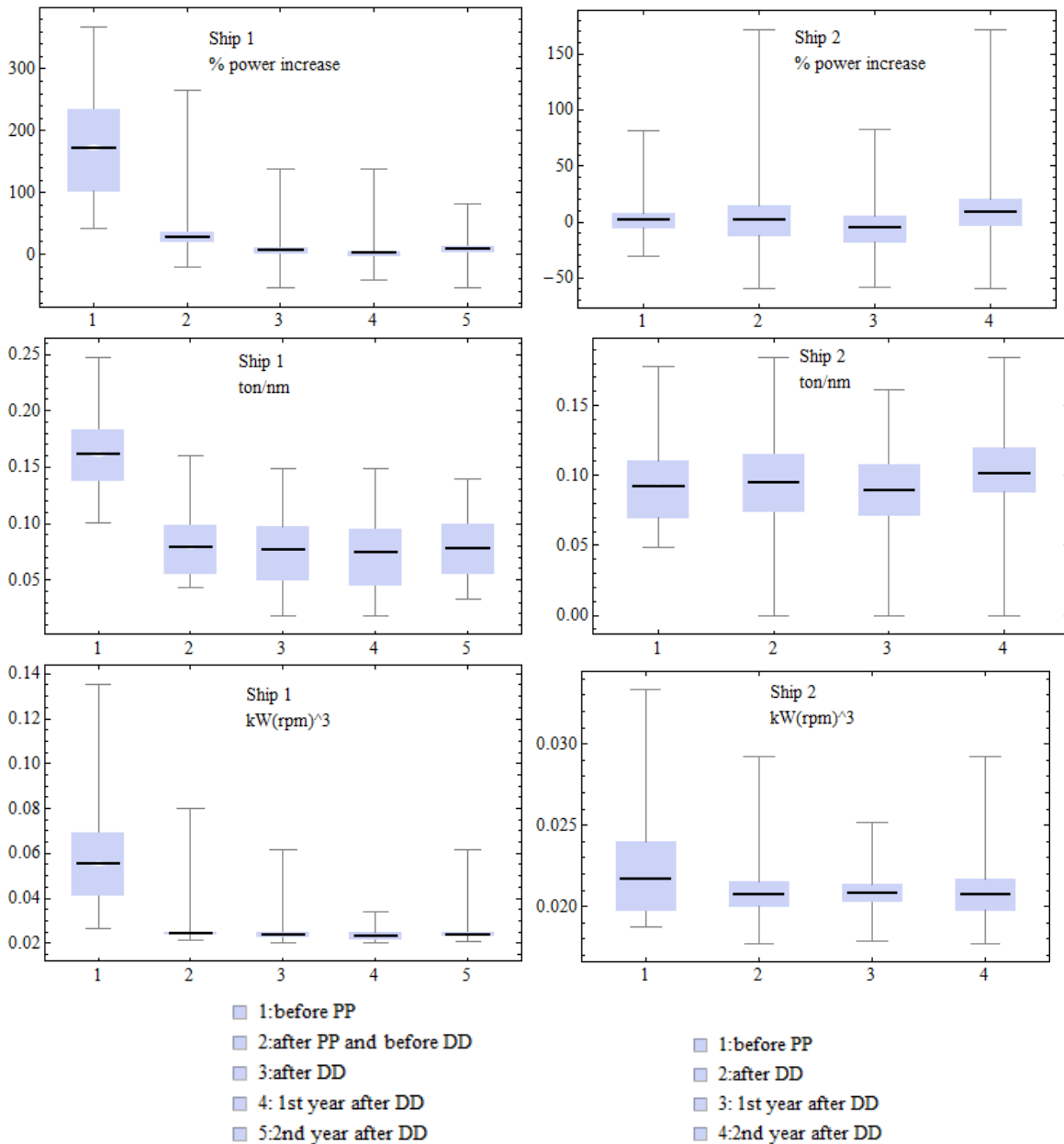


Fig.9: Synopsis of the distribution of KPI values in box and whiskers type of diagrams for specific time periods. Horizontal thick black lines correspond to mean values.

For Ship 1, we have included two periods before dry-dock; one before propeller polishing (named with the number 1 in Fig.9) and the other stands for the period among propeller polishing and dry-dock (named with number 2). Fig.9 includes also a case that include all the period following dry-dock (named as 3 and 2 for Ship 1 and 2, respectively). It can be derived that propeller polishing/cleaning resulted in

a significant decrease of KPI values. For power increase (KPI_a), Ship 1 presented less deviated KPI values, while for year 2 achieved less increase than the respective one of Ship 2. Similar results present the analysis of KPI_b, whereas KPI_c does not indicate significant difference between the ships.

Therefore, in order to focus on KPIs trend, we produce through LAROS Analysis Engine the data sets used for the graphs of Fig.10 which show the statistical trend zone of the KPIs for three key periods: before dry-docking, for the first and second year after dry-docking. For Ship 1 we have selected the period before dry-docking to correspond to the one between propeller polishing/cleaning and dry-dock. For KPI_a (% power increase), we can observe that both ships present a decrease with the one of Ship 1 to be more pronounced, while after year 1 the power increase of Ship 2 is sharper by an amount of 3.5% in average. A similar trend increase between year 1 and 2 occurs also for KPI_b, where Ship 2 presents a severer increase. If we compare at a ship's speed of 12 kn and equal percentage of time for loading conditions at ballast and design draft, then the difference in fuel oil consumption would be in the range of 0.8-1.5 tons/day or else 3.5-5%. This difference is increasing to a range of 5-7% as time is passing further from dry-dock. Such effect could be attributed to the mewis duct as it comparatively seems to be more effective in the later stages of the monitoring period, where probably hull fouling were increased. On the other hand, this trend cannot be verified when using the third KPI of the study, where for year 1 both ships present similar behaviour, while for the year 2, Ship 2 had a steadier KPI trend.

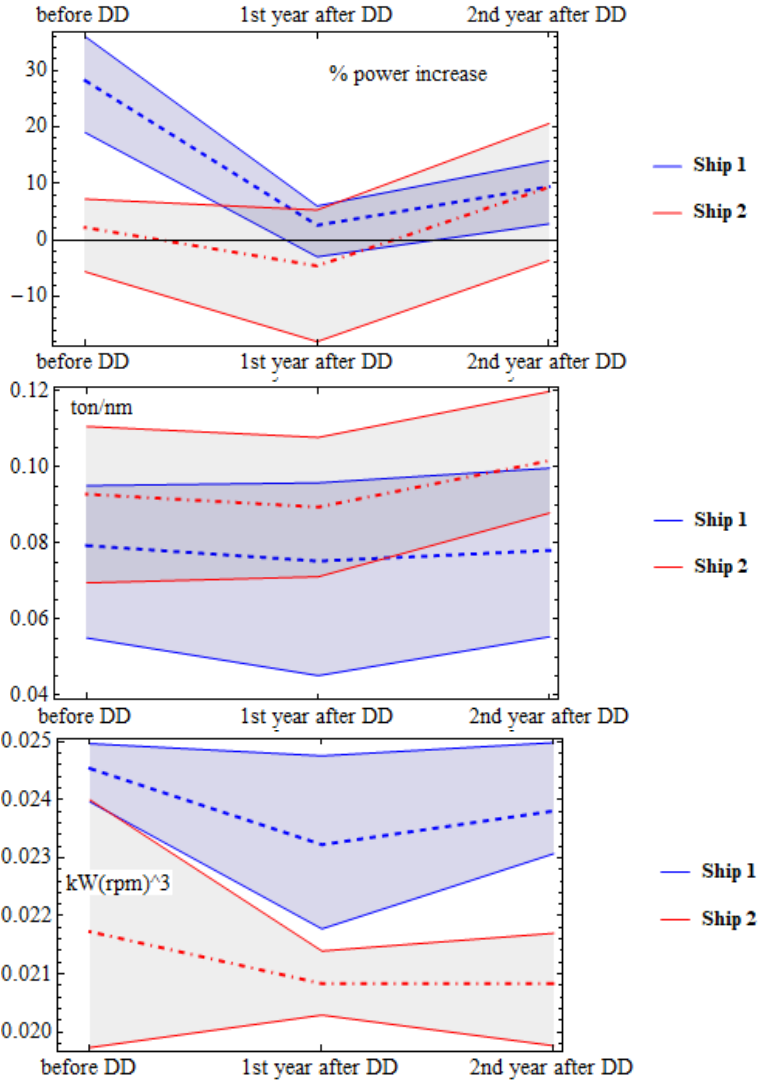


Fig.10: KPIs statistical trend zones in time. Dashed lines correspond to mean values, while the upper and lower lines to the 75% and 25% percentile, respectively.

5. Concluding remarks

We examine the capability of a practical performance monitoring framework to quantify the effect of an energy saving device such as a mewis duct. The key output of the framework is a set of KPIs, whose calculation is relied on the LAROS platform for the collection, processing and analysis of high-frequency data. The case study examined refers to two sister vessels, where one of them had been fitted with a mewis type duct. The effect of other interventions aiming at increasing the energy efficiency of the ships and specifically hull and propeller cleaning were also quantified within this assessment framework.

Our aim is to analyse whether such a quite practical approach could identify any fuel consumption gains provoked by the mewis type duct by comparing the performance of the ships for the period following dry-dock. Fuel savings of the order of 3.5-5% were identified with an increasing trend as hull and propeller fouling is increasing. Such a difference could be owed to the presence of the mewis duct, but we suggest that this result deserves a more detailed examination. Dynamic speed profiling of the vessel may produce a better result for this energy saving device. Therefore, as a next step, an analysis targeting in the separation of the hull and propeller effect in performance in real operating conditions is planned to be carried out, where the option of directly measuring thrust shall not be ignored as an option to the problem. Furthermore, issues such as the performance of such devices in conditions deviating significantly from calm sea is also a subject that needs attention.

References

- BOUMAN, E.; LINDSTAD, E.; RIALLAND, A.; STRØMMAN, A. (2017), *State-of-the-art technologies, measures, and potential for reducing GHG emissions from shipping – A review*, Transportation Research Part D, 52, pp.408-421
- BERTRAM, V. (ed.), (2018), *Proceedings of 3rd Hull Performance & Insight Conference*, Redworth
- GRIGOROPOULOS, G.J.; THEODOSIOU, D.K.N. (2012), *Harmonising SEEMP with effective vessel operation*, SNAME 4th Int. Symp.
- ISO, (2016), *ISO19030: Ships and marine technology - Measurement of changes in hull and propeller performance. Part 2 – Default method*, ISO, Geneva
- LOGAN, K.P. (2011), *Using a Ship's Propeller for Hull Condition Monitoring*, ASNE Intelligent Ships Symp. IX, Philadelphia
- SCHNEEKLUTH, H.; BERTRAM, V. (1998), *Ship design for efficiency and economy*, Butterworth-Heinemann
- SPANDONIDIS, C.C.; THEMELIS, N.; CHRISTOPOULOS, G.; GIORDAMLIS, C. (2018), *Evaluation of Ship Energy Efficiency predictive and optimization models based on Noon report and Condition Monitoring datasets*, Proceedings, 7th Int. Conf. on Data Analytics, IARIA
- THEMELIS, N.; SPANDONIDIS, C.C.; CHRISTOPOULOS, G.; GIORDAMLIS, C. (2018), *A Comparative Study on Ship Performance Assessment based on Noon Report and Continuous Monitoring System datasets*, Proceedings, 12th Conf. Hellenic Institute of Marine Technology, pp.55-64

From Bow to Stern: Hydrodynamic Measures for Increased Hull Performance

Florian Kluwe, Lars-Uve Schrader, Herbert Bretschneider, HSVA Hamburg Ship Model Basin,
Hamburg/Germany, kluwe@hsva.de

Abstract

This paper reviews a comprehensive set of innovative technologies for improved ship-hull performance which have been studied at HSVA in the past or are currently under investigation. The focus is on the reduction of frictional drag, the dominant component of the total hull resistance for large slow-speed vessels. Fundamentally, all concepts build on a modification of the boundary layer via different physical mechanisms such as stabilisation for transition delay through compliant coatings, manipulation of coherent flow structures by grooved surfaces, injection of a low-friction fluid via air lubrication and momentum transport through deflector vanes. They often follow bionic principles inspired by nature, e.g. by dolphins, sharks and penguins, and are associated with a preferred region of application along the hull – from bow to stern. The individual drag-reduction potentials range from about 2% to well above 5% such that the technologies may in combination yield savings in excess of 10%. Whereas some technologies are on the market, others are still a matter of fundamental research. The results have been obtained through in-house studies and within the publicly funded research projects FLIPPER, HAI-TECH, eSHaRk and TARGETS. Finally, an outlook on a new concept based on super-hydrophobic surfaces is given which is currently being studied in the EU project AIRCOAT. New ideas of boundary-layer separation control are discussed as well.

1. Introduction

IMO emission-reduction targets will definitely require a fundamental change in seaborne trade patterns. As alternative fuels will come at a substantially higher price than the present marine fuels, investment into efficiency improvements will become more attractive and solutions currently failing to prove their return on investment will likely stimulate the market in the near future. The efficiency of shipping is among other aspects determined by the hydrodynamic performance of the merchant fleet, with ship-hull resistance and propulsive efficiency being the key factors. The hull resistance of large, slow-speed vessels such as bulk carriers, tankers and general-cargo ships is dominated by the viscous resistance components; these are composed of the friction between the hull surface and the water – including three-dimensional effects – and the friction-induced pressure resistance caused by head loss along the streamlines past the hull. Since the aforementioned ship types make up a large portion of the worldwide fleet, Fig.1, a reduction of viscous hull resistance will significantly contribute to a more ecological and economical seaborne transportation.

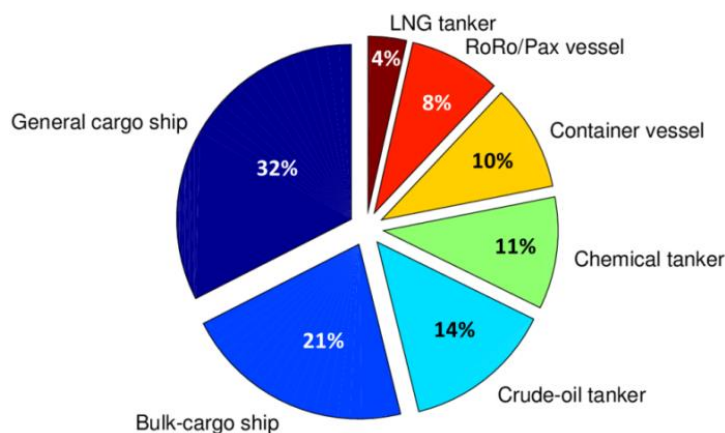


Fig.1: Fraction of different vessel types among the world's merchant fleet of 52,183 vessels as of January 2017 (data source: statista.com)

The frictional forces on the ship hull are confined to a limited region, the boundary layer, which changes its state along the hull: at the bow, the initially laminar flow quickly transitions to the turbulent regime associated with higher skin friction. Towards the stern, the boundary-layer flow decelerates, loses energy and may even separate from the hull surface. All these phenomena cause increased drag. This paper considers four different technologies, of which three directly act on the hull surface and inside the boundary layer to provide reduced skin friction and thus improved hydrodynamic performance. The fourth technology also modifies the boundary layer but focusses on an improved interaction between the hull-wake flow and the propeller. These four hull-performance enhancement technologies are tailor-made for different hull zones, Fig.2, and are illuminated in the subsequent chapters.

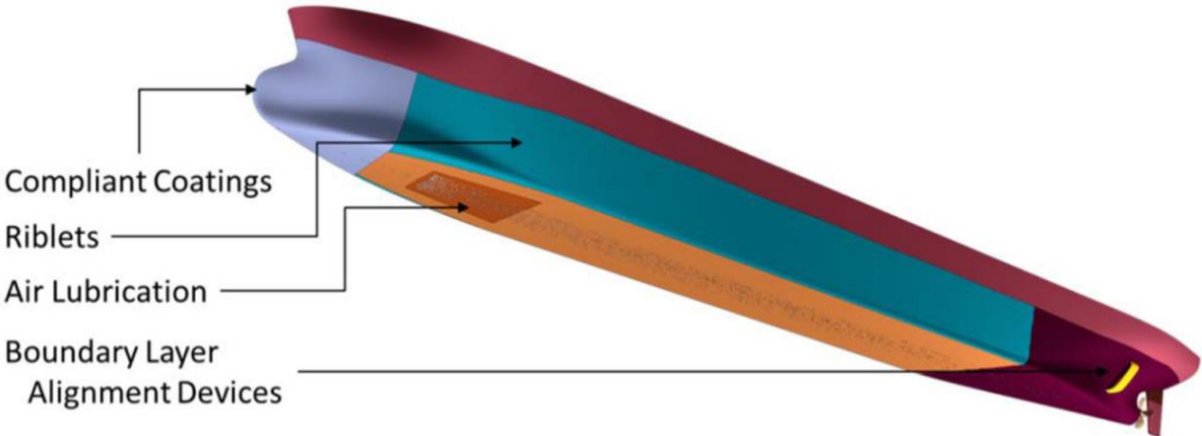


Fig.2: From bow to stern: different concepts of drag reduction for improved hull performance

2. Compliant coatings

In the research project FLIPPER (2014-2017), HSVA joined forces with the Fraunhofer Institute for Manufacturing Technology and Advanced Materials (Fraunhofer IFAM), the Hamburg University of Technology (TUHH) and the chemicals manufacturer ARKEMA in order to investigate the potential of compliant ship-hull coatings to increase the hydrodynamic hull performance. Thanks to their softness and responsiveness, compliant coatings are able to interact favourably with the boundary layer along the ship hull (fluid-structure interaction). Two principal physical mechanisms are at play: (i) a delay of laminar-turbulent boundary-layer transition and (ii) an attenuation of coherent flow structures in fully turbulent flow. FLIPPER focussed on the former mechanism, drawing inspiration from dolphins and their soft, pliable skin, Fig.3a.

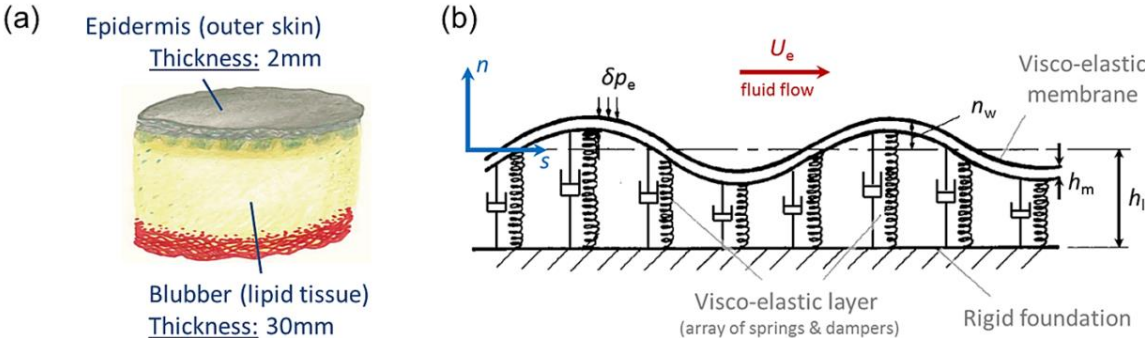


Fig.3: (a) Schematic and (b) mechanical model of dolphin skin; reproduced after *Carpenter and Garrad (1985)*

The project goal of FLIPPER consisted in the development of an “artificial dolphin skin” for ship hulls with the ability to postpone the boundary-layer transition to turbulence at the bow of the vessel.

To this end, numerical calculations of the fluid-structure interaction between the laminar boundary layer at the bow and the compliant coating were conducted using a mechanical model of dolphin skin, Fig.3b, see also *Carpenter and Garrad (1985)*. This model was coupled to a numerical solver of the Orr-Sommerfeld equation governing the development of the so-called Tollmien-Schlichting (TS) waves, *Schmid and Henningson (2001)*. TS waves are minute flow disturbances inside the laminar boundary layer which grow in amplitude when travelling downstream and eventually break down to the fully turbulent state. The role of the compliant coating is to attenuate the growth rate of these TS waves such that the laminar state can be maintained along a longer stretch of the boundary layer, leading to lower skin friction and reduced frictional hull resistance. The compliant-coating model and the Orr-Sommerfeld solver were used to identify suitable coating parameters – layer thickness, stiffness (Young’s modulus) and damping – for effective transition delay. The procedure was applied to the laminar boundary layer along the bow of a small search-and-rescue (SAR) vessel, Fig.4, in model scale 1:3.2 (5.72 m length). The details of the computations are described in *Schrader (2019)*.



Fig.4: SAR vessel of the German Maritime SAR Association DGzRS (source: fassmer.de). The FLIPPER coatings were designed for a 1:3.2 scale model of this ship (5.72 m length). HSVA thanks the Fassmer group and DGzRS for their permission to use the hull geometry in FLIPPER

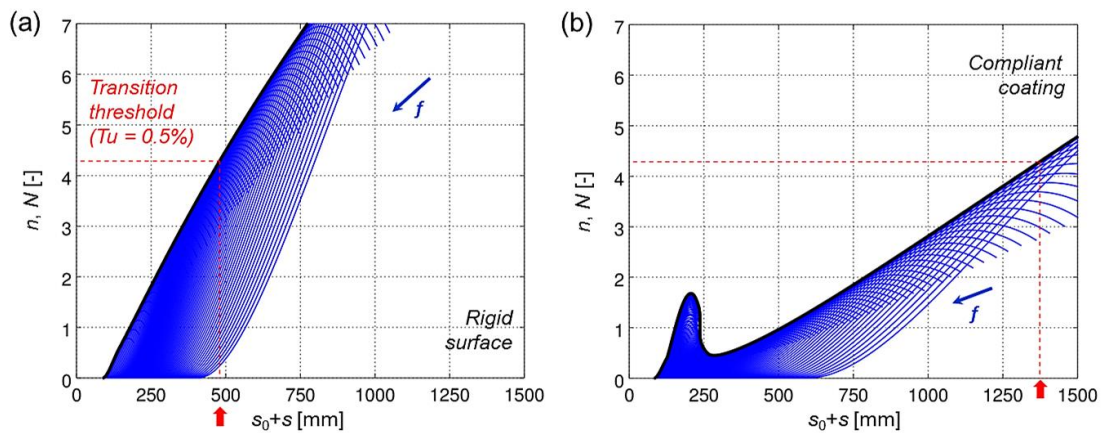


Fig.5: TS-wave growth curves (blue) in laminar flow past the bow of a 1:3.2 SAR ship model and envelope (black) of total disturbance growth. Transition prediction at a ship-model speed of 10 m/s according to the e^N method for (a) a rigid hull surface and (b) a 9.16 mm-thick compliant coating

TS-wave growth curves for a rigid and a coated bow surface of the SAR ship model were computed, Fig.5. The calculations assumed a coating made of a 9 mm-thick soft silicone layer covered by a 0.16 mm-thick polyethylene foil mimicking the thick blubber and the thin epidermis of dolphin skin, Fig.3a. The TS waves amplified at a substantially slower rate on the compliant surface, Fig.5b, than on the rigid counterpart, Fig.5a, such that the transition threshold as per the e^N prediction criterion was reached farther downstream. In this particular example, transition to turbulence occurred 1.37 m downstream of the stem for the compliant coating versus 0.48 m for the rigid surface (red arrows in

Fig.5). This transition shift allowed for a calculated friction-drag reduction by almost 56 N corresponding to 5.6% of the frictional drag of the hull model (see *Schrader (2019)* for details).

The FLIPPER project culminated in coating tests for proof of concept in HSVA’s Hydrodynamics and Cavitation Tunnel (HYKAT). A wooden 1:3.2-scale model of the SAR-ship hull was used, featuring a removable bow segment with an integrated load cell for drag-force measurement, Fig.6a. Several compliant coatings of different thickness and stiffness were formulated and manufactured by HSVA’s partner Fraunhofer IFAM. It could be demonstrated in the experiments that these “artificial dolphin skins” were indeed able to reduce the drag force on the bow with respect to the uncoated reference. At a tunnel speed of 10 m/s (design speed used in the calculations), the 9.16 mm-thick coating led to a drag reduction by almost 21 N, Fig.6b which is less than the predicted value of 56 N. This discrepancy is explained by inherent simplifications of the transition-prediction method, the mechanical coating model and the numerical setup as well as some uncertainty in the experimental determination of the viscoelastic coating parameters, *Schrader (2019)*.

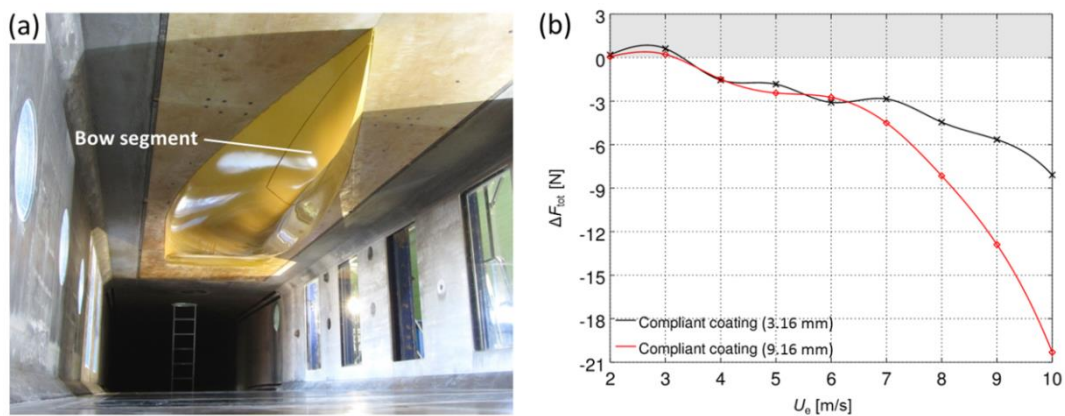


Fig.6: (a) SAR ship-hull model in HYKAT test section. Coatings applied on the bow segment only. Drag force on the bow is measured by an integrated load cell. (b) Frictional drag reduction on the bow w.r.t. the rigid surface thanks to compliant coatings of 3.16 mm and 9.16 mm thickness

In summary, the FLIPPER project successfully demonstrated the functionality of compliant coatings as a means of frictional drag reduction in marine applications. The physical mechanism behind these coatings is a passive boundary-layer control via delayed laminar-turbulent transition. The passive nature of the “artificial dolphin skins” renders this technology particularly attractive because no energy is needed to operate the system – in contrast to active technologies such as air lubrication (see Sec. 4). The obtained frictional drag reduction is moderate but it was also shown in FLIPPER that there is potential for further optimisation of the coating parameters such that a drag reduction by 2-3% based on the total hull resistance is deemed realistic. The compliant-coating technology is applied at the bow of ships where the transition to turbulence occurs. It is best-suited to small vessels as the relative savings through the technology decrease with increasing ship size, *Gad-el-Hak (1996)*. It is also pointed out that the compliant-coating technology is not yet market-ready because practical aspects such as robustness, anti-fouling properties and application technologies on shipyard scale still need to be investigated.

3. Riblet surfaces

Riblets are micro-textured surface protrusions aligned with the flow which impose an anisotropic roughness distribution on a surface. The original idea of using riblets was inspired by the skin of fast-swimming sharks (“shark skin”) and was first applied in the aerospace, automotive and energy industries. The application to Olympic rowing shells (Los Angeles 1984) and racing yachts (America’s Cup 1987) resulted in banning this technology from these disciplines. Extensive experimental investigations on various geometries have been made in a limited range of Reynolds numbers, *Bechert et al. (1997)*, indicating a drag reduction of up to 10% for plane micro-textured

surfaces compared to hydraulically smooth flat surfaces. Although the mechanism is not yet fully understood, a reduction of turbulent fluctuations and a decrease in turbulent shear stress is supposed.

In the German research project HAI-TECH (2009-2011), *Wilke et al. (2010)*, a consortium of Fahrion Engineering, Blohm + Voss Naval, Beluga Shipping, LimnoMar and HSVA led by Fraunhofer IFAM developed a coating technique combining paint application with micro-texturing in a single continuous production process (“Dual-Cure-Paint”) for ship hull applications, Fig.7a. The trials were carried out on an 8 m-long torpedo-shaped body in the HYKAT water tunnel at HSVA, Fig.7b. The comparison between riblet-structured and smooth surfaces revealed a reduction of frictional resistance by more than 5% at near-operational test conditions at ab. 20 knots flow speed. This demonstrated the enormous potential of adapted surface structuring on ship hulls in terms of fuel savings and fuel cost reductions for the shipping industry.

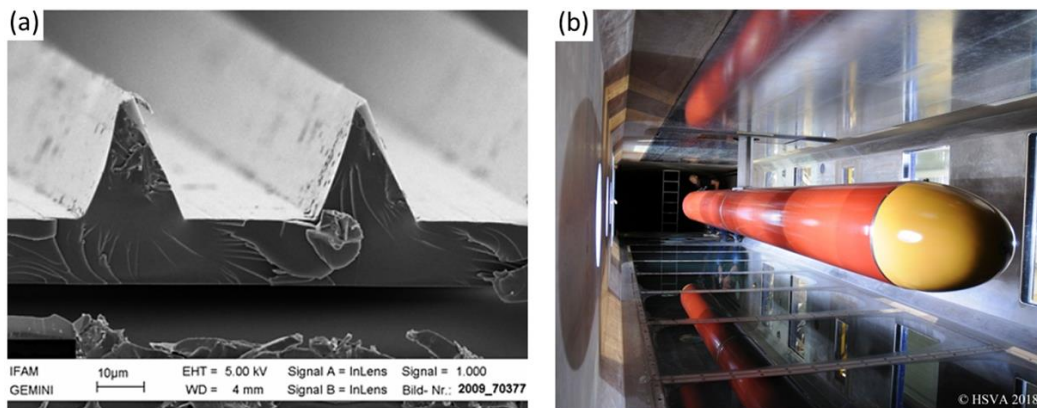


Fig.7: (a) HAI-TECH riblet structure (© Fraunhofer IFAM). (b) Development and testing of the ribleted foils in the HYKAT water tunnel using a cylindrical test body

In the European research and innovation project eSHaRk (2015-2019), PPG (hull paint supplier, coordinator), Mactac (adhesive-film manufacturer), ND Coating/Meyer Werft (hull coating and anti-corrosion services), VertiDrive (robotic solutions for ship hull treatment) and HSVA formed a consortium to develop and manufacture a self-adhesive, non-toxic fouling release foil, produced by applying a state-of-the-art fouling release coating on top of a self-adhesive plastic film. The micro-texture of the film surface for friction reduction was accomplished by appropriate embossing during the manufacturing process. Three test campaigns in the HYKAT water tunnel demonstrated a friction reduction of ab. 4% compared to standard fouling-release paint; moreover, a sufficient strength of the film system and appropriate adhesion forces of the self-adhesive layer could be verified.

4. Active air lubrication

For the last eight years HSVA has been investigating air lubrication systems in the HYKAT water tunnel (partial model in full scale) for application to the flat-bottom area of ships in order to reduce the surface friction force, the propulsion power and the GHG emissions. These studies have been conducted on behalf of a company which has since then equipped several new buildings with air lubrication systems and is nowadays the leading provider of that technology on the market.

The working principle is as follows: the air lubrication system generates small air bubbles and introduces them into the turbulent water boundary layer on the ship hull, producing a fluid-gas mixture of lower viscosity than pure water. The bubbles reduce the wetted hull surface and may also favourably interact with the turbulent flow structures in the boundary layer, thereby significantly diminishing the frictional hull resistance. Although the effect of skin friction reduction of air-lubricated plane surfaces – often referred to as micro-bubble drag reduction (MBDR) – has been tested on a laboratory scale by various researchers for about 40 years, see e.g. *Madavan et al. (1984)*, HSVA was among the first to investigate the system in full scale, using partial models integrated into a flat plate of 8 m by 2 m, Fig.8a, connected to a force balance to measure the friction force at the top of the HYKAT test section

(dimensions: 11 m × 2.8 m × 1.6 m). Apart from different geometries of the air-release openings, ship draughts of 2-13 m, air flow rates up to 120 m³/h and water flow speeds (ship speeds) up to 18 knots were tested with focus on the bubble creation and carpet behaviour, Fig.8b. For the partial model of the air lubrication system a friction reduction of 40% was achieved compared to a flat plate of the same dimensions. Since the air lubrication system is an active system the total power balance needs to include the necessary power for providing the required compressed air.

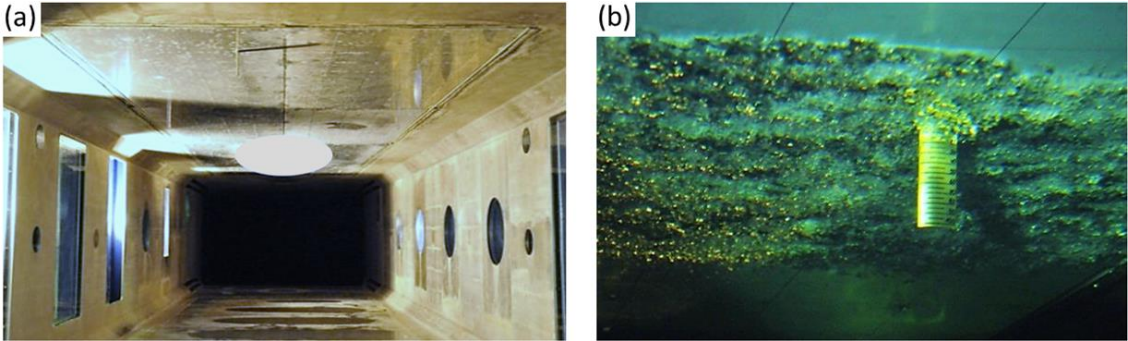


Fig.8: (a) Air lubrication model in the HYKAT. (b) Bubble carpet during testing

In 2014 HSVA participated in the sea trial of a medium-range chemical tanker of 40,000 DWT which had been refitted with the HSVA-tested air lubrication system during the dry-docking period. The installation of the system took two weeks and could be accomplished within the standard docking schedule. Net average energy savings of 4.3% for the vessel in ballast and 3.8% in laden condition could be confirmed based on a conservative interpretation of the speed-power measurements, *Shell and Silverstream (2015)*.

5. Boundary-layer alignment

The wake flow behind a ship plays a crucial role for the propulsive efficiency. Especially the bulky hull forms of full-block vessels suffer from massive axial-momentum losses above the propeller shaft; in addition, rotational losses occur in the propeller slipstream. In order to address these two sources of loss, HSVA developed a novel type of hull appendage in the research project TARGETS (2010-2014) – the boundary-layer alignment device (BLAD) consisting of a pair of flow deflectors, Fig.9.

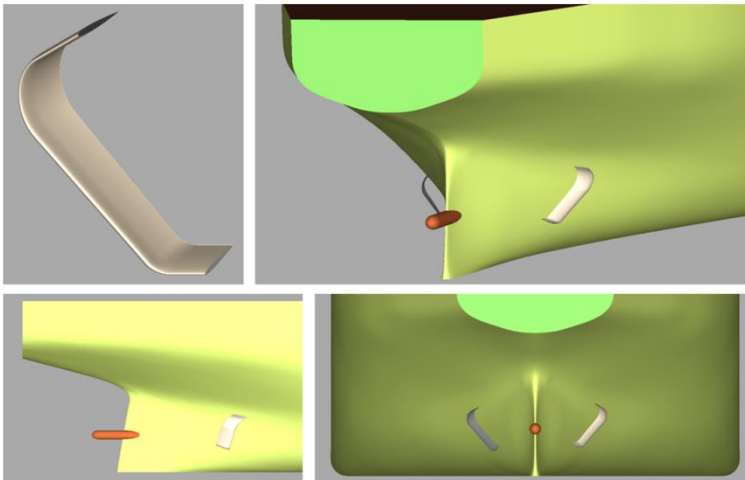


Fig.9: BLAD deflector and position on the aft ship of a Capesize bulk carrier. The two deflectors on the port and starboard sides feature different profiles and are asymmetrically arranged

The purpose of the BLAD is to deflect the streamlines towards the hull surface in order to accelerate the wake flow locally and reduce the boundary-layer thickness for a more homogeneous flow through the propeller. Moreover, the BLAD deflectors are intended to create a swirling flow against the pro-

propeller rotation for diminished rotational losses in the slipstream along with extra thrust at a given engine power. This swirl is accomplished by different profile shapes and an asymmetric arrangement of the two deflectors.

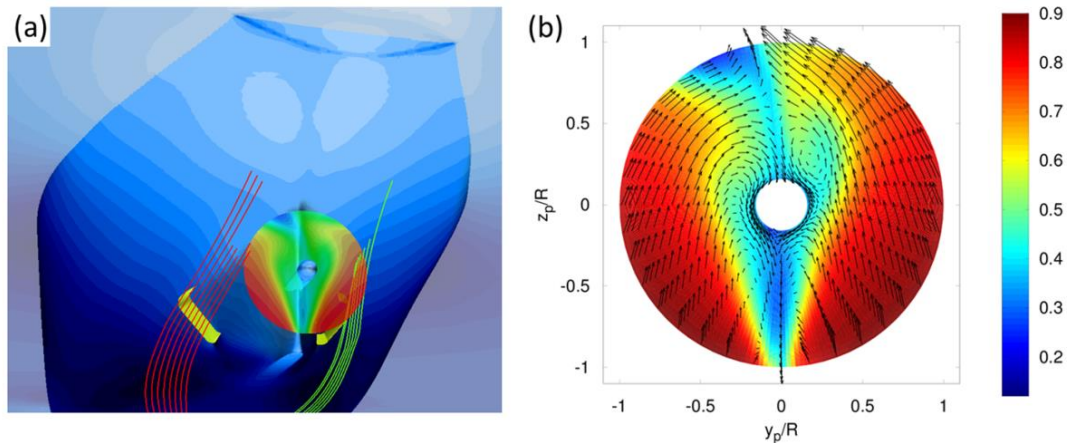


Fig.10: (a) BLAD deflectors “in action” on a Capesize bulk carrier at 14 knots speed: improvement of wake homogeneity and swirl generation. (b) Nominal wake in the propeller plane

The BLAD was developed and tested for a Capesize bulk carrier at 14 knots speed with an 8.5 m-diameter four-bladed propeller, using CFD simulations with HSVA’s in-house codes FreSCo⁺ and QCM. Thanks to the asymmetric deflection of the port and starboard sided streamlines towards the propeller, Fig.10a, a nominal wake with increased homogeneity and a swirling flow component could be achieved, Fig.10b. The flow acceleration into the propeller plane led to an increased advance number at which the propeller could be operated more efficiently, Fig.11a. This effect in combination with diminished rotational slipstream losses allowed for a lower required power to obtain the same ship speed, Fig.11b. Three different retrofit scenarios were considered: (i) a refit of BLAD deflectors only, (ii) a BLAD retrofit plus cutting and grinding of the propeller-blade trailing edges and (iii) a BLAD retrofit along with a new tailor-made propeller. As expected, the most expensive retrofit option (scenario iii) allowed for the largest savings of propulsive power of almost 7%, Fig.11b. The details of the BLAD development and achievements are compiled in *Schrader and Marzi (2017)*.

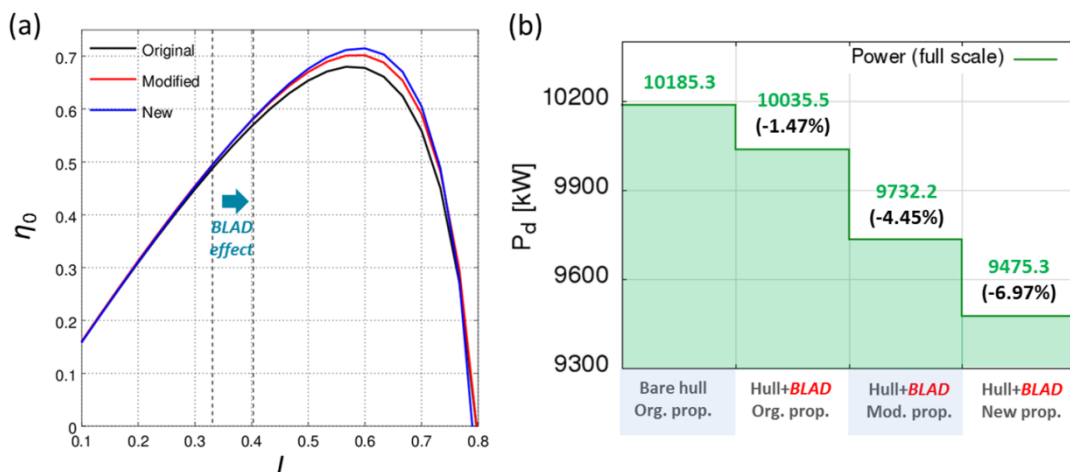


Fig.11: (a) Open-water efficiency and (b) delivered propulsive power at a speed of 14 knots for three different propellers of a Capesize bulk carrier: (i) original propeller, (ii) original propeller with cut and ground blade trailing edges, (iii) new propeller – each combined with the BLAD deflectors in comparison to the baseline (original propeller, no BLAD)

Apart from a power reduction, the BLAD deflectors also led to a more symmetric distribution of the mean propeller-thrust force with a reduced peak value, Fig.12. This is expected to yield lower

propeller-blade loads along with reduced cavitation risks as well as a better course stability of the vessel. The latter aspect will allow for fewer course corrections by rudder manoeuvres such that additional fuel savings are anticipated.

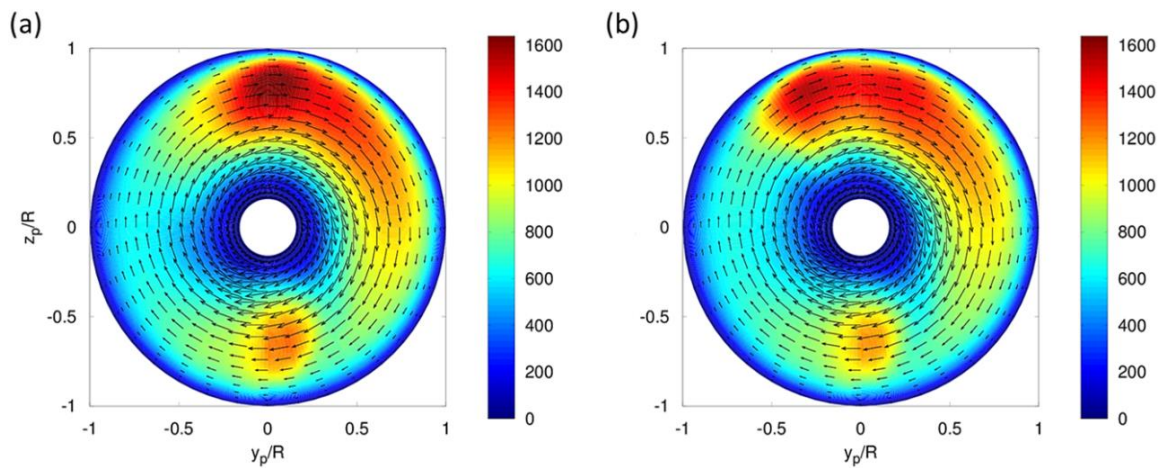


Fig.12: Mean thrust distribution across the propeller disc for a Capesize bulk carrier at 14 knots speed using the original propeller: (a) without and (b) with BLAD deflectors

In summary, the BLAD concept provides an attractive technology for improved hull-propeller performance along with reduced fuel costs and emission of pollutants. The design of the BLAD deflectors is considerably less complex than that of established energy-saving devices like stator fins or various duct products. Since the deflectors are mounted quite far upstream of the propeller they are hardly exposed to the unsteady propeller-induced flow field and the associated dynamic loads, reducing the risk of fatigue and failure.

6. Conclusion and discussion

For many years ship designers have focussed their efforts on the wave-making resistance when optimising the efficiency of their hull designs. Viscous flow was largely out of the focus for various reasons: in pre-CFD times the wave-making resistance was the only component that could be studied in detail by visual observation while measurements delivered integral values for the total resistance only. Technologies like CFD simulations allow for a much more straightforward decomposition of hull resistance and therefore open the opportunity to include these aspects into the optimisation process.

Even more important, the growing ship sizes, the trend of “slow steaming” and the focus on hull lines excessively optimised for minimum wave-making resistance have increased the relative contribution of the viscous drag components to the total hull resistance. Consequently the last years have seen a lot of new and improved paint products that are aiming to reduce the frictional resistance by keeping the surface roughness at a minimum. Looking beyond these approaches, this paper presents several technologies that also target the reduction of viscous resistance by different approaches. Their state of maturity is quite diverse: while technologies like the boundary-layer alignment device (cf. Sec. 5) are close to production readiness, other ideas like compliant coatings (cf. Sec. 2) are still mainly fundamental research.

Experimental model testing plays an important role in these research studies. Model basins provide the large-scale experimental facilities needed to conduct hydrodynamic investigations at Reynolds numbers with practical relevance for the shipping industry. Numerical studies are certainly an attractive alternative at low to medium Reynolds numbers (see Sec. 2); however, fully turbulent high-Reynolds number boundary layers are mostly beyond the scope of industrial CFD and therefore still need to rely on physical testing.

An important aspect is to identify which technology fits to which type of ship. Taking for example the boundary-layer alignment device the effect will be most prominent in the case of blunt full-block vessels like tankers and bulkers while the impact will be limited in the case of slender hulls such as RoRo or passenger vessels – at least with respect to resistance reduction. Air bubble injection (cf. Sec. 4) can be placed only in regions with fairly horizontal, large surfaces and thus becomes more difficult to be applied on vessels with significant deadrise. The previous example also demonstrates another crucial aspect: to make best use of the measures they need to be placed at the right position on the ship's hull. The transition-delaying compliant coatings, for instance, need to be located in the bow region and would not make much sense in the aftbody region. The same applies to air bubble systems as already discussed above. Hence, the ship designers' task and their know-how do not only become manifest in a mature, reliable and resilient technical solution but also in developing hull designs which allow for a beneficial placement and combination of these technologies as illustrated in Fig.2.

The experience shows that the main market barrier for these technologies is often the durability under service conditions. This includes their resilience against mechanical failure as well as the robustness of the working principle against dirt and fouling, which is an obvious challenge in the case of grooved surfaces (cf. Sec. 3). In order to generate trust into these new approaches, continued research and – even more important – prototype installations are needed to demonstrate their practical feasibility. The overall savings that are assumed realistic based on the currently available data on the total resistance reduction of ship hulls amount to 10% and more in total. This is an order of magnitude above the potential for further improvements in wave resistance reduction – a very clear motivation towards extended research on the technologies presented in this paper.

7. Outlook

HSVA is involved in – or is currently setting up – additional research projects dealing with passive and active boundary-layer flow control. The EU project AIRCOAT (May 2018-April 2021) deals with a bionic principle of drag reduction, too: a team of ten European science and industry experts led by the Fraunhofer Center of Maritime Logistics and Services (Fraunhofer CML) is currently developing a passive air lubrication technology that utilises the biomimetic *Salvinia* effect, *Barthlott et al. (2010)*. Nature has developed this effect through evolution, which allows the *Salvinia* plant, a fern floating on the water, to breathe even when submerged by maintaining a permanent layer of air. This ability builds on a complex surface composed of super-hydrophobic and hydrophilic structures. The project partners are implementing the *Salvinia* mechanism on a self-adhesive foil system which is able to trap air on surfaces in water. A ship equipped with such an AIRCOAT foil will produce a thin permanent air layer reducing the overall frictional resistance significantly while at the same time acting as a physical anti-fouling barrier between the water and the hull surface. The project is a prime example of a biomimetic application where scientists and engineers learn from nature. The potentials of the AIRCOAT project are enormous: initial estimates indicate that the AIRCOAT technology may reduce the main-engine fuel oil consumption and exhaust gas emission by at least 25%. The major advantage over existing air lubrication technologies is that the ship hull is passively lubricated, i.e. no energy for operation is needed. Also, if successful the AIRCOAT retrofit technology will be immediately applicable to the entire fleet in the form of a foil system. Through a combination with the latest self-adhesive foil technology, AIRCOAT has the potential to revolutionise the maritime coating sector, promising a ground-breaking future energy-efficiency and emission-reduction technology.

Passive and active boundary-layer separation control is another path of research and development in HSVA's focus. Nature gives again inspiration: the flippers of humpback whales feature a wavy leading edge formed by so-called tubercles, *Aftab et al. (2016)*. These enhance the whales' manoeuvrability through a postponement of flow separation to larger angles of attack. This passive principle can be transferred to ship rudders, stabiliser fins or highly loaded propeller blades in order to increase the lift and the lift-to-drag ratio. Even larger gains in lift at almost no drag penalty can be expected from active separation control. The focus is here on fluidic oscillators for boundary-layer momentum enhancement and energisation, *Kim et al. (2017)*. These devices are an elegant, mechanically simple way of postponing the angle of stall to very large values and can be beneficially applied to hydro-

dynamic surfaces prone to separation such as ship rudders and manoeuvring ship hulls. The main benefit of fluidic-oscillator based active flow control lies in the possibility of turning off the system when not needed – a clear advantage over vortex-generator fins which permanently create drag. Fluidic oscillators have indeed been successfully used for separation control on aircraft rudders, *Lin et al. (2016)*.

Apart from a continued development of the present and of novel friction-reducing technologies, the assessment and validation tools need further attention. Although established EFD and CFD procedures for the flow analysis around ship hulls are available, including the determination of the various resistance components, the incorporation of friction-reducing measures into these procedures is not at all straightforward: the theoretical challenges ahead include the lack of scaling laws – e.g. for model tests with micro bubbles – and the incorrect boundary-layer thickness owing to the violation of Reynold’s similarity. Numerical hurdles consist in a lack of boundary-layer resolution in practical CFD models or in the challenges associated with fluid-structure interaction and many more multi-physics aspects.

Acknowledgements

In this paper, HSVA presents results from several publicly funded research projects: FLIPPER and HAI-TECH received funding from the Federal Ministry for Economic Affairs and Energy of Germany (BMWi). The European Commission funded the projects TARGETS, eSHaRk and AIRCOAT. HSVA gratefully acknowledges these funding bodies for their financial support. The authors thank Dr. Jochen Marzi (HSVA) for giving inspiration to the basic theme of this paper.

References

- AFTAB, S.M.A.; RAZAK, N.A.; MOHD RAFIE, A.S.; AHMAD, K.A. (2016), *Mimicking the hump-back whale: An aerodynamic perspective*, Progress in Aerospace Sciences 84, pp.48-69
- BARTHLOTT, W.; SCHIMMEL, T.; WIERSCH, S.; KOCH, K.; BREDE, M.; BARCZEWSKI, M.; WALHEIM, S.; WEIS, A.; KALTENMAIER, A.; LEDERER, A.; BOHN, H.F. (2010), *The Salvinia Paradox: Superhydrophobic Surfaces with Hydrophilic Pins for Air Retention Under Water*, Advanced Materials 22(21), pp.2325-2328
- BECHERT, D.W.; BRUSE, M.; HAGE, W.; VAN DER HOEVEN, J.G.T.; HOPPE, G. (1997), *Experiments on drag-reducing surfaces and their optimization with an adjustable geometry*, J. Fluid Mech. 338, pp.59-87
- CARPENTER, P.W.; GARRAD, A.D. (1985), *The hydrodynamic stability of flow over Kramer-type compliant surfaces. Part 1. Tollmien-Schlichting instabilities*, J. Fluid Mech. 155, pp.465-510
- GAD-EL-HAK, M. (1996), *Compliant Coatings: A Decade of Progress*, Applied Mechanics Review 49(10), part 2, pp.S147-S157
- KIM, J.; MOIN, P.; SEIFERT, A. (2017), *Large-Eddy Simulation-Based Characterization of Suction and Oscillatory Blowing Fluidic Actuator*, AIAA Journal 55(8), pp.2566-2579
- LIN, J.C.; ANDINO, M.Y.; ALEXANDER, M.G.; WHALEN, E.A.; SPOOR, M.A.; TRAN, J.T.; WYGNANSKI, I.J. (2016), *An Overview of Active Flow Control Enhanced Vertical Tail Technology Development*, Tech. Rep. NASA 20160007653, pp.1-13
- MADAVAN, N.K.; DEUTSCH, S.; MERKLE, C.L. (1984), *Reduction of turbulent skin friction by microbubbles*, Phys. Fluids 27(2), pp.356-363
- SCHMID, P.J.; HENNINGSON, D.S. (2001), *Stability and Transition in Shear Flows*, Springer

SCHRADER, L.-U.; MARZI, J. (2017), *A Novel Power-Saving Device for Full-Block Vessels*, 20th Numerical Towing Tank Symposium, Wageningen, pp.205-210

SCHRADER, L.-U. (2019), *Passive Drag Reduction via Bionic Hull Coatings*, J. Ship Research

SHELL; SILVERSTREAM (2015), *Silverstream Air Lubrication Technology Delivers Significant Energy Savings*, <https://www.shell.com/business-customers/trading-and-supply/trading/news-and-media-releases/silverstream-air-lubrication-technology.html>

WILKE, Y.; STENZEL, V.; PESCHKA, M. (2010), *Haifischhaut für Flugzeuge, Schiffe und Windenergieanlagen*, https://www.ifam.fraunhofer.de/content/dam/ifam/de/documents/IFAM-Bremen/presse/2010/presstext_2010_haifischhaut.pdf

ISO 19030: Onboard Monitoring System for Real-time Performance Feedback, Prediction and Optimization

Paolo Becchi, CETENA, Genova/Italy, paolo.becchi@cetena.it

Abstract

The evaluation of the effective ship power performances during commercial operation and in particular after main maintenance events represents an important feedback for the owner, making it possible to optimize the ship efficiency and management. For this reason, CETENA recently improved its own Ship Performance Monitoring System including what prescribed by the international procedure ISO 19030, that is the evaluation of both the effective ship performances (speed and power corrected data) and the prescribed Performances Indicator (KPI). The system provides to the crew and to the owner indication of the effect of maintenance events on ship performances together with all the other parameters already included in the real time data acquisition. The software has been implemented keeping into account the possibility for further improvements in order to guarantee a quite fast and reliable maintenance any time the international procedure will be updated. Because of the application of S&P data corrections requires environmental conditions together with the navigation ones, the system is directly connected with the remote CETENA own weather forecast system that gives the possibility to know all data needed (wind, sea state, current, depth). The ISO 19030 procedure has been also included in the Sailing Assistant Module of the system aimed to optimize future voyages. The system will optimize the voyage on a minimal consumption basis with the ship affected by reduced environmental-related added power. The application of ISO 19030 procedure in the system thus allows to take under control ship performances and management and brings about a reduction of fuel and pollutant emissions.

1. CETENA's monitoring system PMOTE

In the last years CETENA has implemented its own Performance Monitoring System, designed for the automatic check and storage of data related to the performances of the ship in navigation. The number and type of data to be acquired can be modified for any ship depending on the signals available onboard or from the arrangement of custom sensors. The system has been developed in order to continuously monitor the data and provide a real time feedback to the crew. In addition, if an internet connection is available the system will automatically send all collected data to the owner headquarter making it possible for the technical department to check the ship performances in real time.



Fig.1: Performance Monitoring arrangement on wheelhouse console

Together with hardware components and custom sensors, the system is structured by the following two software modules:

- Data acquisition module (Core), that is usually located on a standalone machine connected to custom sensors and ship automation. This PC is usually an autonomous industrial PC, directly connected to the ship LAN, too.
- Repeater consoles (Repeater). The repeater console is aimed to load the collected data from the

core module and to show to the user all the information needed for the evaluation of the current ship performances. There is no restriction for the repeater console that can be arranged onboard (wheelhouse, chief engineer cabin, ECR, ...).

Fig.2 shows a usual layout of the “Performance Monitoring” system, with the core PC and three repeater consoles.

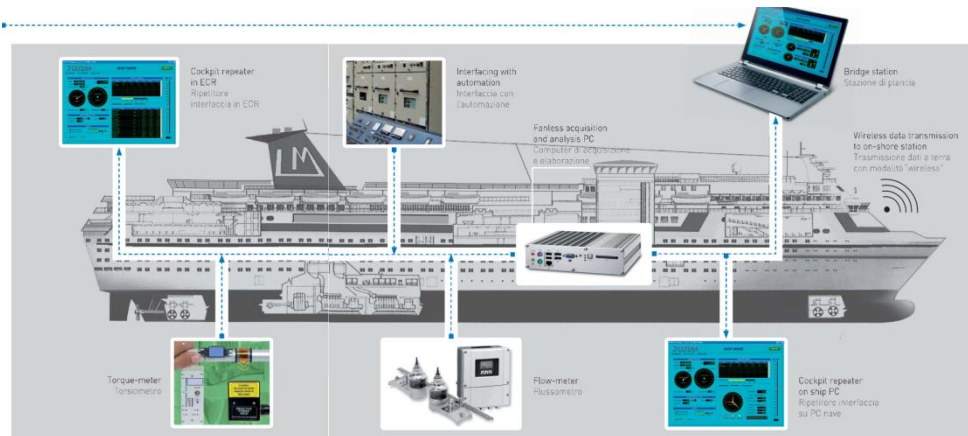


Fig.2: Usual "Performance Monitoring" system layout

The Performance Monitoring system (PM) collects all data needed for the ship performance analysis and any other data required by the crew/technical dept. In detail, the collected data concern both the sailing conditions:

- time and location
- speed over ground, course over ground and heading
- propulsive conditions (propeller pitch, shaft rate of revolutions, torque and power)
- environmental conditions (wind state, sea state, sea current, ...)
- ship loading conditions (draft, trim, displacement)
- anti-roll stabilizer fin status (on/off) from automation system
- rudder angle
- ship operating status (at sea, manoeuvre, docking/anchor) by means of a dedicated signal or by a proper association of ship automation signals

and the energy generation aspects:

- fuel consumption for main engines and diesel generators
- current status of MMEE and DDGG
- electric power generated by DDGG
- electric power generated by Shaft Generator

Fig.3 represents the data collector module of the system, aimed to collect the above-mentioned data and to show them through the repeater console. The window is subdivided into different areas, each one is aimed to show data related to different aspects: navigation, environment conditions, analog channels, shaft, wave radar and extra signals acquired. The system stores the data collected in text files, with a data record every 5 minutes and a single file per day.

The system is also equipped with the optional module named “optimum trim” that gives the crew a real time feedback about the propulsive efficiency depending on the current trim measured. This module requires some preliminary tests at sea to identify the referenced speed and power curves to be used for direct estimation. The module provides a direct indication of the efficiency of the trim and a difference from the best trim curve computed at the same ship displacement. Fig.4 shows the user interface of the

Optimum Trim module, including the chart of the current performance (white line) and the two thresholds defining the good, the acceptable and the bad conditions areas (green, yellow and red area).



Fig.3: Data collector module

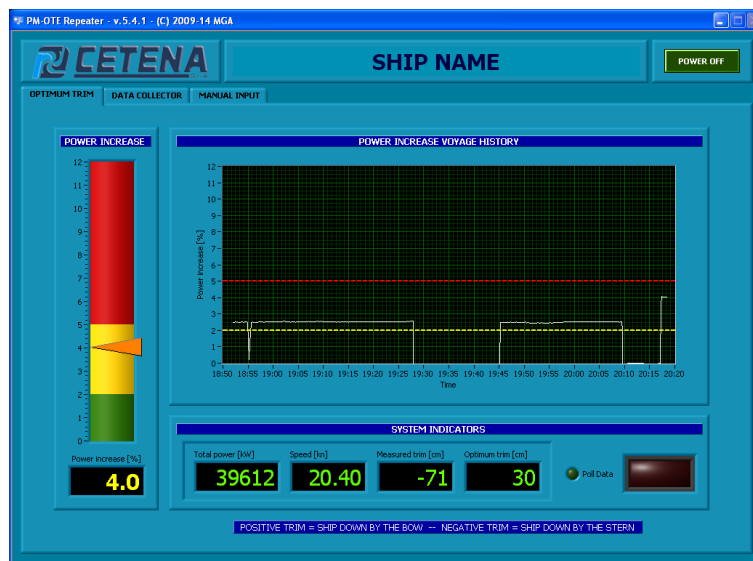


Fig.4: Optimum Trim module console



Fig.5: Analysis software console

The system is usually required for propulsive performance monitoring during ship life, the evaluation of ship management and fuel consumption. In order to make easy this kind of analysis, a custom software has been developed for the analysis of the collected data. The user has the possibility to see history chart of the acquired signals, compare trips performed in different periods (like before and after dry-dock activity) and save the analysis performed in a worksheet format. Fig.5 shows the main console of the analysis software, on which all the data collected and the trips performed can be filtered and compared in order to check all the aspects of the ship's propulsive performances.

2. Computation module for ISO 19030 correction

The “Performance Monitoring” system has recently been implemented by including a computation module aimed to analyze the ship performances in accordance with the international procedure ISO 19030. This normative gives indications for the evaluation of the propulsive efficiency increase due to maintenance events as dry-dock, hull/propeller cleaning, reblading. From this point of view the propulsive efficiency is strictly related to a well-known correlation involving many elements related to the hydrodynamics of the propulsion, that are: hull roughness/fouling, propeller, displacement, trim and environment conditions. The scope of the ISO 19030 is to define a practical method for the measurement of ship performances, their analysis and correction and to evaluate a practical set of indicators related with the real efficiency increase. From the point of view of data collection and analysis, this normative looks to be very close to the ISO 15016 that is aimed to evaluate the real propulsive performances for ship at official sea trials, and hence including many corrections like water density, current effects through multiple runs, and added wave resistance. As the ISO 19030 aims at the data monitoring of ship in operation, at the moment the ISO 19030 prescribes only few corrections like wind resistance effects, shallow water and so on, but it cannot be excluded that further editions might recommend other correction algorithms. Despite what recommended in ISO 15016, the system used for the performance monitoring of ships of different type, size and age in operation must be completely autonomous. It includes not only the detection of a stable condition for data recording but also the storage, backup, data transmission and analysis. The ISO 19030 international normative is structured into the following main steps:

- Monitoring of the sailing and propulsive condition
- Data recording, storage and analysis (including correction and performance value computation)
- Estimation of the four Performance Indicators (PI)

2.1. Virtual Weather Station for environment condition data

The evaluation of the ship performance values and hence the performance indicators, requires the acquisition of data related both to ship sailing and local environmental conditions. As previously described, the current version of the normative prescribes only corrections for the effects of displacement, shallow water and added resistance due to the wind. For this reason, at the moment the use of a custom anemometer and the eco-sounder may be enough for the evaluation of the real ship performances. However, a more accurate investigation of the weather conditions will lead to perform a more detailed analysis of data, including information about the current magnitude and direction and the sea state (significant wave height, direction and period). For this reason, CETENA has developed its own Virtual Weather Station (VWS) aimed to provide indication of past, current or expected conditions for ships sailing in any ocean or sea. It is “virtual” because it is not directly interfaced with instrumentation/sensors measuring the weather conditions, but it collects data from many weather/forecast services and rebuilds a single database with the more accurate spatial resolution and a time step equal to 1 hour. The considered data set is the result of simulations based on numerical models used for forecast and finally tuned with local direct measurements. For each sea/ocean the data set needed for a complete description of the weather conditions are checked in advance, and made consistent with the database units and entity already considered. The VWS is currently configured in order to provide the following entities:

- **Water depth**
- **Sea state**
 - significant wave height
 - wave direction from
 - wave period
 - stokes drift components
- **Current**
 - Eastward component
 - Northward component
- **Wind**
 - Eastward component
 - Northward component

Furthermore, the current component can be provided at different drafts, in order to identify the more significant effect on the ship motion. All the water entities describe the average value on one hour time step. Otherwise, the wind data are related to an average 6 hours because of the lack of more accurate data sets. Anyhow, any ship with the Performance Monitoring System is also equipped with at least one anemometer that provides really accurate data, every minute averaged.

The decision of CETENA to develop a service for the weather condition provision, is based on its experience on both sea trials and computational fluid dynamics. Some years ago, CETENA was asked to perform S&P sea trials on a ship in service, and then without the possibility to carry out the traditional multiple runs. In that occasion it has been decided to correct the ship speed using current data coming from a meteorological service. Thanks to the results have been obtained, it was possible to reduce the spread of the ship speed values from 0.5 knots up to 0.3 knots; this value is considered acceptable by all other international partners involved in the project.

The empowerment of the VWS system aims to query and provide the required data directly through other own systems requiring environmental conditions for their needs. Together with the Performance Monitoring system, also the software aimed for the Speed&Power sea trials analysis consistently with ISO15016 has been developed including the possibility of a direct connection with VWS. So, this system has not a direct user interface for the majority of the services provided. Anyhow it is also possible to query the weather database for any other reasons by using a custom user interface, Fig.6. This console gives the possibility of a direct investigation of weather conditions. Furthermore, if the ship sailing conditions (speed and heading) are detailed for each required point, the apparent environment conditions will be automatically computed showing apparent wind, wave magnitudes and direction.

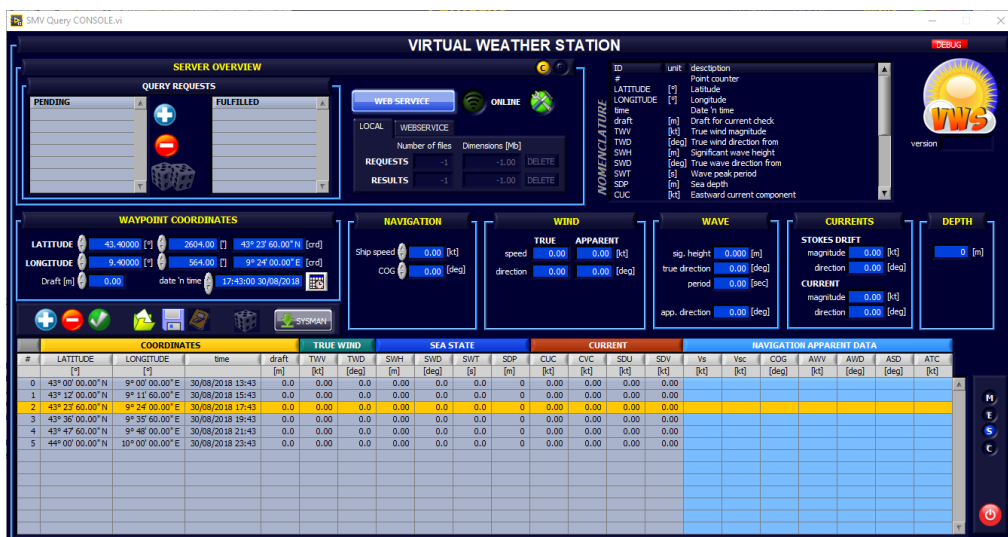


Fig.6: VWS main console

2.2. Performance Monitoring process

From the point of view of the Performance Monitoring System, the computation module automatically proceeds with the sailing condition monitoring, run measuring and storing. As previously mentioned and about the environment conditions, the current version of normative requires only wind state, that can be acquired through an anemometer arranged onboard and directly connected to the acquisition system. However, if further revisions of the recommended procedure will require additional weather data, thanks to internet connection the system will submit the measured run data to the VWS in order to firstly characterize them with proper environment conditions, and then finally compute the corrected propulsive values together with the Performance Indicator. Fig.8 represents the flowchart of the Performance Monitoring from the sailing condition monitoring to the evaluation of the Performance Indicators, represented in Fig.7 that is the “ISO 19030” recently included in the Repeater console. The page shows the four indicators prescribed by the normative and described in Table 1.

Table 1: Basic hull and propeller Performance Indicators

DD	Dry Dock	Determining the effectiveness of the dry-docking (repair and/or retrofit activities) <i>Change in hull and propeller performance following present out-docking (evaluation period) compared with the average from previous out-docking (reference periods)</i>
IS	In Service	Determining the effectiveness of the underwater hull and propeller solution (including any maintenance activities that have occurred over the course of the full dry-docking interval) <i>The average change in hull and propeller performance from a period following out-docking (reference period) to the end of the dry-docking interval (evaluation period)</i>
MT	Maintenance Trigger	Trigger under water hull and propeller maintenance, including propeller and/or hull inspection <i>Change in hull and propeller performance from the start of the dry-docking interval (reference period) to a moving average at any chosen time (evaluation period)</i>
ME	Maintenance Effect	Determining the effectiveness of a specific maintenance event, including any propeller and/or hull cleaning <i>Change in hull and propeller performance measured before (reference period) and after (evaluation period) a maintenance event.</i>

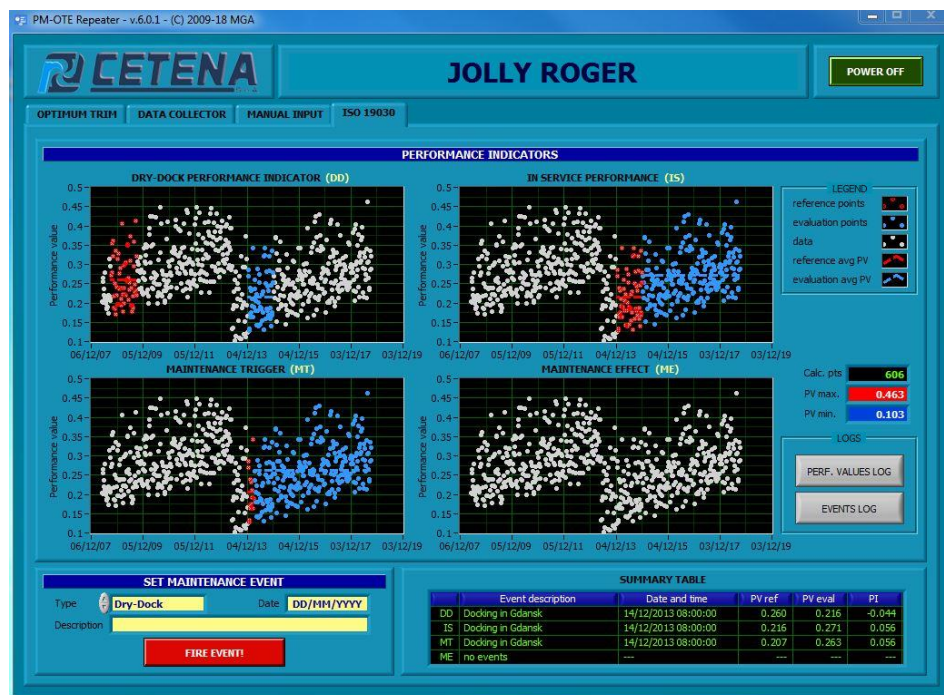


Fig.7: Performance Monitoring - Repeater console: Performance indicator window

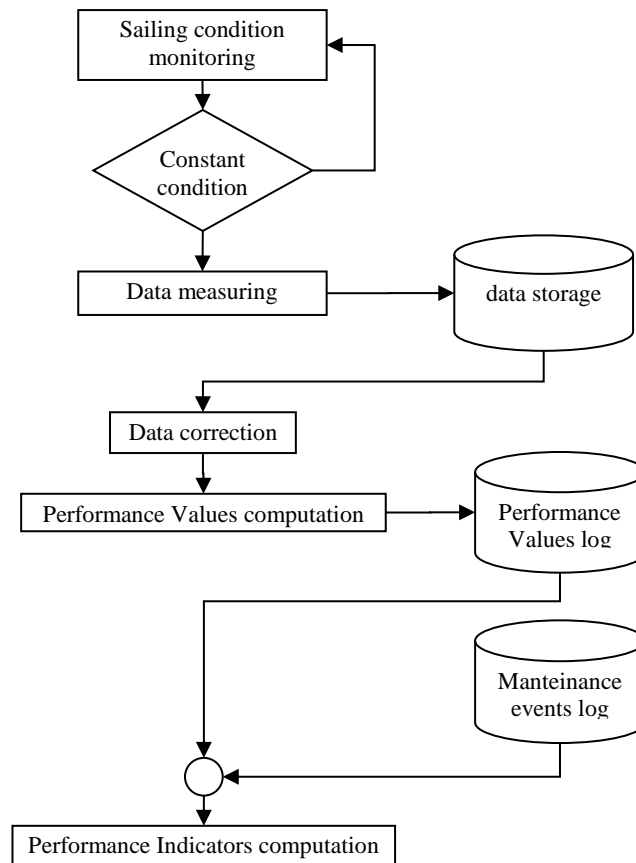


Fig.8: Performance Monitoring System flowchart

For each indicator, all the Performance Values are plotted in accordance with the following representation:

- the grey points are the PV not considered for the indicator computation
- the red points represent the PV included in the reference period
- the blue points represent the PV related to the evaluation period

Furthermore, the console shows some further information:

- the total number of PV computed
- the overall PV value, maximum and minimum
- the last maintenance event set

If required, the system can send all the computed data to the owner's headquarters in order to make it possible to check the ship performance indicator and performance and change the maintenance scheduling if necessary. At the moment of the drafting of this paper, the ISO 19030 had been released in beta version and the tests were already in progress on a merchant ship used as testcase.

3. Sailing Assistant module for voyage optimization

The integration between the ISO 19030 module and the VWS service gave the opportunity for an additional module, aimed at the optimization of a single voyage from the point of view of the required propulsive energy. The idea of this system consists in the evaluation of the added resistance due to the expected weather condition during a voyage and the optimization of both the waypoints location and the ship power configuration. All that allows to respect the required estimated time at arrival and minimize the total propulsive energy needed. The necessity to evaluate all added resistance components according to the environment conditions has brought a modification of the ISO 19030. Furthermore,

the propulsive performance of the ship must be characterized by the speed-power curve and power setting configurations, and the VWS must also be able to provide weather forecast at least up to 36 hours in advance.

The ISO 19030 has then been implemented in order to perform a more accurate prediction of the added power and speed variation, and it has been included in an optimization algorithm together with the request of weather forecast for each waypoint/solution analyzed. The voyage must be configured in advance, just before leaving and include the departure time, the expected time at arrival, all the waypoints describing the trips of the whole voyage is structured by and the maximum ship speed value on each trip, if needed. The configuration of the voyages can be directly performed through a custom user interface, Fig.9, that prepares the configuration files and uploads them in the Performance Monitoring System. The console makes it possible to configure all the voyages, stating the waypoints representing the trips in which a voyage is subdivided, and the maximum speed admitted on a single trip, if necessary. Furthermore, it is also possible to compute the raw scheduling of each voyage by setting the actual time at departure (ATD) and the expected time at arrival (ETA). In this way, the console shows the average speed to be set during the unrestricted trip in order to respect the arrival time.

The console is equipped with four main pages, aimed to define:

- The maximum speed allowed depending on the experienced sea state. This setup must be defined one time by the owner and it will be considered in order to adjust the computed ship speed depending on the sea state expected on each trip
- Voyages configuration, that gives the opportunity to define all the voyages the ship has to do, as previously described
- The extra-propulsive load, that makes it possible to define the power amount required by the propulsive engines for any other business. This setup is really important for ship with diesel-electric propulsion, because the diesel generator shared with all the other power needs. The amount of power required during the day is important for the overall definition of the optimum engine configuration, and hence of the minimum fuel consumption.

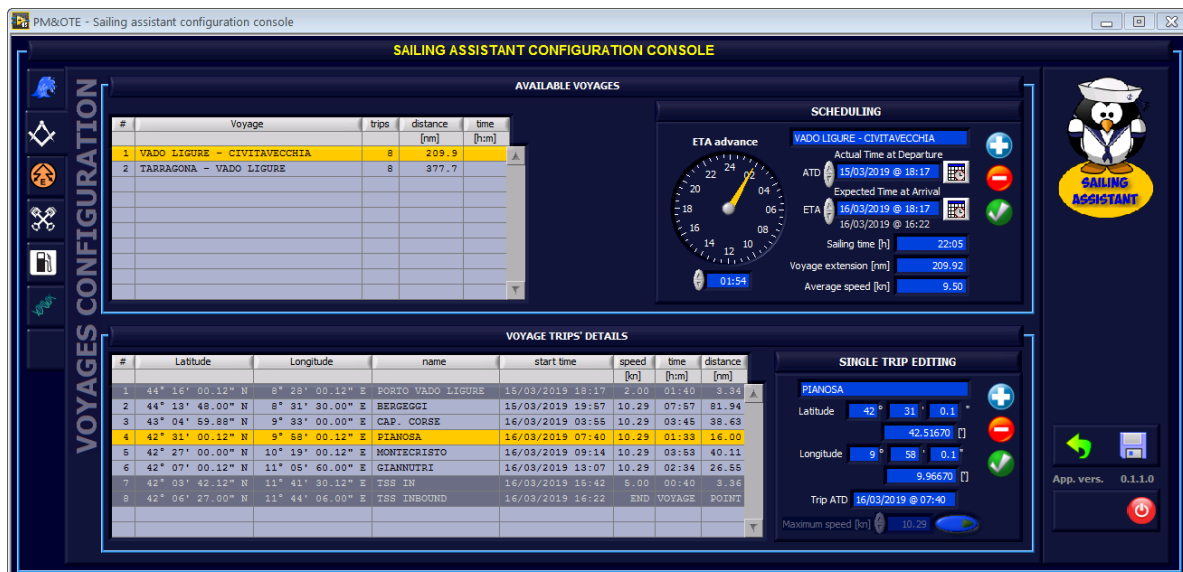


Fig.9: Sailing Assistant configuration console – voyages configuration page

The approach on which the sailing assistant is based on consists in the evaluation of the added resistance due to weather conditions along each trip, the evaluation of the power configuration, that is required to respect the overall power's request at the minimum consumption point and then the modification of the waypoints' coordinates in order to minimize the fuel consumption. The following figure represents a test performed on a rectangular sea area where the distribution of the wave height (and hence the sea

state) is represented by two Gaussian distributions, while the wind is constant. The white line represents the initial voyage that passes through the two high wave areas; the yellow line represents the optimized voyage. The chart shows how the module modified the waypoints' location in order to define trips characterized by lower expectation of added resistance.

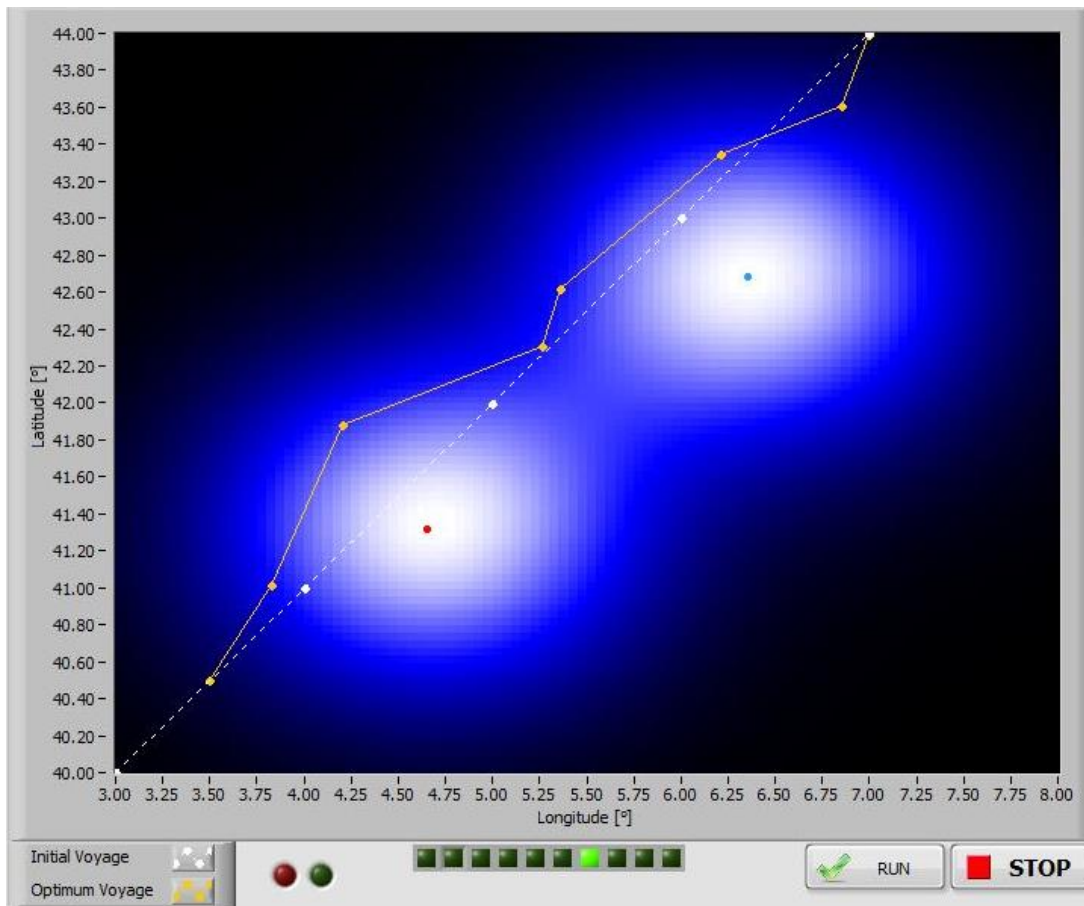


Fig.10: Sailing Assistant – voyages' optimization simulation

4. Conclusions

CETENA's Performance Monitoring system has been developed with the objective to monitor all the relevant propulsive parameters on board and provides ad hoc processed information to increase energy efficiently and reduce operating costs. PM collects data from the vessel's automation and navigation systems together with ad hoc sensors, and is able to filter and integrate data, display all relevant data to ship master and provide customized voyage reports according to customer needs.

Recently, the PM system has been implemented with the addition of the ISO 19030 computation module, that is aimed to compute and plot the prescribed performance indicators showing the propulsive efficiency increase due to maintenance activity. Furthermore, another module under finalization has already been developed for the fuel consumption optimization of any voyage, keeping into account the expected weather conditions in accordance with the international normative. These two PM skills are directly connected with the CETENA's Virtual Weather Station that is aimed to provide a service for the evaluation of historical or expected weather conditions in a defined time and geographic coordinates.

The new version of the CETENA's Performance Monitoring system provides powerful and promising skills for both the evaluation of the current ship propulsive performances and the optimization of voyages and ship management for what concerns the fuel consumption.

References

ISO 19030-1 – *Ship and marine technology – Measurement of changes in hull and propeller performance – Part 1: General principles* – Edition 2016

ISO 19030-2 – *Ship and marine technology – Measurement of changes in hull and propeller performance – Part 2: Default method* – Edition 2016

ISO 19030-3 – *Ship and marine technology – Measurement of changes in hull and propeller performance – Part 3: Alternative methods* – Edition 2016

Real Ship Maritime Big Data Analysis for Prediction of Fuel Consumption

Miyeon Jeon, Pusan National University, Busan/ Republic of Korea, myjeon0725@pusan.ac.kr

Yoojeong Noh, Pusan National University, Busan/Korea, yoonoh@pusan.ac.kr

Kyung Hwan Jeon, POSSM, Busan/Republic of Korea, khjeon@possm.com

Sang Bong Lee, Lab021, Busan/Republic of Korea, sblee@lab021.co.kr

Inwon Lee, Pusan National University, Busan/Republic of Korea, inwon@pusan.ac.kr

Abstract

A big data analysis of a smart ship's performance is important in that it can achieve both economical ship management and eco-friendly effect by reducing the ship's fuel consumption, thereby maximizing the fuel efficiency through optimization of the ship's operation. However, if collected maritime and ship data contain abnormal data such as outliers and bias, it is difficult to accurately estimate the ship's fuel consumption. Actual maritime and ship data are mostly missing and include abnormal data, so it is difficult to obtain accurate big data analysis results for them. Therefore, it is necessary to develop a big data analysis method to predict the ship performance based on real maritime and ship data. The main objective of this research is to develop real ship and maritime data analysis method for prediction of ship's fuel consumption, which consists of big data preprocess and big data analysis process. The big data pre-processing improves the data quality and also obtains the feature selection through rule-based data imputation, denoising, clustering, and compression. The proposed big data preprocess enables the ship and maritime data to be used to accurately predict the ship's fuel consumption by using an ensemble model combined with multiple machine learning models. The proposed big data analysis can be used to plan the navigation strategies and improve energy efficiency for real maritime and ship data with intelligent decision support capabilities.

1.Introduction

A smart ship is actively being studied as the next generation ship, which is capable of effective ship management such as engine monitoring, route optimization, ship diagnosis and remote control in marine and onboard with development of Internet of Technology (IoT). A big data technology including collection, processing, cleansing, and analysis of a large-scaled data is key-element of the smart ship to support the ship's intelligent decision making based on data.



Control

the integrated system in the ship



Diagnosis

ship's health condition, navigation strategy

OUTPUT 1 : Main Engine Fuel L



Monitoring

ship engine & controller status, navigation information

Fig.1: Smart ship in shipbuilding and maritime industry

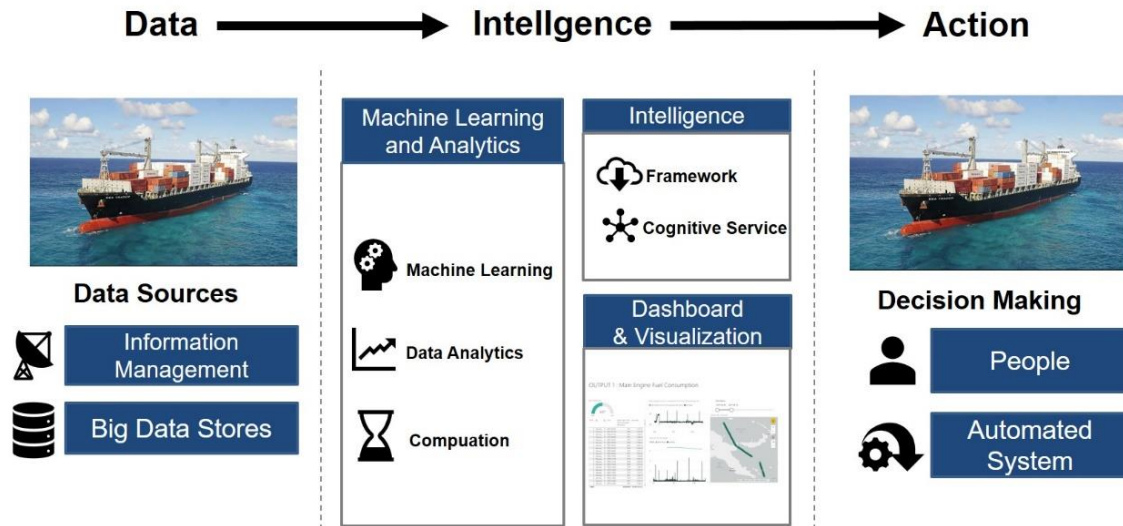


Fig.2: Overall scheme of a big data analysis for smart ship

As shown in Fig.2, after data including engine and navigation information are collected from onboard ship using digital acquisition system (DAQ), a large-scaled data is stored in a data storage. These data are used to predict and diagnose the ship's state through various machine learning models and data analytics methods. The framework enables to allow operators to use machine learning and analytics and amplify sophisticated intellect through cognitive service, and then, dashboards is designed to visualize and make insight of ship and maritime data. An intelligent system helps people or automated system to act through these decision-making systems.

Data analysis of ship performance monitoring for the smart ship is especially has been expanded to enable to improve energy efficiency and eco-friendly operate the ship from the relationship with ship and maritime data including ship's engine, navigation information, ship's state, weather and ship's fuel consumption. Since accurate prediction of ship's performance enables operators to control ship's engine and navigation, it is important to develop the prediction model for ship's fuel consumption by performing big data analysis of the ship and maritime data. Likewise, prediction of ship's fuel consumption can be also useful for optimizing the ship's operation thereby reducing ship's fuel consumption and maximizing the fuel efficiency.

In previous studies, the prediction of ship performance including ship's fuel consumption have been studied by many researchers. A regression analysis of ship's energy consumption using the gaussian process was performed by *Yuan and Nian (2018)*, also prediction of ship's fuel consumption was studied by using artificial neural network in *Jeon et al. (2018)*. *Soner et al. (2018)* used a decision tree model, which is a decision-making tool using tree structure, to predict the ship's energy consumption. However, the previous studies have not used real ship and maritime data for prediction of ship's fuel consumption, and used statistical method or machine learning method has been applied only for small amount of real ship maritime data. Thus, these methods have some limitations to be generally used for large amounts of data including various errors and bias.

In this study, big data analysis framework based on real ship and maritime data is proposed to predict ship's fuel consumption using various machine learning models with optimized hyperparameters. In the framework, original data with various types of errors collected from bulk carriers are refined through data imputation based on rule-based policy, data cleaning, clustering, and data compression. The proposed framework is validated using large scale data in real ship marine field and meta-learning using several regression models is proposed for accurate prediction of real ship and maritime data.

2. Methodology

This framework consists of two parts: data preprocessing for improving data quality and data regression process for using meta-learning. Data preprocessing include a rule-based data imputation, data clustering, data denoising, and data compression for feature extraction. After the data preprocessing is carried out, the data regression process is performed to predict ship's fuel consumption using meta regression. The data regression includes initial data regression process to make three machine learning models such as Generalized Linear Model (GLM), Gradient Boosting Regressor (GBR), and Multivariate Adaptive Regression Splines (MARS), and Bayesian optimization process is used to tune hyperparameters of each machine learning model. Then, the meta regression process is performed to combine three machine learning models to one meta model.

As using meta-regression model through this framework, each machine learning model has different weights to predict the ship's fuel consumption according to its accuracy. In this study, meta-regression models yields more stable predictions results each model alone, and this regression process can be successfully worked for accurate predictions of fuel consumption in real ship maritime data.

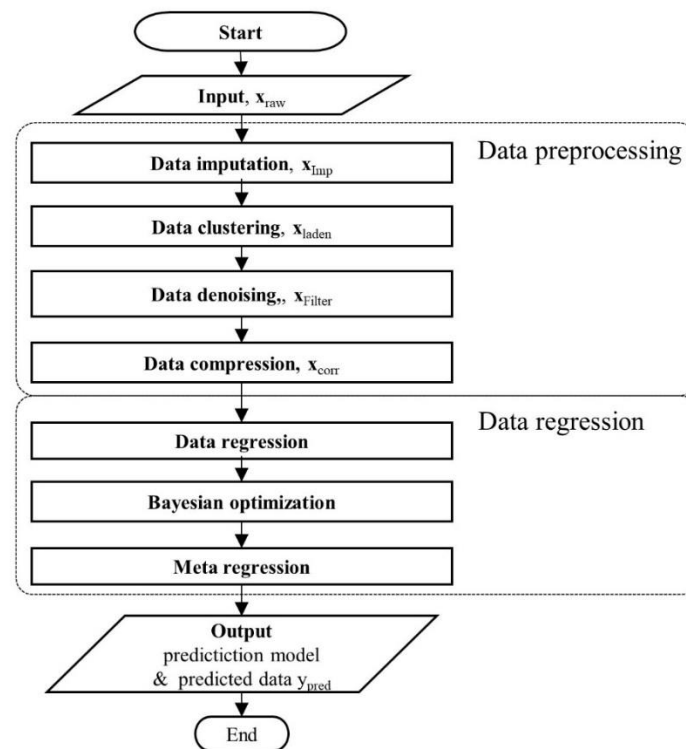


Fig 3: Big data analysis framework of prediction of ship's fuel consumption

3. Case Study

3.1. Data preprocessing

Real ship maritime data are used to validate the proposed framework in this case study. The time series data sets are collected once every ten seconds for three months from a bulk carrier. A detailed vessel information such as ship's length, beam, and maximum rated speed, is skipped for security reasons of the shipping company. The used data have 41 variables about ship operation, navigation, ship state, and weather condition as follows.

- Engine Operation: Main engine fuel consumption, engine power, shaft speed, etc.
- Navigation Speed: Speed Through Water(STW), Speed Over Ground(SOG), Ship heading, etc.

- Ship state: Forward draft, After draft
- Weather Condition: Relative wind speed, Relative wind direction, Wave speed, etc.

The collected raw data x_{raw} includes the corrupted data such as noise, error and bias data. To refine the corrupted data, data imputation process is performed to remove the outliers and select the needed operation region where used data set in this case study include abnormal data occurred while vessel moored or anchored. Since the purpose of this study aims to accurately predict ship's fuel consumption as controlling ship's state on navigation, the data sets also include vessel navigation data during navigation at the sea. Table I shows the rule-based policy for data imputation.

If the collected datum is not in range with lower and upper bound of limits defined in the policy, datum is considered moored ship condition, thus, this datum is imputed as a value defined in the solution. In this study, two input variables, shaft revolution and Speed Over Ground (SOG), are used for data imputation to conserve a large-scale data though rule-based policy as shown in Table 1. In the event of docking or anchoring in these data, the data sets outside of the range in Table 1 were replaced with the ones at a low speed to remove abnormal data, and only dataset with high-speed operation x_{imp} were used to predict ship's fuel consumption. Figure. 4 shows the scatter plot of SOG according to shaft revolution and portion of given data sets either at navigation or moored status.

Table I: Rule-based policy for data imputation

Code	Input variables	Range	Error	Solution	Category
Moor1	Speed Over Ground(SOG)	$-v_{LB} < v < v_{UB}$	$v > v_{UB}, v < v_{LB}$	$v = 0$	Ship Speed
Moor2	Shaft Revolution	$-x_{LB} < x < x_{UB}$	$x > x_{UB}, x < x_{LB}$	$x = 0$	Engine Operation
⋮					

After the data set x_{imp} are refined, features are extracted to classify high frequent draft operation regions in data clustering process. In this study, the k-means clustering algorithm, which is a method of unsupervised learning, was used to separate the two subsets of laden and ballast vessels using forward draft and aft draft affecting ship's fuel consumption as shown in Fig.5.

The number of cluster K needs to be selected by users through K-mean clustering, and silhouette analysis is performed to measure the performance of the clustering by calculating the separation distance between the obtained clusters. The silhouette plot displays a measure of how close each point in one cluster to points in the neighboring clusters, and thus, its value can assess the appropriate number of clusters. In Fig.6, when the number of cluster K is two, the data sets are clustered into two subsets of laden and ballast vessels and their silhouette values are more than 0.7, which means that the data clustering is well performed and data are distributed in a dense region. A large scale data sets, thus, can be effectively classified and used to perform regression analysis through data clustering process. In this study, the subsets x_{laden} are considered as laden data sets, which are used for prediction of ship's fuel consumption.

In the next step, data denoising process is performed to remove the outliers in the resulting classified subset (x_{laden}) and smooth them using Kalman filter. The Kalman filter is a method of filtering data based on a priori state estimated from previous times and posterior state using update information as combining with current observation information and priori state. Figure 7 shows the plot of the denoised data for SOG.

The initial and variance values of the parameters in Kalman filter used the mean and variance values of the dataset, and the covariance matrix of progress noise and measured noise has 100 and 0.01 as default values, respectively. The denoised data follows the trend of previous data and their curve become

smoother in rapidly increasing or decreasing region. All data related to engine operation, navigation, and weather condition were cleaned or smoothed through de-noising preprocessing as well as the SOG data.

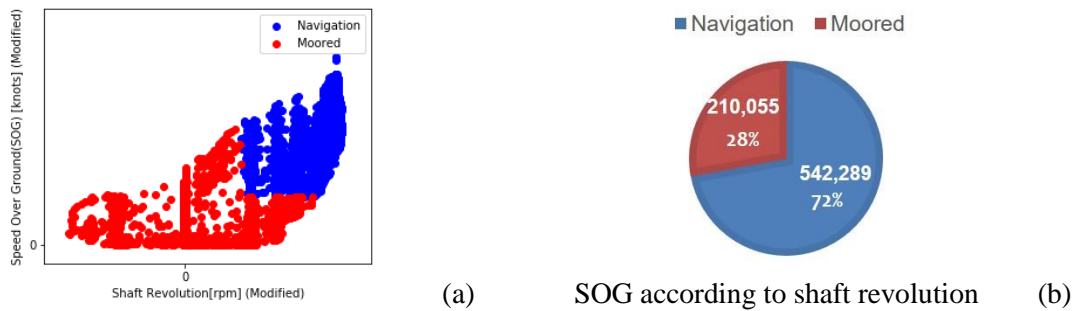


Fig.4: Data imputation process for selection of navigation dataset

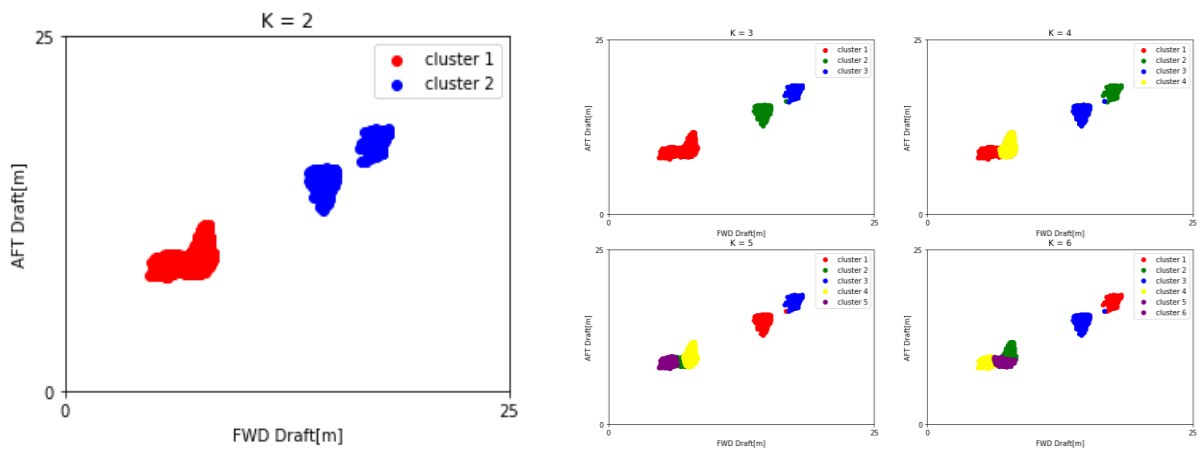


Fig.5: Data clustering of draft following the number of cluster K

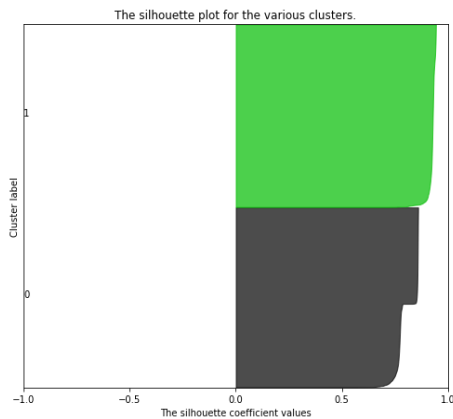


Fig.6: Silhouette values for K = 2

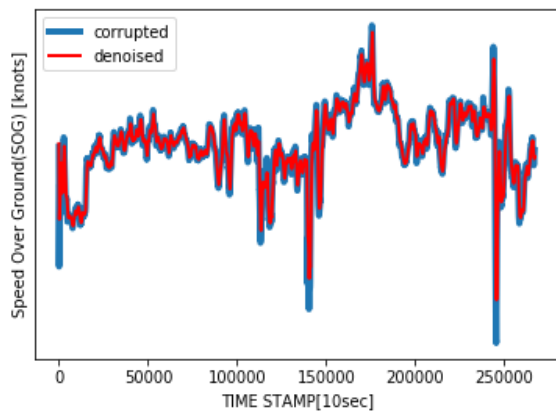


Fig.7: Data denoising of SOG

However, the number of input variables is still high to generate machine learning models, so that it need to be reduced. In the data compression process, the denoised data x_{filter} using Kalman filter is compressed to reduce the dimension of data, and correlated variables are combined through Principal Component Analysis (PCA) and correlation Analysis. As results of PCA and correlation analysis, the input variables are reduced to four variables such as shaft torque, main engine power, shaft revolution, and speed through water, which much affect the ship's fuel consumption.

3.3 Regression model of ship fuel consumption by using meta-regression

With preprocessed dataset x_{corr} , regression analysis is performed to predict ship's fuel consumption using various machine learning models. All data are divided into training data sets for learning model, valid data sets for tuning the parameter of regression model and test data sets for evaluating model's performance with ratio 4:1:1, respectively. Test data sets are split into sequential time-series data sets for evaluating and comparing with each model's performance, and training and valid data sets are randomly selected.

In this study, the predictive model is generated from the machine learning regression analysis: Generalized Linear Model (GLM), Gradient Boosting Regressor (GBR), and Multivariate Adaptive Regression Splines (MARS). It is because they yield the most reliable and accurate prediction results as results of validation tests for various machine learning models, which are widely used in ship and maritime data analysis.

The GLM model is one of additive models using different basis functions, which is based on an assumption that input variables follow normal distribution. The GLM model is a non-parametric model and has the advantage of expressing nonlinearity as reason that each input variable can have a different type of basis function. In general, since ship and maritime data have highly nonlinearity between input and output variables, the GLM model is known to have the high accuracy for predicting the ship performance.

The GBR model is an ensemble model combined with weak learning predictive model such as decision tree by using error correction and tuning hyperparameter of next models. Accordingly, the GBR model can possibly generate regression models with extremely fast computations or extremely high accuracy depending on hyperparameters. In ship maritime big data, this method has some merits in terms of having characteristics of the decision tree as insight of deterministic method and having extremely high accuracy.

The MARS model is a predictive model using a linear combination of base functions in a non-parametrical way. Since MARS model automatically models nonlinearity and interaction between variables, it has advantages especially for high dimensional data with high nonlinearity. Further, it can prevent generating overfit models, and thus, it can be generally used for ship maritime big data.

Each parameter has different hyperparameters and its performance could be different depending on hyperparameter values, so that it is necessary to optimize the hyperparameters of each model. In this study, Bayesian optimization method is used. The Bayesian optimization repeatedly performs the exploitation and exploration steps to find the optimum hyperparameters. The exploitation step is a process of finding the most uncertain and the most likely to be improved observation point by minimizing the acquisition function based on the observed hyperparameter values. The observation points are updated by performing model training using evaluation function such as R^2 or Mean Squared Error (MSE) in exploration step. When the stopping criteria are satisfied in the loop of exploitation and exploration step, the optimal hyperparameter with the highest evaluation function is obtained. Bayesian optimization method is more often used than other typical methods of tuning hyper parameters such as grid search and random search because the optimization process is very efficient especially for high-dimensional hyperparameters. For Bayesian optimization, the lower and upper bounds for each hyperparameter are given in Table II.

As the optimum parameters for each machine learning model are extracted, it is possible to generate more accurate machine learning models for ship's fuel consumption. Even though optimized hyperparameters could improve accuracy of models, it cannot still guarantee reliability and accuracy of each model because machine learning models have different characteristics depending on data quality, data quantity, dimension of input and output variables, and their linear/nonlinear relationships.

For example, GLM model has the advantages of expressing nonlinearity, but it has the disadvantages of having difficulty to overfit some models. In the GBR model, although high accuracy is mostly observed, the GBR model sometimes yield high errors in modeling highly nonlinear data in a deterministic way. The MARS models is simple to use and easy to be generalized, but it might have the relatively large errors for highly nonlinear data.

Thus, a meta regression needs to be performed to guarantee reliability and accuracy of models regardless of data errors, dimensions, or etc. The meta regression is an ensemble model that combines multiple machine learning models to robustly predict ship's the fuel consumption in real ship maritime big data. Each machine learning model is obtained using valid data, and then, a linear regression is performed to get weights on each machine learning model. After the meta regression is performed, the predicted results for fuel consumption are obtained, and then, big data analysis process for predicting ship's fuel consumption is now finished.

Table II: Search domain for Bayesian optimization

Algorithm	Hyperparameter	Lower bound	Upper bound
Generalized Linear Model(GLM)	Number of splines	10	100
	Spline order	1	9
	Smoothing parameter	0.0001	1
Gradient Boosting Regressor(GBR)	Maximum tree depth	100	1000
	Minimum samples leaf ratio	0.001	0.5
Multivariate Adaptive Regression Splines(MARS)	Minimum search points	10	5000
	Thresh	0.001	0.1
	Penalty parameter	1	10
	Maximum order	1	5

4. Results and Discussion

The results of the regression analysis are presented to verify the accuracy of each machine learning model by calculating error between the measured (target) data and predicted data with 4 error measurements: Mean Absolute Percentage Error (MAPE), Relative Root Mean Square Error (RRMSE), Coefficient of residual Mass (CRM), and Coefficient of determination(R^2) as shown in Table III.

Each error measure represents various characteristics of errors between the target data and predicted data. The MAPE calculates the variance of errors with percentage, and the RRMSE measures the degree of the error deviation with percentage where errors of less than 10% indicate the prediction model is reasonably accurate, *Despotovic et al. (2016)*. The CRM is a measure of the tendency of the model to overestimate or underestimate the target data. If the CRM value is close to zero, it means that the model accurately predicts the target data. If it is larger or less than zero, the model underestimates or overestimate the target data, respectively, *Li et al. (2013)*. The R^2 is a measure of how close the data are to the fitted regression line. Values of each error measure are estimated for three machine learning models and ensemble model to verify the accuracy of each model for the valid data set and the test data set.

The results of regression models for different machine learning techniques are repeatedly obtained 50 times from the same training and valid data sets before the hyperparameters are adjusted, and then, the variation in the initial model is examined and the accuracy of each model is compared.

Table III. Error measures

MAPE	RRMSE	CRM	R ²
$\frac{100\%}{n} \sum_{i=1}^n \left \frac{y_i^t - y_i^*}{y_i^t} \right $	$\frac{\sqrt{\frac{1}{n} \sum_{i=1}^n (y_i^t - y_i^*)^2}}{\frac{1}{n} \sum_{i=1}^n y_i^t} \times 100$	$\frac{\sum_{i=1}^n y_i^t - \sum_{i=1}^n y_i^*}{\sum_{i=1}^n y_i^t}$	$1 - \frac{\sum_{i=1}^n (y_i^t - y_i^*)^2}{\sum_{i=1}^n \left(y_i^t - \frac{1}{n} \sum_{i=1}^n y_i^t \right)^2}$

y_i^t : the true value of i-th datum, y_i^* : the predicted value the true value of i-th datum

The results were presented using box plots for each model as shown in Fig.8 (a)-(d). The MAPE and RRMSE values in Fig.8 (a) and (b) show similar performance in estimating errors, and all machine learning models has good fit to actual data because MAPE and RRMSE have errors of less than 5% and 10%, respectively. The GLM model has the smallest variation of errors, and thus, it shows the best accuracy among all machine learning models when comparing all error measure values. On the other hand, the GBR model has the largest variation of errors depending on hyperparameters, and MAPE, RRMSE, CRM, and R² indicate the GBR has the worst accuracy among all models. The MARS model and GLM model has similar accuracy, but MARS model has a disadvantage in the large variation of the errors comparing with the GLM model. Unlike GBR, two models tend to underestimate the fuel consumption based on CRM values, so that they can conservatively estimate it in the economic evaluation of ship operation. Although MARS model has less accuracy than GLM in this case study, but the computational time needs to be taken into account in order to analyze real time ship and maritime data. Therefore, MARS model is still advantageous over other models in practical aspects.

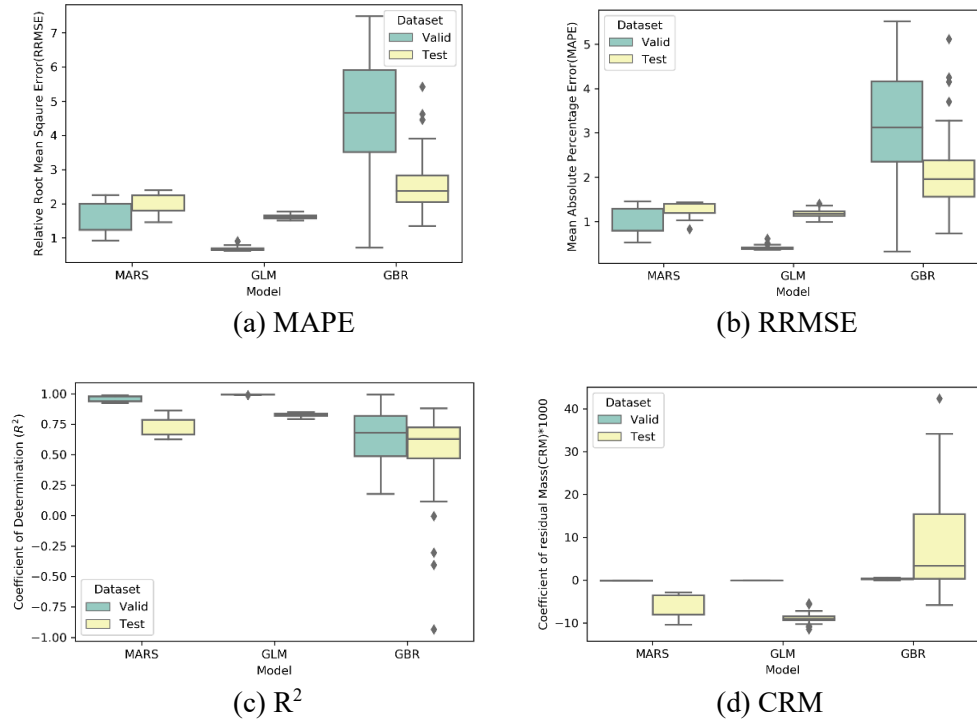


Fig.8 Various error measure values for MARS, GLM, and GBR

The error values of the initial model and optimized models with tuned hyperparameters are compared in Table IV to check how much Bayesian optimization improves the model accuracy where the data sets with the highest R² value were selected. The parameter tuning is performed in the valid data sets, and the test data set is used to verify the accuracy of each model. Thus, most models have the lowest error values for the valid data sets rather than for the test data sets. As shown in Table IV, the model accuracy is improved by parameter tuning using Bayesian optimization for all three models. In particular, the GBR model was the least accurate in Fig.8, but its accuracy is significantly improved

after the parameter tuning because it is the most sensitive to hyperparameter values among all three models. On the other hand, the GLM and MARS model has slightly increased the accuracy due to less sensitivity to the hyperparameter values. However, it is still difficult to select an appropriate model for general ship data because each model could have different performance according to data quality and quantity, data preprocessing process, etc. Thus, it is necessary to derive a model with consistently good accuracy regardless of data state.

Table IV: Comparison of error values before and after Bayesian optimization

		MAPE		RRMSE		CRM*1000		R ²	
		Valid	Test	Valid	Test	Valid	Test	Valid	Test
GLM	Initial	0.4138	1.1897	0.6863	1.6142	-0.0468	-8.9344	0.9930	0.8285
	Optimum	0.3652	0.9568	0.6270	1.4834	-0.0573	-4.3303	0.9942	0.8554
GBR	Initial	2.7433	1.9813	4.0192	2.4825	0.2266	8.0011	0.7091	0.5323
	Optimum	0.0265	0.7254	0.1095	1.2508	0.0043	-4.9935	0.9998	0.8972
MARS	Initial	0.9868	1.2740	1.5195	1.9734	-0.0980	-6.7485	0.9623	0.7383
	Optimum	0.4361	0.9349	0.7270	1.5200	-0.0412	-7.5679	0.9922	0.8481

Fig.9 shows the results of GLM, GBR, MARS, and meta regression models with tuned parameters for estimating the ship’s fuel consumption. The GLM model tends to follow the overall target data as a whole, but the predicted data differ greatly from the target data in some regions. The GBR model shows a tendency to increase or decrease rapidly for a certain region, but it shows accurate prediction for most target data. The MARS model better describes nonlinearity of target data than other models, and the meta model accurately predicts the target data similar to the most accurate GBR model.

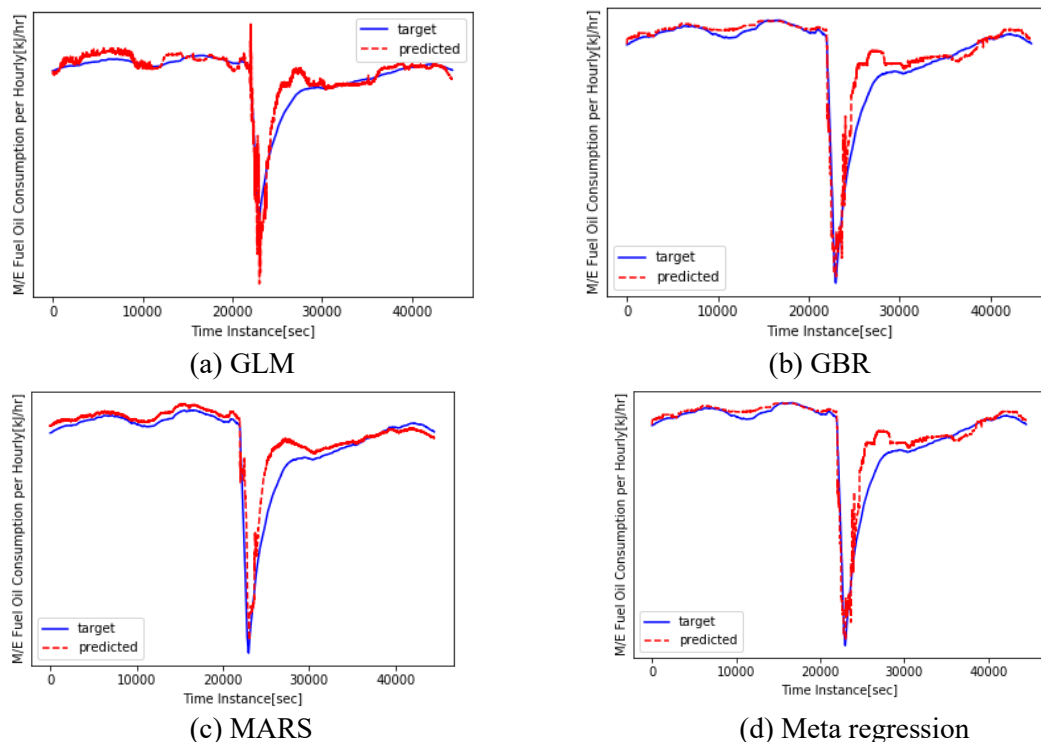


Fig.9: Prediction results on main engine fuel oil consumption per hourly for MARS, GLM, GBR, MARS and Meta regression models

Numerical comparison results of each model accuracy show that the GBR model and the meta model are the most accurate, and the MARS model shows the most conservative prediction for fuel consumption. Although the meta model shows the most similar results with the GBR model, it still has similar characteristics to the MARS model, which tends to overestimate target data and well describe nonlinearity.

In this case study, each single model alone can accurately predict the ship's fuel consumption through parameter tuning, but the meta regression model can show more robust performance rather than using a single model for large amount of real ship data including many errors and missing data.

Table V: Error values for GLM, GBR, MARS and meta regression models

	MAPE	RRMSE	CRM*1000	R ²
GLM	0.9568	1.4834	-4.3303	0.8554
GBR	0.7254	1.2508	-4.9935	0.8972
MARS	0.9349	1.5200	-7.5679	0.8481
Meta	0.7241	1.279	-5.0213	0.8976

5. Summary & Conclusions

In this study, big data analysis based on real ship maritime data is performed to predict ship's main engine fuel consumption through data preprocessing and regression analysis. In the data preprocessing, ship maritime big data were refined by sequential data preprocessing including data imputation using rule-based policy, clustering, denoising and expansion. The regression analysis uses a meta(ensemble) model combining three machine learning models (GLM, GBR, and MARS) to obtain a more stable and reliable prediction model for ship's fuel consumption regardless of data quality or quantity. Each machine learning model is more refined to improve its accuracy through Bayesian optimization of its hyperparameters, and also contributes to improve the accuracy of the meta model.

Although the meta model requires the time-consuming process with large computations including hyperparameter tuning and meta-regression, it is expected to be more accurate and reliable in predicting ship performance, which leads to stable ship's operation and management. From this study, the predicted fuel consumption can be used to support intelligent decision-making in real ship big data analysis, and thus, optimize the economic strategy on ship's consumption for future smart ships.

Acknowledgement

This work was supported by the National Research Foundation of Korea (NRF) grant funded by the Korea government(MSIP) through GCRC-SOP (No. 2011-0030013), Korea government(MSIT) (No. 2018R1D1A1A02086093), and National Innovation Cluster Program (P0006887, Build on Cloud Intelligence Platform based Marine Data) funded by the Ministry of Trade, Industry & Energy (MOTIE) and Korea Institute for Advancement of Technology (KIAT).

References

- JEON, M.; NOH, Y.; SHIN, Y.; LIM, O. K.; LEE, I.; CHO, D. (2018), *Prediction of ship fuel consumption by using an artificial neural network*, J. Mechanical Science and Technology 32(12), pp.5785-5796
- DESPOTOVIC, M.; NEDIC, V.; DESPOTOVIC, D.; CVETANOVIC, S. (2016), *Evaluation of empirical models for predicting monthly mean horizontal diffuse solar radiation*, Renewable and Sustainable Energy Reviews 56, pp.246-260

LI, M. F.; TANG, X. P.; WU, W.; LIU, H. B. (2013). *General models for estimating daily global solar radiation for different solar radiation zones in mainland China*, Energy Conversion and Management 70, pp. 139-148

SONER, O.; AKYUZ, E., & CELIK, M. (2018), *Use of tree based methods in ship performance monitoring under operating conditions*, Ocean Engineering 166

YUAN, J.; NIAN, V. (2018). *Ship Energy Consumption Prediction with Gaussian Process Metamodel*, Energy Procedia 152, pp.655-660

A Short History of Hull Cleaning and Where Do We Go Now

Simon Doran, HullWiper, Dubai/United Arab Emirates, simon.doran@hullwiper.co

Abstract

This paper describes in brief how traditional hull cleaning methodology has developed from Ancient times to the now Robotic and Semi-Autonomous 21st Century, what the associated risks are when hull cleaning is carried out and what the future look like with regards to Hull Cleaning or “Grooming” and general safety and the Ocean Environment.

1. Introduction to Hull Cleaning

Around the world upwards of USD\$5.7 billion is spent every year to prevent and control marine fouling and we all know now that marine Biofouling is associated with the largest percentage of invasive issues, while Ballast Water is the second largest. Invasive Species are now an environmental emergency and as you will know the IMO calls invasive species: “One of the greatest threats to the ecological and the economic well-being of the planet.”

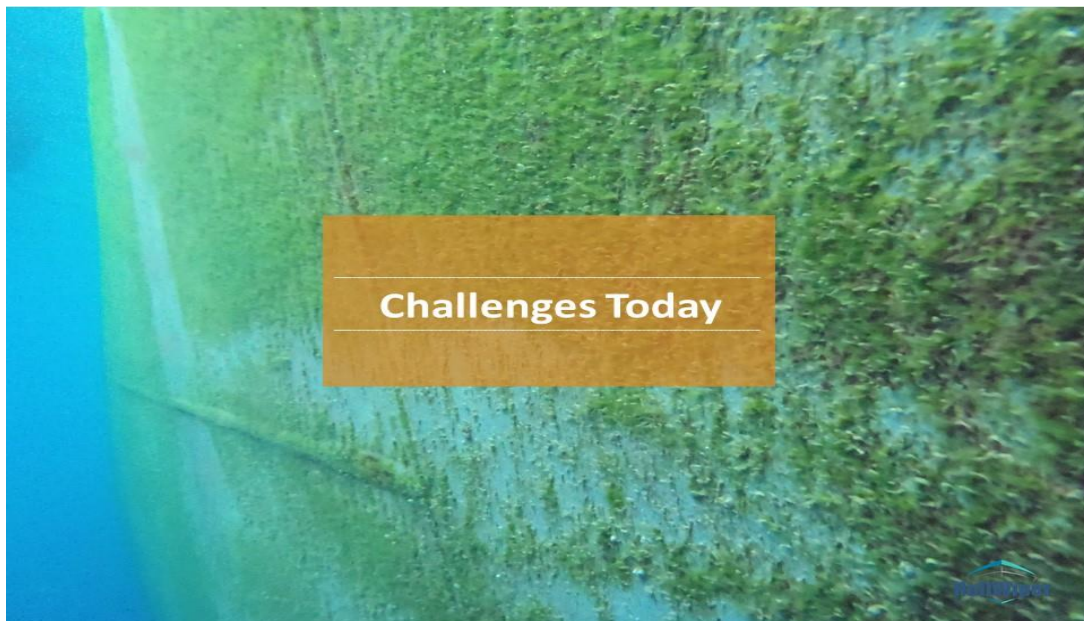


Starting in Ancient Egypt. The most famous example of their shipbuilding skills was the Khufu ship, a vessel 44m in length. An example was found intact in 1954, entombed at the foot of the Great Pyramid of Giza, and carbon dated to around 2500 BC, made from cedar wood brought from region that is now Lebanon. The first recorded treatment for ship efficiency comes from an Aramaic scroll dated about 412 BC which stated “the arsenic and Sulphur have been well mixed with Chian oil...with the mixture evenly applied to the vessels sides so that she may speed through the blue waters freely and without impediment.”

By the 3rd century the Romans and Greeks were leading the way with shipbuilding and sea exploration, and it is recorded that they were using tar and wax to coat their ships' bottoms.

Between the 8th and 11th century, the rampaging Vikings are recorded as being vigilant in cleaning the hulls of their ships for speed and efficiency of sailing and with it came the use of pitch, oil, resin and tallow for hull treatment. Between the 13th and 15th centuries, the Chinese were pushing exploration from the East on bigger and faster ships and they had the hulls of their ships coated with lime mixed with poisonous oil to protect the wood from worms. Christopher Columbus also recorded similar attempts to deal with this invasive problem for his ship, the Santa Maria, stating "all ships bottoms were covered with a mixture of tallow and pitch in the hope of discouraging barnacles and teredo (the worms), and every few months a vessel had to be hove down and graved on some convenient beach." This was the same for Buccaneers and Pirates who recognized the benefits of a clean ship. Having "careened" their ships on low lying bays of the Caribbean islands to clean the hulls, they knew that they were then faster in the water so they could the catch commercial vessels trying to run away, or outrun Navy vessels sent to sink them.

Lord Horatio Nelson was a supreme tactician, even though the admiralty did not always agree with his unconventional tactics. Prior to the battle of Trafalgar, he is known to have ordered his entire fleet of 27 vessels to be hull cleaned. Since he was at a numerical disadvantage in fleet size (with only 27 against the 33 French and Spanish ships), he knew he needed the advantage a clean hull gave him in speed to even the odds. He then used his fleet's superior speed and agility to famously maneuver into two columns directed perpendicular against the French and Spanish and delivered a decisive "broadside", the result being 22 lost French and Spanish ships to not a single British loss. So, the speed advantages of a clean ship were known then as they are today.



BUT What wasn't uppermost in Pirates or Nelsons thinking was the spread of invasive species.

Charles Darwin raised the first questions about the risks in transfer of invasive species attached to ship hulls when in 1836 sailing on HMS Beagle around the Galapagos Islands he recorded "Fouling of a ship's hull could be the other means of transport of marine organisms from one location to another". It was around these times that ships were starting to advance from wood and sails into iron and steam.

The finest example of this was the SS Great Eastern, an iron sailing steamship designed by Isambard Kingdom Brunel. When she was built in 1858, she was by far the largest ship ever at 211m (and with

a carrying capacity of 4,000 passengers to be transported from England to Australia, without the need for refueling). Over the next century, all sorts of antifouling paints were used, with varying ingredients such as lacquer, powdered iron, red lead, tannin, shellac, hot plastic paints then cold plastic paints, to name a few, and by the 1960s the leaching antifoulings were introduced.

The most effective and well-known ingredient used in the anti-fouling paints, TBT, was eventually banned worldwide in 2003



Today the marine coating business is a multi-billion-dollar and very powerful industry, but it's not all plain sailing as the coating industry faces challenges, with some quarters asking for heavy metals to be removed from all coatings. So even here new solutions are needed.

But despite this long journey and all of these advancements, the problems that have been around for thousands of years still exist today, and no clear and present solution is in place which is agreed globally.

- Biofouling is still an invasive species risk.
- Biofouling still impacts speed and performance

Added to the above, hull cleaning and hull cleaning methodology is/was woefully behind. Traditional cleaning goes on in many locations. This consists of Divers with hand held scrubbers, or driving underwater brush carts, marine fouling is aggressively removed from the submerged areas and the coatings are damaged to varying degrees dependent on the cleaning system and operator controls. The brush pressure during cleaning can additionally remove upwards of 100microns of coating in one clean. These cleaning systems are effective to a degree however most, if not all, lack fouling collection systems, and as a result increase inherent risks to both the environment and to life. The fouling is scrubbed off the submerged area along with heavy metals and allowed to fall within the tidal stream. In the past two years at least 4 x divers have been killed whilst hull cleaning.

The importance of environmental standards and HSSE has dramatically increased within corporate culture to the point where the marine industry now considers this to be the norm ... or is it? Some ship

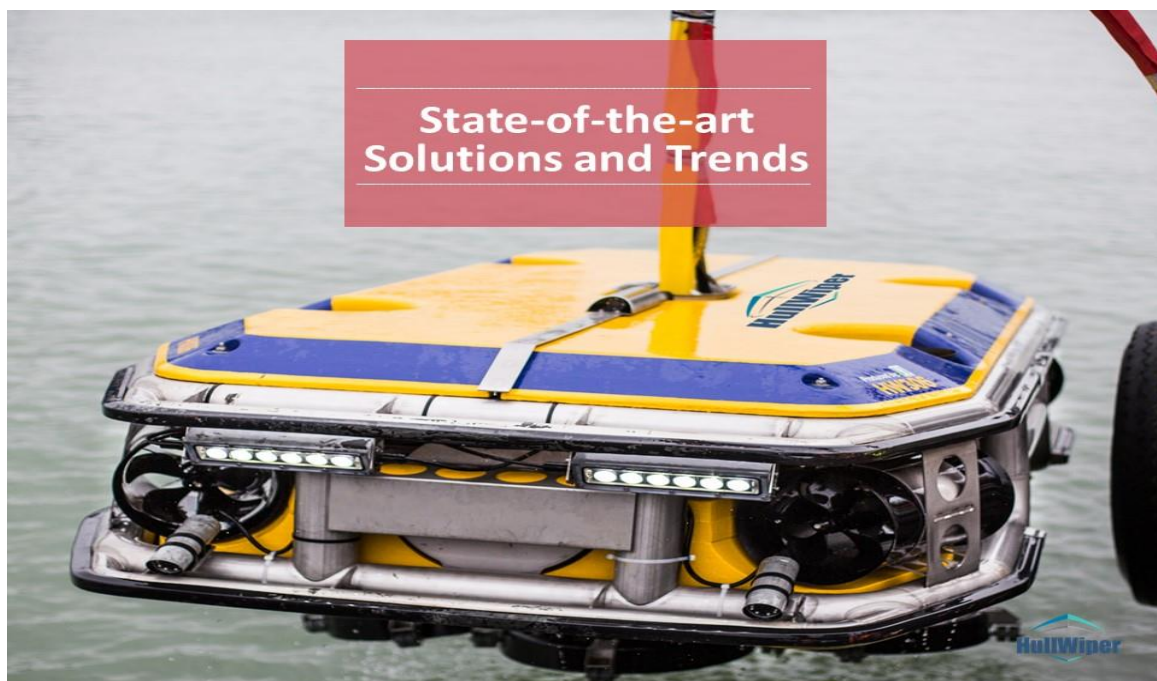
owners, even Oil majors with very robust corporate cultures who set the highest of standards, are often still driven by the cheapest solution.

By 2003 the first Remotely Operated Vehicle (ROV) with marine fouling capture technology was introduced to commercial shipping and ROV hull cleaning became an option, whilst at first limited, now there are known to be 6 x commercially viable ROV Hull Cleaning service providers and more than another 5 x companies undergoing development and testing. Hull Cleaning with marine fouling capture systems are here now, and some of these systems do not require divers to drive them, as they are ROV's

HullWiper and others similar to HullWiper are becoming more and more an option and are diver-free, cost-effective and environmentally friendly ROVs. Most ROVs are equipped with water jets and designed to clean from 1000m² up to 2000m² per hour. Utilizing salt water under variable pressures as the cleaning medium Collects pollutants removed from the vessel's submerged areas for ashore disposal in an environmentally approved and eco-friendly manner and can clean ships whilst taking bunkers or during loading/discharging cargo, saving valuable time for vessels

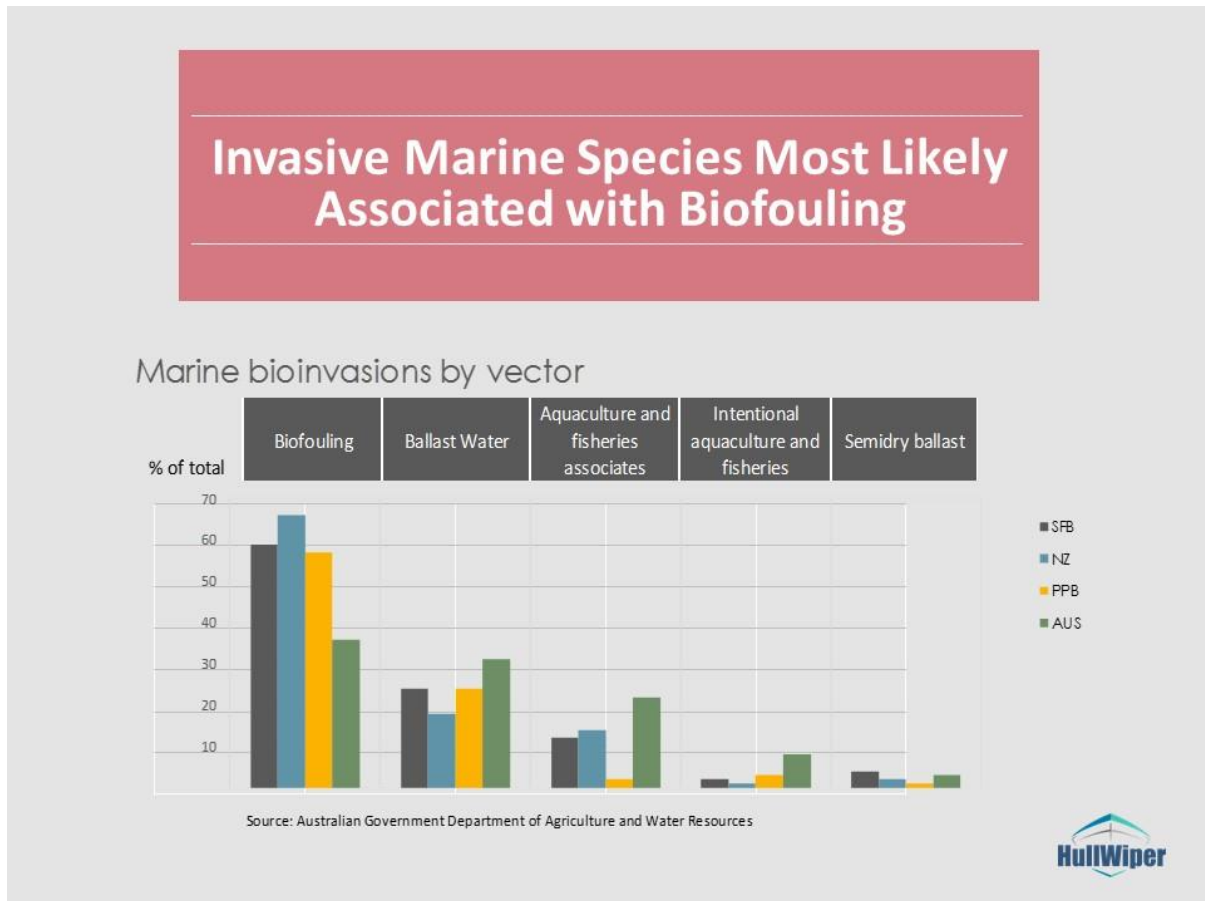
Hull Cleaning is seen as a necessary evil but regulations are now changing, by prohibiting hull cleaning in ports or restricting divers to daylight hours only, this is proactively influencing development of ROV hull cleaning with fouling capture systems as an added requirement.

State, federal and international regulators will positively affect the hull cleaning industry and if more biofouling regulations are implemented and enforced, hull cleaning with fouling capture units may become the only acceptable option.



Add to the pot, the IMO GloFouling Partnership project, launched in November 2018, is focused on dealing with the transfer of invasive aquatic creatures on ship hulls. This is aligned with the Ballast Water Management convention; however, the Ballast Water convention took the best part of 20 x years to complete and has/will cost vessel owners millions to comply with. The IMO will potentially complete the GloFouling directive in 2023, which will then help to push stricter regulations worldwide.

Secondly BIMCO are progressing forwards to bring together different stakeholders including HullWiper and our friendly competitors to provide input on new hull cleaning standards that will enable ports to understand who has been cleaned properly by who and all associated data. This will help in providing a filter to the relevant authorities to check more effectively and will align well with SEEMP - the Ship Energy Efficiency Management Plan released by the IMO in 2013.



So what does the future look like for Hull Cleaning and biofouling?

Once upon a time, fossil fuel engines were the future, now today they are a problem and cost so much to run. Global trade was the future; but no one anticipated that invasive species would wipe out fishing industries and cost governments billions each year. Antifouling paints were the solution, but no one fully understood the impact of TBT and or heavy metals deposited into the oceans. For coatings what is the future? Will there be pressure for strictly, an organic, non-metal compound coating on ships hulls which removes the threat of heavy metals in the oceans?



Tomorrows Challenges

1. Change
2. Cleaning or Grooming
3. Niche areas

HullWiper

No one really knows what options will be available in the future and what problems they will bring, but ROV Hull Cleaning such as HullWiper amongst others is one solution that gets to the root of the problem which can have a positive impact.

- Together we can save you money,
- Together we can help save the environment
- Together we help save lives.

A Digital Business Model for Vessel Performance Monitoring

Serena Lim, Ascenz, Singapore, serena.lim@ascenz.com
Roger Teo, Ascenz, Singapore, roger.teo@ascenz.com
Teck Chong Sia, Ascenz, Singapore, sia.teckchong@ascenz.com

Abstract

Hull and propeller performance monitoring is an important aspect of the overall vessel performance monitoring and management, which is driven economically towards optimised fuel consumption and environmentally towards a reduced carbon footprint throughout the operational life of a vessel. Research and development is carried out continuously to improve operational performance, for example to increase reliability of measurements in terms of sensor technology and data integration as well as understanding the effects of vessel draft, trim, speed, seaway and wind. Benchmarking capabilities are also being constantly improved to enable users to apply standards for vessel performance monitoring such as the development of ISO 19030. These multi-directional research approaches for optimising vessel operations, using new sensor technologies and applying machine learning techniques can result in the slow adoption of new vessel performance solutions. We therefore propose here adoption of a digital business model for vessel performance monitoring and to provide a clear direction to drive the industry towards a sustainable and successful digital ecosystem, which delivers solutions more rapidly than traditional approaches. The benefits and contribution of different players in the industry will be highlighted and the digital business model will be discussed as the sector moves towards Industry 4.0. Results and analysis will be presented to demonstrate the state of implementation of various standards as part of the business model and to highlight specific development needs.

1. Introduction

As the shipping industry moves towards an era of increasing digitalization, a deeper awareness of available resources and solutions in the market to support this trend is important. An ecosystem describes a community of interacting organisms and their physical environment, in a broader business context, it can be viewed as a complete network of interconnected systems and businesses. A digital ecosystem is one in which systems are digitally connected, and the success or failure of each component will affect those systems to which it is connected. A successful digital ecosystem in the maritime industry is a distributed, adaptive, open socio-technical system with properties of self-organisation, scalability and sustainability, inspired by natural ecosystems, *Zhu (2015)*. Digital ecosystem models are informed by knowledge of natural ecosystems, especially for aspects related to competition and collaboration among diverse entities.

The root of a successful digital ecosystem lies in the availability of high-quality data and information that can be generated from databases. Data can be presented qualitatively or quantitatively; the quality of the data depends of the intended use of data in operations, decision making and planning. Data accuracy, compatibility and completeness remain a major problem for most companies and industries, since datasets that are flawed or corrupted can lead to wrong information and incorrect forecasts being made, *Crandell (2017)*.

Data Acquisition Systems (DAS) have been installed on vessels to acquire high frequency data which record the performance of the vessel. These data can be used to develop standards, improve efficiencies of operation and used to develop advice on future designs. The European Union Monitoring, Reporting and Verification system (EU MRV) and International Maritime Organization Data Collection System (IMO DCS) were developed to reduce the greenhouse gas (GHG) emissions of shipping activities, focusing on ships operating within the EU area and in international shipping operations respectively, *EU (2015), IMO (2016)*. These reports also provide useful inputs and guidance for policy making. The data collected can also be used to measure improvements in the energy efficiency of ships as part of the

Ship Energy Efficiency Management Plan (SEEMP), *IMO (2012)*, which feeds the data into Energy Efficiency Operational Indicator (EEOI) to benchmark ship performances, *IMO (2009)*. The data from a DAS are also used to influence ship designs and retrofitting, *Peri (2016)*.

The performance of ships during different operations can be evaluated in real time. Vessel performance monitoring (VPM) products and services can be viewed in terms of three categories. The first is a Data Acquisition System (DAS) which logs data collected from sensors on a common database, which can be viewed on-board the vessel, and telemetry data to shore for real time display of data, *Rødseth et al. (2016)*. The second is added information that can be provided through monitoring sensors, such as total fuel consumed in each operation, efficiency of machinery that is monitored, *Perera and Mo (2017)*. The third is advanced analysis to generate additional information from the available databases, such as for maintenance base monitoring purposes, hull degradation and vessel performance monitoring. The third category could also include services with advance data processing such as using machine learning techniques and artificial intelligence, which could lead to advisory systems, *Coraddu et al. (2019)*.

Preparation for the development of a digital ecosystem framework for ship performance monitoring is proposed. A background understanding for stakeholders is also provided so that choice of VPM services and the expected outputs of such systems when choosing providers with different business models can be facilitated. Areas where there is a need for further development towards an ecosystem driver, which can provide a cyber physical network (Industry 4.0) for the VPM system are also highlighted.

2. Digital business model framework

A digital business model is therefore proposed for vessel performance monitoring to provide clear direction and to drive and guide the industry towards a sustainable and successful digital ecosystem, which delivers solutions more rapidly than traditional approaches. The benefits and contributions of different players within the digital ecosystem will be highlighted and the digital business model will be discussed, as the sector moves towards Industry 4.0, a cyber-physical system that connects automation and data exchange in manufacturing technologies.

The framework proposed for a digital business model for vessel performance monitoring (VPM), shown in Fig.1 is adapted from ‘Four business models for the digital age’ and ‘Thriving in an increasingly digital ecosystem’ by Peter Weill and Stephanie Woerner. An understanding of the types of digital business models will help develop a more holistic VPM that serves the needs of the shipping industry in terms of data acquisition systems (DAS) design and development, as well as data processing and analysis. In addition, users of such systems can be informed of the type of business models that are available in the industry and can make the informed decisions when choosing suitable providers.

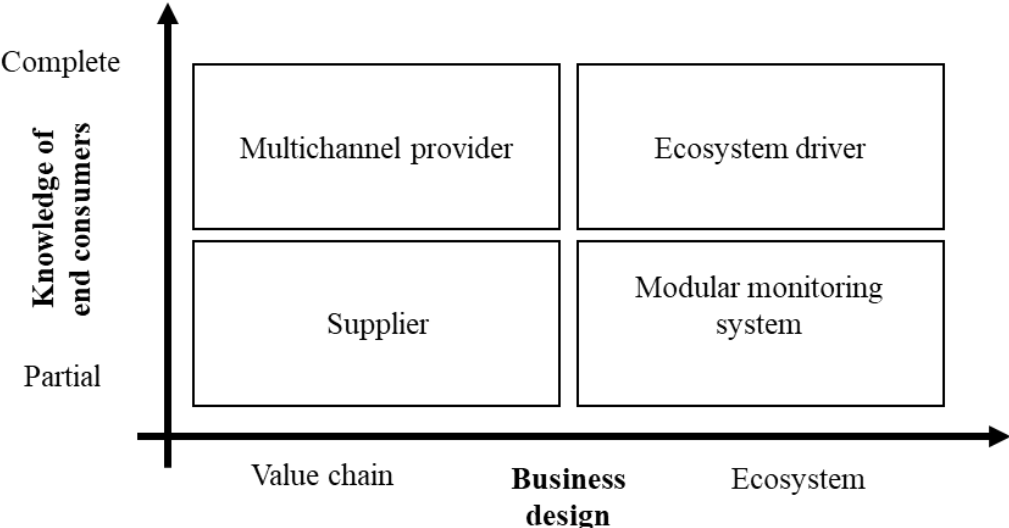


Fig.1 Business models for the digital era

Different business models can be derived from two critical dimensions, namely, the knowledge of end consumers and the business design. The business models depend on the extent of knowledge of the end consumer needs, from a lower end of partial familiarity with end consumer's needs towards a higher level of complete understanding. The business model also depends on the business design, whether to focus as a value chain business, such as those which add value to the customers and provide for example, training and after-sales services, or to further develop into an ecosystem to create a network of interconnected systems. These dimensions combine to form four business models for creating value, these are businesses as a supplier, a modular monitoring system provider, a multichannel provider or an ecosystem driver.

2.1 Supplier

Suppliers, depicted at the lower left quadrant of Fig.1 typically have little knowledge of preference for selecting their end customer, and usually sell the product through distributors or wholesale to businesses that use the supplied product or services. The product can usually be mass produced, or the service can be duplicated with repetition. In order to be sustainable as a supplier, efficiency and price plays a big role if substitutes can be easily found in the market. This type of business model must continue to provide reliable products/services and innovate to stand out from other suppliers.

Examples of such businesses in the vessel performance monitoring sector are sensor makers, where the sensors are designed to measure specific parameters and able to transmit data in a digital form. These include fuel meter makers and torque meters, sensor makers are also good examples of suppliers of products that are important components of the VPM system. Data storage companies and businesses that specialise in machine learning using data collected are examples of suppliers of services that support the VPM system.

The benefit of being a supplier business is that specialised product/services can be developed. The ability to mass produce components reduces the cost of product/services. The downside of suppliers is that often the product/services including analytics or diagnostics are available for the part supplied and do not generally deliver system wide integrity. For example, companies that provide machine learning solutions to data can provide statistical reliability of the methodology used but often cannot validate data sensibility of the source of data.

2.2 A modular monitoring system

A company that adopts a business model approach to provide modular monitoring systems lies in the lower right quadrant of Fig.1. Such a business model offers a wide range of distinct solutions. The solution of plug-and-play systems can usually work with several different partners. However, such systems are limited to specific functions and may not be freely integrated for information transfer.

Examples of such business models adapted to provide VPM systems include companies that only deal with specific type of monitoring system. The company might only specialize in fuel consumption monitoring, where a line of products is available to accommodate all sizes of pipelines, all system configurations and different fuel types. However, due to the complexity of ship systems which are made up of interconnected systems such as the hot water system, sea water system, fresh water system, propulsion system, fuel oil system etc., solely relying on such plug and play fuel monitoring systems does not allow the provision of a wider picture of vessel performances, especially when data errors in the fuel monitoring arises from different systems such as faults in the fuel injection or faults in engine misalignment. To be able to measure overall vessel performance, an integrated modular monitoring system that collects data under one single platform and is able to carry out an overall analysis is needed.

The benefit of such a business model is that a fast set up system is achievable, and specific information can be connected to the DAS within a short period of time. However, additional advanced analysis is usually not available and the data output is usually in a rigid format.

2.3 Multichannel business provider

A multichannel provider lies in the upper left quadrant of Fig.1. This type of business usually has a good knowledge of customer needs and has direct relationships with a wide customer database. Products and services of multichannel businesses are often available online with a friendly user interface.

Examples of a VPM multichannel business provider are those that provide products and services using a more rounded approach. These companies usually offer sensor selection advices, approved and reliable sensor installations, DAS to communicate with the sensors, systems for visualisation of data on-board and on-shore. The level of VPM services can usually be customised and adapted depending on the available budget and system type. Protected and safe long term and short term data storage solutions usually accompany such products. Advanced analysis of data using different techniques, including machine learning techniques are usually offered. More mature companies that adopt such models also provide advice and consultancy services to support the analysis to improve vessel performance.

The benefit of such systems is that system assurance and accountability of system integrity is usually part of the package. The products/services are usually customisable to suit specific customer's needs. Training to use the VPM system are usually available for customers to enhance the added value of the system installed. Such businesses however come with higher costs because additional research and innovation is usually carried out to meet the need of the customers, changes in market and for customised solutions. More specialised engineers, software designers, and data analysts are usually needed to support such a business model.

2.4 Ecosystem driver (Industry 4.0)

The VPM system, like the maritime industry is moving towards cyber physical system integration (Industry 4.0), where the business model of an 'ecosystem driver' is desirable. Such a business model provides a platform that connects customers needs and inter-connects all products and services available in the industry. Such a system is constantly updated with new technology and services that can be offered.

A business which acts as an ecosystem driver has a certain level of smartness embedded which advises users of the options and services that are available that best fit their needs. For example, a monitoring system with machine learning abilities can detect the need for hull cleaning of a certain vessel. Different available options to meet and solve such needs will be suggested to the customers. When the option of a self-cleaning robot is selected, the robot will be sent to solve the problem, where the location of the ship is known, and the extent of cleaning required is known. Or when there is a faulty sensor, a database of suitable sensors that can be used as a replacement will be available almost immediately. Although industry 4.0 sounds futuristic, it is rapidly becoming a reality and systematic steps must be taken in the marine industry to ensure that this is achieved.

Such an ecosystem requires sharing of reliable information on a large database, where data from an engine manufacturer is available for integration with other plug-and-play devices for data processing. This business model relies on the provision of reliable databases by different players. The maritime industry is moving towards such systems, where the data and system security of such systems is still being investigated. The creation of such an ecosystem will none the less promote the creation of new businesses and form new social networks, *Bock et al. (2017)*. Successful digital leaders in the industry have proven to have systematic data acquisition strategies and stand out based on the data platform created, to allow successful prediction and decision making based on reliable and validated data.

2.5 Summary of digital business framework

A good understanding of the type of digital business model selected will also allow better allocation of resources such as training of employees, allocation of employee's time, strategy for business expansion,

networking activities to participate in, and technology to invest in. The ecosystem driver aims to connect systems and connect processes to satisfy supply and demand in the industry. The characteristics, benefits, limitation and examples of these four digital business model frameworks introduced can be summarized in Table 1. The ecosystem (industry 4.0) encourages interaction of customers, partners, adjacent industries and government. Allows all users to tackle cyber security at all levels. A business ecosystem delivers products and services through both competition and cooperation. A healthy ecosystem inspires collaboration which aims to provide mutually beneficial results to all parties involved, encourages diverse thinking and innovation whereby the industry can benefit from provision of quick solutions. The idea is to create a collection of flexible services that can shift around and quickly be adapted to the ever-changing needs of customers.

Table 1: Characteristics, benefits, limitations and examples of digital business models

	Supplier	Modular monitoring system	Multichannel provider	Ecosystem driver (Industry 4.0)
Characteristics	Mass production of offerings, usually sold to distributors and subjected to commoditization	Plug and play product or services that are easily adaptable to the wider ecosystem	Stands out as big players in the industry, usually meets customer’s needs and provides integrated value chain	Provides a branded platform which ensures an excellent multifaceted customer experience.
Benefits	Specialised product/service Low cost producer Incremental innovation	Constant innovation of product is needed to keep up with market competition Fast set up system, able to integrate with common sensors	Provides system integrity Knowledge to customize product and services to meet customer’s needs Provides training to maximise use of product	Allows plug-and-play third party product Information sharing between customers and providers
Limitations	Usually only provides analytics on product/service developed and not as an overall system	Provides non-specific data analysis or single goal data analysis	Higher costs associated with intensive research and innovation	System security
Examples	Sensors makers Data storage providers Machine learning companies	DAS for individual system. Offers generic data analysis	DAS system with advanced analytics and advisory systems	VPM system with offers of solutions from other sectors (i.e. robotics, blockchain, new technologies)

3. Challenges in moving towards an ecosystem of interconnected VPM systems

A review of the different digital business models available shown in section 2 enhances our

understanding of components needed to achieve an ecosystem of connected VPM systems, where the knowledge of end users is important and that an ecosystem needs to be established. The challenges of moving towards the ecosystem driver business model are now presented so that steps can be taken to overcome these challenges. In order to develop a holistic vessel performance system, good management and the centralised use of information from different parties is required. The development must also be inclusive of knowledge from the seafarers who have first-hand experience at sea and the naval architects and marine engineers who have design experience, with a good knowledge base of structures, hydrodynamics, material science and engine performance to check for data sensibility range and data validity before data analyses is carried out, and to explain results from analysed data. There is also the need for mathematicians, and computer scientists who understand coding and development of software and cyber security. To achieve an advisory system, the system must also be properly informed of the policies of different parties, both local and global. A successful ecosystem driver draws power from the diversity of different skilled individuals.

All knowledge and expertise from different aspects relating to the development of VPM systems must be integrated to increase reliability of measurements in terms of sensor technology, data integration as well as understanding the effects of vessel draft, trim, speed, seaway and wind. The VPM system should be able to provide services to improve operational performance and be constantly updated to comply with standards and be adaptable to changes of technology. These data can be processed using deterministic approaches such as using industrial standards, using statistical approaches and using various machine learning techniques. Benchmarking capabilities using standards are being constantly improved to enable users to apply standards for vessel performance monitoring such as the development of ISO 19030 and applying data filters using ITTC recommendations.

This multi-directional research of optimising vessel operations, sensor technology and applying machine learning techniques can result in the slow adoption of vessel performance solutions. Research is a core activity which enables the adoption of new technology and the creation of a resilient system with regularly updated security systems.

Data reliability and data standardization remain one of the major challenges for a successful VPM ecosystem. The sharing of information is not yet readily transparent, data collected from vessels are not synchronised and not readily comparable between different ships and fleets. A multichannel VPM system can take the lead in ensuring reliable data sharing is available, which will allow delivery of solutions more rapidly than traditional approaches. Tools must also be developed to measure performance, for research, for improvements, and to identify key performance indicators.

The digital business model adapted for vessel performance monitoring provides an indication that understanding end consumer's needs and importance of sharing of information will drive the industry towards a sustainable and successful digital ecosystem. Using the data from vessel does not focus on one component but looks at the overall performance of the vessel. Understanding the business models allows providers to achieve long term investment potential.

4. Reliable databases for further development

Most vessel performance monitoring systems available on the market to date can act as a modular monitoring system or a multichannel provider. The VPM system design will play an important role in the transition of the marine industry into Industry 4.0, where reliable databases are required to feed into the ecosystem. An example of a multichannel provider is Ascenz's Shipulse, a leading maritime VPM system, particularly in Asia, and is demonstrated here. In addition, the deliberate efforts taken by the company to encourage the move towards an ecosystem driver business model are highlighted.

4.1 A structured and reliable database

Standardisation of data architecture is one of the key challenges for industries to move towards an ecosystem driver model, *Weyer et al. (2015)*. Fig.2 shows a methodology adopted for ships to ensure a

structured and reliable database is available for use and for integration with other databases. Row A shows the categorisation of the database, row B shows the required qualitative and quantitative time stamps of each data set, row C shows the independent data validation step needed for each category and row D shows examples of analysis that can be carried out in each category. The categories of data can be broken down into data output from individual sensors, data from an individual system and integrated systems within the ship and immediate data collected from external systems. The on-board data acquisition unit and computer can process these different data categories. The time stamp of each parameter is recorded and the unit is standardised to enable further integration of this database into external databases.

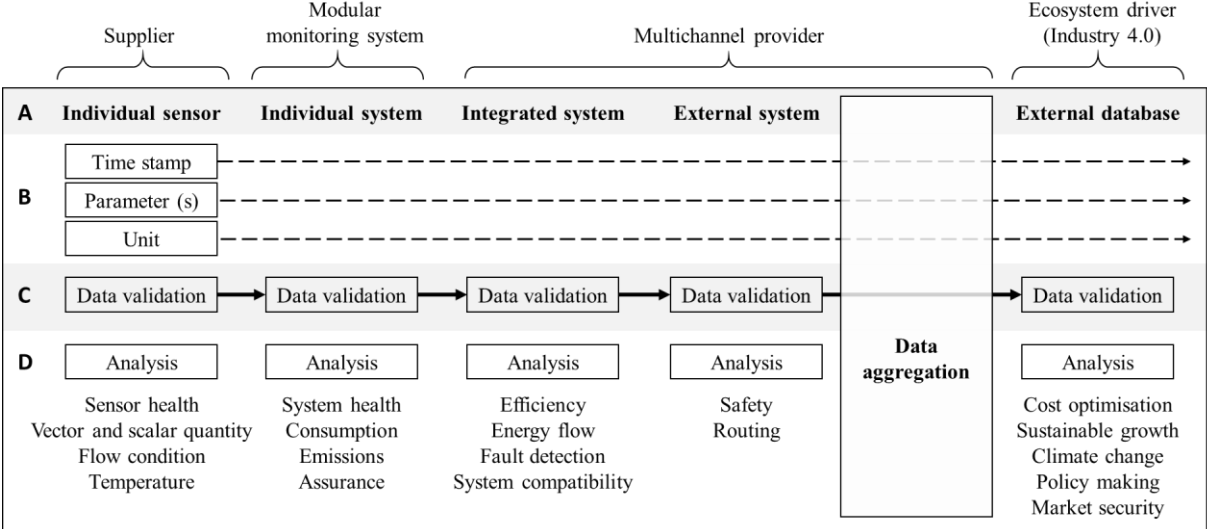


Fig.2 Developing a structured and reliable database

Independent data validation is required for each category to ensure that the data is reliable when carried forward for further analysis. After independent data validation, each category will be able to provide separate information on the ship. A detailed example is further shown in Fig.3. For example, in an individual sensor category, such as a Coriolis flow meter, the data collected from an individual sensor can be analysed to provide information about the health of the sensors and to inform operators if any calibration is required, or if the sensor integrity has been compromised. The vector and scalar quantity of the parameter monitored can be derived, and information such as flow condition and temperature changes at the location of the sensor can be monitored. Analysis that can be derived from an individual system such as the fuel consumption system can be used to inform the actual fuel consumption during each operation and allows understanding of the system health and assurance of the system. The data can also be used to further inform the estimated emissions.

When this system is integrated with other ship systems such as the propulsion system and the engine system, analysis can be carried out to inform the efficiency of the machinery. Further detailed analysis of frequency, noise and vibration can be used for fault detection. This information can be used to understand system compatibility and test the possible boundaries for system improvement. Higher levels of analysis can be carried out using data from integrated systems, such as to understand the energy flow throughout the entire vessel under different conditions and to provide recommended optimum operational advices. An example of a common external system integration is the metocean data which is useful when directly integrated within the ship data system, to provide instantaneous operational analysis and forecasted routing to ensure safety, comfort and minimise fuel consumption.

A multichannel provider must have a good grasp of the market and customer needs and is able to provide a structured and reliable database of a ship. This can be done by standardising the data collection process and by interaction with suppliers and customers. Every category must be validated to ensure that the ultimate ship database is reliable and readily available for integration with other databases. The outlook

of an ecosystem driver is the integration of different databases to provide a well connected cyber physical system to provide an overall cost optimisation, ensure sustainable growth of maritime businesses, using data for policy making and to tackle climate change. A systematically thought-out data collection process will generate a reliable database that can be used to make predictions and business decisions as well as ensuring market security.

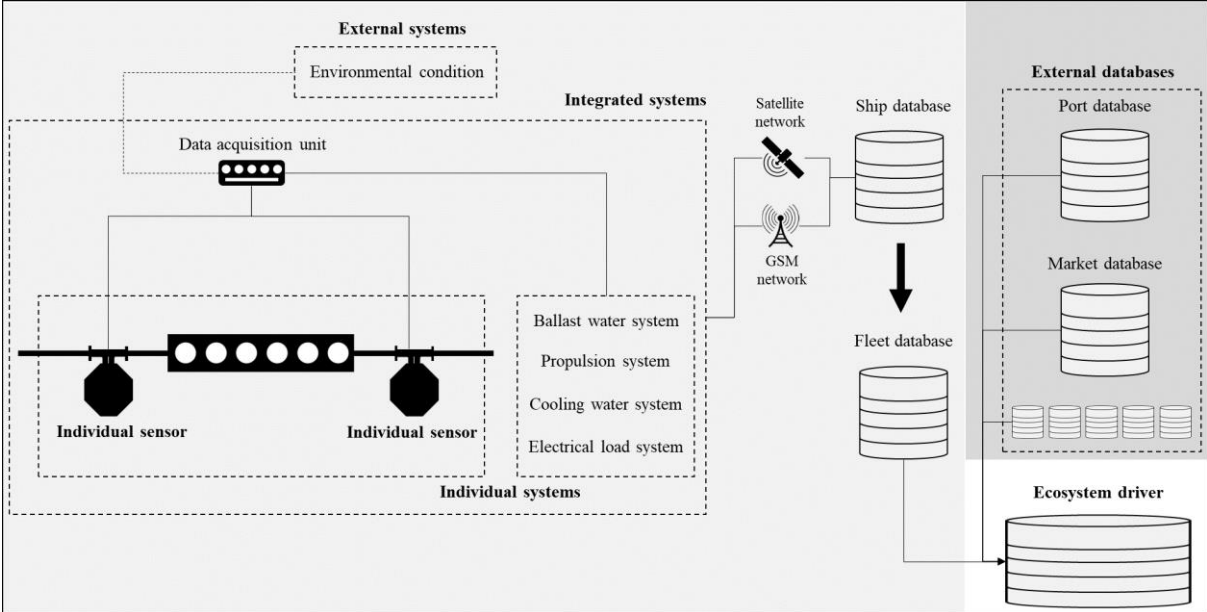
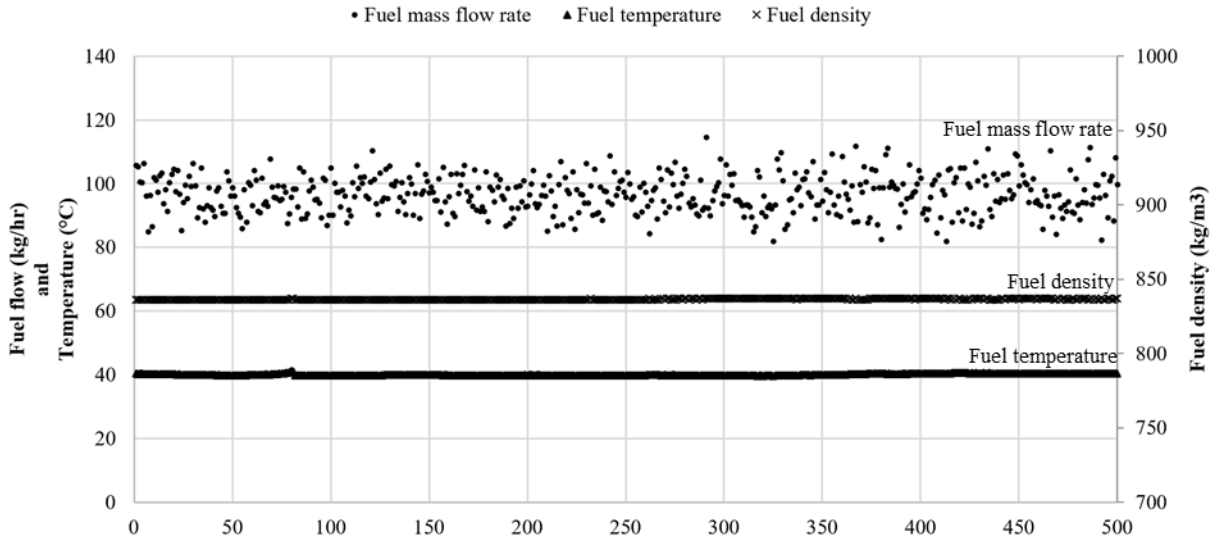


Fig.3 Data integration of individual sensors required for the development of an ‘ecosystem driver’ business model

Fig.3 shows that the data collected from individual sensors makes up the fundamental data for individual systems and is used for integration between different systems. The data collected under a single data acquisition unit is time stamped and sent to an on-shore database, contributing to the fleet database, which will be able to feed into the ecosystem driver for integration with external databases such as port and market databases.

4.2 Database of ship operational parameters

Prior to analysis carried out on vessel data, a good understanding of each data source and also each data validation process must be carried out. An example of data validation for an individual system such as a mass flow meter is to compare the measured fuel density, temperature and flow rate of the sensor. Fig.4 shows an example of data collected from a Coriolis fuel flow meter that is measuring marine gas oil. The data from the sensor shows that the density of the fuel oil is approximately 840kg/m³, which falls within a confidence limit of the expected value. Further validation can be carried when required from the bunkering notes of the vessel. The fuel temperature at the supply line moving through the sensor shows a steady temperature of approximately 40°C. This information indicates that the sensor is providing sensible data and is working in a healthy manner. Boundary conditions can be set to enable alarm triggers when deviation of data from expected levels are recorded, to trigger further investigation into system health. The data collected from sensor can also be used to indicate sensor tampering or situations where the fuel in the pipeline is not a single-phase flow.



Vessel speed over ground (SOG) is derived using global positioning system (GPS) on-board the vessel whilst vessel speed through water (STW) can be obtained using different types of approach such as using electromagnetic, pitometer and Doppler methods. Fig.5 shows histograms that represents the difference in data for SOG and STW using two different sets of data. Table 2 shows the comparison of distribution of data. In reality, not all vessels have a speed through water sensor. Fig.5 and Table 2 show that there could be obvious differences when using SOG and STW to analyse vessel hull and propeller performances.

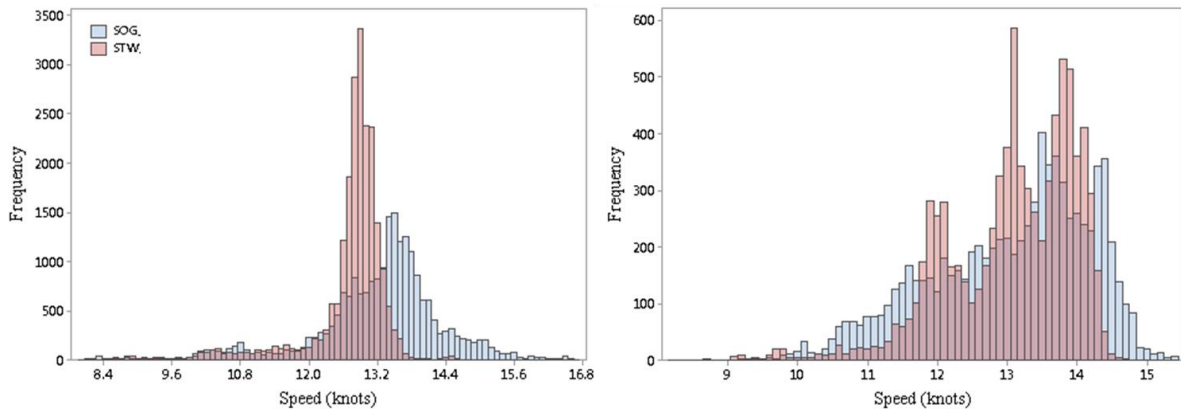


Table 2: Distribution of data using measurement of SOG and STW

Data set	Mean	Standard deviation
1 (left)	13.23	1.162
	12.70	0.752
2 (right)	13.05	1.148
	13.06	0.917

Once all the parameters logged in the data acquisition system are validated, analysis can be carried out using the full data set. An example of useful further analysis is to understand the power needed to move the vessel through the water. The data used to plot Fig.5 were filtered for vessel operations and only considered when the vessel is in transit operation. One month's worth of data is shown in Fig.6. A continuous monitoring of such data trends can be used to estimate the hull and propeller degradation through time, whereby losses in hull and propeller efficiency can be calculated. In addition, the fuel consumption by the engine to generate shaft power is also monitored. The fuel consumption and shaft

power comparison can be used to calculate the specific fuel oil consumption of the engine, this value can be monitored to observe the changes in engine efficiency and acts as a tool to prompt maintenance services and measure changes of engine efficiency after maintenance works are carried out.

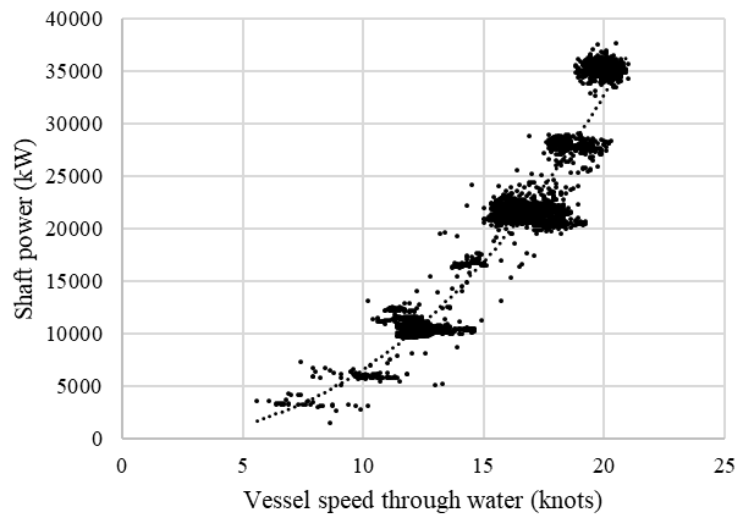


Fig.6 Example of shaft power vs vessel speed through water

5. Conclusions

The sustainable way of moving forward towards an ecosystem driver business model for interconnected VPMs is to carefully but quickly bring together and integrate the expertise of people with emerging technologies. A sustainable digital business model can improve performance of operations, provide economic incentives for different stakeholders, and even provide data-bases which provide evidence to underpin and justify advice given on shipping conduct within a complex and ever changing political and environmental industry landscape. From the examples given, it is clear that a well thought through digital ecosystem business model can be further enhanced by using carefully structured databases, improving the quality and performance of individual ships, the entire fleet, and the businesses themselves. The next step is to take advantage of reliable databases developed from VPM systems and to integrate them safely and efficiently with other systems such as port authorities and systems within the supply chain of trades and services.

References

BOCK, R.; IANSITI, M.; LAKHANI, K.R. (2017), *What the companies on right side of the digital business divide have in common*, Harvard Business Review

CORADDU, A.; LIM, S.; ONETO, L.; PAZOUKI, K.; NORMAN, R.; MURPHY, A.J. (2019), *A novelty detection approach to diagnosing hull and propeller fouling*, Ocean Engineering

CRANDELL, C. (2017), *The problem with data is too much the wrong stuff*, Forbes, <https://www.forbes.com/sites/christinecrandell/2017/06/26/the-problem-with-data-is-too-much-of-the-wrong-stuff/#1d429a12d5f4>

EU (2015), *Regulation (EU) 2015/757 of the European Parliament and of the Council of 29 April 2015 on the monitoring, reporting and verification of carbon dioxide emissions from maritime transport, and amending Directive 2009/16/EC*, Official Journal of the European Union, L 123/55, 19.5.2015

IMO (2009), *Resolution MEPC.1/Cric.684, Guidelines for the voluntary use of the ship energy efficiency operational indicator (EEOI)*, International Maritime Organization, London

IMO (2012), *Resolution MEPC.213(63), 2012 Guidelines for the development of a ship energy efficiency management plan (SEEMP)*, International Maritime Organization, London

IMO (2016), *Resolution MEPC.278(70) Data collection system for fuel oil consumption of ships*, IMO Doc MEPC.70/18/Add.1., International Maritime Organization, London

PERERA, L.P.; MO, B. (2017), *Marine Engine-Centered Data Analytics for Ship Performance Monitoring*, J. Offshore Mechanics and Arctic Engineering 139(2), p.021301

PERI, D. (2016), *Robust Design Optimization for the refit of a cargo ship using real seagoing data*, Ocean Engineering 123, pp.103-115

RØDSETH, Ø.J.; PERERA, L.P.; MO, B. (2016), *Big data in shipping - Challenges and opportunities*, 15th COMPIT Conf., Lecce

WEYER, S.; SCHMITT, M.; OHMER, M.; GORECKY, D. (2015), *Towards Industry 4.0 - Standardization as the crucial challenge for highly modular, multi-vendor production systems*, IFAC - Papersonline 48(3), pp.579-584

ZHU, P. (2015), *Digital Master: Debunk the Myths of Enterprise Digital Maturity*, Lulu Press

Distributing Real-Time Measurements of Speed Through Water from Ship to Shore

Gunnar Prytz, Miros, Asker/Norway, gp@miros-group.com

Rune Gangeskar, Miros, Asker/Norway, rg@miros-group.com

Vemund Svanes Bertelsen, Miros, Asker/Norway, vsb@miros-group.com

Abstract

This paper describes how latest generation radar-based remote sensing solutions give high-quality information about ocean wave parameters such as wave heights, directions and periods, surface current magnitude and direction and ship Speed Through Water (STW). Combining the sensing technology with Internet-of-Things technologies allows making accurate sea state data available in real-time both onboard and onshore. This enables significant improvements in such applications as hull fouling estimation and speed optimization. This paper will present such a solution in detail together with some examples from testing on vessels.

1. Introduction

The shipping industry is currently undergoing a transformation due to digitalization. A strong focus on cost of operations, operational efficiency and on the environmental aspects associated with shipping are some of the main driving forces behind this development.

Situational awareness is a necessary ingredient in the digitalization process. One area that has seen considerable improvements recently is within real-time sea state measurements. Recent developments within radar-based technologies have given access to accurate sea state data that can be used to optimize ship operations, Gangeskar (2017,2018a,2019), Gangeskar et al. (2018). State-of-the-art radar-based sea state measurements can measure both ocean waves and ocean currents accurately under widely varying conditions and with high availability, reliability and accuracy.

Sea state has a significant impact on ship performance. This holds true for both ocean waves and ocean currents. There are intricate relationships between waves and ship performance requiring advanced models that take into account such factors as 3D hull properties and loading conditions. The situation is somewhat simpler when it comes to ocean currents. Currents coming against the direction of ship motion means that more water needs to be displaced per time unit compared to a situation with no current. Similarly, currents travelling in the direction of ship motion means that less water needs to be displaced per time unit. Hence, the current component going in the direction parallel or antiparallel to the vessel heading has a major influence on vessel performance. Currents travelling perpendicular to the ship motion might also lead to a need to spend energy to counter the forces inflicted by the currents. Thus, the presence of ocean currents has a profound influence on the performance of the vessel.

The Speed Through Water (STW) parameter is the vessel speed with respect to the water. STW is equal to the Speed Over Ground (SOG) when there is no ocean current present. SOG is easily measured by means of a GPS receiver. STW, however, has not been easily measured in an accurate and reliable way until now, Gangeskar (2019).

Ocean surface current measurements from moving vessels by traditional underwater (in-situ) instrumentation are associated with challenges and data heavily influenced by noise. Systems measuring the speed through water (STW) are equally influenced by similar disturbances affecting the vessel speed log, Antola et al. (2017), Baur (2016), Bos (2016), Fritz (2016). Wave measurements from underwater instrumentation are only available on rare occasions. The following items are relevant for both acoustic Doppler current profilers (ADCPs), Flagg et al. (1998), King et al. (1993), New (1992), and other instruments based on traditional in-situ measurement principles.

- Underwater equipment generally involves installation and maintenance procedures being both time-consuming and expensive.
- Underwater equipment is exposed to fouling, *Carchen et al. (2017)*, *Goler et al. (2017)*, *Kelling (2017)*.
- Measurements are disturbed by air bubbles, turbulence, and inhomogeneous hydrodynamics caused by the vessel motion and propellers, *Bos (2016)*, *Carchen et al. (2017)*, *Brown et al. (2001)*.
- Measurements are disturbed by other instruments, for instance acoustic echo sounders and vessel speed logs.
- The surface current itself is considerably affected by the vessel motion.
- Sensors are frequently inadequately calibrated, *Antola et al. (2017)*, *Bos (2016)*, giving systematic errors in certain speed ranges, *Antola et al. (2017)*.

A vessel has an optimal speed which in simple terms depends on the speed vs. fuel relationship of the vessel and the efficiency characteristics of the propulsion configuration (e.g. the propellers). Ocean currents of up to several knots can exist on the oceans which means STW might be quite different from SOG. It is therefore STW and not SOG that should be used as the basis for vessel performance calculations, i.e. how fast is the vessel moving with a given supply of fuel. Thus, STW is a very important parameter in ship performance optimization.

There are several vessel applications that will benefit from accurate STW measurements. Hull performance is often analyzed by investigating the amount of fuel consumed at a given speed. Hull fouling will lead to increased friction and thus increased fuel consumption at a specific speed. This is typically based on SOG measurements from a GPS or heavily filtered STW measurements from underwater sensors. Hull cleaning can be a very expensive process and thus it is important to estimate the actual hull condition as accurately as possible. Thus, accurate STW measurements can be used to improve planning of hull cleaning or to investigate the effectiveness of hull cleaning procedures or hull coatings. Related use cases might be related to performance degradation of parts of the drivetrain, e.g. the propellers.

While hull performance estimations can be made in retrospect with historical data of medium to low time resolution, there is another very important application that benefits from having access to real-time STW measurements. A vessel has an optimal speed where the fuel consumption is the lowest. The optimal speed is measured relative to the water, i.e. accurate STW measurements are required. Whenever possible, there is a significant potential for fuel savings by making sure that the vessel STW is optimal. The fuel savings potential can range up to tens of tons per day for large vessels in areas with currents of 1-2 knots. Due to the accuracies required, it is in most cases not feasible to rely on theoretical models of surface current. The actual speed optimization can be done either manually by the crew or automatically by an autopilot system.

Traditionally, speed control or autopilot systems have been based on GPS input as the STW sensors have not been reliable enough. With the recent STW solution from Miros it is now possible to have access to STW measurements that are reliable and accurate enough to be used in real time for speed optimization, *Gangeskar (2018,2019)*, <https://www.miros-group.com/wp-content/uploads/2017/11/Wavex-v5.7-Datasheet.pdf>.

Traditionally, information from sensors and automation systems onboard ships have been available mainly for local use by various onboard systems and users. Remote connections have been limited in bandwidth and functionality, complex to install, manage and use and connected to highly proprietary platforms with limited usability for end customers. This no longer needs to be the case. An abundance of cloud platforms, modern communication technologies and Internet-of-Things solutions makes it considerably easier to build end-to-end solutions that are cost-efficient and easy to use. A powerful example of such a technology platform is Microsoft Azure, which offers a very wide set of services and functions to enable seamless integration of sensors, data handling, processing, visualization and

distribution, both locally (i.e. on the Edge) and remotely (i.e. in the Cloud). Particularly, the strong combination of Edge and Cloud computing, often referred to as hybrid computing, means that Microsoft Azure is a very attractive platform to build applications related to the Internet-of-Things and digitalization.

In the rest of this paper, we shall focus on describing the system based on imaging X-band radar that can provide reliable STW measurements. Furthermore, the results from a verification study onboard a vessel will be presented in detail. Finally, the integration aspects will be discussed with focus on how modern IoT technologies can simplify the distribution of STW data from ship to shore.

2. Measurement principle for STW based on imaging X-band radar

Wavex provides current measurements with high accuracy, *Gangeskar (2018a,b,c)*. Measuring the STW has much in common with measuring currents, and the two measurements are generally based on the same physical principles. The major difference is what the measured water speed is referred to: the vessel when measuring the STW, and a fixed position when measuring currents.

The vessel's velocity through water and current velocity are related through:

$$\vec{v}_{STW} = \vec{v}_{SOG} - \vec{U}, \quad (1)$$

where \vec{v}_{SOG} is the vessel's velocity over ground. Therefore, obtaining reliable current measurements implies that also STW measurements will be reliable, as they are related to each other (at the same depth) through the speed over ground (SOG), which can easily be extracted from GPS data.

Fig.1 shows the basic components in a Wavex system on a moving vessel. Specialized, DNV type approved hardware is connected to the analog video signal output from a marine navigation X-band radar. This hardware digitizes the analog radar video and outputs a radar image timeseries. Each radar image includes a sector covering the STW measurement area.

Digitized images can also be acquired directly from radars with digital data output, commonly known as IP (Internet Protocol) radars. This eliminates the need for additional digitalization hardware.

The Wavex system requires certain radar image meta-data from a GPS and a gyro compass.

To provide STW estimates, all required data are collected, synchronized and processed on the system computer.

Optimum STW measurement performance requires radar images with sufficient spatial resolution. The radar's range resolution is determined by the radar pulse width, and the azimuth resolution is determined by the radar antenna beamwidth. For optimal accuracy, the radar should be operated in short pulse mode. (If a solid-state X-band radar, utilizing pulse compression techniques, is used, the spatial resolution in the STW measure area can be sufficient without compromising the radars navigation performance.) In addition, a wind speed of at least 2 – 3 m/s is required. At this wind speed, the sea surface gets sufficiently rough to create sufficient electromagnetic backscatter, *Skolnik (1980)*. Gravity waves modulate the ocean surface backscatter. A radar image with a clearly visible wave pattern is shown in Fig.2.

Wavex bases its measurements on radar images covering local areas of interest, in a reasonable distance from any disturbing structures, including the vessel hull. Fig.3 shows how the STW measure areas are extracted from the radar images. The measure areas are called Cartesian image sections and are defined during system commissioning through software configuration. Dedicated algorithms process these images to provide the user with real-time STW data. The measure areas can be changed by software reconfiguration at any time.

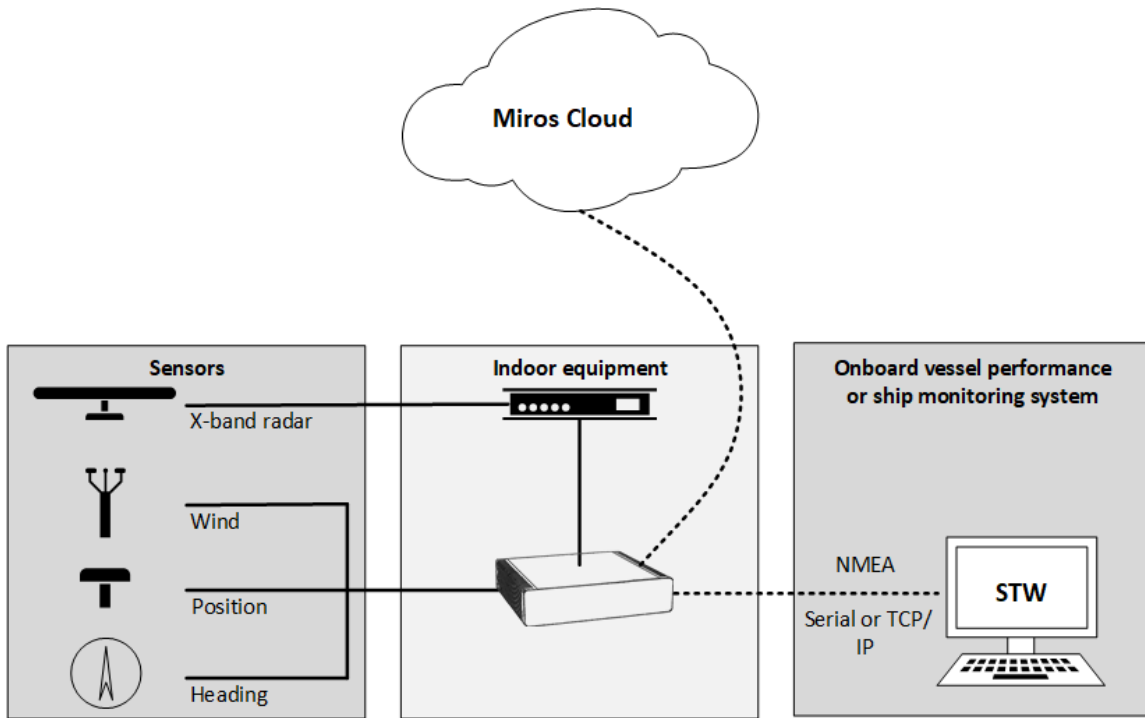


Fig.1: Schematic diagram of system based on imaging X-band radar

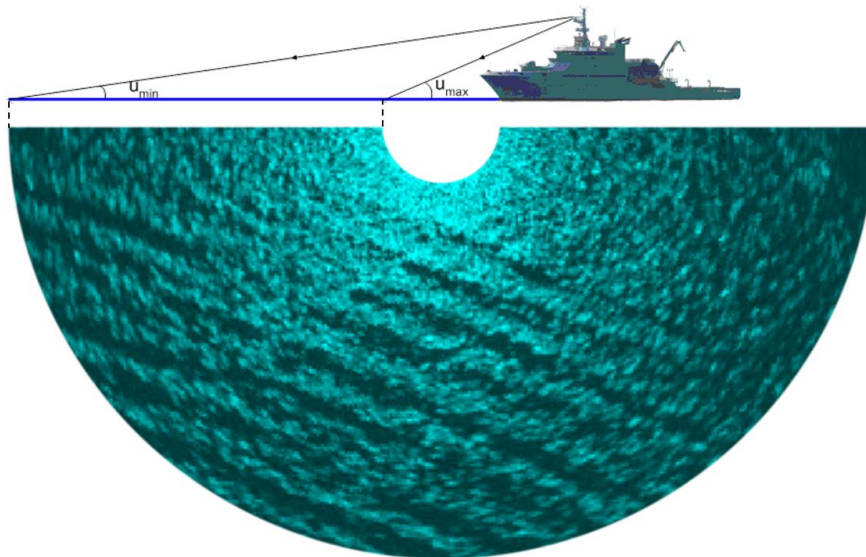


Fig.2: Imaging radar

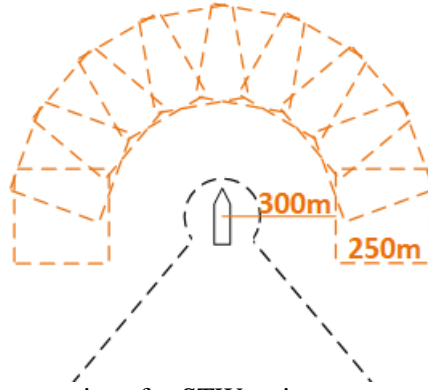


Fig.3: How Cartesian image sections for STW estimates are extracted from a radar image.

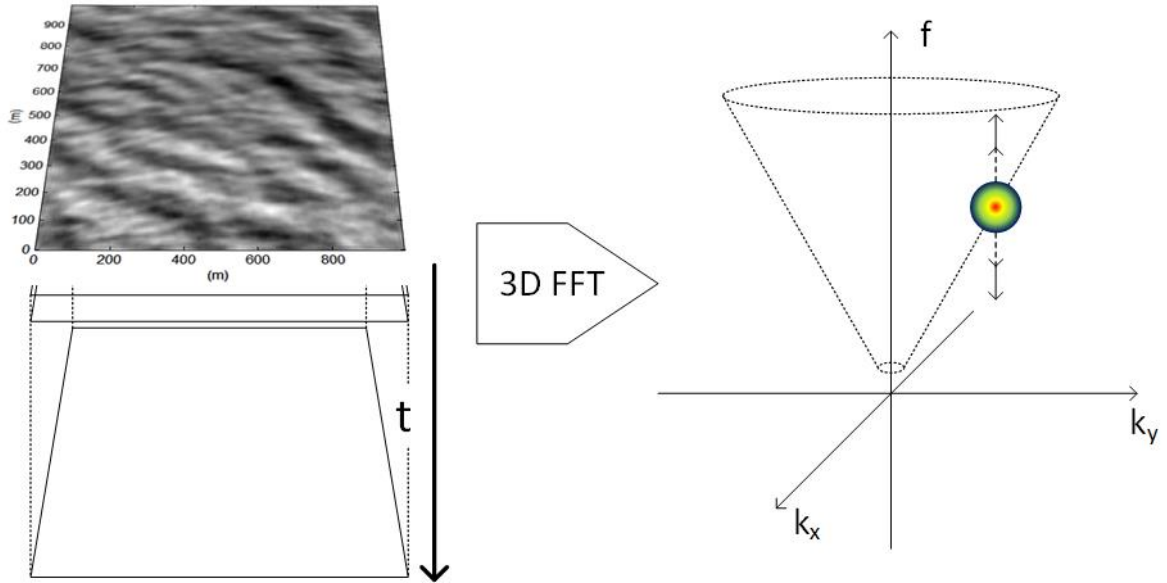


Fig.4: Cartesian image section time series are transformed into a wavenumber-frequency spectrum.

Fig.4 illustrates how 3-D fast Fourier transforms (FFTs) are applied to time series of Cartesian images, giving 3-D spectra with information about the power present at various wavenumbers and frequencies, *Young et al. (1985)*. Various sorts of noise filtering are applied before STW is estimated from the wavenumber-frequency spectra using an improved method developed by Miros. The method is, as previously known methods, based on our already existing knowledge about the relation between wavenumbers and frequencies of ocean gravity waves for zero current, i.e. the dispersion relation, *Pond et al. (1983)*:

$$\omega_0^2 = g|\vec{k}| \tanh(|\vec{k}|d) \quad (2)$$

where ω_0 is the wave frequency, \vec{k} is the wavenumber vector, d is the water depth, and g is the gravity of Earth. If there is a surface current \vec{U} relative to the radar, a Doppler frequency shift is introduced in the wave frequency:

$$\omega = \omega_0 + \vec{k} \cdot \vec{U} \quad (3)$$

This Doppler shift causes the energy in the 3-D spectra frequency planes to be located on ellipses, rather than circles. Based on the power distribution in the wavenumber-frequency spectra, the current vector can be estimated.

Miros has recently developed further improvements to the method used for estimating ocean surface currents from X-band radar images. This includes an improved method utilizing the full power distribution properties, improved motion compensation, as well as several improvements increasing performance under conditions with high current speeds and low signal-to-noise ratios. The method also includes various functionalities to automatically detect and tag data with respect to quality.

3. Pilot verification of speed through water functionality at Arctic Lady

A number of Wavex pilot systems have been installed on various vessels using various sorts of X-band radars. The system reliability and the accuracy of radar-based STW measurements have been examined and verified by comparing with theoretical models and standard speed logs over large geographical areas in a wide range of weather conditions and sea states.

3.1. Data acquisition

The following examples, based on data acquired from the LNG carrier Arctic Lady, were published in *Gangeskar (2019)* in agreement with the vessel's owner Høegh LNG. With help from the crew, months of data were made available from their travels between Hammerfest in Norway and Marseilles in France. In addition to Wavex measurements, simultaneous data were acquired from the on-board acoustic speed log, from the Norshelf model by the Norwegian Meteorological Institute, and from the Irish Marine Institute Northeast Atlantic Model. Fig.5 shows the route during a period of simultaneous data from all sources, from September 15 to October 31.

The **acoustic speed log** on Arctic Lady is a JLN-550 Doppler Sonar (SDME) provided by JRC, <http://www.jrc.co.jp/eng/product/lineup/jln550/pdf/JLN-550.pdf>, which is an advanced and widely used instrument for measuring the STW from vessels. It is a two-axis, four-beam pulse Doppler Sonar with optional rate of turn gyro, operating at 2 MHz (for water tracking), measuring a few meters below the hull bottom. Information about the STW longitudinal component is obtained via the VBW (dual ground/water speed) NMEA string. This is the STW component parallel to the vessel heading, with positive values when the vessel moves forward relative to the water.

The **Norshelf model**, *Röhrs et al. (2018)*, provides ocean current data for the Norwegian Shelf Sea. The model has been set up at the Norwegian Meteorological Institute (MET) and includes the Skagerak in the southeast, the northern parts of the North Sea, the shelf sea off western Norway including the shelf slope, and parts of the Barents Sea in the north, that is, a considerable part of section 1 of the route, Fig.5. The model provides data at a horizontal resolution of 2.4 km at a temporal resolution of 1 hour. Data are available from MET Norway Thredds Service, <http://thredds.met.no/thredds/fou-hi/norshelf.html>, in NetCDF files. Model data representing 5 m depth were chosen because this is close to the effective measurement depth of the radar-based system.

The dataset **Irish Marine Institute Northeast Atlantic Model** provides surface current vectors for the Irish waters in the northeast Atlantic, *Dabrowski et al. (2016)*, that is, a considerable part of section 2 of the route, Fig.5. The ROMS hydrodynamic model (Regional Ocean Modeling System) uses a mean horizontal resolution of 1.9 km and provides data at a temporal resolution of 1 hour. Data for the last week are available via Thredds and ERDDAP servers in various formats, https://erddap.marine.ie/erddap/griddap/IMI_NEATL.html. Older data were ordered from and delivered directly by the data steward at the Irish Marine Institute in Matlab format.

3.2. Statistics and time series

Current data from the models were extracted at times and positions of interest, indicated by the route in Fig.5, using time and position data from the vessel and linear interpolation. This is partly similar to what was done in *Gangeskar (2018a)* when defining a dynamic tidal model following the vessel's route. As already stated above, the accuracy of STW measurements is closely linked to the accuracy of current measurements, defined by (1). Hence, for convenience, as the models and the Wavex system already

provides current data, we chose to consider current values as the basis for statistical measures (Table I). The STW longitudinal component output from the speed log was simply converted to the current longitudinal component using (1).

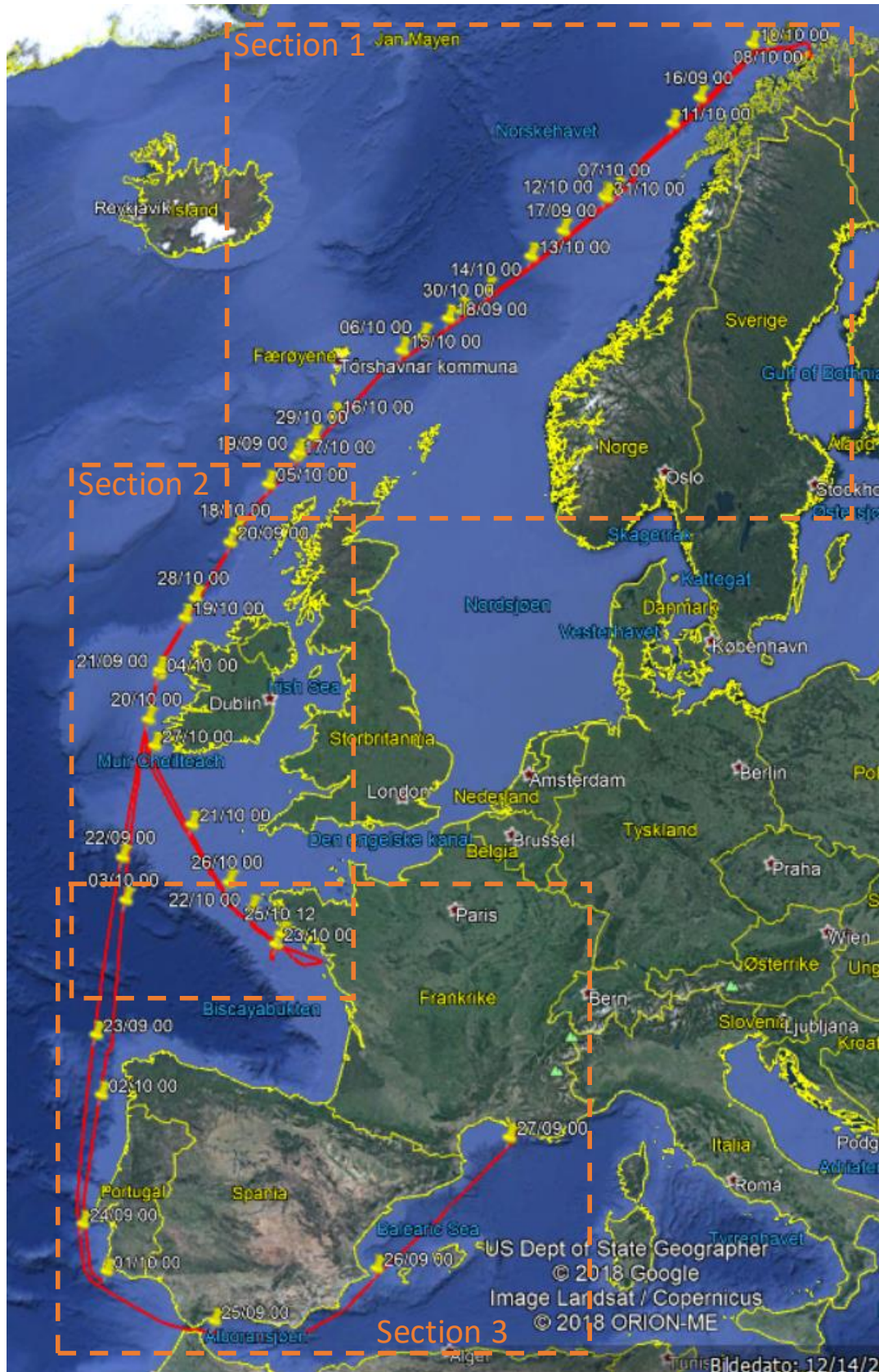


Fig.5: Route from September 15, 2018 to October 31, 2018, indicated by red lines in Google Earth

In order to compensate for different averaging strategies, to make statistical comparison more balanced, to smooth out any minor temporal offsets between various data sources, and to make measured data more comparable to model data, an additional temporal averaging of measured data was performed before calculating statistics. For this purpose, a 40-min centered average filter was applied to the time series. Mean and root-mean-square (RMS) deviations between individual data sources were calculated.

Fig.6 provides an overview of longitudinal current components and STW during the entire route shown in Fig.5. No additional averaging is applied to these data. Data are missing in three periods because most of the measurement systems were turned off when the vessel was at rest in Hammerfest (Norway), Marseilles (France), and Saint-Nazaire (France). Apart from these periods, the data capture is complete. The rate of defined STW data from the Wavex system is 99.94 % during the periods with available radar images. In the following, we will look further into the details for a couple of shorter periods.

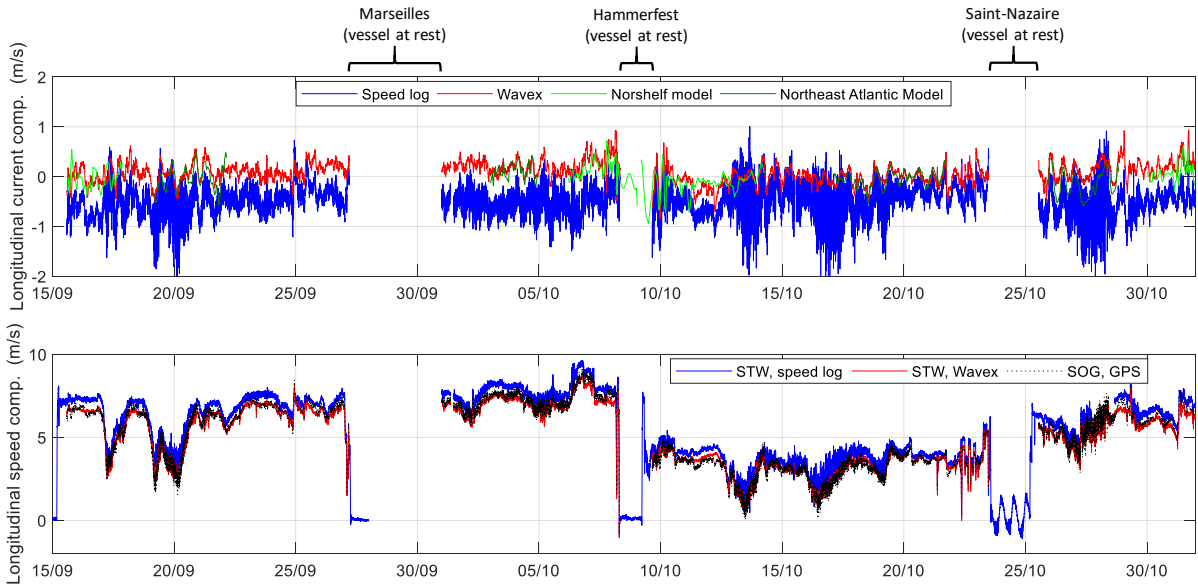


Fig.6: Overview of longitudinal current components and STW during the entire route shown in Fig.5
No additional averaging.

Table I: Deviations between longitudinal current components from radar-based system, speed log, and models, based on all available data

	Radar-based vs.		Speed log vs.		Radar-based vs. speed log
	Norshel model	Northeast Atlantic Model	Norshel model	Northeast Atlantic Model	
Offset (m/s)	-0.08	-0.11	0.49	0.46	-0.56
RMS dev. (m/s)	0.24	0.20	0.55	0.49	0.59

Fig.7 shows five days of current and wind data from a period covered by the Northeast Atlantic Model. The wind speed varies from 0 to 15 m/s, and the surface current in the area is dominated by the tidal contribution, making it easy to visually observe the agreement between model data and measurements. Currents in this area are more homogeneous and stable, with less eddies and stronger tidal dominance, than for instance in the region covered by the Norshel model. This may make this model more accurate, and it makes comparison easier, because different averaging strategies and possible remaining temporal and spatial offsets will make less influence on the results. Table I (based on all available data) shows that measurements agree slightly better with the Northeast Atlantic Model than with the Norshel model.

Fig.8 shows the longitudinal current component and the STW during the same period, without any additional averaging. It is evident that the radar-based system produces considerably smoother data than the speed log. The reason for the varying amount of noise observed in speed log data is not known. It is also clear that the speed log measurements are systematically erroneous, with an offset of approximately 0.5 m/s. This can also be observed from the statistics in Table I (despite additional averaging before calculating statistics), in which data from the radar-based measurements are considerably more consistent with model data (comparing green and red columns). Current magnitudes in the range 0–0.5 m/s are expected in this region and period. In the context of fuel optimization, the observed offset in speed log data could mean an additional fuel cost corresponding to tens of tons of fuel a day for one ship.

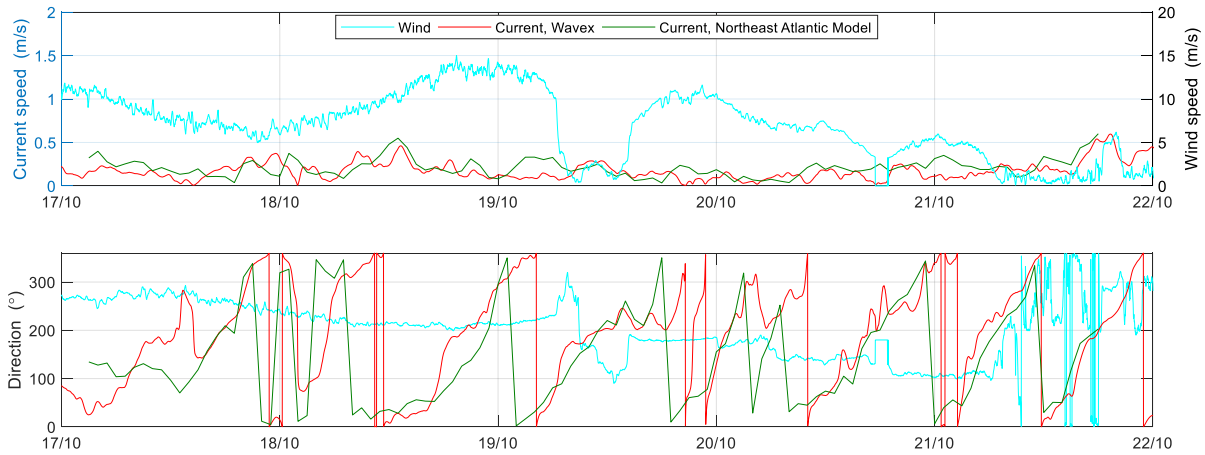


Fig.7: Time series of current and wind data from Arctic Lady, during a period covered by the Northeast Atlantic Model; radar-based compared to Northeast Atlantic Model.

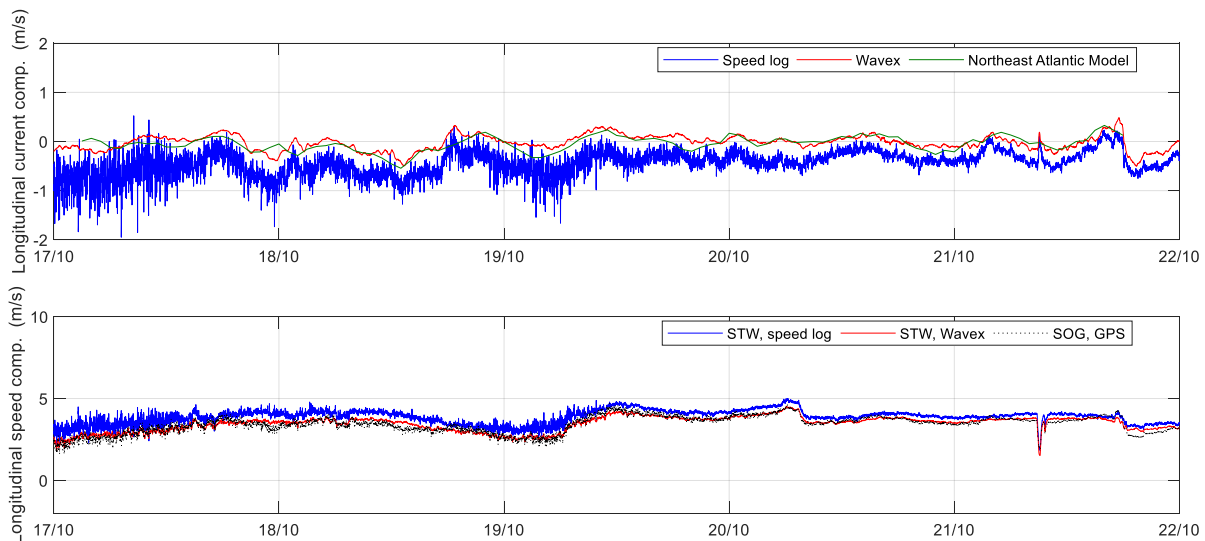


Fig.8: Time series of longitudinal current components and speeds, during a period covered by the Northeast Atlantic Model; radar-based compared to Northeast Atlantic Model, speed log, and GPS (partly covered by radar-based). No additional averaging.

Fig.9 shows the longitudinal current component and the STW during a period covered by the Norsshelf model, without any additional averaging. The wind speed varies from 1 to 19 m/s. Less homogeneous currents and more local eddies, combined with different averaging strategies, make comparison more difficult, because both model data and measurements vary relatively quickly with position and time. Still, clearly the radar-based system produces considerably smoother data than the speed log; the speed log data are influenced by an offset-like error, though the covariance between the two sensors looks relatively consistent. Current magnitudes in the range 0–0.5 m/s are expected in this region and period.

Some possible explanations for observed deviations between various data sources are:

- differences in spatial and temporal averaging strategies;
- differences in effective measurement depth;
- minor temporal offsets between various data sources;
- inaccurate environmental data input to models;
- finite resolution and accuracy in models;
- measurement errors in sensors.

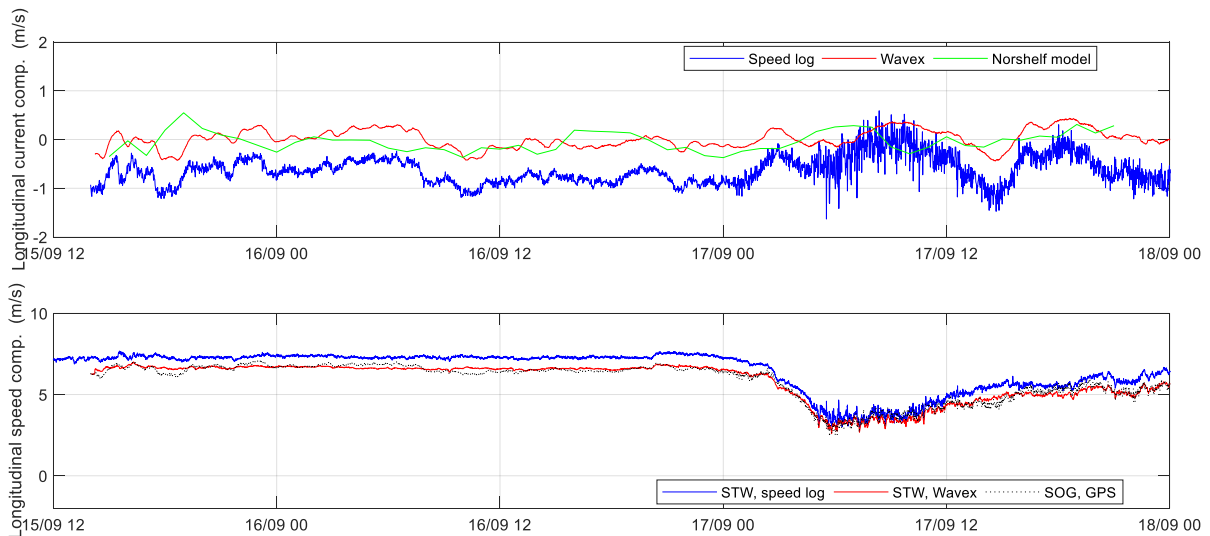


Fig.9: Time series of longitudinal current components and speeds, during a period covered by the Norshel model; radar-based compared to Norshel model, speed log, and GPS. No additional averaging.

4. Making STW data available onboard and onshore

Easy access to vast amounts of data from a multitude of sources is currently driving a wave of innovation that impacts how vessels are designed, built, operated and maintained. Processes that used to be largely based on manual observations and retrospective analysis based on incomplete data sets can now be improved and automated with the access to detailed, reliable and accurate data. Modern technologies make sure that the information can be made available both on the vessel and onshore and thus enables a wide range of improvements.

In order to support the various application use cases mentioned above, *Gangeskar (2019)*, there is a need to have a flexible solution that allows easy access to the STW data both onboard the vessel and onshore. The onboard requirement is particularly related to real-time usage for speed optimization. The onshore requirement is related to hull and propeller performance estimations and the optimization of hull cleaning activities. In addition, there are use cases for fleet management, including comparing and optimizing vessel fleets, as well as reporting.

4.1. Access to STW data onboard

The STW data from a system such as the Miros system discussed in this paper can easily be made available onboard the vessel either on dedicated displays, on web displays or via integration into a 3rd party system onboard, *Miros AS (2017)*. Traditionally, such integration has been based on simple transmission of NMEA (National Marine Electronics Association) formatted data on serial links or embedded in TCP or UDP transmissions on an Ethernet connection. A UDP transmission can be seen as a simple push type of communication whereas a TCP connection can be seen as a pull connection as it has to be initiated by the receiver. Sending NMEA data over a serial or Ethernet connection is still a very common way to integrate sensors and systems.

Modern technologies facilitate integration between sensors and systems. One common technology found in this domain is the MQTT (Message Queuing Telemetry Transport) protocol. MQTT is a publish-subscribe type of protocol where a sensor (MQTT client) can send data to a server (often called an MQTT broker). The broker is then responsible for distributing the information. Any MQTT client can both send and receive data from the broker. MQTT is one of several commonly used IoT protocols. One of the major advantages of MQTT over legacy solutions is that the sensor does not have to know who the receivers of the data are, it only needs to relate to the broker. This increases reliability as the remaining system continues to work when a client (receiver) goes down or has intermittent connectivity. MQTT communication can be set up to buffer data in case of connectivity issues or other periods with downtime on the receiver side. MQTT is a bandwidth-efficient protocol. The core MQTT protocol is using TCP ports 1883 and 8883 which typically might be outbound blocked by firewalls. A good solution is therefore to use MQTT over Websockets which is using TCP port 443. This port is commonly open outbound or can easily be opened as it is typically used by many secure services based on TLS (Transport Layer Security) communication, e.g. secure https websites, online banking etc.

Traditionally, it has been challenging to get access to real-time data from distributed assets. This has been due to many factors including limited connectivity, lack of suitable protocols, lack of suitable interfaces to send and receive data from and lack of platforms that can handle data efficiently and seamlessly. Particularly, for seagoing vessels the lack of connectivity with sufficient and reliable bandwidth has been a serious hinderance. This has changed in recent years due to a number of factors, including:

- satellite connections with reliable and cost-efficient connectivity;
- efficient and modern communication protocols suitable for real-time transmission of telemetry data across the internet;
- data platforms that can handle large amounts of incoming data in a cost-efficient manner;
- scalable and flexible processing platforms that can process incoming telemetry data;
- security solutions utilizing mechanisms such as Public Key Infrastructure (PKI) encryption (e.g. https);
- authentication and authorization mechanisms based on Active Directory.

4.2. Access to STW data onshore

The STW data from a system, such as the Miros system discussed in this paper, can easily be made available onshore via web displays or via integration into 3rd party system using push or pull functionality. The described solution is based on using Microsoft Azure to collect, store, visualize and distribute the data from the vessels in a secure manner.

The communication of STW data from the vessel to Microsoft Azure is made via secure communication using modern protocols such as MQTT over Websockets, as described above. The STW system onboard the vessel will initiate a secure connection to Microsoft Azure. Both sides (the vessel STW system from Miros and the Miros environment in Microsoft Azure) is authenticated and authorized to avoid any possibility for illegal access to data or tampering with data. Communication is established outbound from the vessel, thus there is no need to open inbound ports in firewalls. Depending on the vessel network configuration, there might be a need to open outbound firewall ports. If needed this can be set up to only allow communication with Microsoft Azure to avoid any other services to utilize this outbound open port.

On the receiving side the access to data is governed by Microsoft Azure security mechanisms based on Active Directory. This means that only authorized personnel will be able to access the data via download mechanisms or web displays. Furthermore, any automated data transfer will be secured in a similar fashion.

Utilizing Microsoft Azure means that the STW data can be combined with other types of information, such as data from other types of instruments and systems, sea state forecasts from weather providers etc. It is also easy to get an overview of the status and history for a fleet of vessels.

Device management can also be supported by utilizing the functionality found in Microsoft Azure. In this way it is possible to remotely configure the STW system and provide firmware update features. This dramatically simplifies the commissioning and maintenance of the solution. With a transparent solution it is straightforward to identify possible issues related to the configuration or the maintenance of the physical equipment. This results in improvements in data quality and data availability. Software updates and configuration changes can be implemented in several ways. One common use case is to trigger a software update or configuration change from a remote location, i.e. by the equipment vendor (Miros in this case). Microsoft Azure then makes sure that this change is applied in the most seamless way. Software updates are then downloaded from the vessel via https communication which is again authenticated, authorized and encrypted.

The various options for how to integrate the Miros STW solution is shown in Fig.10, starting with using the STW solution as a standalone system onboard, via integrating the STW solution into an onboard system to integrating the STW solution to an onshore party via Microsoft Azure. The onboard system could be a vessel performance system or the vessel control system containing functionality such as an autopilot or automated speed optimizer.

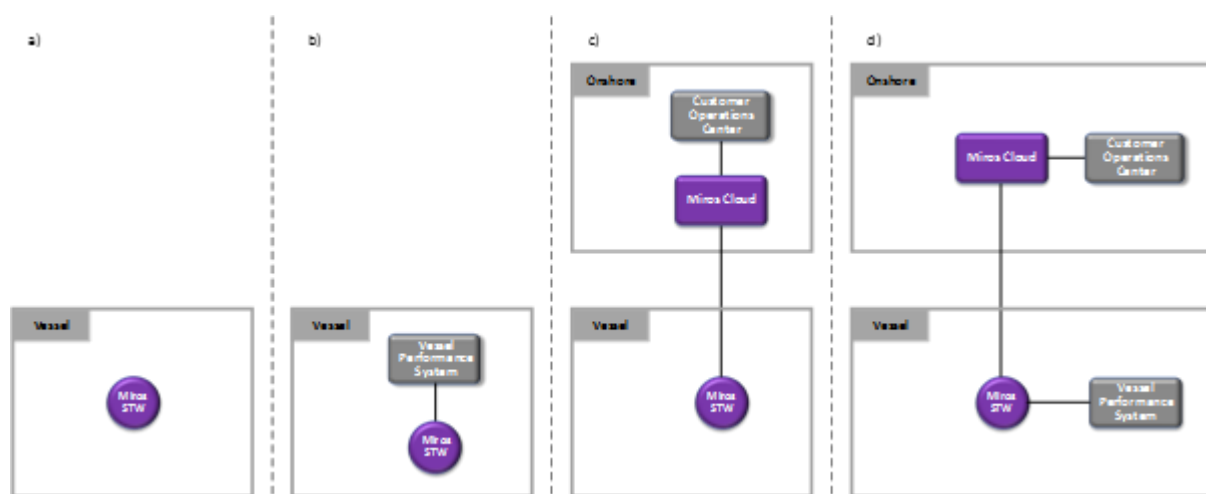


Fig.10: Various options for how to use the Miros STW solution. a) Miros STW system used as a standalone solution onboard a vessel, b) Miros STW system integrated into vessel performance system onboard, c) Miros STW system integrated with an onshore customer system via the Miros Cloud, d) combining options b) and c).

5. Conclusion

Information about surface currents and STW is of great value for many purposes, for instance as input to fuel optimization systems and hull performance estimation (detection of fouling). Thanks to considerable work and progress within the field of radar remote sensing during the recent decades, such ocean surface measurements can now be performed with a high reliability and accuracy using radar sensors. Hence, challenges like data heavily influenced by noise and costs related to installing and maintaining traditional underwater equipment can be avoided. By means of radar remote sensing techniques, the user can measure the current and the STW in the water of interest, sufficiently far away from structures and the chaotic conditions close to a vessel hull that would otherwise disturb the measurements. Combining the sensing technology with technologies from the Internet-of-Things domain means that the data can be made easily and securely available anywhere in real time.

Acknowledgements

Miros would like to thank Höegh LNG and the crew of Arctic Lady for making available and approving data to be used in this work and paper. Miros would also like to thank the Irish Marine Institute and their data stewards for well-organized model output provision, and the Norwegian Meteorological Institute for making model data available from their servers.

References

- ANTOLA, M.; SOLONEN, A.; PYÖRRE, J. (2017), *Notorious speed through water*, 2nd HullPIC, Ulrichshusen, pp.156-165
- BAUR, M. (2016), *Acquisition and integration of meaningful performance data on board - challenges and experiences*, 1st HullPIC, Pavone, pp.230-238
- BOS, M. (2016), *How MetOcean data can improve accuracy and reliability of vessel performance estimates*, 1st HullPIC, Pavone, pp.106-114
- BROWN, J.; COLLING, A.; PARK, D.; PHILIPS, J.; ROTHERY, D.; WRIGHT, J. (2001), *Ocean Circulation*, The Open University, Milton Keynes (130 pages)
- CARCHEN, A.; PAZOUKI, K.; ATLAR, M. (2017), *Development of an online ship performance monitoring system dedicated for biofouling and anti-fouling coating analysis*, 2nd HullPIC, Ulrichshusen, pp.90-101
- DABROWSKI, T.; LYONS, K.; CUSACK, C.; CASAL, G.; BERRY, A.; NOLAN, G. D. (2016), *Ocean modelling for aquaculture and fisheries in Irish waters*, Ocean Sci. 12, pp.101-116
- FLAGG, C. N.; SCHWARTZE, G.; GOTTLIEB, E.; ROSSBY, T. (1998), *Operating an acoustic Doppler current profiler aboard a container vessel*, J. Atmospheric and Oceanic Technology 15, pp.257-271
- FRITZ, F. (2016), *Practical experiences with vessel performance management and hull condition monitoring*, 1st HullPIC, Pavone, pp.128-136
- GANGESKAR, R. (2017), *Automatically calibrated wave spectra by the Miros Wavex system – Accuracy verified*, Miros AS, Asker
- GANGESKAR, R.; PRYTZ, G.; SVANES BERTELSEN, V. (2018), *On-Board Real-Time Wave & Current Measurements for Decision Support*, 3rd HullPIC, Redworth, pp.223-233
- GANGESKAR, R. (2018a), *Verifying High-Accuracy Ocean Surface Current Measurements by X-Band Radar for Fixed and Moving Installations*, IEEE Trans. Geosci. Remote Sens. 56/8, pp.4845-4855
- GANGESKAR, R. (2018b), *Ocean Surface Current Measurement by the Miros Wavex System*, Miros AS, Asker
- GANGESKAR, R. (2018c), *Surface Current Measurements from Moving Vessels by Wavex – Verified*, Miros AS, Asker
- GANGESKAR, R. (2019), *Measuring the speed through water by Wavex[®]*, Miros AS, Asker
- GOLER, H.; BOSKURT, K. (2017), *Speed loss analysis of high-speed ro-ro vessels coated with new antifouling technologies*, 2nd HullPIC, Ulrichshusen, pp.173-193

- KELLING, J. (2017), *Ultrasound-based antifouling solutions*, 2nd HullPIC, Ulrichshusen, pp.43-49
- KING, B. A.; COOPER, E. B. (1993), *Comparison of ship's heading determined from an array of GPS antennas with heading from conventional gyrocompass measurements*, Deep Sea Research Part I: Oceanographic Research Papers 40/11-12, pp.2207-2216
- NEW, A. L. (1992), *Factors affecting the quality of shipboard acoustic Doppler current profiler data*, Deep Sea Research Part A: Oceanographic Research Papers 39/11-12, pp.1985-1996
- POND, S.; PICKARD, G. L. (1983), *Introductory Dynamical Oceanography*, Butterworth-Heinemann, pp.207-219
- RÖHRS, J; SPERREVIK, A. K.; CHRISTENSEN, K. H. (2018), *NorShelf: An ocean reanalysis and data-assimilative forecast model for the Norwegian Shelf Sea*, Norwegian Meteorological Institute
- SKOLNIK, M. I. (1980), *Introduction to radar systems*, McGraw-Hill, pp.474-482
- YOUNG, I. R.; ROSENTHAL, W.; ZIEMER, F. (1985), *A three-dimensional analysis of marine radar images for the determination of ocean wave directionality and surface currents*, J. Geophys. Res. 90/C1, pp.1049–1059

Exploring the Effect of Vessel Performance Information Barriers on Decision-Making Practice: A Time Charter Application

Jean-Marc Bonello, UCL Energy Institute, London/UK, jean-marc.bonello.15@ucl.ac.uk
Tristan Smith, UCL Energy Institute, London/UK

Abstract

Several technological solutions are available to improve vessel efficiency. However, despite short payback periods, uptake remains low due to several market barriers and failures. Information related barriers in particular, introduce uncertainty during technology appraisal through poor performance data quality and use. Furthermore, information asymmetry can exist between stakeholders regarding vessel performance more generally, and result in a challenge identifying the efficiency and performance of a ship relative to its peer group or competitors for a charter. This paper explores these problems in practice and attempts to evaluate the effect of information related shortcomings related to vessel efficiency and decision making in deep sea cargo shipping. The work is aimed towards creating an evidence base for targeted commercial tools and policy designed to promote and reward vessel efficiency by bridging the information gap between technical and commercial sides of shipping.

1. Introduction

After many years of debate, the International Maritime Organisation (IMO) set the course for the reduction of greenhouse gas (GHG) emissions from shipping by at least 50% of 2008 levels by 2050 at MEPC 72 (IMO MEPC, 2018). Efficiency is one of the routes by which ships can reduce their emissions which can be achieved through operational or technological interventions, *Bouman et al. (2017)*. Despite efforts from the IMO Maritime Environment Protection Committee (MEPC) to increase energy efficiency (EE), the uptake of these technologies is still found to be low even for measures with short payback periods, *Wang et al. (2010)*, *Faber et al. (2011)*, *Poulsen and Sornn-Friese (2015)*, *Rehmatulla and Smith (2015a)*. (The implementation of the mandatory Energy Efficiency Design Index (EEDI), Ship Energy Efficiency Management Plan (SEEMP) and voluntary Energy Efficiency Operational Index (EEOI) put in place by the MEPC have not been seen to improve efficiency and some studies finding vessels being designed less efficiently since the implementation of these measures, *Stevens et al. (2015)*, *Faber and 't Hoen (2017)*). This EE gap in shipping between the hypothetically achievable and the actual attained vessel performance has been most commonly interpreted through classical economic barrier theory, *Rehmatulla and Smith (2015b)*, *Johnson and Andersson (2016)*.

Information barriers are consistently found to be one of the more significant market failures hindering decision-making for EE technology (EET) uptake. The lack of access to the right information, low quality data and, paradoxically, information overload makes technology appraisal challenging, *Eppler and Mengis (2004)*, *Jafarzadeh and Utne (2014)*, *Rehmatulla and Smith (2015b)*. Another layer of complexity is added due to stakeholder relationships and influencers in shipping involved at various phases of decision-making. Information asymmetry causing lack of transparency and split incentives, intrinsic to shipping chartering practices, increases uncertainty thus discouraging EET uptake, *Agnolucci et al. (2014)*, *Poulsen and Sornn-Friese (2015)*, *Poulsen and Johnson (2016)*. This is particularly the case in the time charter (TC) market where the charterer incurs bunker costs that are determined by the condition and performance of the vessel which they have limited information about. A consequence of this is that more efficient ships are not seen to be rewarded on the market for their better performance, *Tamvakis and Thanopoulou (2000)*, *Prakash et al. (2016)*, *Adland et al. (2017)*, thus creating a two-tier market which plays in favour of worse performing vessels creating the theoretical market for lemons, *Akerlof (1970)*.

This paper sets out to:

- 1) Identify a number of sources of information barriers and asymmetries between owners and charterers with regards to vessel performance

- 2) Propose a game theoretic framing of the charterer-owner dynamic at the pre-fixtured stage to capture information asymmetry for a TC scenario
- 3) Set up a quantitative model to represent the charterer-owner dynamic

Through the evidence produced by achieving the above, this paper aims to determine the effect of uncertainty due to identified information asymmetry and barriers in economic terms for both parties.

A discussion on information barriers related to vessel performance is followed by a brief review of current chartering practices. This leads to the proposal of the game-theoretic framework that is used to build a probabilistic model to quantify the uncertainty different stakeholders are exposed to and associated financial risks. Readers should note that the terms 'energy efficiency' and 'vessel performance' are used interchangeably in this paper. This is since a performance model looks at energy use therefore a vessel with better performance is analogous with a vessel being more efficient.

2. Information barriers in vessel performance

Performance modelling and monitoring is fundamental to any ship owner and has gained much higher importance in the last decade with significant human and financial resources dedicated to it. This is mostly driven by shrinking margins (due to increased fuel costs and oversupply of tonnage in some markets) and more recently, due to the advent of high frequency data acquisition systems and access to relatively cheap data processing power. Technical departments and companies are increasingly seen to be developing complex proprietary models using statistical analysis, multivariate regression and artificial neural network based models to model and predict vessel performance. *Haranen et al. (2016)* give a good summary of the different approaches available with some recent applied examples being *Bocchetti et al. (2015)*, *Bal Beşikçi et al. (2016)*, *Jeon et al. (2018)*; *Yoo and Kim (2019)*.

With the increasing complexity of these methods and a lack of standardization, comes the penalty of reduced transparency where black box models for specific vessels are developed which cannot be used to communicate vessel performance externally. Although ISO 19030, *ISO (2016)*, provides some basis for standardisation, it is increasingly used market ISO-compliant performance monitoring solutions which go beyond the standard including proprietary additions. This creates opacity that occurs especially when third-parties are contracted to undertake performance monitoring where the ship owner may not understand fully the way performance is being measured and modelled due to lack of expertise and resource.

The solution that shipping has embraced for years is the use of speed-consumption benchmarks for vessels. These simple relations are fundamental to daily commercial operations and are the widely accepted method of communicating vessel performance outside of the ship owner's technical department. Once again there is no standardised procedure for creating these curves which are compiled at the discretion of the owner most commonly based on noon reports. *DNV-GL (2015)* found that half the respondents (N=80) of a survey only keep manual daily reading of data, ranging from fuel consumption to metocean conditions. The use of low frequency data has been shown to lead to high uncertainty when assessing performance, *Aldous et al. (2015)*, *Lund and Gonzalez (2017)*, due to associated measurement uncertainty and averaging errors.

The four basic measurements that are required for compiling this curve are speed through water, fuel consumption, draught and weather condition. Speed logs have a relatively good precision of around 1% however they do suffer from bias and drift, *Aldous et al. (2015)*. In the absence of flow meters, fuel consumption is measured by tank soundings which carry a significant uncertainty due to various factors including inaccuracies in tank geometries, human error, and trim correction factors leading to an precision of around 5% on average, *Hunsucker et al. (2018)*. With manual fuel consumption measurement, human error is difficult to avoid altogether and also some incentive to misrepresent daily readings in order to cover for operational decisions taken by the master or chief engineer which they may not want to have on record. While draught sensors are notoriously unreliable due to various factors, this problem is circumvented by the parametrisation of curves for ballast and laden conditions. Similarly for weather, curves are compiled using data up to a particular threshold (nominally BF4)

above which is considered to be heavy weather operation. While this has been shown to be effective to allow comparison of performance below the weather threshold, *Hudson and Daniels Galle (2017)*, it leaves the charterer with no indication of vessel performance in rough weather which can make up for a significant amount of the operating profile on certain routes.

Once some basic filtering is undertaken to remove clear outliers stemming from instrumentation or human error, heavy weather days are removed and the data set is split to represent the two loading conditions, the amount of data loss usually results in a very small number of data points. A quadratic fit, *Bialystocki and Konovessis (2016)*, is usually found to be the best fit for this relation, Fig.1, for which some basic fitting parameters can be determined. In the example below, an uncertainty of ± 2.5 TPD (at a 95% confidence interval) is associated with any consumption estimated using the curve. Thus, when such a curve is used to determine the warranted performance on a charter party at a given speed, the uncertainty related to the modelling technique used (in this case the confidence interval for the quadratic curve) is omitted.

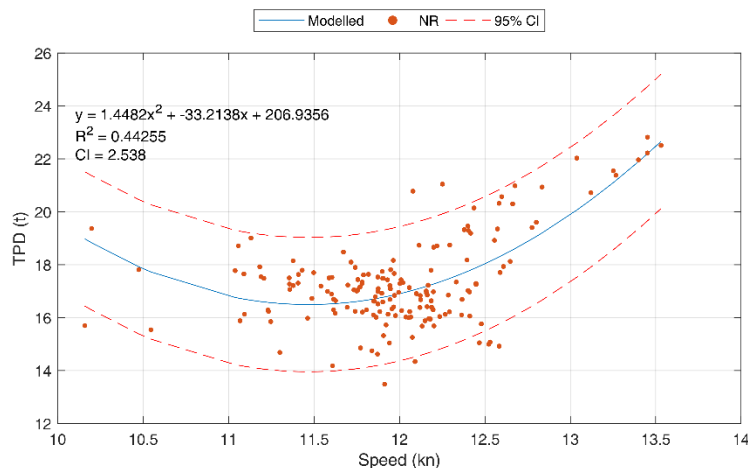


Fig.1: Typical speed-consumption curve [laden, \leq BF4]

3. Information asymmetry: stakeholder dynamics in time chartering

Most vessels engaged in deep-sea shipping are owned and operated by different parties who come to a contractual agreement defining the terms and conditions under which a charter is undertaken. In TC, the vessel is hired out for a fixed period of time on a \$/day charter rate during which the owner is responsible of all operating costs while the charterer incurs voyage costs, *Stopford (2009)*. This sets up a split incentive barrier where, any efficiency investment undertaken by the owner will be beneficial to the charterer. The chartering routine can be described in five discrete steps; pre-fixture, fixture, execution of charter, post-fixture and claims handling, *Plomaritou and Nikolaidis (2016)*. At the pre-fixture stage orders and positions are matched, usually via brokers, which then leads to a series of negotiations via offers and counteroffers between the owner and charterer.

Once an agreement is reached, all the details of the charter are made official through the signing of a charter party contract defining the fixture, *Gorton et al. (2009)*. The role of the charter party is fundamental as it sets up an agreement on terms with an understanding that each party commits to financial obligations under a legally binding contract, *Assimenos (2017)*. These contracts are based on well-established standard forms issued by institutions such as BIMCO and NYPE or, in the case of larger companies chartering in, compiled inhouse making them more specialized to the requirements of the charterer (SHELLTIME and EXXONTIME being some common examples of the latter). Amongst the clauses agreed upon in a TC party is the warranted performance that is defined at a loading condition and a within a weather threshold. A typical speed and consumption clause would specify the warranted vessel performance as follows:

“... capable of steaming, fully laden, under good weather conditions about ___ knots on a consumption of about ___ tons of ___”, *ASBA (1981)*

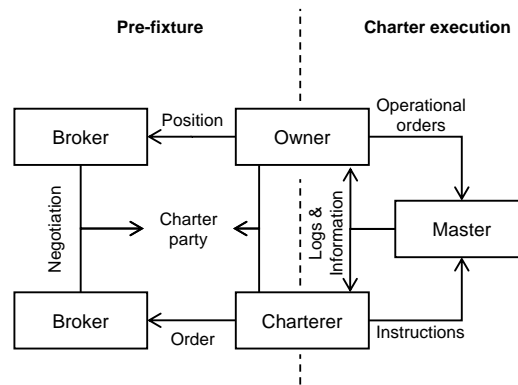


Fig.2: Typical TC stakeholder interaction

Given that the charterer is responsible for voyage cost, the largest portion of which is cost of bunkers posing the biggest commercial risk during the execution of the fixture, it is in their interest to have the best information possible related to vessel performance. The above clause leaves the charterer with limited possibility to evaluate their exposure to risk due to operation in rough weather, sailing under any draught other than fully laden or at any speed other than the warranted velocity. The latter is particularly relevant considering the increasing popularity of slow steaming being instructed by the charterer for commercial reasons. Moreover, under English Law, this clause is not understood as a guarantee over the whole charter period but implies that the vessel is capable of the quoted performance at the time of negotiation and fixture, *Gorton et al. (2009)*. Given the speed under which the above negotiations are conducted and the fact that they are treated as standard practices, there is little scrutineering of this clause which raises difficulties in the post-fixture phase when performance claims can be filed by the charterer. This is not normally a part of the negotiation process which is mainly focused on the charter rate and other logistical such as delivery time and location, *Veenstra and van Dalen (2011)*.

Additionally, there is no way for the charterer to ensure that the vessel performance that is being quoted is representative of the performance they are to expect in operation. *Veenstra and van Dalen (2011)* were able to show that owners strategically change the warranted performance from one charter to another and were being fixed at a performance worse (higher consumption at a lower speed) than their design performance. Anecdotally, in discussions with industry players, a tendency for owners to warrant lower performance than observed in practice was encountered in several cases. (One exception that has been encountered by the author is when owners are entering their vessel into a charter pool. Owners tend to quote their vessels performing better as some charter pools allocate higher proportions of profits for higher efficiency.) This information asymmetry regarding vessel performance leads to a significant level of uncertainty forcing the charterer to make “rule of thumb” estimates when considering their commercial risk exposure due to bunker cost. During the charter commences, noon reports are communicated to the charterer who can then start to assess performance only after having committed to the fixture. The degree of transparency in these reports can also be dubious as there are clear incentives for misreporting consumption, *Poulsen and Johnson (2016)*.

Another legacy term that introduces uncertainty is the consistent use of the term “about” before any number is specified in a charter party. *Gorton et al. (2009)* explains that this is generally accepted to mean “given without guarantee but in good faith and believed to be correct” which in practice is seen to be interpreted as a 5% margin on the warranted consumption and a 5% or 0.5kn margin on warranted speed, *Coghlin et al. (2014)*. This is invariably a point of contention when speed or consumption claims are taken up to arbitration which gives the owner a margin for underperformance.

Having had a closer look at the specific information related barriers and asymmetries in the previous two sections, the elements discussed are summarised in Table I along with the associated artefacts to be included in the framework designed to assess the uncertainty propagation due to each. The selection of these elements strives to capture both the epistemic uncertainty associated with the information

barriers but also the aleatoric uncertainty stemming from the information asymmetry. The bottom line is that when estimating the possible bunker cost over a fixture, charterers are not provided with information about the possible range of the cost (through information barriers) as well as the accuracy of the value they are given (through information asymmetry).

Table I: Information barrier categories and artefacts

Barrier category	Barrier artefact
Data quality and acquisition method	Data collection frequency Instrumentation and measurement error
Performance modelling	Performance modelling (speed-consumption curve based)
Information asymmetry	Communication of vessel performance between owner and charterer

4. Proposed game theoretic model

In order to capture some of the TC dynamics described above including both information barriers and asymmetry, a simple game theoretic model is proposed that has been previously used to frame similar problems. Game theory (GT) is originally a mathematical framework that has been embraced by economics and also environmental disciplines to describe strategic behavior between different stakeholder and assess the outcome for each based on the effect of their decisions on each other, *von Neumann and Morgenstern (1944)*. Information asymmetry is tackled in a particular branch of GT which uses principal agent theory to describe problems of adverse selection (where one party is better informed than another before entering a contract) and moral hazard (where one party is better informed about the actions that will take place after signing a contract). More information can be found in *Rasmusen (2007)*. Several studies related to energy efficiency have identified the owner-charterer dynamic as a principal-agent problem, *IEA (2007)*, *Kontovas and Psarftis (2013)*, *Rehmatulla (2014)* expressing it through GT, *Bergantino and Veenstra (2002)*, *Suh and Park (2010)*, *Psarros (2016)*.

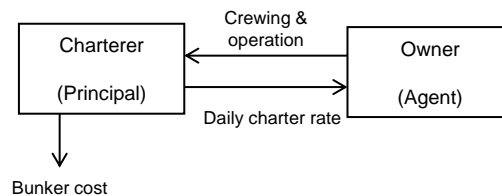


Fig.3: Principal-agent relationship in TC (adapted from *Rehmatulla and Smith (2015a)*)

Thus, drawing on the examples above, an adverse selection game is proposed as an appropriate model of charterer/owner dynamics and set up with the owner acting as the agent that has better information regarding the vessel performance than the charterer who is the principal Fig.4. The game is envisaged to represent the fixture stage when the owner and charter agree the terms in the charter party including the warranted performance specified in the performance clause. The charterer will circulate an offer which an owner will fulfill with their vessel which they can accept or reject. It is assumed that no negotiation takes place because to the best of the authors knowledge, the performance clause is normally not negotiated upon. (Large companies that charter in a high volume of vessels may build up an internal database based on historic performance which will allow them to compare warranted performance across owners, sister ships and peers which is not possible for smaller charterers.)

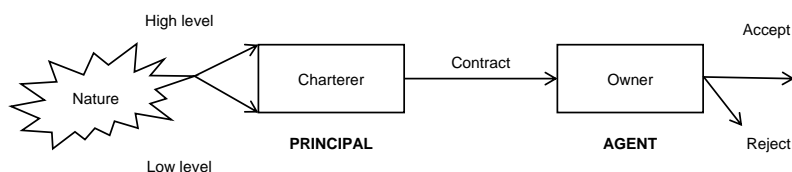


Fig.4: TC fixture represented as an adverse selection game

In this case, nature sets the actual performance of the vessel which the charterer has no way of knowing except through the information provided by the owner in the performance clause. It is assumed that the owner accepts the contract if the conditions of the contract reach some level of expected utility for both parties. The charterer assesses the contract with some level of trust based on the expectation of transparency with regards to vessel performance. Thus, assuming the extremes of these player types, the owner can be modelled as acting with high or low transparency while the charterer can have high or low trust. This allows to set up different scenarios based on the four possible behavior combinations to assess the effect on the utility for both players (in this case, operating profit) under the four different scenarios proposed can be evaluated to analyse the outcome of each case. In the next section, this framework is used to constrain a quantitative model that sets out to illustrate the risk due to uncertainty that parties are exposed to when taking chartering decisions under uncertainty regarding vessel performance. The assumptions regarding vessel performance information use and communication for these four base cases are described in Table II. From the observations in current chartering practice presented in Sections 2 and 3, the business-as-usual (BAU) is understood to be Case 2.2 which implies low transparency from the owner and low trust by the charterer. The three other counterfactuals are set up to represent the other possible combinations and associated assumptions.

Table II: Description of modelling scenario assumptions

	Case 1.1	Case 1.2	Case 2.1	Case 2.2 (BAU)
Trust	High	Low	High	Low
Transparency	High	High	Low	Low
Performance modelling	Speed-consumption curves based on noon report data up to BF4 weather threshold			
Measurement uncertainty	Considered		Not considered	
Warranted performance	Based on historic experience		Strategically compiled	
Performance communication	Provision of speed-con curve including associated confidence interval		Provision of warranted speed-consumption at laden condition	
Charterer bunker estimate method	Probabilistic: Based on speed-consumption curve and expected probability distribution of speeds		Deterministic: Based on warranted performance communication and expected operational profile during fixture	
Charterer bunker estimate margin	None	Included	None	Included

Charterer Owner

5. Quantitative modelling

A utility function to evaluate each players payoff under the different scenarios must be devised. A common approach looks at cashflows for owners and charterers to define operating profits over a fixture period which can be defined as (Factors such as historic relationships, location of vessels and market conditions are not considered. A transactional relationship is assumed taking the charter as a one-off event not being affected by any past charters and not influencing future ones. Brokerage fees on both sides are also not included.):

$$E(OP_o^T) = \sum_{t=1}^T [R_t - CO_t] \quad 5.1$$

$$E(OP_C^T) = \sum_{t=1}^T [-R_t - CV_t - E(B_t) + E(RF_t)] \quad 5.2$$

Where for a charter period T days long, OP_o^T is owner operating profit, R_t is daily charter rate, CO is the average daily operating costs, OP_C^T is charterer operating profile, RF_t is freight revenue from transport work, CV_t is voyage costs. It should be noted that the cost of bunker B_t is normally in integral part of voyage cost however in this case it is being represented separately for clarity as this work focuses on energy efficiency. The notation $E()$ is used to denote an expected term that can only be estimated when the vessel fixture is agreed. It is assumed that both players are rational and will strategically act to maximise their respective operating profit.

Operating profit for the owner can easily be evaluated as a good knowledge of operating costs is assumed and the revenue from the charter is fixed. The charterer payoff however carries uncertainty in bunker cost and freight revenue which stems partially from market conditions (future utilisation, freight rates and bunker cost) and factors affecting bunker consumption (vessel performance, hull condition, weather). The owner is exposed to some risk stemming from performance claims that the charterer may raise based on the warranted consumption agreed upon in the charter party. However, at the pre-chartering stage neither the owner nor the charterer can include these payouts in their assessment of costs throughout the fixture. Only at the end of the charter period T the realised operating profit can be determined as:

$$OP_o^T = \sum_{t=1}^T [R_t - CO_t] - PC^T \quad 5.3$$

$$OP_C^T = \sum_{t=1}^T [-R_t - CV_t - B_t + RF_t] + PC^T \quad 5.4$$

Where PC^T is the total value of any performance claims over the charter period T . The total value and probability of occurrence of performance claims is directly related to how conservative the owner is in warranting the vessel. Following the equations above, the financial risk that the charter is exposed upon fixing a vessel can be described as the difference between the expected and the realised operating profit. Linking back to the scenarios described in Table II:, the four cases infer different information available to evaluating the term $E(B_t)$ under the different actor types, levels of transparency and trust which in turn leads to a different evaluation of $E(OP_C^T)$.

An applied case study is presented for a 50,000DWT chemical/product tanker for which a three-year long continuous monitoring (CM) data set (10-minute frequency) was made available. This vessel was used to set up a counterfactual game to illustrate the effect of the information barrier artefacts presented in Table I.

5.1. Data collection and performance modelling

The data was resampled over 24 hour periods to simulate noon-reporting and, given draught was not part of the data set provided, Automatic Identification System (AIS) data was used to determine if the vessel was in ballast or laden condition. After outlier removal, speed through water (STW) and fuel consumption (TPD) values were used to compile speed-consumption curves for both loading conditions for fair weather conditions up to BF4. In order to simulate the measurement errors associated with noon reporting, a random error (following a Beta distribution) of 5% and 1% was applied to TPD and STW respectively as specified by Aldous *et al.* (2015). This yielded a quadratic relationship with an associated confidence interval that could be applied to any value estimated using the performance model.

5.2. Communication of performance

Based on the historic vessel performance, the warranted TPD and speed value set by the owner is to be determined. Upon observation of the speed distribution when operating in the laden condition Fig.5:, the mean velocity at around 12kn which implies that the master strives to keep to this velocity for most of the time. Assuming a 12.5kn warranted speed, the performance model suggests a consumption of 17.8 ± 2.5 TPD (at a 95% confident interval). Assuming a conservative owner the performance is strategically quoted to be 18.5 TPD at 12kn laden for fair weather up to BF4 following findings by Veenstra and van Dalen (2011).

With regards to the weather condition, Fig.5: illustrates that the vessel spends around 45% of time sailing above BF4 which falls outside of the warranty. The histogram also suggests the speed of the vessel is not affected by weather condition indicating that higher fuel consumption is expected due to the rougher weather.

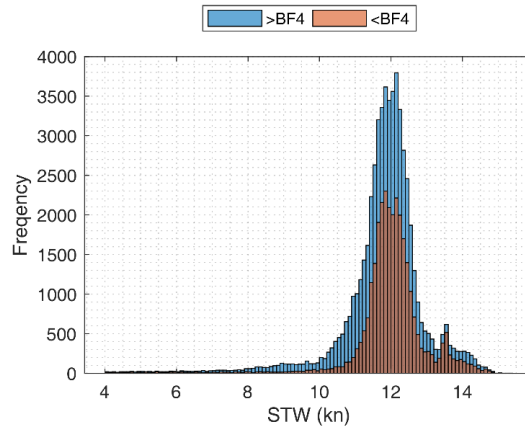


Fig.5: Speed distribution for laden condition

5.3. Expected bunker consumption estimate

Once the charter is presented with the warranted performance, they can use this to estimate the expected profit from the charter having some experience of operating similar vessels and knowledge of the expected operating profile over the fixture period. In order to populate Equation 5.2, some assumptions must be made which are presented in Table III.

The upper bound bunker cost that the charterer expects based on the warranted performance assumes maximum operation throughout the fixture period with some margin for rough weather operation. This method would represent an extremely risk-averse charterer or one with no previous experience.

$$E(B_t) = 365 \cdot \beta \cdot TPD_w (1 + \gamma) \cdot B_p \quad 5.5$$

Table III: Baseline assumptions for fuel consumption estimate

Parameter	Symbol	Value	Description	Source
Charter rate	R_t	13,500	Charter rate for peer group for a one-year fixture in \$/day	(Clarksons, 2018)
Freight rate	f_r	50	Freight rate for Easychem cargo in \$/t	(Clarksons, 2018)
Parcel size	f_q	38,000	Typical parcel size of cargo from previous voyages in t	(Clarksons, 2018)
Voyages (pa)	n_v	6	Average number of voyages undertaken per annum since 2014	Historic data
OPEX	CO_t	6300	Daily operating cost based on OPEX index	(Clarksons, 2018)
Load	α	0.6	Ratio of laden and ballast time	Historic data

utilisation				
Time utilisation	β	0.85	Utilisation of vessel, sailing days per annum	Historic data
Bunker price	B_p	450	Bunker cost for IFO 380 at Port of Rotterdam (Q1 2018) in \$/t	(Clarksons, 2018)
Weather margin	γ	0.05	Additional margin to account for rough weather	(Gorton <i>et al.</i> , 2009)
Low trust margin	μ	0.05	Additional bunker margin to represent a conservative approach under low trust scenario	Author assumption
TPD ratio	δ	0.9	Ratio of mean bunker consumption for ballast condition compared to laden conditions	Historic data
Warranted TPD	TPD_w	18.5	As derived in previous section in t [Based on speed of 12.5kn with an additional 0.5t]	Historic data
Warranted Speed	V_w	12	As derived in previous section in kn	Historic data

The above assumes that consumption is not sensitive to loading condition and all sailing is conducted at the warranted speed. Assuming a charterer with some previous experience, a slightly more sophisticated bunker estimate may be represented as follows:

$$E(B_t) = 365 \cdot \beta \cdot [(TPD_w \alpha) + (\delta TPD_w (1 - \alpha))] (1 + \gamma) \cdot B_p \quad 5.6$$

Equation 5.6 accounts for expected utilisation, time spent in ballast and laden condition and decreased consumption for the laden condition and is used as method for charterer consumption estimation in the low transparency scenarios.

In the high transparency case, it is assumed that the speed-consumption curves for both ballast and laden conditions are shared with the charterer including the associated model uncertainty (standard deviation for a 95% confidence interval). This allows the charterer to use a probability distribution of expected speeds rather than relying on the warranted speed which allows for a probabilistic estimate to be created rather than a deterministic one. The speed consumption curves used include all weather conditions in order to account for increased consumption due to rough weather operation and are used for the high transparency scenarios.

5.4. Expected operating profit estimate

The bunker consumption estimations as described are used in Equation 5.2 which will be evaluated for a one-year fixture. The expected freight revenue can be defined as:

$$E(RF_t) = f_r f_q n_v \quad 5.7$$

For the case presented in this paper, the values provide in Table III: are used to determine freight revenue and charter cost. Voyage costs CV_t are approximated using costs adapted from *Stopford (2009)* to be equal to half the bunker cost B_t .

6. Results

The model described is run for a 12 month long fixture and Fig.6: illustrates the preliminary results for the baseline parameters presented in Table III: showing expected bunker consumption and charter operating profit. The attained performance estimate B_t for comparison is obtained from historical data for an equivalent operating profile and is presented in Table IV: along with the modelling results.

6.1. Charterer perspective

Bunker consumption estimates move further away from the baseline historic performance as transparency and trust decrease as expected which is also reflected in expected operating profits. With single point performance communication in the low transparency cases, only a discrete value can be estimated compared to the probabilistic range from the higher transparency case. This may be a driver for charterers to take a more conservative approach to estimating expected operating profits and take decisions based on the worst perceived outcome due to lack of information. In the high-performance case, even through only noon reports and simplistic performance modelling was used, an accurate bunker estimate can be observed with the mean being within 3% of the historic baseline.

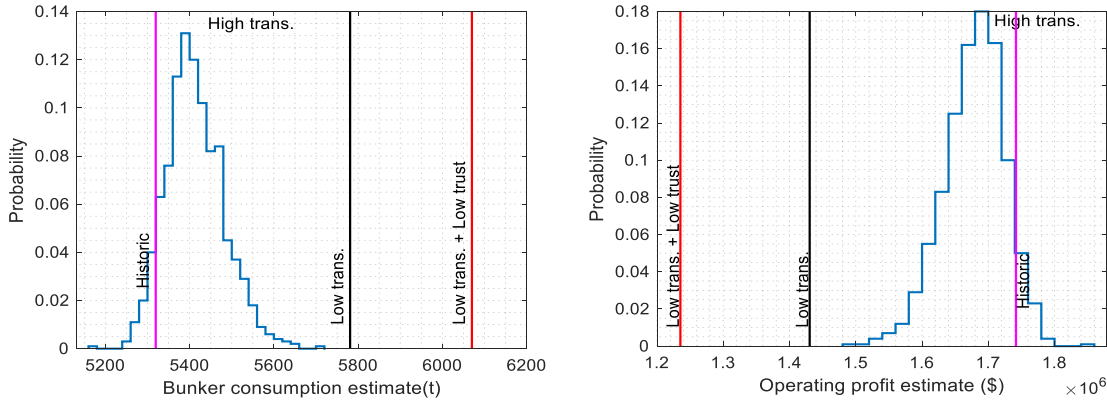


Fig.6: Bunker and charterer operating profit estimates under different transparency regimes (Results of Case 1.2 are not show for clarity. The distributions are similar to those for Case 1.1 with means and standard deviations as specified in Table 6 1.)

Table IV: Bunker and charterer operating profit estimates under different transparency regimes

Case	Description	$E(OP_C)$	% of Historical	$E(B_t)$	% of Historical	$E(OP_O)$
Historical	Attained performance estimate	1.74*	1	2.39*	1	2.63*
1.1	High transparency, high trust	1.68 (0.048)**	0.97	2.44 (0.032)**	1.02	2.63
1.2	High transparency, low trust	1.49 (0.048)**	0.86	2.56 (0.032)**	1.07	2.63
2.1	Low transparency, high trust	1.43	0.82	2.60	1.09	2.63
2.2	Low transparency, low trust	1.24	0.71	2.73	1.14	2.63

*Baseline attained values as defined in Equation 5.4 rather than expected. **Mean (standard deviation)

Fig.7 illustrates the effect on bunker cost estimate based on variations in warranted speed and strategic warranted TPD changes under the low transparency regime. At no change, the warranted TPD is equal to the actual TPD obtained from the speed-consumption model derived from noon reports. The accompanying parallel lines describe the variation expected by strategic changes in TPD in steps of 0.5 t. Given the quadratic nature of the relationship, the bunker estimate increases at a higher rate as warranted speed increases. This brings to light the effect of the “about” clause as used in performance clauses which allows for a 1kn window around the warranted speed creating a significant amount of uncertainty when attempting to estimate bunker cost over a fixture.

Recalling the assumption that the charterer is a rational actor looking to maximise operating profits, the results show that this is the least optimal option compared to the baseline for various reasons. Firstly, it effectively ties up a significant amount of cash that is expected to be spent on bunker which will not which becomes a significant issue in tight markets when positive cashflows become paramount in day-

to-day operations. Alternatively, that money could be put towards better use through investments or towards chartering another vessel with a higher charter rate but better performance.

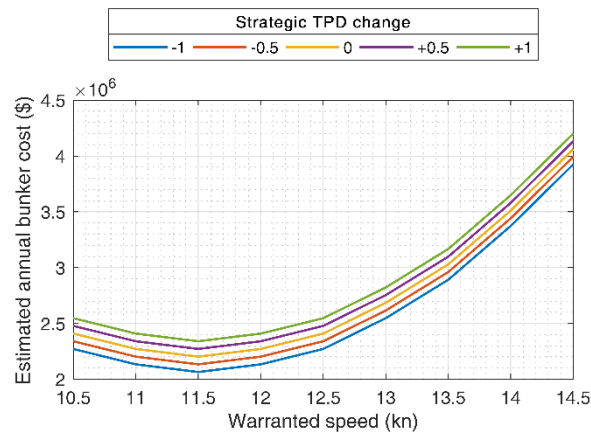


Fig.7: Effect of owner strategic warranty declaration on bunker consumption estimate

Secondly, the results in Fig.6: show that the owner has a large margin within which they are still within the warranted performance which can be used strategically in various ways due to the lack of information on the charterer side. This may lead to reduce the efforts of the master and crew to operate the vessel efficiently as well as reducing the urgency for hull maintenance or other interventions that will have a positive effect on efficiency. Alternatively, an opportunity is provided for misreporting of fuel consumption by the master to cover deviations from the agreed instructions or any skimming of bunker by the crew to be sold on the black market for which *Poulsen and Johnson (2016)* found evidence in their interview-based study. (This situation gives rise to another two instances of the principal-agent problem: i) a second level problem between the owner and the charterer with respect to the provision of fuel consumption information during the charter and ii) one between owner and the master on board with regards fuel consumption reporting. These provide fertile ground for further research.)

6.2. Owner perspective

On the owner side, the expected operating profit is only affected by the reported future operation of the vessel and any related performance claims. The number of days that are liable for claims is dependent on the warranted performance as selected by the owner and on the reported performance once the vessel is in operation which can be used strategically by the owner to their advantage. Fig.8 illustrates the extent to which strategic warranted performance selection can virtually absolve the owner of risks associated with claims. For the dataset used in this study, only 45% of the days used were within the performance clause with the remaining days being at a speed higher than warranted, over BF4 or in clear breach of warranty. Only 1% of these days were in clear breach of warranty which is negligible in terms of claim value explaining why the $E(OP_O)$ in Table IV: is constant. As warranted performance is increased (vessel made more efficient), the liability for performance claims increases in likelihood and value. *Veenstra and van Dalen (2011)* suggest that the strategic changes in warranted performance are not bargained upon at the negotiation phase but are used to build a safety margin to protect against performance claims. Fig.8 can also draw upon the effect of the “about” clause as used in the performance clause as the number of days liable for performance claims decreases significantly as warranted TPD increases (or warranted speed decreases).

On the owner side, higher transparency does not have a direct benefit to operating profit as modelled above however it can be used as a strategy to increase the likelihood of winning more charterers at a possibly higher rates as charters are empowered to make more informed decisions when leading to better operating profit estimates. This may become especially relevant in periods of higher bunker cost or weak markets where bunker consumption contributes to additional costs.

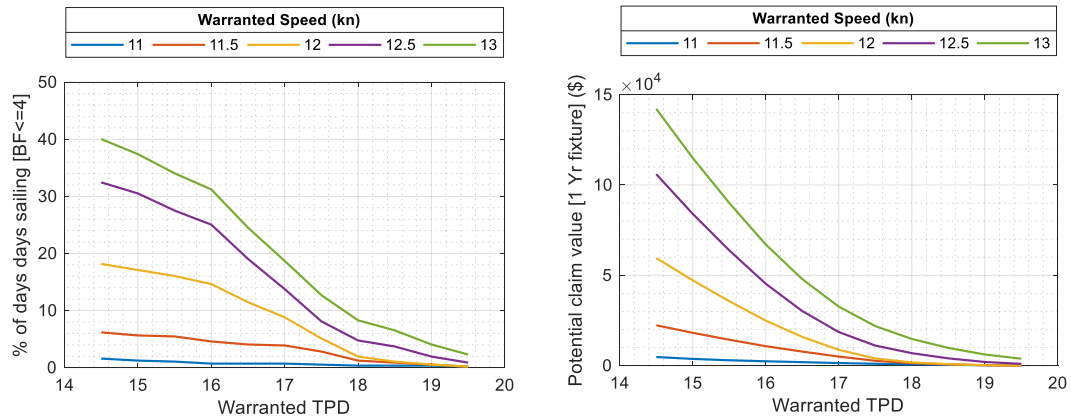


Fig.8: Percentage of days sailing liable to performance claims and prospective claim value

7. Conclusion

This work proposes a novel way of bringing together the technical and commercial regimes in vessel chartering which are usually treated in isolation both in academic literature and in industry. The use of GT has been shown to have potential as a good framework to build an analytical model that transparently considers the perspective of both charterer and owner and their expected economic outcomes based on their respective strategies. By tackling information barriers and asymmetries specifically, this techno-economic model can empower charterers and owners to quantify the effect of these market failures when making chartering decisions and policy makers to test the potential outcome of measures by also considering the behaviour of industry players. Due to the flexibility offered by the quantitative modelling, it can be developed to test the outcome for various market scenarios, implementation of standardisation or policy, different performance modelling and data collection approaches and performance-based contracting.

The preliminary results presented lead to the conclusion that, in the current scenario, information barriers and lack of trust regarding vessel performance leave charterers with a large uncertainty when determining the commercial viability of a fixture. The strategy chosen to overcome this is being conservative which in turn provides owners with little or no incentive to operate vessels more efficiency or, in the long term, invest in more efficient tonnage especially as these have not been seen to attract higher charter rates. Under a higher transparency regime and increased trust, it is proposed that both parties may stand to make smarter business decisions in the short term whilst also promoting a long-term shift towards more efficient shipping through both technological and operational means.

The next step in this research involves running systematic sensitivity analysis to assess the impact changes in the input parameters and player dynamics have on the outcome for charterers and owners respectively. This will be followed by the addition of another layer of complexity by considering the addition of energy efficiency technologies, energy savings clauses and performance contracting assessing the effect of sharing the associated risks and rewards under the uncertainty.

References

- ADLAND, R. et al. (2017), *Does fuel efficiency pay? Empirical evidence from the drybulk timecharter market revisited*, Transportation Research Part A: Policy and Practice 95, pp.1–12.
- AGNOLUCCI, P.; SMITH, T.; REHMATULLA, N. (2014), *Energy efficiency and time charter rates: Energy efficiency savings recovered by ship owners in the Panamax market*, Transportation Research Part A: Policy and Practice 66(1), pp.173–184.

- AKERLOF, G.A. (1970), *The Market for "Lemons": Quality Uncertainty and the Market Mechanism*, The Quarterly Journal of Economics, 84(3), pp.488–500
- ALDOUS, L. et al. (2015), *Uncertainty analysis in ship performance monitoring*, Ocean Engineering 110, pp.29–38
- ASBA (1981) ASBATIME Type 81 Time Charter Party Agreement, http://www.fleetle.com/a/d/pdf/asbatime_nype_81.pdf
- ASSIMENOS, N. (2017), *Commercial Operations Management*, Shipping Operations Management, Springer
- BAL BEŞİKÇİ, E., KECECI, T., et al. (2016), *An application of fuzzy-AHP to ship operational energy efficiency measures*, Ocean Engineering 121, pp.392–402
- BAL BEŞİKÇİ, E., ARSLAN, O., et al. (2016), *An artificial neural network based decision support system for energy efficient ship operations*, Computers & Operations Research 66, pp.393–401
- BERGANTINO, A.S.; VEENSTRA, A.W. (2002), *Principal agent problems in shipping: An investigation into the formation of charter contracts*, Int. Assoc. Maritime Economists Conf., Panama City
- BIALYSTOCKI, N.; KONOVESSIS, D. (2016), *On the estimation of ship's fuel consumption and speed curve: A statistical approach*, J. Ocean Eng. and Science 1(2), pp.157–166
- BOCCHETTI, D. et al. (2015), *A Statistical Approach to Ship Fuel Consumption Monitoring*, J. Ship Research 59(3), pp.162–171
- BOUMAN, E. A. et al. (2017), *State-of-the-art technologies, measures, and potential for reducing GHG emissions from shipping – A review*, Transportation Research Part D: Transport and Environment 52, pp.408–421
- CLARKSONS (2018), *Clarksons Ship Intelligence Network*
- COGHLIN, T. et al. (2014) *Time charters*. 7th edn. Routledge (Lloyd's shipping law library).
- DNV-GL (2015), *Energy Management Study 2015 Energy efficient operation – what really matters*. <https://www.dnvgl.com/maritime/publications/energy-management-study.html>
- EPPLER, M.J.; MENGIS, J. (2004), *The concept of information overload: a review of the literature from Organization Science, Accounting, MIS, and related disciplines*, The Information Society 20(5), pp.325–344
- FABER, J.; 'T HOEN, M. (2017), *Estimated Index Values of Ships 2009-2016. Analysis of the Design Efficiency of Ships that have Entered the Fleet since 2009*, Delft, http://www.seas-at-risk.org/images/pdf/publications/2017_07_CE_Delft_7L97_Estimated_Index_Values_of_Ships_2009-2016_def_2017.pdf
- FABER, J.; BEHRENDIS, B.; NELISSEN, D. (2011) *Analysis of GHG Marginal Abatement Cost Curves*, Delft, http://www.cedelft.eu/?go=home.downloadPub&id=1155&file=7410_defreportJFSD.pdf
- GORTON, L. et al. (2009), *Shipbroking and Chartering Practice*, Informa
- HARANEN, M. et al. (2016), *White, Grey and Black-Box Modelling in Ship Performance Evaluation*,

1st HullPIC, Pavone, pp.115–127

HUDSON, D.A.; DANIELS GALLE, G.P. (2017), *Investigation of Ship Motions and Fuel Consumption with respect to Charter Party Agreements*, Shipping in Changing Climates Conf.

HUNSUCKER, J.T. et al. (2018), *Uncertainty Analysis of Methods Used to Measure Ship Fuel Oil Consumption*, Fort Lauderdale, http://www.imo.org/en/OurWork/Documents/Uncertainty_Analysis_in_Ship_Fuel_Oil_Consumption.pdf

IEA (2007), *Mind the Gap: Quantifying principal-agent problems in energy efficiency*, Paris

IMO MEPC (2018), *Reduction of GHG Emissions from Ships*, MEPC 72/WP.5, IMO, London

ISO (2016), *ISO19030-1 Ships and marine technology - Measurement of changes in hull and propeller performance - Part 1: General principles*, Geneva

JAFARZADEH, S.; UTNE, I.B. (2014), *A framework to bridge the energy efficiency gap in shipping*, Energy 69, pp.603–612

JEON, M. et al. (2018), *Prediction of ship fuel consumption by using an artificial neural network*, J. Mech. Science & Technology 32(12), pp.5785–5796

JOHNSON, H.; ANDERSSON, K. (2016), *Barriers to energy efficiency in shipping*, WMU J. Maritime Affairs 15(1), pp.79–96

KARLSEN, R.; PAPACHRISTOS, G.; REHMATULLA, N. (2018), *The diffusion of wind propulsion technologies in shipping: an agent-based model*, 9th Int. Sustainability Transitions Conf., Manchester, pp.1–28

KONTOVAS, C.A.; PSARAFTIS, H.N. (2013), *Bridging the Energy Efficiency Gap in Shipping: The case of Principal-Agent Problems in operational emission reduction measures*, IAME Conf., Marseille, pp.1–20

LUND, B.; GONZALEZ, C. (2017), *The Big Data Concept in a Performance Monitoring Perspective*, 2nd HullPIC, Ulrichshusen, pp.76–88

NEUMANN, J.v.; MORGENSTERN, O. (1944), *Theory of Games and Economic Behavior*, Princeton University Press.

PLOMARITOU, E.; NIKOLAIDES, E. (2016), *Commercial Risks Arising from Chartering Vessels*, J. Shipping and Ocean Engineering 6, pp.261–268

POULSEN, R.T.; JOHNSON, H. (2016), *The logic of business vs. the logic of energy management practice: Understanding the choices and effects of energy consumption monitoring systems in shipping companies*, J. Cleaner Production 112, pp.3785–3797

POULSEN, R.T.; SORNN-FRIESE, H. (2015), *Achieving energy efficient ship operations under third party management: How do ship management models influence energy efficiency?*, Research in Transportation Business and Management 17, pp.41–52

PRAKASH, V. et al. (2016), *Revealed preferences for energy efficiency in the shipping markets*, London

PSARROS, G.A. (2016), *Energy Efficiency Clauses in Charter Party Agreements: Legal and Economic Perspectives and their Application to Ocean Grain Transport*, Springer

- RASMUSEN, E. (2007), *Games and information: An introduction to game theory*, Blackwell
- REHMATULLA, N. (2014), *Market Failures and Barriers Affecting Energy Efficient Operations in Shipping*, Thesis, University College London
- REHMATULLA, N.; SMITH, T. (2015a), *Barriers to energy efficiency in shipping: A triangulated approach to investigate the principal agent problem*, *Energy Policy* 84, pp.44–57
- REHMATULLA, N.; SMITH, T. (2015b), *Barriers to energy efficient and low carbon shipping*, *Ocean Engineering* 110, pp.102–112
- STEVENS, L. et al. (2015), *Is new emission legislation stimulating the implementation of sustainable and energy-efficient maritime technologies?*, *Research in Transportation Business and Management* 17, pp.14–25
- STOPFORD, M. (2009), *Maritime Economics*, Routledge
- SUH, S.; PARK, N. (2010), *The Charter Fixing Negotiation Procedure with Asymmetric Impatience in a Game Theory Framework: Case Studies in Coal and Ore Transactions*, *The Asian J. Shipping and Logistics* 26(2), pp.247–261
- TAMVAKIS, M.N.; THANOPOULOU, H.A. (2000), *Does quality pay? The case of the dry bulk market*, *Transportation Research Part E: Logistics and Transportation Review* 36(4), pp.297–307
- VEENSTRA, A.W.; VAN DALEN, J. (2011), *Ship Speed and Fuel Consumption Quotation in Ocean Shipping Time Charter Contracts*, *J. Transport Economics and Policy* 45(1), pp.41–61
- WANG, H. et al. (2010), *Reduction of GHG emissions from ships: Marginal abatement costs and cost-effectiveness of energy-efficiency measures*, MEPC 61/INF. 18, IMO, London
- YOO, B.; KIM, J. (2019), *Probabilistic modeling of ship powering performance using full-scale operational data*, *Applied Ocean Research* 82, pp.1–9

Techniques for the Automated Detection of Anomalies and Assessment of Quality in High-Frequency Data Collection Systems

Carlos Gonzalez, Kyma, Bergen/Norway, cg@kyma.no
David Lara Arango, Webstep, Bergen/Norway, david.lara.arango@webstep.no

Abstract

During the last few years, the advent of big data techniques and their benefits for obtaining valuable insights enabling better decision-making, has been a trend topic in all the industries. One of these benefits has been an increased capability to detect patterns, anomalies and confidence boundaries for different phenomena; which has significantly improved the overall reliability in various processes across multiple industries. At the same time, in the shipping industry, questions have arisen about the reliability of the data gathered automatically from sensors. This is of course vitally important for the industry; for each of the values used to carry out various operational and managerial processes, it is necessary to consider the accuracy of the sensors, the calibration processes and any inherent errors in the measurement process. In recent years, many companies in the shipping industry have decided to invest more resources in the digitalization of their ships; with the goal of gathering valuable data which will lead to better decisions and, in consequence, give an advantage over their competitors. This has been resulted in an improvement of the quantity and quality of the telemetry on board their vessels. By applying machine learning and statistical analysis techniques, this paper shows the anomalies detected and the accuracy of datasets, collected on board several ships, containing data collected every 15 seconds (this being the frequency defined in ISO 19030).

1. Introduction

The maritime industry is facing tighter economic margins, so their top priority is to optimize ship's operations; maximizing benefits by reducing the operational costs. One of the measures used to optimize ship performance is by achieving better fuel efficiency, since fuel consumption may account for 50% of the total ship's voyage costs, *Bialystocki and Konovessis (2016)*. Typically, three strategies are being used for improving ship efficiency, *Wan et al. (2018)*:

- **Technical solutions:** these are technical means to increase the ship performance, such as better hull design, waste recovery system, etc. This strategy may involve large investment by the shipping companies
- **Operational solutions:** these are normally defined in the Ship Energy Efficiency Management Plan (SEEMP). These solutions are taken by the ship operator, and normally do not require a high level of investment. Some examples of operational solutions are the adoption of slow-steaming, trim optimization, etc. In order to optimize any operation, it is critical to have data available to support the changes implemented.
- **Market-Based solutions:** This is the most controversial solution since the potential benefits are not universally accepted. This solution carries more challenges which are covered by different authors, *Wan et al. (2018)*, *Shi (2016)*.

On this study, we paid attention to the *operational solutions* which may be regarded as the most cost-efficient. One of the most topical operational solutions adopted is that of digitalization and data analysis. In this regard, shipping companies are investing a lot of resources in digitalizing their business structures anticipating seeing the benefits of such investments. It has been pointed out that traditional ways of analyzing the ship performance by using low frequency data (noon reports) might be not good enough, *Aldous et al. (2013)*, due to higher uncertainty associated with such low frequency data. The advent of big data techniques and their benefits for obtaining valuable insights enabling better decision-making has been and remains a hot topic across the industry. The companies need to manage the data collected and get insights from that.

Nowadays, vessels are using more and more sensors to measure and capture an extensive set of data including from navigation, cargo, machinery and auxiliary systems. The continual improvement in quality and accuracy of such sensors giving very high level of precision in the measurements and data transmission, *Gonzalez et al. (2018)*.

As part of their digitalization strategy, the shipping companies have realized they need systems to gather and store automatically the various inputs from those sensors, instead of overloading the crews with additional manual reporting requirements. One way of solving this, is by installing Continuous Monitoring (CM) and data acquisition systems. These tools will automatically support better decision making and reporting, with more transparency. However, in order to retain the advantage of CM system, priority must be given to monitoring the quality of the input. Otherwise their results become valueless. One typical example about the benefits and challenges of using high-frequency data and CM systems can be found when an overconsumption is analyzed. The reason for such overconsumption could be found in a decrease of the vessel performance. However, a sensor malfunction, wrong or missing manual recordings, adverse weather, or other external factors can also cause it. Therefore, automatic data collection, filtering, repeatability and transparency in a performance monitoring system are critical elements for the credibility of the CM system. Once the input quality is assessed, the combination of displaying instant performance values together with investigating the long trend of important key performance values are keeping the crew and the management continuously and accurately updated on a vessel's performance status, *Hagestuen et al. (2016)*.

Besides the beforementioned, the ship-to-shore communication and internet availability on board has been significantly improved, making it easier to transfer data from ship to shore. As such, it helps the shore staffs to perform deeper data analysis and even anticipate to a problem on board. Before 2025, many ships, systems, and components will be linked to the Internet, making them accessible from almost any location in the world. Maritime connectivity will advance significantly, forcing to the industry to be ready for using and getting insight from such huge volume of data and at such high velocity, <https://to2025.dnvgl.com/shipping/digitalization/>.

One factor to be considered as essential when the companies are defining their digitalization strategies and data management plans is, what they need to monitor to get valuable results.

Different vessel's type, trade or operator are some parameters that affects the required parameters to monitor the ship performance. In this regard, ISO, by means of the standard 19030, is trying to homogenize and define the required parameters and methods to evaluate the hull and propeller performance in a standard way.

One of the bases for the ISO 19030 is the automatic high-frequency data collection from sensors on board. This is a delicate issue due to the controversies within the industry about the reliability of the data measured by sensors. Adding more complexity to that problem, the growing volumes of data and the increasing number of source systems can lead to possible data errors, duplicates, missing values, incorrect formatting and contradictions in data analysis, *Azeroual et al. (2018)*.

In this study, we focus on the automated detection of anomalies and assessment of quality in the high-frequency data collected by continuous monitoring system. The technique used for this study is a machine learning technique called Long-Short-Term-Memory (LSTM) neural networks, which are applied on four ships with four datasets formed by high-frequency data (15 s) according the ISO 19030 standard. Other metrics applied on statics are being applied in order to show the quality of the datasets.

2. Methodology and data acquisition

The methodology used is based on the collection of high frequency in-service data automatically from on board the by a Continuous Monitoring system (CM) system installed on four ships. The CM collects data from different sensors (Table 1) at 15 s intervals which is averaged into hourly readings for increasing the performance in the data quality assessment.

Table 1: Parameters and sensors used on this study

Variable	Sensor	Error Associated
Shaft Power	Torque-meter	0.5 % (a)
Shaft RPM	Torque-meter	0.1 % (a)
ME Fuel consumption	Mass flow meter	0.1-0.2 % (b)
Speed Through the water	Doppler log	3 % (c)
Speed over ground	GPS	5 % (c)
Draft astern and forward	Draft sensors	+0.1 m (c)
Rudder Angle	Rudder Angle Indicator	N/A
Ship heading	Gyrocompass	N/A
Depth of water	Echo-sounder	N/A
Wind relative speed and direction	Anemometer	N/A

(a): Kyma Power Meter, (b): Hunsucker et al. (2018), (c): ISO (2016)

ISO 19030 defines two levels of parameters, primary and secondary parameters. Primary parameters are two and they are the Shaft Power and the Speed through water. In Table 1, the primary parameters are in green font and the secondary in blue fonts.

Once the high-frequency data is collected on board by the CM system, it is stored in a database and then the data is averaged into hourly values. Following to this averaged, the data is filtered eliminating outliers and, as a final step to assess the data quality, machine learning technique is applied on the data sets in order to detect anomalies on the inputs from sensors. The whole process is described in Fig.1.

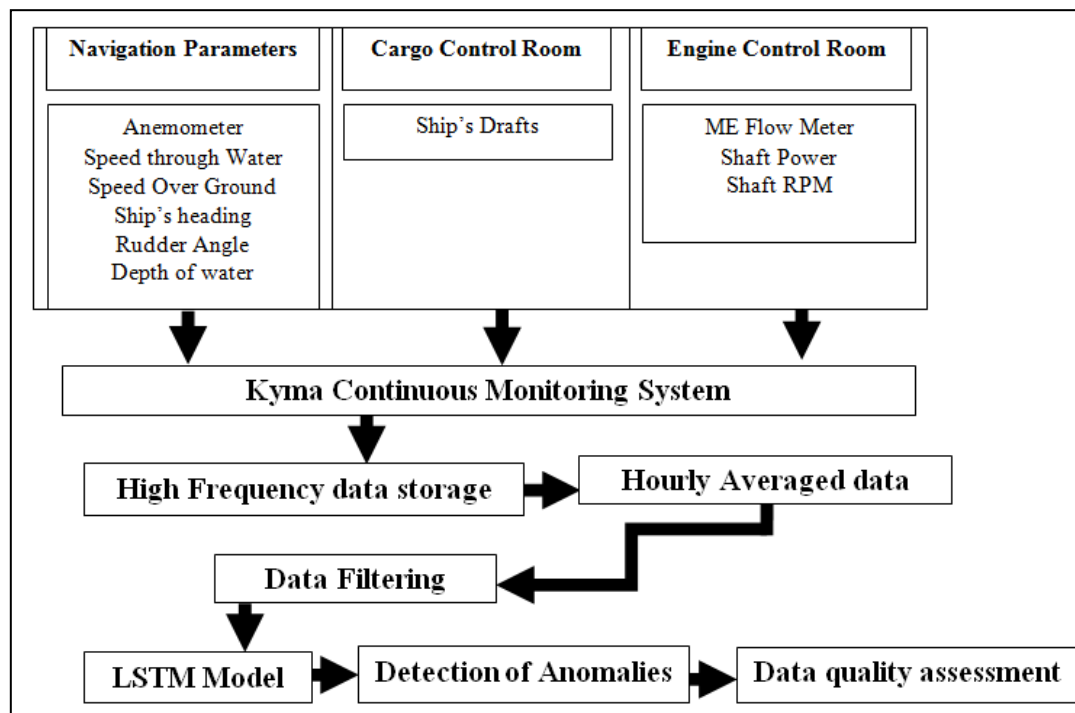


Fig.1: Methodology and data acquisition flow diagram

On this study, we only focus on data quality assessment and anomalies detection for the parameters Speed Through Water, Shaft Power, Shaft RPM and Speed Over Ground.

2.1. Data Filtering applied on the raw data

The raw data collected by the CM system, is automatically filtered as it is shown in Table 2, to avoid outliers. These conditions are the only filters applied on the datasets subject of this study.

Table 2: Data filtering applied on datasets

Condition	Output
If Shaft RPM < 2 rpm	SOG = 0
	STW = 0
	SP = 0
	ME Fuel = 0
If Shaft Power < 100 kW	SOG = 0
	STW = 0
	RPM = 0
	ME Fuel = 0

SOG: Speed Over Ground
STW: Speed Through Water
SP: Shaft Power

2.2. Data quality assessment

There are multiple approaches to assess data quality. These approaches can be differentiated based on the level of control one has over the data generation process. In this sense, data quality assessment can be either experimentally based or real-performance based. In this paper we focus on the latter. Among the available real-performance based quality assessment approaches, we make a distinction between two modelling paradigms, statistical modelling and machine learning modelling (also known as algorithmic modelling; see *Breimann (2001)* for a thorough discussion on these two modelling approaches from an ontological point of view). Statistical modelling is based on mathematical proofs and widely accepted. Statistics collect, arrange and analyse data sets, providing information about the instruments used for gathering the data. However, they frequently fail when dealing with complex and highly nonlinear, *Karlaftis and Vlahogianni (2011)*.

Machine learning modelling (ML) approaches are more flexible; include learning processes, offer better performance processing outliers and mitigating noisy inputs, *Ma et al. (2015)*. These approaches are currently accepted as a method to manage high dimensional and non-linear relationships.

In this study, we have decided to assess the data quality of our inputs (values from sensors) using the Machine learning. Specifically, we make use of a type of Deep learning model, which specializes in dealing with time-series data, namely Long Short-Term Memory (LSTM).

LSTMs belong to a class of neural networks currently referred to as Recurrent Neural Networks (RNNs). RNNs are neural network-based models that are particularly geared towards processing time series type data. A neural network is a group of interconnected nodes (neurons) organized in layers. Each layer of neurons receives input from the previous layer such that each of the neuron's output is the result of a non-linear combination of the weighted input it receives from neurons in the previous layer. Therefore, the more the neurons per layer are the higher the order of the neurons' non-linear outputs will be. In this sense, we can roughly categorize neural networks based on this metric (neurons per layers) or, in other words their "depth". This concept gives rise to the nowadays quite popular Deep learning denomination, where "Deep" represents the existence of multiple layers of neurons. Although there is no universal consensus on how many layers are needed in order to consider a neural network to be deep, the difference between a deep neural network and a shallow (not deep) neural network is often depicted as in Fig.2.

The interaction between neurons across layers is regulated by activation functions. Activation functions take in the inputs from previous neurons and produce a non-linear output. Some examples of these functions are Sigmoid, RELU and Tanh, see *Mohammed et al. (2018)* for an application-based discussion on these functions.

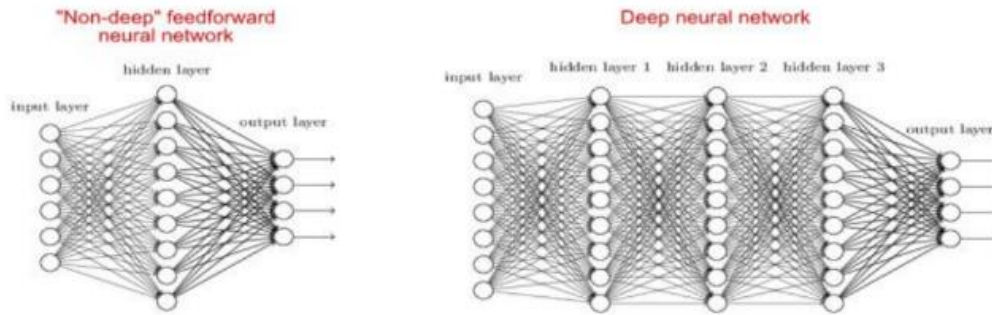


Fig.2: Non-deep and deep neural networks

Once all the neuron layers have been activated through a succession of activation functions, the outputs of the output layer are contrasted with a real variable. In our case, the output layer is contrasted with the measurements we have for each of the variables we have included in this study. By performing such contrast, a prediction error is calculated, and departing from this error, the weights of all neurons are changed such that this error is minimized.

This process is often referred to as back-propagation. Specifically, the error is treated as an objective function to be minimized by adjusting all the networks' weights. This minimization process can be carried out using multiple optimization algorithms, which are often based in the mathematical process of gradient descend, *Friedman (2011)*. In order to use neural networks to process time series data, it is necessary to somehow keep track of time and transfer learning from one-time instance to another i.e. it is necessary to include memory into the neural network. RNNs do exactly that, they give memory to neural networks by creating stacked, sequential architectures that can capture time, *Georgiopoulos et al. (2011)*. While creating such architectures gives neural networks the ability to deal with time-dependent data, it also creates non-trivial mathematical challenges to ensure that the back-propagation process is able to minimize the prediction error, *Hochreiter (1998)*. In order to solve these challenges, a type of neural network with a more sophisticated memory mechanism that received the name of Long Short Term Memory (LSTM). The models we design and implement of this paper are LSTM neural networks. For the LSTM model used in this study, dependent variables have been defined in order to train the model to predict the results and see how far or close these are from the real values, assessing the data quality by determine the R-square of the series for each input from sensors. The LSTM approach is well explained on different works, *Ma et al. (2015)*, *Bodén (2002)*, *Jaeger (2002,2012)*, *Ordóñez and Roggen (2016)*. In order to train and validate the LSTM model, the data was split into two sets: the training set and the test set. The training set was used to train the LSTM, while the test set was used for prediction only. The variables defined for the training model are shown on the Figs.3-6.

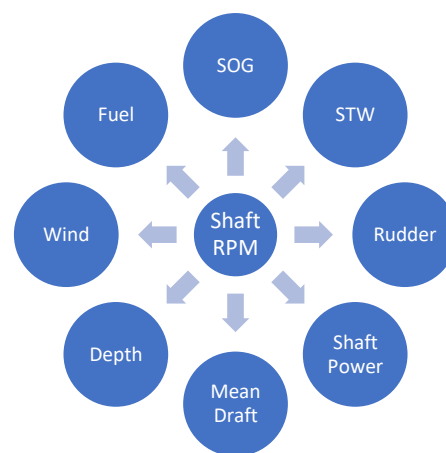
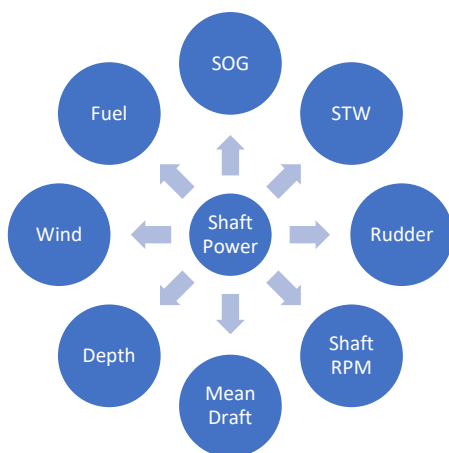


Fig.3: Dependant variables for “Shaft Power” Fig.4: Dependant variables for “Shaft rpm”

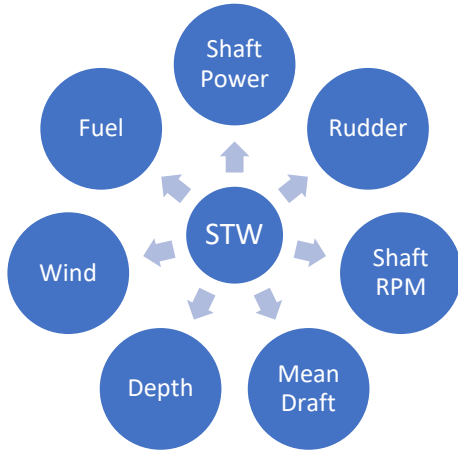


Fig.5: Dependant variables for “STW”
STW: Speed Through Water

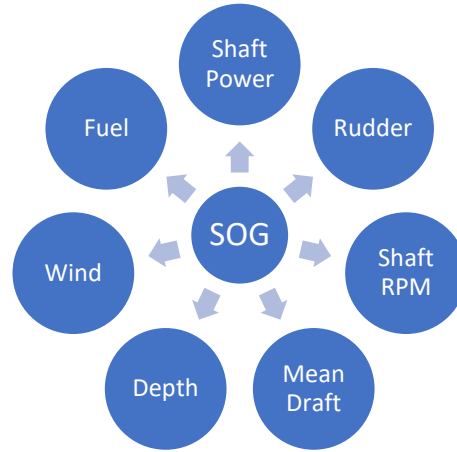


Fig.6: Dependant variables for “Shaft SOG”
SOG: Speed Over Ground

For the numerical analysis, three metrics are used on this study in order to assess the data quality of the inputs. These are:

- **Mean Absolute Error (MAE):** it is a measure of difference between two continuous variables. It is one of the most common metrics used to measure accuracy for continuous variables. MAE measures the average magnitude of the errors in a set of predictions, without considering their direction. It’s the average over the test sample of the absolute differences between prediction and actual observation where all individual differences have equal weight.
- **Mean Square Error (MSE):** The mean squared error tells you how close a regression line is to a set of points. It does this by taking the distances from the points to the regression line (these distances are the “errors”) and squaring them. The squaring is necessary to remove any negative signs. It also gives more weight to larger differences. It is called the mean squared error as you are finding the average of a set of errors.
- **Coefficient of Determination (R-Square):** R-squared is a statistical measure that’s used to assess the goodness of fit of our regression model. In R-squared we have a baseline model which is the worst model. This baseline model doesn’t make use of any independent variables to predict the value of dependent variable Y. Instead it uses the mean of the observed responses of dependent variable Y and always predicts this mean as the value of Y. Any regression model that we fit is compared to this baseline model to understand its goodness of fit.

2.3. Anomalies detection

In this study, anomalies are defined as a function of predictions and real values. More specifically, the difference between real and predicted values i.e. the prediction error, is used as a base for determining whether a particular observation in the data can be considered an anomaly. In this sense, an anomaly is identified as such if the error term exceeds one of a given set of upper and lower thresholds where these thresholds are given by the error’s mean and standard deviation values across a specific time span. In this study, we defined four main parameters, namely a rolling window (time span), and three multipliers for the standard deviation of the error. In this specific study, we used a rolling window of 3 hours (i.e. predictions for a specific time are made using data from the time in question together with data from up to three hours before), and multipliers (K) of 1.5, 1.75 and 2.0 for the standard deviation. The upper and lower thresholds for anomaly detection are therefore written as shown in the Eq.(1):

$$Threshold_t = \frac{\sum_{i=t-3}^t error_i}{4} \pm K \left(\sqrt{\frac{\sum_{j=t-3}^t x_j - \frac{\sum_{i=t-3}^t error_i}{4}}{3}} \right) \quad 1$$

K takes the values of 1.5, 1.75 and 2.0. This results in three pairs of thresholds, one for each K. An anomaly is defined as an observation that exceeds at least one of such thresholds by being either lower or higher than the threshold. This should provide an acceptable basis for anomaly detection, provided our predictions can be trusted and the model predictions are unbiased (i.e. the model's error prediction are normally distributed with mean zero).

While this methodology directly allows to classify anomalies according to their severity (e.g. anomalies could be classified based on what threshold they have exceeded in the likes of branding them as “serious anomalies”, “suspicious anomalies”, “mild anomalies” should they exceed the $K=2.0$, $K=1.75$ or the $K=1.5$ respectively), we decided to plot their severity directly instead. Therefore, anomalies are depicted in our graphs results if and only if they have exceeded the lowest threshold ($K=1.5$) and their severity (e.g. their error term value) is plotted as is in red.

3. Vessel Characteristics

The data from four ships have been used on this study. The ships characteristics are shown in Table 3.

Table 3: Ships characteristics

Vessel No	Group	Ship type	Construction Year	Built in	DWT
1	A	COT	2016	DSME	300 000
2		COT	2016	DSME	300 000
3	B	LNG carrier	2017	DSME	95 785
4		LNG carrier	2017	DSME	95 785

The ships are sister ships between each ship type, therefore ship 1 – 2 (group A) and the vessels 3 – 4 (group B) are sister between them.

4. Results

The data quality and detection of anomalies in the inputs from sensors are detailed graphically and numerically for each group of ships in this section. It is shown on Figs.7 and 8 and in Table 4.

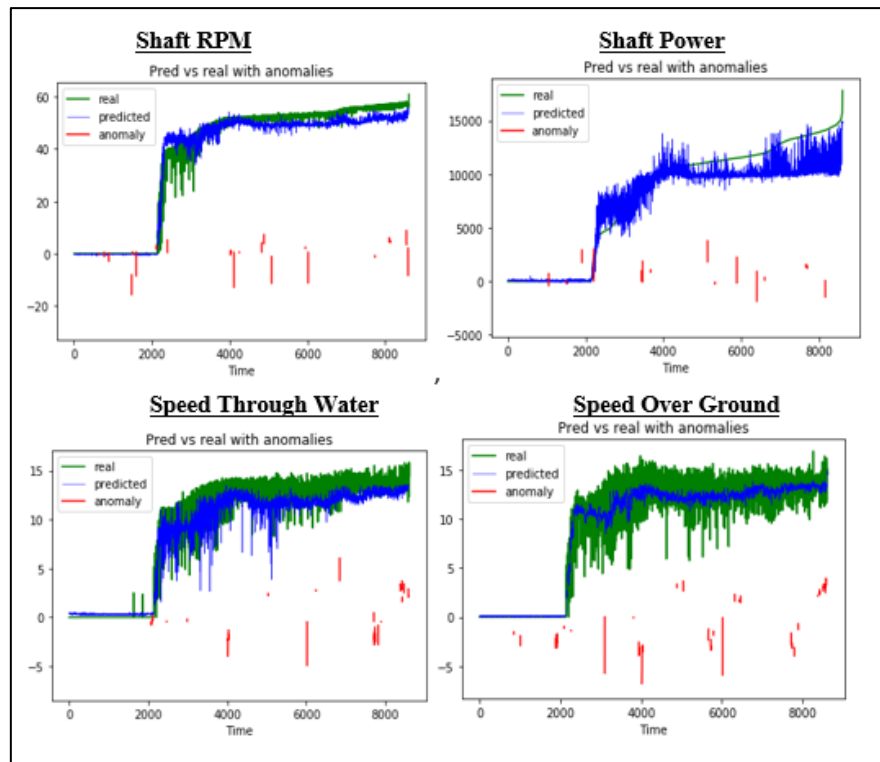


Fig.7: Data prediction and anomalies for vessel group A

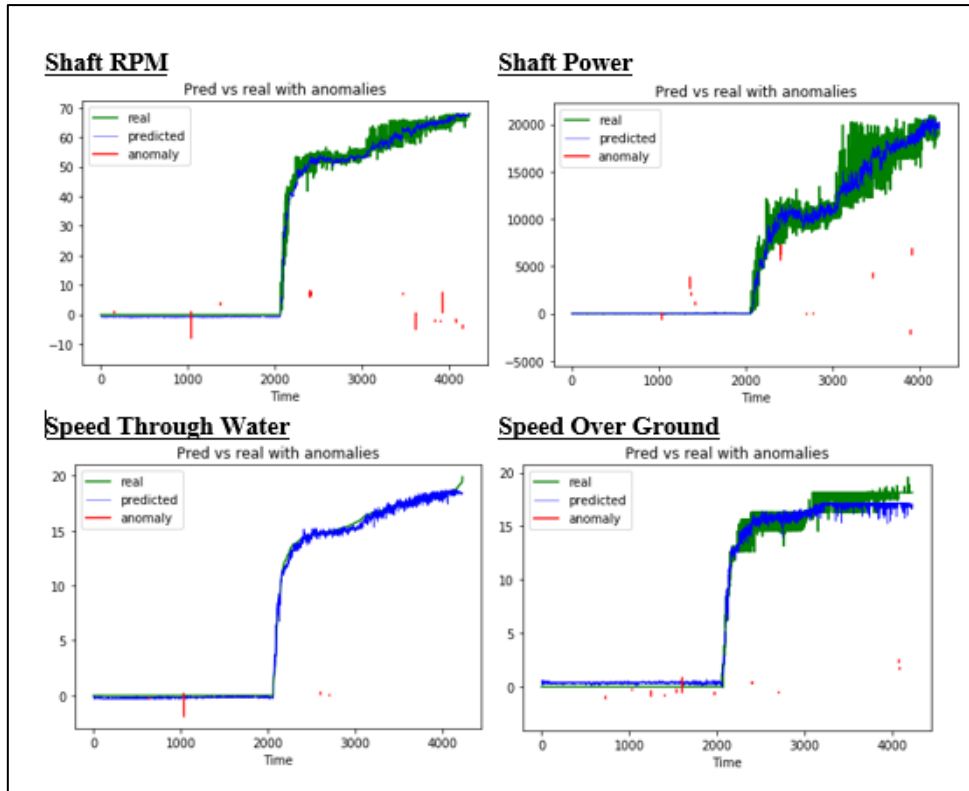


Fig.8 Data prediction and anomalies for vessel group B

Table 4: Data quality – Numerical results

Group	Metric*	Shaft power ⁽¹⁾	Shaft RPM	Speed over ground	Speed through water
A	MSE	31016.1	0.08	0.02	0.03
	MAE	15.03	0.02	0.01	0.02
	R-squared	0.99	0.99	0.99	0.99
B	MSE	13636.2	0.03	0.01	0.01
	MAE	7.33	0.01	0.08	0.01
	R-squared	0.99	0.99	0.99	0.99

(1) The results are expressed as a magnitude of the variable's units.

The data quality on these two ships (vessel group A) is good due to the prediction calculated by the LSTM model (blue line) is very close to the real values measured by the sensors (green lines) for the four parameters. This means that the data quality for this vessel group and these parameters is fairly good as far as real performance tests enable us to determine. A full assessment of the data quality requires experimental tests to complement these findings.

On the graphs, the red vertical-lines represent when the difference between the predicted and real values is significant (anomalies), and the magnitude of the red lines shows how big the difference between both values is. Then, checking the number and the length of these red lines determine the number and magnitude of the anomalies detected. The fewer red lines the less anomalies found.

For the vessel group A, there are not so many anomalies and they are relatively short, indicating that the sensors reliability is quite good. For the vessels group B, the data quality is also fairly good, going the predicted and real values very close. And, very few anomalies were detected by the model, therefore the sensor data is accurate enough to provide good data analysis.

Besides of the graphical data, numerical analysis is done by checking out the three metrics selected and explained on the section 2.2. The results are presented in Table 4.

Concentrating only on how goodness fit is for the variables, it is demonstrated that the four parameters for these four ships analysed are very good, been the R-square values very close to “1” (perfect condition). Comparing both groups, the data quality for the group B is slight better than the quality on vessel group A, according to the metrics MSE and MAE. The R-squared is the same for all the parameters.

5. Conclusions

- a) Confidence of anomalies are very related to the quality of the predictions.
- b) On this study, only one data set is used for training and another one is used only for prediction. It is reasonable to expect that more data, for both training and testing, would generate better, more accurate models.
- c) The data quality on the two primary parameters defined by ISO 19030 is fairly good for the ships analysed
- d) The data quality for the other two parameters analysed, Ship Over Ground and Shaft RPM is also good enough.
- e) The number of anomalies detected is not so high, suggesting a good quality of the sensors installed on board
- f) The ships are operating on real situations; therefore, the data collection is done under an uncontrolled environment.
- g) Due to the uncontrolled environment, it is not possible (on this study) to determine if the anomalies are caused by sensor bias or because the actual ship operation.
- h) A data quality assessment is essential for validating the further data analysis.
- i) Detection on sensor anomalies can also be used for making an automatic sensor status-check.
- j) The current model used can be extended in complexity to assess many more components, providing additional results and insights about the data quality and sensor quality.
- k) For future work, data analysis of other ship performance parameters should be considered for getting the whole data quality assessment of the data sets.

References

- ALDOUS, L.; SMITH, T.; BUCKNALL, R. (2013), *Noon report data uncertainty*, Low Carbon Shipp. Conf., pp.1–13
- AZEROUAL, O.; SAAKE, G.; SCHALLEHN, E. (2018), *Analyzing data quality issues in research information systems via data profiling*, Int. J. Inf. Manage. 41, pp.50–56
- BIALYSTOCKI, N.; KONOVESSIS, D. (2016), *On the estimation of ship's fuel consumption and speed curve: A statistical approach*, J. Ocean Eng. Sci. 1/2, pp.157–166
- BODÉN, M. (2002), *A guide to recurrent neural networks and backpropagation*, Dallas Proj. SICS Tech. Rep. 2, pp.1–10
- BREIMAN, L. (2001), *Statistical Modeling: The Two Cultures*, Stat. Sci. 16/3, pp.199–231
- FRIEDMAN, J.H. (2011), *Greedy function machine: A gradient boosting machine*, Statistics 29/5, pp.1189–1232
- GEORGIOPOULOS, M.; LI, C.; KOCAK, T. (2011), *Learning in the feed-forward random neural network: A critical review*, Perform. Eval. 68/4, pp.361–384
- GONZALEZ, C.; LUND, B.; HAGESTUEN, E. (2018), *Case Study: Ship Performance Evaluation by Application of Big Data*, 3rd HullPIC, Redworth, pp.104–119
- HAGESTUEN, E.; B. LUND, B.; GONZALEZ, C. (2016), *Continuous Performance Monitoring – A*

Practical Approach to the ISO 19030 Standard, 1st HullPIC, pp.49–61

HOCHREITER, S. (1998), *The Vanishing Gradient Problem During Learning Recurrent Neural Nets and Problem Solutions*, Int. J. Uncertainty, Fuzziness Knowledge-Based Syst. 6/2, pp.107–116

HUNSUCKER, J.T.; PRZELOMSKI, D.; BASHKOFF, A.; DIXON, J. (2018), *Uncertainty Analysis of Methods Used to Measure Ship Fuel Oil Consumption*, January

ISO (2016), *ISO 19030 - Part 1*, ISO, Geneva

JAEGER, H. (2002), *A Tutorial on Training Recurrent Neural Networks, Covering BPPT, RTRL, EKF and the “echo state network” approach*, German National Research Center for Information Technology

JAEGER, H. (2012), *Long Short-term Memory in Echo State Networks: Details of a Simulation Study*, Jacobs University

KARLAFTIS, M.G.; VLAHOGIANNI, E.I. (2011), *Statistical methods versus neural networks in transportation research: Differences, similarities and some insights*, Transp. Res. Part C Emerg. Technol. 19/3, pp.387–399

MA, X.L.; TAO, Z.M.; WANG, Y.H.; YU, H.Y.; WANG, Y.P. (2015), *Long short-term memory neural network for traffic speed prediction using remote microwave sensor data*, Transp. Res. Part C Emerg. Technol. 54, pp.187–197

MOHAMMED, M.A.; NAJI, T.A.H.; ABDULJABBAR, H.M. (2018), *The effect of the activation functions on the classification accuracy of satellite image by artificial neural network*, Energy Procedia, pp.164–170

ORDÓÑEZ, F.J.; ROGGEN, D. (2016), *Deep convolutional and LSTM recurrent neural networks for multimodal wearable activity recognition*, Sensors (Switzerland) 16/1

SHI, Y. (2016), *Reducing greenhouse gas emissions from international shipping: Is it time to consider market-based measures?*, Mar. Policy 64, pp.123–134

WAN, Z.; EL MAKHLOUFI, A.; CHEN, Y.; TANG, J. (2018), *Decarbonizing the international shipping industry: Solutions and policy recommendations*, Mar. Pollut. Bull. 126, pp.428–435

Study on Additional Ship Resistance due to Roughness using CFD

Anders Östman, SINTEF Ocean, Trondheim/Norway, anders.ostman@sintef.no

Kourosh Koushan, SINTEF Ocean, Trondheim/Norway

Luca Savio, SINTEF Ocean, Trondheim/Norway

Abstract

The additional resistance due to roughness is studied by means of CFD simulations. The KVLCC2 hull at full-scale Reynolds number is considered as a test case. A wall function formulation is used to model the rough wall turbulent boundary layer, where the roughness function is based on data from towing flat plates coated with paint of similar roughness as for the full-scale vessel. The additional resistance for coatings with various roughness heights is studied, with roughness heights ranging from less than 10 μm to more than 60 μm . Also, the potential in low-cost reduction of frictional resistance is investigated. High-quality paint coating (with low roughness) can be applied at given locations where the skin friction is high, while using cheaper coating and application procedures (resulting in larger surface roughness) at other locations where skin friction is of less importance.

1. Introduction

Resistance due to fouling and poorly applied antifouling coating can have a significant contribution to the total resistance of a ship. This is especially true for ships operating at low Froude numbers, where skin friction resistance is the dominating component of the hydrodynamic resistance and could account for 60% or more of the total resistance. Reliable estimations of added resistance due to rough hull surfaces are important in order to be able to perform speed prediction of the vessel. Also, insight into the relative importance of roughness at different parts of the hull can be used to give guidance on where and how to apply antifouling coating on the ship.

Numerical simulations of rough surface friction drag are traditionally based on roughness functions that relies on finding an equivalent sand grain height that fits *Nikuradse (1933)* pipe flow experiments, examples can be found in *Vargas and Shan (2016)* and *Deminel et al (2014)*.

In the present paper a different approach is applied, the roughness function is based directly on experimental resistance test of the specific surface coating. The roughness function is derived based on experimental flat plate towing tank tests. Plates with various surface roughness were towed at constant speeds, *Savio et al (2015)*, and the results were post processed using methods proposed by *Granville (1987)*. The roughness levels of the different plates were related to typical real applications processes used in the marine industry. Results from these tests were implemented in customized rough wall functions in the OpenFOAM flow solver, and presented in a validation study, *Östman et al (2017)*. The validation showed very good agreement of computed flat plate resistance against experiments.

The method is in the present paper applied on a full-scale ship hull. The coatings and roughness models developed in the 2D validation study is used to model the rough surface ship hull. The computed total friction resistance of the various coatings is compared. Also, the effect of applying the highest quality coating at limited areas, selected based on the computed friction coefficient, is studied.

2. Formulation of the roughness wall function

The implemented physical model that is used to model rough surfaces in the CFD simulations relies on measured flat plate resistance experimental results. Flat plates with various surface roughness were towed at constant speed while resistance was recorded, *Savio et al (2015)*. The roughness on the plates was due to paint applied on the surface of the plates with various quality of application process. The aim was to mimic typical real application processes used in the marine industry. Three roughness levels (denoted A, B and C with increasing order of roughness) were considered. Roughness level A represents

an optimal new build or full blast dry docking application of the paint. Roughness level B corresponds to dry dock situation with some underlying spot repair roughness and poor coating application of the paint. Finally, the plate with the most severe roughness was denoted level C, which could simulate an extreme case with severe underlying roughness accumulated from several dry dockings and very poor application of the paint. In addition, a set of smooth blank plates were used in order to have a reference to the theoretical smooth boundary layer friction drag.

The measured drag was post-processed following methods proposed by *Granville (1987)* and presented in terms of inner variables, Fig.1. The graph shows the shift ΔU^+ of the velocity profile in the logarithmic part of the boundary layer as a function of the non-dimensional roughness height, k^+ , where k^+ is defined by $k^+ = kU_\tau/\nu$. The height, k [m] is a typical roughness height of the rough surface, U_τ is the friction velocity and ν is the fluid kinematic viscosity. The variable, k^+ , can be interpreted as a local Reynolds number for the surface roughness in the boundary layer. The value of typical roughness height, k , is found from a statistical analysis of the actual rough surface and defined as the rms (root mean square) of absolute heights of the surface, and denoted S_q in the following. The statistics of the surface is found from analyzing high-resolution laser scans of imprints of the surface. The measured rms roughness height of the plates is presented in Table 1. Visualisations of the surface from the laser scan is shown in Fig.2.

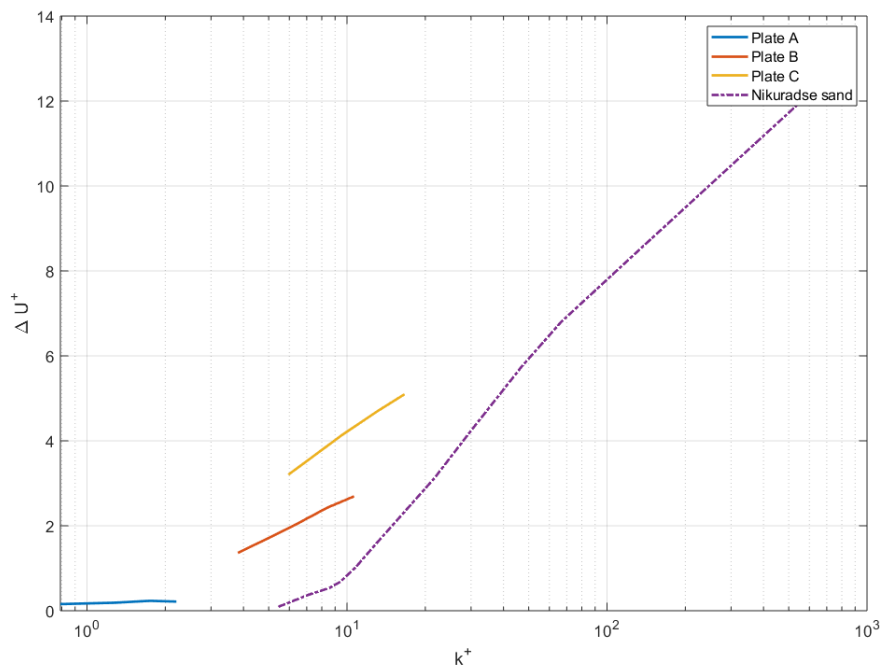


Fig.1: Presentation of the experimental data in terms of inner variables

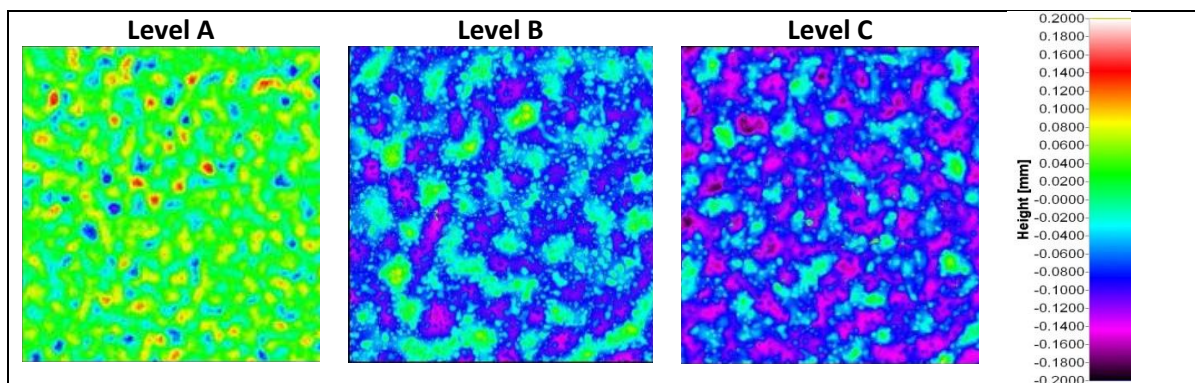


Fig.2: Visualization of surface scans of the plates

Table 1: Measured root mean square of absolute heights of the surface roughness (Sq) of the plates

Plate	$Sq[\mu m]$
PlateA	8.51
PlateB	41.15
PlateC	64.44

The towing test results of the rough plates was used to derive the roughness function that is implemented in the CFD solver. The experimental results, Fig.1, show that each plate has a linear relation between velocity shift and $\log(k^+)$. Based on this observation, the idea of developing dedicated roughness functions for each surface coating was considered.

The velocity profile in the log law region is described by the equation, *Cebeci and Bradshaw (1977)*:

$$U^+ = \frac{1}{\kappa} \ln(E y^+) \quad (1)$$

where $\kappa=0.41$ is the von Karman constant and E is a constant which equals 9.8 for smooth walls. For rough walls the velocity profile is switched downward in the logarithmic region. This can mathematically be expressed by substituting E with a modified variable E' defined as

$$E' = \frac{E}{f} \quad (2)$$

Where the roughness function, f , can be found directly based on experimental results of the velocity shift (ΔU^+). The procedure on how to estimate f directly from measurements are described in the following. Inserting the expression given in Eq. (2) into Eq. (1) gives:

$$U^+ = \frac{1}{\kappa} \ln\left(\frac{E}{f} y^+\right) = \frac{1}{\kappa} \ln(E y^+) - \frac{1}{\kappa} \ln(f y^+) \quad (3)$$

The last term in the equation is the velocity shift, ΔU^+

$$\Delta U^+ = \frac{1}{\kappa} \ln(f y^+) \quad (4)$$

ΔU^+ is defined to be positive when the velocity profile is shifted downwards. The roughness function f can now be found directly from Eq. (4):

$$f = e^{(\kappa \Delta U^+)} \quad (5)$$

As seen in the experimental results for the velocity shift that are presented in Fig.1 as a function of k^+ , it is evident that a logarithmic fit can be found for each plate. An expression of the velocity shift can be formulated as:

$$\Delta U^+ = a_0 + a_1 \log_{10}(k^+) \quad (6)$$

where a_0 and a_1 are constants of the curve fit. The best fit for different plates are shown in Fig.3.

4. CFD solver

The flow solver used is the simpleFOAM mono fluid solver included in the OpenFOAM package. The solver solves the steady-state fluid flow using the SIMPLE algorithm, *Ferziger and Peric (2002)*. The k-omega SST turbulence model is used to model turbulence. The flow over the rough surfaces is modeled by means of modifying the smooth wall function as described in the previous section.

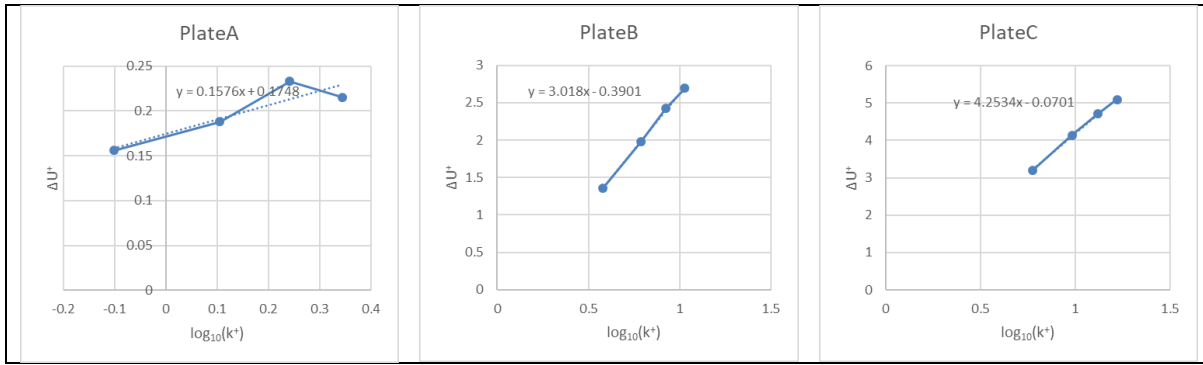


Fig.3 Curve fit of measured velocity shift for the plates

5. Flat plate validation study

The flat plate validation study, presented in *Östman et al (2017)*, is in the following shortly summarized. The problem is simplified in the CFD analysis by neglecting wave generation and end-effects of the towed plates. This is done by solving the equations for a mono-fluid flow field in a 2D dimensional flow domain. Separate meshes were generated for each speed, the meshes were generated with a target for the near wall mesh spacing that results in $y^+ \approx 60$ for the cell center of the wall adjacent cells, Fig.4.

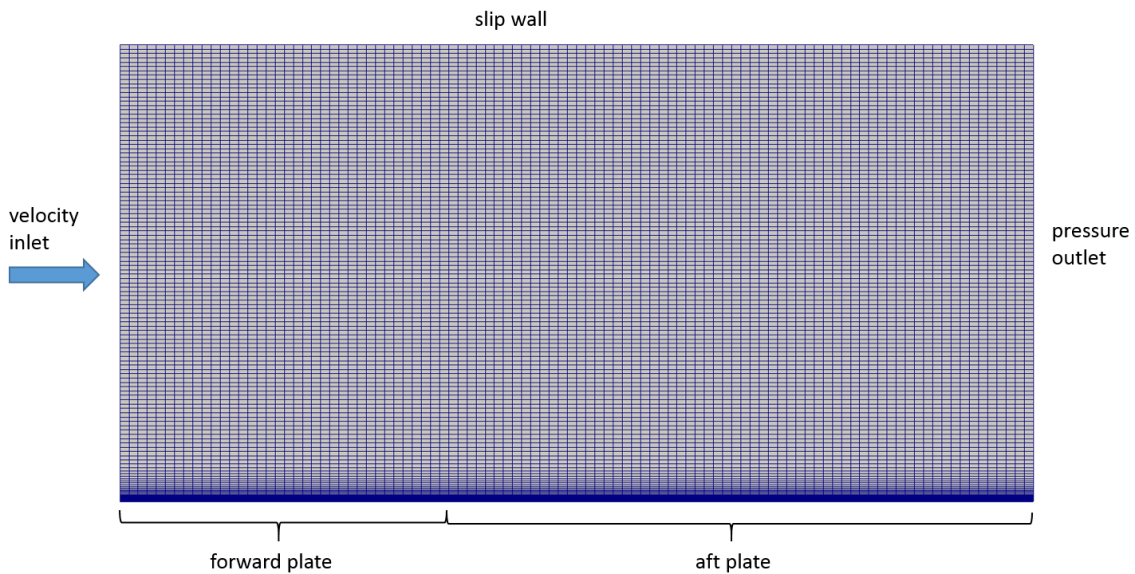


Fig.4: Mesh in the flow domain and boundary conditions

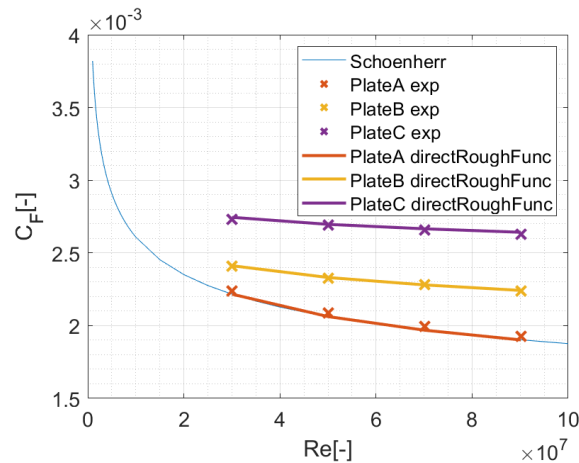


Fig.5: Skin friction resistance coefficient. Comparison of CFD results using the direct roughness function formulation Eq.(5) against experimental results.

The simulations were performed for the same speeds as tested in the towing tank, $U=3, 5, 7$ and 9m/s . The computed results are compared against experiments in Fig.5. The comparison is very good for all plates. The implemented roughness function is thus able to accurately model the behavior of the rough surfaces.

5. Full scale ship hull simulations

Simulation of the full scale KVLCC2 hull is performed at 15 kn . The length between perpendiculars of the vessel is 320 m , resulting in a Reynolds number of 2.08×10^9 and Froude number 0.137 . The same rough hull coatings as in the flat plates experiments is assumed. At this low Froude number, wave resistance is of less importance, while skin friction resistance being the dominant resistance component. The purpose of the present study is to quantify the increase in resistance due to hull surface roughness. It was therefore decided to simplify the simulation setup by replacing the free surface with a fixed slip surface. The motivation for this simplification is: (i) Changes in wave resistance due to hull surface roughness is assumed to be very small. The wave pattern, and hence, the wave resistance is not expected to be influenced by the hull surface roughness. (ii) We are only interested in the difference in resistance due to hull roughness, thus, the actual level of resistance is of less importance as long as the difference in resistance is captured by the simulation setup. (iii) The wave resistance is anyhow a small component of the total resistance due to the small Froude number.

The rough surface was modelled using the direct roughness function with the same parameters as for the flat plate simulations. The 3D volume mesh was generated using the HEXPRESS™ grid generator. Illustrations of the flow domain and mesh on the hull surface in the symmetry plane are shown in Fig.6 and Fig.7. The mesh is refined in the boundary layer in order to accurately capture the boundary layer profile. The aim is to have a y^+ value in the range $40-100$ at the cell centre in vicinity to the hull surface. Based on boundary layer theory the size of the first cell normal to the hull surface is chosen as 0.6 mm . The total number of grid cells was approximately 6.2M .

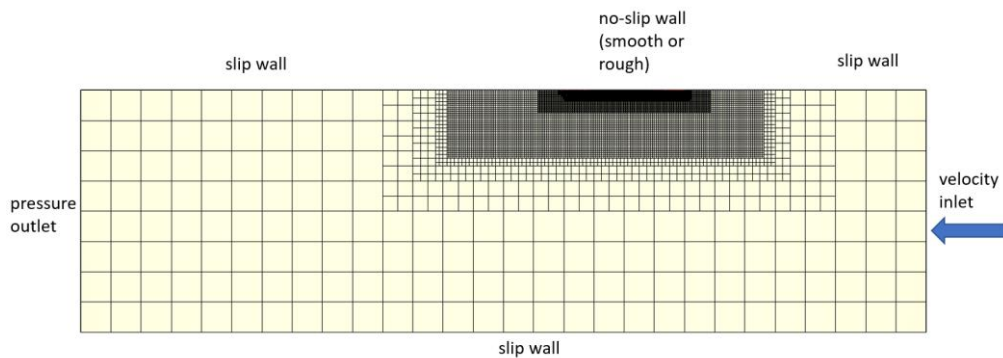


Fig.6: Illustration of mesh on the hull surface and in the symmetry plane

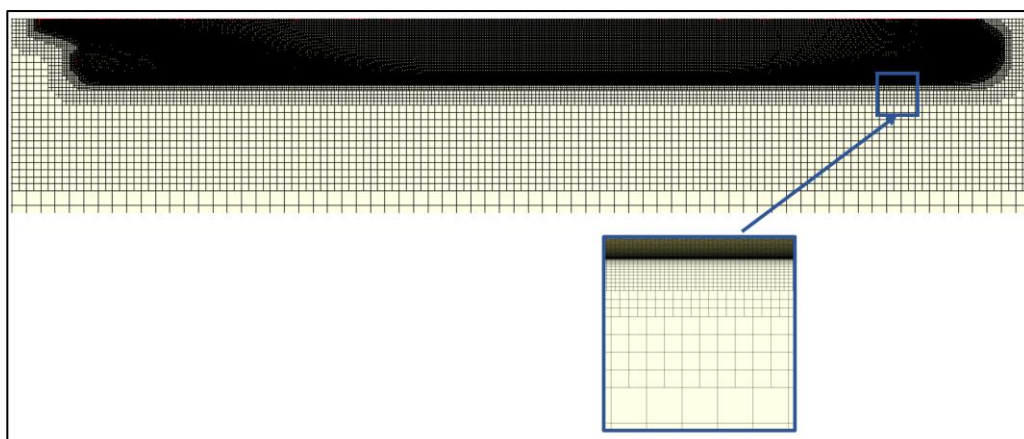


Fig.7: Mesh on the hull surface and in the symmetry plane in vicinity to the hull

The computed wall shear stress on the hull for the different surface coatings is presented in Fig.8. For simplicity, the surfaces are denoted to have different coatings, this is strictly not correct, all surfaces are treated with the same coating, but using different quality of the application process, resulting in different surface roughness. However, the term "coating" is in the following used to simplify the presentation.

As expected, the wall shear increases with increasing surface roughness. Moreover, the increase in shear stress is seen on the entire hull surface. As was also observed in the flat plate simulations, the smoothest coating is very smooth, which results in a shear stress that is very similar to the stress on the hydraulic smooth reference surface. The largest values of wall shear stress are seen in areas with accelerations in the flow, such as around the shoulder and at the bilge in the bow area. The computed friction resistance coefficients are compared in Table 2. The increase in resistance for coating A, compared to the smooth surface, is only 0.9%. Coating B results in about 11% increase, while the increase in resistance for coating C is 24% compared to the smooth surface.

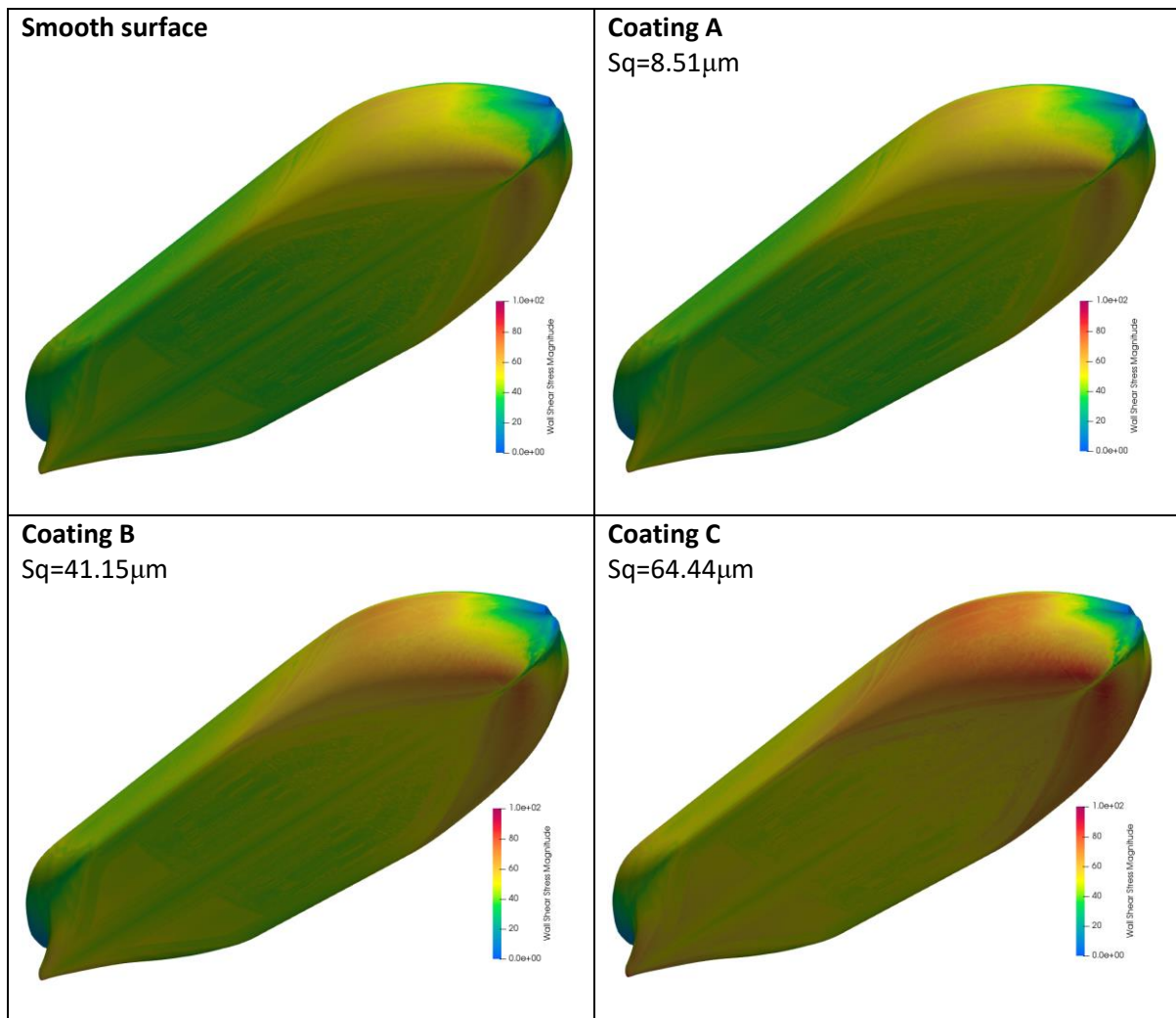


Fig.8: Computed wall shear stress at the hull surface for the different coatings

In an attempt to investigate the relative importance of surface coating quality at different parts of the hull, the hull surface was split based on shear stress threshold values. Using coating C as a basis, areas with shear stress exceeding 60, 65 and 70 Pa were identified. The hull surface was thereafter split in two parts based on these threshold values. The splits are shown in Fig.9. The red part illustrates areas with high wall shear stress. The size of the area of the high shear part of the hull depends on the threshold value. The area of the part of the hull where $\tau_w > 70$ Pa is 134 m², this corresponds to approximately 0.5% of the total wetted hull surface area. Threshold $\tau_w > 65$ Pa results in an area of 798

m² (3%), while $\tau_w > 60$ Pa results in an area of 2433 m² (9%). Simulations was thereafter performed using the high quality coating A at the part of the hull where the shear stress exceeds the threshold value, while the remaining part of the hull has the rough coating C. The computed wall shear stress on the hull surface is also shown in the figure. The shear stress is significantly reduced at areas where the smooth coating is applied.

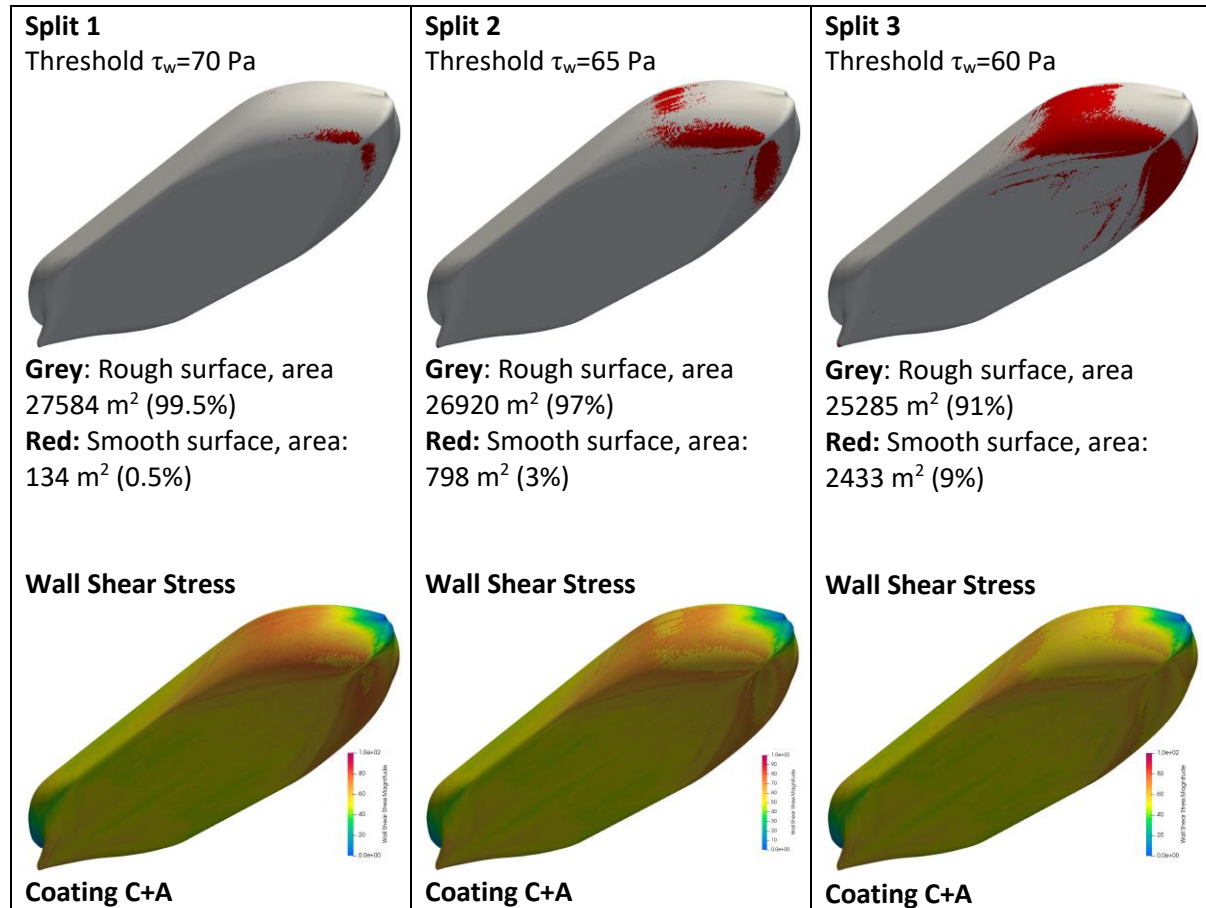


Fig.9 Above: The hull surface splitted based on a wall shear stress threshold. Below: Computed wall shear stress at the hull surface. Simulations using different coatings. Surface coating C is applied on the grey part of the hull, coating A is applied on the red part.

Table 2: Computed friction resistance coefficient of hull with different coatings. The increase relative to the smooth hull is also presented.

Surface description	C _F *1000 [-]	% Increase
Smooth	1.3096	0.0 %
Coating A	1.3216	0.9 %
Coating B	1.4502	10.7 %
Coating C	1.6240	24.0 %
Split 1, Mixed Coating C+A	1.6219	23.8 %
Split 2, Mixed Coating C+A	1.6151	23.3 %
Split 3, Mixed Coating C+A	1.5905	21.4 %

The computed friction resistance coefficients are presented in Table 2. The resistance is reduced for the hull with mixed coatings compared to the hull with coating C. However, the reduction is not very large. For Split 1, where only 0.5% of the hull is treated with coating A while the rest of the hull consist of coating C, the increased resistance compared to the smooth reference is 23.8%, instead of 24% for the hull with coating C on the entire wetted surface. This corresponds to approximately 1% "reduction of

increase" (0.2% of 24%). That is, by treating 0.5% of hull with a high-quality coating, the increase in resistance is reduced by 1%. By increasing the area of the part which is coated with coating A the resistance is further reduced. For Split 3, where 9% of the hull is treated with coating A, the increase in resistance is reduced to 21.4 % compared to the smooth surface hull simulations. The computed resistance of the various surface coatings is also compared in Fig.10.

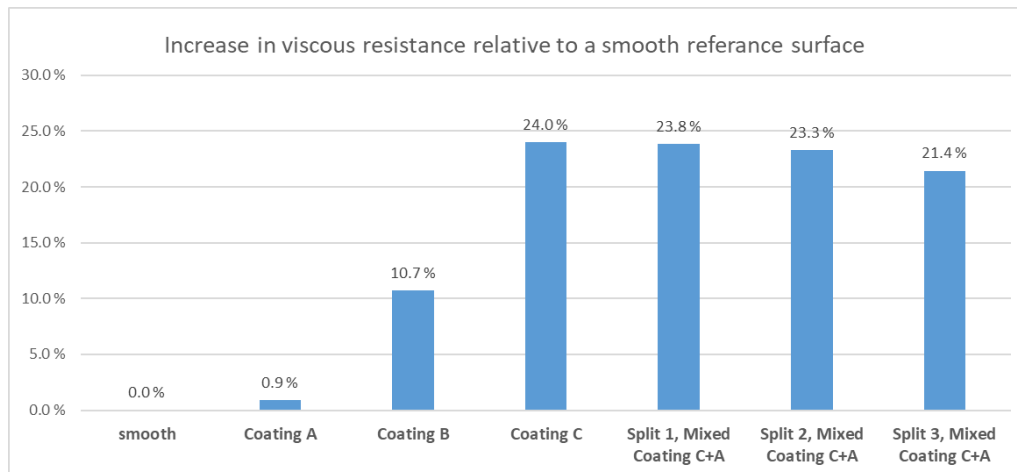


Fig.10: Computed increase in viscous resistance for the different coatings

6. Conclusions

The additional viscous resistance due to surface roughness on a full-scale ship hull has been studied using CFD simulations. Three different rough coatings were modeled, the rough surfaces correspond to realistic hull surface conditions found in the marine industry. Parameters in the numerical implementation of the roughness function, which is used in the turbulent wall function, relies on towing tank experiments conducted on coated sample plates.

The simulations showed, for the roughest coating, an increase in viscous resistance of 24%, compared to a smooth hull surface. The potential of low-cost reduction of frictional resistance was also investigated. When a low roughness coating was applied at locations where the shear stress is high, while the rest of the hull had a high roughness coating, the resistance was reduced compared to having the same rough coating on the entire hull. However, the reduction of viscous resistance was not very large. When 9% of the hull has a low roughness coating, while the rest of the hull is coated with the roughest coating, the increase in viscous resistance was computed 21.4%, instead of 24%, which is the increase in resistance when the entire hull is coated with the roughest coating.

Acknowledgements

Part of this work was supported by the EU FP7 Project "Low-toxic cost-efficient environment-friendly antifouling materials" (BYEFOULING) under Grant Agreement no. 612717.

References

- CEBECI, T.; BRADSHAW, P. (1977), *Momentum Transfer in Boundary Layers*, McGraw-Hill
- DEMIREL, Y.K.; KHORASANCHI, M.; TURAN, O.; INCECIK, A. (2014), *A CFD model for the frictional resistance prediction for antifouling coatings*, Ocean Engineering 89, pp.21-31
- FERZIGER, J.H.; PERIC, M. (2002), *Computational Methods for Fluid Dynamics*, Springer
- GRANVILLE, P.S. (1987), *Three Indirect Methods for the Drag Characterization of Arbitrarily Rough Surfaces on Flat Plates*, J. Ship Research 31, pp.70-77

GRIGSON, C.W.B. (1992), *Drag losses of new ships caused by hull finish*, J. Ship Res. 36, pp.182–196

NIKURADSE, J. (1933), *Laws of flow in rough pipes*, NACA Technical Memorandum 1292

ÖSTMAN, A.; KOUSHAN, K.; SAVIO, L. (2017), *Numerical and Experimental Investigation of Roughness Due to Different Type of Coating*, 2nd HullPIC, Ulrichshusen

SAVIO, L.; BERGE, B.O.; KOUSHAN, K.; AXELSSON, M. (2015), *Measurements of added resistance due to increased roughness on flat plates*, 4th Int. Conf. Advanced Model Measurement Technology for the Maritime Industry, Istanbul

VARGAS, A.; SHAN, H. (2016), *A numerical approach for modeling roughness for marine applications*, FEDSM2016-7791, ASME 2016 Fluids Engineering Division Summer Meeting, Washington

Influence of Data Sources on Hull Performance Prediction

Daniel Schmode, DNV GL, Hamburg/Germany, daniel.schmode@dnvgl.com
Ole Hympendahl, DNV GL, Hamburg/Germany, ole.hympendahl@dnvgl.com
Francesco Bellusci, Scorpio, Monaco, fbellusci@scorpiogroup.net

Abstract

Hull Performance assessment is done based on very different data sources. Basic noon reporting is already implemented on all vessels. Specific reporting software is guiding crew and reducing reporting mistakes. Complex auto-logging systems reduce the human factor and deliver higher data frequencies. All sources have pros and cons. Here we present ways to combine these sources with 3rd party data. Best combination of sources with respect to value to cost ratio is differing depending on vessels equipment and operation. A scoping exercise is always recommended before engaging in any project to properly define objectives (improve commercial performance, improve technical performance, etc.) and invest as consequences.

1. Introduction

All commercial vessels report data in different formats. Some are also equipped with automatic data acquisition systems. Owners, managers and operators are interested in assessing vessel performance. The quality of the performance assessment depends on the input data which differs in quality and quantity.

We are following the discussion arguing either to do analysis based on simple noon or on high-end auto-logged data. In reality, things are not just black or white; we see many shades of grey. In the following, we discuss the pros and cons of different data sources as well as options to combine them to get better results.

2. Available data sources

We see a wide spectrum of reporting regimes on-board vessels today. They are driven by different stakeholders, such as vessel owners, technical managers, operators, routing companies, etc. Because stakeholders have different aims, reporting systems vary in scope and technology. Often vessels are required to report similar information to different stakeholders through different systems at the same time.

Below we try to categorize the reporting systems we have seen. Here we categorize from the hull performance prediction perspective. Thus, we might skip information relevant for other tasks. For other purposes, a different categorization might be more suitable.

2.1 Noon reporting

All commercial vessels do noon reporting due to SOLAS requirements. Typical noon reports contain time, position, speed, draft/trim, weather and fuel RoB/consumption data. Noon reports are sent every noon. Thus, their frequency is once in 24h. In case the time zone changes, the period between two reports can be either 23 or 25 hours. This needs to be accounted for if consumption rates are calculated. Most noon reports include the current operational status (sea/port), but do not differentiate consumptions by operation modes like sea passage, maneuvering or anchoring.

Data format varies from simple free text email to complex spreadsheet forms. Free text email is hard to process for a computer, since small differences (e.g. comma instead of decimal point) can irritate the parsing algorithm. Spreadsheet forms with automatic format validation overcome the issue.

Operational modes are not separated; thus, consumption cannot be mapped to operational modes. This is a substantial intrinsic inaccuracy. Typically, crews do not get feedback on the reporting quality, which can lead to inaccurate reporting. Manual reporting is open to misuse, typically for fuel consumption, as to justify inefficiencies or increase efficiencies.

Once forms are developed, documented and deployed, there are no further costs related to data recording. Due to a lack of structure in the data, parsing and analyzing the data might cause high costs.

2.2 Event reporting

Some vessels have implemented an event-based reporting using complex spreadsheet or html forms or specialized reporting software. Typical event reports contain time, position, speed, draft/trim, weather and fuel RoB/consumption data. Often also basic voyage planning (next port, ETA, distance to go, ...), Cargo and SOF related data, engine RPM and running hours, and lube oil and sludge RoBs is reported precisely. Often also detailed fuel quality is reported from bunker delivery notes including sulfur content and LHV.

Event reports are sent at least every noon. Thus, the minimum frequency is once in 23h/24h/25h. If the vessel changes operation mode (sea passage, maneuver, port) a specific event is reported. Typical events are: arrival/departure, begin/end of sea passage (BOSP/EOSP), begin/end of anchoring/drifted. Advanced systems also allow having special events for bunkering, sounding, disposal, cargo operations, etc.

Event reporting systems differentiate between port, sea passage, maneuvering, drifting, anchoring, ballast, laden. Consumptions/RoBs are recorded for every change of operational mode.

Data format varies from complex spreadsheet/html forms to specialized reporting software with RoB bookkeeping and plausibility checking.

Operational modes can be analyzed separately. Systems with built-in plausibility checks avoid typos or unit mismatch. Risk of involuntary or voluntary error is always present, a vessel tracking system service tends to reduce certain inaccuracies.

When 3rd party software is used typically some license costs for reporting and aggregation of events. Analyzing the results is then straightforward.

2.3 Snapshot reporting

Event reporting allows reporting average numbers (e.g. speed, power, wind) between the events. These numbers are not always constant over the reporting period. With respect to hull performance evaluation, averaging over a 24h period introduces substantial noise. Thus, DNV GL introduced the concept of snapshot reporting. Here figures are averaged over a short period (15-30min) and reported in a special snapshot event. Crews are advised to do this measurement when weather and vessel are in steady state.

Typically, GPS data, heading, speed log, draft/trim, wind, RPM, shaft power, fuel flow and often M/E parameters like T/C speed, exhaust gas temperature, etc. On sea passage, reports are created 1-3 times per day, and only on sea passage.

The reports are transmitted as spreadsheet or reporting software. Trained and motivated crews typically deliver good quality data which is sufficient for hull performance evaluation. There are no additional cost involved, just crew time to carry out measurements.

2.4 Automatic data acquisition systems

Especially modern and complex vessels have many sensors connected to an automatic data acquisition system. Typical sensors are GPS data, gyrocompass for heading, speed log, draft/trim, wind, RPM, shaft power, fuel flow and often M/E parameters like T/C speed, exhaust gas temperature, etc. Fuel quality is usually not available. If the fuel flow measurement is based on volume, density and temperature are required but usually not measured.

Typically, the data aggregation period is 1 to 15 minutes. Automatic data acquisition systems do not differentiate between operational mode (port, sea, etc.). Data format varies from text/csv (comma separated value) files to compressed binary formats such as hdf5. The quality depends on sensor maintenance/accuracy. The same applies for manual reading, but we see that through manual reporting broken or imprecise sensors are detected and fixed earlier. Draft sensors do not give reliable results in many cases due to their working principle based on static water head. Here manual readings or loading computer data is more reliable.

Sensors and data loggers in the maritime environment are complex technology. They require substantial CAPEX and OPEX. Nowadays also simple solutions are available at a lower cost which are only connected to an existing NMEA bus. These might lack relevant channels such as power and consumption.

2.5 Third-party sources

Available data is weather (wind and waves), currents (sea and tidal), water temperature, water depth and AIS signals. Data is collected from once per minute (AIS close to shore) to once per 6h (weather models) and comes through APIs, with weather data in complex binary formats. Weather models deliver good quality hindcast. Close to the coast, substantial deviation might occur due to local weather effects and tidal currents. AIS is a cheap auto logging of the GPS signal. The quality is very good. Many weather sources are available free of cost. Converting and interpolating to vessel position is complex. For AIS data a subscription is required.

3. Requirements for vessel reporting schemes

In the classical commercial setup, a vessel owned by one party (owner) is managed by another (manager), who is responsible for the maintenance of the ship. The vessel is chartered by the owner to an operator, who usually pays the fuel. The different parties have different requirements which we summarize here. The list is by far not complete, but we focus here on what is motivating the reporting in many cases.

3.1 Requirements from the ship owner

Ship-owners need to have a clear view on the technical performance of their vessel in order to

- a) define a competitive C/P description that has a low risk of successful claims,
- b) make correct investment decisions e.g. for retrofitting and high-performance coating,
- c) benchmark the technical manager,
- d) ensure asset protection.

We also see a growing demand for transparency related to vessel efficiency from financial institutions.

3.2 Requirements from the ship manager

The ship manager works on behalf of the owner and needs to support him with regards to his

requirements listed above. He has to educate and support the crew on a day-by-day basis to operate the vessel in the most efficient way. The focus areas, which require daily monitoring, are speed, trim, A/E and boiler utilization. Also, long term degradation processes such as propeller, hull and engine fouling need to be tracked.

3.3 Requirements from the operator

The operator is responsible for the transport of cargo or passengers and the interaction with the surrounding supply chain. His priority is typically to maintain a schedule or meet a laycan. His highest cost is often the fuel-cost. Thus, he is closely checking C/P compliance and is requesting the crew to report consumption, speed and weather. C/P vessel description and guaranteed performance are anyhow generic (up to Beaufort 5, no matter wind direction and current, based on SOG) thus getting affected by external factors not depending on the owner/manager. Often another 3rd party such as weather routing providers are involved to perform post voyage calculations which can then lead to a claim.

3.4 Requirements for MRV

Vessels (above 5000GT) trading to, from or inside the European Union need to hand in basic voyage, consumption and cargo data for those voyage legs. Different to commercial C/P reporting, where only the sea passages are separated and analyzed, EU MRV separates port and under-way consumption. With standard noon reporting as described above, this is not possible because sea and port consumptions are mixed. Also, some traditional C/P reporting schemes only require reporting events at begin/end of sea passage. (Sometimes the BOSP/EOSP are named arrival/departure in those schemes. MRV in contrary refers to arrival/departure at times were the vessel reaches or leaves the berth.) These schemes also do not comply with MRV requirements because maneuvering and port times are not separated. Systems purely relying on automatic data acquisition systems usually do not have all the required information. Cargo data and precise arrival/departure times need to be reported manually.

3.5 Requirements for IMO DCS

IMO DCS requirements are similar to EU MRV but data needs to be reported for all voyage legs, not only those to or from EU ports but without specifying cargo figures.

3.6 Overlap of requirements

On most vessels all requirements described above need to be met. Most reporting solutions do not meet all requirements. Also, stakeholders tend to insist on their in-house system to be used. Thus, crews often must report the same data via multiple systems.

4. Data Quality

The accuracy of the analysis based on reported data depends on the quality of the reported data. In the following, we share our subjective view on some typical issues and how they can be mitigated.

4.1 Sensor quality

Most sensors need maintenance, calibration and regular plausibility checking. In case the crew reports data manually, sensor failure can be detected by the crew. Reporting software may facilitate plausibility checking. When automatic data acquisition systems are used, we recommend establishing an automatic plausibility checking as well. These checks should include missing signals, physical range limits, and plausibility against baselines. For example, the measured torque and rpm can be checked against a curve taken from the shop test. Here some tolerance needs to be applied due to the influence of added resistance and fouling.

To identify the faulty sensor, data points that have substantial deviation can be checked against measured consumption. If RPM and consumption are close to the shop test curve we conclude the torque measurement inaccurate, if torque and consumption are close to shop test we would conclude the RPM measurement is wrong. Fig.1 illustrates an example where torque is measured inaccurately for a certain period.

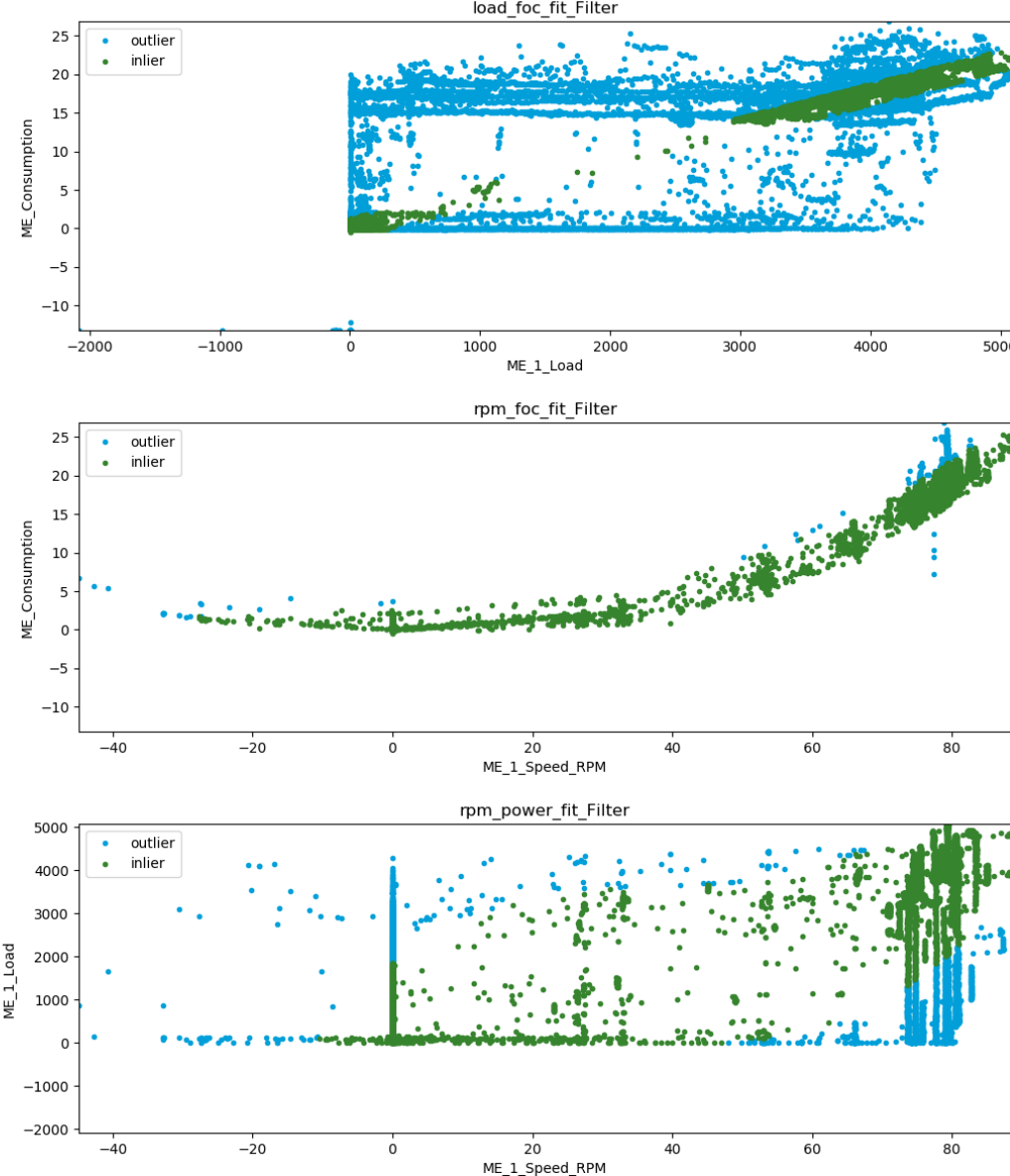


Fig.1: RPM, power and consumption in relation to baseline data

Even well-maintained sensors have certain uncertainties. For example, draft sensors based on hydrostatic pressure perform well in port but are biased by hydrodynamic effects at sea.

4.2 Human factor

The operator orders the speed (maybe indirectly by defining an ETA) which has a huge impact on the consumption. Other measures that influence fuel consumption are in the responsibility of the technical manager. To ensure that the vessel is managed efficiently, the operator and the manager agree on a target consumption which is defined in the charter party agreement. In container shipping these are speed/consumption curves for 2-3 drafts. In tanker and bulker shipping, it is a table with speed, draft and consumption points. Additional weather limits are defined which are considered ‘good weather’.

After each voyage the reported consumption is compared with the consumption described in the charter party agreement. Here only ‘good weather’ days are considered. If the reported consumption exceeds the described consumption the operator can claim some money for over-consumed fuel, or, if the ordered speed was not reached, for the lost time.

Traditionally many ship-to-shore reporting systems are designed and applied to facilitate the process of managing charter party compliance. In cases where vessel performance is poor due to fouling or missing maintenance, the crew might be tempted to report more wind than observed or less consumption than measured to avoid a claim from the operator. Extra consumption can then be recovered during uncontrolled activities (vessel discharging, tank cleaning, bad weather etc.) If we use this data to predict hull performance, we will overrate the vessels performance, or underestimate the fouling.

4.3 Comparison of manually reported and automatically logged data

In Fig.2, reported and auto-logged main engine work is plotted over a period of 10 months. The auto-logged data has been aggregated to the reported events for better comparability. We see that manual reported work is significantly higher. Applying both datasets to hull fouling evaluation would result in differences of more than 20%.

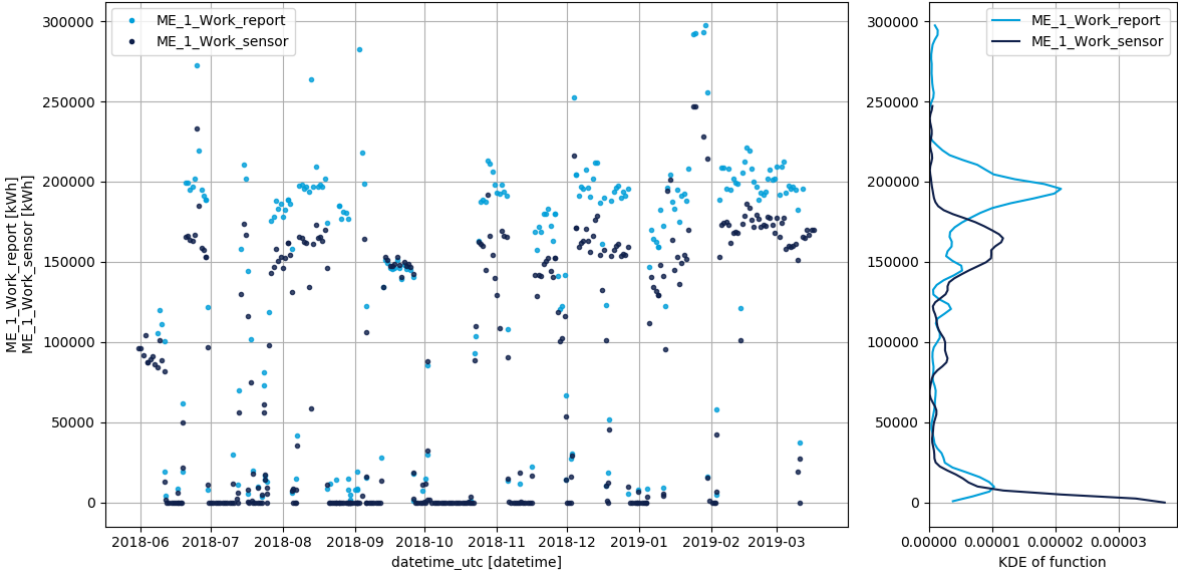


Fig.2: Work, reported vs. auto-logged data aggregated to events

In Fig.3, the work is related to the reported consumption by computing a specific fuel oil consumption (SFOC). We see the auto-logged data scatters around an average of 205g/kWh which, depending on fuel quality and environmental condition, is a realistic value. The SFOC based on manual reporting data is constantly 179 g/kWh in the first 3 months. It is similar to auto-logged data in the next 2 months and, finally, in the remaining 6 months it is constantly 170 g/kWh. We suspect here the crew did not have access to the torque measurements and has calculated the work based on the measured fuel consumption. The basis for this calculation has been an assumed SFOC of 179 g/kWh in the first period. Then, after a crew change, the new chief engineer has calculated with an assumed value of 170 g/kWh.

When looking into speed/power relation for hull performance evaluation, we need to exclude periods where the vessel is accelerating (speeding up or speeding down). In manual reporting we only see average rpm and average power. Here acceleration phases cannot be excluded. In pure auto-logged data, the BOSP and EOSP times are not available. Here we need to check derivatives of e.g. rpm. Fig.4 shows auto-logged RPM over 4 days in time. Grey dots mark periods out of the sea passage

(identified by manual reporting). Green dots mark the periods identified as constant rpm. Blue dots mark data which has been identified as acceleration phase based on the time derivative of rpm. We recommend applying such kind of filtering on auto-logged data to reduce scatter on hull performance evaluation.

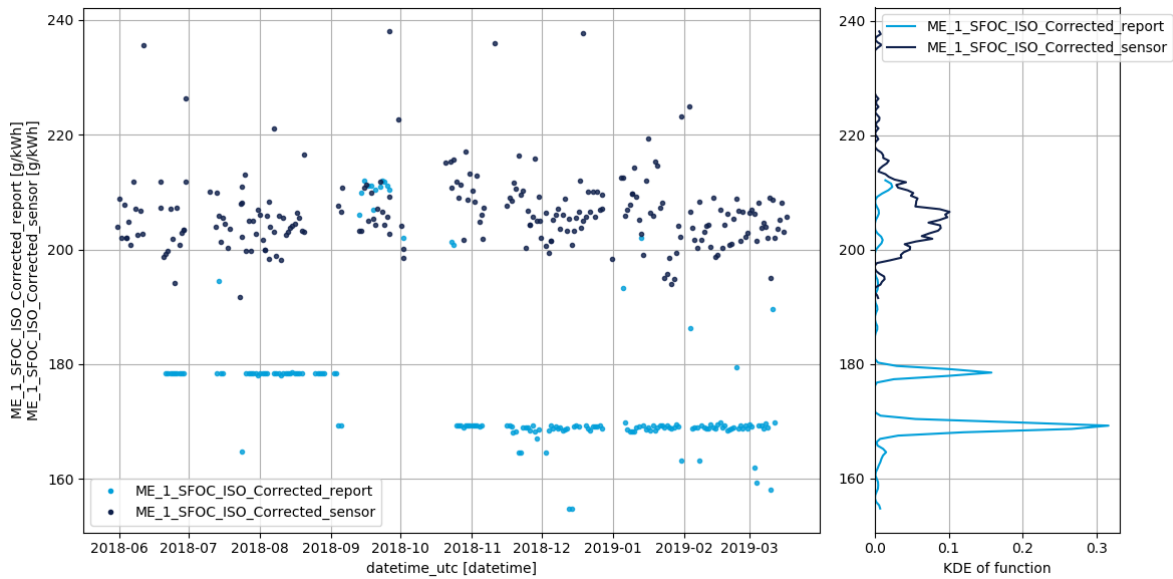


Fig 3: Specific fuel oil consumption, reported vs. auto-logged aggregated to events

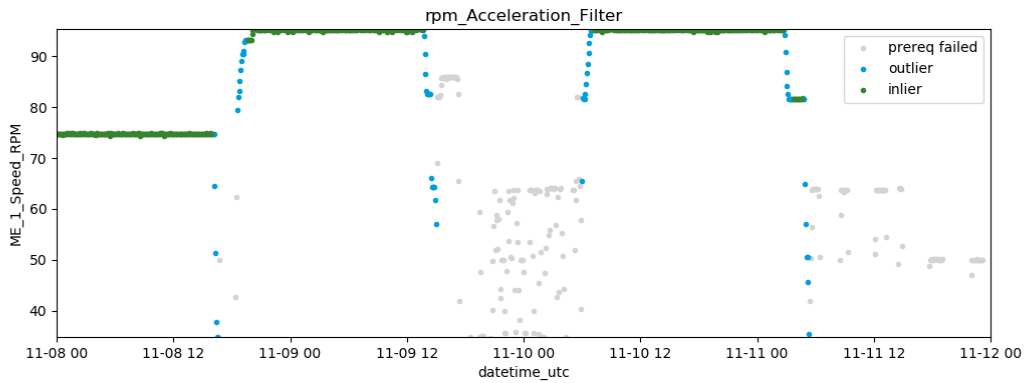


Fig.4: RPM over time. Grey are periods out of sea passage, blue dots are detected acceleration phases, green points indicate steady-state

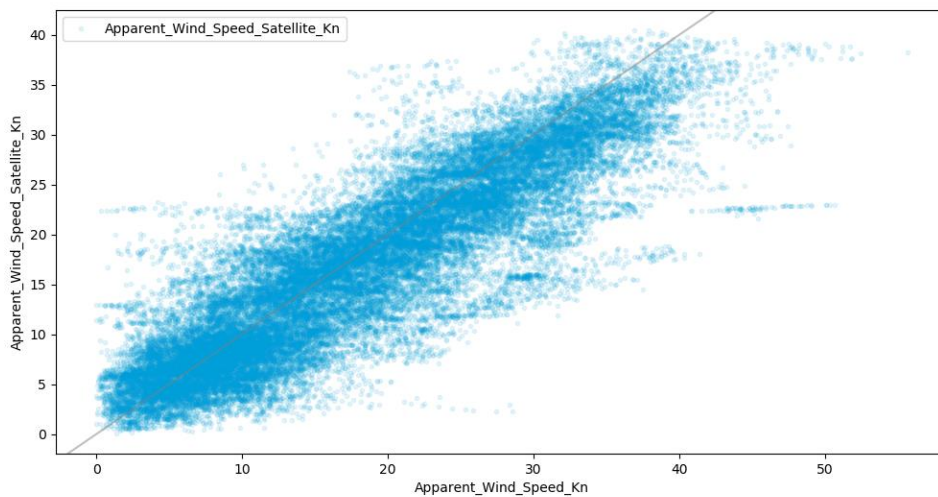


Fig.5: Auto-logged apparent wind plotted over data from hindcast indicating good correlation

Specific focus needs to be put on measured and reported wind, because the added resistance due to wind has a large impact on the power demand. Different reporting systems have different definitions. Some use apparent wind (typically measured by automatic data acquisition systems), some manual reporting systems use true wind since it is often reported in the log book. Some use m/s, some knots, others use Bft. Some systems do not give clear guidance and it changes with the crew. We recommend comparing data from the vessel with hindcast data to ensure proper transformation. Fig.5 shows such a comparison with what we consider a good correlation.

5. Hull Performance evaluation

Hull and propeller fouling can cause an increase in consumption by more than 30%. Depending on the paint, the trading and off-hire periods, the degradation rate is very different. Thus, all stakeholders have the interest to predict and manage hull condition properly.

5.1 Requirements from hull performance evaluation perspective

ISO 19030 gives clear requirements for its standard method. These cannot be met by many vessels. Thus, many companies make use of part 3 of the ISO standard and apply similar methods based on what data is available. Below is a list of the minimum requirements based on our experience:

- To assess hull performance, we need speed (GPS and/or log), draft/trim, wind (speed and direction), waves, shaft power, water depth, water temperature.
- From one snapshot report per day to one reading per hour is suitable. The benefit of higher frequency is limited.
- The vessel should sail at constant speed, RPM and weather should be constant during the measurement period.
- Every structured format is usable.

5.2 Best possible combination of data sources

DNV GL together with Scorpio has developed a new approach combining high-quality auto-logged data with event reporting, initially introduced for commercial performance evaluation and various third-party data sources. We use the following data sources for the main input data:

- Speed: Here we take speed through water and over ground from the auto-logging system and validate it against AIS and hindcast current data. Periods where these sources do not agree, we exclude from the analysis.
- Power: Power is taken from auto-logged torque meter and compared with rpm and consumption. When these values are not in line with the expected relation from the shop test we exclude these periods.
- Weather: We compute added resistance based on onboard measured data and compare it with added resistance computed based on hindcast data. If not in line, we exclude.
- Draft: Draft sensors have their limitation at sea. Since values do not change much between events, we take values from event reporting.

By this combination of data sources, and by intelligent filtering, we achieve a very high evaluation quality. Fig.6 shows calculated hull performance over a period of one and a half years. The kernel density function illustrates very low scatter.

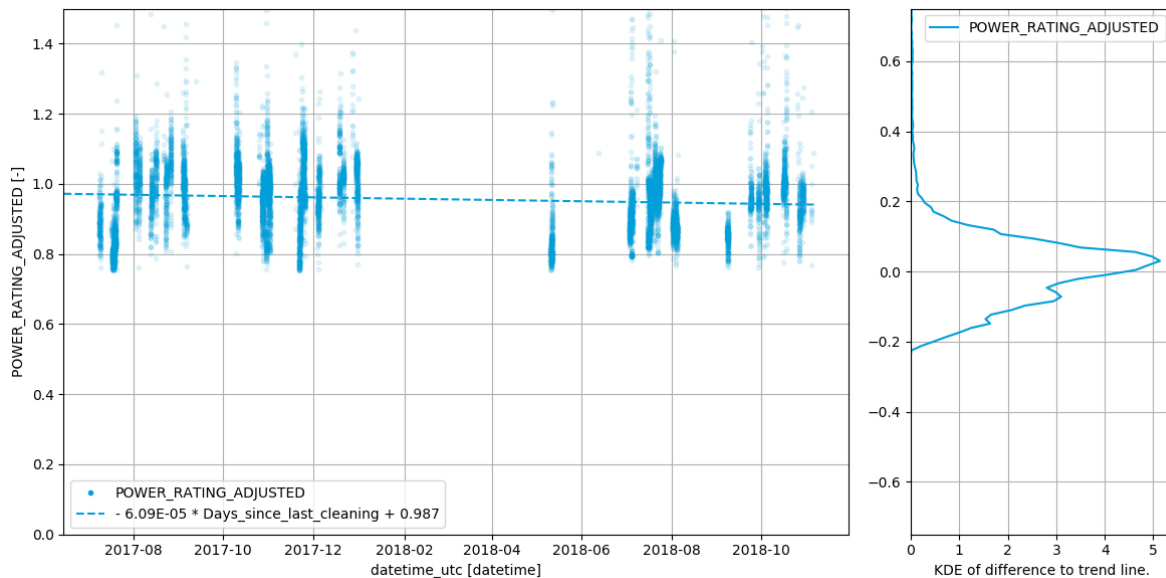


Fig.6: Hull performance index over 1.5 years

6. Conclusion

All commercial vessels report performance data to various stakeholders. Content and data quality vary. When it comes to analyzing the data, this needs to be considered. To assess the vessel performance in many cases additional data needs to be recorded. Ideally, auto-logged or snapshot data should be collected. To ensure good data quality we recommend to train crews and establish an immediate feedback loop for data quality. The best results can be achieved by combining available data sources.

References

- BAUR, M.v. (2016), *Acquisition and integration of meaningful performance data on board challenges and experiences*, 1st HullPIC Conf., Pavone, pp.230-238, <http://data.hullpic.info/HullPIC2016.pdf>
- BERTRAM, V. (2012), *Practical Ship Hydrodynamics*, Butterworth & Heinemann
- BERTRAM, V. (2016), *Added Power in Waves – Time to Stop Lying (to Ourselves)*, 1st HullPIC Conf., Pavone, pp.5-13, <http://data.hullpic.info/HullPIC2016.pdf>
- BERTRAM, V. (2017), *Some Heretic Thoughts on ISO 19030*, 2nd HullPIC Conf., Ulrichshusen, pp.4-11, http://data.hullpic.info/HullPIC2017_Ulrichshusen.pdf
- BOS, M. (2016), *How MetOcean data can improve accuracy and reliability of vessel performance estimates*, pp.106-115, <http://data.hullpic.info/HullPIC2016.pdf>
- DÜCKERT, T.; SCHMODE, D.; TULLBERG, M. (2016), *Computing hull & propeller performance: ship model alternatives and data acquisition methods*, 1st HullPIC Conf., Pavone, pp.23-28, <http://data.hullpic.info/HullPIC2016.pdf>
- FREUND, M. (2013), *Holistic analysis of onboard consumption and efficiency of the energy systems of ships*, PhD thesis, Helmut-Schmidt University, Hamburg, http://edoc.sub.uni-hamburg.de/hsu/volltexte/2013/3004/pdf/2012_Freund.pdf
- JONSSON, S.; FRIDRIKSSON, H. (2016), *Continuous estimate of hull and propeller performance*

using auto-logged data, 1st HullPIC Conf., Pavone, pp.332-338, <http://data.hullpic.info/HullPIC2016.pdf>

SCHMODE, D. (2017), *Influence of Noise and Bias on the Uncertainty of Data-Based Hull Performance Prediction*, 2nd HullPIC Conf., Ulrichshusen, pp.19-24, <http://data.hullpic.info/HullPIC2017.pdf>

ISO 19030-1:2016 *Ships and marine technology – Measurements of changes in hull and propeller performance*, International Organization for Standardization, Geneva

Full-Scale Measurement of a Flow Field at Stern using Multi-Layered Doppler Sonar (MLDS)

Tomoki Wakabayashi, Yasuhiko Inukai, Japan Marine United Corporation, Yokohama/Japan,

{wakabayashi-tomoki, inukai-yasuhiko}@jmuc.co.jp

Takeshi Yonezawa, Norihide Igarashi, MTI, Tokyo/Japan,

{takeshi_yonezawa, norihide_igarashi}@monohakobi.com

Masahiko Mushiake, Satoshi Kawanami, Furuno Electric, Nishinomiya/Japan,

{masahiko.mushiake,satoshi.kawanami}@furuno.co.jp

Abstract

This paper introduces the ongoing joint research project on full scale measurement of a flow field at stern with Multi Layered Doppler Sonar (MLDS). Full scale measurement was conducted on a 14,000 TEU container ship with multiple MLDSs and the interim results are shown here. It was confirmed that the full scale Computational Fluid Dynamics (CFD) agreed well with the measurements in wide region. And our new plan to apply MLDSs on VLCC is shown as well.

1. Introduction

A flow field around a ship at full scale is different from that at model scale due to so-called “scaling effect” even though the geometry of the model is completely scaled. While a model test is usually performed to know a ship performance and is a well-established technique, the scaling effect is still not fully understood. A direct calculation with full scale Computational Fluid Dynamics (CFD) is expected to solve this problem. If the technique of the full scale CFD is established, it is also expected to enhance the practical applications of an optimization of a hull form, an energy saving device and a propeller at full scale to reduce GHG emission. However, verification and validation works for full scale CFD are not enough at this moment. The number of full scale measurements, especially related to a flow field, is very limited.

In this background, Nippon Yusen Kaisha (NYK), MTI Co, Ltd. (MTI), Furuno Electric Co. Ltd. (FURUNO) and Japan Marine United Corporation (JMU) started a joint research project on full scale measurement for 14,000 TEU container ships using Multi-Layered Doppler Sonar (MLDS). MLDS developed by FURUNO and MTI is an acoustic Doppler sonar capable of measuring relative water velocity at multiple arbitrary depths along ultra-sonic beams, <https://www.furuno.com/files/Brochure/161/upload/ds-60.pdf>. A full-scale measurement using a MLDS was conducted in 2017 as the world first application to a flow field at the stern. It was confirmed that the MLDS works well and the fruitful result was reported at HullPIC 2018. Subsequently, we continue this project and installed three MLDSs on the sister ship in order to enlarge the measurement area than that in 2017. In this paper, a quick report of the measurement is presented. And our new plan to apply MLDSs on VLCC is shown as well.

2. Full scale measurement of a flow field at stern of 14000TEU container ship

2.1. Particulars and measurement location

The subjected ships in the measurement in 2017 and this time have same hull form with particulars shown in Table 1. Hereafter, we call them Ship-A and Ship-B respectively. Both are built by JMU and operated by Ocean Network Express Ltd. We plan the measurements on SHIP-B two times. The first was performed during a voyage from Southampton Port to Suez Canal in February 2019 with 1m deeper draft than that in the measurement on Ship-A . The second is scheduled in summer 2019.

Table 1: Particulars of 14000TEU container ship

Length overall	364m	Depth	29.5m
----------------	------	-------	-------

Breadth	50.6m	Summer load draft	15.8m
---------	-------	-------------------	-------

2.2. Measurement system

Fig.1 shows the configuration of MLDS equipped on SHIP-A and SHIP-B. The commercial Doppler Sonar, Model: DS-60, *FURUNO 2019*, developed by FURUNO in 2010 is used in the system. The detail is described in *Inukai (2018)*. The differences between both ships are shown in Table 2. The aims of the change from SHIP-A are as follows,

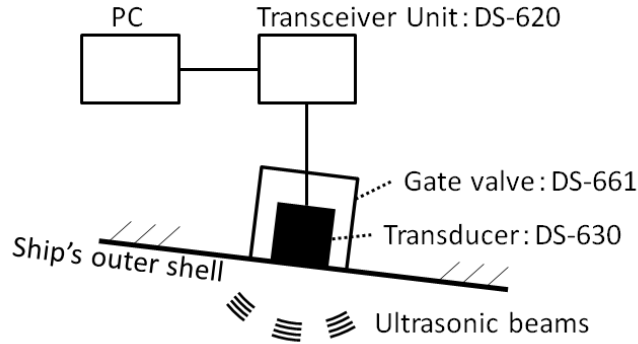


Fig.1: Configuration of system for MLDS equipped on 14,000 TEU container ships

1) Expansion of measurement area

The number of MLDSs increases from one to three (TD1, TD2, TD3) to measure the velocity in the wider area than SHIP-A. The locations of MLDSs and measuring area on SHIP-B are shown in Fig.2. The location of the MLDS on SHIP-A was between TD1 and TD2 of SHIP-B. By using three MLDSs, it is possible not only to enlarge measurement area but also to obtain three velocity components at the intersection of ultrasonic beams transmitted from three MLDSs.

Additionally, the number of beam directions in which velocity can be measured increases from six to twelve as shown in Fig.3. It is realized by rotation of the transducer by 90° in the Gate Valve. The solid lines show the original directions, i.e. SHIP-A, and the dotted lines show directions added for SHIP-B. The number of measurement layers in depth direction is also increased from nine to eighteen by changing the software.

2) Reduction of the interaction between beams

MLDS transmits beams in three directions (beam 1, 2, 3 or 4, 5, 6) at the same time. It was found in the measurement on SHIP-A that when one beam hits the propeller or the hull, the velocities in the other two directions were affected by it. Thus, we limit the number of ultrasonic beams transmitted simultaneously from three to one in order to eliminate interaction between beams.

Table 2: Measurement system equipped to SHIP-A and SHIP-B

	SHIP-A	SHIP-B
Number of MLDS equipped at stern	1	3
Number of directions ultrasonic beams are transmitted by each transducer	6	12
Number of measurement layers in depth direction of each ultrasonic beam	9	18
Number of ultrasonic beams transmitted at same time	3	1

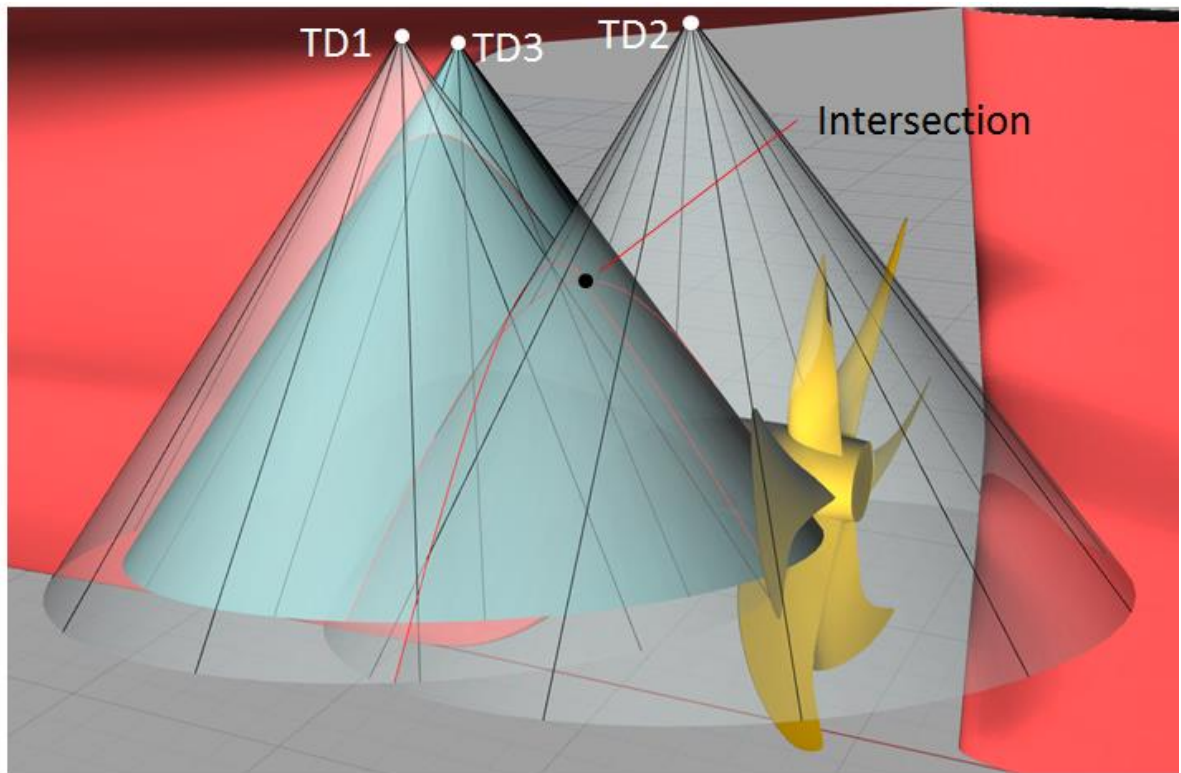


Fig.2: Measurement range with three MLDSs

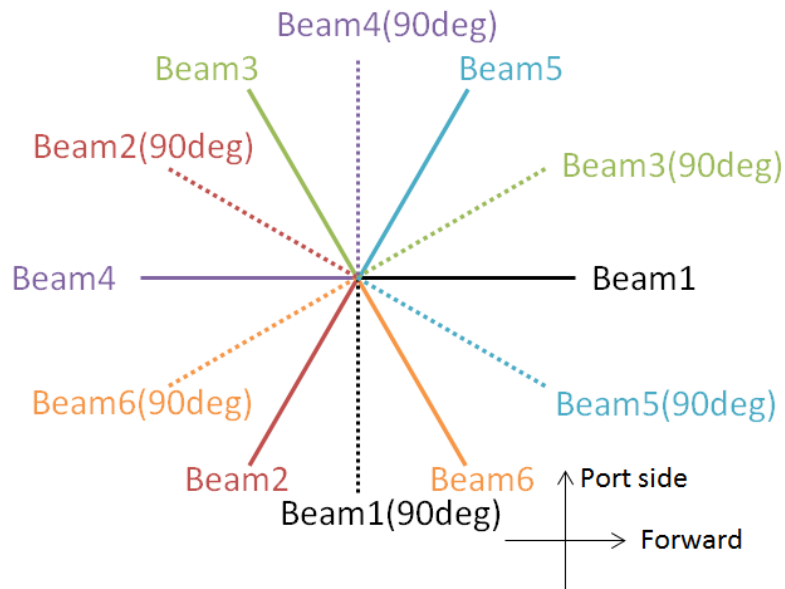


Fig.3: Directions ultrasonic beam transmitted to

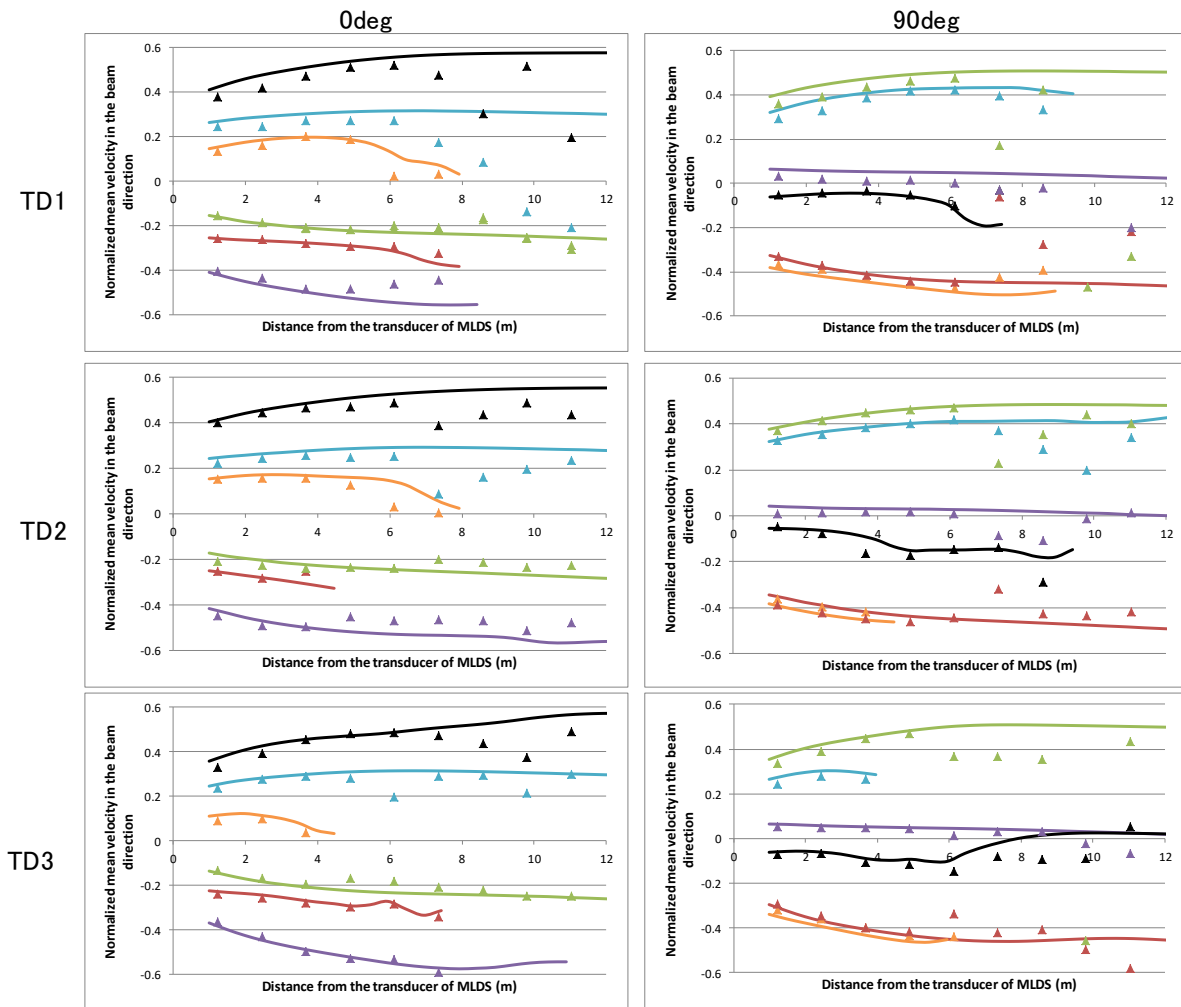
2.3. Measurement results

Full-scale measurement on SHIP-B was carried out from 8th to 10th February 2019 in the Mediterranean Sea. Fig.4 shows an example of measurement result on 8th February. The figures on left show measurement result when beam 1 was transmitted forward (corresponding to solid lines shown in Fig.3) and the figures on right show measured result when the transducer was rotated by 90° (corresponding to dotted line in Fig.3). The measurement results of TD1, TD2 and TD3 are shown in order from the top. Horizontal axis indicates a distance from the transducer to measuring point and vertical axis indicates the velocity in the beam direction which is normalized by ship log speed

measured by “DS-60” equipped at the bow. The marks show measurements and the lines show CFD calculation. The colors of each line correspond to those in Fig.3.

1) Near field

In the range of within about 6 m from the transducers, the measured velocity agrees well with the estimation by CFD. Fig.5 shows the contour plot of the difference between the measurement and the calculation within this range. It can be seen that the difference is less than 2% of ship speed in the most part. On the other hand, the deviation in the frontal area of TD1 was a little bit larger. The reason of the deviation that the measured velocity was slower than the calculation is not clear at this moment. We will investigate the quality of both measurement and calculation through not only this measurement but also the second measurement scheduled in summer.



Beam1(black) Beam2 (red) Beam3 (green) Beam4 (purple) Beam5 (aqua) Beam6 (orange)
 Lines: CFD, marks: Measurement

Fig.4: Comparison between measurement and CFD for velocity in direction of each beam

2) Far field

In the far field, the difference between the measurement and the calculation became much larger. Although we intended to transmit only single beam in order to eliminate the interaction with the other beams, the interaction obviously remained. For example, the velocity in the beam 1 of TD1 was disturbed in the region 6m far from the transducer as shown in the upper

left figure in Fig.3 despite the fact that the beam couldn't hit any obstacles. It can be thought to be influenced by the other beams which hit hull or propeller. Because it is difficult to form a beam in completely one direction, there are beams transmitted to unexpected direction no matter how weak they are. While the signal level from the reflection against small particles is attenuated as the distance gets large, one from the reflection against hull or propeller remains strong. Thus, even if the power of the transmitted ultrasonic beam toward the hull or propeller is small, the influence of the beam is not negligible. We are trying to find a solution to reduce the influence by the second measurement.

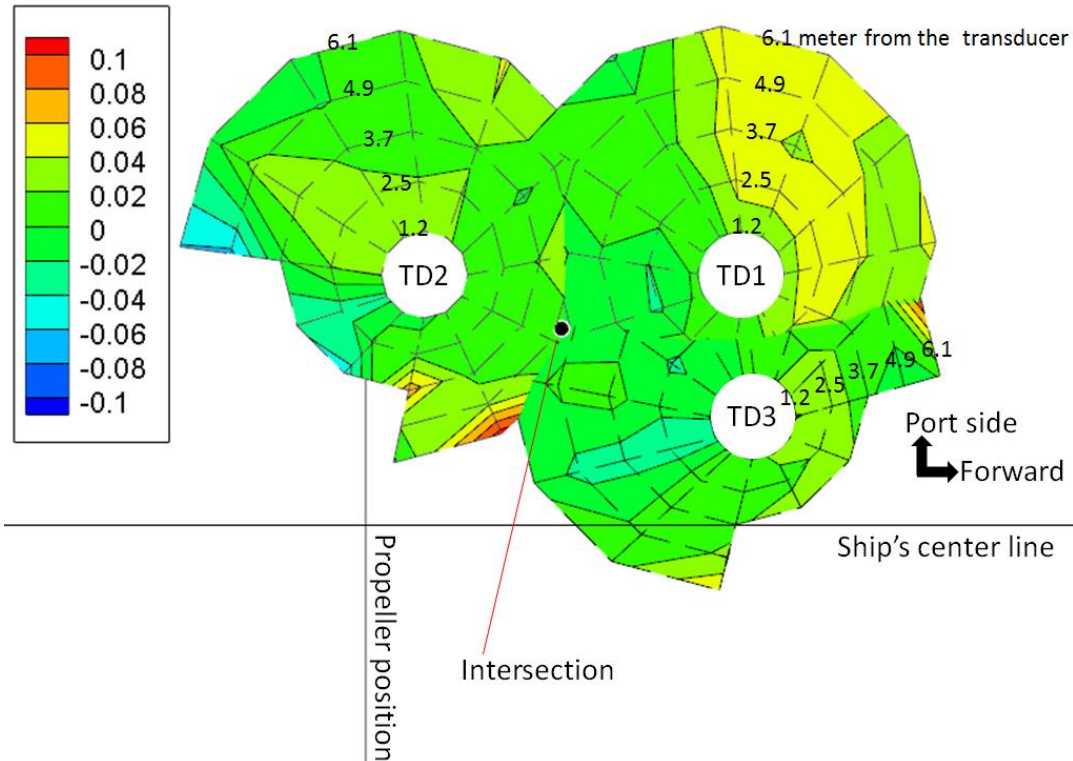


Fig.5: Contour plot for difference between measured velocity and CFD

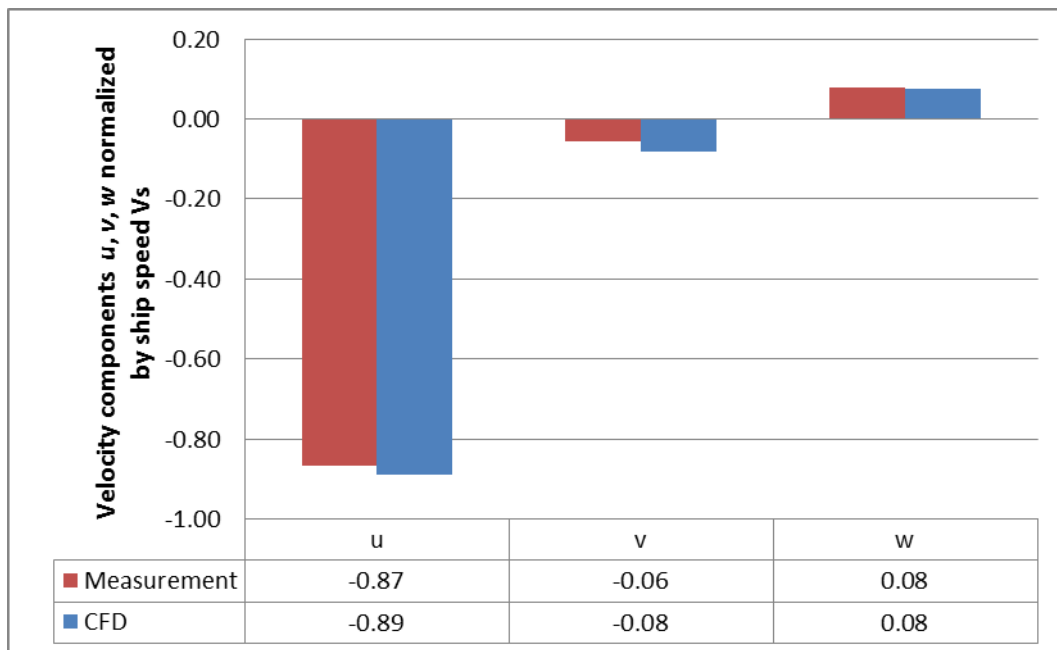


Fig.6: Comparison of three components of velocity at intersection

3) Three velocity components

Three velocity components u , v , and w in x , y , and z direction, can be derived at the intersection of the beams transmitted from the three MLDSs. The intersection is plotted as dot in Fig.2 and Fig.5. Velocities of beams which pass through the intersection are interpolated with measured data because it is difficult to locate MLDSs so that the beams cross at one point. Fig.6 shows the comparison of velocities in three components between the measurement and the calculation. Vertical axis indicates the velocity normalized by ship speed. The sign of u , v and w are positive respectively forward, toward port and upward. The differences in all the components are less than 2% of ship speed and the calculation agrees well with the measurements at the intersection.

2.4. Second measurement

The second measurement on SHIP-B is scheduled in summer 2019. A close investigation will be made over the quality of measurement by increasing the sampling data. We look for a solution against the problem that the interaction among beams still remains and will try it in the second measurement.

3. Full scale measurement of a flow field at stern of VLCC

Flow field at stern of blunt ship like VLCC is different from that of slender ship like container ship because of the existence of strong vortex generated from the bilge part. Fig.6 shows examples of velocity contours calculated by CFD. The upper and lower figures show flows at model scale and full scale, and the left and right figures show the flow of blunt ship and slender ship respectively. It can be seen from the figures that the boundary layer of blunt ship is thicker and the scaling effect is larger than those of slender ship. Because some physical models are used in CFD calculation, e.g. turbulence model, the proper model should be set up for accurate calculation. The different flow pattern may require the different model. Thus, the validation of CFD should be made for as many kinds of ship as possible.

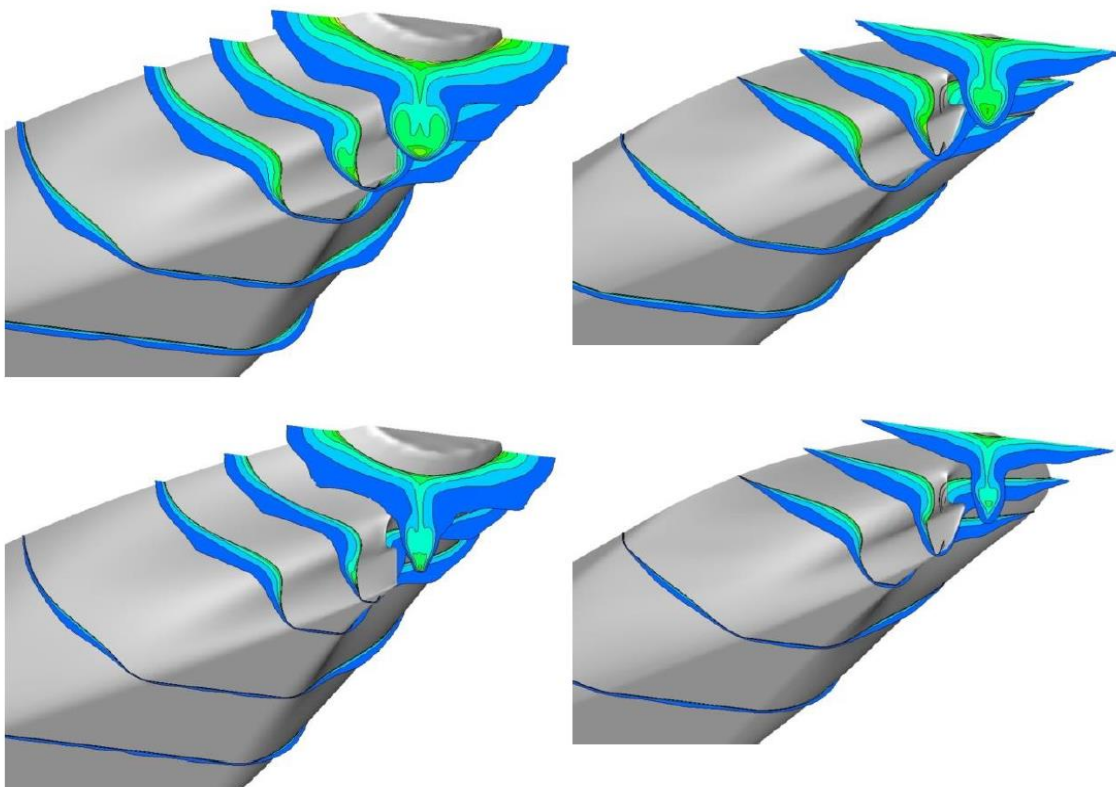


Fig.6: Difference of flow field at stern between blunt ship and slender ship

Accordingly, we decided to expand the application of MLDSs to VLCC as the next challenge. Classification Society of Nippon Kaiji Kyokai (NK) has joined the current research group and we plan the measurement in 2020.

4. Conclusion and future work

Full scale flow field measurement with three MLDSs has been carried out on a 14000TEU container ship. This paper shows just quick report because the measurement is ongoing. Following the report at HullPIC 2018, a good agreement between the measurement and the calculation were confirmed. Compared to the last report for the measurement with a MLDS, the velocity in wider area could be measured by installing three MLDSs. The second measurement is scheduled this summer in order to accumulate more data and investigate qualities of the measurement and the calculation deeply.

In addition to that, we will carry out a full-scale measurement for VLCC. Class NK joined the project so as to develop the MLDS as widely applicable measuring system. Our goal is to contribute to reduction of GHG emission by practical application of full scale CFD to the ship design. More validation data is necessary to achieve the goal. MLDS has a great potential as a measuring system of flow field at full scale because it has favorable features of being inexpensive and easy to handle. Therefore, we continue works to establish the technology of MLDS.

References

INUKAI, Y.; SUDO, Y.; OSAKI, H. ; YANAGIDA, T. (2018), *Extensive Full-Scale Measurement on Propeller Performance of 14000TEU Container Ship*, 3rd HullPIC, Redworth

Case Study on Performance Improvement using Advanced Hull Performance Analysis Methodologies

Jason Stefanatos, DNV GL, Piraeus/Greece, Jason.Stefanatos@dnvgl.com
André Kauffeldt, DNV GL, Potsdam/Germany, Andre.Kauffeldt@dnvgl.com
Eirinaios Petoumenos, PPG, Athens/Greece, Petoumenos@ppg.com

Abstract

DNV GL and PPG performed an assessment of the hull degradation on various vessels when using energy saving coating systems based on low friction materials. The scope of this exercise was to use already existing data in various formats avoiding to perform targeted measurement campaigns and, thus, allowing the methodology to be replicated for any vessel manager irrespective of the data collection followed. Working with various levels of data qualities and reporting systems enabled DNV GL to define the boundaries of the methodology steps including the hull degradation calculations. The method used by DNV GL and delivered already to more than 2,000 vessels either through Trim optimization (ECO Assistant), Fleet Performance Management (ECO Insight), or both, is based on ISO 19030 but further expanded to cover all conditions in a more granular way by incorporating the latest developed techniques (phenomenological modelling combined with data-driven methods and machine learning techniques). On this project, the methodology was applied for different vessel types, including cruise vessels, LNG carriers, bulk carriers and crude oil tankers over a combined period of 30 years of operation and using approximately 165,000 data points, gathered through both manual and automatic data acquisition systems. This paper presents the methodology and indicative results derived from the performance analysis of two LNG carriers and one cruise vessel.

1. Introduction and project overview

Energy efficiency is an important factor in the life cycle costs of a ship. With rising fuel oil prices, an increasingly competitive market and new environmental regulations, like the recent IMO Green House Gas (GHG) strategy aiming for a 50% reduction of CO₂ by 2050 compared to 2008 (MEPC.304(72), 2018), improving energy efficiency is vital. The maritime sector is known for sometimes being reluctant to embrace change and tends to stick with proven concepts and best practices, which have been developed and applied for a long time. However, times change and today many shipping companies invest in energy efficiency improvement, whose importance is steadily growing. It is realized that a holistic view on the vessel performance is important to continuously lift the remaining potential of performance improvement.

There are various approaches to improving fuel consumption, and hence CO₂ emissions. *Bouman et al. (2017)*, aggregated results from various publications indicating a wide range of solutions covering hull design, power and propulsion systems, alternative fuels, alternative energy sources, and operation. Fig.1 depicts the potential improvement that could be achieved through each solution. It is observed that there are solutions of different nature, which are not available or feasible for all ship types.

Hybrid power propulsion for instance is a good solution for small scale of vessels with specific trade routes, while it would be an infeasible solution for a large oil tanker. Other solutions can provide significant improvement of CO₂ emission but at a very high cost, which make them non-feasible options, for the time being, e.g. fuel cells. The low hanging fruits were already harvested through different stages of energy efficiency improvement measures in the last years, Fig.2:

- 1st wave: slow steaming
- 2nd wave: trim optimization and other tools
- 3rd wave: retrofits now the monitoring and controlling gains importance
- 4th wave: managing operations and performance management

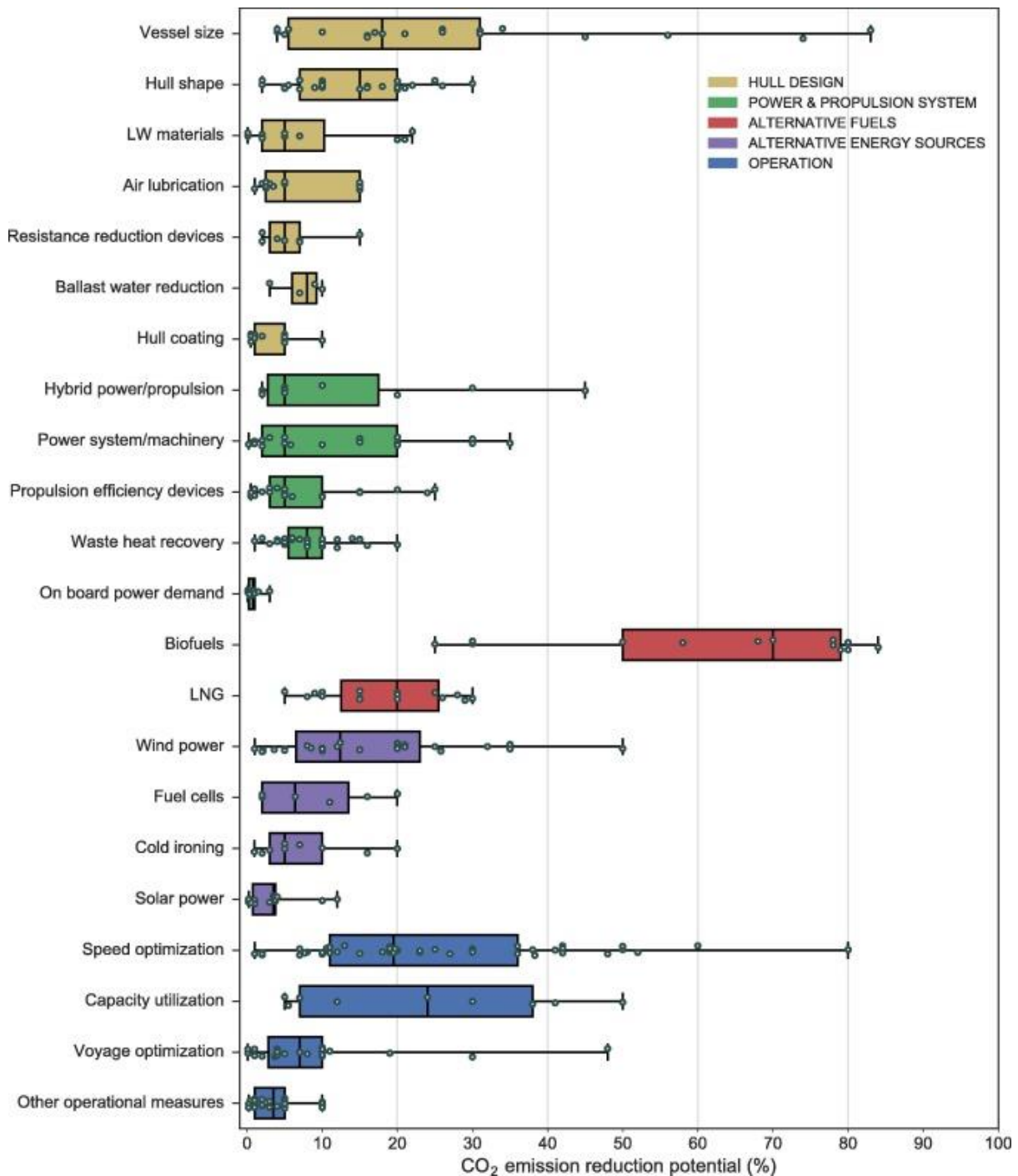


Fig.1: CO₂ emission reduction potential from individual measures, classified in 5 main categories of measures, *Bouman et al. (2017)*

During the first stages, specific energy efficiency topics were addressed, while now the focus shifts to ensuring that vessels operate efficiently all the time by addressing the whole spectrum of measures affecting the vessel performance. To achieve this a good and detailed understanding of the vessel is important. This is where performance management comes into play.

Fuel consumption evaluations of similar sized vessels during the sea passage show that there are huge differences between the best performer and the average of the peer group, Fig.3. Depending on the vessel type the differences may account for up to 36%, *Kauffeldt and Hansen (2018)*.

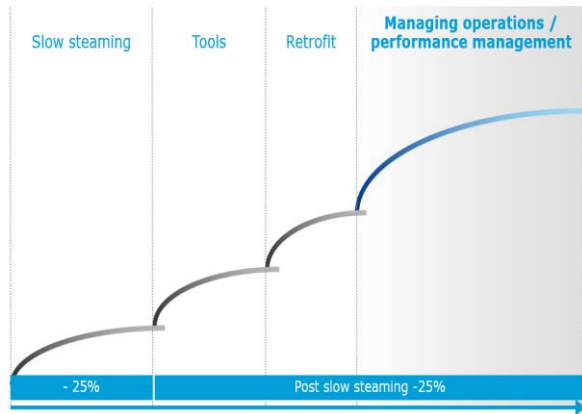


Fig.2: Steps of energy efficiency improvement measures

Fuel oil consumption/Nm during sea passage

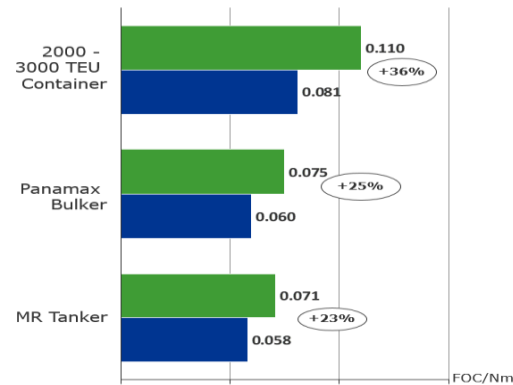


Fig.3: Remaining potential of performance improving measures: class average (green), best performer (blue)

An important parameter of the vessel performance is hull degradation as well. The hull protective coating is a key element that determines hull performance and the levels of potential degradation, having an impact on the Energy Efficiency Design Index (EEDI) and Energy Efficiency Operation Index (EEOI) of a vessel.

More specifically, on energy saving coating system solutions, according to studies, silicone-based coatings decrease hull drag resistance, improving the hydrodynamic performance of a vessel, *Schultz et al. (2010)*. Silicone-based fouling release coatings provide optimum fouling anti-adhesion due to hydrophobicity and low surface energy properties, *Baier (2015)*, capable to minimize the adhesion of marine organisms on coated surfaces, *Eduok et al. (2017)*. Analysis shows skin frictional drag reduction by 9–22%, in different velocities (6.5–22.7 Knot), when compared to SPC technologies, *Mirabedini et al. (2006)*, along with high durability, antifouling and anticorrosive effectiveness, *Marceux et al. (2014)*, *Peres et al. (2018)*.

Investigation on the fuel consumption of tin-free SPC coatings and foul-release coatings illustrated that the latter can decrease speed-adjusted fuel oil consumption by 22%, *Corbett et al. (2011)*. Overall, improved vessel operational costs, fuel oil consumption and energy savings are to be expected, as studies suggest, *Selim et al. (2017)*.

In this article, the results of a joined effort between DNV GL and PPG to assess hull degradation of various vessel types, and different operational profiles, when using PPG energy saving coating systems based on low friction materials, are presented.

There are various ways to assess the performance of a coating over-time, e.g. towing tank model tests, CFD calculations, etc. Further to this, hull performance depends on various factors, such as the environmental and sailing conditions, vessel operational profile, coating application specifications, hull pretreatment, etc.

In this study, a methodology developed by DNV GL (described in Section 2) was applied. This is relying on the technical specifications of the vessel, i.e. design data and operational data. This enables to efficiently apply the method to a large number of vessels without the need of costly and time-consuming installations and infrastructures, e.g. sensors, experimental setup, or physical model building.

By using already existing data in various formats it was additionally avoided to perform elaborated measurement campaigns. Thus, the developed methodology can be easily applied to any vessel, irrespective of the data collection process defined by the managing company. Due to the fact that various companies utilize different data acquisition methods and reporting systems, data of a wide range

of quality were received and used for calculations. Access to these big data source enables DNV GL to define the boundaries of the methodology steps including the hull degradation calculations and its filter settings, thus providing more accurate quality analysis.

The project included studies of four series of different sister vessel groups; cruise vessels, LNG carriers, bulk carriers, and crude oil tankers. The owning and managing companies of the vessels are located in different geographical regions while the vessels trade globally, under different operational profiles and conditions. Section 3 describes the detailed specifications of this project along with the key results.

2. Methodology

From the operator's point of view, performance management covers a wide range of aspects and considers the ship as a holistic system. This approach can become very complex and involve monitoring a wide range of parameters. It can be extended almost indefinitely depending on the operator's approach. However, most performance analyses consider the following main aspects:

- Efficient main engine operation (power, fuel oil consumption (FOC), RPM, etc.)
- Efficient management of auxiliary engines (combination, power, FOC, etc.)
- Controlling of other auxiliaries (boilers, separators, etc.)
- Hull and propeller performance considering:
 - Resistance
 - Weather
 - Propulsion
 - Trim
 - Hull degradation
- Voyage management (Optimized routing, consumptions, weather, speed, legs)
- Bunker statistics
- Port/supplier rating
- Emissions and disposals
- Maintenance and survey interval optimization

This list is not exhaustive and shall only demonstrate the complexity of the topic. The paper focuses on hydrodynamic performance, considering resistance, propulsion, hull degradation as well as propeller effects.

Vessel performance assessment cannot provide safe conclusions by simply plotting the measured power demand during operation over time. The scatter observed in such plots is dominated by speed and draft variations in operation, which have a much bigger impact on the power demand than the rather small effect of hull degradation. Hence, to identify trends in hull degradation, it is necessary to normalize the power measurements to eliminate the effects of different operating conditions regarding speed, draft and trim. Basis of such a normalization could be the ideal power demand determined for the same condition. It can be used as a reference, representing the theoretical power demand of the vessel at this condition. Measured power and reference power demand together allow conclusions about the hull performance and, therefore, the hull degradation.

Simply put, looking at the impact of the hull, a performance analysis compares a measured power demand for a certain operating condition to a reference value valid for that condition.

Here, the relevant condition is mainly defined by the following parameters:

- Operating conditions:
 - Draft
 - Trim
 - Vessel speed

- Environmental conditions:
 - Wind (force and direction)
 - Sea state (height and direction)
 - Swell (height and direction)
 - Temperature (air and water)
 - Current (speed and direction)
 - Water depth

By comparing the measured with a reference power of a comparable condition, a performance index can be deduced, which enables operators to easily infer conclusions about the vessel performance.

Many factors influencing performance make it difficult to distinguish effects and hence understand the parameters that drive performance. Therefore, for a meaningful and accurate performance analysis it is crucial to have a matching reference condition for all measured operating conditions. Hence, comprehensive baselines covering the entire operating range regarding draft, trim and speed are prerequisite to get the most out of the performance analysis. Or the other way around, the further an existing reference condition must be extrapolated to meet a measured operating condition, the less accurate the result of the performance analysis would be.

2.1 The right baseline for the right ship

For assessing ship performance, speed-power curves of the individual vessels serve as a reference. They reflect the calm water power demand of the corresponding vessels under ideal conditions:

- Clean hull
- Deep water
- No wind
- No waves

There are several well-known ways to determine speed-power curves for a vessel, which can serve as reference in a performance analysis. As summarized in Fig.4, each approach has its own advantages and disadvantages:

- **Empirics:**
Based on generalized equations this approach is not intended to fit a specific vessel. Neglecting the individual characteristics of a vessel, this approach delivers a general idea of the magnitude of the power demand only.
 - *Pro:* Very quick and therefore cheap
 - *Contra:* Inaccurate and not suited for ship specific comparison due to neglecting of individual vessel characteristics
- **Model scale measurements:**
A well-established approach, which is based on measurements in model scale. Since these measurements are conducted under laboratory conditions, the accuracy of the model scale results is generally high.
 - *Pro:* The widely accepted approach with its accurate results is well suited for the comparison of different hull shapes.
 - *Contra:* Building of a scale model, preparation and execution of each test is time consuming and expensive. Due to uncertainties when extrapolating to full-scale, the results are not fully consistent across different test facilities. Possible scaling effects are not considered.
- **Full-scale measurements:**
General accepted approach to validate the performance predictions for a newly delivered ship. With additionally installed measuring equipment the power results are very accurate. However,

the measurement quality strongly depends from the environmental conditions. It is not the first choice for comparative measurements.

- Pro: Accurate power results without scale effects.
- Contra: Often only conducted at ballast draft and under non-ideal conditions. The correction of the environmental conditions as well as the extrapolation to the design draft lead to uncertainties. Depending on the used correction and extrapolation methods the results are not fully consistent across different test facilities or yards.

Empirics	Model test	Sea trial	CFD
<ul style="list-style-type: none"> ▪ Quick ▪ Cheap 	<ul style="list-style-type: none"> ▪ Accurate ▪ Analyze ▪ Compare ▪ Accepted 	<ul style="list-style-type: none"> ▪ Accurate ▪ Analyze ▪ Accepted 	<ul style="list-style-type: none"> ▪ Accurate ranking of form variants ▪ Capturing of flow details
<ul style="list-style-type: none"> ▪ Inconsistent ▪ Inaccurate ▪ Not suited for comparisons and benchmarks 	<ul style="list-style-type: none"> ▪ Time consuming ▪ Expensive ▪ Inconsistent across test-facilities 	<ul style="list-style-type: none"> ▪ Only ballast draft ▪ No ideal conditions ▪ Inconsistent across yard 	<ul style="list-style-type: none"> ▪ Inconsistent across setups

Fig.2: Methods of power demand analysis

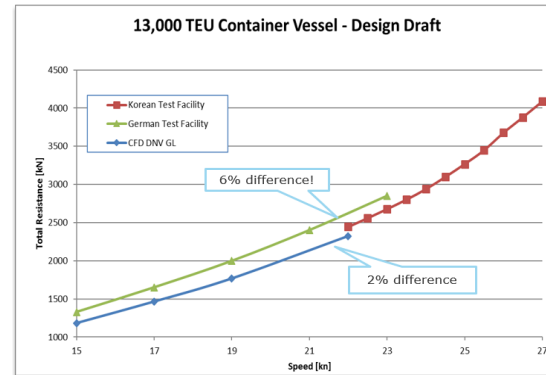


Fig.3: Differences in power prediction

- **Computational Fluid Dynamics (CFD) simulations:**

CFD has become a well-established tool for relative comparison of different designs, configurations and operating conditions. The absolute accuracy still depends on the CFD setup and available resources.

- Pro: A fast and effective approach to conduct full-scale simulations and, thus, become independent of scaling effects. Well suited tool for comparative studies.
- Contra: There are still substantial computing capacities required to conduct large-scale studies efficiently. The absolute accuracy depends on the CFD setup and the experience of the user.

Probably none of the common methods is perfectly suited to meet all requirements of the maritime industry. Fig.5 visualizes the mentioned inconsistencies of absolute power predictions, which not only vary between model test and CFD but also between different model test facilities. In some cases, differences of up to 10% are reported between different model test facilities using the same model.

When generating baselines, it is indispensable to cover all relevant operating conditions of a vessel regarding draft, speed and trim to get reliable performance information. More precisely, the operational profile must be closely covered by the reference simulations to minimize the uncertainties due to extrapolation from the available reference to the recorded operating condition. This means that a large amount of reference conditions is required to produce accurate power baselines.

Figs.6 and 7 show a typical operating condition of a large container vessel (red cross) relative to the reference points based on different data sets. Fig.4 presents an example with a dense grid of reference points based on comprehensive CFD simulations. A matrix of 7 trims, 11 speeds and 8 drafts results in 616 reference points covering the operational profile of the vessel. Fig.5, on the other hand, shows a reduced data set based on a standard model test of the same vessel. Here, the matrix contains only 3 drafts (scantling, design and ballast), 1 trim and 6 speeds resulting in 18 reference points inhomogeneously distributed over part of the operating range. The example with the reduced data set shows impressively the distance between the measured operating condition and reference points.

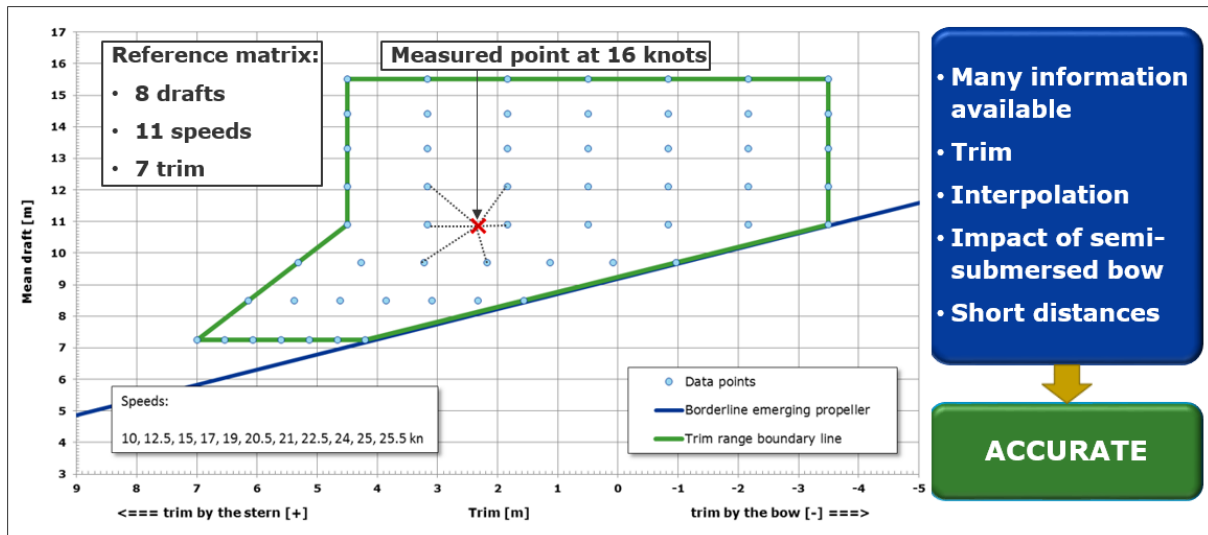


Fig.4: Interpolation of a measured conditions using a dense grid of CFD-based reference points

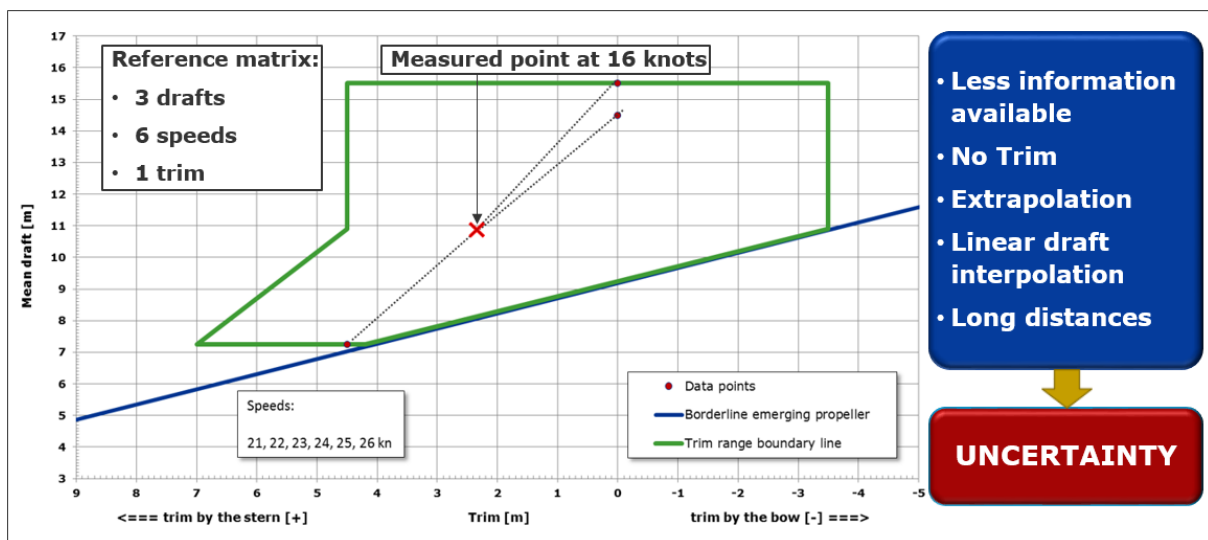


Fig.5: Extrapolation to a measured condition using a reduced data base referring to a standard model test with ballast, design and scantling draft available

For container vessels with their extremely large operating range far from design condition regarding draft, trim and speed, Fig.8, the use of CFD approaches is strongly recommended. Today, standardized CFD setups ensure high comparability. The application of state-of-the-art fully viscous, free surface CFD approaches using Volume of Fluid (VoF) and Reynolds averaged Navier Stokes equations (RANSE) in combination with standardized prediction methods as well as full-scale computations (no scale effects), provide reliable results. Beside the significant technical enhancement, the constantly growing computing power and the resulting reduction in lead time and cost means that large numbers of simulations can be conducted efficiently – a crucial factor when developing comprehensive baselines for performance analysis of container vessels.

However, the operating profile of many vessel types is much less extensive and easier to predict than that of container ships. Bulk carrier and tanker for example, mainly operate at ballast or laden condition reducing the draft-trim combinations significantly.

Cruise vessels even operate at one draft only. In addition, the speed range of these vessel types is significantly reduced compared to that of container vessels. Thus, it is not necessarily required to use the same comprehensive CFD baselines for all types of vessels. Often, it might be more efficient to use existing model test and sea trial results to create appropriate baselines for certain vessel types.

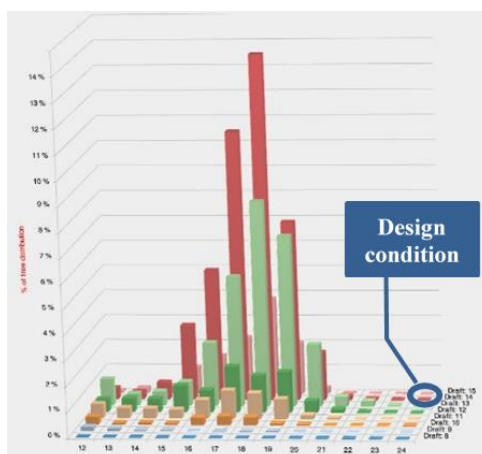


Fig.6: Typical operating profile of a large container vessel far from design condition

2.2 Calculation of the Hull Performance Index

The hull performance index is based on:

$$Performance\ index = \frac{reference\ power}{corrected\ measured\ power} \quad (1)$$

The reference power reflects the power demand under ideal conditions, whereas the corrected measured power is based on the measured power corrected for the influence of the weather. The weather correction is mostly based on empirics and often includes the following corrections:

- wind
- sea state
- swell
- water temperature
- current

Using Eq.(1) to determine performance means, that the vessel performs at 100%, if the corrected measured power is equal to the reference power. If the corrected measured power is twice as large as the reference power, the vessel only performs at 50%. Hence, using this performance index it is expected that the performance is ideally close to 100%.

Plotting the calculated HPIs of all reported events over time results in a hull degradation trend, which is the key parameter for deciding whether the next hull cleaning is advised. It may also provide insight on the performance of various hull coatings and may support the decision process for the best suited product depending on the characteristics of the operating area and profile. Depending on that, the corresponding decisions can vary significantly.

In general, the HPI plots tend to scatter more or less strongly. Besides the data base quality, the scatter could also be the result of uncertainties with respect to long-term measurements during normal operation. For example, if the measuring equipment is not calibrated on a regular basis, the accuracy of the reported measurements decreases with time. In addition, reporting environmental conditions is obviously still a challenge for many crews causing uncertainties in the weather correction.

2.3 Corrections and filter settings as main differentiator

The ISO 19030 is intended to provide a methodology for assessing changes in hull performance. It is organized in three parts, where part 2 describes the default method, which stipulates high-frequency data capturing. Changes in hull and propeller performance are quantified in terms of KPIs, which are

designed to evaluate the effect on performance over time of different maintenance, repair and retrofit activities. As stated in ISO19030, the method is not intended for determining “absolute” levels of performance in order to, for instance, compare different ship types, but only to compare performance changes over time for a given ship.

The weather corrections in ISO19030 are relatively simple. There are no explicit corrections for wind speed and swell provided. Instead, the default filter recommendations strictly limit the wind speed, which is corrected based on generic wind corrections with wind force coefficients taken from open literature, potentially leading to increased inaccuracy of the attained results.

The DNV GL method follows the default method in ISO 19030 Part 2 up to an extent, but deviates in other elements using the leeway given in Part 3. The main differences between DNV GL approach and ISO 19030 methodology can be summarized as follows (details can be found in *Schmode et al. (2018)*):

- No certain data frequency is required in order to use all available data, irrespective of the data collection process, but always applying data quality assessment criteria.
- A correction for sea water temperatures is applied to reduce scatter and increase accuracy.
- Vessel group specific weather corrections make the performance index less weather dependent. Smaller scatter equates better accuracy.
- The application of smart wind filters leads to many more surviving data sets without global loss of accuracy.
- The speed dependency in the performance indicator is reduced to give more realistic and less speed dependent values.
- A machine learning correction is applied to account for effects not modelled.

On top of above, AIS data are used as well to identify and verify each vessel’s operational profile and conditions.

Apart from the calculation of baselines based on design data, another set of baselines was calculated based on reported data from the first year of the studied period, as per ISO 19030. The design baselines were modified to take the actual performance of the first year into account.

Finally, it should be noted, that the results were normalized based on reported data from the first year of operation, i.e. first year of operation is equal to 100% performance.

3. Case studies and indicative results

The methodology described in Section 2 was applied for various vessel types, including cruise ships, LNG carriers, bulk carriers and crude oil tankers. A combined period of over 30 years of operation and approximately 165,000 data points, gathered through both manual and automatic data acquisition systems. In this paper, the key results of 2 LNG carriers and 1 cruise vessel are described. For the development of the baselines, data from the sea trials included as presented in Table 1.

Table 1: Sea trial data used for model development

	LNG Carriers	Cruise vessel
Draft	Two drafts Since all vessels are mainly operated on the provided drafts, no major disadvantages due to the interpolation are to be expected here	One draft Introduction of a draft band according to ISO 19030 in which the power extrapolation is allowed. Valid draft band range: 7.75-8.57m (\pm 5% displacement change)
Speed Range	A large speed range is provided (13-22 kn) minimizing the need to extrapolate the results.	A limited speed range (22.5kn -25kn) Extensive extrapolation of lower speeds was required.

Trim No trim information.

No trim information.

Vessels operated near level trim and therefore the missing trim consideration is acceptable

AIS data were used to identify the trade areas and operational profile of each vessel, as shown in Table 2, Figs.9-11. Key parameters that may affect the hull performance significantly are the sailing speed, the time spent in anchorage, and the idle time. For this reason, AIS data were used to identify the average sailing speed, the time spent annually in anchorage (speed less than 8kn) as well as idle time for more than 15 consecutive days, Table 2.



Fig.9: Trade route of LNG carrier



Fig.10: Trade route of LNG carrier 2

Table 2: Operating profile of vessels: trade areas, anchorage, idling time

Vessel	LNG Carrier 1	LNG Carrier 2	Cruise Vessel
Winter trade areas	Global trade	Global trade	New Zealand Australia Indonesia
Summer trade areas	Global trade	Global trade	Canada USA
Avg. sailing speed	14.6 kn	15.1 kn	16.1 kn
Anchorage yearly	15.8%	11.4%	33.1 %
Idling time (<15 consecutive days)	2 times: S.E. Asia: 17 days S.E. Asia: 22 days	1 time: S.E. Asia: 15 days	N/A

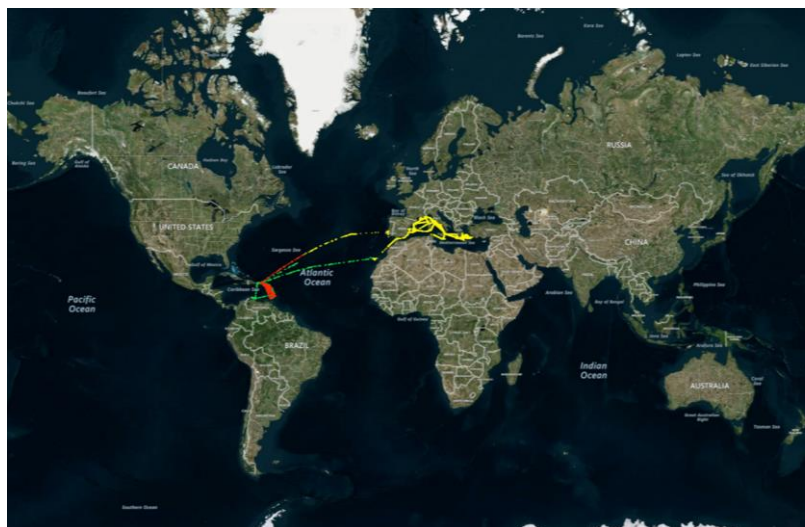


Fig.11: Trade route of Cruise Vessel

The analysis of the LNG carriers operation demonstrated good hull performance over the studied period, considering the sailing and idling conditions. More specifically, LNG Carrier 1 Hull Performance Index (HPI) degraded on an average annual rate of 3.7%, Fig.12, while the average speed drop was calculated at 1.2%, Fig.13. LNG Carrier 2 demonstrated an average annual HPI rate of -4.0%, Fig.14, and an average speed drop of 1.2%, Fig.15.

Table 3 summarizes the operational conditions and hull performance results. The negligible performance deviation between the two case studies, could be explained by different average speed, anchorage time and idling for more than 15 days.

Table 3: Overview of sailing pattern and hull performance versus 1st year performance

	Avg. Sailing Speed, [kn]	Avg. Sailing Draft, [m]	Anchorage per year, [%]	Annual HPI rate, [%]	Speed reduction, [%]
LNG Carrier 1	14.6	10.4	15.8%	-3.7%	1.2%
LNG Carrier 2	15.1	10.7	11.4%	-4.0%	1.2%

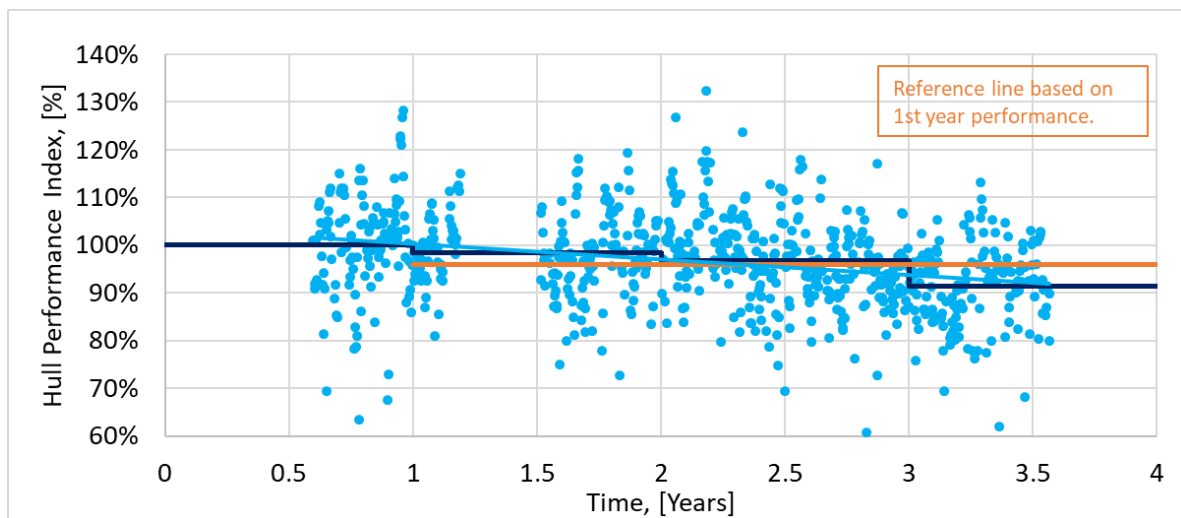


Fig.7: LNG Carrier 1 Hull Performance Indicator (HPI) vs time

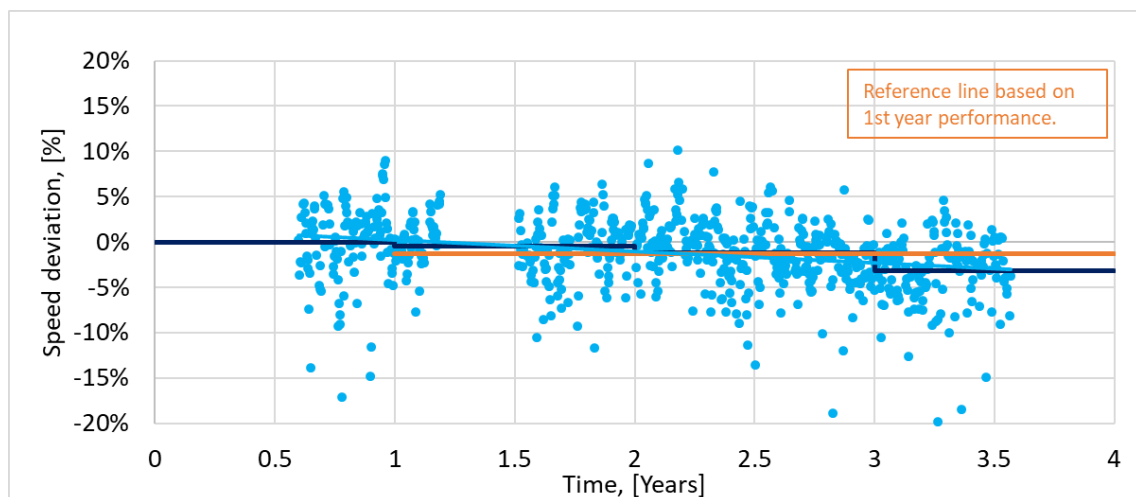


Fig.8: LNG Carrier 1 Speed deviation vs time

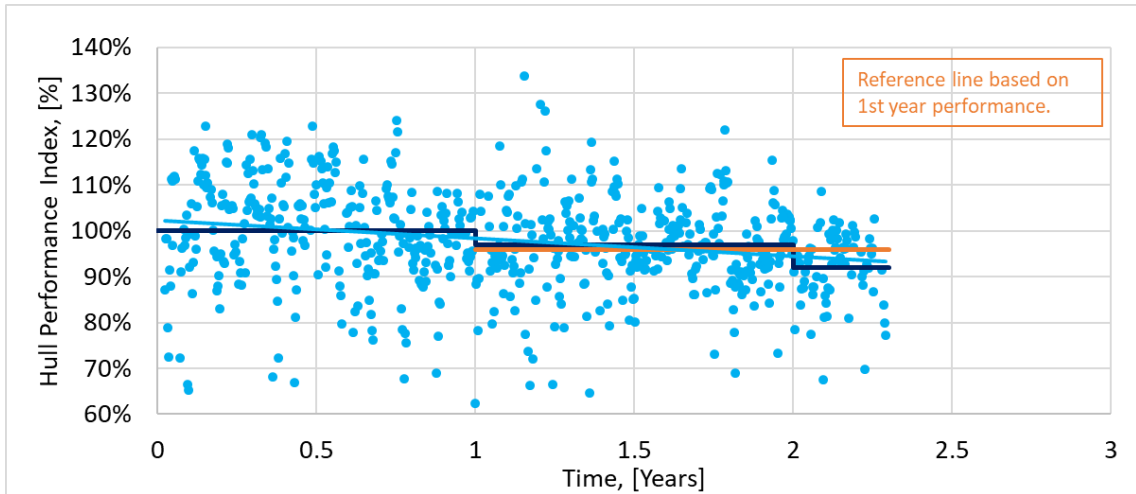


Fig.9: LNG Carrier 2 Hull Performance Indicator (HPI) vs time

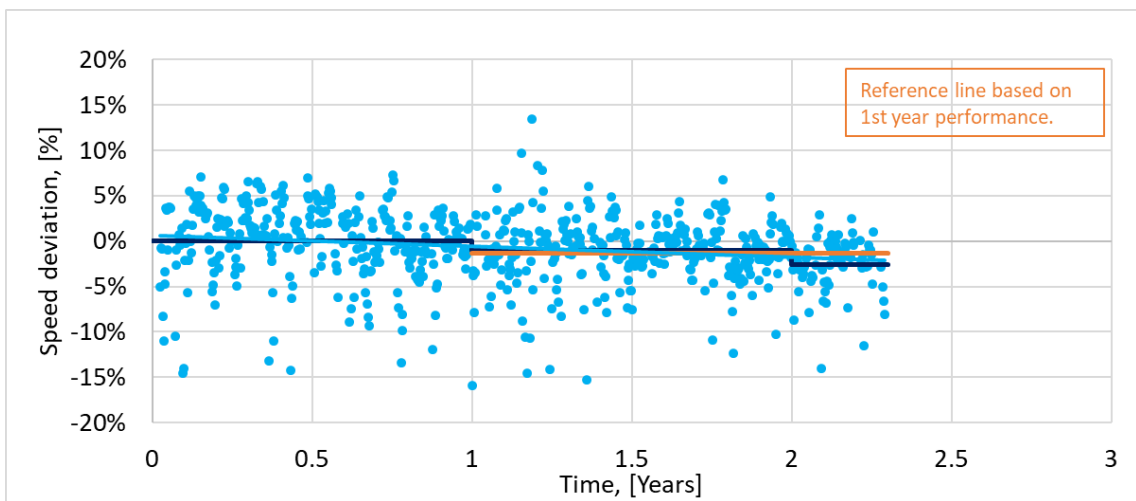


Fig.10: LNG Carrier 2 Speed deviation vs time

For the cruise vessel, the analysis was performed using the vessel ideal/design (based on sea trials) conditions as reference; a speed and power improvement were observed that may be attributed to improved performance of the new applied coating. More specifically, the Cruise Vessel demonstrated a speed increase of 0.5% and HPI improvement of 3.2% compared to the sea trials.

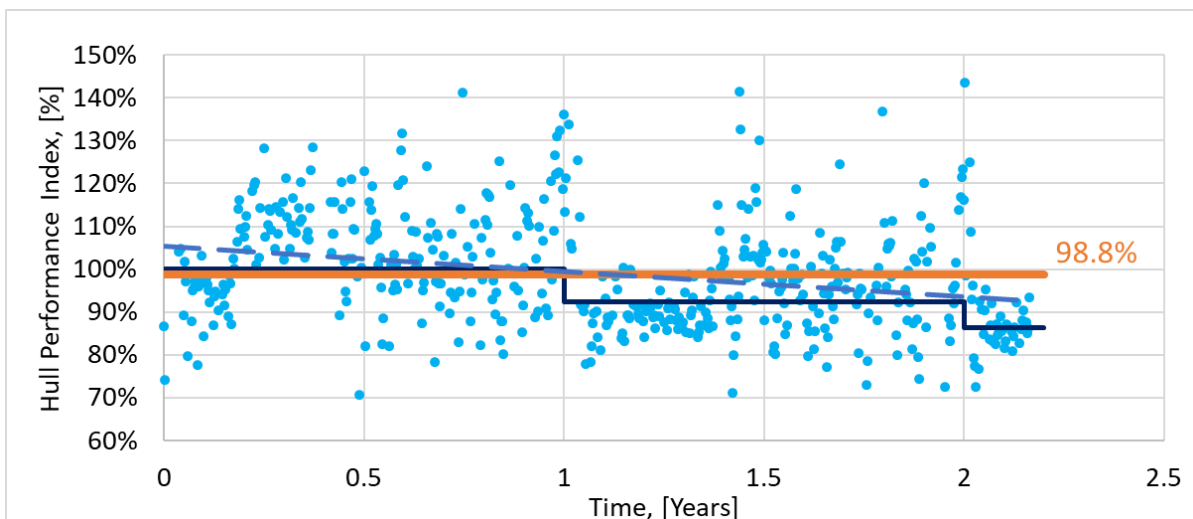


Fig.11: Cruise vessel Hull Performance Indicator vs. time (Initial improvement against the sea-trials)

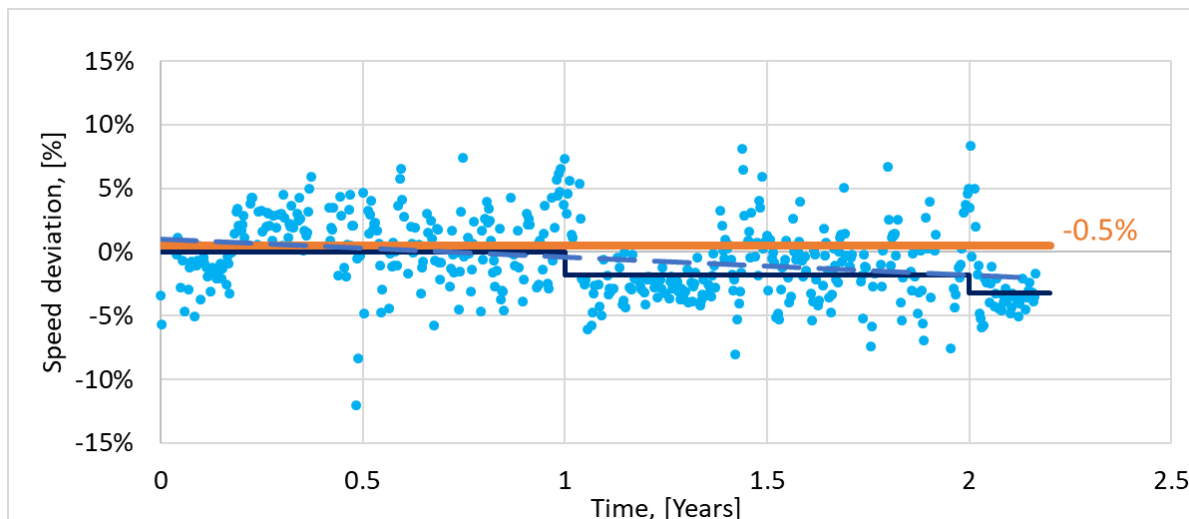


Fig.12 – Cruise vessel Speed deviation vs. time (Initial improvement against the sea-trials)

Table 4: Overview of sailing pattern and hull performance versus vessel design data

	Avg. Sailing Speed	Avg. Sailing Draft	Anchorage per year	Speed deviation vs sea trials	Speed reduction	HPI vs sea trials	Hull Perf.
Cruise vessel	16.1 kn	8.5 m	33%	+0.5%	0.5%	+3.2%	98.8%

4. Conclusions

In this article, the joined project between DNV GL and PPG on assessing the hull degradation of vessels was discussed. The advanced hull performance analysis methodology developed by DNV GL, was applied on various ship types of different sister vessel groups. Indicative results were presented, referring to a specific coating system based on low friction materials, developed by PPG.

Analysis was based in different reporting systems. Design data, e.g. sea trials, but also actual operational data were used to create the baselines and reference periods of the case studies. In addition, AIS data were utilized, in order to gain a holistic view of each vessel operational profile and conditions. Indicative results were presented; 2 LNG carriers with constant hull performance over the studied period. Furthermore, 1 cruise vessel showing speed and power improvement compared to the sea trials, which could also be attributed to the improved performance of the new applied coating.

References

BAIER, R.E. (2015), *Correlations of Materials Surface Properties with Biological Responses*, J. Surface Engineered Materials and Advanced Technology 5, pp.42-51

BENDICK J.A.; SCHULTZ M.P.; HOLM E.R.; HERTEL W.M. (2010), *Economic analysis of underwater hull coatings and maintenance*, NSWCCD-63-TR-2010/17, NSWC-CD, Bethesda (MD)

BOUMAN, E.A.; LINDSTAD, E; RIALLAND, A.I.; STRØMMAN, A.H (2017), *State-of-the-art technologies, measures, and potential for reducing GHG emissions from shipping – A review*, Transportation Research Part D: Transport and Environment 52/A, pp.408-421

- CORBETT, J.J.; WINEBRAKE, J.J.; COMER, B.; GREEN, E. (2011), *Energy and GHG Emissions Savings Analysis of Fluoropolymer Foul Release Hull Coating*, Energy & Environmental Res. Assoc.
- EDUOK, U.; FAYE, O.; SZPUNAR, J. (2017), *Recent developments and applications of protective silicone coatings: A review of PDMS functional materials*, Progress in Organic Coatings 111, pp.124-163
- KAUFFELDT, A.; HANSEN, H., *Enhanced Performance Analysis and Benchmarking with CFD Baselines*, 3rd HullPIC, Redworth
- MARCEAUX, S.; BRESSY, C.; PERRIN, F.-X.; MARTIN, C.; MARGAILLAN, A. (2014), *Development of polyorganosilazane-silicone marine coatings*Sandra, Progress in Organic Coatings 77, pp.1919-1928
- MEPC.304(72), *Initial IMO Strategy on Reduction of GHG Emissions From Ships*, 72nd MEPC, IMO
- MIRABEDINI, S.M.; PAZOKI, S.; ESFANDEH, M.; MOHSENI, M.; AKBARI, Z. (2006), *Comparison of drag characteristics of self-polishing co-polymers and silicone foul release coatings: A study of wettability and surface roughness*, Progress in Organic Coatings 57 421-429
- PERES, R.S.; ZMOZINSKI, A.V.; BRUST, F.R.; MACEDO, A.J.; ARMELIN, E.; ALEMÁN, C.; FERREIRA, C.A. (2018), *Multifunctional coatings based on silicone matrix and propolis extract*, Progress in Organic Coatings 123, pp.223-231
- SCHMODE, D.; HYMPENDAHL, O.; GUNDERMANN, D. (2018), *Hull Performance Prediction beyond ISO 19030*; 3rd HullPIC, Redworth
- SCHULTZ, M.P.; BENDICK, J.A.; HOLM, E.R.; HERTEL, W.M. (2011), *Economic impact of bio-fouling on a naval surface ship*, Biofouling 27 1, pp.87-98
- SELIM, M.S.; SHENASHEN, M.A.; EL-SAFETY, S.A.; HIGAZY, S.A.; SELIM, M.M.; ISAGO, H.; ELMARAKBI, A. (2017), *Recent progress in marine foul-release polymeric nanocomposite coatings*, Progress in Materials Science 87, pp.1-32

Application of an ISO 15016:2015 based Method in Analysing Ship's Performance

Beom Jin Park, KRISO, Daejeon/Republic of Korea, bjpark@kriso.re.kr
Myung-Soo Shin, KRISO, Daejeon/Republic of Korea, msshin@kriso.re.kr
Gyeong Joong Lee, KRISO, Daejeon/Republic of Korea, gjee@kriso.re.kr
Min Suk Ki, KRISO, Daejeon/Republic of Korea, mski@kriso.re.kr

Abstract

ISO 19030 was developed in order to prescribe practical methods for measuring changes in ship specific hull and propeller performance. ISO 19030 was expected to give a set of relevant performance indicators for hull and propeller maintenance, repair and retrofit activities. However, as presented in previous HullPIC conferences, results of ISO 19030 is not yet fully verified to give reliable performance indicators. On the other hand, ISO 15016 was developed to provide a set of standard methods to analyse results of speed trials of newly built ships with the accuracy of 2% in shaft power and 0.1 knots in speed, if all requirements are met. However, as ISO 15016 is intended to be used for sea trials, which are run on somewhat controlled environment with as low environmental forces as possible, some part of ISO 15016 is not applicable to ships' operational data. This paper proposes a new method based on ISO 15016:2015 and presents results of applying to operational data of bulk and container carriers and identifies benefits over ISO 19030 in ship performance.

1. Introduction

ISO 19030 standard was developed to prescribe practical methods for measuring changes in ship specific hull and propeller performance. The emphasis was laid on practical methods and many analysis techniques, such as calculating added resistance due to waves, was not included in the standard since there was no practical means to collect data necessary to apply such techniques at the time. Filtering and averaging were introduced instead to deal with environmental effects that was not accounted for in the standard. The results were a practical method the measure a ship's performance with limitation that it can only be used relatively to compare ship specific changes and unsuitable to be used to compares different ships, with rather coarse time resolution. (Averaging period should be at least 3 month or more and typically a year).

On the other hand, ship operators need means to analyse their fleet's performance each leg of the journey and often day by day to retain their competitiveness to survive in ever challenging business environment. Decision to increase a ship's efficiency are made day to day and three months averaged value of a ship's performance is too late and too coarse to be used in decision-making process.

This paper tries to identify possible alternatives to meet ship operators' needs, while not losing the practicality of the analysis method. ISO 15016:2015 is the new amended standard of ship speed trial analysis method. Its accuracy objective of 2% in shaft power and 0.1knots in speed was verified from many sources during its development process as it is used in contracts and mandatory regulations such as the reference speed in EEDI calculations. ISO 15016:2015 was also considered during ISO 19030 development and many parts in ISO 19030, such as wind correction, was directly referenced. In this paper, a new analysis method based on ISO 15016:2015, but retaining practical applicability as in ISO 19030 is proposed and application results to ship operation data is discussed.

2. Analysis methods

2.1. Overall process

The overall process of the new proposed method is basically the same as ISO 19030 and ISO 15016:2015. First, outliers and unwanted data, such as when turning direction or in shallow water is

removed by filtering. Then resistance increase due to environmental forces are estimated by the same method used in ISO 15016:2015. These resistance increases are then used to correct power using direct power method used in ISO 15016:2015. For comparing purposes, the analysis results are further corrected to standard displacement.

2.2. Filtering

In ISO 19030, filtering is used to remove outliers and only leave the part of data when the ship is steadily cruising. However, as noted in *Park et al. (2017)*, filtering in ISO 19030 have unwanted effects. In ISO 15016:2015, no filtering on data is applied as speed trial is only conducted in very calm environment and very few measurements are taken.

The proposed method uses only very simple filters to avoid any unwanted effects:

- Remove too low or high speed. Usually the speed range in model test is used as reference and any speed outside the range is discarded.
- Remove when rudder angle is larger than 5° to remove when changing direction.
- Remove when the ship is operating in shallow water.

2.3. Estimating resistance increase

As in ISO 15016:2015, resistance increase due to wind, wave and difference in water density is estimated with the same method used in ISO 15016:2015. For wind resistance, ISO 19030 and ISO 15016:2015 basically uses the same method. For wave resistance, it was not included in ISO 19030 as no practical means to measure wave parameters are not available. However, as noted in *Park et al. (2018)* there are publicly available wave data for sources such as National Oceanic and Atmospheric Administration (NOAA). ISO 15016:2015 includes STAWAVE II and theoretical method for wave resistance calculation, but since theoretical method requires more detailed ship geometry data and requires more time for calculation, STAWAVE II, even with its limitation of only calculating waves within ±45° of the ship's heading, is more practical method to use.

Resistance increase due to difference in water density can be calculated from water temperature, which is also available from weather services even if the ship is not equipped to record the data.

2.4. Power correction

When all resistance increases are estimated, they are used in correcting the measured power value. The corrected delivered in ideal condition is calculated using Eqs.(1) and (2).

$$\Delta P = \frac{\Delta R \cdot V_s}{\eta_{Did}} + P_{Dms} \left(1 - \frac{\eta_{Dms}}{\eta_{Did}} \right) \quad (1)$$

- ΔP is the required correction for power in watts;
 ΔR is the total resistance increase in newtons;
 V_s is the ship's speed through the water in metres per seconds;
 P_{Dms} is the measured delivered power in the operating condition;
 η_{Dms} is the propulsive efficiency coefficient in the operating condition;
 η_{Did} is the propulsive efficiency coefficient in the ideal condition.

Then, the corrected power is calculated by:

$$P_{Did} = P_{Dms} - \Delta P \quad (2)$$

P_{Did} is the corrected delivered power in the ideal condition.

Unlike ISO 15016:2015, current correction is not included in the new method. Current correction method in ISO 15016:2015 assumes that the measurements are taken in the same geographical location and therefore current can be expressed as periodic function dependent on time. However, for operating ships, geographical location is always changing and the current affecting the ship's performance is changing as well. How to account for the current is left as future work at this time.

2.5. Displacement correction

Each leg and journey of the operating ship has different displacements and in order to compare analysis results, the difference in displacements has to be accounted for. In the proposed method, this is achieved by first defining standard displacements for typical loading conditions such as laden and ballast for bulk carriers and 80% or 90% displacements for container carriers and then using displacement correction method in ISO 15016:2015 to correct power to standard displacements. After displacement correction, analysis results can be compared to each other and even with model test or sea trial results, if such data is available for the same loading conditions.

3. Data collection

During ISO 19030 development, particular care was given so that only practically available data is used in the standard. The proposed method uses the same basic principles. All data is typically available in most ships. The data used in the proposed method is summarised in Table 1.

Table 1: List of operational data used in the proposed method

Data item	Mainly used in	Typical source
Speed over ground	Wind resistance calculation	Onboard measurements
Speed through water	Power correction Wave resistance calculation	Onboard measurements
GPS heading	Wind resistance calculation	Onboard measurements
Gyro heading	Wave resistance calculation	Onboard measurements
Rudder angle	Filtering (changing direction)	Onboard measurements
Water depth	Filtering (shallow water)	Onboard measurements Weather service data
Shaft power	Power correction	Onboard measurements
Wind speed	Wind resistance calculation	Onboard measurements Weather service data
Wind direction	Wind resistance calculation	Onboard measurements Weather service data
Air temperature	Wind resistance calculation	Onboard measurements Weather service data
Sea wave height	Wave resistance calculation	Weather service data
Sea wave period	Wave resistance calculation	Weather service data
Sea wave direction	Wave resistance calculation	Weather service data
Swell height	Wave resistance calculation	Weather service data
Swell period	Wave resistance calculation	Weather service data
Swell direction	Wave resistance calculation	Weather service data
Sea water temperature	Wave resistance calculation Water density resistance calculation	Weather service data
Static draught	Displacement correction	Onboard measurements Port inspection

4. Analysis results

The proposed method is applied to two ships – one 176K bulk carrier and one 8600TEU container carrier. Figs.1 to 4 shows typical analysis results of the bulk carrier and shows those of the container

carrier. Unlike ISO 19030, the results are expressed in a point cloud. Its dispersion trends and slope show much more information of the performance of the ship than one averaged value of ISO 19030. In all figures, after power correction, the point cloud resembles a line similar to the reference speed power graph obtained from model test. Basically, the difference in the performance from the reference condition, similar to the Performance Indicator in ISO 19030 can be identified by the location of the point cloud in reference to solid line, which represents model test results. But unlike ISO 19030, this analysis can be done for each leg of a journey or combined data of several legs or journeys, as long as the loading condition is the same.

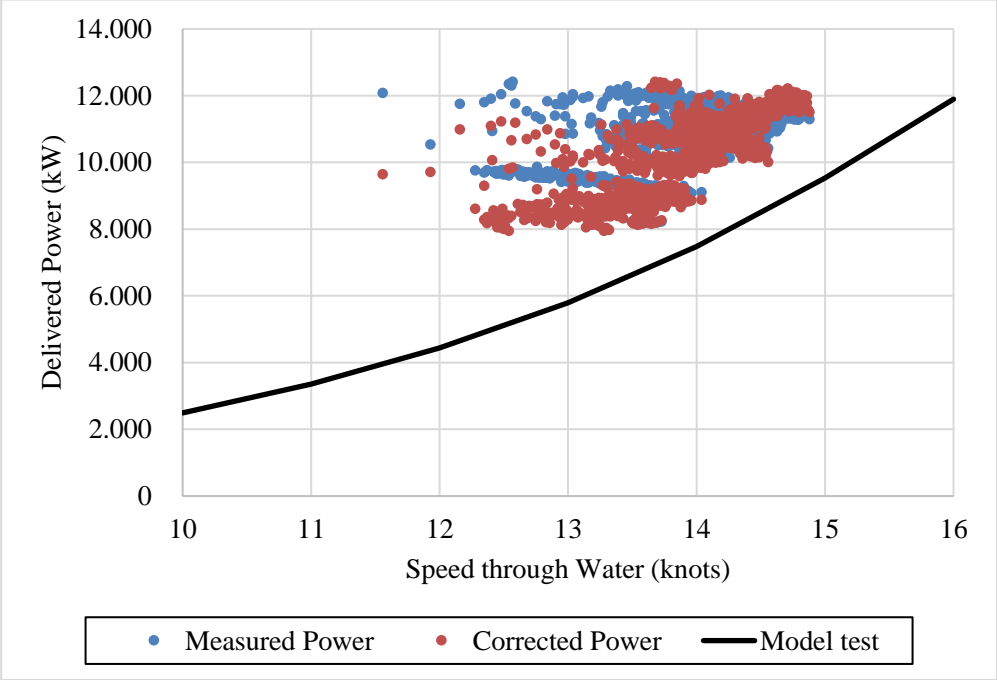


Fig.1: Typical analysis results of bulk carrier in ballast condition

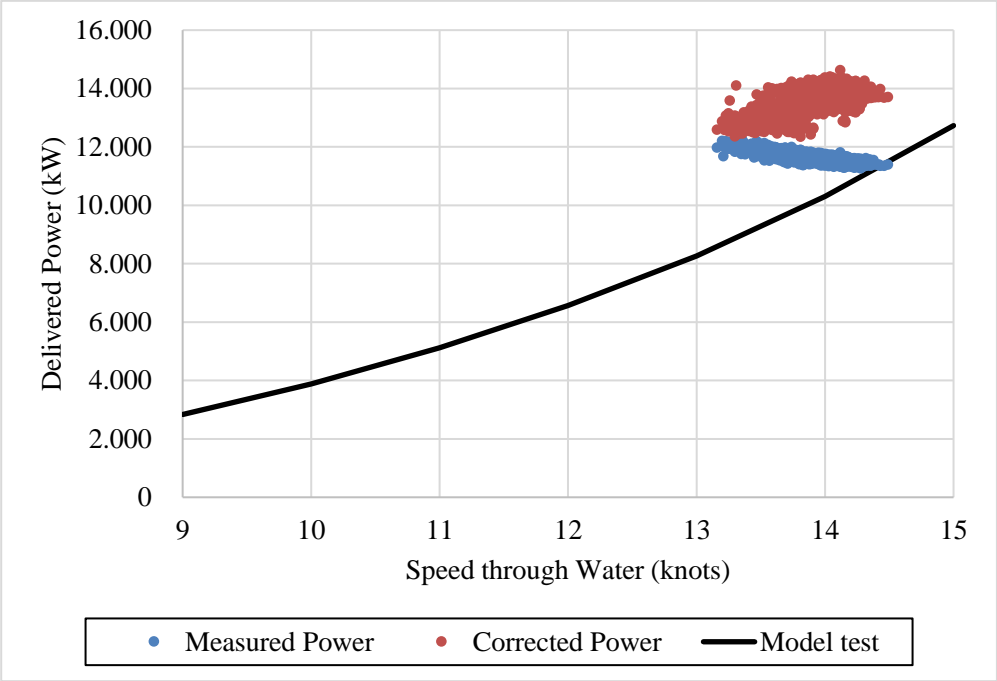


Fig.2: Typical analysis results of bulk carrier in laden condition

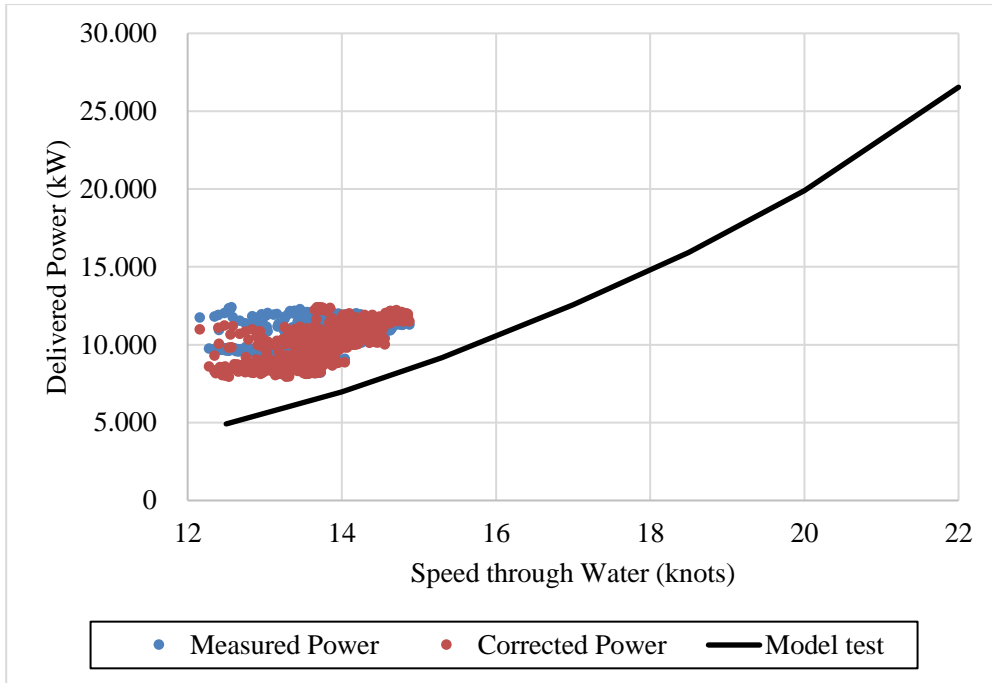


Fig.3: Typical analysis results of container carrier in 80% loading condition

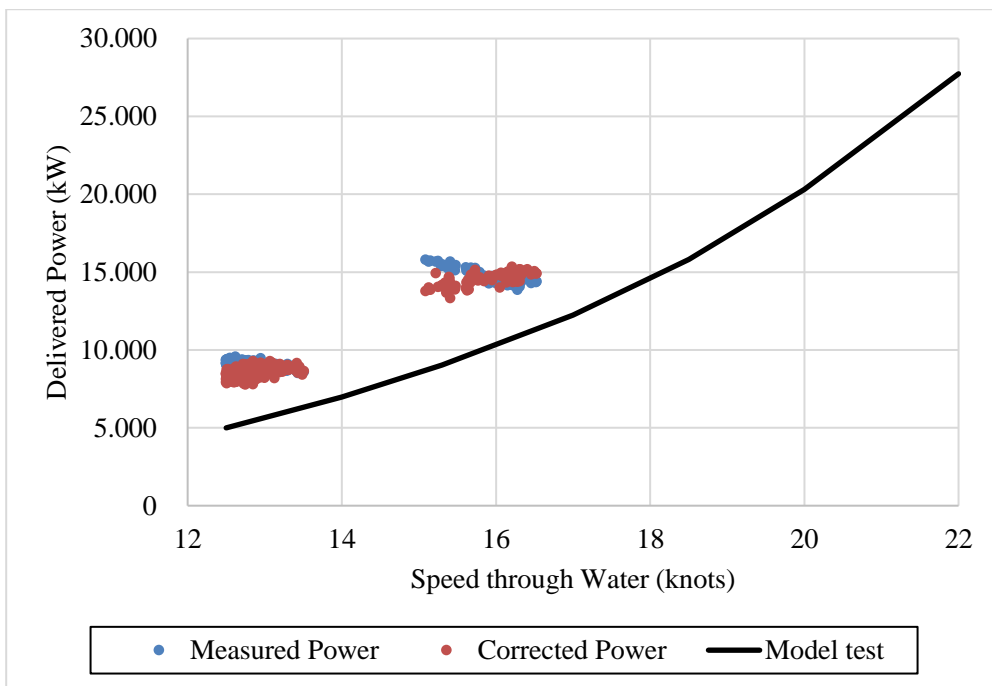


Fig.4: Typical analysis results of container carrier in 90% loading condition

Fig.5 shows analysis results of 4 journeys with same departure and destination of the bulk carrier in ballast condition. The legend shows the dates when each journey is made. There is a noticeable difference in the performance of the bulk carrier between each journey and journey made in February, 2017 have distinctively better performance than the journey made in July of the same year. Fig.6 shows the same results of container carrier in 90% loading conditions. Unlike the bulk carrier, the container carrier does not show distinctive difference in performance between April and October, 2018.

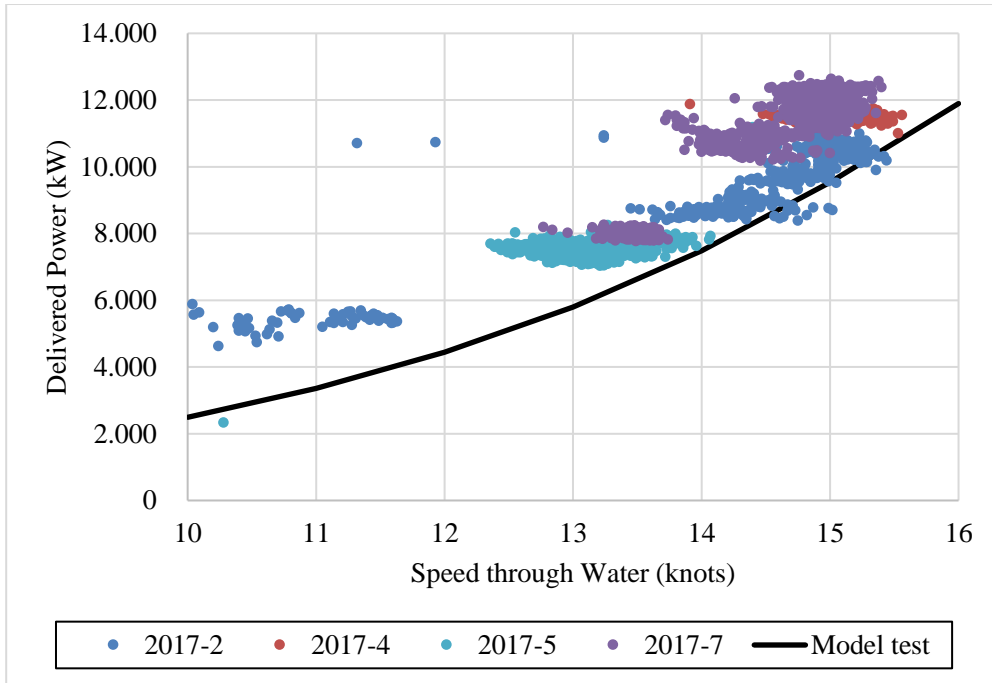


Fig.5: Comparison of analysis results of bulk carrier in ballast condition

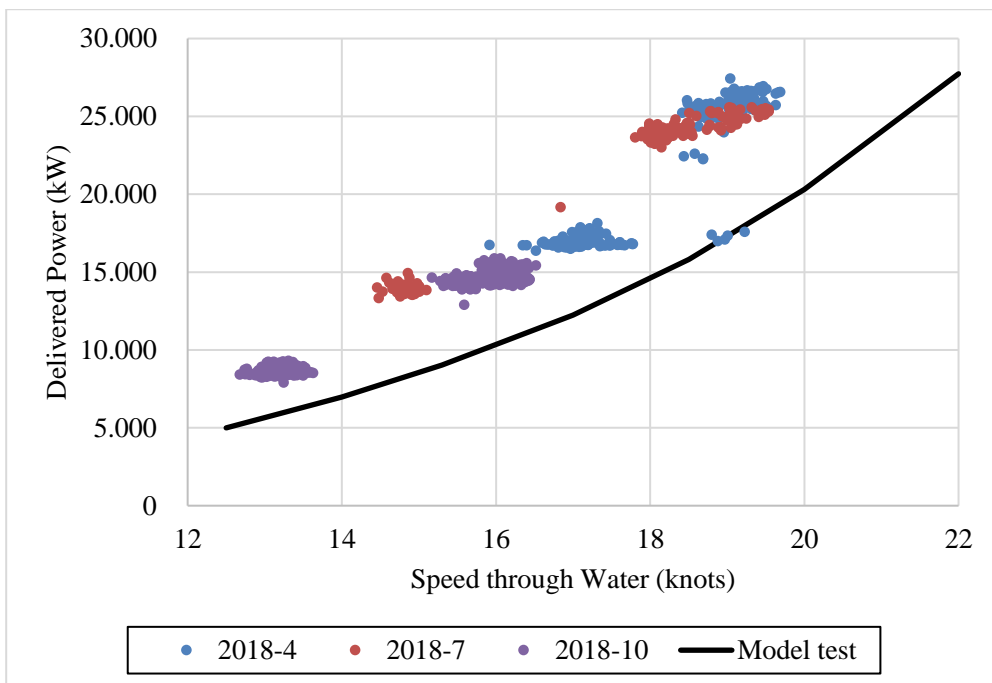


Fig.6: Comparison of analysis results of container carrier in 90% loading condition

In ISO 19030, in order to analyse change in performance before and after a dry docking or a maintenance event, at least 6 months of data (3 months before and 3 months after) is required. However, in the proposed method, it can be analysed even with only one journey before and after dry docking as shown in Fig.7 to Fig.9. Fig.7 shows analysis results of one journey before and after dry docking in laden condition of the bulk carrier and Fig.8 in ballast condition. Fig.9 shows analysis results of one journey before and after dry docking in 80% loading condition of the container carriers. They all show noticeable difference from dry docking and may even describe the effects dry docking more accurately as the time period is very short, within two months for total period.

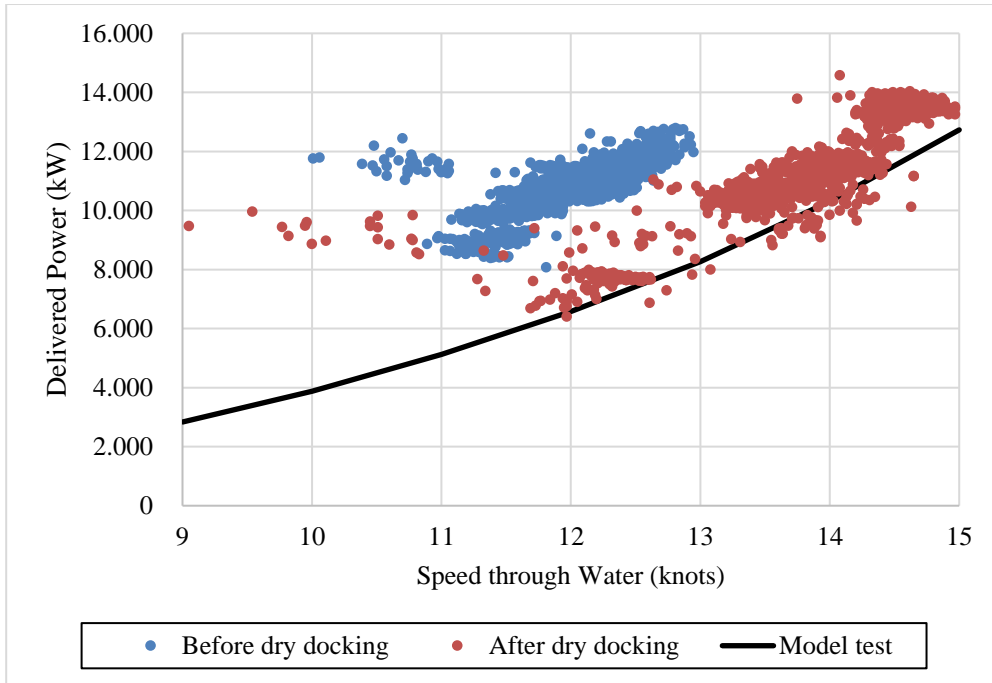


Fig.7: Comparison of before and after dry-docking performance of bulk carrier in laden condition

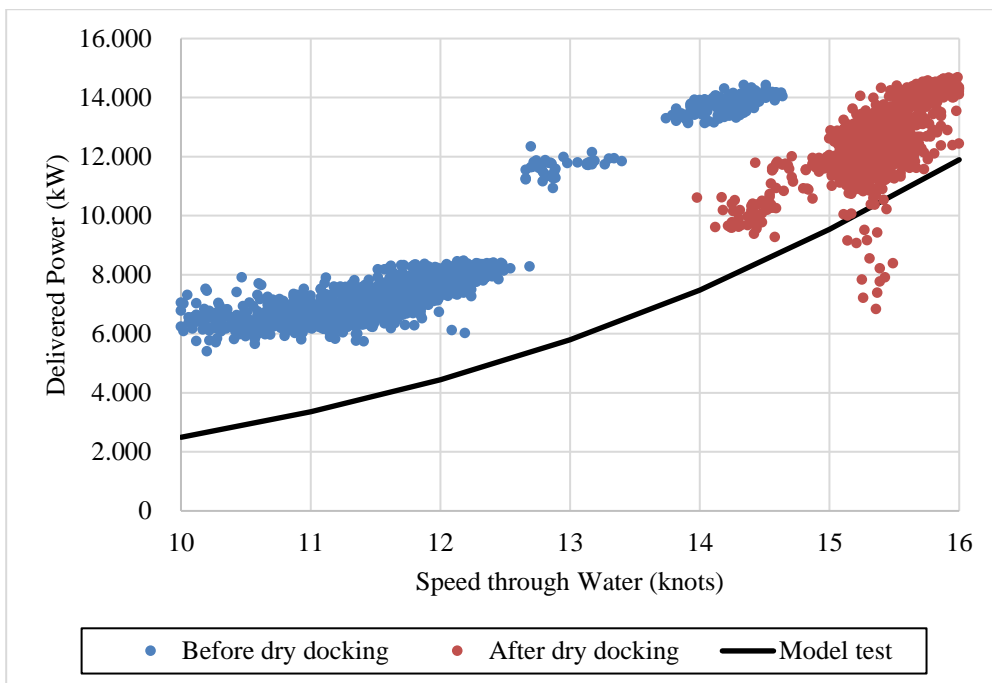


Fig.8: Comparison of before and after dry-docking performance of bulk carrier in ballast condition

5. Conclusions

This paper proposes a new method based on ISO 15016:2015 that can give more detailed analysis results on the changes in the performance of a ship than ISO 19030. Specifically, the proposed method does not need averaging as it takes account of major environmental effects and therefore can analyse the performance of a ship with data collected in shorter period of time than ISO 19030 and provide more insights on the performance the ship as it gives more than a single averaged value.

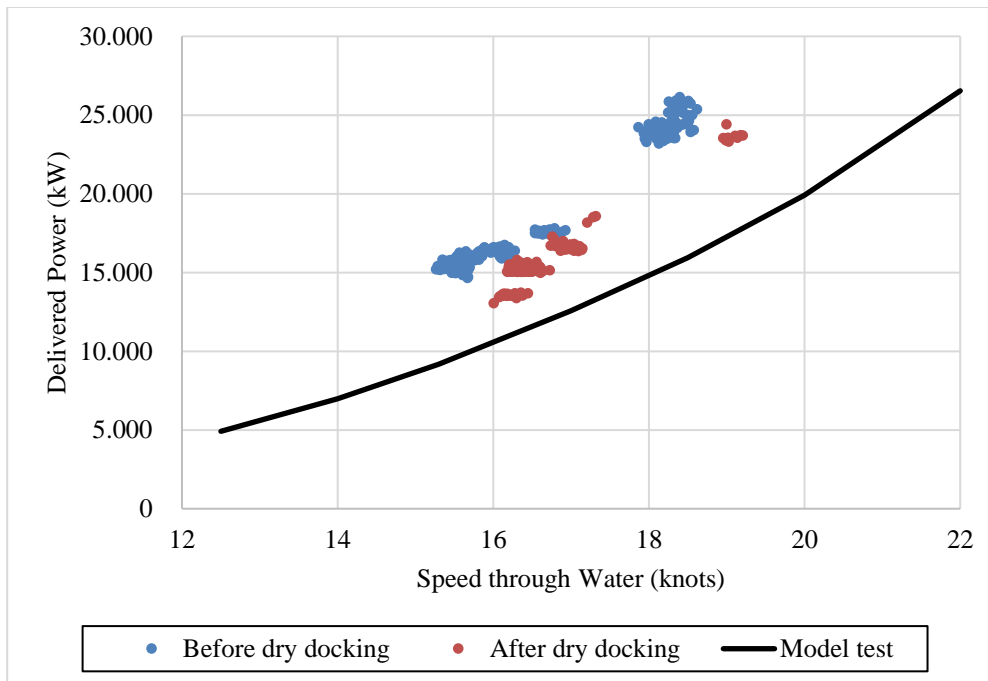


Fig.9: Comparison of before and after dry-docking performance of container carrier in 80% load

While the proposed method shows good promises, more validation is required to many different types of ships. Also, one major environmental effect that is not accounted in the proposed method still remains – currents. A reliable method to estimate resistance increase will improve the accuracy of the proposed method further.

Acknowledgements

This research was sponsored by the Ministry of Trade, Industry & Energy (Korea Government) under the project “Accuracy enhancement of model-ship correlation based on the ship performance measurement (PNS3370)” and “Development of advanced speed-power analysis technology to attain high energy efficiency and GHG reduction of operating ships under real sea condition (PNS3190)”.

References

- PARK, B.J.; et al (2017), *Experience in Applying ISO 19030 to Field Data*, HullPIC 2017, Ulrichshusen, pp.150-155
- PARK, B.J.; et al (2018), *Ideas on How to Improve ISO 19030 based on the Results of Applying to Field Data*, HullPIC 2018, Redworth, pp.178-184
- ISO 15016:2015 (2015), *Ships and marine technology – Guidelines for the assessment of speed and power performance by analysis of speed trial data*, Int. Organization for Standardization
- ISO 19030-1 (2016), *Ships and marine technology – Measurements of changes in hull and propeller performance – Part 1: General Principles*, Int. Organization for Standardization
- ISO 19030-2 (2016), *Ships and marine technology – Measurements of changes in hull and propeller performance – Part 2: Default method*, Int. Organization for Standardization
- ISO 19030-3 (2016), *Ships and marine technology – Measurements of changes in hull and propeller performance – Part 3: Alternative methods*, Int. Organization for Standardization

Full-Scale Performance Measurement and Analysis of the Silverstream Air Lubrication System

Luke De Freitas, Silverstream Technologies, London/UK, luke.defreitas@silverstream-tech.com

Noah Silberschmidt, Silverstream Technologies, London/UK,
noah.silberschmidt@silverstream-tech.com

Takis Pappas, Silverstream Technologies, London/UK, takis.pappas@silverstream-tech.com

David Connolly, Silverstream Technologies, London/UK, david.connolly@silverstream-tech.com

Abstract

In this paper, Silverstream Technologies will discuss and present their experience in executing performance measurement and analysis of the company's proprietary Air Lubrication System; the Silverstream® System. Experiences discussed are drawn from execution of commercial installations on a chemical tanker and two cruise ships. The intent is not to present the mathematical nuances of trials data analytics but to provide an informative script as to the challenges encountered with on-board data collection and the reality that one defined method is not fit for evaluating performance of Energy Efficiency Technologies (EETs). The discussions encompass the accuracy of measurement instruments, methodologies applied in determining in-service performance, applicability of ISO 19030 and uncertainties that changing environmental factors introduce in full-scale performance monitoring. The experiences fall against the backdrop of a unique hydrodynamic EET that has the capability of being switched ON and OFF greatly simplifying the baseline against which performance is measured.

1. Nomenclature

The following words and/or expressions used in this paper shall have the meaning as defined below:

ARU	Air Release Unit(s)
ALS	Air Lubrication System
BF	Beaufort Wind Scale
C _{AA}	Air Resistance Coefficient
EET	Energy Efficiency Technology
Gross	Total reduction in power
HSVA	Hamburgische Schiffbau-Versuchsanstalt (Hamburg Ship Model Basin)
hh:mm:ss	Timestamp in hours, minutes and seconds
kn	Values given in Knots
kW	Values given in Kilowatts
LR	Lloyds Register
Net	Total reduction in power after deduction of compressor power
RPM	Revolutions Per Minute
Run	Consecutive block of ON and OFF data
SOG	Speed Over Ground
STW	Speed Through Water

2. Introduction

A vessel's resistance when moving through the water is made up of multiple components, of which frictional resistance is the most dominant. Injection of air into the boundary layer (between the stationary and moving water) can reduce the frictional resistance of the hull, *Liem et al. (2013)*. The concept of using air lubrication has been considered a viable method for reducing frictional resistance of ocean-going vessels for decades with the first patent; US5644 A filed in 1848 for increasing vessel speed, *Stevens and Stevens (1848)*. Many methods have been proposed and tested since then, but no single method of achieving the desired net energy reduction has been readily adopted by the industry.

Silverstream have spent the last decade perfecting the Silverstream® System which has been based on full-scale testing at research facilities in combination with full-scale testing on three shipboard installations deployed over the last 5 years. Full-scale testing is essential for proving air lubrication as accurate scaling of microbubbles and air layers from full to model-scale is practically impossible due to the widely known Reynolds number scaling problem, *Molland et al. (2017)*. Consequently, caution is required when inferring full-scale performance from the basis of model tests only. As a result, Silverstream Technologies have adopted a split development programme encompassing full-scale testing at HSVA using their cavitation tunnel to experiment and demonstrate the formation of the microbubble carpet in the vessel's boundary layer. The experimentation work allows for measurement of the reduction of frictional resistance on a plate immediately aft of the ARU. This translates to reduction in hull surface frictional resistance requiring full-scale trialing to capture the coverage achieved and adherence of the microbubble carpet formed by the ARU to the hull which underpins the importance of measuring performance at ship scale.

The Silverstream® System utilises a natural phenomenon known as the Kelvin-Helmholtz instability as shown in Fig.1, using uniquely designed and patented ARUs to generate microbubbles with minimal energy input, *Johannesson et al. (2015)*.

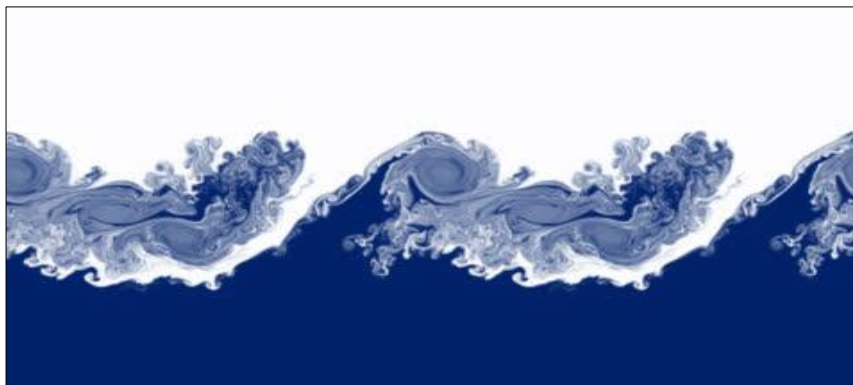


Fig.1: Kelvin Helmholtz Instability

A shearing mechanism is created by the passing of fast-flowing water across a stationary air interface resulting in the formation of microbubbles in the boundary layer which is then carried along the flat bottom of the hull as the vessel moves through the water. The layer of microbubbles remain in the boundary layer reducing the frictional resistance of the vessel.

This gives a reduction in shaft power and an increase in speed for a constant RPM as the thrust/resistance ratio associated with the specific hull reaches a new equilibrium. The increase in speed can also be translated into a change in shaft power based upon the vessels measured speed/power curve which provides three (3) possible scenarios for Ship Owners/Operators:

- RPM is maintained as constant and benefit of technology is taken as a combination of fuel savings and increase in speed
- Shaft power is maintained as constant resulting in an increase in RPM allowing the full benefit to be taken as speed gain
- Speed is maintained as constant reducing the required engine power and RPM allowing the full benefit to be taken as fuel savings

The first prototype Silverstream® System was sponsored by Shell and retrofitted to the relatively unsophisticated 40,000 DWT chemical tanker MT Amalienborg in 2014, *Silberschmidt et al. (2016)*, (renamed to MT Shandong Zihe) which demonstrated average net savings of 4.3% during extensive trials post installation with many confirmed double runs exceeding net savings of 6% and with a maximum of 12%. During these sea trials, 52 runs consisting of 26 double runs were executed over 3 days in near perfect metocean conditions (i.e. flat calm with minimal wind and waves) which is rarely

afforded within a commercial installation scenario. Within these trials, care was taken to measure impact of the bubble carpet upon performance of the ships propeller to remove concerns relating to loss of propeller thrust and risk of cavitation, neither of which was experienced. Long term in-service monitoring in the fully-loaded condition then demonstrated savings of 5.1% and the results of both trials were independently verified by Shell, LR and Southampton University.

More recently, the Silverstream® System was installed on two cruise vessels, one newbuild and one retrofit for major owners which demonstrated savings in the range of 4-6%, the results of which have been also been independently verified by LR and HSVA.

These vessels encompass state of the art technologies with modern sensor units, integrated ship management systems and sophisticated performance monitoring equipment. In theory, given the availability of these technologically advanced systems onboard geared to monitor all aspect of vessel performance, analysis of the performance of an EET should be straightforward and simple. However, the complexity of system integration poses issues in terms of ensuring that sensor signals are provided uncorrupted since it is inevitable that they will pass through multiple systems before connection to the control and monitoring system of the EET. Additionally, irrespective of the complexity involved, vessel performance is still heavily dependent upon simple measurement instruments such as a speed log for STW which has been seen to provide inaccurate and unreliable signals in many cases. Additionally, the commercial pressure to return these vessels to service immediately after dry-docking is also such that execution of dedicated trials like those conducted on MT Amalienborg, *Silberschmidt et al. (2016)*, is rarely a viable option.

As a result, trials conducted in-service can introduce many issues such that the effort involved in data collection onboard and performance analysis to determine the simplified net savings effect from ALS requires on average 100-man days for each vessel.

3. Performance Monitoring & Data Analysis

The complexity of conducting performance trials can also be somewhat daunting as there are various circumstances which should be considered such as the ship's operational schedule and navigating traffic in shipping lanes which introduces variations in ship's heading, rudder angle and RPM as a minimum. Additionally, changing weather conditions also cause fluctuations in conditions such as wind direction, speed and current. For many ships, the above is unavoidable as it is often not possible to conduct trials in isolated conditions outside of ship operations i.e. during dedicated shipyard trials which could improve accuracy of results.

However, one of the advantages with trials on cruise vessels is the simplification of operating at a single draught as hull flow lines can change dramatically especially when the waterline on the bow differs in the presence of a bulb. With small changes in draught (typically in the range of 10-20mm), the hull can move to non-optimum operating conditions due to additional submergence of the bulbous bow thereby increasing the residual resistance on the hull and care should be taken when considering results where there have been any variations in draught, *Gorski et al. (2013)*.

3.1. Analysis Methodology

The Silverstream® System, unlike other EETs, has the added benefit of being able to be switched ON and OFF which greatly simplifies measurement of system performance. This functionality provides the added benefit of being able to isolate the impact of the technology from other effects on the ship such as change in fin stabiliser deployment particularly relevant for cruise ships.

The Silverstream Performance Monitoring System integrates with ship systems collecting high frequency data from other systems to accurately measure changes in performance between system OFF and ON conditions as shown in Fig.2.

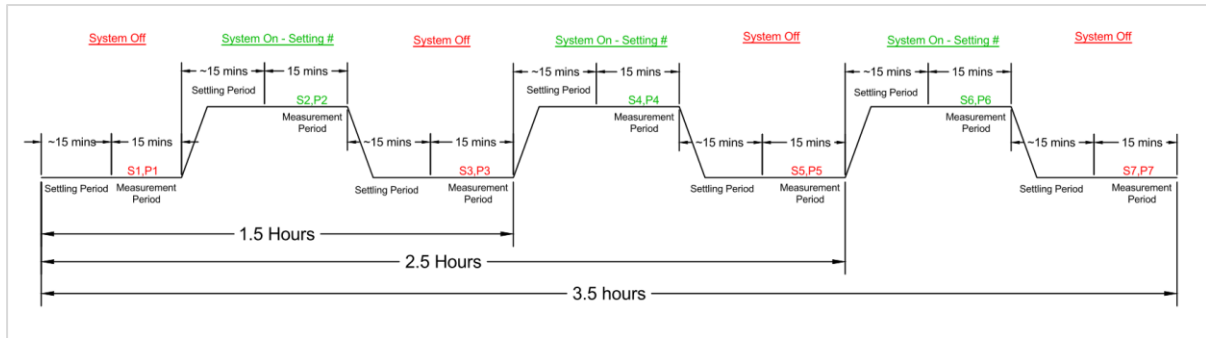


Fig.2: Silverstream Procedure for Switching System ON/OFF

The settling and measurement periods shown in Fig.2 have been developed based on Silverstream's experience during performance trials which identified that a period of 10-15 minutes is enough to allow for the vessel's speed to stabilise following a change in the condition from OFF to ON or vice versa. The settling period however may be adjusted up or down during the testing phase as required to increase accuracy of measurements being taken onboard. Data inputs to the Silverstream computer are logged upon any change in an input outside the prescribed limits. This is above the required frequency given in ISO 19030, *ISO (2016)*, as some parameters such as fin stabiliser and rudder angle positions can be required to be recorded at a higher frequency to sufficiently capture the variation and account for measurable changes between ON and OFF periods.

The two most critical parameters required to evaluate performance of the Silverstream® System are shaft power and vessel speed as for a constant RPM, the shaft power required is reduced resulting in an increase in speed in the system ON condition when compared with the corresponding OFF condition. Typically, a total gross power reduction of 500-600 kW can be seen at 14-15 kn whilst at 17-18 kn, the power reduction is usually in the region of 800-1000 kW as seen on large cruise ships. On average, the ratio between shaft power reduction and equivalent power from the speed increase has been identified as a 40:60 split but this can vary based on changing conditions. This means that at a constant RPM, 40% of the power reduction is seen at the shaft and 60% of the power reduction is gained from a speed increase of 0.1-0.7 knots.

Both speed and shaft power data inputs were found to have varying reliability over the period of analysis which introduced a level of uncertainty in the results as discussed in the next section.

3.2. Data Quality & Accuracy

In this section, some examples of data quality issues and actions taken relating to the main parameters affecting accuracy of the performance evaluation are provided.

3.2.1 Shaft RPM

Data from the torque meters is usually received at a high frequency and the signal is assumed to be sufficiently accurate with the expectation that it is routinely calibrated and for simplicity, the calculated power is usually fed to the onboard datalogger. In a given period during trials, some inaccuracies in the power was noticed and forensic analysis driven by inconsistency between the two shafts showed that shaft 2 RPM measurements fluctuated by 1-2 RPM as shown in Fig.3, such that power measurements derived from these RPM readings were unreliable in comparison to shaft 1 which kept constant throughout performance testing. Given the averaging of data, it was not obvious that shaft 2 RPM was fluctuating but instead showed that the readings were constant at one 1 RPM higher leading to warped results. Only after RPM measurements were analysed in detail, the fluctuations of 1-2 RPM became apparent. Consequently, as we were confident that both engines were balanced, inconsistency in the data was minimised in this instance by doubling the power from shaft 1 in calculation of the overall performance to increase accuracy of results pertaining to RPM and shaft power measurements.

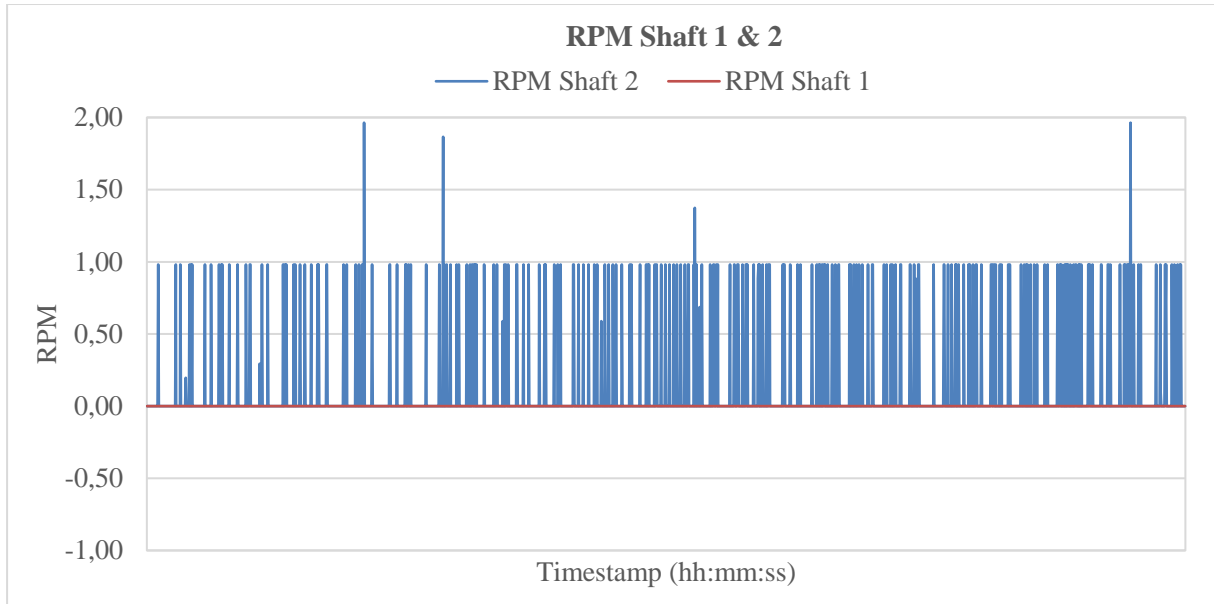


Fig.3: RPM Fluctuation over time

3.2.2 Speed Measurement

Experience from several trials also identified that there can be intermittent issues with readings from the speed log. Fig.4 shows a time plot of STW vs. SOG signals over a 6-hr period whilst at sea which identified that the STW signal dropped out frequently throughout performance testing.

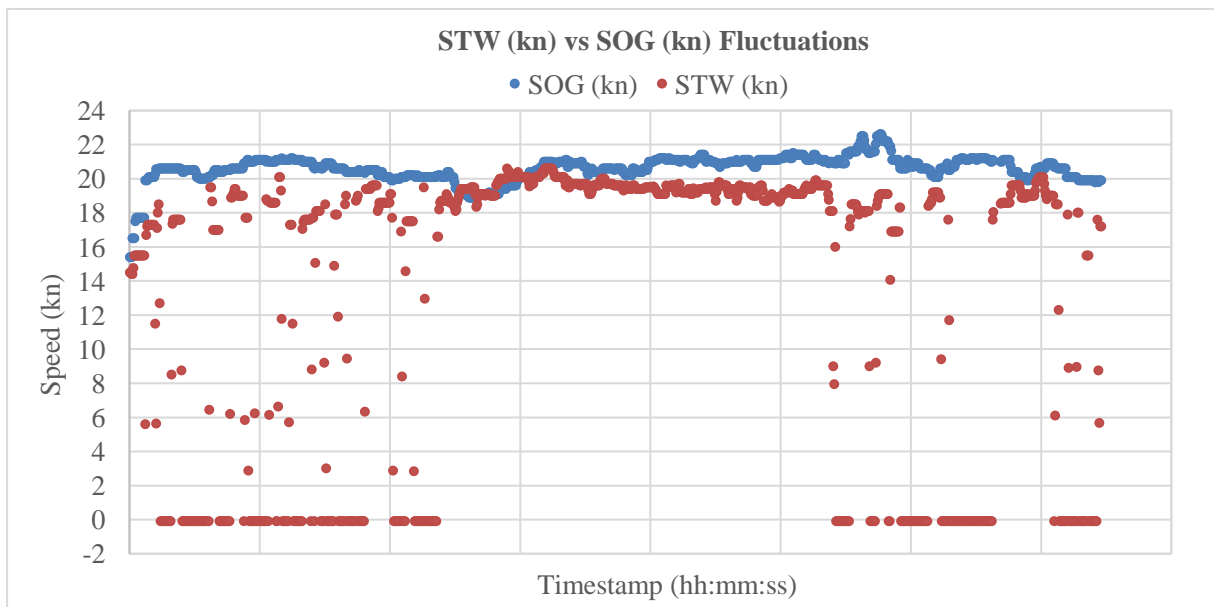


Fig.4: STW vs. SOG Fluctuation over time

This provided the greatest source of inaccuracy as the speed gain provided by the Silverstream® System makes up approximately 60% of the shaft power savings as discussed earlier. It should also be noted that if there are no changes in current, the SOG can be more accurate and reliable in measuring the speed gain achieved between OFF and ON conditions. However, the changes in current within a measuring period can also affect the accuracy, but if large datasets are available the confidence can be increased as the variation can be reduced. Hence, if the STW signal is seen to be temperamental, but SOG and STW are similar, the confidence level achieved can be higher.

3.2.3 Wind Speed & Direction

Environmental factors are also crucial to accurately determine vessel's performance with EETs. Analysis showed that weather conditions measured by the ship's anemometer can introduce another level of uncertainty as large and frequent changes in relative wind direction were identified in recorded values compared to small changes in wind speeds for corresponding times as shown in Fig.5.

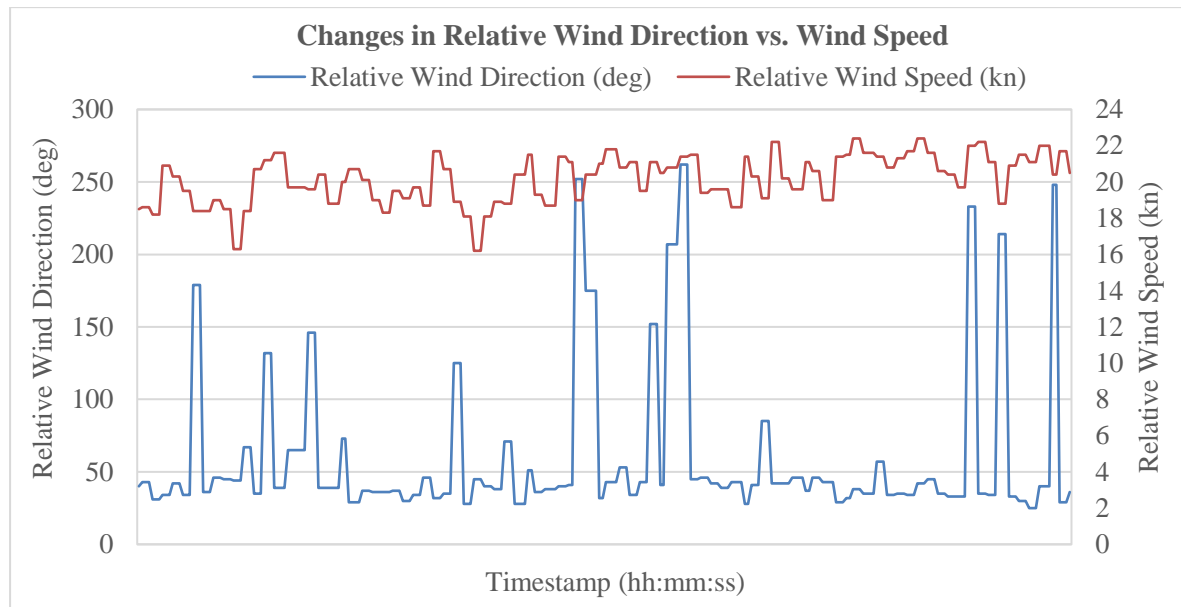


Fig.5: Wind Direction and Speed Fluctuation over time

These environmental changes play an important part as fluctuations in weather conditions very often introduce large data scatter in results. It is also worth pointing out that the effect of changes in wind speed and direction will vary across ship types as wind on a cruise ship will have a larger effect on the resistance impact than on a fully laden tanker/bulk carrier. C_{AA} for vessels with up to 5 decks can be in the region of 0.04 – 0.07, *Kristensen and Lützen (2013)*, whereas on cruise ships with 10-20 decks, the coefficient will be significantly larger. Additionally, height of the anemometer on cruise vessels are often located greater than 50m above the waterline thus introducing varied results. Hence, ISO19030 should be used as guidance and applied where applicable for type of ship being considered when filtering out for changes in weather and wind conditions.

4. Data Filtering & Analysis

Data quality also plays an instrumental part in determining performance of EETs as described above. Fig.6 shows unfiltered ON and OFF data collected onboard a cruise ship during 2 separate sea trials over a total trial period of 10 days. The large scatter in data can be attributed to changing parameters, environmental conditions as well as varying levels of accuracy in the data collected from several onboard instruments and sensors.

In accordance with the Silverstream's Performance Testing Procedure, data is analysed in 10-15 min blocks where each block is made up of 10 or 15 x 1 min average data points. Runs are then analysed and eliminated where there are any significant changes in rudder angle, shaft rpm, wind speed and wind direction between ON and OFF periods. The time interval is dependent mainly on the ship size/type as it is based on the time required for the ship to come to a new equilibrium condition following a change in operation which initiates an effect on the resistance forces acting on the hull whilst sailing in system ON vs. OFF conditions. Similar changes will also occur when variations in RPM and main engine power settings are made by the crew. The criteria for filtering runs between ON and OFF conditions in Table 1 has generally been used within which specific data points that comply with the criteria below are retained.

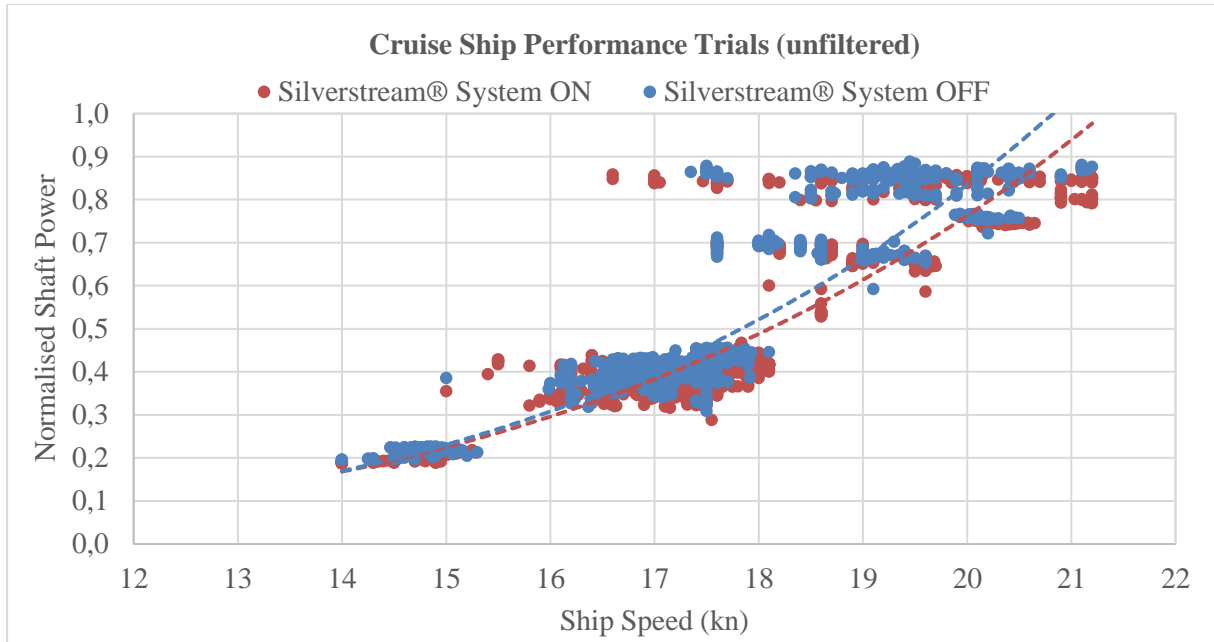


Fig.6: Cruise Ship Performance Trials (unfiltered data)

Table 1: Criteria for filtering data between ON/OFF periods

Rudder Angle (rate of change)	< 1°(in accordance with ISO 19030-2:2016 Annex I & J for outliers)
RPM	< 1 RPM
Wind Direction	< 30°
Wind Speed	< 10 kn
Water Depth	> 60 m
Max Wind Speed	All valid runs < BF 5 wind scale (change in conditions of ≤ 1 BF scale)

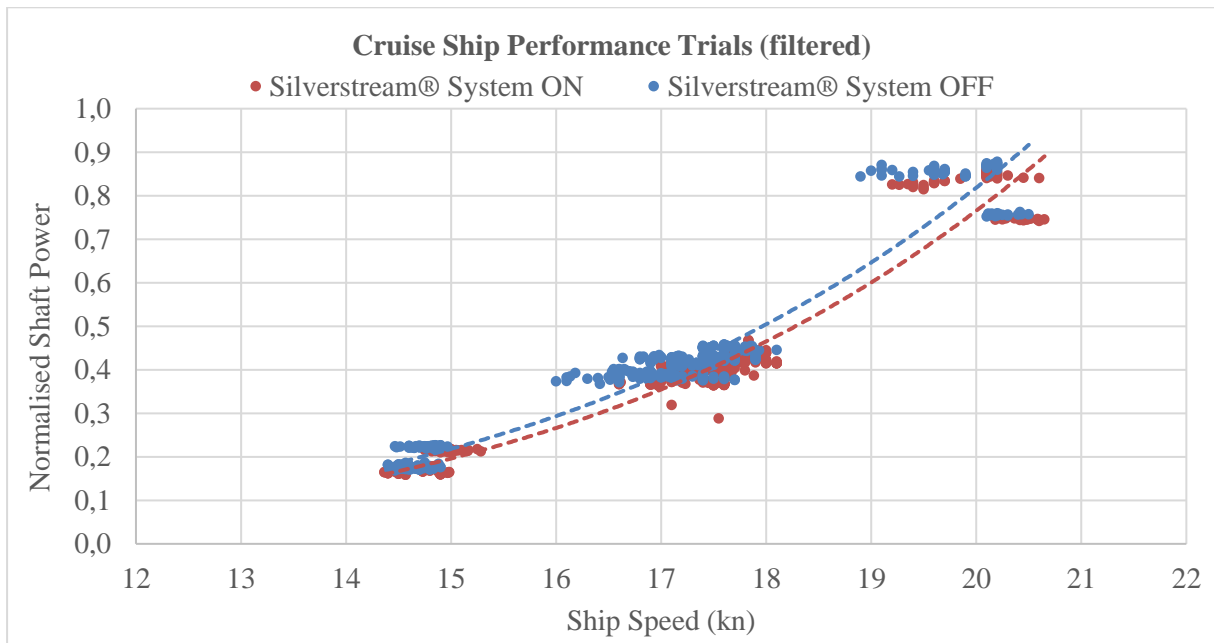


Fig.7: Cruise Ship Performance Trials (filtered data)

In addition to filtering using the above basic criteria, data points which showed inaccuracies due to errors from instruments (such as the speed log) were discarded to increase the confidence in perfor-

mance achieved from the system. In the below example, a total of 131 runs were conducted during commercial operations which resulted in 76% of the data points (100 runs) being discarded once filtering was applied. Performance of the system was then evaluated using 24% of the data points (31 runs) which were found to be valid as shown in Fig.7.

Although filtering was carried out to account for all known inaccuracies and changes in conditions, it is evident that there are still some unknowns in the data remaining which confirms the complexity of being able to accurately measure and evaluate performance savings for hydrodynamic based EETs even with the added ON/OFF functionality of the Silverstream® System.

Another factor which should be considered based on Fig.7 is the need for additional data points at higher speeds i.e. above 18 knots. This can have an effect on the speed/power curve as fitting of the curve can be influenced by the lower speeds due to the large quantity of data points in the range of 16-18 kn. Hence, to accurately determine performance impact of the technology at higher speeds, a separate speed/power curve should be fit to points at higher speeds if it is not possible to collect additional data.

5. Discussion

Although the Silverstream® System has the added benefit of switching ON and OFF, there are several other factors and non-linear environmental parameters which introduce a large scatter of data. These increase complexity in filtering, analysis and determining performance of the system.

One of the main areas that can introduce uncertainty is the quality of data being received onboard. Data is received from various instruments and then routed through several onboard systems before being received in the Silverstream Control and Monitoring System. This increases complexity significantly as it is often not clear how data is processed before being received. With the large quantity of instruments and sensors providing data and not being able to check the accuracy of each one, it is often difficult to determine the quality of data being received.

Data in 15 min blocks has been filtered out to remove inaccuracies and separated into the main categories as shown in Fig.8.

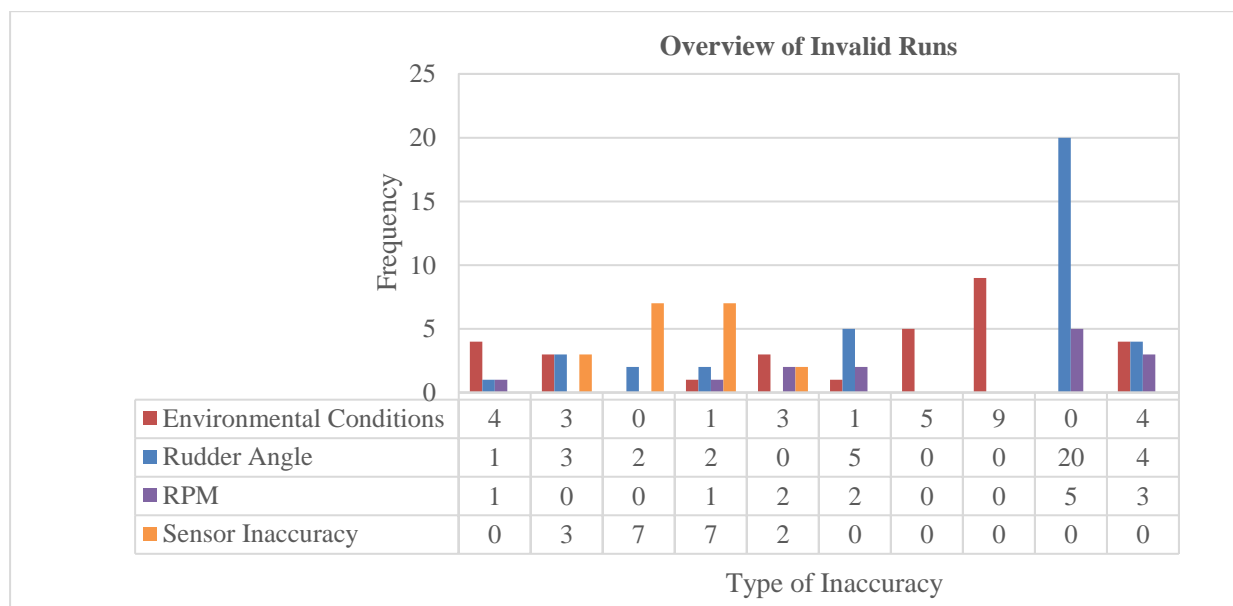


Fig.8: Cruise Ship Performance Trials (filtered data)

Most of the data scatter can be attributed to unavoidable environmental factors. However, another major contributor to data inaccuracy is the unreliability of data received from onboard instruments which is

often only identified after testing has been completed and data is interrogated during analysis. Despite the above, the Silverstream® System offers an advantage that can increase confidence in the accuracy attained as savings can also be verified by analysing runs in near ideal environmental conditions with stable parameters. Hence, any miscalibration or inconsistency of signals over time can be cancelled out by comparing consecutive ON and OFF performance within a specific time interval.

6. Recommendations

To improve the accuracy and confidence in savings attributed to EETs, it is recommended that the following steps are taken:

- Use of reliable and calibrated torque and thrust meters.
- Regular checks of all data feeds and measurement accuracy to be considered with focus on speed logs and shaft torque meters.
- Utilise signals directly from the sensors/instruments (if possible) thus avoiding any processing or rounding of values and loss of accuracy in transmission.
- Greater fidelity in data capture, quality of signals and data collection may demonstrate increased performance.
- Real time analysis of data collected during performance trails to check that data signals being received from onboard instruments are providing accurate readings in adequate frequency.
- Utilising hindcast metocean data to cross check measurements at ship where data permits.
- Long term analysis can serve to give further confidence in sea trials results, but care should be taken not to mix data from different conditions such as ballast/laden draughts and the issue of hull degradation over time should also be considered.

The above points would help to address some of the uncertainties encountered in performance trials with the hope of having greater confidence in performance results measured onboard.

7. Conclusions

Although the Silverstream® System has the distinct advantage over other hydrodynamic based EETs in that it can be switched OFF allowing a baseline to be established in a significantly more controlled manner, measuring and demonstrating performance can be extremely complex. This can be attributed to changes in ship parameters, environmental conditions and sensor/instrument inaccuracy because of:

- Variations in rudder angle, RPM, fin stabiliser positions due to ship operational schedule and navigating in shipping lanes.
- Inability to conduct dedicated trials outside of commercial operations in near ideal conditions
- Changing environmental conditions and inaccurate readings from ship's anemometer providing large scatter of results.
- Inaccurate measurement signals recorded from onboard ship instruments.
- Reduced data quality and clarity as data is processed, received from various instruments and then routed through many onboard systems.
- Increase in data scatter and uncertainty when different draughts are being considered.
- Lack of data points at certain speeds can introduce inaccurate curve fitting through these points.
- SOG measurements over the years have become extremely accurate while the STW technology available has remained relatively stationary and does not provide accuracy to the desired degree increasing the uncertainty in recording accurate STW.

Additionally, ISO 19030 can offer a sound base document for evaluating performance but there is the need to differentiate between reported results based on the sophistication introduced and going forward the following should also be considered:

- One should not underestimate the effort and quantity of data required to analyse/conduct trials and that a single trial with a couple of runs is unlikely to provide a true indication of an EET's performance.
- ISO 19030 and basis of data filtering is currently the only viable means of executing analysis performance of an EET.
- Time should be spent to check and verify that sensors are operable and reading accurately, a recommendation which is already encompassed within ISO 19030.
- Investing in technology to improve efficiency onboard requires robust sensors and systems which can be sufficiently integrated with EETs to provide a reliable route of measuring performance and advancing the EET to provide additional benefits to both the owner and the environment.

Considering the above factors and through our experience of performance testing, achieving high confidence levels requires large sets of high frequency data with minimal instrument/sensor inaccuracy which can be difficult to achieve on many occasions especially during ship trials in commercial operations.

References

GÓRSKI, W.; ABRAMOWICZ-GERIGK, T.; BURCIU, Z. (2013), *The influence of ship operational parameters on fuel consumption*, Maritime Univ. of Szczecin, Vols. ISSN 1733-8670, p. 6

ISO (2016), *ISO 19030: Ships and Marine Technology - Measurement of changes in hull and propeller performance*, Int. Organization for Standardization, Geneva

JOHANNESSON, J.; SILBERSCHMIDT, N.; CLAUSEN, J. (2015), *Air Lubrication System and Vessel Comprising such a System*, Int. Patent WO2015/133900a1

KRISTENSEN, H.O.; LÜTZEN, M. (2013), *Prediction of Resistance and Propulsion Power of Ships*, TU Denmark, Lyngby, p. 52

LIEM, H.C.; TODA, Y.; SANADA, Y. (2013), *Effect of Air Lubrication Method on Frictional Resistance of Ship*, ASEAN Eng. J. 4/A, p.9

MOLLAND, A.F.; TURNOCK, S.R.; HUDSON, D.A. (2017), *Ship Resistance and Propulsion*, Cambridge University Press

SILBERSCHMIDT, N.; TASKER, D.; PAPPAS, T.; JOHANNESSON, J. (2016), *Silverstream® System – Air Lubrication Performance Verification*, Low Carbon Shipping, p.12

STEVENS, R.L.; STEVENS, F.B. (1848), *Improvement in apparatus for the increase of the speed of vessels*, USA Patent US5644 A

Autolog Data Processing for Vessel Performance Application

Najmeh Montazeri, Vessel Performance Solutions, Lyngby/Denmark, nmo@vpsolutions.dk
Jakob Buus Petersen, Vessel Performance Solutions, Lyngby/Denmark, jbp@vpsolutions.dk
Søren Vinther Hansen, Vessel Performance Solutions, Lyngby/Denmark, svh@vpsolutions.dk

Abstract

This paper describes the procedure that has been developed to use autolog datasets in the analysis of hull and propeller performance for ships. The datasets have been received from the sensors onboard the ships and the data have been validated through different processes. The influence of this data processing on the scatter of added resistance is investigated and the results of performance trends are compared with manual (noon) data.

1. Introduction

During the last couple of years, VPS has developed an advanced Vessel Performance Decision Support system (VESPER) that provides information about fleet fuel efficiency using traditional noon reports. Noon reports will continue in the shipping industry to be the main source of data exchange between vessels and operators for quite some time. Therefore, we have to develop robust methods for performance analysis of noon reports. However, those manual data have the disadvantage, that they typically cover a period of 24 hours where, in many cases, the important parameters that influence the propulsion of the vessel are not stable. Moreover, the data are averaged and subject of human interpretation especially the evaluation of the waves, wind and currents over the noon reports. This, inherently, has the consequence that the determination of the vessels hull and propeller performance over time deals with some uncertainty and a relatively long evaluation time is required to determine the hull and propeller degradation slope over time.

Using autolog data for performance management has been thoroughly discussed in recent years and more ships are being equipped with sensors. The sensors measure operational data with a very high frequency. However, the use of autolog data does not necessarily solve the above-mentioned uncertainty, one issue is for example that the vessel is often experiencing periods of acceleration. Environmental forces are constantly fluctuating causing constant accelerations. Engine response is also not constant, most evident is variations in RPM when the engine is not running at optimum conditions (engine overload). Since most methods for analysis of performance data are based on the assumption of quasi-steady state forces, such accelerations may cause scatter in the results when analyzing over shorter periods of time. Moreover, faulty or drifting sensors can significantly mislead the performance evaluation. Therefore, sensor reliability becomes a major issue for the analysis.

Towards the industry prospects, VPS has started to investigate how the VPS performance management platform VESPER can be improved to reasonably support autolog data. In order to get a valuable and efficient assessment of the vessel performance based on autolog data, filtration, averaging and plausibility checks are important. The objective of this work (in the scope of iSea project funded by EU program, <https://www.era-learn.eu/network-information/networks/eurostars-2/eurostars-cut-off-5/isea-intelligent-telematics-and-safety-solution-for-sea-vessels>) is to develop the algorithm that determines stable periods without significant accelerations and faulty signals. If successful, we will be able to establish the performance of vessel faster and more reliable than using traditional noon reports or averaged-unfiltered autolog data sets. On the other hand, using noon data for performance management is still unavoidable. So, we will try to combine the results of noon and autolog data. The evaluated performance indicators of the vessel are expected to be less scattered and more reliable. Further, we expect to learn more about the influences of the environment acting on the ship itself and to learn more about the baseline ship model itself with more accurate stable periods from high frequency autolog data. Information that we can learn from and utilize in our daily analysis of the less precise noon data.

The method of stable period detection takes its origin in an approach for automatic fault diagnostics, *Lajic (2010)*.

2. Input parameters

Multiple measurements/signals are received from different sensors. Depending on the performance indicator that needs to be analysed, the different signals are optional to be used in the filtration procedure. In this paper, we focus on hull and propeller performance. Therefore, the following channels are used:

- Speed over ground
- Logged speed
- Ship heading
- Wind speed
- Wind direction
- Fuel consumption from fuel flow meter
- Shaft RPM
- Power from torsion meter

For many vessels, the draft data are not provided. So, in the analysis, the drafts are transmitted from the noon reports in the same periods. A good example of how noon data and autolog data can supplement each other. It should be noted that more channels can be used, for instance, water temperature, turbocharger RPM, rudder angle, etc, if they are available.

A table of parameters is predefined for each vessel as filtration criteria. The parameters that are used to define the stable periods depend on the available sensors and the ship characteristics. Therefore, the parameters set needs to be defined for each vessel type and/or vessel segment individually. The optimization of the parameters is not automated yet. Therefore, verification based on visual observations of samples of stable periods that come out of the algorithm is required for each dataset.

The signals are filtered preliminarily based on physical range checks. In addition to filtration of non-physical outliers, the algorithm looks for spikes. A spike is recognised as a single point, the deviations of which from the previous and the next points are higher than $X\%$ of the predefined $[\max - \min]$ value for that sensor. X is considered as a parameter.

The following parameters are used as criteria for individual time series:

1. Minimum mean (min mean)
2. Maximum mean (max mean)
3. Maximum standard deviation (max std)
4. Mean deviation threshold
5. Standard deviation threshold

Each parameter corresponds to a check that is applied on the time series. Every check can be included/excluded through a flag for individual signals.

3. Filtration algorithm

The first step is to go through the data, point by point. The window size (the period that is considered at each step) is defined as another parameter. The mean value and the standard deviation of the first window is calculated. Then the mean value is checked to be between the “min mean” and “max mean” (parameters 1 and 2 respectively). The standard deviation value is checked to be less than “max std” (parameter 3). If any of the checks fail, the next window is looked at. The first window the statistical parameters of which, passes the above criteria is considered as the reference window.

Then the next window is considered, and the mean and standard deviation are calculated. We wish to find periods when the ship responses are stable according to our predefined criteria. In order for time series to be stationary, the mean value and standard deviation have to remain the same as the reference window over time. Therefore, the theory of probability of detection of a change in the mean and standard deviation is utilized, *Lajic (2010)*. In this step, mean deviation threshold and standard deviation threshold (parameters 4 and 5) are used to compare the statistical parameters of the current window with the reference window.

An output matrix is defined with an equal size to the number of data points in time series. If any of the stability criteria checks fails, the elements in the output matrix become “red”. In this case, the algorithm resets the reference statistical parameters in the next step. In other words, the 3 former checks will apply on the next windows until a new valid reference window is found. If the measurement point passes through all checks, all points in the specific window become “green” in the output, meaning that the window is a stationary period.

Since the outliers are removed from the time series, the time gap between every two consecutive time stamps are checked. If this time gap is longer than 20% of the window size, the output becomes “red”.

The above procedure applies on every signal from section 2.

4. Averaging

When stationary periods are detected for all measurements, we focus on the “mutual stable periods”, which we define as a period when all the time series are simultaneously stationary. In those periods, the average of individual time series is calculated over those periods. If the mutual period is longer than the output sampling rate (set as a parameter), the average is calculated over that specific period. For instance, if the output sampling rate is 60 min and the mutual stationary period is 130 min, the average value is calculated every 60 min and therefore, 3 average points will be calculated for each sensor. Correspondingly, the report durations for the new points will be 60, 60 and 10 minutes.

The averaged values and the corresponding report durations are stored in the database. Another parameter used as a constraint is the “minimum mutual period”. If the report duration is less than this value, the average points are removed from the data.

Beside the detection of stable periods, there is an algorithm to calculate the average of every sensor measurement every Y hours without doing any filtration. Y is another arbitrary parameter defined by the user. This averaging of autolog data is, today, a common method in the industry. The 24-hours averages are used in section 8.

5. Case study

The case study in this paper is a tanker, Table 1.

Table 1: Vessel properties

Property	Value
L _{OA}	244.60 m
L _{PP}	233.00 m
Beam	42.00 m
Design Draft	12.00 m
Design Deadweight	107640 t
MCR	15260 kW

The sampling frequency of the input data is 2 minutes.

6. Stable period results

Fig.1 shows an example of stable time series detection. The blue lines show the input data. The green points indicate the detected stationary time series for individual signals. The black points appear when a change is detected in the mean or standard deviations of the stationary time series. The red points are the average points over the period of mutual stable time series. In this example, 5 different signals have been considered for the analysis.

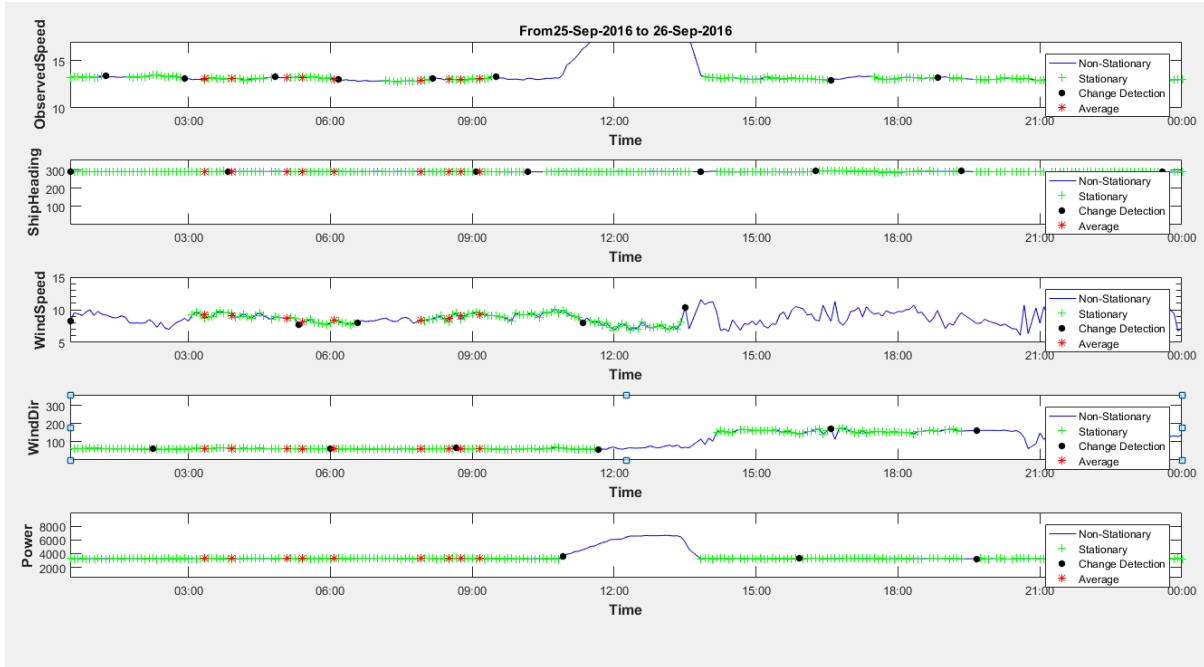


Fig.1: Stable period detection and average evaluation

The average values of stable periods are stored in VESPER for analysis and calculation of performance trends. The following sections show some of the findings.

7. Validation analysis

In order to assess if the dataset is valid and worthy for performance analysis, we need a validation process from a physical point of view. The parameters relative to each other are checked based on physical boundaries or a range perspective. The ship model (baseline) determines what is possible and what to expect for the boundaries of the parameters.

Fig.2 compares the SFOC values with the shop test results. It can be observed that autolog data and noon data are quite conforming and the values and the scatter are reasonable. There are other technical validation procedures that can be carried out manually regarding the engine related data, but they are out of the scope of this paper.

The data also get through the validation engine that is designed in VESPER. There are many rules that can be set by the user to check the validity of data depending on the point of interest. For the considered autolog dataset in this paper, rules for missing fields and range checks of the sensor measurements are set up. The output of the validation engine will help to detect and diagnose problems in the received data, i.e. sensor reliability.

In Fig.3, the data quality is assessed through the VESPER validation engine. Red output shows the amount of failed data point through a specific rule. Yellow output shows the number of warnings coming out of a specific rule. The bars on the left show the total percentages of errors and warnings

among all rules for the specific vessel. The bars on the right show the results per rule. It can be concluded that the data quality is very promising in this case. The draft rule has triggered 100% because the drafts are missing in the autolog data and they are enriched with noon data in the analysis, as mentioned before.

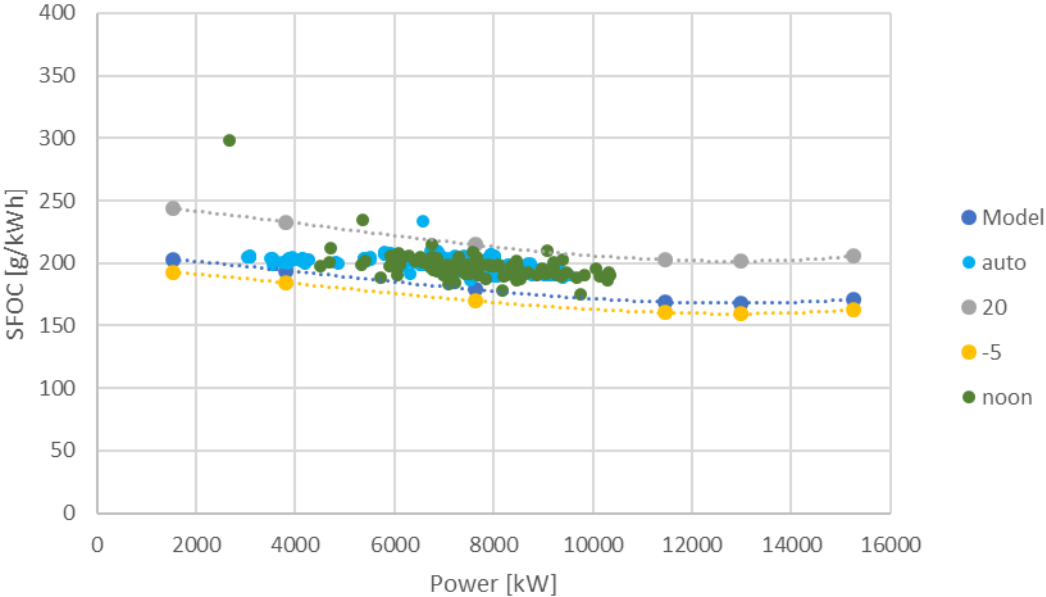


Fig.2: SFOC values vs the model



Fig.3: Validation output for autolog data set

Through this validation check, the users can find out whether or not the autolog data are worthy for analysis and if not, they can recognize the problems and investigate the reasons and possibly resolve them. It is noteworthy that during our studies, we have found a couple of vessels for which, the autolog data included invalid values from sensors. In that case, the results of performance evaluation have to rely on noon results only.

8. Performance trends- Comparison with noon reports

In this section, the performance trend results are shown. In the previous section, it is shown that the data set has very good quality and delivers sensor values within acceptable ranges. For comparison purpose, beside the stable periods, we also make the analysis based on the unfiltered autolog data which are averaged every 24 hours and compared with the conventional noon data. In this section, we use three different input data for deriving the added resistance:

1. Autolog results using stable periods
2. Autolog results (unfiltered) using 24 hours averages
3. Noon reports

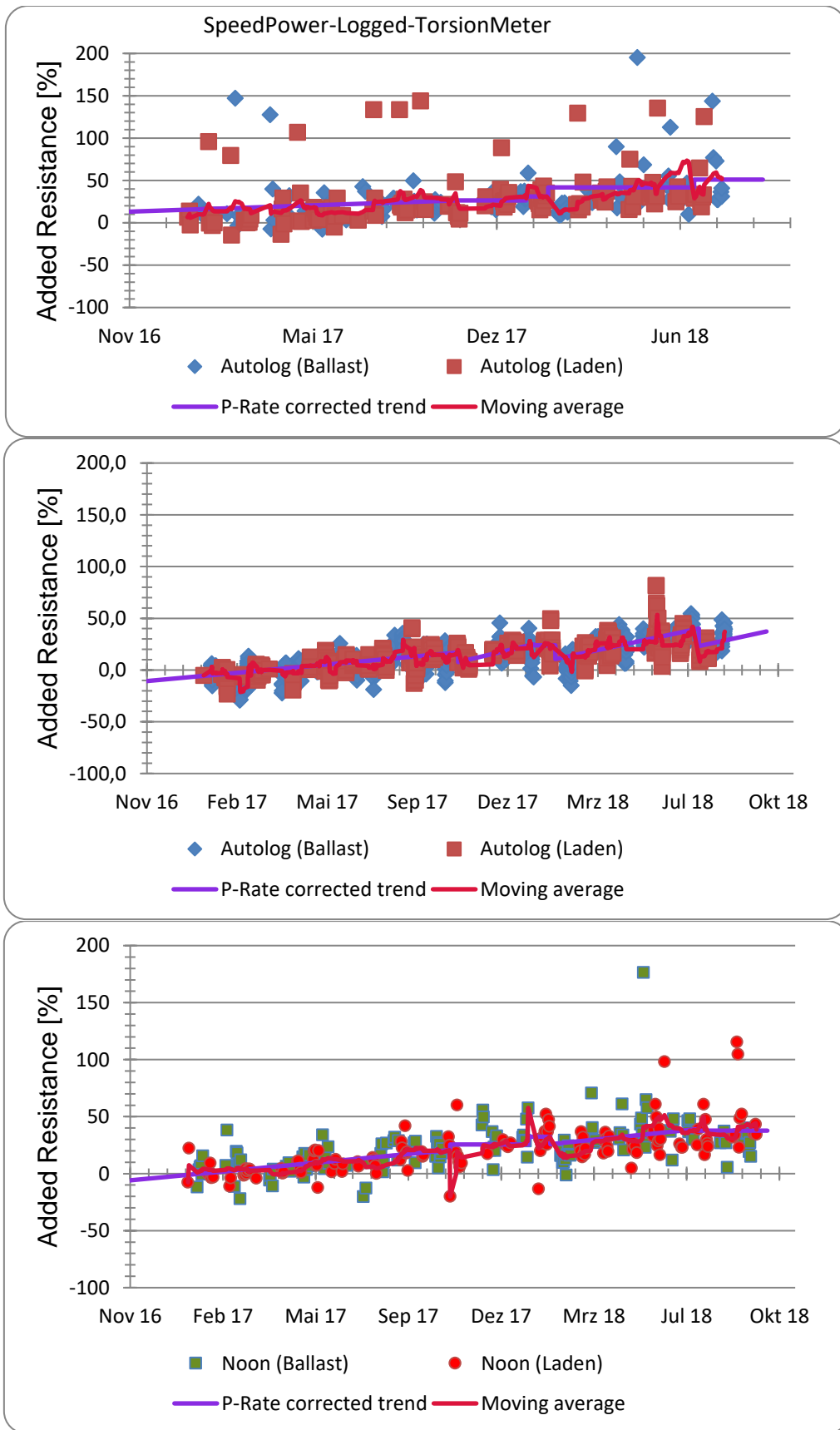


Fig.4: Comparison of added resistance (Logged speed-TorsionMeter) between unfiltered autolog (top), stable autolog (middle) and noon (bottom) data

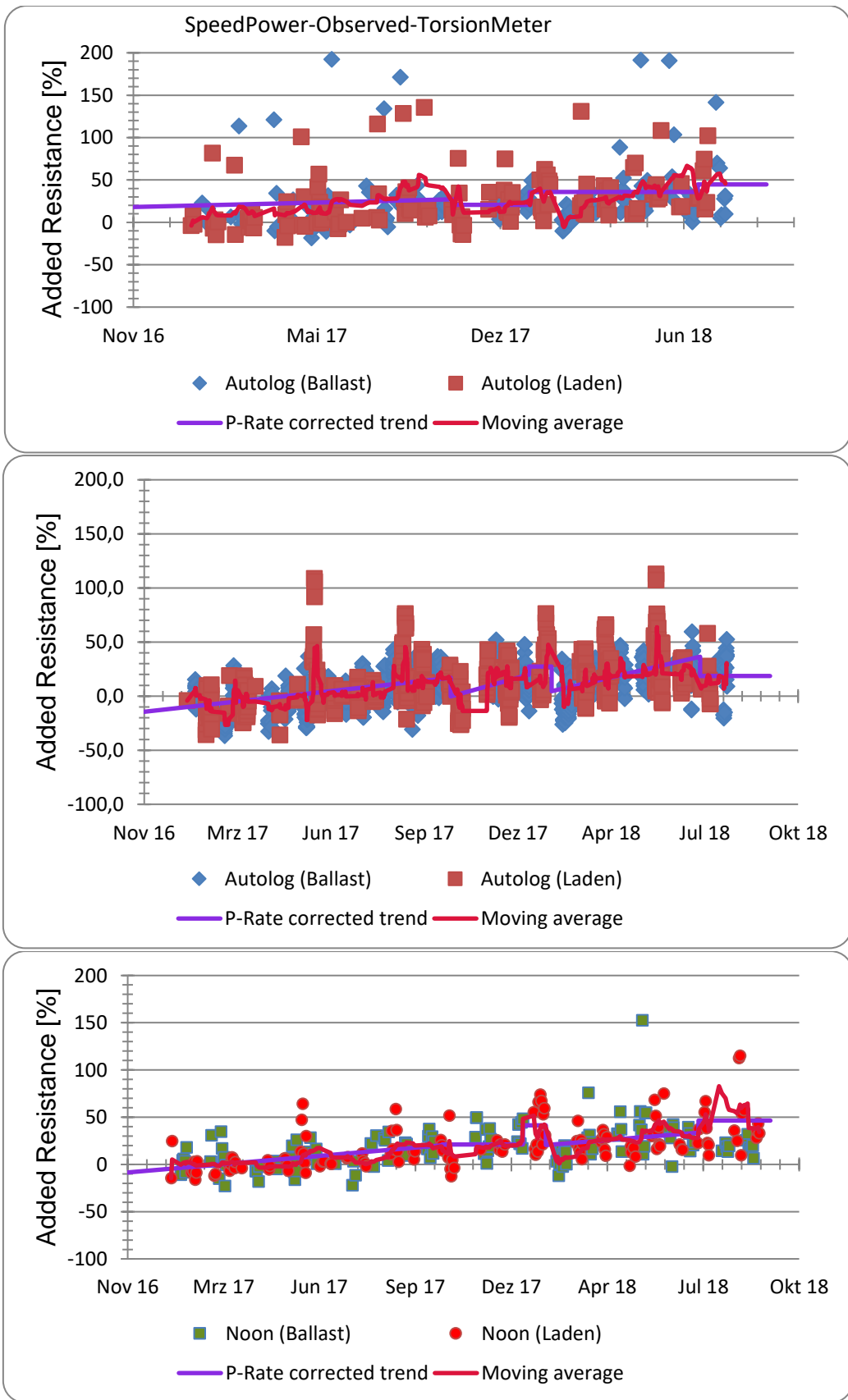


Fig.1: Comparison of added resistance (Observed speed-TorsionMeter) between unfiltered averaged autolog (top), stable autolog (middle) and noon (bottom) data

Added resistance is a major performance indicator in VESPER. This value represents the relative discrepancy between the actual and the expected resistance. The expected resistance is calculated based on the propulsion model for the specific vessel plus the calculated resistance due to the environmental conditions/weather. The actual resistance is calculated based on the measured fuel/power. The added resistance trend indicates the level of fouling/damage on the hull and propeller over time since the last event on the vessel. The trend evaluation is started over, once an event/treatment is registered.

VESPER can calculate the added resistance trend based on different methods. Here, we show only the best results which are based on power from torsion meter and the vessel speed (both observed speed and logged speed). The added resistance based on logged speed and torsion meter was found to have the lowest scatter and the results are very close to noon data. Fig.4 and 5 show the trends of added resistance using torsion meter-logged speed and torsion meter-observed speed, respectively. The trends are calculated based on the P-Rate method which is a modified linear trend depending on the prediction reliability. As mentioned before, for the same vessel within the same period, we extracted also noon reports to calculate added resistance. The results are shown in these figures for comparison. As mentioned above, the unfiltered data are averaged every 24 hours. The filtered (stationary) data are averaged every 1 hour.

Tables 2 and 3 show the resulting added resistances from Figs.4 and 5. Two trends are considered before and after the propeller polish on 14/7/2018. “AR” stands for added resistance. The prediction reliability function is a VESPER internal function which depends on both the number of valid reports within the trend period and the scatter (STD) around the least squared fitted trend line. The more data points and the less scatter in added resistance, the higher prediction reliability would be obtained. In both tables, by using the logged speed, the magnitudes of added resistance, which is the performance of vessel at the evaluation date, for filtered autolog data are very close to noon data Table 1. The scatter (STD) is significantly decreased by use of filtered autolog data, approximately half the standard deviation of the noon reports and significantly more data points. The prediction reliability is 20-30% higher than noon as the number of points are higher and the scatter is lower.

Table 1: Comparison between results of autolog data and noon reports- Added resistance based on torsion meter- Trend before propeller polish on 14/7/2018

Method	Source	Valid reports	Prediction Reliability	Prediction reliability Score	P-Rate corrected trend AR%	STD of AR%
Logged speed – torsion meter	Autolog (avg. 24 h)	76	25	Low	42	39
	Autolog (Stable periods)	449	80	High	40.2	9.3
	Noon	74	53	Medium	39.2	22
Observed speed-torsion meter	Autolog (avg. 24 h)	76	25	Low	35.7	40
	Autolog (Stable periods)	449	77	High	36.4	17
	Noon	74	55	Medium	33.5	22

Table 2: Comparison between results of autolog data and noon reports- Added resistance based on torsion meter- Trend after propeller polish on 14/7/2018

Method	Source	Valid reports	Prediction Reliability	Prediction reliability Score	P-Rate corrected trend AR%	STD of AR%
Logged speed – torsion meter	Autolog (avg. 24 h)	16	5	Low	51	36
	Autolog (Stable periods)	41	43	Medium	37.2	6.5
	Noon	30	23	Low	37.8	22
Observed speed-torsion meter	Autolog (avg. 24 h)	16	1	Low	44.7	36
	Autolog (Stable periods)	41	20	Low	18.6	19
	Noon	31	0.4	Low	46.4	71

By using the observed speed, the added resistance value just before the propeller polish is very close between stable autolog and noon reports. But at the end of the next period (after the propeller polish), the added resistance is much lower for the stable period's autolog data than for the noon data. However, reliability of the noon data is skeptical here which can be seen by very low prediction reliability (0.4) and the very high scatter around the trend line (71) in the added resistance. The scatter from observed speed and torsion meter is twice compared to the results from logged speed and torsion meter which could be due to the ocean currents and, for once, a well-functioning speed log.

Using stable periods based on logged speed seems in this case to be significantly superior to both 24 hour average autolog data and noon reports with respect to standard deviation and prediction reliability. The performance evaluation seems to be consistent between the three methods in the first period, whereas the three methods are less consistent in the second period. VPS will further investigate the reasons for this in the future. Reduction of scatter is important, but we must not forget the main objective, which is to determine the performance of the vessel.

9. Summary and Conclusion

VPS has developed a tool for analyzing ship-based autolog data to be integrated into the VESPER performance application. The target is to investigate how the sensors that are already invested in and installed onboard vessels all around the world can be utilized for performance management. Human errors in the manual data can somehow be compensated by combining the noon data with reliable autolog data.

The parameters set for stable period detection should be vessel specific and still needs to be fine-tuned manually. The stable periods will be identified based on the theory of probability of detection of a change in the mean and standard deviation, *Lajic (2010)*. The average signals are stored to be transferred to the analysis platform. The program is also capable of calculating the average measurements over the requested period without any filtration. This gives the user the ability to compare the results of filtered and unfiltered data.

Validation engine in VESPER needs to be run to check the data quality. If the data are not in the expected physical ranges, the sensors need to be inspected or calibrated. The data from the tanker that is used in this paper show, relatively, a very good data quality.

Hull and propeller performance is analyzed based on the filtered and unfiltered autolog data. The method of stable periods is superior to noon data and unfiltered 24 hours-averaged autolog data. However, the results of performance evaluation are not necessarily the same as noon data, which indicates that more thorough investigation is required. In general, the logged speed has been found to give more consistent performance compared to noon results for this vessel.

In the "ShippingLab" project, <http://shippinglab.dk/en/front-page/>, VPS will continue the work for further investigation of autolog-based performance analysis and also improvements of modelling in VESPER.

References

LAJIC, Z. (2010), *Fault-tolerant onboard monitoring and decision support systems*, PhD thesis, TU Denmark, Lyngby, pp.50

When ISO19030 Fails: Utilizing Basic Machine Learning/Data Fitting Methods for Performance Analysis without Reference Data

Ditte Gundermann, Hempel, Copenhagen/Denmark, DIGU@hempel.com
Danny McLaughlin, Hempel, Copenhagen/Denmark, DaMcL@hempel.com

Abstract

ISO 19030 compares in-service data with reference data such as sea trials and model tests. Non-conclusive results are common when there is not enough reference data to match the in-service data or when the filters have removed a large part of the in-service data. An alternative analysis method based on a multiple linear regression model is tested for different ship and data types. The linear model is fitted to in-service data only and requires no reference data. The predicted speed power curves are evaluated against available reference curves, and the predicted performance trend in time is compared to the performance trend found by the ISO 19030 method. Despite some limitation and uncertainty, the model is found to give good prediction of the power at different loading conditions and at different points in time. Some suggestions for improving the uncertainty are given.

1. Introduction

The ISO 19030 standard on performance monitoring describes how to evaluate the hull and propeller performance of a ship by comparing data measured on board the ship (in service data) with reference data such as sea trials or model tests. In the common case that the reference data cannot be related to most operational conditions of the vessel, the ISO19030 method gives no or inconclusive results. Also, even with adequate reference data, there are other aspects of the ISO 19030 standard analysis that can give rise to misleading results. One of these aspects is the well-known speed (and draft) dependence of the performance values, *Bertram (2017)*, which can be quite significant and give false impressions of performance variations, *Schmode et al. (2018)*. Using a mathematical model of the ship at reference condition can help solve these problems by expanding the reference data significantly and by normalizing the performance values to a single condition (draft/trim/speed), but such models often require the same information in terms of reference data as the ISO standard, and are thus not always a possibility. Another limitation of the results of the ISO19030 method is that they describe relative performance changes over long periods, rather than actual performance at a specific time. Further, it does not specify how to get actual consumption/power curves for different drafts or at a given point in time.

The increase in the availability of high frequency data has provided new possibilities for utilizing mathematical algorithms for analyzing ship performance based on in-service data alone. Many different methods and algorithms exist and are used also by some performance monitoring service providers who specialize in these methods, but ready-made tools are available in many open source and commercial software packages making it increasingly possible for a wider range of users to utilize machine learning for data analysis.

Apart from not needing reference data, an advantage of such methods is the prediction of the performance and consumption/power requirement at any time, speed, draft and weather condition. A disadvantage compared to the ISO 19030 method is obviously the lack of transparency and the risk of receiving misleading results due to lack of understanding of interdependencies in the data.

With the aim of determining the hull and propeller performance of a vessel using only in-service data, we examine the feasibility of using a multiple linear regression model for the dependency of power on different input variables. Although linear models may be considered less accurate than other machine learning methods for vessel performance analysis, *Pedersen (2014)*, the advantage of linear models are that they are simple, give a continuous output and make it possible to interpolate and extrapolate outside of the measured data ranges.

The linear model has been tested on data of different frequency ranging from noon reports to high frequency auto-logged data from 6 ships of different types. The vessels' type and data frequency are shown in Table 1.

Table 1: list of vessels and data used in this study

<i>Vessel</i>	<i>Data Frequency</i>
LNG Tanker	1/15 sec autologged
VLCC	1/5 min autologged
Passenger Carrier	1/5 min autologged
Crude Oil Tanker	1/24 hour manual
Container A	1/24 hour manual
Container B	1/24 hour manual

2. Method

The linear model can be described by the following general expression:

$$f = C_0 + C_x x + C_y y + C_z z + \dots$$

Where x, y, z, \dots are different input variables that affect the output f , and $C_0, C_x, C_y, C_z, \dots$ are constants. The number of input variables depend on the given case (type of vessel, data availability and data frequency). Most significant variables are usually speed, draft, weather and time. Other inputs could be waves, trim and sea water temperature. In order to fit the model to the data, the data has to be linearized. In the case of using speed (v), draft (d), weather (w) and time (t) as input the equation becomes:

$$\log\left(\frac{p}{p_0}\right) = C_0 + C_v \log\left(\frac{v}{v_0}\right) + C_d \log\left(\frac{d}{d_0}\right) + C_w \left(\frac{w}{w_0}\right).$$

where $p_0, v_0, d_0,$ and w_0 are normalization factors.

The model is applied to in-service data of different frequencies, ranging from noon data to high frequency auto-logged data. In the case of high frequency data some filtering has to be done on the raw signals in order to remove non-steady state data points. This is done to minimize autocorrelation effects. Fig. 1 shows an example of the filtering.

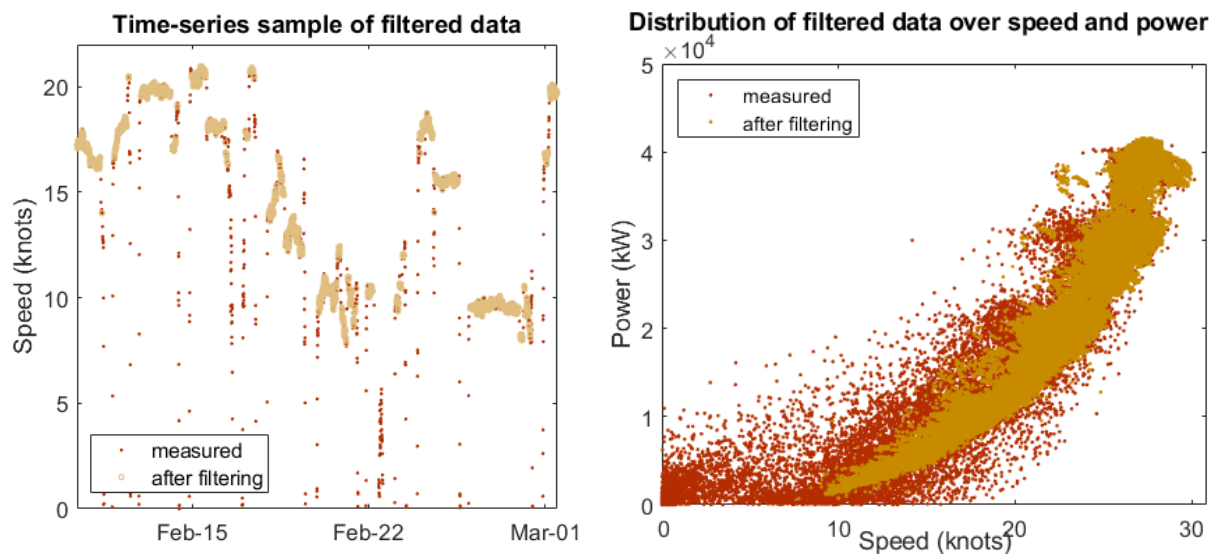


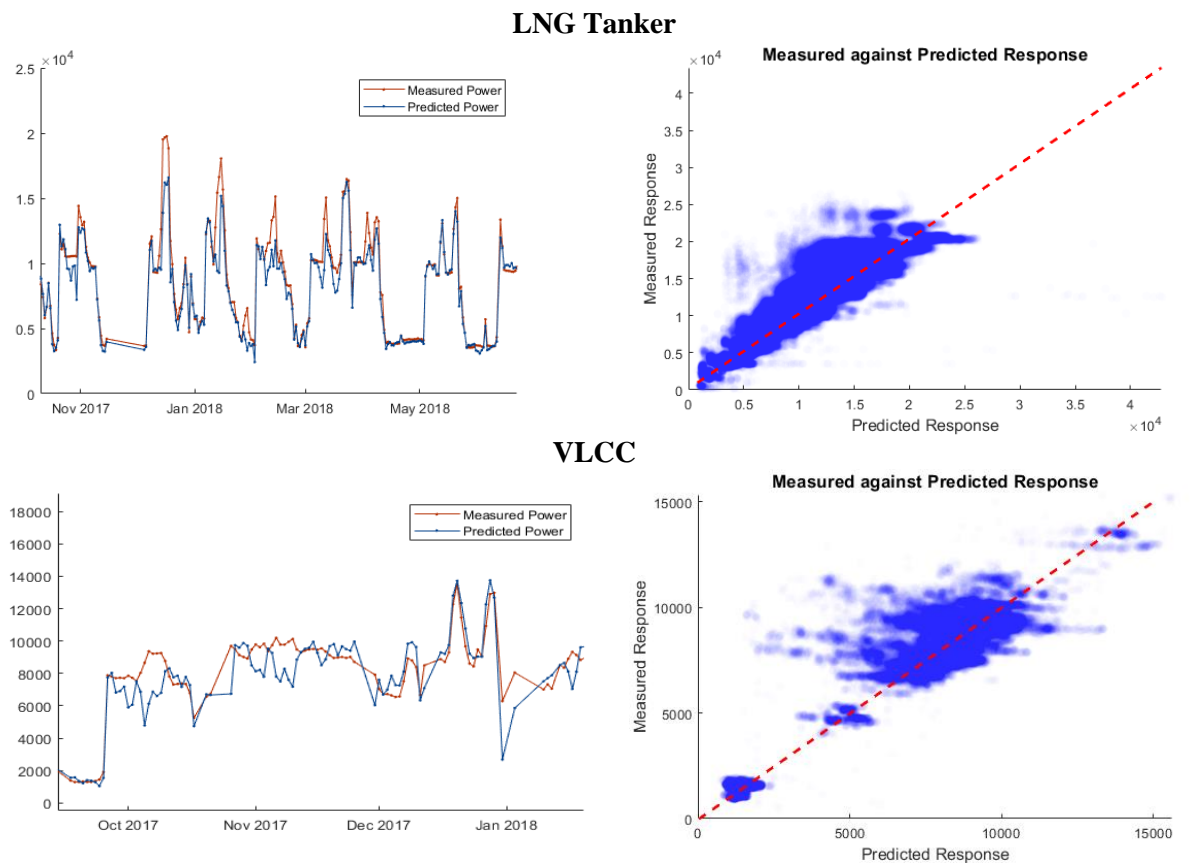
Fig. 1: Raw (red) and post-filtering (orange) speed data. Left: selection of time series data. Data measured while the ship is accelerating is not used for modelling. Right: speed power plot of entire raw and filtered data sets. Times when the vessel was accelerating are seen in the low speed/power range, where the scatter is much higher than at higher speed/power values.

The linear expression is then fitted to the data to find the coefficients C_θ , C_v , C_d , and C_w . Once the coefficients are found, the predicted power for any input variable combination can be found. This means that we can for instance plot the time development of power for a certain speed and draft in no wind, or we can find speed power curves for any draft at any time and for any weather (wind speed and direction) condition.

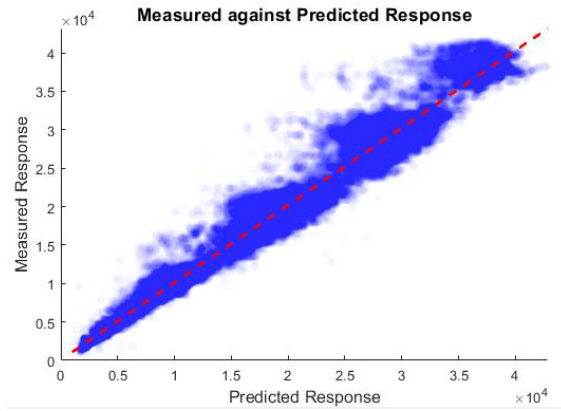
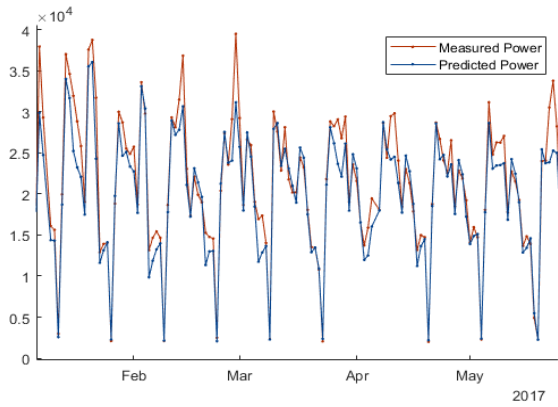
3. Results

3.1. Model prediction vs measured

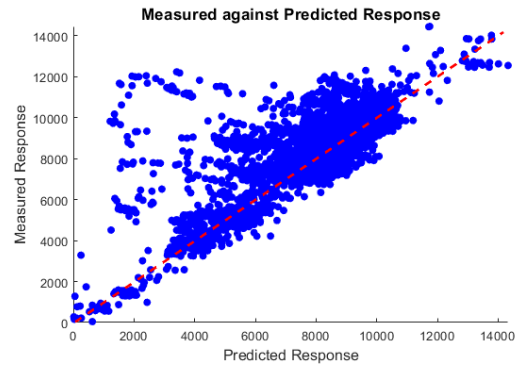
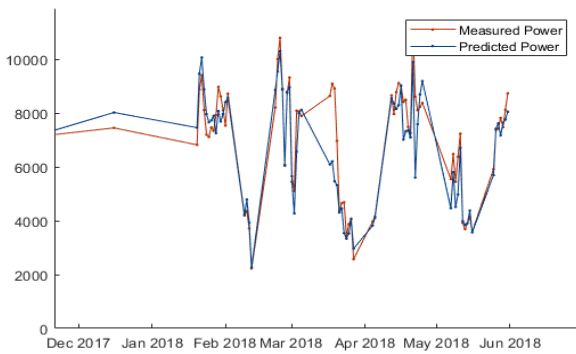
Fig. 2 left shows a time series plot of measured and predicted power for the entire available time period for all the vessels (after filtering described in section 0). Fig. 2 right shows the same data in a scatter (correlation) plot. The closer the points are to the red line, the better match between predicted and measured power. The values are for most data sets evenly distributed around the red line, showing that the model on average predicts the power well and that the use of a linear relationship between input variables and the dependent variable power is acceptable. There is some scatter in the measured power that is not captured by the model. This is also seen in the time series plots, where some measured values are not well reproduced by the model. This probably reflects the fact that not all relevant input variables are included in the model. Perhaps the most significant effect not captured by this model is that of waves. Table 2 shows the coefficients of determination (R^2) and the root mean squared error (RMSE). The R^2 values for the noon data-based models are generally lower than the values for the auto-logged data based models. Similarly, the RMSE values are generally higher for noon data than for auto-logged. This shows - not surprisingly - that the model performance is better for high frequency auto-logged data.



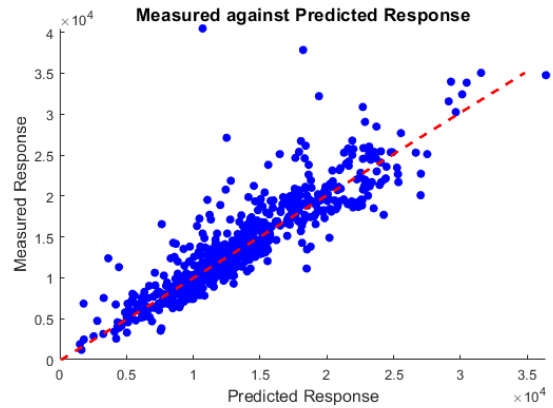
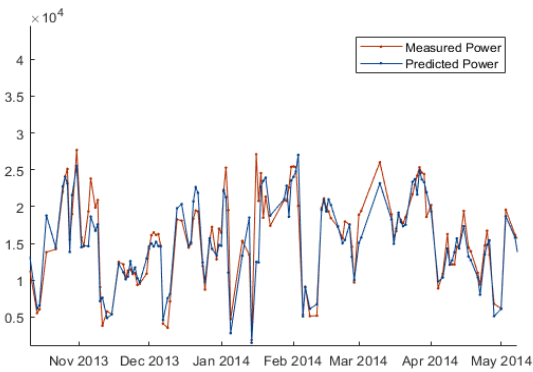
Passenger Carrier



Crude Oil Tanker



Container A



Container B

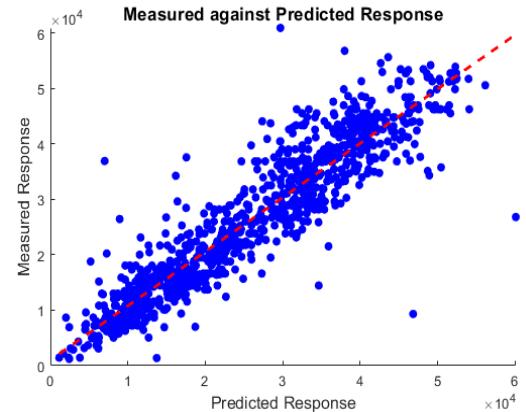
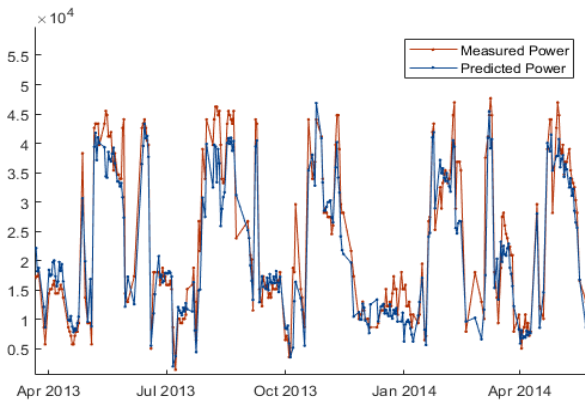


Fig. 2: Measured and predicted power for all vessels. Left: time series plot, right: correlation scatter plot. Transparent dots are used for high frequency data, while solid dots are used for noon data in the correlation scatter plot.

Table 2: Model performance measures for all ships

<i>Vessel</i>	<i>Dry Docking Interval</i>	<i>Measure</i>	
		<i>R²</i>	<i>RMSE</i>
LNG Tanker	1	0.9598	0.1036
VLCC	1	0.9598	0.1505
Passenger Carrier	1	0.9778	0.0878
Passenger Carrier	2	0.9772	0.0857
Crude Oil Tanker	1	0.9415	0.1853
Container A	1	0.9588	0.1353
Container A	2	0.8902	0.1586
Container A	3	0.8703	0.1659
Container B	1	0.9160	0.1901
Container B	2	0.9338	0.2426

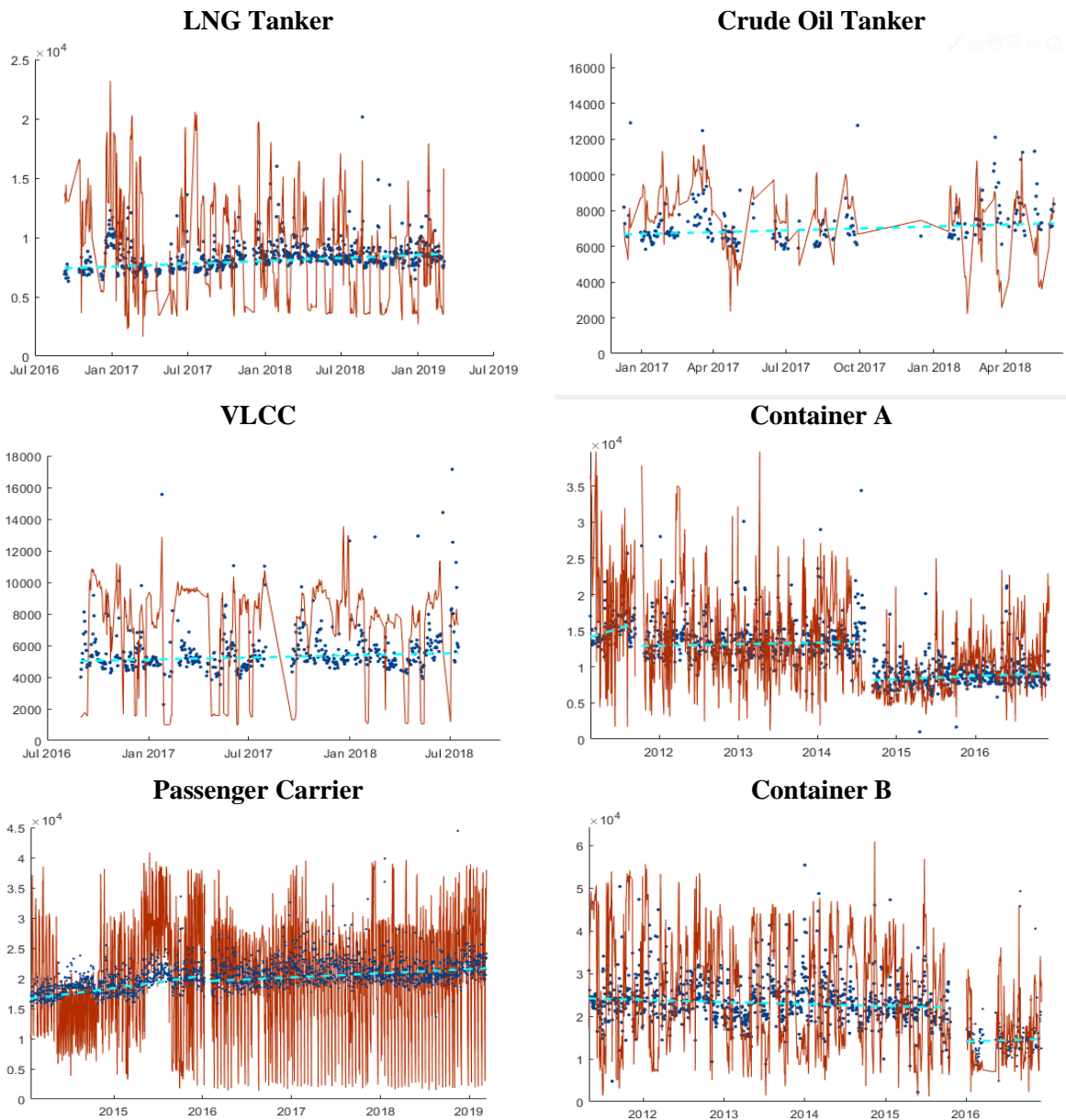


Fig. 3: Measured (red) and corrected power (blue) for most common draft and speed, calm weather. Predicted trendline in turquoise). The auto-logged data on the left-hand side has been averaged to 24 hours, while the noon data on the right are untreated.

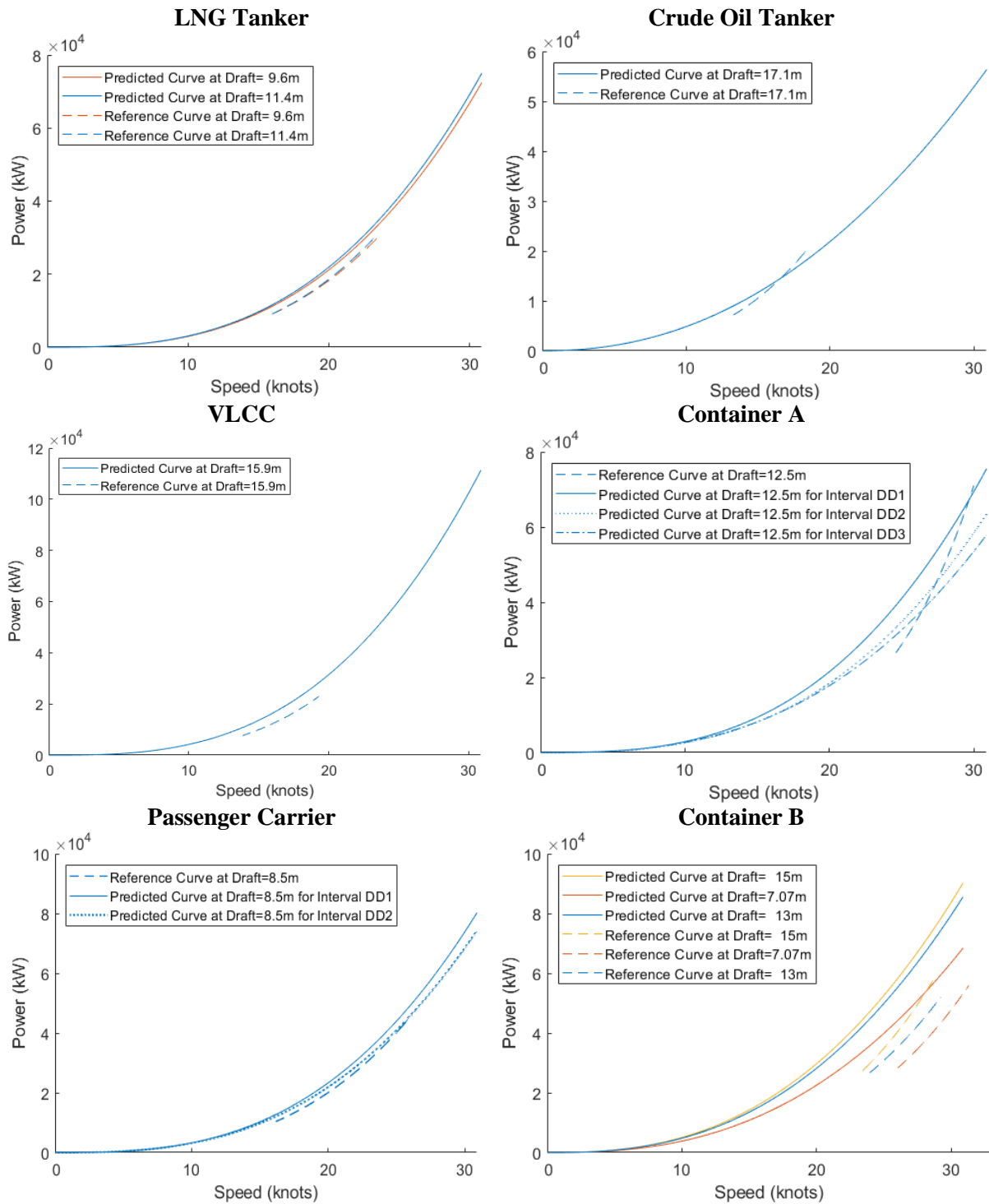


Fig. 4: Predicted speed power curves for different loading conditions and times in calm wind conditions. Reference curves are shown for comparison (dashed curves). Different colors refer to different loading conditions while different line styles in same color refer to different dry docking intervals.

3.2. Time series plots

After the dependencies (coefficients) of power on the input variables have been found, it is possible to determine the theoretical predicted power at any time, draft, speed and wind condition. Fig. 3 shows time series plots of all the measured power values and the predicted trendline for the most common draft and speed, at calm wind conditions. The predicted trendlines shows a realistic trend of slowly

increasing power over time, reflecting hull and propeller performance deterioration over time. The effects of dry dockings are also seen as a discontinuous shift in the trendlines. One data set (bottom right) shows a declining power (indicating increasing performance) over time, which could reflect that events such as hull cleaning and propeller polishing activities which are not taken into account. The plots also show the measured power values after correcting for the variation in draft, speed and wind. The measured power has been corrected to the same draft, speed and wind condition as the predicted line, and agrees well with the trendline (as it should).

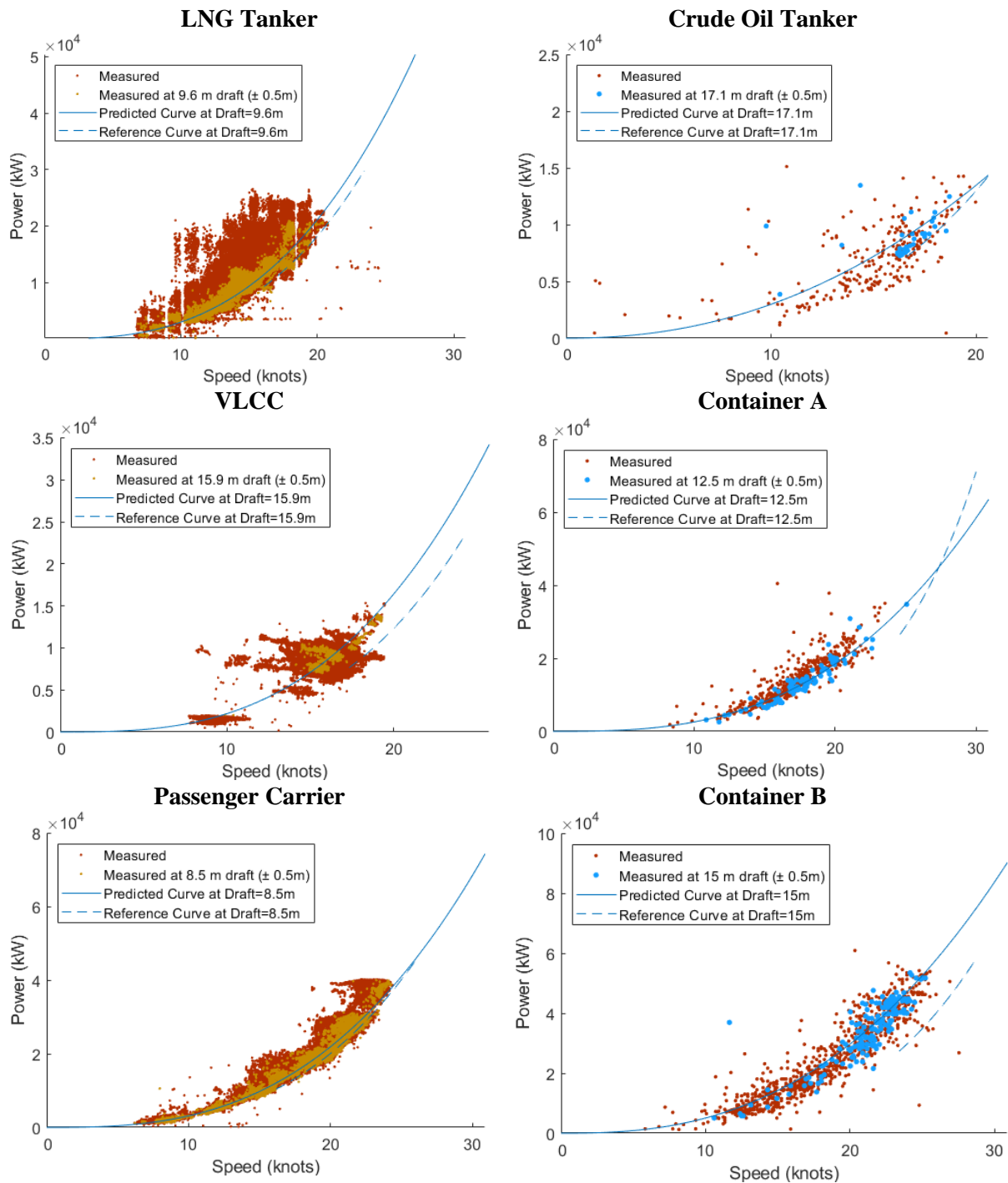


Fig. 5: Predicted speed power curves for one loading condition (blue lines) at time 0 compared to measured data points at the same loading condition (orange or light blue dots). Reference curves for the same loading condition are also shown for comparison.

The correction reduces the variation in the power significantly for most data points, but there are some outliers among the corrected values showing higher values than the measured. Again, the scatter is likely due to the power-dependent physical phenomena not taken into account in the model, such as the effect of waves.

3.3. Speed-power plots

One purpose of using the linear model was to produce speed power curves for any condition and at any point in time. Fig. 4 shows the predicted curves for each ship for one to three loading conditions at the beginning of the dry docking or data period.

In order to evaluate how realistic these predictions are they are compared with the available reference curves (sea trial or model test) for the same loading conditions. The predicted curves are similar in shape to the reference curves for most ships, but are shifted up reflecting a higher power consumption compared to the new build ship. This agrees with well with expectations.

A few of the predicted curves in have a different speed power relationship (shape of the curve) than the reference curves at high speeds. When considering the speed range of the measured data in Fig. 5, this difference in shape probably arises from lack of data in the high-speed range.

In Fig. 5 the predicted curves are shown together with measured raw data points at the same loading condition ($\pm 0.5\text{m}$ of draft). The predicted curves appear to represent the data points quite well in the measured speed range.

3.4. Comparison of results with ISO 19030

A final comparison is done to an ISO 19030 standard analysis for the single ship where the ship is actually trading inside the reference speed and draft range. Fig. 6 shows ISO 19030 defined Power Performance Values for the passenger carrier together with linear regression lines through those points. The trendlines from the linear model shown in purple are very similar to the regression lines through the ISO 19030 Power performance values.

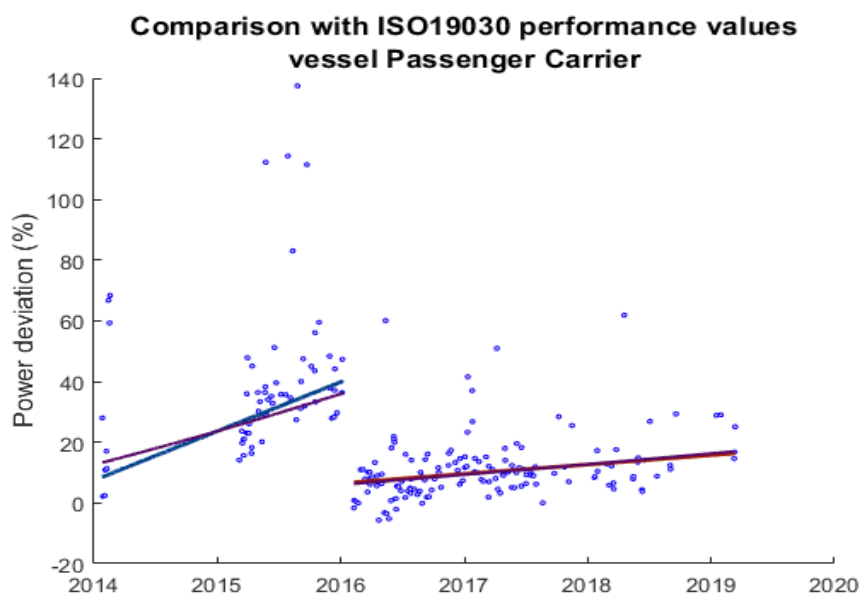


Fig. 6: ISO 19030 Power Performance Values (dark blue dots) and linear regression trendlines through the points (blue and red). The purple lines are predicted time development of Power Performance from the linear model.

4. Conclusion

A linear model was tested on in-service data of different frequencies for a number of vessel types. The results of the model were evaluated by:

- Comparing the predicted and measured power values. The agreement between measured and predicted power values is generally better for auto-logged data.
- Evaluating the time development found from the model and dry-docking effects of predicted power. All vessels (except possibly one) show realistic time developments.
- Comparing speed power curves, calculated from the model results, to available reference curves. The predicted curves were found to agree well with the reference curves in the measured speed range for all ships.
- Comparing speed power curves, calculated from the model results, with measured data at some loading condition. The predicted speed-power curves agreed well with measured data for all ships.
- Comparing the predicted time development of power deviation to a linear regression line through ISO 19030 defined Power Performance Value data. The linear model trendline is very similar to the trendline of the ISO 19030 Power Performance Values.

The model was found not to work in cases not shown in this report, where:

- Ship is trading within a narrow speed range (especially for noon data).
- There is strong correlation between input variables. If for instance ship is systematically reducing or increasing speed over time.

Besides from these cases, in order for the model to work, some amount of data have to be available. This means that it can only be used after the ship has been trading for some time in various loading conditions and speeds. In order to improve the uncertainty of the model, an obvious suggestion would be to include more input variables. Waves, trim and water temperatures are probably the most significant.

Despite the limitations and uncertainties, the linear model can be useful first of all for estimating speed-power curves at different loading conditions, and second for monitoring long-term performance trends. In cases where reference curves are not available, or the ship operates outside the speed-power range of the reference curves, the ISO 19030 standard analysis is not applicable and the linear model is a good alternative. It can also be used to supplement the ISO 19030 method, because of the possibility for producing speed-power curves for any loading condition and at any point in time. This is very useful for operational purposes, where the alternative is often to divide data into two different loading conditions, remove the points with wind above some limit and then fit a speed-power curve for each condition at certain time intervals. The linear model uses all the data for fitting rather than dividing into different groups and fitting fewer data separately with higher resulting uncertainty.

References

BERTRAM, V. (2018), *Some Heretic Thoughts on ISO 19030*, 2nd HullPIC Conf., Ulrichshusen

ALDOUS, L.G. (2015), *Ship Operational Efficiency: Performance Models and Uncertainty Analysis*, PhD Thesis, University College London

PEDERSEN, B.P. (2014), *Data-driven Vessel Performance Monitoring*, PhD Thesis, Technical University of Denmark

SCHMODE, D.; HYLPENDAHL, O.; GUNDERMANN, D. (2018), *Hull Performance Prediction beyond ISO 19030*, 3rd HullPIC Conf., Redworth

Application of Sensor Fusion to Drive Vessel Performance

Angelos Ikonomakis, Maersk Line Fleet Performance, Copenhagen/Denmark, angelos.ikonomakis@maersk.com

Roberto Galeazzi, DTU Electrical Engineering, Copenhagen/Denmark, rg@elektro.dtu.dk

Jesper Dietz, Maersk Line Fleet Performance, Copenhagen/Denmark, jesper.dietz@maersk.com

Klaus Kähler Holst, Maersk Digital Research, Copenhagen/Denmark, klaus.holst@maersk.com

Ulrik Dam Nielsen, DTU Mechanical Engineering, Copenhagen/Denmark, udn@mek.dtu.dk

Abstract

Typically, slow steaming is adopted to lower ship's resistance, which in turn reduces exhaust gas emissions due to lower propulsion power demands. Fine tuning of the underlying hydrodynamic models is key to the reliable forecasting of fuel consumption. Accurate knowledge of the vessel's speed-through-water (STW) is paramount to estimate the actual resistance of the vessel. The paper presents a feasibility study about the use of sensor fusion methods for real-time estimation of STW based on inertial measurements of ship motions and measurement of sea current. By combining a purely kinematic model together with linear Kalman filtering, the paper addresses the challenge of designing an optimal STW estimator by detailing the fundamental design choices. The proposed STW estimator is verified on simulated data and tested with measured data from an in-service container vessel.

1. Introduction

1.1. Background and motivation

At sea the speed of a moving craft is measured either relative to the seabed (speed over ground - SOG) or relative to the water flowing past the hull (speed through water - STW). Both of these speed types apply in modern navigation systems. The STW is a crucial source of data for the performance monitoring of a container vessel. Hull and propeller fouling estimation derive from the knowledge of the STW, hence its accurate observation is a key element towards energy efficiency. Traditionally, maritime speed logging devices use either of the following measurement principles to obtain the STW: water pressure, electromagnetic induction, or the transmission of low frequency radio waves *Tetley and Calcutt (2007)*. The latter refers to as the Doppler velocity log (DVL), which is the speed log used by the vessels dealt with in this paper. A range of environmental factors can sometimes influence the accuracy of the measured speed log, *Litton (1998)*. In addition to that, speed log manufacturers always provide distinct information concerning the possible accuracy.

The speed log measurements cannot be categorically trusted, *Griffiths and Bradley (1998)*. Occasionally, offsets occur when measured STW is compared with computed STW, obtained through post-processing of hindcast and propulsion data. This observation, along with other influences, such as trim, aeration, sensor fouling and water clarity, are factors that diminish the confidence of the measured STW. Therefore, the availability of tools for reliably estimating the STW based on either already available measurements or measurements deriving from potentially installed sensors, is of interest to fleet managers for the optimization of fleet performance. The scope of this work is to estimate STW with an accuracy significantly higher than that of the signal measured by the Doppler velocity log. This is achieved by fusing both onboard inertial measurements and external data into a kinematic model of vessel motions. The virtual sensor can be used as input for associated applications such as data-driven fuel tables, trim optimization and accurate hull cleaning predictions.

1.2 State-of-the-art

The analysis of the data provided by onboard sensors is a complex and necessary task, in order to get a clear picture of the ship's behavior and condition. When data derives from sensors, there is always some uncertainty on the measurements, hence it is necessary to analyze each sensor with respect to its

type. Besides the manufacturer information on the sensor uncertainty, several uncertainty analyses have been published. With regard to the ITTC Powering Prediction Method, *ITTC (2002)*, an analysis has been conducted on the uncertainty assessment of the performance parameters during sea trials, *ITTC (2005)*. The results of the trials include errors due to measurements, hull form production and corrections of environmental conditions.

It is noted in the literature, *ITTC (2005)*, that, as speed increases, both bias and precision errors decrease. Bias errors are 5% for all speed range and 3% at the design speed, while the precision errors are 9% at lower speeds and 7% at the design speed. Concerning STW, there is a claim from *Boom et al. (2013)* which states that the speed log is one of the most inaccurate onboard measurement devices. *Bos (2016)* identifies situations where STW data can result in misleading performance trends. These statements have to be investigated and different values of uncertainty should be tested for STW before reaching conclusions.

Numerous researchers have pinpointed the various difficulties in STW estimation including *Pyörre (2012)* and *Antola et al. (2017)*. *Antola et al. (2017)* proposed a Bayesian approach to the STW estimation combining an extended Kalman filter with a mixed kinematic-kinetic model of the vessel. Despite the very promising results showed through validation on almost 200 vessels, three main elements are pointed out that could impact negatively the STW estimate: (i) the model assumes knowledge of the vessel's calm water resistance; (ii) to exploit measurements of shaft torque it is assumed that the vessel STW equals the propeller speed of advance, thereby neglecting wake effects that for ships with a single propeller may account for reductions in the range of 20% to 45% for the speed of advance; (iii) the vessel accelerations due to wave motion are neglected. Power-resistance curves are available for each operating vessel; however this data, usually obtained through model tests, reflects the characteristics of the vessel as new and does not necessarily account for changes in the hull due to retrofits or simply aging. For a given shaft rotational speed switching the speed of advance of the propeller with the vessel STW gives rise to a larger advance ratio, which may determine a systematic mismatch between measured and modelled shaft torque. For a vessel sailing in waves a thrust-resistance balance to achieve zero surge acceleration is rather unrealistic since it demands the thrust/torque/shaft speed control systems to completely compensate for wave-induced speed variations. Therefore, a vessel in seaway can experience substantial accelerations that, at least locally, influence the vessel's STW. These elements can potentially introduce systematic errors in the estimate of the vessel's STW.

1.3 Novelty and contribution

This paper addresses the reliable estimation of the STW within the linear Kalman filtering framework by combining a purely kinematic model of vessel dynamics with inertial measurements of the vessel's position, velocity and acceleration as well as velocity of the sea current. The vessel kinematic model is favored because it does not require partial or full knowledge of vessel hydrodynamics or propulsion characteristics. The available STW measurement is not considered in the estimation, while it is used for the evaluation of the estimated STW. Although the adopted model may be used to estimate the speed through water for a vessel sailing in an arbitrary sea state, this feasibility study focuses on calm water condition to determine the potential estimation performance in absence of major disturbances affecting the vessel dynamic behavior.

The paper details the modeling procedure towards the design of an optimal estimator of STW and illustrates a systematic approach for the evaluation of the obtained estimate. The STW estimator is evaluated both on simulated and full-scale data from an in-service container ship. Preliminary results confirm the possibility to improve the knowledge of the STW with respect to the DVL measurement.

2. Problem Formulation

For a correct formulation of the problem the following assumptions are made:

Assumption 1: The motion of the vessel in the horizontal plane is described by three degrees-of-freedom (DOF), namely surge, sway and yaw.

Assumption 2: Two reference frames are used to represent the motion of the vessel: the North-East-Down (NED) coordinate frame $\{n\}$ is the inertial frame used to describe the pose of the vessel; the body-fixed coordinate frame $\{b\}$ is the non-inertial frame fixed to the vessel used to describe linear and angular velocities.

Assumption 3: The ocean current in the inertial frame $\{n\}$ $\mathbf{V}_c^n = [V_x, V_y, 0]^T$ is constant and irrotational, i.e. $\dot{\mathbf{V}}_c^n = 0$.

Assumption 4: The vessel is equipped with a GNSS (global navigation satellite system) receiver providing synchronous measurements of vessel position (N, E) and speed over ground U_s at the rate $0 < f_p < 1$ Hz. The position measurement in the North and East directions is affected by zero mean white Gaussian noise with variance σ_p^2 , i.e. $w_N \sim \mathcal{N}(0, \sigma_p^2)$ and $w_E \sim \mathcal{N}(0, \sigma_p^2)$. The SOG measurement is affected by zero mean white Gaussian noise with variance σ_s^2 , i.e. $w_{U_s} \sim \mathcal{N}(0, \sigma_s^2)$. It is further assumed that the noise sources w_N , w_E and w_{U_s} are uncorrelated among each other.

Assumption 5: The vessel is equipped with a tri-axis accelerometer providing measurements of linear accelerations $\mathbf{a}^b = [a_u, a_v, a_w]^T$ along directions parallel to the axes of the body-fixed frame at the rate $f_a \geq f_p$ Hz. Each measured acceleration is affected by zero mean white Gaussian noise with variance σ_a^2 , i.e. $w_{a_i} \sim \mathcal{N}(0, \sigma_a^2)$ with $i = \{u, v, w\}$. The three noise sources are uncorrelated among each other.

Assumption 6: The vessel is equipped with a compass providing a measurement of heading at the rate $f_\psi \geq f_p$ Hz. The heading measurement is affected by zero mean white Gaussian noise with variance σ_ψ^2 , i.e. $w_\psi \sim \mathcal{N}(0, \sigma_\psi^2)$

Assumption 7: A prediction of the sea current velocity vector \mathbf{V}_c^n is available through an external provider at a rate $0 < f_c \ll 1$. Each predicted component of the velocity vector is subject to zero mean white Gaussian noise with variance σ_c^2 , i.e. $w_{V_j} \sim \mathcal{N}(0, \sigma_c^2)$ with $j = \{x, y\}$. The two noise sources are uncorrelated between each other.

Remark 1. The noise sources impacting the GNSS measurements of position and SOG are strongly correlated when the SOG is computed by differencing two consecutive position measurements. This is the case in low-end receivers that are usually not adopted in motion control applications of marine crafts. Medium to high-end receivers provide the SOG measurement based on either the Doppler frequency shift of the received signal due to vessel-satellite relative motion or the time differenced carrier phase, *Freda et al. (2015)*, *Gaglione (2015)*. Here the uncertainty of the SOG depends on the quality of the phase measurements (affected by measurement noise and multipath) as well as on the accuracy of the computed position, although to a minor degree. Hence in this case the noise source w_{U_s} can be assumed uncorrelated with the noise affecting the position measurement.

Let $\boldsymbol{\eta}^n = [N, E, \psi]^T \in \mathbb{R}^3$ be the pose vector in the $\{n\}$ frame and $\mathbf{v}^b = [u, v, r]^T \in \mathbb{R}^3$ be the velocity vector in the $\{b\}$ frame. Then the 3-DOF maneuvering model reads, *Caharija et al. (2012)*, *Moe et al. (2014)*.

$$\dot{\boldsymbol{\eta}}^n = \mathbf{R}_b^n(\psi) \mathbf{v}_r^b + \mathbf{V}_c^n \quad (1)$$

$$\mathbf{M} \dot{\mathbf{v}}_r^b + \mathbf{N}(\mathbf{v}_r^b) \mathbf{v}_r^b = \boldsymbol{\tau} \quad (2)$$

where $\mathbf{M} = \mathbf{M}_{RB} + \mathbf{M}_A$ is the total mass given by the sum of the rigid body contribution and the added mass/inertia; $\mathbf{N}(\mathbf{v}_r^b)\mathbf{v}_r^b$ is the sum of centripetal and frictional forces; $\boldsymbol{\tau} = [\tau_x, 0, \tau_\psi]^T \in \mathbb{R}^3$ is the vector of generalized forces and moments; $\mathbf{v}_r^b = \mathbf{v}^b - \mathbf{v}_c^b = [u_r, v_r, r]^T \in \mathbb{R}^3$ is the relative ship speed, i.e. the speed through water. $\mathbf{v}_c^b = (\mathbf{R}_b^n(\psi))^T \mathbf{V}_c^n$ is the velocity vector of the current in the $\{b\}$ frame. The transformation of coordinates between the reference frames $\{b\}$ and $\{n\}$ is achieved through the rotational matrix

$$\mathbf{R}_b^n(\psi) = \begin{bmatrix} \cos\psi & -\sin\psi & 0 \\ \sin\psi & \cos\psi & 0 \\ 0 & 0 & 1 \end{bmatrix} \quad (3)$$

Based on the Assumptions 4 – 7, the output model is given as

$$y_1 = N_m = N + w_N \quad (4)$$

$$y_2 = E_m = E + w_E \quad (5)$$

$$y_3 = \psi_m = \psi + w_\psi \quad (6)$$

$$y_4 = U_{s,m} = U_s + w_{U_s} \quad (7)$$

$$y_5 = V_{x,p} = V_x + w_{V_x} \quad (8)$$

$$y_6 = V_{y,p} = V_y + w_{V_y} \quad (9)$$

$$y_7 = a_{u,m} = a_u + w_{a_u} \quad (10)$$

$$y_8 = a_{v,m} = a_v + w_{a_v} \quad (11)$$

where the subscripts m and p indicate “measured” and “predicted”, respectively.

Problem statement: Consider a ship sailing in calm water along a piecewise continuous path with SOG $U_s(t) = \sqrt{u^2 + v^2}$ and heading $\psi(t)$. The vessel is subject to an ocean current with speed $U_c = \sqrt{V_x^2 + V_y^2}$. Exploiting asynchronous inertial measurements of vessel motion and predictions of the ocean current velocity, generate an estimate of the vessel’s STW $U_r(t) = \sqrt{u_r^2 + v_r^2}$.

3. STW Estimator Design

Sensor measurements are noisy and their accuracy proportionally relates to cost. To overcome the limitations introduced by each individual measurement system, in multi-sensor applications the overall quality of the information is improved by using sensor fusion methods. In *Elmenreich (2002)*, sensor fusion is defined as “the combining of sensory data or data derived from sensory data such that the resulting information is in some sense better than would be possible when these sources were used individually”. Some of the most common sensor fusion methods are the Weighted Least Squares, the Maximum Likelihood, the Maximum Posterior, the Particle Filter, and the Kalman Filter, *Castanedo (2013)*. In this paper the Kalman filter is adopted because in the presence of uncertainty it provides the optimal estimate of the quantities of interest in the sense of minimum variance.

Designing an estimator of STW based on the maneuvering model (1)-(2) requires detailed knowledge of the vessel hydrodynamic characteristics, which in general might be unavailable or simply outdated due to aging of the hull or hull modifications. Therefore, robustness of the estimation could be achieved only through the parallel estimation of $U_r(t)$ and model parameters. This will obviously increase complexity of the estimation scheme.

An alternative approach, which conjugates both simplicity and robustness, based on only the vessel kinematics (1) and exploiting the available measurements of ship motion and predictions of current velocity. Since an estimate of STW is sought, rather than its projection onto the body axes, u_r and v_r , then the estimation problem can be formulated in terms of traveled distance and cruising speeds, $U_s(t)$ and $U_r(t)$.

Let $\hat{\mathbf{x}} = [\hat{d}, \hat{U}_s, \hat{U}_r, \hat{U}_c]^T \in \mathbb{R}^4$ be the state estimation vector, where \hat{d} is the estimate of the traveled distance $d = \sqrt{N^2 + E^2}$ and \hat{U}_c is the estimate of the speed of the current $U_c = \sqrt{V_x^2 + V_y^2}$. Then the discrete time state space model at the core of the estimator is given by

$$\hat{d}(k+1) = \hat{d}(k) + \hat{U}_s(k)T_s + \frac{1}{2}A_s(k)T_s^2 \quad (12)$$

$$\hat{U}_s(k+1) = \hat{U}_s(k) + A_s(k)T_s \quad (13)$$

$$\hat{U}_r(k+1) = \hat{U}_s(k) - \hat{U}_c(k) + A_s(k)T_s \quad (14)$$

$$\hat{U}_c(k+1) = \hat{U}_c(k) + v_c \quad (15)$$

where $T_s = 1/\max\{f_p, f_a, f_c\}$ is the sampling time, A_s is the total ship acceleration, i.e. $A_s = \sqrt{a_u^2 + a_v^2}$, and v_c is a zero mean white Gaussian noise source with variance $\sigma_{v_c}^2$.

Remark 2: Eqs. (14)-(15) are valid only when the vessel sails with constant heading, i.e. $r \approx 0$. During heading alterations the equations should also account for fictitious accelerations due to centripetal forces, *Fossen (2011)*, [Section 8.3].

Remark 3: Based on the direct measurements (10)-(11) the indirect measurement of total ship acceleration is given by $u_A = \sqrt{y_7^2 + y_8^2}$, which is a stochastic process whose characteristics are in general non-Gaussian. When the acceleration components a_u and a_v are both zero, then u_A will be a Rayleigh distributed random process. However, when the acceleration along the surge and/or sway directions is different from zero then the random component of u_A is still well approximated by a Gaussian distribution. For the sake of simplicity and in order to apply standard results in Kalman filtering, it is assumed that the measured total ship acceleration can be approximated as $u_A \approx A_s + v_A$, where v_A is zero mean white Gaussian noise with variance σ_d^2 . Hence the total ship acceleration A_s in Eqs. (12)-(14) is given by $A_s = u_A - v_A$.

Based on the output model (4)-(11) and considering asynchronous measurements the following measurement models are defined

$$\mathbf{z}(k) = [y_d, y_4, y_c]^T + \mathbf{w}_1(k) \quad k = LT_c/T_s \quad (16)$$

$$\mathbf{z}(k) = [y_d, y_4]^T + \mathbf{w}_2(k) \quad k \neq LT_c/T_s \quad (17)$$

where $y_d = d$ is the measured traveled distance, $y_c = \sqrt{y_5^2 + y_6^2}$ is the predicted sea current speed, $T_c = 1/f_c$ and $L \in \mathbb{N}$ is a counter.

The measurement noise vectors $\mathbf{w}_1 = [w_d, w_{U_s}, w_c]^T$ and $\mathbf{w}_2 = [w_d, w_{U_s}]^T$ are described by independent and uncorrelated Gaussian distributed stochastic processes, i.e. $\mathbf{w}_1 \sim \mathcal{N}(0, \mathbf{R}_1)$ with $\mathbf{R}_1 = \text{diag}\{\sigma_d^2, \sigma_s^2, \sigma_{U_c}^2\}$ and $\mathbf{w}_2 \sim \mathcal{N}(0, \mathbf{R}_2)$ with $\mathbf{R}_2 = \text{diag}\{\sigma_d^2, \sigma_s^2\}$.

Remark 4: The measurement y_d of the travelled distance d is indirect since it is computed from the direct GNSS measurements y_1 and y_2 . Similarly, the measurement y_c of the speed of the current is indirectly computed based on the predicted V_c^n . Both y_d and y_c are in general non-Gaussian stochastic process due to the nonlinear processing of the white Gaussian noise affecting the direct measurements. Applying the same line of reasoning of Remark 3, the measurement models (16)-(17) are adopted.

Remark 5: Deviations of the true measurements from the proposed approximations in Remarks 3 and 4 will determine a poorer performance of the Kalman filter with respect to the theoretical expectation.

In particular, the estimation error covariance will be larger than the theoretical expected value and correlation may appear in the estimation error.

Based on the estimator model (12)-(15) and measurement model (16)-(17) the discrete time state transition matrix \mathbf{F} , the input matrix \mathbf{G} , the process noise input matrix \mathbf{G}_v and the output matrices \mathbf{H}_1 and \mathbf{H}_2 can be set up:

$$\mathbf{F} = \begin{bmatrix} 1 & T_s & 0 & 0 \\ 0 & 1 & 0 & 0 \\ 0 & 1 & 0 & -1 \\ 0 & 0 & 0 & 1 \end{bmatrix}, \quad \mathbf{G} = \begin{bmatrix} \frac{1}{2}T_s^2 \\ T_s \\ T_s \\ 0 \end{bmatrix}, \quad \mathbf{G}_v = \begin{bmatrix} -\frac{1}{2}T_s^2 & 0 \\ -T_s & 0 \\ -T_s & 0 \\ 0 & 1 \end{bmatrix} \quad (18)$$

$$\mathbf{H}_1 = \begin{bmatrix} 1 & 0 & 0 & 0 \\ 0 & 1 & 0 & 0 \\ 0 & 0 & 0 & 1 \end{bmatrix}, \quad \mathbf{H}_2 = \begin{bmatrix} 1 & 0 & 0 & 0 \\ 0 & 1 & 0 & 0 \end{bmatrix} \quad (19)$$

The last step towards the implementation of the STW estimator based on linear Kalman filtering is to define the process noise covariance matrix \mathbf{Q} . Given the estimator model (12)-(15) two process noise sources are identified, namely v_A and v_c , which are assumed to be uncorrelated between each other. Therefore, the process noise covariance matrix is given by $\mathbf{Q} = \text{diag}\{[\sigma_a^2, \sigma_v^2]\}$. Whilst the variance of the process noise component v_A as well as the variances of the measurement noise \mathbf{w}_1 are given by the noise characteristics of the individual sensors, the variance σ_v^2 is a tuning parameter for the Kalman filter that can be used to determine the trade-off between smoothness of the estimation and promptness to changes in the operational conditions of the system to perform estimation on. The linear optimal STW estimator in its predictor-corrector formulation reads *Lewis et al.(2017)* [Section 2.3]

Time update

$$\hat{\mathbf{x}}^-(k+1) = \mathbf{F}\hat{\mathbf{x}}(k) + \mathbf{G}u_A \quad (20)$$

$$\mathbf{P}^-(k+1) = \mathbf{F}\mathbf{P}(k)\mathbf{F}^T + \mathbf{G}_v\mathbf{Q}\mathbf{G}_v^T \quad (21)$$

Measurement update

- $k = LT_c/T_s$

$$\hat{\mathbf{x}}(k+1) = \hat{\mathbf{x}}^-(k+1) + \mathbf{K}_1(k+1)[\mathbf{z}(k+1) - \mathbf{H}_1\hat{\mathbf{x}}^-(k+1)] \quad (22)$$

$$\mathbf{P}(k+1) = [(\mathbf{P}^-(k+1))^{-1} + \mathbf{H}_1^T\mathbf{R}_1^{-1}\mathbf{H}_1]^{-1} \quad (23)$$

- $k \neq LT_c/T_s$

$$\hat{\mathbf{x}}(k+1) = \hat{\mathbf{x}}^-(k+1) + \mathbf{K}_2(k+1)[\mathbf{z}(k+1) - \mathbf{H}_2\hat{\mathbf{x}}^-(k+1)] \quad (24)$$

$$\mathbf{P}(k+1) = [(\mathbf{P}^-(k+1))^{-1} + \mathbf{H}_2^T\mathbf{R}_2^{-1}\mathbf{H}_2]^{-1} \quad (25)$$

where $\mathbf{K}_i(k) = \mathbf{P}(k)\mathbf{H}_i\mathbf{R}_i^{-1}$, $i = \{1,2\}$, is the Kalman gain. During the time update the state prediction $\hat{\mathbf{x}}^-$ and the a-priori estimation error covariance \mathbf{P}^- are computed based on the linear time invariant discrete time model $(\mathbf{F}, \mathbf{G}, \mathbf{G}_v)$ and the process noise covariance \mathbf{Q} . When a new measurement becomes available, the state estimate $\hat{\mathbf{x}}$ and the a-posteriori estimation error covariance \mathbf{P} are updated based on the measurement model \mathbf{H}_i , the Kalman gain \mathbf{K}_i , and the measurement noise covariance \mathbf{R}_i .

4. Implementation on Simulated Data

The simulations are carried out using the Marine Systems Simulator (MSS), *Fossen (2011)*. The simulator is a Matlab/Simulink library for marine systems that includes models for ships, underwater vehicles, and floating structures, <https://github.com/cybergalactic/MSS>. The library also contains guidance, navigation, and control functionalities for real-time simulation. The library has been translated

to Python and then focused on the model for coupled motion of steering and rolling of a high-speed container ship, introduced in *Son and Nomoto (1981)*. The simulation study case represents a $L = 175$ m vessel, which travels with variable SOG U_s , subject to a sea current coming from astern with constant speed $U_c = 1$ m/s.

The simulation environment has been configured to run with an integration time step of 0.01 seconds, in order to mimic the continuous time nature of the vessel motion and enable further resampling of the data due to simulated measurement processes. To verify the ability of the designed estimator to converge in mean value towards the true value as well as to track time-varying behaviors, the vessel has been initialized with $U_s(0) = 10$ m/s and the shaft angular velocity $n(0) = 70$ rpm, which gives rise to a non-stationary condition when n is increasing or decreasing over time.

The measurement process has been set up by simulating sensors with sampling rates and noise characteristics as stated in Table 1.

Signal	Frequency [Hz]	Noise [std]
N_m	0.033 [30s]	2.5 [m]
E_m	0.033 [30s]	2.5 [m]
U_{OG}	0.033 [30s]	0.065 [m/s]
U_{curr}	0.008 [20min]	0.2 [m/s]
a_x	0.033 [30s]	0.05 [m/s ²]
a_y	0.033 [30s]	0.05 [m/s ²]

Table 1: Sampling frequency and noise intensity (1σ) of each sensor used by the estimator

Fig.1 shows the estimate of the speed through water \hat{U}_r (virtual STW). The true STW obtained from the simulation is indicated by the dashed-blue line. It is evident by checking the log lines that the data is asynchronous meaning that it resembles a real-world scenario where the measurement of the current speed U_c is acquired with a different frequency than the SOG measurement from the GPS sensor.

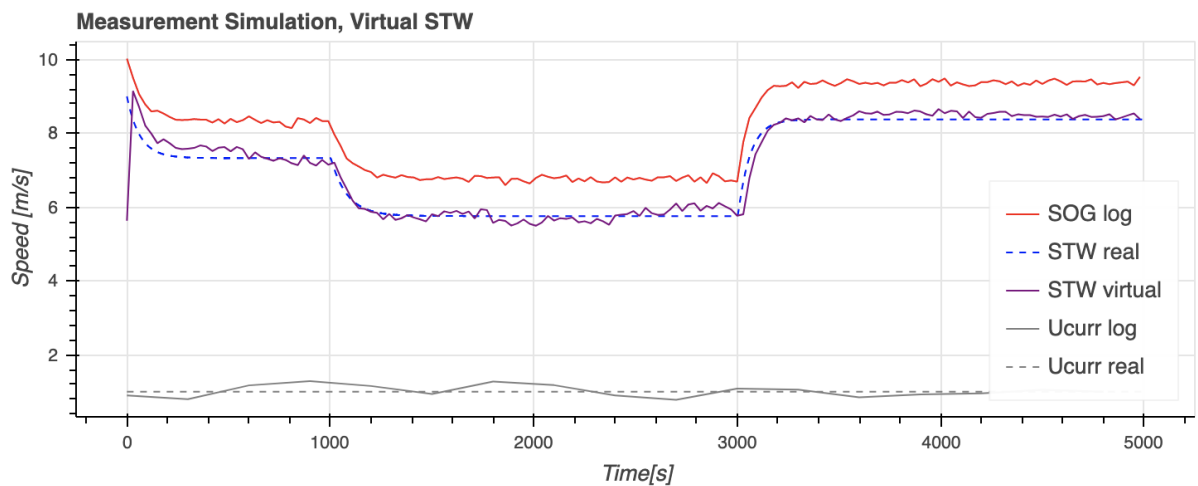


Fig.1: Estimation of speed through water in comparison to other speed signals obtained in simulation

Simulated results show that the designed estimator performs well in reconstructing the STW: although there is a noticeable phase lag, in only a few iterations it is visible that despite the noise and the asynchronicity of the sensor rates, the STW estimator converges in mean value to the true value of the relative ship speed U_r .

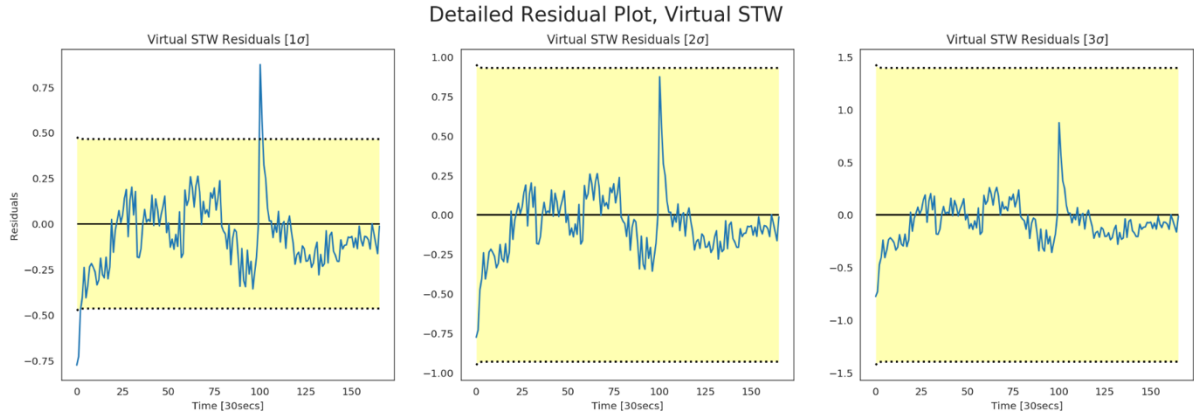


Fig.3: Virtual STW residual within 1σ , 2σ and 3σ confidence bounds

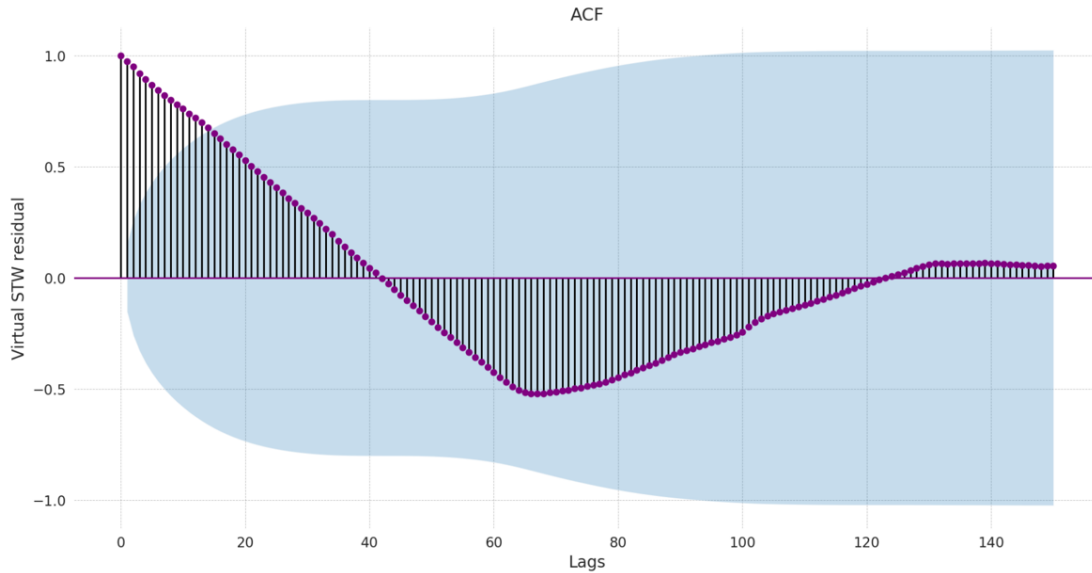


Fig.3: Autocorrelation function of virtual STW residuals. Lags are displayed in x-axis.

To qualify and quantify the performance of STW estimator an analysis of the estimation error $\tilde{U}_r = U_r - \hat{U}_r$ is carried out. Fig.2 illustrates the estimation error \tilde{U}_b with the 1σ , 2σ and 3σ confidence bounds. Fig.3 shows the autocorrelation function of the estimation error.

Under ideal conditions, if the STW estimator correctly reconstructs the vessel's STW then \tilde{U}_b should be a white noise process with zero mean and bounded small variance. Figs.2 and 3 show that the residual is well within the 3σ confidence bound and that the autocorrelation falls within its confidence bound as soon as the stationary condition is achieved. Therefore, the estimation error \tilde{U}_b can be considered a white sequence, meaning that the designed estimator reconstructs the dynamics of interest.

5. Implementation on full-scale data

The data originates from a 10,500 TEU container vessel owned and operated by Maersk Line. Only relevant vessel information and values are included. Fig.4 illustrates the vessel route and speed profile for a 1-month sample data of the vessel. It can be noticed that along the route there are periods when the speed is switching from high to low values and vice versa. Sea currents affect the STW either positively or negatively according to their angle of attack. When $U_c < 0$, it refers to head currents.



Fig.4: Vessel service route with measured speed-through-water (left) and sea current speed (right)

When measuring and analyzing data, it is desirable that the underlying measured process is wide sense stationary, i.e. its statistical properties are time invariant. In practice, the measured process and, thereby, the collected data will often display non-stationary features over certain periods of time. Changes in environmental or operational conditions over time, such as variations in current speed magnitude and direction or ship's heading alterations, result to changes in vessel's speed leading to non-stationary data. It is possible, though, to find cases where the ship can be assumed to operate in a stationary condition.

An inspection on the whole 1-month-dataset has been conducted to ascertain how stationary the STW sensor is overtime; always keeping in mind to maintain the mean draught in the same level and the trim close to zero (even keel). Additionally, the sea state was loosely inferred by checking both roll and pitch angles so as to focus on calm water conditions. Moreover, when visualizing the sea current speed U_c and the speed over ground U_s , it is clear that their patterns do not always match, which is probably due to the fact that sea currents are not accurately predicted, especially in open waters. By checking Fig.5 one can see that the two signals have a strong match only in days 18-19.

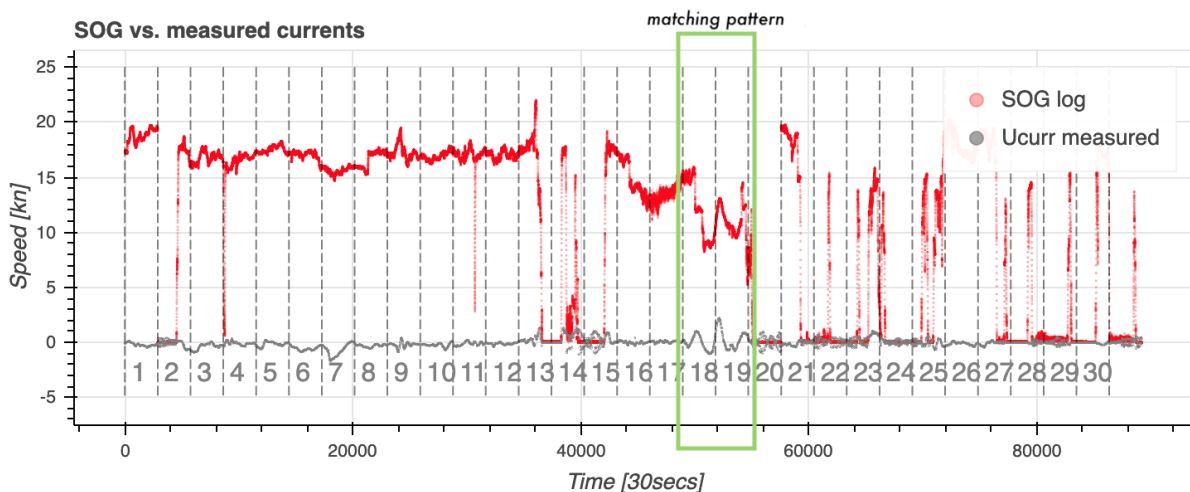


Fig. 5: SOG vs predicted sea current speed, within the 1-month-dataset. Index refers to day number.

Thus, the estimator is applied to data collected while the vessel passed through the English Channel, which refers to day 19 of the dataset. Fig.6 shows location and direction of the vessel when operating on this specific trip. Based on the small amplitude of the roll and pitch angles it is assumed that the vessel sailed in calm weather conditions. The ship's heading angle is considered constant for most of the time (the variance of heading angle is $\text{var}\{\psi\} \approx 3 \text{ deg}^2$ in between indicated turns in Fig.6). Noteworthy that for the selected vessel the only measurement of acceleration is not provided by an inertial measurement unit, but it is given by processing the GNSS outputs. This introduces correlation between the measurements used in the Kalman filter, which as stated in Remark 5 potentially determines a poorer performance of the estimator.

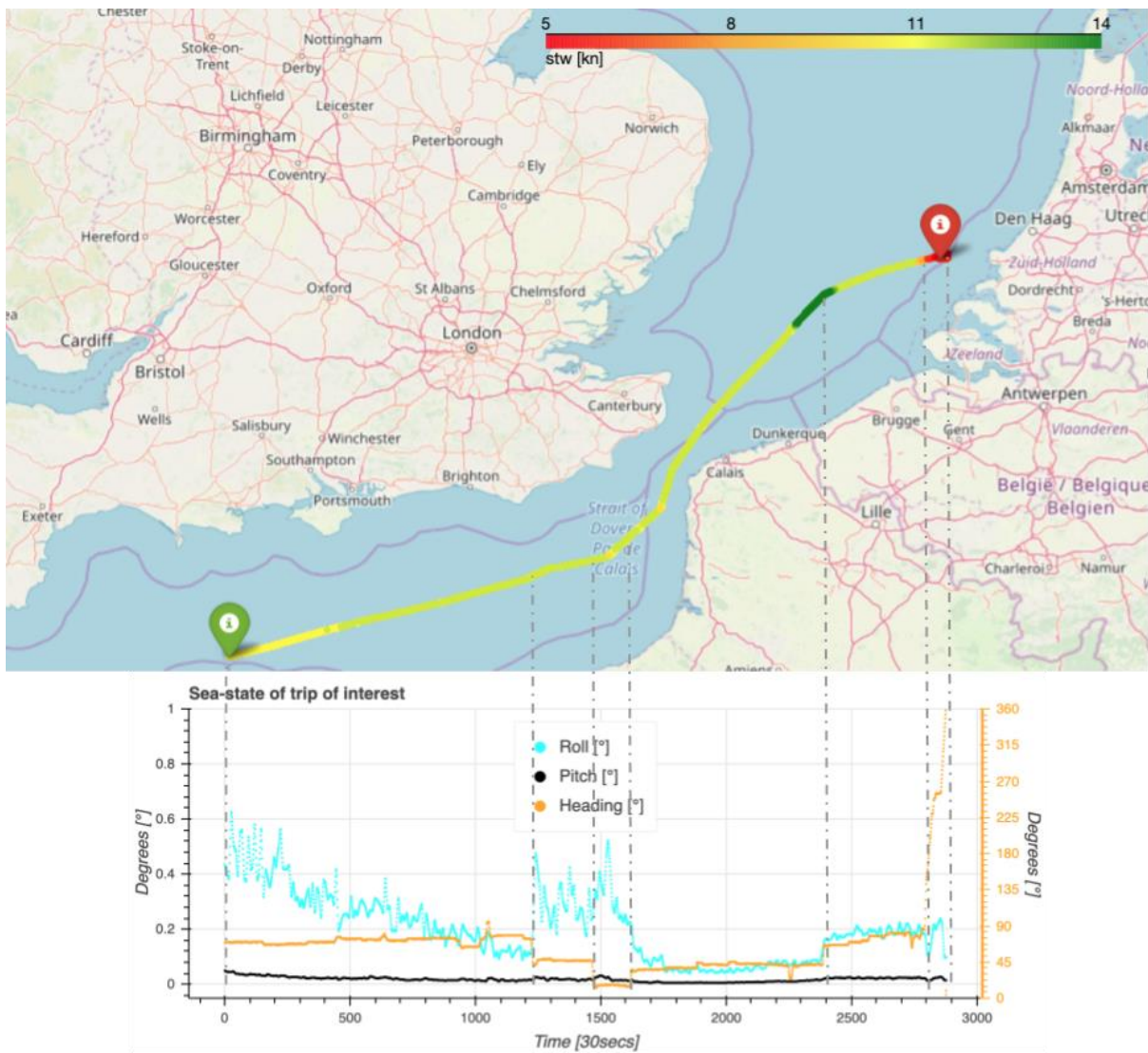


Fig. 6: On top the trip of interest drawn on a map. On the bottom, map is connected with the sea state characteristics (roll, pitch on the left y-axis and true heading on the right y-axis).

Fig.7 shows the speed profiles of the "trip of interest". It is evident from the measurements that the STW is not stationary and there are strong and changing sea currents.

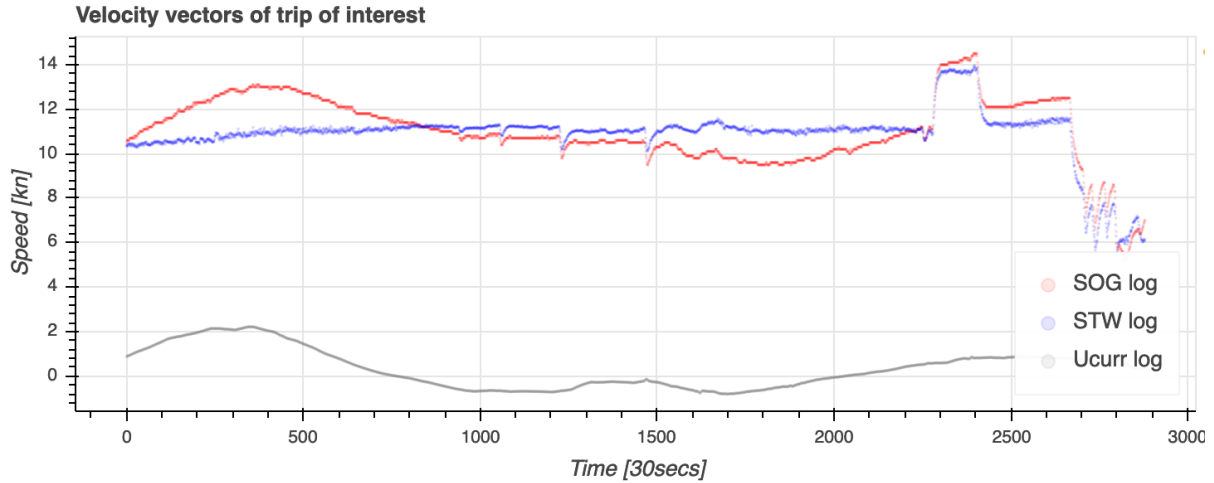


Fig. 7: Speed profiles of the "trip of interest"

The STW estimator has been applied to a synchronous sensor rate implementation and then to an asynchronous one, similar to the simulation implementation where the predictions of the sea current speed were invoked at a lower frequency than the rest of the signals. The synchronous implementation outcome is shown in Fig.8. The estimated STW \hat{U}_r (virtual STW in the plot) shows some significant deviations from the measured STW, up to approximately 0.5 m/s, and in general seems to better account for variations in current speed.

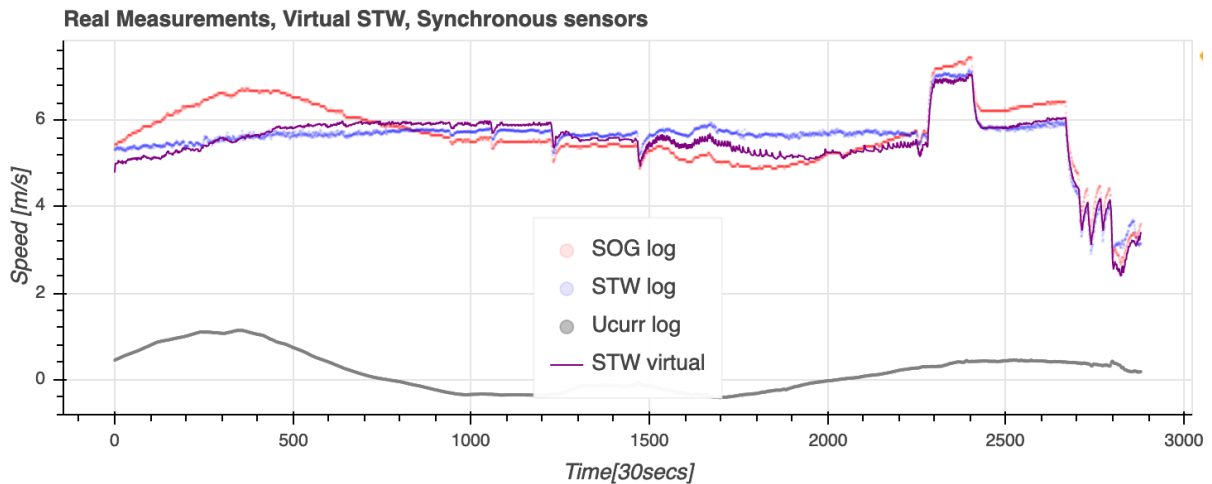


Fig. 8: Estimation of the STW \hat{U}_r (virtual STW) throughout the "trip of interest" based on the synchronous implementation of the measurement model

In Fig.9 the asynchronous implementation of the filter is depicted, when current speed is provided every 20 minutes, which is standard for most of the hindcast data providers. This time the estimated STW \hat{U}_r (virtual STW in the plot) shows a more fluctuating behavior induced by the more sporadic knowledge of the current speed. The jerky variations are related to each measurement update performed by the estimator whenever a new prediction of the current speed is available. Despite the reduced smoothness, the estimated STW is in line with the results obtained through the synchronous implementation both in terms of maximum deviations from the measured STW and the overall trend of the estimate.

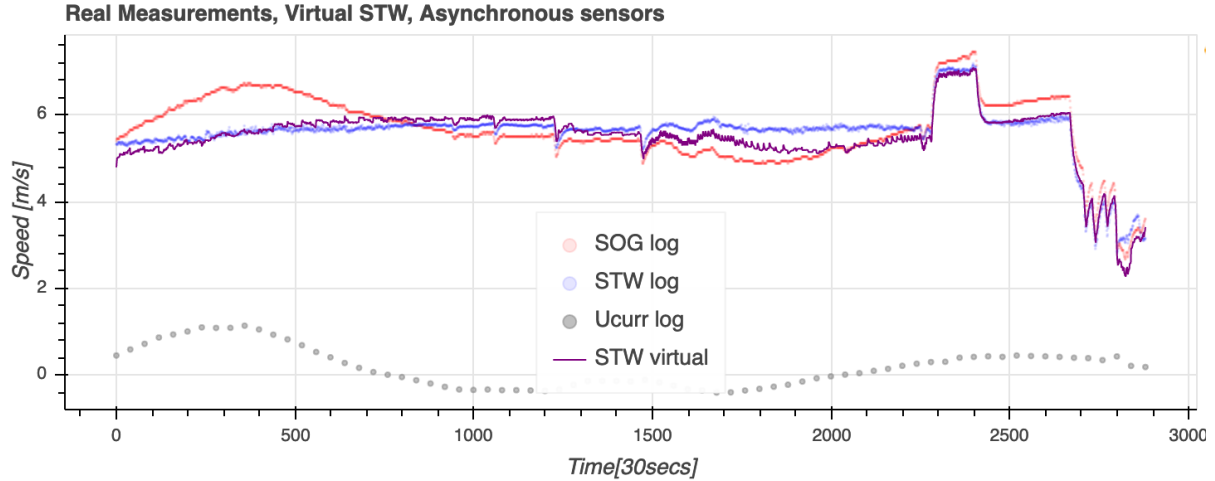


Fig. 9: Estimation of the STW \hat{U}_r (virtual STW) throughout the "trip of interest" based on the asynchronous implementation of the measurement model.

6. Discussion

Throughout the paper, the methodology, the model design, the application as well as the results, have all been described and meticulously assessed. The outcome of the implemented filter is highly dependent on the input parameters, i.e. the auto-logged vessel data. On a literature basis study, the indicated total of errors can be expected up to 9% for the auto-logged data, *ITTC (2005)*. However, it is believed that precision errors are limited, due to the extended data processing.

The Kalman filter is a mathematical tool that conjugates the knowledge about physical phenomena formalized in a model with measurements of quantities directly or indirectly related to that phenomena in order to provide estimates of unmeasured states as well as to improve the signal-to-noise ratio of the measured quantities. Hence its performance is tightly coupled with the accuracy of the model and the quality of the available measurements.

In order to provide a simple solution that could be used as reference for future studies, some assumptions have been made concerning linearity of models, Gaussianity and uncorrelation of noise sources. However, these assumptions are not always satisfied in reality giving rise to performance deterioration of the estimation process. Accounting for correlation among the available measurements can potentially improve the estimation in terms of lower estimation error covariance, however this will come at the cost of a somewhat more complex implementation.

The STW estimator was tested on simulated data, before being applied to full-scale data. The availability of high-fidelity simulators able to produce numerical data capturing the phenomena of interest facilitates the design and tuning of the Kalman filter, especially when the true value of the variables to be estimated is in reality unknown. In the addressed study case a measurement of the STW was actually available but considered untrustworthy, thereby it was not included in the estimator design. Despite the simplifying assumptions, the evaluation of the designed STW estimator on the full-scale data is positive and it shows the feasibility of using a pure kinematic model to estimate a STW signal, which appears more aligned with the other inertial measurements than that one provided by the DVL.

7. Conclusion

A kinematic-based linear Kalman filter was designed to compute an estimate of the STW based on onboard inertial measurements and external hindcast sea current measurements of a large container vessel sailing in calm water. The analysis of the results obtained by processing full-scale measurements indicates an improvement of estimated STW with respect to the measurement provided by the onboard DVL, that is the estimate explains better changes in vessel's SOG and sea current's speed.

However, these results are preliminary and an extended investigation should be conducted by e.g. broadening the analysis to various container vessels of different characteristics, including more comprehensive and extended analyses made during sailing in seaway.

References

- ANTOLA, M.; SOLONEN, A.; PYÖRRE, J. (2017), *Notorious speed through water*, 2nd HullPIC Conf., Ulrichshusen, pp.156-165
- BOOM, H.V.D.; HUISMAN, H.; MENNEN, F. (2013), *New guidelines for speed/power trials: Level playing field established for IMO EEDI*, SWZ Maritime, Schip en Werf de Zee Foundation, Rotterdam
- BOS, M. (2016), *How MetOcean data can improve accuracy and reliability of vessel performance Estimates*, 1st HullPIC Conf., Pavone, pp.106-114
- CAHARIJA, W.; CANDELORO, M.; PETTERSEN, K.Y.; SØRENSEN, A.J. (2012), *Relative velocity control and integral LOS for path following of underactuated surface vessels*, IFAC Proc. Vol. 45.27, pp.380-385
- CASTANEDO, F. (2013), *A review of data fusion techniques*, The Scientific World J. 13
- ELMENREICH, W. (2002), *An introduction to sensor fusion*, TU Vienna, 502
- FOSSSEN, T.I. (2011), *Handbook of Marine Craft Hydrodynamics and Motion Control*, John Wiley & Sons
- FREDA, P.; ANGRISANO, A.; GAGLIONE, S.; TROISI, S. (2015), *Time-differenced carrier phases technique for precise GNSS velocity estimation*, GPS Solutions 19.2, pp.335-341
- GAGLIONE, S. (2015), *How does a GNSS receiver estimate velocity?*, Inside GNSS, pp.38-41
- GRIFFITHS, G.; BRADLEY, S.E. (1998), *Correlation speed log for deep waters*, Sea Technology 39, pp.29-36
- ITTC (2005), *Final Report and Recommendations to the 24th ITTC*, Manoeuvring Committee et al., 24th ITTC, pp.137-198
- ITTC (2002), *Final report and recommendations to the 23rd ITTC*, Propulsion Committee et al., 23rd ITTC
- LEWIS, F.L.; XIE, L.; POPA, D. (2008), *Optimal and robust estimation: with an introduction to stochastic control theory*, CRC press
- LITTON (1998), *Srd-500 dual axis doppler speed log. Operation Manual*, Litton Marine Systems
- MOE, S.; CAHARIJA, W.; PETTERSEN, K.Y.; SCHJØLBERG, I. (2014), *Path following of under-actuated marine surface vessels in the presence of unknown ocean currents*, IEEE American Control Conf., pp.3856-3861
- PYÖRRE, J. (2012), *Overcoming the challenges in vessel speed optimisation*, HANSA 149, pp.130-135
- SON, K.H.; NOMOTO, K. (1981), *On the coupled motion of steering and rolling of a high speed container ship*, J. Society of Naval Architects of Japan 150, pp.232-244
- TETLEY, L.; CALCUTT, D. (2007), *Electronic navigation systems*, Routledge, pp.45-87

Using CFD to Predict Ship Resistance due to Biofouling, and Plan Hull Maintenance

Abel Vargas, Hua Shan, Eric Holm, Naval Surface Warfare Center, Carderock Division, West Bethesda/USA, abel.vargas@navy.mil

Abstract

Computational fluid dynamics (CFD) was used to investigate the impact of biofouling roughness on ship resistance, for the DTMB 5415 hull form at full scale. The ship hull form was divided into sections to allow for the evaluation of both homogeneous and heterogeneous distributions of roughness. Total resistance C_T , and frictional resistance C_F , associated with biofouling increased with hydrodynamic roughness (as represented by equivalent sand grain roughness k_s). Local values of C_F varied across the hull with higher values observed at the bow. Ranking of the hull sections in terms of C_F was bow > sides > flat bottom > stern > transom when scaled by the proportion of the wetted surface area of the hull accounted for by the section of interest. Several scenarios associated with heterogeneous accumulation of biofouling were investigated, including increased growth at the waterline, and sequential cleaning of the hull. The benefits of carrying out partial cleaning of the hull (for example, bow + sides, bow + sides + flat bottom) were observed to depend on the initial biofouling condition. As biofouling roughness increased, cleaning of more of the hull (from bow to stern) was required to attain a particular reduction in C_T . These results demonstrate the potential use of CFD to efficiently evaluate alternative biofouling control strategies.

This paper is provided for information only and does not constitute a commitment on behalf of the U.S. government to provide additional information on the program and/or sale of the equipment or system.

1. Introduction

That hull biofouling degrades a ship's performance has been understood for centuries, if not millennia, *WHOI (1952), Townsin (2003)*. The ability to accurately predict the impacts of biofouling, and thus evaluate the potential benefits of biofouling control strategies is, however, still in development. Although powering trials or towing tests have been used since the 1920s (at least) to quantify the effects of biofouling on vessel operations, the attached communities (or other sources of drag-producing roughness) would now be considered to be poorly described (if described at all), or the extent of biofouling to be well beyond that which would currently be tolerated, e.g. *Visscher (1927), Davis (1930), Izubuchi (1934), Kempf (1937), Kan et al. (1958)*. More recently, *Townsin et al. (1981), Lewthwaite et al. (1984); Hundley and Tsai (1992)*, trials have been linked to detailed inspection of the hull, substantially improving understanding of the relationships between particular types of biofouling or roughness and their effects on vessel performance.

Although ship trials, when combined with thorough inspection of the hull, provide the best information on the impact to ship performance of biofouling, such efforts are expensive, can require taking a ship out of service, and are limited in the number or diversity of cases that can be investigated in a reasonably short amount of time. Mathematical approaches may provide an efficient alternative. *Schultz (2004, 2007), Schultz et al. (2011)* used *Granville's (1958)* procedure to predict the effect of roughness (including biofouling) on the resistance of two classes of naval vessels, (see *Oliveira et al. (2018)*, for a model commercial vessel). This procedure assumes that biofouling is homogeneously distributed across the hull surface, and thus cannot be used to investigate impacts associated with heterogeneous roughness distributions, such as may occur if accumulation of biofouling varies with location on the hull either due to biological processes (for example, differential attachment of propagules, growth, or mortality) or management practices, e.g. targeted hull cleaning, *Hundley and Tsai (1992)* or use of different biofouling control coatings on different parts of the hull, *Swain and Lund (2016)*. *Townsin et al. (1981)* and *Monty et al. (2016)* presented calculation methods that allowed for heterogeneous biofouling along the length of the hull. *Townsin et al. (1981)* used their method to demonstrate outsized benefits for reducing roughness on the forward quarter of a containership, much as *Hundley et al.* (see *Hundley and*

Tsai (1992)) showed using targeted hull cleaning combined with detailed biofouling assessments and powering trials.

Recently, computational fluid dynamics (CFD) methods have been applied to the hull biofouling problem, *Leer-Andersen and Larsson (2003)*, *Demirel et al. (2014, 2017)*. These methods offer certain advantages over those of *Granville (1958)*, *Townsin et al. (1981)*, and *Monty et al. (2016)* in that they take into account details of the form of the hull, at the cost of being much more computationally intensive. *Leer-Andersen and Larssen (2003)* and *Demirel et al. (2014,2017)* used CFD to evaluate the impact of coating and biofouling roughness distributed homogeneously on a ship hull. Herein an alternative CFD formulation, to modelling the frictional resistance of a rough ship hull, is employed to examine the effects of both homogeneously-distributed biofouling and heterogeneous accumulations, such as might be associated with differential growth of biofouling or targeted hull maintenance strategies. The results demonstrate the potential for use of CFD to evaluate the efficacy of alternative biofouling control strategies in terms of effects on ship performance, or to plan hull maintenance activities so as to extract the greatest benefit.

2. Computational Fluid Dynamics

Computational fluid dynamics (CFD) was carried out in NavyFOAM, *Shan et al. (2011)*, an integrated CFD package based on OpenFOAM, and developed at Naval Surface Warfare Center, Carderock Division under funding by the Department of Defense High Performance Computing Program (HPCMP) CREATE Ship's Hydrodynamics Program. Details of this solver, modifications made to the turbulence model to account for roughness due to biofouling, and validation of the approach, can be found in *Vargas and Shan (2017)*. Within the turbulence model, biofouling roughness is represented by the equivalent sandgrain roughness height, k_s . In the simulations described below, the k_s values used were obtained from *Schultz (2007)*, although additional values associated with various types and configurations of biofouling have been determined experimentally, e.g. *Monty et al. (2016)*, *Murphy et al. (2018)*, and can be readily employed in the simulations.

2.1. Computational Domain: DTMB 5415

The DTMB 5415 hull form was chosen to carry out CFD at full scale. This hull form resembles that of a US Navy surface combatant. Details of the hull form (see *Olivieri et al. (2001)*, *Larsson et al. (2014)*) include the following: length between perpendiculars (L_{pp}) = 142 m; wetted surface area = 2976.2 m²; and Froude Number (Fr) = 0.28. The hull was tested at a draft of 6.15 m with a fixed sinkage and trim of $-1.82 \times 10^{-3} L_{pp}$ and -0.108° , respectively, and without any appendages. Fluid properties of sea water included density = 1026.02 kg m⁻³, and kinematic viscosity = 1.1892 m²/s. After carrying out a study of grid sensitivity, a grid size of 10×10^6 cells was chosen. The computational domain, discretization methods, and numerical schemes for all simulations were as described previously for model-scale evaluations, *Vargas and Shan (2017)*.

3. Results

3.1 Homogeneous Biofouling

As a first step in evaluating the impact of biofouling on resistance, homogeneous biofouling roughness was added to the hull form. For small values of biofouling roughness k_s less than 1000 μm , such as those associated with slime or biofilm biofouling, the total resistance coefficient C_T increases rapidly, Fig.1, Table 1. As larger or rougher biofouling ($k_s > 1000 \mu\text{m}$) is added to the hull, the slope of the relationship between k_s and resistance decreases, Fig.1, Table 1. Numerical simulation allows for the estimation not only of the total resistance of a rough ship hull (R_T), but also components of the total resistance associated with frictional (R_F) and residuary resistance including pressure and wave resistance (R_R) (*Vargas and Shan 2017*). The force components can be written in dimensionless coefficients defined as follows:

[1]

[2]

$$C_T = \frac{R_T}{\frac{1}{2}\rho U^2 S}$$

$$C_F = \frac{R_F}{\frac{1}{2}\rho U^2 S}$$

$$C_R = \frac{R_R}{\frac{1}{2}\rho U^2 S},$$

where ρ is the fluid density, U is the ship speed, and S is the wetted surface area of the hull. In the current computations, appendage drag and still air drag are not added to C_T , and only C_F and C_R are used to compute the total resistance ($C_T = C_F + C_R$).

Residuary resistance C_R is relatively unaffected by the presence of biofouling roughness on the hull. Instead, variation in C_T is driven by increases in frictional resistance C_F with k_s , Fig.1. Based on biofouling conditions and associated values of k_s from *Schultz (2007)*, accumulation of bacterial biofilms (light slime, heavy slime) results in increases in C_T of 15%-30% over the hydraulically smooth condition, and 10%-25% over the as painted condition, Table 1. The worst case investigated by *Schultz (2007)*, heavy calcareous biofouling, increases C_T by approximately 93% relative to the hydraulically smooth condition, and 85% relative to the as painted condition, Table 1.

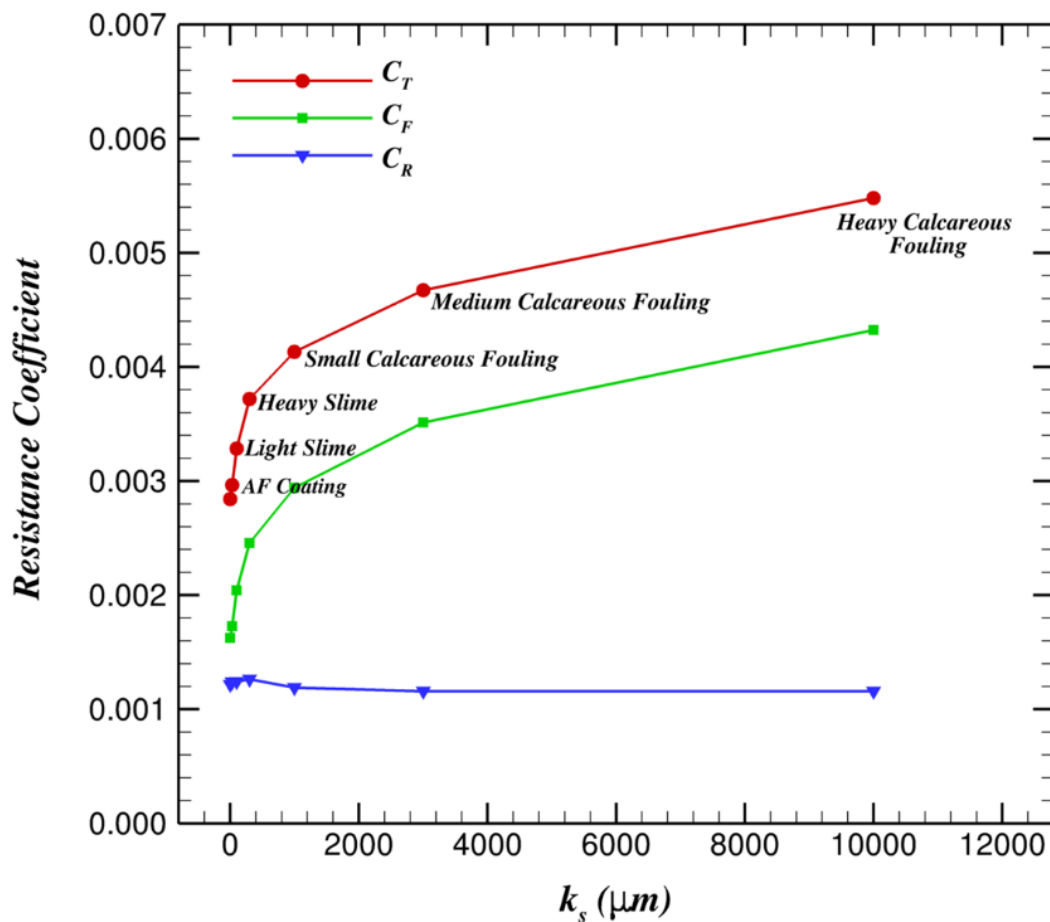


Fig.1: Change in resistance with biofouling roughness k_s , for homogeneously-distributed biofouling roughness. C_T = total resistance coefficient; C_F = frictional resistance coefficient; C_R = pressure resistance coefficient.

Table 1: Impact of roughness on total resistance C_T , relative to a hydraulically smooth hull and a hull painted with a typical antifouling coating

Biofouling/Roughness Condition	% Change in C_T Smooth Hull as Reference	% Change in C_T Painted Hull as Reference
Hydraulically-smooth hull	-	-
Typical as-applied antifouling coating	4.35	-
Light slime	15.53	10.72
Heavy slime	30.86	25.41
Small calcareous biofouling	45.36	39.31
Medium calcareous biofouling	64.36	57.51
Heavy calcareous biofouling	92.82	84.78

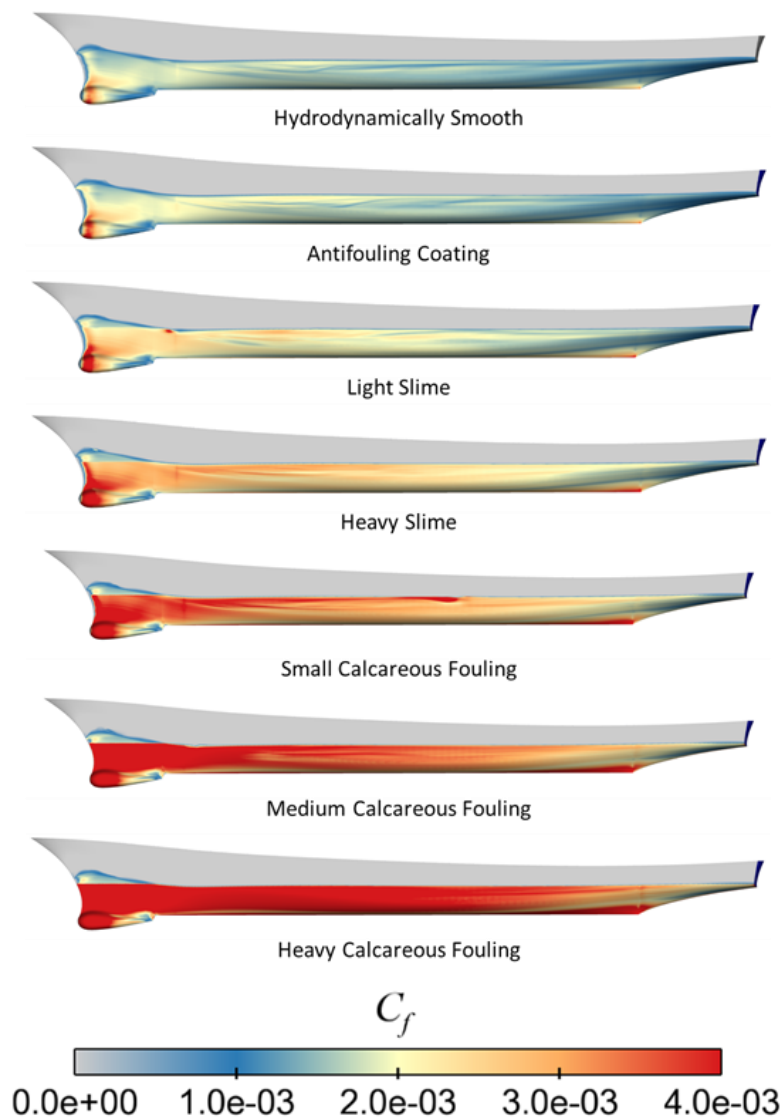


Fig.2: Distribution of local skin friction values for homogeneous biofouling roughness of varying k_s , for a ship speed of 20 kn.

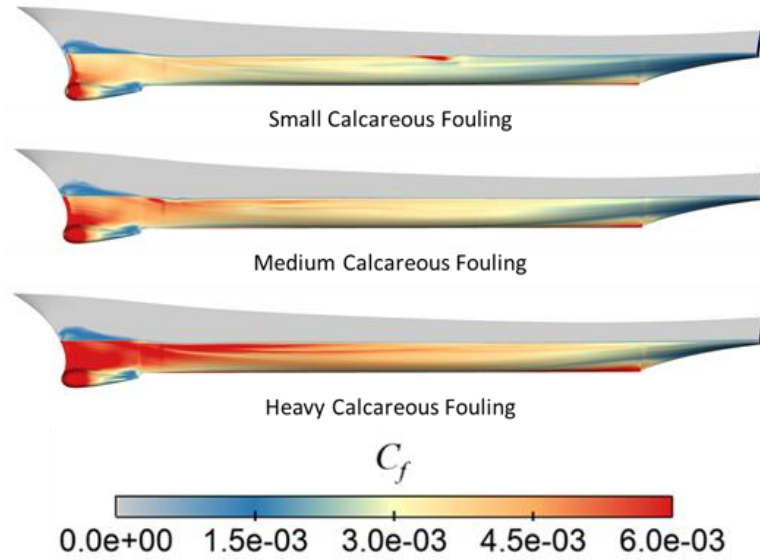


Fig.3: Distribution of local skin friction values for homogeneous biofouling roughness of varying k_s , for a ship speed of 20 kn. C_f is rescaled from Figure 2 in order to visualize spatial variation in skin friction for larger values of k_s .

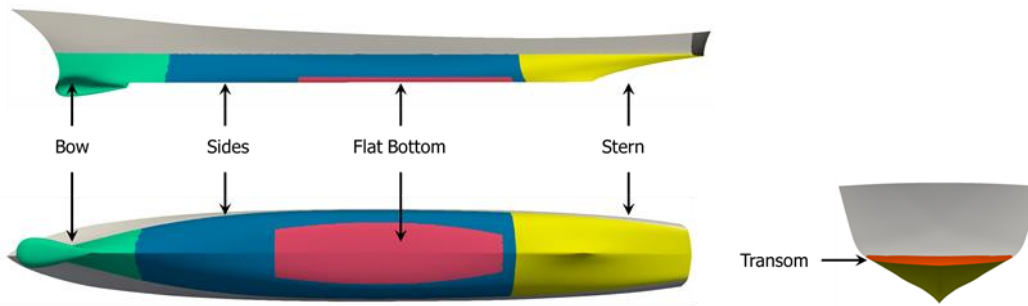


Fig.4: Division of the DTMB 5415 hull form into sections

Values of local frictional resistance (C_f) defined as:

$$C_f = \frac{\tau_w}{1/2 \rho U^2},$$

where τ_w is the wall shear stress, ρ is the fluid density, and U is the ship speed, as associated with biofouling roughness, are heterogeneously-distributed across the hull, Figs.2 and 3. The contours indicate that various sections of the hull contribute differentially to the overall impact of biofouling roughness on resistance. This phenomenon has been demonstrated previously in ship trials using sequential hull cleaning (for example, *Hundley and Tsai (1992)*), and computationally by *Townsin et al. (1981)*, but CFD provides the opportunity to evaluate the nature and magnitude of these effects for any case of biofouling roughness which can be represented by k_s (as opposed to the specific cases associated with ship trials, for example).

Unlike a flat plate where high skin friction is concentrated at the leading edge and then monotonically decreasing along the streamwise direction, *Vargas and Shan (2016)*, the curvature of the hull changes the local velocity thus the wall shear stress. This change in wall shear stress is reflected in the skin friction contours in Figs.2 and 3, where changes in C_f not only occur in the streamwise direction, but also from the waterline to the keel. Skin friction is higher at the bow for all roughness conditions, but as k_s increases, regions of high frictional resistance extend further aft and beyond midships, Fig.2 and 3. Minimal change in skin friction is observed near the stern section, even at high values of k_s .

The impact of biofouling roughness on frictional resistance (C_F), for individual ship hull sections, was investigated by dividing the hull into parts or sections (bow, sides, flat bottom, stern, transom) corresponding to the inspection plan used by divers to evaluate the biofouling condition of in-service US Navy vessels, Fig.4. The hull sections were created by assigning the faces of each grid cell that were inside a specified bounding box which intersected the hull into the corresponding section. The bounding boxes were defined by hull locations defined in diver inspection plans. The dividing of the hull was carried out during the pre-processing phase of the CFD setup. The resulting hull sections accounted for the following percentage of the total wetted surface area of the hull: bow – 16%; sides – 42.9%; bottom – 18%; stern – 22.9%; and transom – 0.2%.

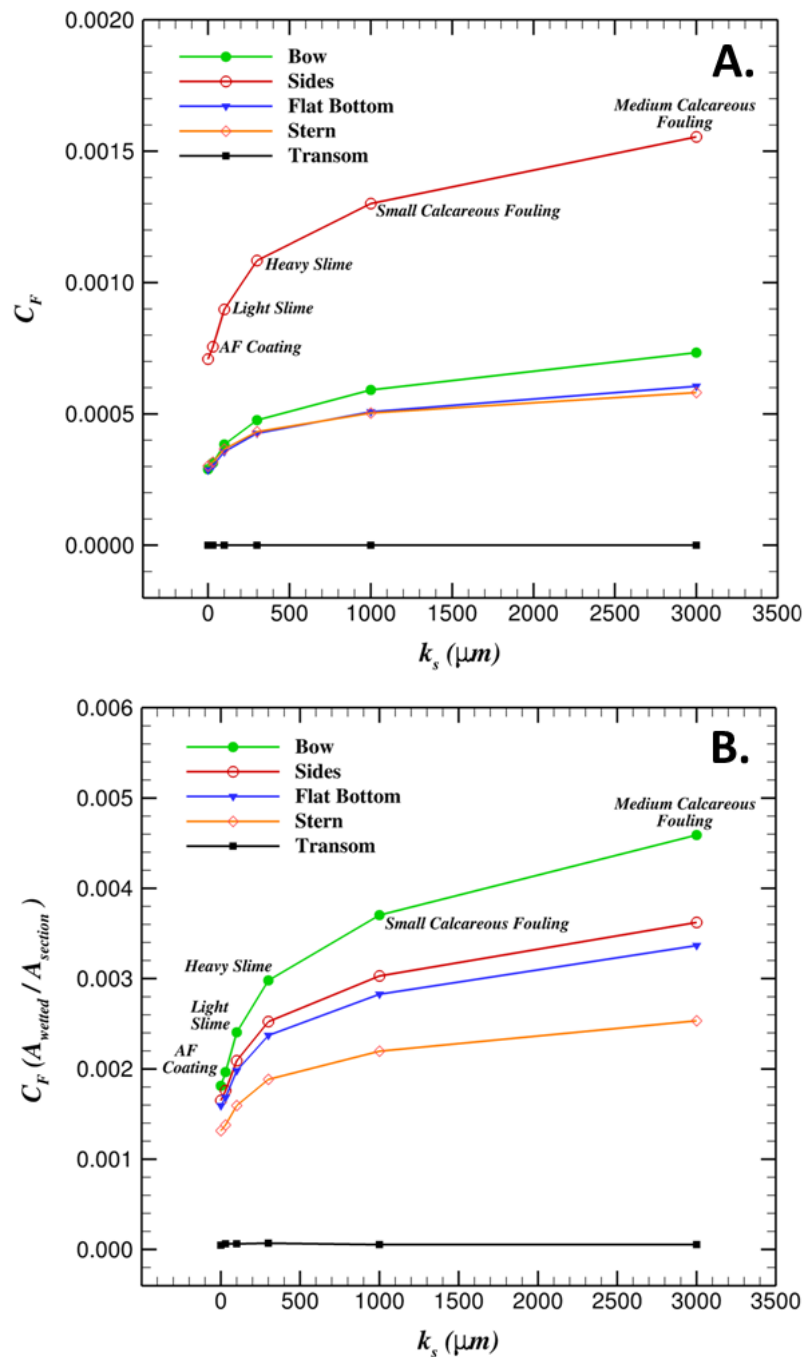


Fig.5: Frictional resistance (as C_F) associated with sections of the DTMB 5415 hull form, for varying levels of biofouling roughness (k_s). A. Absolute values of C_F for each section. B. Values of C_F scaled by the proportion of the hull wetted surface area accounted for by each section.

Frictional resistance generated by biofouling roughness on the sides of the hull is much larger than that for the other hull sections, while biofouling of the transom generates no, or very little, frictional resistance at all, Fig.5A. Biofouling of the bow, flat bottom, and stern produce comparable absolute values of C_F at a given level of k_s , Fig.5A. If, however, frictional resistance is scaled by the proportion of the wetted surface area of the hull accounted for by the section of interest, Fig.5B, the importance of biofouling of the bow to ship-wide frictional resistance stands out. On a per unit area basis, biofouling on the ship's bow has a greater impact on resistance than any of the other hull sections. As well, the rate of increase in C_F from one biofouling condition to another is greater for the bow than any other section; a given change in k_s results in a greater change in C_F for the bow than the other hull sections (Figure 5B). The rate of change in C_F with k_s for the sides and flat bottom are comparable once biofouling progresses beyond the light slime condition. These scaled results match predictions which may be drawn from the contour plots of local values of frictional resistance, Figs.2 and 3. Regardless of the biofouling condition (as represented by k_s), the ranking of the hull sections in terms of C_F remains bow > sides > flat bottom > stern > transom, on a per unit area basis, Fig.5B.

3.2 Heterogeneous Biofouling Case Study – Effect of Biofouling at the Waterline

The ability to divide the hull form into sections further enables the use of CFD to investigate the impact on total resistance of heterogeneous accumulation of biofouling roughness. In order to demonstrate this capability, an evaluation of the effects of biofouling at the waterline was undertaken. Accumulation of biofouling at a ship's waterline may be greater than for other sections of the hull due to a number of factors including the availability of light (affecting growth of macroalgae) and the presence of degraded or ineffective antifouling coatings (as a result of abrasion or other types of physical damage, or the harsh environment represented by the air-water interface). A k_s value equivalent to light slime ($k_s = 100 \mu\text{m}$) was applied homogeneously to the DTMB 5415 hull form. Biofouling of varying roughness was then applied to a zone on the hull form extending from the waterline to 1.83 m (6') deep, representing approximately 23% of the total wetted hull area. Total resistance C_T was estimated, and compared to corresponding values for biofouling distributed homogeneously across the hull (Figure 6). Results indicate that increasing roughness at the waterline from a k_s value equivalent to light slime to one equivalent to medium calcareous fouling increases ship-wide C_T by 10%, to a level comparable to that for a hull supporting homogeneous biofouling roughness equivalent to heavy slime (Figure 6).

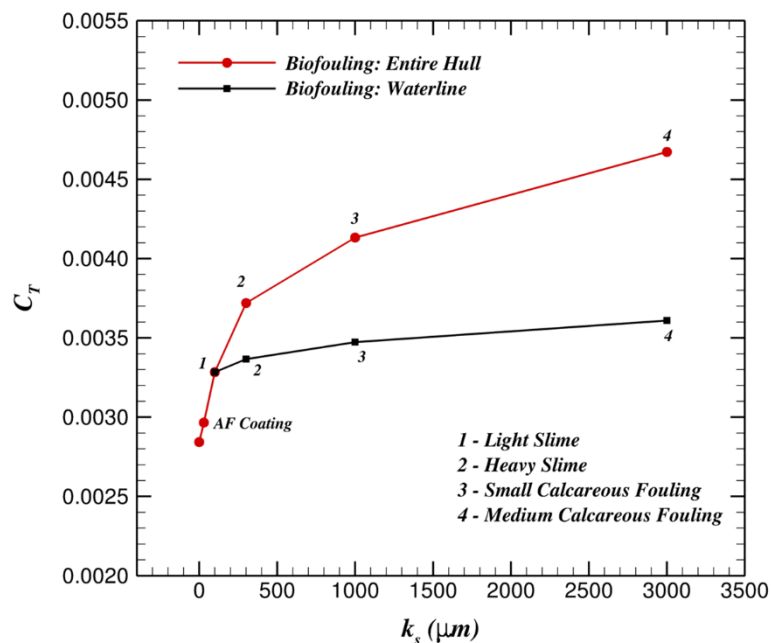


Fig.6: Effect of biofouling roughness (as represented by k_s) on the total resistance coefficient C_T , for biofouling at the waterline and over the entire hull.

3.3 Heterogeneous Biofouling Case Study – Effect of Cleaning Individual Hull Sections

The divided hull form and CFD can also be used to evaluate the benefits of hull cleaning. In this case, a k_s value equivalent to medium calcareous fouling ($k_s = 3,000 \mu\text{m}$) was applied homogeneously to the DTMB 5415 hull form. The impact of cleaning the bow, sides, flat bottom, or stern was then quantified by reducing the k_s value for that section to that for light slime, while keeping biofouling roughness on all other sections constant. Results parallel those for the evaluation of each hull section's contribution to frictional resistance when biofouling roughness is homogeneously distributed across the hull. Cleaning of the sides produces the greatest percentage reduction in C_T , Fig.7. When scaled, however, by the proportion of wetted surface accounted for by the cleaned section, cleaning of the bow results in the greatest reduction in resistance. Hundley (see Hundley and Tsai 1992) demonstrated a similar effect using ship powering trials paired with partial/sequential cleaning of the underwater hull, and Townsin *et al.* (1981) by computation.

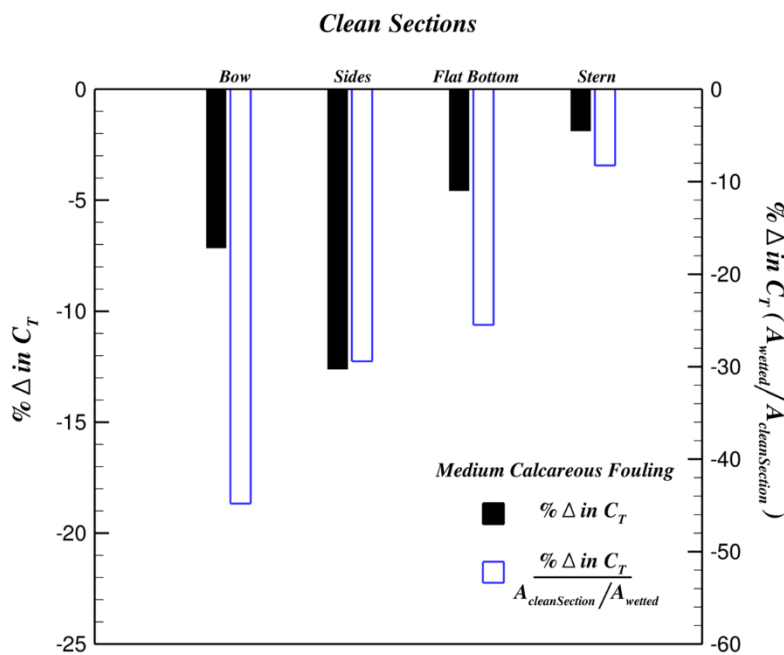


Fig.7: Effect of cleaning of individual hull sections on the percentage change (reduction) in total resistance C_T , and percentage change in C_T scaled by the proportion of the hull wetted surface area accounted for by each section. Cleaned hull sections are assumed to support biofouling by light slime.

3.4 Heterogeneous Biofouling Case Study – Effect of Sequential Cleaning of the Hull

The divided hull form and CFD were further employed to investigate the benefits, in terms of reduced resistance, of cleaning multiple sections of the hull in sequence. The change in resistance with the cleaning of additional hull sections was quantified for three values of k_s , corresponding to small ($k_s = 1,000 \mu\text{m}$), medium ($k_s = 3,000 \mu\text{m}$), and heavy calcareous fouling ($k_s = 10,000 \mu\text{m}$), applied homogeneously to the DTMB 5415 hull form. As with the case for cleaning of individual hull sections (see Section 3.3 above), hull cleaning was assumed to reduce k_s on the affected sections to that representative of light slime. For all biofouling conditions, total resistance C_T decreased with the cleaning of additional hull sections, Fig.8A. When scaled by the proportion of wetted hull surface area cleaned, however, the impact of cleaning on C_T decreased with each additional section, Fig.8B, reflecting the distribution of local skin friction observed previously, Fig.2 and 3. The greatest reduction in C_T (on a per unit area basis) was observed with cleaning of the bow, and no change in this proportional reduction was apparent beyond cleaning the bow and sides, Fig.8B. The pattern of change in C_T itself, with sequential

cleaning of hull sections, suggests that the pattern of benefits accruing from hull cleaning depends on the initial biofouling condition, Fig.9. For hulls fouled by small or medium calcareous fouling, cleaning of the bow and sides reduces C_T to a value equivalent to that of a hull supporting homogeneous coverage of heavy slime. For hulls fouled with heavy calcareous fouling this level of total resistance can only be attained after cleaning of the bow, sides, and stern, Fig.9.

4. Discussion

Previously, full-scale predictions of ship performance penalties associated with the accumulation of biofouling have been generated from limited ship powering trials, e.g. *Hundley and Tsai (1992)*, or have been calculated using boundary layer similarity law methods, e.g. *Schultz (2007)*, *Schultz et al. (2011)*, *Oliveira et al. (2018)*. Computational fluid dynamics methods, e.g. *Demirel et al. (2017)*, offer an alternative approach which allows the details of both the hull form, and the distribution of biofouling roughness across the hull, to be taken into account. Together, these features may allow for more accurate estimation of performance penalties. The ability to represent spatial variation in biofouling growth may be particularly important. Results presented above demonstrate that local values of frictional resistance differ across the hull, even for hydrodynamically-smooth hulls. These effects may be amplified, or diminished, if distribution of biofouling roughness is spatially correlated with the ship hull features that contribute to the variation in local skin friction in the smooth condition – for example, if more hydrodynamically-rough biofouling were to preferentially develop on the bow. Under such scenarios, representation of the biofouling on the entire hull by a simple mean roughness value could result in either under- or over-estimation of performance penalties. Methods such as that of *Monty et al. (2016)* may to some extent mitigate this problem.

The ability of CFD to account for spatial variation in roughness enables the evaluation of impacts to ship performance of either natural processes or control practices that generate heterogeneity in occurrence of biofouling (for example, see Sections 3.2-3.4 above). Increased biofouling of the waterline is a common problem that may be amenable to control through targeted in-water hull cleaning. Simulation of waterline biofouling for the DTMB 5415 hull form suggests that accumulation of medium calcareous fouling in this zone increases ship-wide C_T by 10%. The potential benefit of reducing this penalty by targeted cleaning can be estimated by comparing the cost of the cleaning effort to the value of the fuel saved through reduction in the resistance associated with the biofouling. Such an analysis may not be possible using similarity law methods that base their calculations on homogeneous roughness. Simulations of sequential hull cleaning indicate that full hull cleaning may not be required to recover acceptable vessel performance such as that associated with typical biofilm growth. CFD, however, also shows that the details of this result depend on the initial level of biofouling; the presence of greater biofouling roughness requires more of the hull (from bow to stern) to be cleaned to attain a given reduction in resistance.

Comparable results to those described above have been obtained from ship powering trials, e.g. *Hundley and Tsai (1992)*. Computational fluid dynamics, however, allows the simulation of a greater range of biofouling or maintenance scenarios without the expense of ship trials, the need to wait for a particular configuration of biofouling to develop on the hull, or the need to take a vessel out of service. Thus, CFD can form the basis for more efficient evaluation of the costs and benefits of alternative, novel, biofouling control strategies.

Acknowledgements

This research was funded by the Naval Surface Warfare Center Carderock Division as part of the Naval Innovative Science and Engineering (NISE) program under the direction of K. Michalis. Many thanks to J. Gorski, P. Chang, and S. Aram for providing useful insights and technical support. The rest of the team members from the project ‘Hydrodynamic Modeling of Biofouling-associated Roughness and Drag’ are also acknowledged.

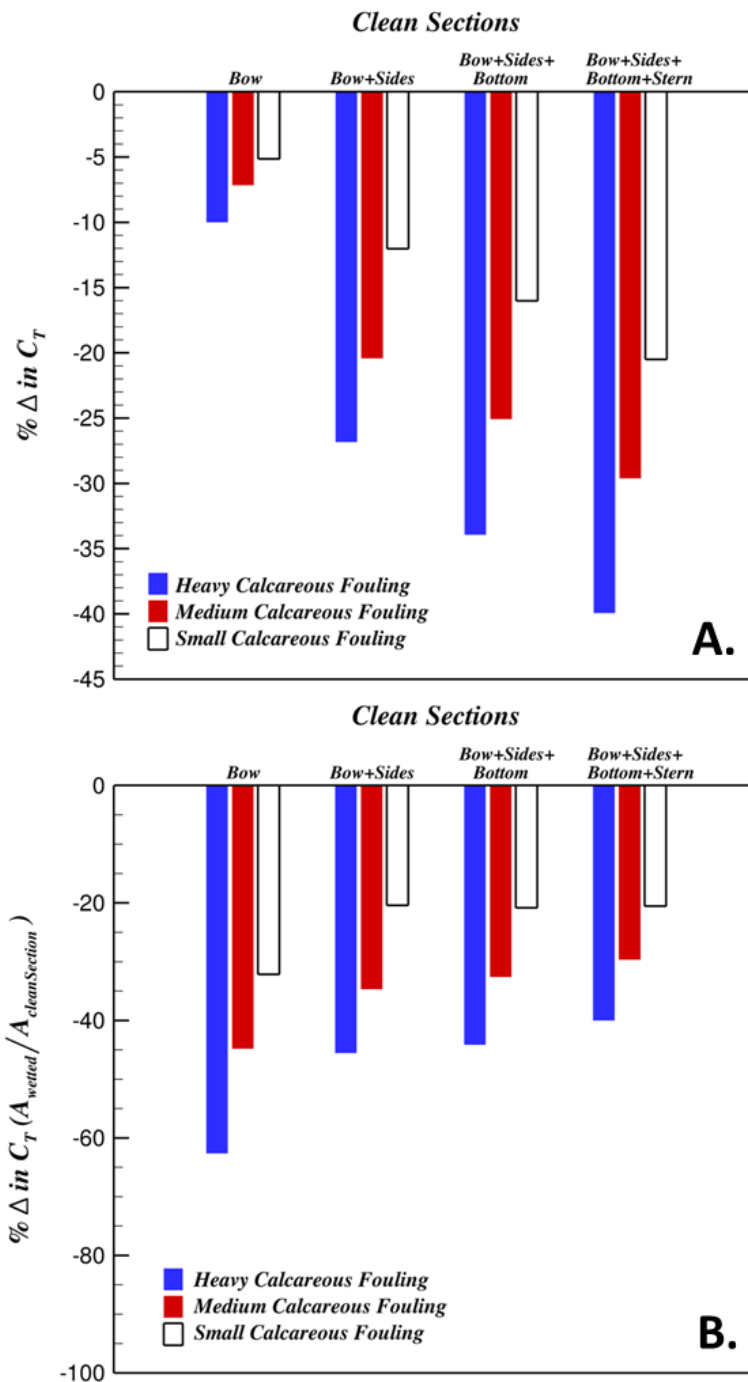


Fig.8: Effect of sequential cleaning of the hull on change in total resistance C_T . A. Percentage change (reduction) in C_T with cleaning. B. Percentage change (reduction) in C_T with cleaning scaled by the proportion of the hull wetted surface area accounted for by the cleaned section(s). Results plotted for three different levels of biofouling roughness. Cleaned hull sections are assumed to support biofouling by light slime.

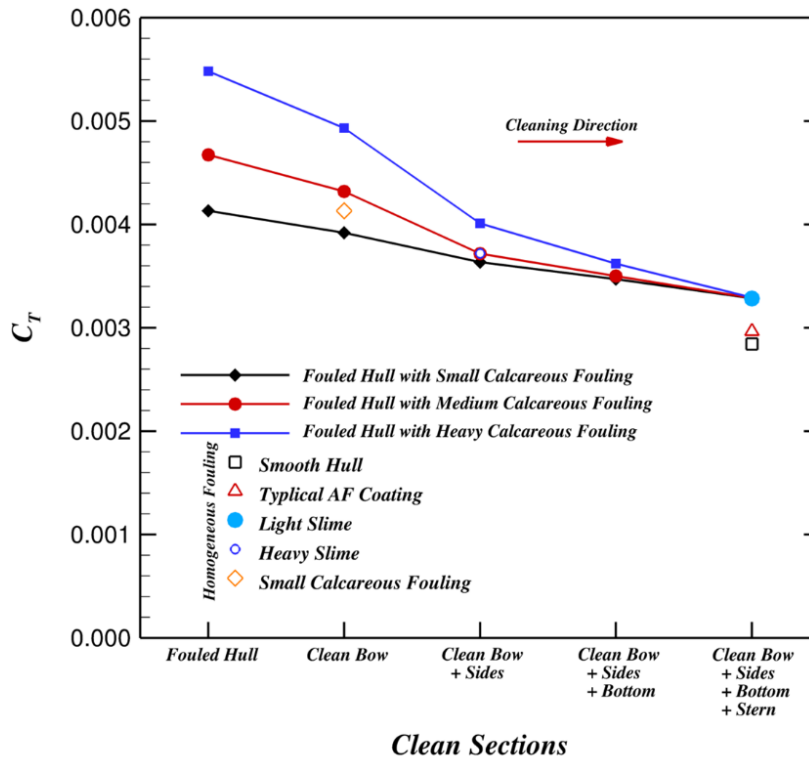


Fig.9: Effect of sequential cleaning of the hull on change in total resistance C_T , for three different levels of biofouling roughness. Cleaned hull sections are assumed to support biofouling by light slime.

References

- DAVIS, H.F.D. (1930), *The increase in S.H.P. and R.P.M. due to fouling*, J. American Society of Naval Engineers 42, pp.155-166
- DEMIREL, Y.K.; KHORASANCHI, M.; TURAN, O.; INCECIK, A.; SCHULTZ M.P. (2014), *A CFD model for the frictional resistance prediction of antifouling coatings*, Ocean Engineering 89, pp.21-31
- DEMIREL, Y.K.; TURAN, O.; INCECIK, A. (2017), *Predicting the effect of biofouling on ship resistance using CFD*, Applied Ocean Research 62, pp.100-118
- GRANVILLE, P. S. (1958), *The frictional resistance and turbulent boundary layer of rough surfaces*, J. Ship Research 2, pp.52-74
- HUNDLEY, L.L.; TSAI, S.J. (1992), *The use of propulsion shaft torque and speed measurements to improve the life cycle performance of U.S. naval ships*, Naval Engineers Journal 104(6), pp.43-57
- IZUBUCHI, T. (1934), *Increase in hull resistance through ship bottom fouling*, Zosen Kiokai 55
- KAN, S.; SHIBA, H.; TSUCHIDA, K.; YOKOO, K. (1958), *Effect of fouling of a ship's hull and propeller upon propulsive performance*, International Shipbuilding Progress 5, pp.15-34
- KEMPF, G. (1937), *On the effect of roughness on the resistance of ships*, Trans. INA 79, pp.109-119
- LARSSON, L.; STERN, F.; VISONNEAU, M. (2014), *Numerical ship hydrodynamics: an assessment of the Gothenburg 2010 workshop*, Springer
- LEER-ANDERSEN, M.; LARSSON, L. (2003), *An experimental/numerical approach for evaluating skin friction on full-scale ships with surface roughness*, J. Marine Science and Technology 8, pp.26-36
- LEWTHWAITE, J.C.; MOLLAND, A.F.; THOMAS, K.W. (1984), *An investigation into the variation of ship skin frictional resistance with fouling*, Trans. RINA 127, pp.269-284
- MONTY, J.P.; DOGAN, E.; HANSON, R.; SCARDINO, A.J.; GANAPATHISUBRAMANI, B.; HUTCHINS, N. (2016), *An assessment of the ship drag penalty arising from light calcareous tubeworm*

fouling, Biofouling 32, pp.451-464

MURPHY, A.K.; BARROS, J.M.; SCHULTZ, M.P.; FLACK, K.A.; STEPPE, C.N.; REIDENBACH, M.A. (2018), *Roughness effects of diatomaceous slime fouling on turbulent boundary layer hydrodynamics*, Biofouling 34, pp.976-988

OLIVEIRA, D.; LARSSON, A.I.; GRANHAG, L. (2018), *Effect of ship hull form on the resistance penalty from biofouling*, Biofouling 34, pp. 262-272

OLIVIERI, A.; PISTANI, F.; AVANZINI, A.; STERN, F.; PENNA, R. (2001), *Towing tank experiments of resistance, sinkage and trim, boundary layer, wake, and free surface flow around a naval combatant INSEAN 2340 model*, IIHR Technical Report 421

SCHULTZ, M.P. (2004), *Frictional resistance of antifouling coating systems*, Journal of Fluids Engineering 126, pp.1039-1047

SCHULTZ, M.P. (2007), *Effects of coating roughness and biofouling on ship resistance and powering*, Biofouling 23, pp.331-341

SCHULTZ, M.P.; BENDICK, J.A.; HOLM, E.R.; HERTEL, W.M. (2011), *Economic impact of biofouling on a naval surface ship*, Biofouling 27, pp.87-98

SHAN, H.; DELANEY, K.; KIM, S.E.; RHEE, B.; GORSKI, J.; EBERT, M. (2011), *Guide to NavyFOAM VI.0*, NSWCCD-50-TR-2011/025, Naval Surface Warfare Center Carderock Division, West Bethesda

SWAIN, G.; LUND, G. (2016), *Dry-dock inspection methods for improved fouling control coating performance*, J. Ship Production and Design 32, pp.186-193

TOWNSIN, R.L. (2003), *The ship hull fouling penalty*, Biofouling 19(Supplement), pp.9-15

TOWNSIN, R.L.; BYRNE, D.; SVENSEN, T.E.; MILNE, A. (1981), *Estimating the technical and economic penalties of hull and propeller roughness*, SNAME Trans. 89, pp.295-318

VARGAS, A.; SHAN, H. (2016), *A numerical approach for modeling roughness for marine applications*, ASME 2016 Fluids Eng. Division Summer Meeting, Washington DC

VARGAS, A.; SHAN, H. (2017), *Modeling of ship resistance as a function of biofouling type, coverage, and spatial variation*. 2nd HullPIC, Ulrichshusen

VISSCHER, J. P. (1927), *Nature and extent of fouling of ships' bottoms*, Bulletin of the US Bureau of Fisheries 43, pp.193-252

WHOI (1952), *Marine fouling and its prevention*, Woods Hole Oceanographic Institution, US Naval Institute, Annapolis, MD, USA

Reducing the Resistance of Container Ships with a FLUME® Roll Damping Tank

Bastian Marquardt, Alessandro Castagna, Amirhossein Rahimi, Aaqib Gulzar Khan, Johanna Marie Daniel, Christian Voosen, Nikhil Mathew, Hoppe Marine, Hamburg/Germany, ba.marquardt@hoppe-marine.com

Abstract

Hoppe Marine GmbH, an international specialist for anti-rolling tank systems having over 60 years of expertise, designs and outfits all kind of vessels with passive damping systems. The company is taking part in the Joint Research Project HERMes (Improvement of the Harmonic Excitation Roll Motion Procedure). This project is cooperation with the Hamburg Ship Model Basin (HSVA), the Hamburg University of Technology and the Peter Döhle Schiffahrts-KG. The project is founded by the Federal Ministry for Economic Affairs and Energy. Within the framework of this project, numerous model tests and CFD simulations have been carried out for a modern 9,000 TEU container vessel design with and without the passive roll damping system. Additionally full-scale measurements on a 5000 TEU container vessel of Peter Döhle Schiffahrts-KG are still ongoing. The aim of this project is the investigation of roll damping with respect to different roll damping devices and their influence on the roll motion behavior as well as resistance of the ship hull. New possibilities to quantify benefits of having a passive roll damping system aboard of modern vessel have been used and developed. This paper focusses on the investigation of influences of a passive roll damping tank on the reduction of ship resistance and consequently the possible fuel savings. The advantage of a passive roll damping tank over conventional bilge keel setups will be shown through the example of a modern container vessel.

1. Introduction

Passive roll damping systems are distributed by Hoppe Marine under the brand name FLUME® Roll Stabilization Systems. The main purpose of installing a FLUME® Roll Stabilization System is the reduction of roll motion and the associated accelerations aboard a vessel. This is consequentially leading to more crew comfort & safety and a reduction in forces, increasing the cargo capacity and reducing the risk of cargo damage and loss. However, the reduced roll motions due to the FLUME® tank also have a direct influence on the resistance of the vessel and this influence is quantified in this paper. Beforehand a short explanation about the different damping possibilities and the functionality of a FLUME® tank is given.

Generally, the natural damping of a vessel for the roll degree of freedom is low and thereby necessitating the use of additional equipment to enhance the roll damping. The most common way to achieve the additional roll damping is the use of bilge keels. However, the biggest disadvantage of the bilge keels is that they have a negative effect on the resistance of the vessel and usually offer a marginal roll reduction of 5-20% only. Active devices such as fin stabilizers can be used to achieve a much higher damping, but they are quite expensive in purchase, operation and maintenance, making them irrelevant for container vessels or commercial shipping in general. Since, the FLUME® Roll Stabilization System is passive and has no moving parts, no maintenance and operational costs occur. Moreover, a FLUME® Roll Stabilization System does not increase the resistance and at the same time there is a significantly higher reduction in roll of the vessel. This roll reduction is usually 30-70% in resonance and depends on the design and the operational conditions of the vessel. Parametric roll can be even completely eliminated.

2. FLUME® Roll Stabilization System

The FLUME® Roll Stabilization System is essentially a tank running across the beam of the ship containing ballast water that can flow from one side to the other, driven by the roll motion of the

vessel itself. The damping effect is based on the existence of a travelling wave that has a phase lag with respect to the roll motion of the vessel, providing a counteracting moment. Ideally the water motion has a delay of a quarter cycle behind the roll motion of the ship, which itself is delayed about a quarter cycle behind the wave excitation at resonance, *Journée and Massie (2001)*. Thus, the liquid in the tank will directly oppose the upward buoyant force of the wave. This is reducing the roll motion as shown schematically in Fig.1.

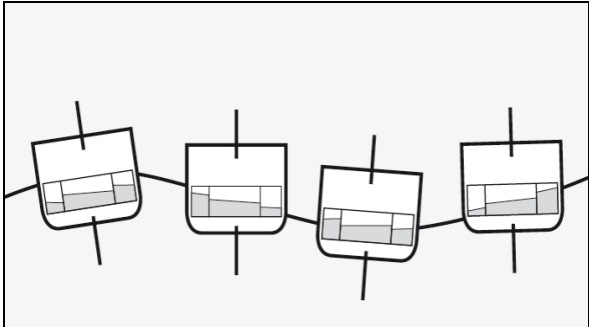


Fig.1: FLUME® tank working principle

The liquid level inside the tank can be changed in order to tune the tank to the different loading conditions of the ship. The internal wave is travelling faster with higher water levels, thus a tank must be designed and operated in a way that the water depth and consequently travelling wave speed is in accordance with the roll period of the vessel. This ensures that the roll resonance period of the tank is the same as that of the ship for the optimum damping effect. In theory a FLUME® tank can be installed anywhere on the vessel. However, there are some optimum positions that minimize the impact on the cargo intake and the general arrangement of the vessel thereby making the installation more economic and efficient. These optimum positions are shown in red in Fig.2. FLUME® tanks have been installed or investigated aboard different container vessels in all these positions by Hoppe Marine. The tanks can be installed for a newbuilding and can also be retrofitted.

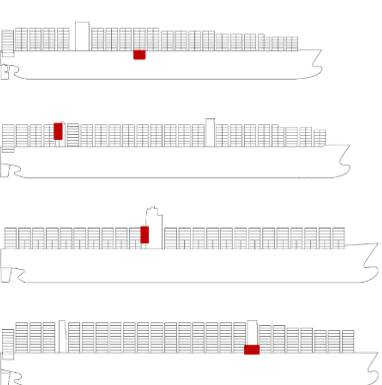


Fig.2: Optimum positions for installation



Fig.3: FLUME Tank on a modern Container Ship

Fig.3 shows a practical FLUME® Roll Stabilization System installation aboard a modern 15500 TEU container vessel. Hoppe Marine has designed and installed systems on 52 modern container vessels varying from 2100 TEU to 20000 TEU in size. The FLUME® tanks have proven to be a very effective solution especially for ULCVs with a large variation in GM values in many operational scenarios.

3. Influence of FLUME Tank on Ship Resistance

The main purpose of a FLUME® tank on container vessels is to reduce the roll motions in order to increase the vessel capacity, comfort and safety. However, this reduction in roll motion reduces the

resistance of the vessel as well. The reduction in roll and resistance of the 9000 TEU container vessel that was especially designed for the research project was quantified in a specialized model test program. These model tests were carried out by one of the partners of the joint research project, the Hamburg Ship Model Basin (HSVA). The model was self-propelled and equipped with bilge keels along with the FLUME® tank. Four different bilge keel sizes were tested: 0 mm (no bilge keel), 200 mm, 400 mm and 800 mm. Within this paper, only the results of no bilge keels and 400 mm bilge keels in combination with the FLUME® tank are presented. The ship model installed with the FLUME® tank in the area of the deckhouse is shown in Fig.4.

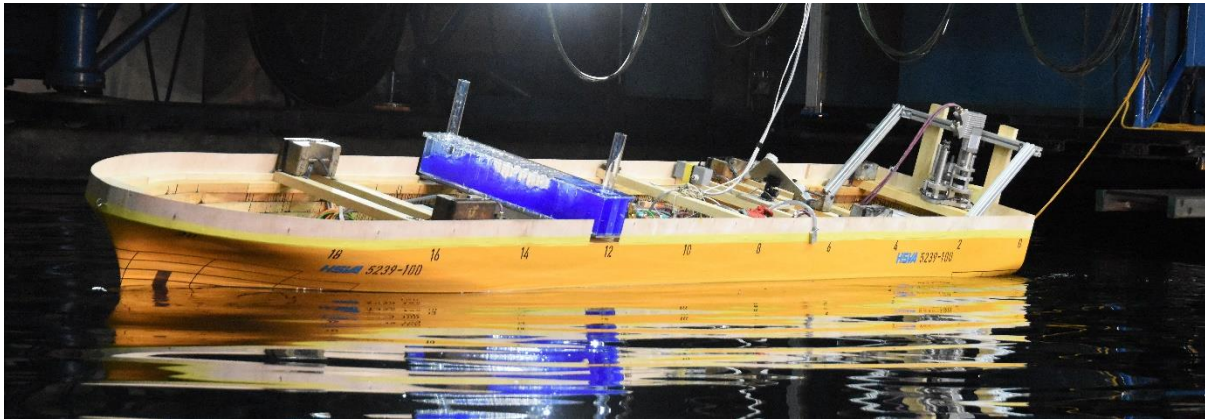


Fig.4: Model of the 9000 TEU Container Vessel

The model tests conducted are different from usual seakeeping model tests in the sense that the ship model was not excited by regular or irregular waves. Instead a gyroscopic excitation machine that oscillates the model at a given frequency and amplitude has been used for these tests. The water surface is flat and undisturbed prior the tests. The application itself is called HERM test and was developed as a part of the research project in a cooperation between HSVA and Hamburg University of Technology (TUHH). The advantage of using the HERM test rather than tests in regular or irregular waves is that the roll degree of freedom can be studied independently without the influence of other degrees of freedom. Additionally this procedure offers the possibility to repeat tests with almost absolutely identical environmental and physical conditions, offering a great opportunity to compare different scenarios as e.g. the influence of different bilge keel sizes.

In this model test program different excitation moments are generated corresponding to different wave heights at 4 different test speeds (0.0, 7.0, 14.0 and 21.0 kn). The vessel was tested always at the design draft of 13.0 m and with two different GM values of 2.0 m and 7.0 m. The results presented here correspond to a stability of 7.0 m and a ship speed of 14.0 kn. The excitation period was always set to the natural roll period of the vessel leading to resonant roll only.

The roll angle is a direct result from the measurements and is not subject to any scaling laws, why it can be directly used for the results of the full scaled ship. The roll damping coefficients are estimated based on the conservation of energy approach over one roll period, *Handschel and Abdel-Maksoud (2015)*, but it is not further important for the results shown in this paper and therefore only mentioned for completeness. The delivered power is calculated by the mean over one steady excitation level (constant roll amplitude) and extrapolated to full scale in order to correct the overestimated friction from the model. The main problem for the precise transmission of the power to full scale is the different propulsion point. Therefore, from the Froude extrapolated thrust difference between the HERM test and calm water test the additional resistance is calculated taking the thrust coefficient into account. The full scale delivered power is estimated using the open water diagram from the 9000 TEU container vessel estimated from separately conducted propulsion tests, *Daniel (2018)*.

The estimation of the corresponding wave height from the HERM test excitation moment is based on the calculation of an effective wave slope (EWS). This method was already developed by William

Froude and is fairly valid for longer beam sea waves, *Tupper (2013)*. The EWS method is seen to be sufficient to give a good correlation between the moments generated from the HERM application and a corresponding regular beam sea wave.

The results from the model tests that are presented here essentially focus on the comparison of the ship's performance with and without the FLUME® tank. Fig.5 shows the relationship between roll amplitude and wave height, Fig.6 shows the relationship between delivered power and roll amplitude, and Fig.7 shows the relationship between delivered power and wave height, all with and without the FLUME® tank at a speed of 14 kn.

From these results the influence of the FLUME® tank becomes clearly visible. Fig.5 is indicating that the reduction in roll angles for the smaller wave heights (< 3.0 m) is more than 80%. This reduction is around 60% for higher wave heights and is still 40% for largest wave heights of 6.5 m. Fig.6 shows the delivered power as a result of the roll angle of the ship. There is no difference with and without the FLUME® tank. This is because for a given value of roll amplitude, the amount of delivered power is dependent on the resistance created by the hull only. If that certain roll amplitude is occurring with a roll damping tank being present or not has no influence on the roll motion pattern. The purpose of the FLUME® tank is to reduce the roll motion, but when the roll motion is fixed, the delivered power shall remain unchanged for a given draught. During all tests the draught of the ship was same, even when the FLUME® tank was not active, an equivalent weight was installed on the model to have always the save immersion of the hull for better comparison.

If Figs.5 and 6 are compared as done in Fig.7, it can be seen that the resistance of a rolling ship can be reduced significantly, when it is equipped with a FLUME Tank. For the regular waves, at a moderate wave height of 3.0 m the FLUME® tank reduces the delivered power by about 30%.

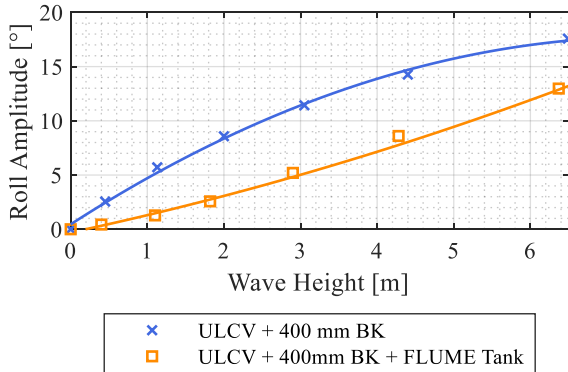


Fig.5: Roll Amplitude vs Wave Height at 14 kn

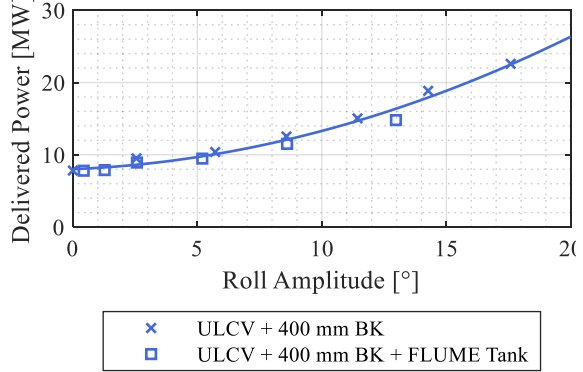


Fig.6: Delivered Power vs Roll Amplitude at 14 kn

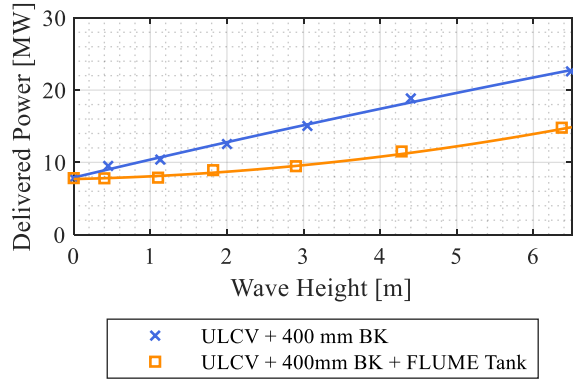


Fig.7: Delivered Power vs Wave Height at 14 kn

Another major task of the research project was to get these results confirmed in reality, by investigating on board measurements taken from the M/V JOGELA (Loa=255.40m; 5000 TEU).

Unfortunately the measurements have been partly corrupted for some data during the 2 years of measurement, thus no clear picture could be yet concluded due to the leak of data. Hoppe Marine is now constantly collecting data and works on a concept to prove the benefits also for a full-scale vessel.

4. Comparison of the Influence of Bilge Keels and FLUME Tank on Ship Resistance

The results from the HERM model tests indicated that the FLUME® tank reduce the roll motion of the ship and at the same time this reduced roll motion leads to a decrease in the resistance of the vessel. The common method to reduce the roll motion of the ship is the installation of bilge keels. Bilge keels dampen the roll motion of the ship to a certain extent, but at the same time they increase the overall resistance of the ship.

It is not possible to achieve a similar amount of roll damping with bilge keels as that of a FLUME® tank, unless their size is huge which would mean that they increase the ship resistance drastically. When the FLUME® tank is installed aboard a vessel there is an additional load on the vessel which increases the draught slightly. This increase in the draught shall also increase the resistance of the vessel and thus it becomes imperative to analyze the phenomenon.

A full-scale Computational Fluid Dynamics (CFD) analysis was done by the Hamburg University of Technology in order to evaluate the additional resistance due to the bilge keel and the FLUME® tank. The analysis was done for the 9,000 TEU container vessel at a speed of 21 kn and a design draught of 13 m. The presence of the FLUME® tank increased the draught of the ship by 0.1 m. The additional immersion due to the weight of the tank was considered as a parallel immersion. Here it is not considered, that in reality in many cases the additional water in the FLUME® tank compensates some of the ballast water that would be used otherwise.

The results are shown in Figs.8 and 9. Fig.8 shows the variation of delivered power with different trim angles. The ship has a length of 312.0 m, therefore a trim angle of 0.25° means 1.5 m trim forward. From this result it is determined that on average for all the considered trim angles, the 400 mm bilge keels requires an additional power of 0.9 %. Even though the FLUME® tank generates an additional immersion, it still requires 0.3 % less power than the bilge keels, for the case that the vessel is always sailing with 21.0 kn. Fig.9 shows the variation of delivered power over draught at 21 kn. It can be seen that the additional resistance offered by the 400 mm bilge keels remains almost independent of the draught. It is assumed that this will be also the case for the other trim angles that might occur.

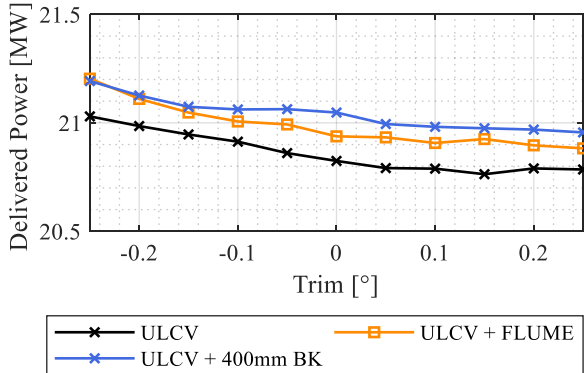


Fig.8: Resistance of a 9000 TEU vessel at 21 kn with & without bilge keels and FLUME® tank at different trim

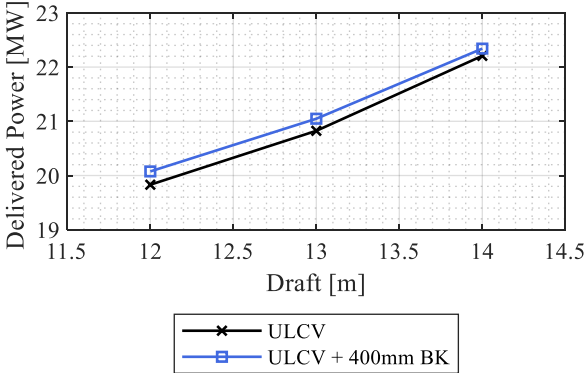


Fig.9: Resistance of a 9000 TEU vessel at 21 kn with and without bilge keels at different draught

5. Commercial Evaluation: Reduced Fuel Consumption due to Reduced Roll Motions

In order to quantify the fuel saving potential of a FLUME® tank two things need to be considered. The magnitude a vessel is rolling at sea during its entire operation profile and the roll reduction that

can be achieved with a FLUME® roll damping tank for all these occurring roll scenarios. Fig.10 shows the evaluation of the quantity of rolling of M/V JOGELA for different roll RMS windows of 0.5° during 1.5 years of operation. It can be seen that the vessel is facing significant roll (RMS below 0.5°) almost on a daily basis. **Error! Reference source not found.** as well gives for different windows of roll RMS the probability of occurrence. These windows are defined according to the roll reductions that can be expected for the different occurring magnitudes of roll, in case a FLUME® tank is present. The possible power savings have been estimated from the results of the HERM model tests, Fig.6, for these different windows. Multiplying these numbers for the possible savings with the probability of occurrence of each of the defined windows leads to the final power savings the vessel could have, in case a FLUME® tank is installed. The sum of these savings gives the overall saving of 1.4%, but the additional resistance due to increase of deadweight is not yet considered.

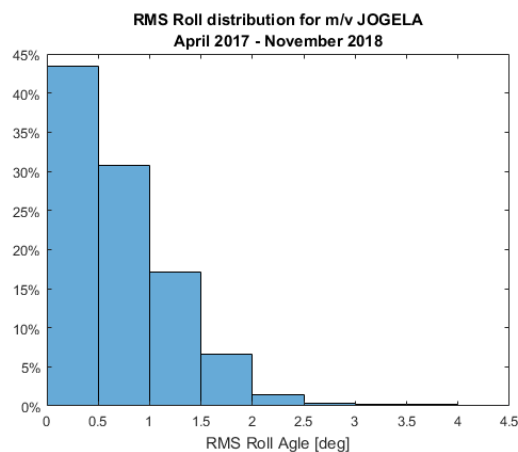


Fig.10: Distribution of RMS roll angles of the 5000 TEU CV M/V JOGELA

Table 1: Distribution of roll angle occurrence and according savings at these roll scenarios due to FLUME® tank

RMS	probability of occurrence	Roll Red.	Possible Power Savings	Savings Power (considering occurrence)
0.0°-0.5°	43%	0%	0.0%	0.0%
0.5°-1.5°	46%	40%	1.4%	0.9%
1.5°-3.0°	10%	60%	4.0%	0.4%
>3.0°	1%	30%	5.1%	0.1%
Avg. Savings				1.4%

The fuel costs of a modern 9000TEU Container vessel are assumed to be approximately 16 Mio USD per year. Consequently the 1.4% less engine power required lead to savings of 224,000.00 USD. Considering at the same time the resistance increases due to an increase in deadweight for all cases the vessel is sailing about 0.6%, because the FLUME® tank is constantly in operation, still 0.8% less engine power are required and the savings are still 128,000.00 USD.

Other potential savings result from the absence of bilge keels presented in section 4. In case an innovative vessel design makes use of a roll damping tank only and dispense on bilge keels the required power is further reduced. In the following commercial evaluation the additional savings are only considered for the 43% of operation time (see Table 1) where the vessel was rolling with an RMS value below 0.5° . As the absence of the bilge keels has still a positive influence on the power for the significantly rolling vessel this is a conservative approach, and will lead to a reduction of 1.7% in case the draft increase due to the FLUME® tank is considered throughout the entire operation time of the vessel. Assuming that the additional weight of the FLUME® tank is compensated by the absence of other ballast water, even 2.3% power savings are possible.

It is uncontested that these numbers vary for different vessel sizes and operation profiles, but it shows that an innovative roll damping concept, making use of a FLUME® tank instead of bilge keels offers vessel owners the possibility to save between 272,000.00 USD and 368,000.00 USD per year for the example given of a modern 9000 TEU container vessel.

6. Other FLUME Tank Benefits

Although these investigations show that the installation of a roll damping tank has a positive effect on the fuel consumption of a vessel, it is only one of many positive effects leading to a much more effective vessel. The other major effects making a FLUME® tank a “must have” on each modern container vessel are:

Commercial benefits:

- Additional container intake (2%-15% per bound, depending on container weight, ship size and route)
- Fewer restows (50%-75% in first harbor of west bound, other scenarios were not investigated)
- Reduced fuel consumption and reduced exhaust emissions per container transported
- Reduction of cargo damage and insurance claims
- Optimization of route planning

Comfort & Safety benefits:

- Reduced risk of losing cargo
- Elimination of parametric roll scenarios
- Increased crew comfort

The installation of a FLUME® tank leads to a more efficient and environment friendly vessel. Investigations have shown that the ROI (Return of Investment) is less than a year for many vessels, even if the tank is retrofitted.

7. Classification

For the benefit of fuel saving the classification society does not need to accept the FLUME® tank in the vessel approval. However, the most valuable benefit for container vessels is the cargo boost possibility resulting from reduced lashing forces. Some classification societies have a provision in the calculation of container lashing forces. There is a reduction factor (f_{ART}) multiplied to the maximum roll angle similar to the coefficient used for bilge keels (f_{BK}). The value of f_{ART} is determined performing hydrodynamic calculations on the tanks using model tests or CFD followed by scatter data evaluations.

References

ABDEL-MAKSOUND, M. (2010), *Seakeeping of Ships*, Lecture Notes, TU Hamburg

DANIEL, J.M. (2018), *Influence of a FLUME tank on the roll damping of a container ship in interaction with different sized bilge keels*, TU Hamburg

HANDSCHEL, S.; ABDEL-MAKSOUND, M. (2015), *Improvement of the Harmonic Excited Roll Motion Technique for Estimating Roll Damping*, TU Hamburg

JOURNEE, J.; MASSIE, W. (2001), *Offshore Hydromechanics*, TU Delft

TUPPER, E.C. (2013), *Introduction to Naval Architecture*, Butterworth & Heinemann

ISO 19030 2.0: How to Improve

Sergiu Paereli, Jotun, Sandefjord/Norway, sergiu.paereli@jotun.com
Manolis Levantis, Jotun, Athens/Greece, manolis.levantis@jotun.com

Abstract

Introduction of ISO 19030 – measurement of changes in hull and propeller performance to the marine industry, contributed significantly in realizing the importance of performance monitoring and the huge potentials on fuel and CO₂ emissions savings that can be achieved. Although the standard is a powerful tool for all relevant stakeholders, there are possibilities for further improvements. This paper describes some approaches suggested for better weather filtering. Among these are: smoothing true wind speed data before filtering for it; accounting for variability in true wind speed; modifying the cut-off value, aggregation of true wind speed data, using wave data in performance analysis filter.

1. Introduction

ISO 19030 has been playing an important role in the marine industry for almost 3 years now. Its publication in 2016 has made it possible for all stakeholders to solve their one of the biggest challenges – lack of measurability. The standard has contributed to the alignment of the parties with regards to not only using a practical approach of quantifying changes in hull and propeller performance, but also reducing costs and GHG emissions. Observations show that there is a clear tendency towards higher investments in premium technologies related to improvement in hull and propeller performance. It seems that the decisive factors determining the change in stakeholders' mindset have been predictable accuracy levels of the savings quantification and transparency of the method.

The majority in marine industry are nowadays collecting data from their ships and, in a way or another, monitoring the performance of the latter. The way in which vessel performance monitoring is done has evolved during the years and today continuous monitoring seems to be more and more popular as it allows people to first and foremost make faster decisions.

Continuous monitoring, as its name suggests, refers to regular collection of data from the ship, and then processing of this data. ISO 19030 describes very well the steps of continuous ship data analysis, among these data acquisition, storage, preparation (here referring mainly to filtering, validation and correction), and calculation of performance indicators. Although, the standard discusses practical and rather simple guidelines, ship performance monitoring, as such, is a complicated job. Challenges come with the need of data preparation for analysis and are mainly related to changes in ship operational profile (speed, loading condition, etc.) and changes in environmental conditions (wind, sea state, currents, etc.). To isolate changes in hull and propeller performance, two main approaches can be considered. It is either that one estimates the contribution of changes in other factors and corrects for these, or data should be filtered for comparable conditions. ISO 19030 describes both approaches.

As mentioned in the standard, variation in loading condition is accounted for by adjusting vessel model (speed-power reference curves). Wind effect can be estimated using wind correction scheme or data can be simply filtered for bad weather (wind and sea state). Wind correction is a good approach but additional data, such as wind tunnel test results, would be needed. These are not always available for analysis, or not meaningful (e.g. for container vessels). Therefore, the simplest approach in data preparation, is to filter the latter for similar conditions. This is, of course, to be done after removing outliers and validation of the dataset.

In ISO 19030 it is suggested that data is filtered for wind speed so that only periods when true wind speed is below 7.9 m/s (BF 4 or 16 knots) are considered for analysis. As practice shows, this condition eliminates a significant amount of data from analysis. It has been found that on average about 40% of data is filtered out.

There is no doubt that the higher the true wind speed is encountered by the vessel, the bigger the impact on apparent performance is. Nevertheless, it remains a question whether the 16 knots standard cut-off would be ideal. This paper discusses whether the proposed cut-off is justifiable and suggests alternative ways of filtering data for bad weather.

2. In-service data

Weather is one of the main factors influencing vessels performance. It does not influence the in-service performance as such, but rather operational performance. Nevertheless, if one is after accurately quantifying changes in hull and propeller performance in time, he needs to somehow deal with variations in weather. There are several aspects one would ideally investigate, among these the impact of wind and sea state (waves and swell). Unfortunately, as of today there are no commonly accepted devices that could be installed on a vessel in service and that could provide sea state data. The latter, though, can be obtained from for example noon reports (crew observations). Another source of sea state data could be observations and model data provided by research institutes. These data are, however, available on a relatively low frequency and resolution and the accuracy level is questionable. The common approach today is to rather focus on wind readings and apply filters on true wind speed. In this way it is expected that wave effects will, to a certain extent, be eliminated as well, since waves development is generally not as spontaneous as wind development.

In this paper, an evaluation of a dataset from a VLCC was performed and the goal was to better understand the impact of filtering data for true wind speed on the accuracy of the performance values (speed deviation). Chosen vessel was equipped with a high frequency data logger, receiving and saving data every 15 seconds. All necessary parameters for speed deviation computation - speed through water, shaft power, draft aft and fore – were logged. In addition, speed over ground, propeller rpm, fuel consumption and wind speed and direction were available, so that data consistency could be concluded to be good and necessary wind filtering to be applied.

From the whole dataset, only the first year of data (after dry-docking) was isolated for analysis purposes. This has been done to ensure stable speed deviation throughout the whole period. Before speed deviation computation, data has been filtered using a basic performance analysis filter. This was based on a certain speed range, shaft power range and mean draft range. In addition, for every simulation, a filter on true wind speed was applied and the impact of this filter on the final speed deviation over a one-year period has been evaluated.

Simulation 1: In Simulation 1 true wind speed has been filtered as per ISO 19030. All periods for which true wind speed was higher than 16 knots have been eliminated from analysis. Calculated speed deviation points and their average are shown in Fig.1.

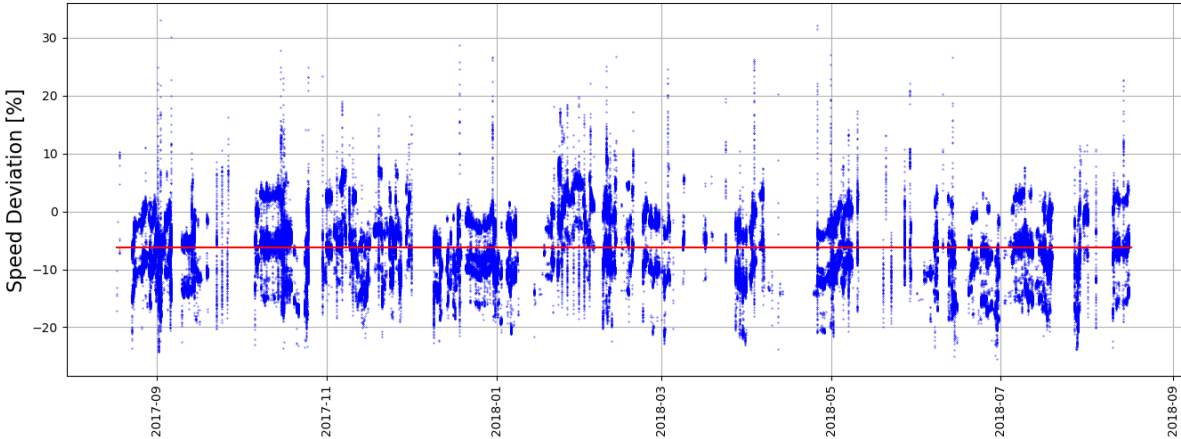


Fig.1 Speed deviation (blue points) and flat average (red line)

The first observation made was the amount of data left for analysis after applying the filter on the initial dataset – 25.8%. This value lies within normal range, as usually after filtering data for speed, shaft power, loading condition and wind speed, there is 20-35% data left for analysis. No significant fluctuations have been noticed in speed deviation and it is concluded to be stable throughout the whole period. In table 1 several statistical parameters describing the resulted performance values are presented. These are mean, standard deviation, mean absolute deviation (MAD).

Table 1: Speed deviation statistics for Simulation 1

Mean	Standard deviation	Mean absolute deviation (MAD)
-6.2	4.60	3.58

Mean is the measure of central tendency. The next two refer to statistical dispersion and talk about data variability. The reason of looking at both measures describing scatter is the fact that unlike standard deviation, mean absolute deviation is a robust measure of scale which means that it is less affected by outliers. “Favorable” standard deviation can be achieved not only by low variance in data, but also changes in “population” size. This is important as by applying difference filters on the same initial 1-year dataset, one could be left with different amount of data for computation of performance value. Simulation 1 is taken as reference and the results of the following simulations are to be compared with results presented in Table 1.

Simulation 2: In this simulation, the same cut-off value for true wind speed as suggested in ISO 19030 has been used. The difference from Simulation 1 is that before filtering data for wind, a very simple low pass filter has been used for smoothing the signal – moving average. When setting the 16-knot threshold on the raw true wind speed data, one aims at eliminating “bad” weather (anything strictly higher than BF4) from analysis. However, it remains a question whether values around this threshold but slightly above or below are really affecting the final performance values. In Fig.2 a couple of examples of these doubtful situations are given.

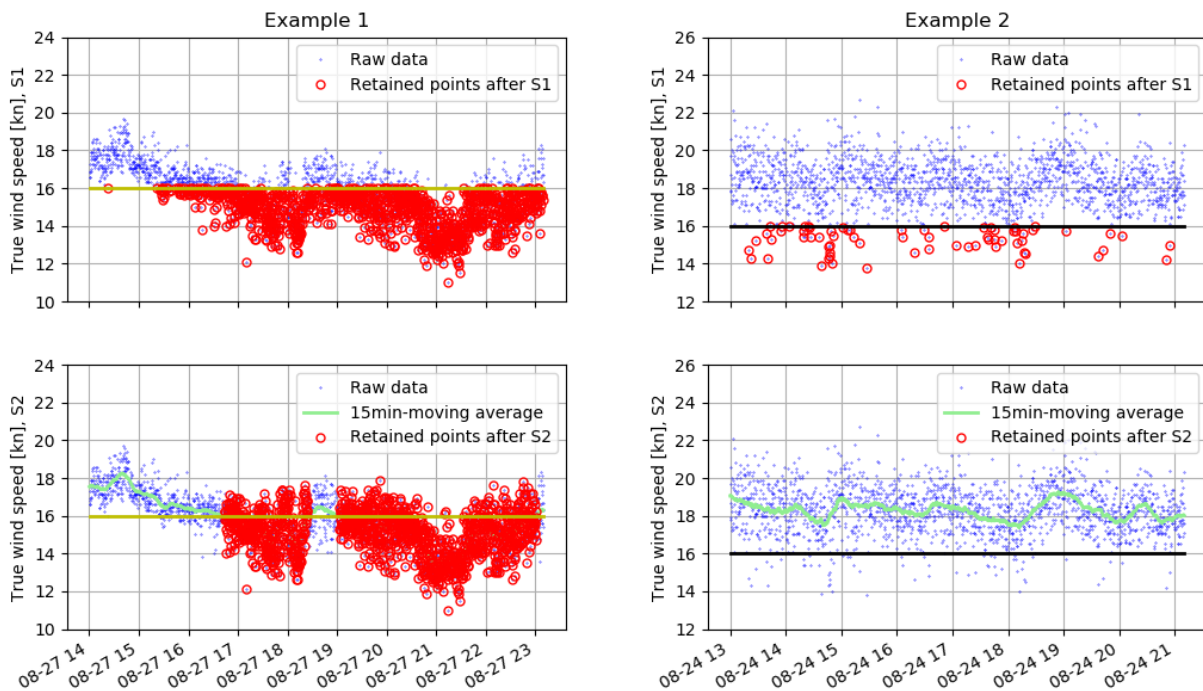


Fig.2: Differences between filters in simulations 1 and 2 (15min moving average)

In example 2 from Fig.2 one could see that some data points that lie within the 16-knot threshold are kept for analysis and the question is whether they should. Wind trend is clearly higher than accepted cut-off value and unless values between BF4 and BF5 throughout the whole period are accepted, it seems that these points can increase the uncertainty of the analysis.

On the other hand, as shown in example 1, when the general wind trend is below and/or very close to the cut-off value, one might consider keeping for analysis those data points that are slightly above the threshold.

Several scenarios have been considered in Simulation 2: 15-minute –, 1h –, 6h – and 1 – day moving average for true wind speed. These are referred to as S2-1, S2-2, S2-3 and S2-4. The amount of data left for analysis in Simulation 2 is shown in Table 2. In Table 3 speed deviation statistics are presented.

Table 2: Data left upon filtering in scenarios 1-4 from Simulation 2.

Window size	Data left for analysis
15min	25.6%
1h	25.6%
6h	25.7%
1day	25.6%

Figs.3 to 5 give more examples of impact of true wind speed smoothing.

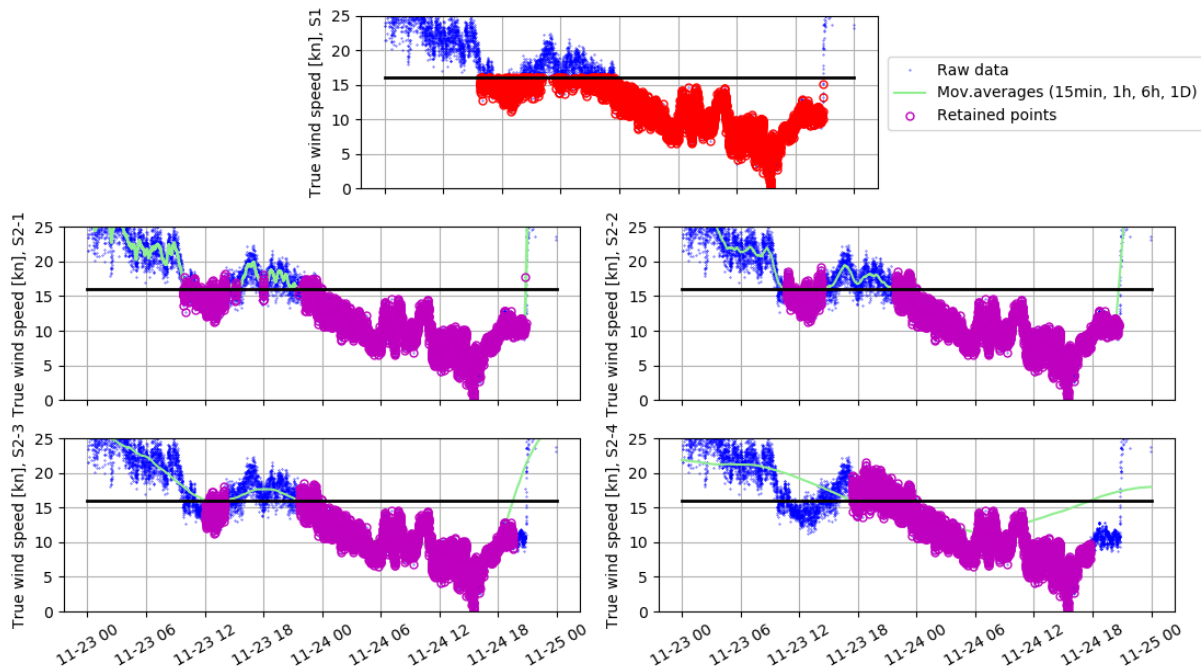


Fig.3: Example 1 - Differences between filters in simulations 1 and 2 (all scenarios: S2-1, S2-2, S2-3 and S2-4)

No big differences in neither amount of data left for analysis, nor statistical parameters have been found and it is therefore difficult to judge whether evaluated filters have any positive impact on the performance analysis precision. Nevertheless, Figs.3 to 5 point again to the idea that it is probably not always meaningful to filter raw true wind speed data but rather first apply a low pass filter on it. There is a significant amount of data around the threshold of 16 knots that could potentially be part of performance analysis if not filtered out.

Table 3: Speed deviation statistics for Simulation 2

Window size	Mean	Standard deviation	Mean absolute deviation (MAD)
15min	-6.2	4.60	3.57
1h	-6.2	4.59	3.57
6h	-6.1	4.56	3.54
1day	-6.2	4.67	3.62

From all three figures, but especially Fig.3, it could be concluded that applying 1-day moving average on true wind speed does not make much sense. Although, over filtering is not concluded, even if somewhat expected, applying 1-day moving average on wind does not make it possible capturing shorter-term fluctuations. Similar percentage of filtered data can therefore be explained by the fact that more data is retained when smooth transitions from “bad” weather (BF>4) to “good” weather or vice-versa occur and less data retained when moving average has a highly negative or highly positive slope around 16-knot threshold.

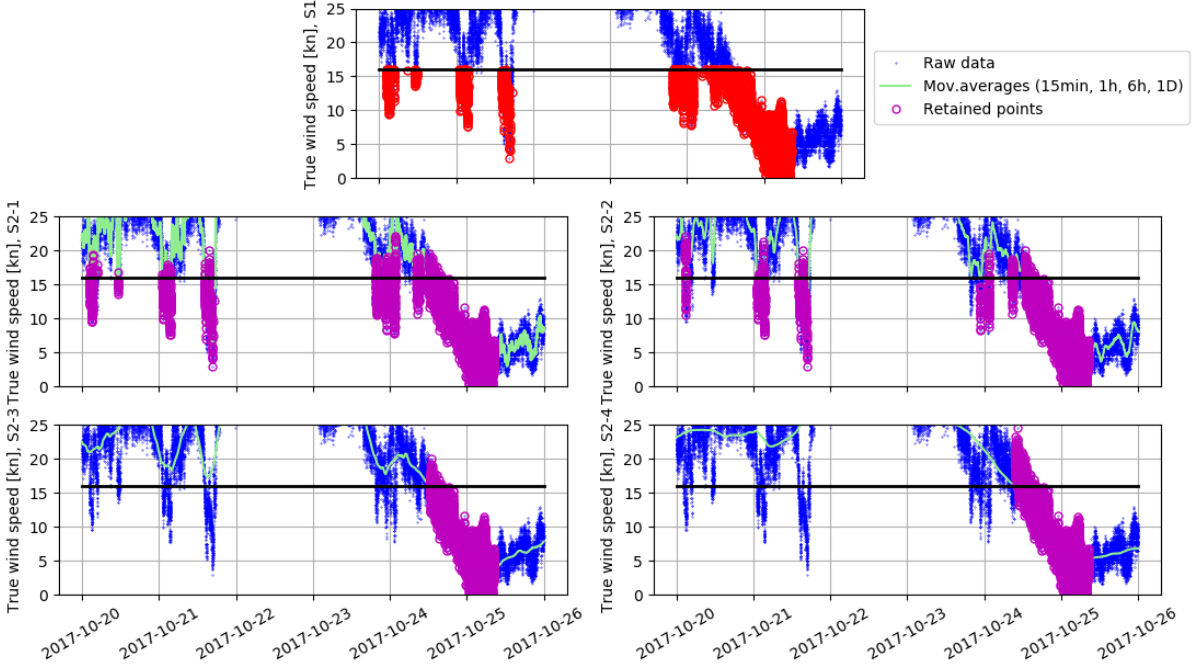


Fig.4: Example 2 - Differences between filters in simulations 1 and 2 (all scenarios: S2-1, S2-2, S2-3 and S2-4)

If wind signal is smoothed by applying 15 minutes moving average, then filtering for the latter leads to sometimes retaining maybe a bit too much data for analysis. When short-term downward fluctuations in true wind speed occur, see figure 4, these are often “captured” by the relatively short 15-minute window size. This might impact the final performance values, especially if those fluctuations are just some noise. It can indeed happen that true wind speed drops short-term, but then it remains a question whether the apparent operational performance of the vessel picks up in those periods.

By looking at Figs.3-5, it could be suggested that instead of following one of the 4 tested scenarios, a combination of them is used. Since using 1-day moving average has been concluded not practical, it is suggested that one proceeds with both 1-hour and 6-hour moving averages before applying the standard filter of 16 knots on true wind speed. This is also supported by speed deviation statistics presented in Table 3. In this way, more data is retained for analysis when wind trend is just below the cut-off value. Furthermore, in many cases, it is believed that the impact of true wind speed values slightly exceeding the threshold does not impact negatively the final performance figure.

If this is implemented for this particular vessel, about 23% of data would be left after filtering.

There are cases, though, when this approach does not work as expected and therefore an additional simulation has been carried out.

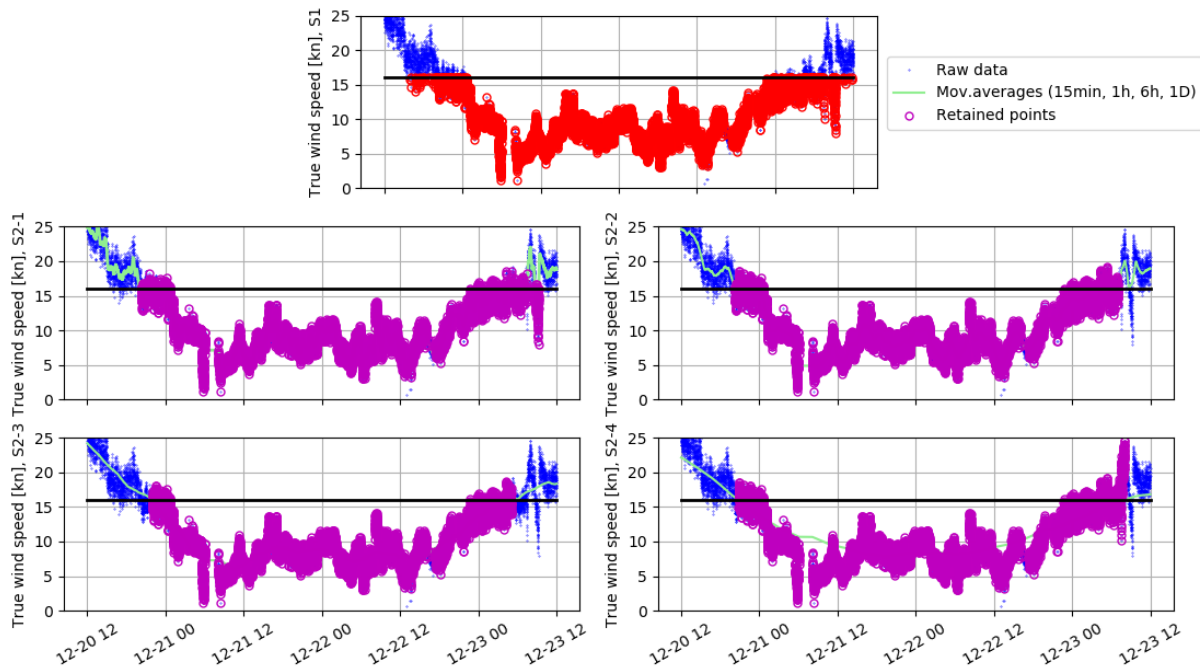


Fig.5: Example 3 - Differences between filters in simulations 1 and 2 (all scenarios: S2-1, S2-2, S2-3 and S2-4)

Simulation 3: Approach tested in Simulation 3 is very similar to the one used in Simulation 2. The purpose of running it is to check how filters mentioned in Simulation 2 would behave if one accounts for the variability in true wind speed. Variability in true wind speed has been evaluated by computing the moving average of standard deviation. Window size used in this sense corresponds to that used for smoothing the wind speed signal. Same window sizes as in Simulation 2 were used. The distributions of moving standard deviations are plotted in Fig.6.

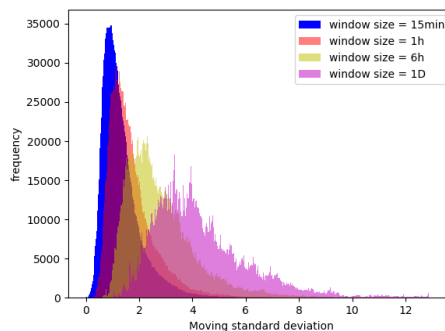


Fig.6: Distributions of moving standard deviations (different window sizes)

As expected, variability in wind speed during 1 day is generally very high. This again confirms that probably using 1-day moving average of true wind speed as filtering parameter makes no sense. The distributions of moving standard deviations in case of 15min – and 1h window sizes are similar. Standard deviations of these distributions are 0.78kn and 0.94kn while the means – 1.3kn and 1.7kn, respectively. The variability in wind speed over 6h lies somewhere in between the described distributions.

By smoothing true wind speed signal (window size 15min and 1h) before using this parameter in filtering criteria, it is expected that more data is retained for analysis when wind trend is just below the cut-off value of 16 knots but, at the same time, less data is retained when wind trend slightly exceeds the threshold. The question of keeping some data points in the first case or filtering them out in the second case is addressed by evaluating the variability of true wind speed values in respective periods.

The threshold for moving standard deviation has been set to the sum of distribution mean and distribution standard deviation. For scenario S3-1 (using 15min window size) threshold is therefore 2.1 kn, for S3-2 (using 1h window size) – 2.6kn and, finally S3-3 (using 6h window size) – 4.2kn. The latter seems a bit to high but, at the same time, if lowering it to 2-2.5kn a lot of data would be filtered out. Nevertheless, it is decided that all 3 scenarios are plotted. Speed deviation statistics are presented in Table 4 and some results from Simulation 3 presented in Figs.7 and 8.

Table 4: Speed deviation statistics for Simulation 3

Window size	Mean	Standard deviation	Mean absolute deviation (MAD)
15min	-6.1	4.56	3.54
1h	-6.1	4.56	3.53
6h	-6.1	4.53	3.51

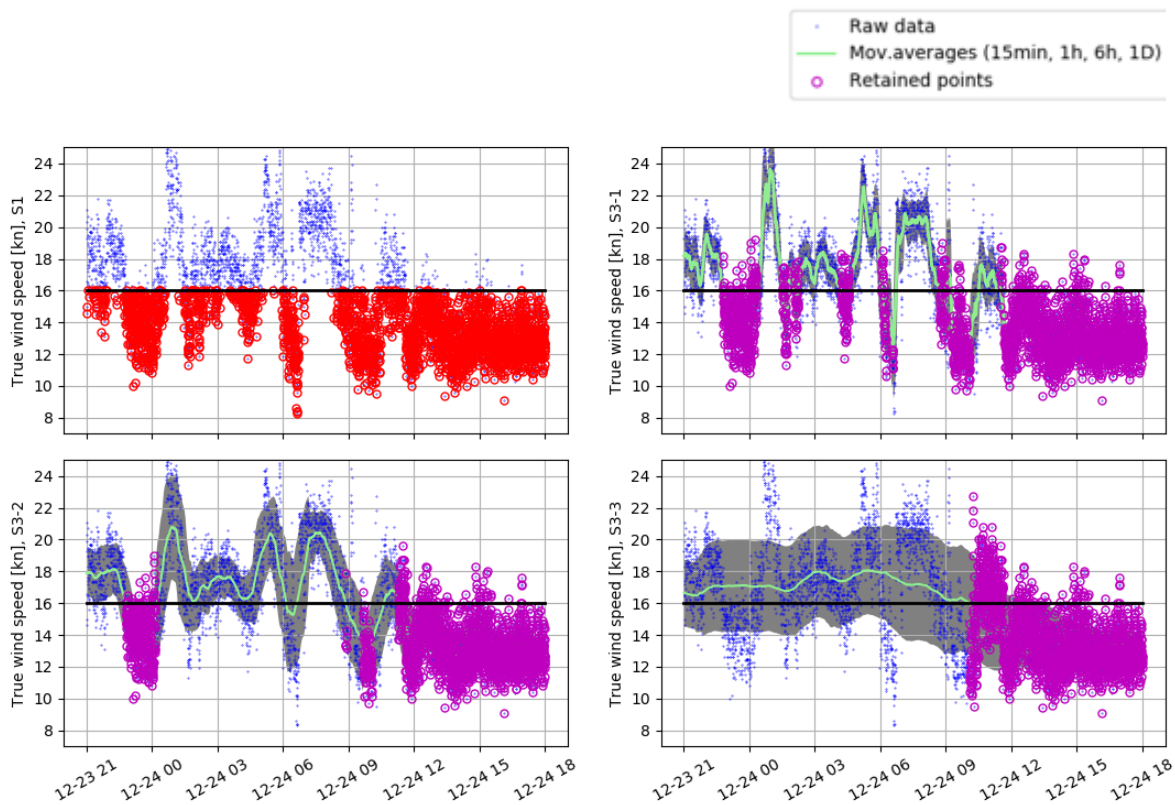


Fig.7: Example 1 - Differences between filters in simulations 1 and 3 (all scenarios: S3-1, S3-2, S3-3)

In Fig.7 is shown a case in which, somewhat more short-term fluctuations in wind occurred. If the initial 1-year dataset is filtered according to ISO 19030 then all the points below 16 knots would be kept for analysis. On the other hand, it could be seen that the general wind trend from midnight to about 9am is above the threshold. Imposing variability limits on true wind speed data enables to filter out such dips which are probably less meaningful. There is no doubt that wind can slowdown but not to forget that wind is the only logged parameter that reflects the weather overall. If the general trend in wind is higher than the accepted threshold over enough long periods, sea state changes as well. On the other hand, fluctuations in sea state condition are not expected to happen as fast as fluctuations in wind speed.

In Fig.8, the opposite case is shown. There is a sudden peak in true wind speed while the overall trend is below the accepted cut-off value. Furthermore, there are some values which are very close to the threshold but slightly above. Normal filter from Simulation 1 would not retain such values, while if averaging true wind speed and then on top impose a variability limit, one could keep more data for speed deviation computation.

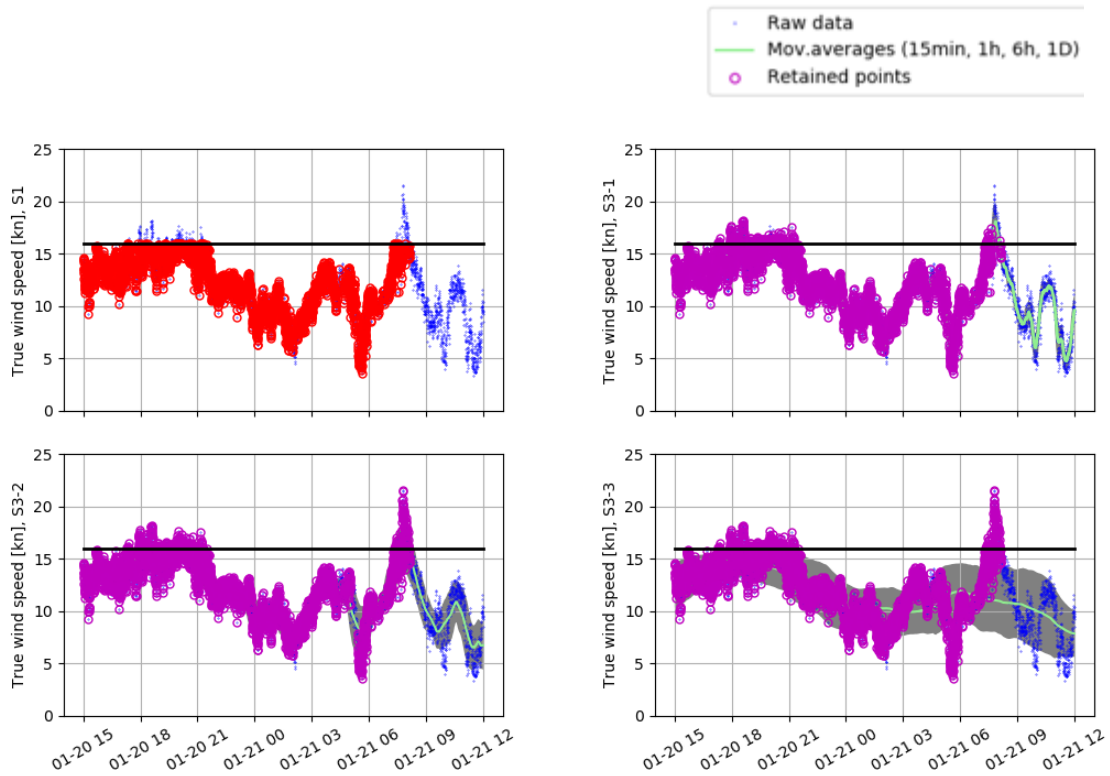


Fig.8: Example 2 - Differences between filters in simulations 1 and 3 (all scenarios: S3-1, S3-2, S3-3)

When simulating chosen scenarios, it has been noticed that sometimes S3-1 and sometimes S3-2 provide desirable results. It is difficult to draw a conclusion, even from table 4, on which approach should be used instead of S1, but probably a combination of the two would work well. It is also to be noted that somewhat less data is kept for analysis after filtering data in Simulation S3 in comparison to simulation S2. The amount of retained data is in between 23.5 – 24.6%.

Simulation 4: If one would like to keep more data for analysis, then one could experiment also with increasing the threshold of 16 knots. In Simulation 4, it has been decided to still average true wind speed (window sizes 15min and 1h) and when filtering for it account for variability in data but increase the cut-off value to 18 knots (scenario S4-1) and 21 knots (scenario S4-2). Statistics for resulted speed deviation are summarized in Table 5. As expected by increasing the threshold, standard deviation and MAD increase slightly but no significant differences have been spotted. It is therefore questionable whether excluding true wind speed values in the range 16-21 knots from analysis is justifiable.

Table 5: Speed deviation statistics for Simulation 4 (S4-1 and S4-2)

Window size	Mean	Standard deviation	Mean absolute deviation (MAD)
15min (S4-1)	-6.2	4.58	3.56
15min (S4-2)	-6.3	4.61	3.62
1h (S4-1)	-6.2	4.58	3.57
1h (S4-2)	-6.3	4.60	3.61

Another scenario considered in Simulation 4 is using wind speed and eventually wave height from research institutes data for filtering purposes. Data is available either from in-situ observations (wind speed) or models (wave height) and could be used especially in cases when anemometer data is not trustful. Wind data is available as 6h averages while wave data – 3h instantaneous values.

First, it has been checked whether there is a correlation between in-situ/model data (wind and waves) and data from anemometer. The correlation of weekly moving averages is shown in Fig.9.

Since logged data is very well correlated with in-situ data, one could try using the latter for filtering bad weather. It is to be noted that no averages have been applied to in-situ wind and wave data. Results of scenario S4-3(only wind), S4-4(only waves) and S4-5(wind and waves) are presented in Table 6.

Index	windspe_a	wind_speed	wave_height
windspe_a	1	0.934672	0.798227
wind_speed	0.934672	1	0.793625
wave_height	0.798227	0.793625	1

Fig.9: Pearson correlation

Table 6: Speed deviation statistics for Simulation 4 (S4-3)

Scenario	Mean	Standard deviation	Mean absolute deviation (MAD)
S4-3	-6.3	4.64	3.62
S4-4	-6.0	4.61	3.55
S4-5	-5.5	4.42	3.42

When in-situ wind speed data is used in performance analysis filter, no big changes in speed deviation are noticed. However, when wave data is included as well, it seems that some more scatter is being removed. The mean value changes significantly, while standard deviation and MAD become the smallest among all previous simulations. The amount of data left for analysis upon filtering in scenarios S4 3-5 ranges between 19.5 – 31.1% with the smallest values corresponding to S4-5. This points to the conclusion that wave data could indeed increase the precision of the analysis. Besides this, one could possibly think of aggregating weather data instead of smoothening the signals by applying a low pass filter. This has been tried and briefly discussed further.

3. Alternative approach

An alternative approach to the above would be to aggregate true wind values into longer period averages. The idea is that speed deviation (performance values) is not significantly affected by temporary fluctuations in true wind speed (ex. gusts), but rather by the overall trend in true wind on a longer period. In addition, aggregating to lower frequencies than 15 seconds is an indirect way to reduce the noise from the sensor (anemometer). In order to check the effect of true wind aggregation, the same initial dataset was used as in previous chapter. Aggregation levels chosen were one minute, 5 minutes, 15 minutes and 1 hour. Padding was selected in order to fill the missing values when projecting true wind values into 15 seconds frequency. Finally, median was selected for aggregation instead of mean as median is less sensitive to outliers and as such more representative of the longer trend of true wind. The effect of wind signal aggregation is shown in Fig.10.

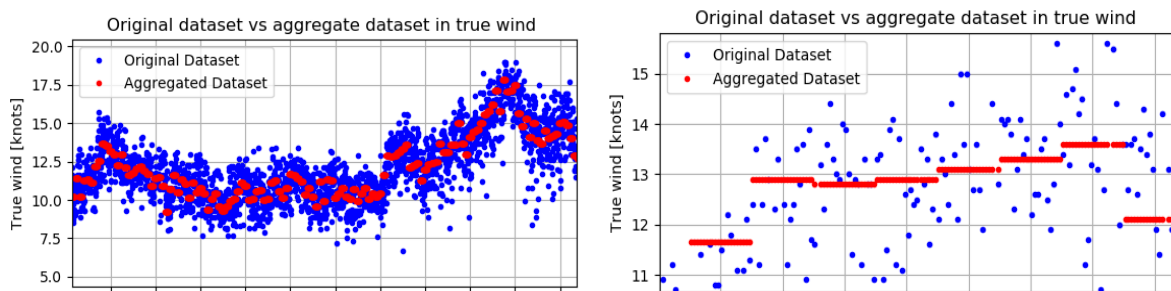


Fig.10: Effect of wind signal aggregation on different scale

In order to measure the impact of this approach on speed deviation, the mean, standard deviation(std) and mean absolute deviation(MAD) of performance values were calculated for each of the selected aggregated

frequencies. By applying the above, the number of points left for speed deviation calculations varies to $\pm 0.5\%$, which means that there is no preferred aggregation frequency which potentially could increase data retention. A possible explanation for this is that the amount of points which are being excluded and at the same time included around the threshold of 16 kn is similar. This could also be a possible explanation of the findings of this simulation. As seen in Table 7, all statistical metrics are surprisingly the same, meaning that there is no significant difference in mean, standard deviation or mean absolute deviation of performance values.

Table 7: Speed deviation statistics for alternative approach

Period Averages	Mean	Standard deviation	Mean absolute deviation(MAD)
15sec	-6.2	4.60	3.58
1min	-6.2	4.60	3.58
5min	-6.2	4.60	3.58
15min	-6.2	4.60	3.58
1h	-6.2	4.61	3.58

For validation purposes one more simulation was carried out with a dataset from an LNG vessel using the same approach. The findings were similar, and all statistical metrics were almost identical. Although further research is needed with several datasets and especially datasets from containers (due to higher impact of true wind in such vessel type), one may conclude that short term fluctuations of true wind (ex. gusts) do not have a significant impact on speed deviation. This conclusion may be used as an argument in order to increase the threshold of 16 knots as imposed by the ISO 19030 standard

Park et al. (2017) mention in their analysis, that once all filtering recommended by the ISO 19030 is applied, then a statistically significant dataset cannot be realized (approximately 90% of the dataset is filtered out). This is not always the case, as many points are being filtered out due to the fact that operational parameters (speed and power) are not within the range of the available external information (speed-power curves). However, threshold of true wind value of 16 knots has a significant role in the number of points which are filtered out. Given the above conclusion one may suggest that increasing the threshold of 16 knots is meaningful and will not have significant impact on calculations. The question remains; which level of threshold should be introduced in order to maintain similar accuracy levels in calculation of speed deviation.

To address this issue, a simple exercise was made for the vessels in question (VLCC and LNG). The simulation was carried out with the alternative approach but a threshold of 18 knots applied. In both cases, the amount of data retained was on average 12% higher. Mean value was affected by $\pm 0.1\%$ in VLCC and by $\pm 0.2\%$ in the LNG case. The other statistical measures (std, MAD) were very similar without a clear indication of improvement. As such, the trade-off between the amount of data and analysis precision seems to pay off.

4. Summary

This paper discusses the possibility of improving data filtering for weather – crucial step in data preparation stage. Weather is a broad term and can be described by many parameters – wind, waves, currents, etc. However, not all are being logged and available for vessel performance monitoring purposes. Therefore, paper focuses on primarily wind data filtering and two approaches have been tried out.

First, wind data signal is smoothed by applying a low pass filter. In this approach several scenarios were tested. It is the window size which was varied, data variability which was accounted for and cut-off value which was changed. When attenuating true wind speed signal, 15min –, 1h –, 6h – and 1-day moving averages have been used. After that wind speed values have been filtered according to the threshold mentioned in ISO 19030 (16 knots). It has been concluded that 1h – and 6h – moving averages

provide somewhat better results, as in those cases less periods with short-term fluctuations in wind are kept for further analysis.

If, besides smoothening wind signal, one attempts to account for wind data variability, then even more scatter can be eliminated. When fixing variability limits on wind speed data, one could filter out either some more noise in data or, as described in the paper, less meaningful periods. Fluctuations in wind speed in time are expected but sudden changes in wind do not necessarily mean changes for example in sea state and, therefore, these probably should not reflect instantly on the performance values. In case wind speed from anemometer is not available, one could use wind and eventually wave data from either in-situ observations or models. This has been simulated and results suggest that somewhat more scatter is eliminated from data. It is believed that there is a two-fold reason for this - filtering data for wave height and using aggregated wind data. Since lower-frequency wind data (from in-situ observations) has shown better results, additional simulations with anemometer wind data aggregation have been carried out.

Wind data has been aggregated to 1min, 5min, 15min and 1h and then used in filtering criteria for performance analysis. Padding was selected to maintain high frequency of the data and median was selected in aggregation as it is less sensitive to outliers. Results suggest that wind aggregation has no significant impact on the final performance values regardless of the selected aggregation level. To validate this, a different dataset from an LNG was used and the same has been concluded. This was not fully expected, since aggregation is supposed to reduce scatter in wind signal.

Finally, since both approaches indicate that there is no big impact on performance values, it has been concluded that by increasing the threshold on true wind speed data from 16 to 18 knots is meaningful. This increases the amount of data retained by about 12% on average whereas it does not affect significantly the statistics of the performance values.

References

PARK, B.J.; SHIN, M.S.; KI, M.S.; LEE, G.J.; LEE, S.B. (2017), *Experience in Applying ISO19030 to Field Data*, 2nd HullPIC Cof., Ulrichshusen

Effects of Hull and Propeller Cleaning on Propulsion Efficiency of an Offshore Patrol Vessel

Kevin Murrant, Allison Kennedy, Rob Pallard, Marcel Montrose,
National Research Council Canada, St. John's/Canada, Kevin.Murrant@nrc-cnrc.gc.ca

Abstract

The effects of hull and propeller cleaning on propulsion efficiency are evaluated for an offshore patrol vessel belonging to the Canadian Coast Guard. Dedicated sea trials were conducted between cleanings to evaluate propulsion efficiency using standard speed and power trial procedures. These results are compared with efficiency analysis performed on continuous operational data. A hull recoat was applied in fall of 2018, and the condition of biofouling and coatings observed at dry dock is discussed.

1. Background

The Canadian Coast Guard Ship (CCGS) Cygnus is an offshore patrol ship that operates out of St. John's, NL. It is the first CCG vessel to be instrumented with a vessel performance monitoring system, developed by OpDAQ. The system measures shaft torque, shaft speed, shaft power, and vessel fuel consumption. The National Research Council (NRC) of Canada has a separate Data Acquisition System (DAS) onboard the CCGS Cygnus since Fall 2015. The NRC DAS stores data from a number of vessel systems such as the navigation system and propulsion system. The NRC has also been obtaining OpDAQ data from the CCGS Cygnus since 2016. The data from the NRC DAS and OpDAQ system is used for the current project to quantify changes in vessel performance as a result of hull and propeller cleaning.

This report summarizes the propulsion efficiency analysis of the CCGS Cygnus operational data prior to and subsequent to cleaning the hull and propeller. This data is used to quantify any changes in vessel performance, specifically the power versus speed relationship. In addition, the vessel fuel consumption at a given power level will be quantified prior to and post cleaning events.

Three dedicated sea trials were conducted to support this project. Each set of trials is a dedicated Speed and Power trial and was planned and conducted in accordance with International Towing Tank Conference (ITTC) guidelines. The first set of trials is a baseline trial to quantify the performance before the hull or propeller are cleaned. The second set of trials is a post hull cleaning trial to quantify the performance subsequent to cleaning the vessel hull only. The third trial is conducted post propeller cleaning and is used to quantify any changes in speed and power performance as a result of cleaning the propeller.

The result of this project suggests how the power and speed relationship for the CCGS Cygnus changes after cleaning events within the scope of the trials. It also quantifies how the power and fuel consumption relationship changes as per the observed data. These changes are quantified using measured data from dedicated sea trials. This information could be used to support planning and optimization of vessel cleaning schedules.

2. CCGS Cygnus – Vessel Details

The CCGS Cygnus is an offshore fisheries patrol vessel that operates out of St. John's. It operates on a two week rotational schedule. This generally involves the vessel departing St. John's, transiting to the Grand Banks area which it patrols and then returning to St. John's for crew change. The day after crew change the vessel departs again for Grand Banks to continue patrolling. The vessel has two main medium speed, diesel engines. The ship particulars of the CCGS Cygnus are outlined in Table 1.

Table 2: Hull fouling characterization – type, rating and percent coverage

Location	Fouling Type	Fouling Rating	Percentage Coverage (%)
1	Soft	30	80
2	Soft	20	50
3	Soft	20	75
4	Soft	20	100
5	Soft	20	80
6	Soft	20	90
7	Soft	20	100
8	Soft	20	50
9	Soft	30	50
9	Soft	20	50
10	Soft	30	70
11	Soft	20	50
12	Soft	20	40
13	Soft	20	80
14	Soft	20	80
15	Soft	20	90
16	Soft	20	90
17	Soft	30	65
18	Soft	30	80
19	Soft	20	90
20	Soft	20	60
21	Soft	20	90
22	Soft	20	100
23	Soft	20	90
24	Soft	20	100
25	Soft	20	95
26	Soft	20	50
27	Soft	20	80

The hull and propeller of the CCGS Cygnus had not been cleaned in two years prior to this project. The level of fouling present was a result of 2 years of operation. The CCGS Cygnus operates year round on a two week rotation with a two day layover. Vessels with an off-season or with long layover periods would likely have more fouling in similar operational and environmental conditions.

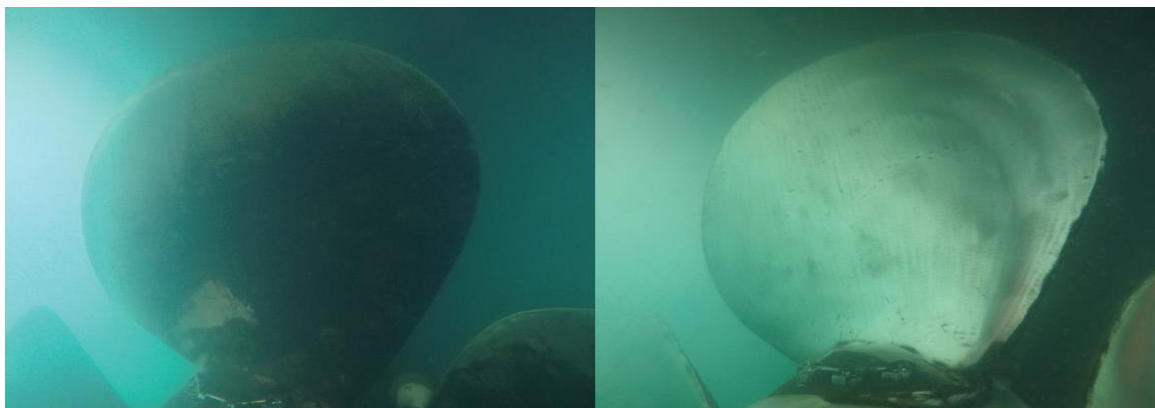


Fig.2: Typical propeller pressure face pre (left) and post (right) cleaning

The propeller was also assessed by divers to quantify the level of fouling present on July 18, 2018. All propeller blade faces were covered in a light to moderate slime which was heavier at the root and tapered towards the tips. Under the slime the propeller blades were covered with a heavy calcium buildup. The level of propeller fouling was measured using a ship propeller roughness gage which characterizes the propeller roughness per the Rubert Comparator scale. The propeller fouling was

rated as Rubert scale E. Once polished, the propeller was rated at a Rubert scale A/B. Post polishing trials were conducted at this polished state. Fig.2 illustrates the pre-cleaning and post-cleaning condition of a typical propeller pressure face of the CCGS Cygnus propeller. This report includes a number of images of pre and post cleaned propeller surfaces.

4. Sea Trials

Three separate sets of sea trials were completed. The first was conducted prior to cleaning the hull or propeller and provides data to use as a baseline. The second set of sea trials were completed after the hull was cleaned and the third set of sea trials were completed after the propeller was cleaned.

All trials followed the same procedure and occurred at the same location. The trials followed ITTC 2014 guidelines for the completion of speed and power trials. These guidelines outline boundary conditions as a cutoff point for the completion of such trials. These boundary conditions relate to location, water depth and environmental conditions and vary based on the vessel size. The specific trials boundary conditions for the CCGS Cygnus, are summarized in Table 3.

Table 3: Sea Trials Boundary Conditions

Parameter	Parameter Detail or Value
Location	Selected location should have minimal vessel traffic and should be sheltered to avoid wind / wave where possible.
Water Depth	Minimum water depth of 52.2 m. Data corrections required for water depths less than 71.8 m.
Wind	Wind shall not be higher than Beaufort 5. Beaufort 5 relates to mean wind velocity between 17-21 knots.
Sea State	The maximum wave height when derived from visual observation should be 1.2 m.
Current	Areas with known large current variations in time or space should be avoided. Small currents will be corrected for by completing tests in two directions, one upwind and the other downwind.

Prevalent weather conditions and vessel traffic intensity were considered when selecting a trials location. The location was selected to be within Conception Bay to reduce the likelihood of heavy sea states when compared to a location along the normal Cygnus operational route. The location was set to north of Bell Island since there was relatively little vessel traffic at this location than other areas of the Bay.

During each trial three or four different power settings were tested. The power settings tested included 50%, 65%, 80%, and 100% of the main engines Maximum Continuous Rating (MCR). All tests were completed in two directions: upwind and downwind. A double run at 65% MCR was conducted once during each set of trials. The double runs completed at 50%, 80% and 100% MCR were conducted twice, as per the ITTC 2014 guideline. The baseline trials included only three power settings (65%, 80%, and 100%) as the original plan did not specify runs at 50% power setting. After analysis of the baseline trial data, it was decided to include runs at 50% power in the subsequent trials to provide additional context for the higher power data points. It was attempted to perform all trials at a consistent displacement and as such there were no significant changes in cargo or machinery between trials.

Fig.3 shows the location of the sea trials. The direction of all trials was along the yellow line, between the points NRC 1 and NRC 2. This track has a total length of ~10 km to provide space for the high-speed runs. Each test required 10 minutes of constant rpm, pitch, and speed settings. As such, some tests were shorter in distance than others. All tests were centered near the subsea acoustic probe (Autonomous Multichannel Acoustic Recorder – AMAR) point in Fig.3. The AMAR point is located at 47°41.757' latitude and -52°56.509' longitude. The direction of the yellow line relates to in and out of the Bay, which corresponds with the prevailing wind direction. Once a test was completed in one direction, the vessel would turn around and complete the same test in the opposite direction.

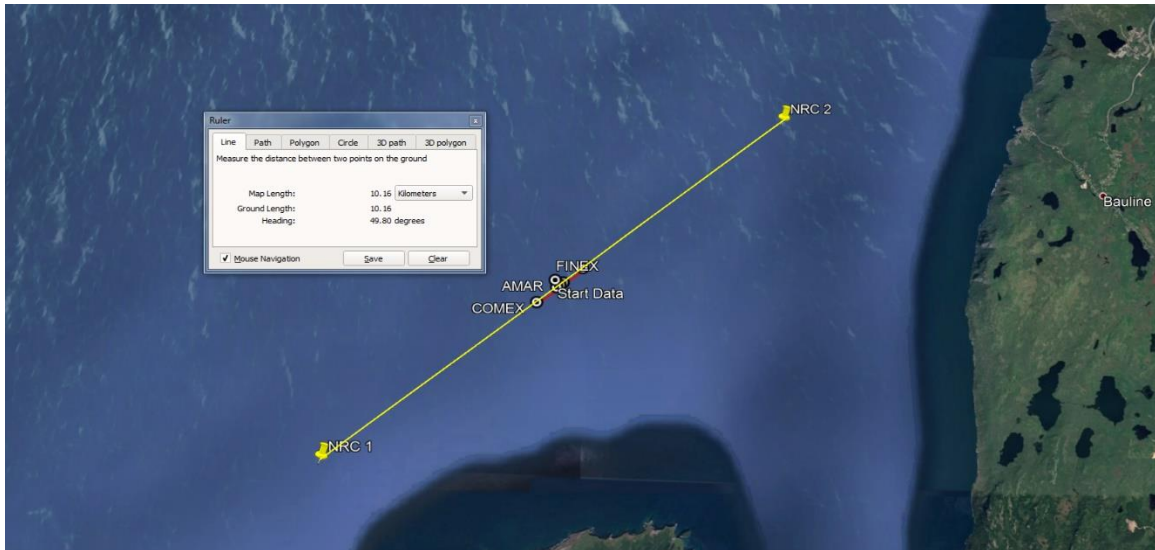


Fig.3: Trials location and direction in Conception Bay, NL

Each trial run involved a period to get up to speed and attain constant settings, a 10 minute constant setting period, and then a Williamson turn to return vessel to opposite direction for subsequent testing. The trial trajectory was similar to that shown in Fig.4.

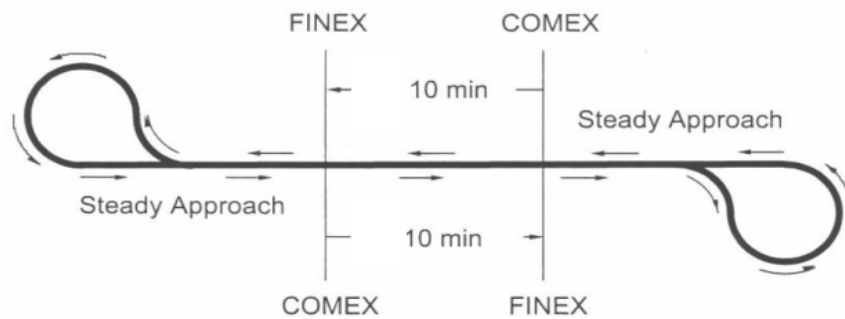


Fig.4: Trial trajectory illustrating the approach for each reciprocal run

4.1 Baseline Trials

Baseline (pre-cleaning) trials were completed on May 23, 2018. The wind and sea conditions during the morning were higher than the boundary conditions for these tests and as such all tests were completed in the afternoon when conditions calmed. The conditions during baseline trials are summarized in Table 4. There were 11 runs completed in total. Two of these were runs at a MCR setting of 65% (upwind and downwind), four at MCR of 80% (two upwind and two downwind) and four at a 100% MCR (two upwind and two downwind). There was a repeat test of the first run which was 65% MCR in the upwind direction. The repeat was conducted because the wave and wind conditions were higher during the first test of the day than they were during the remainder of the tests.

Table 4: Baseline Trial Conditions

Condition	Value
Testing timeframe	13:30 – 16:15
Vessel forward draft (m)	3.35
Vessel aft draft (m)	4.83
Range in true wind speed (kts)	16 - 22
Range in wave heights (m)	0.5 – 1.0
Range in swell height (m)	0 – 0.5
Water temperature (°C)	4.0

During the baseline trials the wave and swell heights were estimated by the vessel Captain. These values were not measured during baseline trials as the wave buoy was not deployed due to morning weather conditions. The water temperature was also estimated for the baseline trial, using historic water temperature values from the area. In addition, the estimated water temperature was compared to water temperature measurements taken from a wave buoy that was located in Holyrood Harbor, which is not too far from the trials site.

4.2 Post Hull Cleaning Trials

The post hull cleaning trials were completed on July 18, 2018. The weather conditions during post hull cleaning trials are summarized in Table 5. There were 14 runs completed in total. Four of these were runs at 50% MCR (two upwind and two downwind), two at a 65% MCR (one upwind and one downwind), four at 80% MCR (two upwind and two downwind) and four at a throttle setting of 100% MCR (two upwind and two downwind).

Table 5: Post Hull Cleaning Trial Conditions

Condition	Value
Testing timeframe	10:30 – 14:00
Vessel forward draft (m)	3.05
Vessel aft draft (m)	4.66
Range in true wind speed (kts)	14 - 25
Range in wave heights (m)	0.2 – 0.4
Range in swell height (m)	0 – 0.25
Water temperature (°C)	10.2

During the post hull cleaning trials the wave and swell heights were estimated by the vessel Captain. These values were also measured by a wave buoy during these trials. Estimated values were compared with those measured. Values estimated were consistently higher than those measured, by approximately 50%. Measured values are summarized in the trials log as well as in Table 5.

4.3 Post Propeller Cleaning Trials

The post propeller cleaning trials were completed on August 1, 2018. The weather conditions during post propeller cleaning trials are summarized in Table 6. There were 14 runs completed in total. Four of these were runs at 50% MCR (two upwind and two downwind), two at 65% MCR (one upwind and one downwind), four at 80% MCR (two upwind and two downwind) and four at 100% MCR (two upwind and two downwind).

Table 6: Post Propeller Cleaning Trial Conditions

Condition	Value
Testing timeframe	11:45 – 15:05
Vessel forward draft (m)	3.02
Vessel aft draft (m)	4.72
Range in true wind speed (kts)	4.5 – 10.2
Range in wave heights (m)	0.3 – 0.6
Range in swell height (m)	0
Water temperature (°C)	14.9

During the post propeller cleaning trials the wave and swell heights were measured by a wave buoy deployed for the test.

5. Measured Speed and Power Data

The measured shaft power versus speed through water for each test during each trial are plotted on the same axes in Fig.5. All collected data points follow a similar relationship that can be fit with an

exponential curve. There is less variation in the post propeller trials data when compared to the other trials results for a given engine setting. This is expected due to the calm wind and sea conditions during the post propeller polishing trials which were lighter than those for the other two trials.

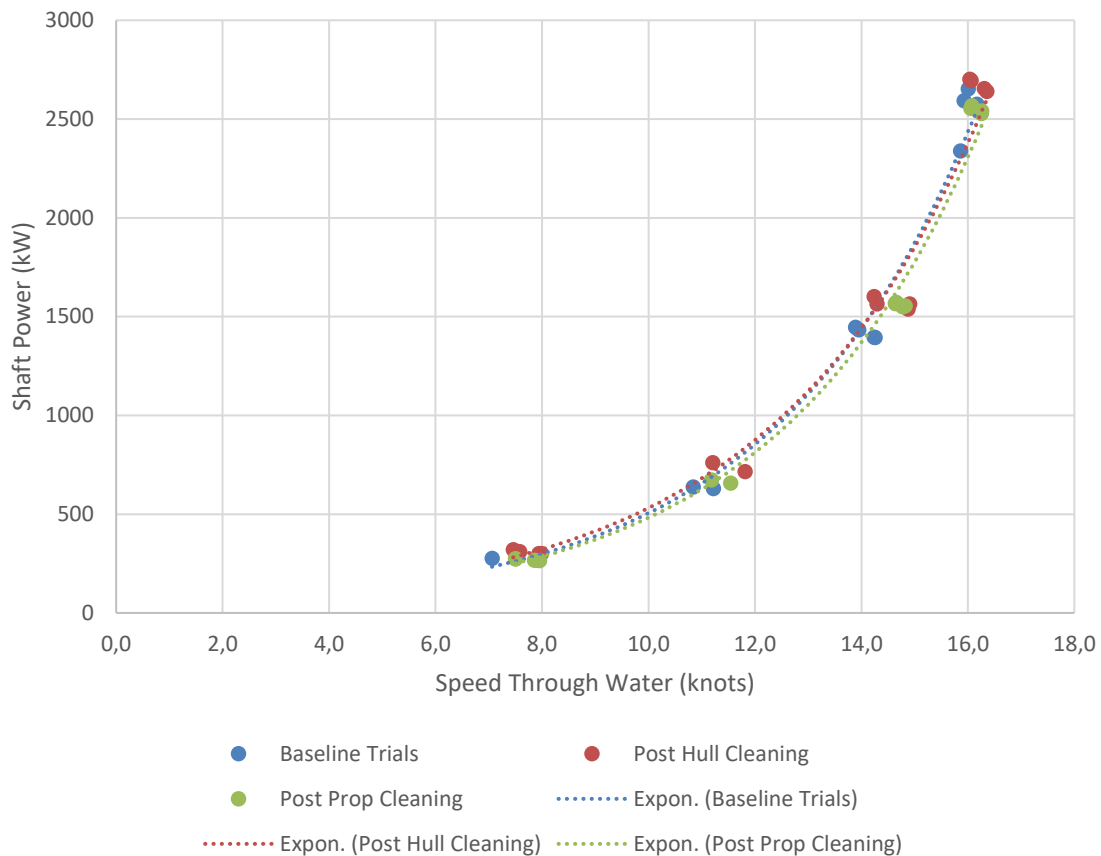


Fig.5: Uncorrected power versus speed data from each test run during each trial. An exponential curve fit is shown to illustrate the trends between trials. The uncorrected data does not show a significant difference between trials in the speed curve.

The measured data was analyzed first using the mean of means method to provide further insight towards data trends between trials. The mean of means method involves taking the mean of consecutive double runs at a given engine setting and then taking the mean of those means to represent the speed and power values at that engine setting. The intent of this method is to eliminate the unidirectional effects of wind and current under the assumption that these effects will average to zero. The mean of means for all trials completed at a given engine setting, within each sea trial, were calculated. The results of shaft power and vessel speed through water for each sea trial were plotted (Fig.6). Trend lines were fitted through the data for each sea trial.

The differences in the relationships between power and speed for the three sea trials is clearer here. The trend line relationships between trials change across the speed range. The post-hull cleaning trials trend line requires approximately 4% less power to attain speeds between 12.5 and 16 knots. In this same speed range, the post-propeller cleaning trials trend line indicates that approximately 5% less power is required to attain a given speed when compared to the post hull cleaning trials. These results indicate that a total of approximately 9% less power is required to attain a given speed (in speed range between 12.5-16 knots) as a result of cleaning both the hull and propeller. For speeds less than approximately 12 knots, more power is required to attain a given speed for the post hull cleaning trials when compared to the baseline trials. This result is unexpected and may be influenced by the higher level of uncertainty involved in the lower engine setting trials.

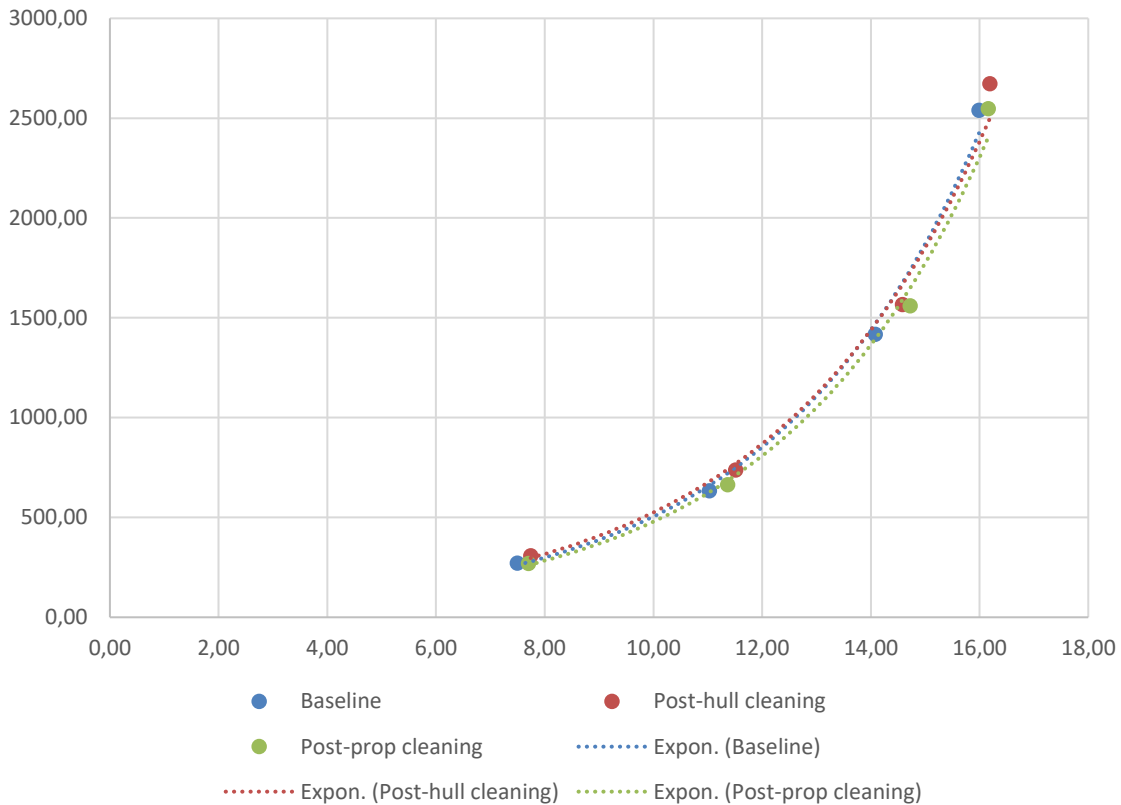


Fig.6: Means of means for each trial. Each data point is the mean of 2-4 runs at that speed in reciprocal runs.

It is also noteworthy to discuss the fact that these results are presented in terms of power versus speed rather than overall resistance versus speed. Overall resistance is more difficult to characterize since it takes into account the propulsion as well as associated efficiencies (hull efficiency, propulsive efficiency, and relative rotative efficiency). The power can be roughly calculated by dividing the resistance multiplied by the vessel speed, by the overall system efficiency. The overall propulsion system efficiency is a combination of multiple complex factors. For example, the propulsive efficiency would increase as a result of cleaning the propeller. Another example is that the hull efficiency, which describes how the water flows around the hull and into the propeller, can affect the propeller efficiency as a result of cleaning the hull. It is therefore possible that the resistance versus speed relationship for each set of trials would not exhibit the same performance gains across the speed range compared to simply comparing power versus speed.

6. Speed and Power Analysis and Results

The speed and power data measured during field trials was analyzed to remove variations due to environmental differences between trials. This was completed following ITTC guidelines for the analysis of full-scale speed and power trials, *ITTC (2005)*. This analysis method was complimented using insight from ISO 15016 when additional guidance was needed. The ITTC guideline requires the conversion of measured power data to vessel resistance in order to apply certain correction factors to account for environmental effects and correct data to a common, calm state. The ITTC guideline describes a method to determine the resistance of each trial run by using the measured torque along with information from associated propeller curves. A major element of uncertainty in this analysis is that the open water propeller curves for the Cygnus propeller are not available to support data analysis. As such, a standard B-Series propeller curve was assumed to be representative of the Cygnus propeller.

The ITTC guideline provides methods to calculate resistance corrections for: wind, waves, deviation

in water temperature and density, water current, shallow water, and displacement variation. Resistance corrections were calculated for each trial run within each specific sea trial. For all cases, the resistance correction to account for water current was not calculated since the vessel speed through water was measured directly. Also, the shallow water correction was not calculated for any trials since the trials were conducted in deep water. The resistance correction to account for variations in vessel displacement were provided only for displacements that varied less than 2%. Based on the forward and aft draft measurements taken at the beginning of each trial, the displacement varied by approximately 8%, exceeding the range of the correction method. As such, there were no corrections added to account for displacement variation and the change in displacement is a source of variability within the results. Note that the forward and aft were estimated by the vessel crew based on draft marks prior to each trial and were not measured directly. Therefore, the variation in displacement could differ than the percentage value calculated using the estimated trim values.

The resistance corrections calculated for each trial were subtracted from the trial resistance that was calculated to reduce the resistance to a calm water baseline which could be used for direct comparison between trials. The corrected vessel resistance was used to calculate the corrected power. The ITTC analysis method required estimation of a number of coefficients specific to the vessel used in trials as well as the estimation of a number of environmental parameters that were not directly measured. Estimation of these parameters leads to a level of uncertainty in the results. A summary of the estimated parameters is provided below.

- Wake fraction, thrust deduction fraction and propeller relative rotative efficiency. These coefficients can be found from model test results for a particular vessel. Model test data for the CCGS Cygnus was not available for this data analysis. As such, the commercial software NavCad was used to model each trial and output the associated coefficients. The measured and predicted shaft power values compared well (within 10%) and thus the coefficients output from NavCad were deemed as reasonable.
- Thrust coefficient and advance coefficient. The ITTC analysis guideline states that the propeller open water thrust and advance coefficients, both required to calculate resistance, are to be retrieved from propeller open water curves. The CCGS Cygnus propeller open water curves were not available for this analysis. As such, standard B-Series open water propeller curves were used to represent the Cygnus propeller. The standard B-Series open water propeller curves were updated to match the pitch (as approximated by NavCad) of each trial run. Each unique set of curves was then used to retrieve the required data associated with the corresponding run. Unfortunately, the actual pitch relating to each test was not known and had to be approximated based on the pitch percentage which was noted from a gage on the bridge of the vessel and using NavCad. This added to the uncertainty involved in using the standard B-Series curve. In addition, the Cygnus propeller is controllable pitch and the standard B-Series propeller is not. The ratio of hub diameter to propeller blade length is larger for a controllable pitch propeller than for a fixed pitch propeller.
- Wetted surface area. The wetted surface area of the CCGS Cygnus was estimated with NavCad using input of the vessel main particulars and selection of representative vessel type.
- Transverse projected area above waterline. The transverse projected area above waterline of the CCGS Cygnus was estimated using measurements from the general arrangement drawing of the vessel and known draft.
- Wind resistance correction. The correction for wind resistance was estimated using recommended equations for the calculation of wind resistance.
- Wave height during baseline trials. The wave height was not measured during baseline trials. It was estimated using the measured wind speed and the fetch limited JONSWAP wave spectrum. The value of fetch used for the trials was 30 km. These estimates were compared to measured wave height data from a nearby (Holyrood) wave buoy and the results matched well (within 10%).
- Water temperature during baseline trials. The water temperature was not measured directly during baseline trials and was estimated based on historic water temperature data during the

same time of year. The estimated value was compared to measured data from a nearby (Holy-wood) wave buoy and the results were similar.

- Water density for all trials. It was assumed that 3.5% salinity was representative of the water density during trials.
- Kinematic viscosity for all trials. The water kinematic viscosity was not directly measured and was estimated using the water temperature and ITTC Salt Water Property tables.

Preliminary results of the analysis showed that the wind resistance correction the most significant factor in comparison to the other corrections, for all sea trials. In addition, for the baseline trials and the post hull cleaning trials, where wind speeds were towards the upper wind speed limits of the trials, the wind resistance correction was very large in comparison to the bare hull resistance, particularly at the lower speeds.

The measured speed and power data was analyzed three separate times to correct for environmental conditions, each using the ITTC 2005 method or a slight variation to the method. The first analysis approach was conducted strictly to the ITTC guideline. The second and third analysis approaches were conducted using the ITTC 2005 guideline with a different estimation of wind resistance correction. The second attempt involved a wind resistance correction estimation using the Fujiwara method. This method was one of the wind resistance predictors recommended in NavCad, a commercially available vessel performance evaluation software. The third attempt involved a wind resistance correction estimation of half the predicted value using the Fujiwara method. Three separate analysis were completed to illustrate the variation in result that occurs due to different estimations of wind resistance correction.

6.1 Results – Baseline Trials

The results of the three analysis methods for all trials data is summarized in Fig.7. The measured trials data have higher power per speed than the corrected data for all test cases except the 11 knot speed. It is expected that the measured power would be higher since the power is being corrected to a calm condition and less power would be required to attain a given speed in calm seas. The measured data is very close to the corrected values at 11 knots which suggests that the wind and wave conditions during these tests were relatively mild. There is not much difference between the corrected results using the ITTC wind correction and the NavCad (Fujiwara) wind correction, for all tests. The corrected data using half the Fujiwara wind correction, lies in between the measured data and the other corrected data.

The measured trials data have higher power per speed than the corrected data for all test cases except the 11 knot speed. It is expected that the measured power would be higher since the power is being corrected to a calm condition and less power would be required to attain a given speed in calm seas. The measured data is very close to the corrected values at 11 knots which suggests that the wind and wave conditions during these tests were relatively mild. There is not much difference between the corrected results using the ITTC wind correction and the NavCad (Fujiwara) wind correction, for all tests. The corrected data using half the Fujiwara wind correction, lies in between the measured data and the other corrected data.

6.2 Results – Post Hull Cleaning Trials

The data corrected using the ITTC wind correction and the NavCad wind correction are similar. The spread between the measured and corrected data increases with speed for the post hull cleaning trials.

6.3 Results – Post Propeller Cleaning Trials

The measured data is very close to the corrected data for the post propeller cleaning trials due to the mild environmental conditions during the trials. There does appear to be one outlier for the tests at speed between 11 and 12 knots for which the measured power is below the corrected power values.

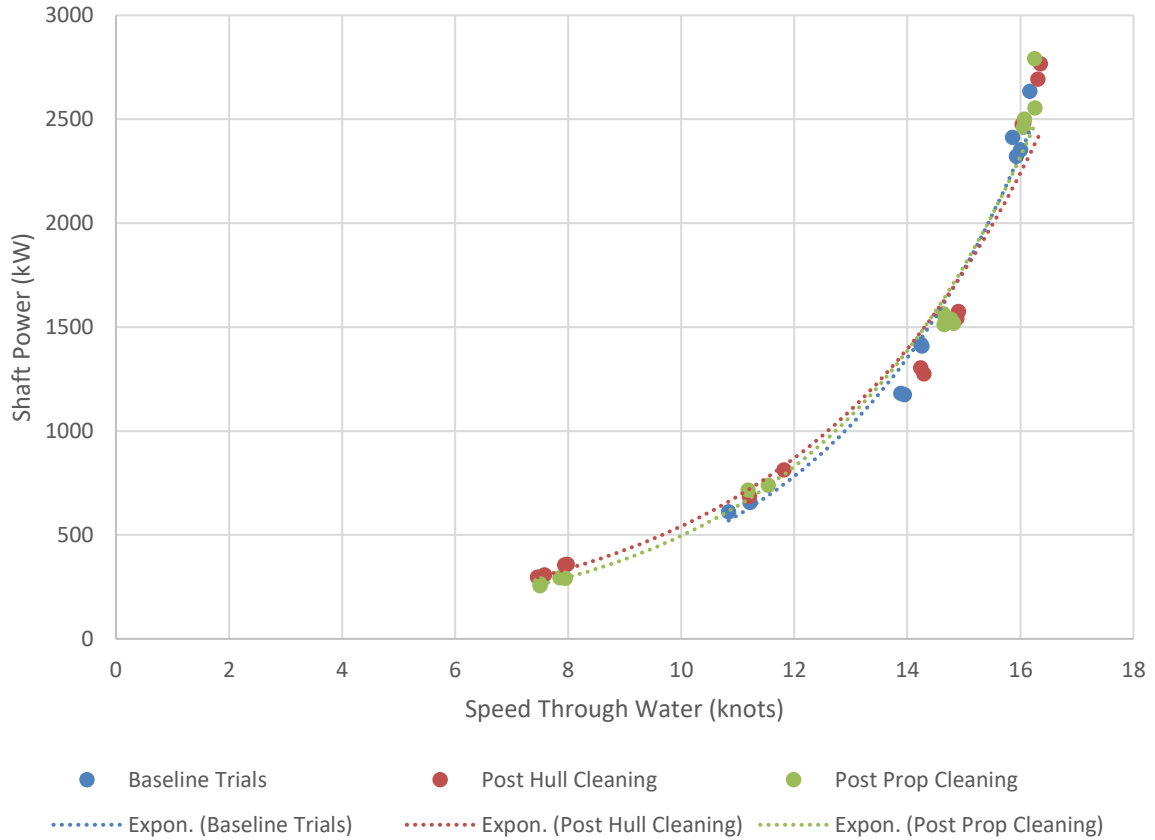


Fig.7: Corrected speed and power data for all trials. Due to the correction, environmental effect is reduced and the data points follow more closely the trend.

Table 7: Corrected speed and power data for all trials

Baseline		Post Hull Cleaning		Post Propeller Cleaning	
Speed (STW)	Power	Speed (STW)	Power	Speed (STW)	Power
(knots)	(kW)	(knots)	(kW)	(knots)	(kW)
		7.6	308	7.9	293
		7.9	356	7.5	264
7	276	7.5	298	7.9	291
8	265	8.0	359	7.5	256
10.8	611	11.2	685	11.5	739
11.2	657	11.8	813	11.2	716
13.9	1182	14.2	1305	14.8	1539
14.2	1418	14.9	1541	14.6	1512
13.9	1175	14.3	1275	14.8	1518
14.3	1409	14.9	1575	14.6	1565
16.0	2353	16.0	2477	16.3	2555
16.2	2635	16.3	2694	16.1	2501
15.9	2323	16.1	2481	16.3	2792
15.9	2413	16.4	2766	16.1	2460

6.2 Results – Post Hull Cleaning Trials

The data corrected using the ITTC wind correction and the NavCad wind correction are very similar.

The spread between the measured and corrected data increases with speed for the post hull cleaning trials.

6.3 Results – Post Propeller Cleaning Trials

The measured data is very close to the corrected data for the post propeller cleaning trials due to the mild environmental conditions during the trials. There does appear to be one outlier for the tests at speed between 11 and 12 knots for which the measured power is below the corrected power values.

6.4 Results – Comparison of Trials

The corrected power results for each sea trial were plotted against speed on the same plot to illustrate differences in performance. This was completed for each of the three wind correction approaches considered. For each analysis method, the results of each trial are relatively similar in terms of the power required at a given speed. Given this, it is difficult to quantify the gain in power associated with cleaning the hull and propeller, from this data. The regression lines for each trial are very similar for all analysis methods used. For each approach, the baseline trial regression line is higher than the post hull and post propeller cleaning regression lines, at speeds higher than approximately 13 knots. This indicates that there is a benefit of cleaning the hull and propeller in these speed ranges in terms of power required to attain a given speed. Below, approximately 13 knots, the regression line for baseline trials falls below the regression line for the other two trials. This change in regression line relationship between trials is consistent to the measured data results and may be due to higher uncertainty at the low speed tests.

The power savings above 13 knots were quantified using the regression line equations from the NavCad wind correction approach. Between 13.5 and 16 knots an average of 5% less power is required to attain a given speed after cleaning the hull, when compared to the baseline power requirements. There is no additional power reduction identified within this speed range as a result of cleaning the propeller which was unexpected. In fact, the performance after cleaning the propeller, in terms of power versus speed, is worse in this speed range.

Note that there is variability within the tests conducted at a given throttle setting for a given trial in terms of speed through water and corrected power. The corrected power for a throttle setting for one trial often falls within the range of corrected power for the same throttle setting in a different trial. For example, at a throttle setting of 10 the speed through water varies between 15.9-16.2 knots for the baseline trials, 16.0-16.4 knots for the post hull clean trials and 16.1-16.3 knots for the post propeller cleaning trials. For this same throttle setting the corrected power (NavCad wind) ranges from 2272-2677 kW for the baseline trials, 2462-2823 kW for the post hull clean trials and 2438-2599 kW for the post propeller cleaning trials. The speed and power values from one trial, fall within the speed and power range for a different trial for this throttle setting. This is consistent for the other throttle settings considered and is true for the measured data as well as the corrected. This may be due to variability between trials (e.g. displacement variation, fouling present) and leads to less reliability in the power savings quantified using this data.

7. Operational Data Analysis

In addition to the sea trials conducted under somewhat controlled conditions, operational data was collected on an ongoing basis throughout the time period of the sea trials. From this data, the data was segmented based on speeds greater than 7 knots, and durations of at least 2 hours. Each segment meeting these criteria was averaged to provide a mean data point. These data points, color coded by period between cleaning events, are illustrated in Fig.8.

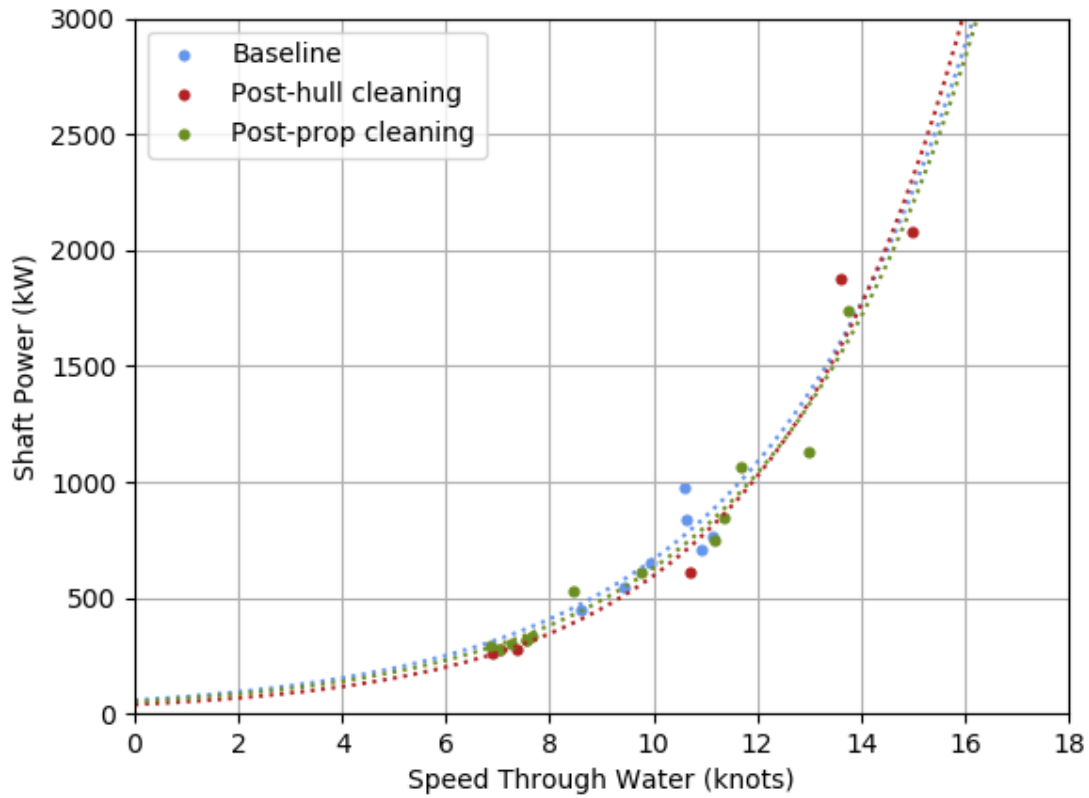


Fig.8: Mean data points extracted from operational data segments greater than 7 knots in speed and 2 hours in duration. Data points are color coded according to the period between cleaning events they correspond with.

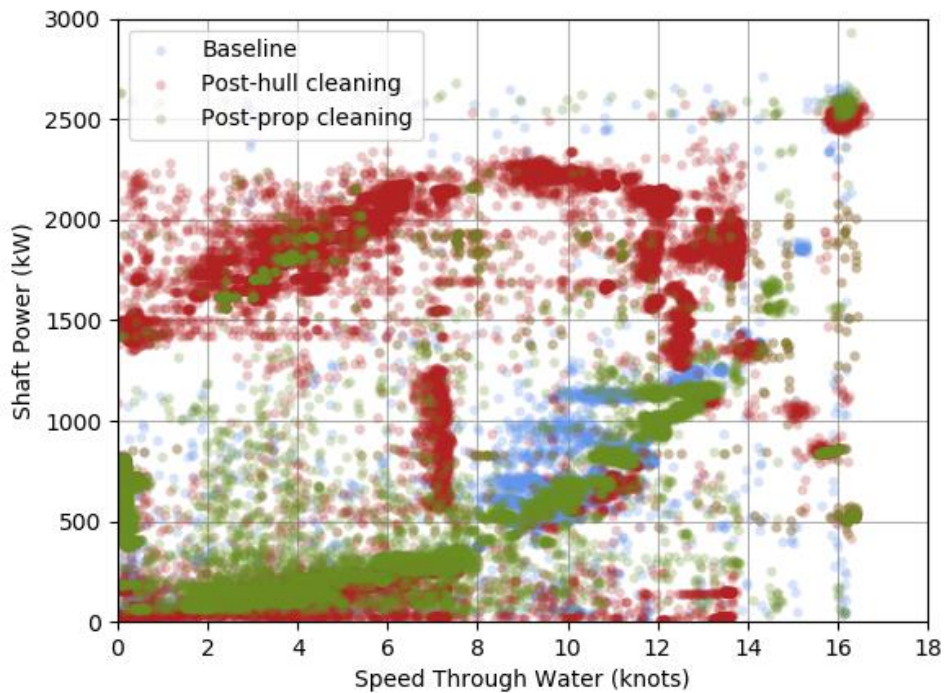


Fig.9: All operational data points throughout time period covering the cleaning trials. Scatter points occur due to operational activities, equipment and instrumentation fluctuation, and environmental condition.

The complete operational dataset is illustrated in Fig.9. This data covers all recorded data points throughout the operational period covering the cleaning trials (May-Aug, 2018). The data points are scattered due to operational activities, such as towing, equipment or instrumentation fluctuations, such as shaft power, and environmental conditions, such as large wind and waves. The open water power to speed relationship is visible, but not easily characterized.

To reduce the extraneous data points, the data set was clipped by a threshold of 300 kW about the approximate power to speed relationship. Fig.10 illustrates the data set with curve fits and comparison to the mean trial data. From this figure, it can be seen that the relationships are apparent, but the trial conditions capture the minimum power to speed curve from the operational data scatter. This is due to the relatively calm conditions under which the trials were conducted versus the typically rougher conditions encountered by the vessel under normal operation.

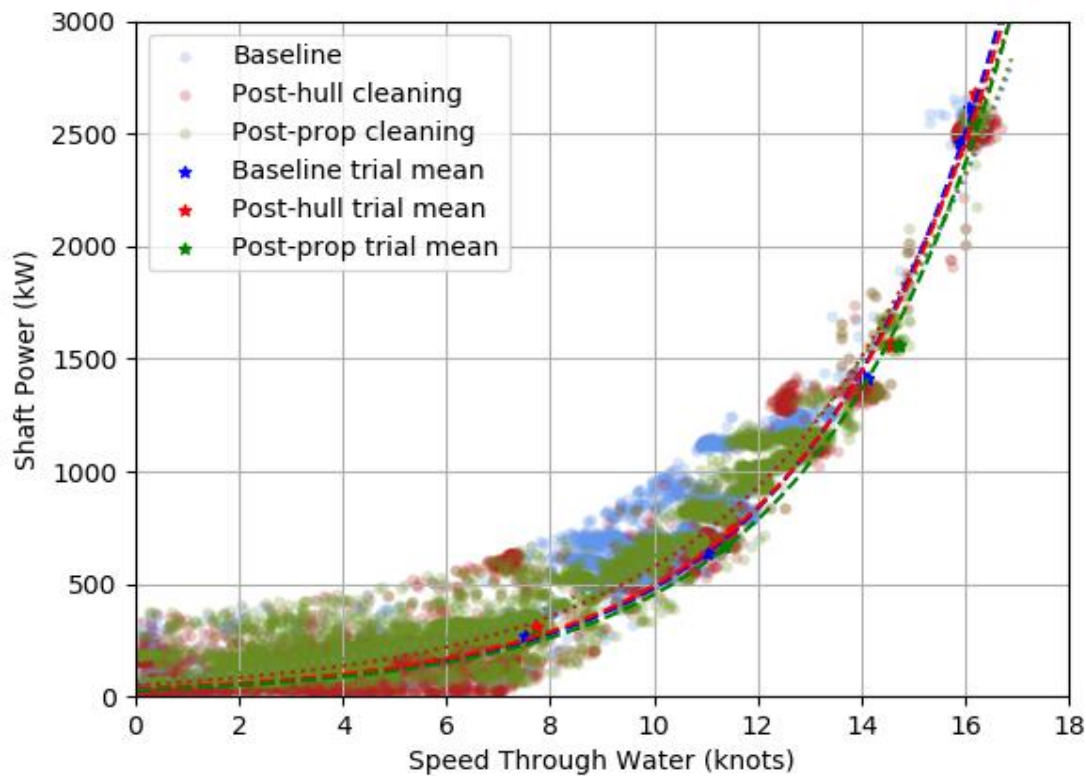


Fig.10: Reduced operational dataset covering trials period. Curve fits are applied for comparison. The mean trial data is shown for comparison with the operational data result.

8. Fuel Consumption and Speed

To identify the fuel curve for the vessel, total main engine fuel consumption versus shaft power was plotted for each trial. The fuel consumption versus power curve should be consistent for all trials since both fuel consumption and shaft power are not affected by external parameters such as environmental condition or hull and propeller condition. The speed attained however, does change as a result of variation in these external parameters. The measured total main engine fuel consumption versus power curve for all trials is shown in Fig.11. For each engine setting tested during trials, the baseline trials and post propeller cleaning trials data aligns well. However, there is an offset when it comes to the post hull cleaning trials data. For these trials there is less fuel required for a given power setting, particularly at higher power values. It is expected that there was some mechanical difference in the fuel measurement system that led to the discrepancy in the post hull cleaning fuel versus power data. A possibility is that one (or more) of the fuel flow meters surrounding one of the main engines was bypassed or partially bypassed or blocked during the post hull cleaning trials. However, the OpDAQ system bypass indicator did not highlight a complete bypass during this, or any of the trials.

The baseline and post propeller trials data for fuel consumption versus power are used to define the general fuel versus power curve for the Cygnus main engines. The post hull cleaning trials data was not used for this purpose due to the discrepancy from the other trials data. The general fuel versus power regression equation (regression equation corresponding to Fig.11) was used to calculate the “corrected” fuel consumption by adding the corrected power values at each engine setting for each trial. The power values corrected using the NavCad wind correction were used in this analysis. There is no quantifiable difference between the fuel consumption rate and speed through water for the different sea trials. This is due to the level of variation in data at single test condition within a given trial and how data from different trials fall within this variability range. For example, at a throttle setting of 8.0, the baseline trials speed through water ranges from 13.9-14.3 knots and the corrected fuel consumption ranges from 373-475 L/h. At this same throttle setting, the post hull cleaning trials speed through water ranges from 14.2-14.9 knots and the corrected fuel consumption ranges from 393-526 L/h. There is overlap in the speed and fuel consumption variability ranges between trials for each engine setting.

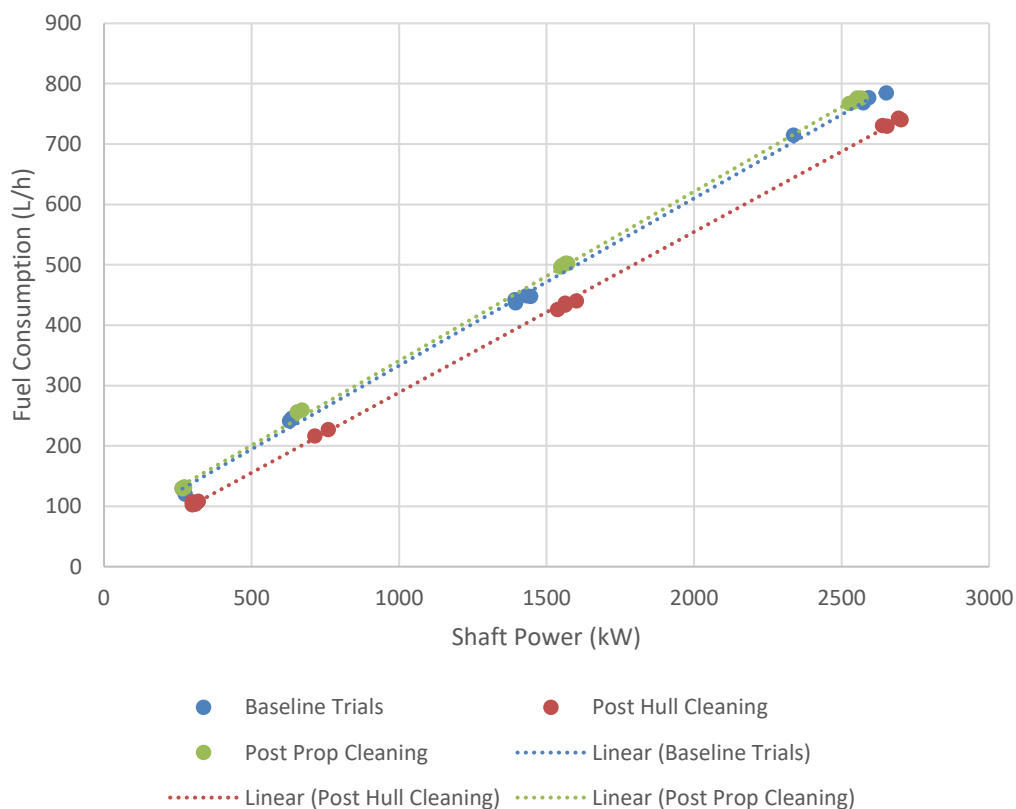


Fig.11: Uncorrected total main engine fuel consumption rate versus shaft power

9. Condition of Cygnus Hull in September 2018

The CCGS Cygnus was taken into dry dock on September 11, 2018 to perform vessel maintenance. When in dry dock, the hull was observed to have a relatively high level of fouling on one side in particular (port). The level of fouling present on the port side was similar to the amount that was present during the underwater survey conducted in May, 2018, prior to cleaning the hull. Specifically, there was slime and sea grass covering a large portion of the underwater hull (Fig.12). These observations were unexpected for two reasons. The first relates to the speed of fouling taking place on the Cygnus hull. Prior to the May hull cleaning, the Cygnus hull had not been cleaned in two years. It was anticipated that the level of fouling present in September, just 3.5 months post hull cleaning, would be much less than that observed during the May survey. Some reasons that could have led to rapid fouling growth during this short period include the relatively warm temperatures during summer 2018 in the region and a depletion in anti-fouling coating.

It is observed that the September hull condition level of fouling differs on the port and starboard sides of the vessel with the starboard side having a higher level of fouling. The May survey results indicated that the starboard side of the hull had a slightly worse level of fouling. It was anticipated that if one side was more fouled than the other in September, it would have been the starboard side to be consistent with earlier results. Increased fouling on one side of the vessel could result from frequent docking on one side (fouling occurs more on side subject to sunlight) or lower quality of anti-fouling coating on one side of vessel. Cygnus Captains were consulted and it was confirmed that the docking side varies. The anti-fouling paint was noted to be highly depleted in September, on both sides of the vessel (see Fig.13). This likely played a role in the high fouling accumulation rate during the summer period.



Fig.12: Images of port side of hull during September, 2018 dry dock. The level of fouling is similar to that encountered in May, 2018.

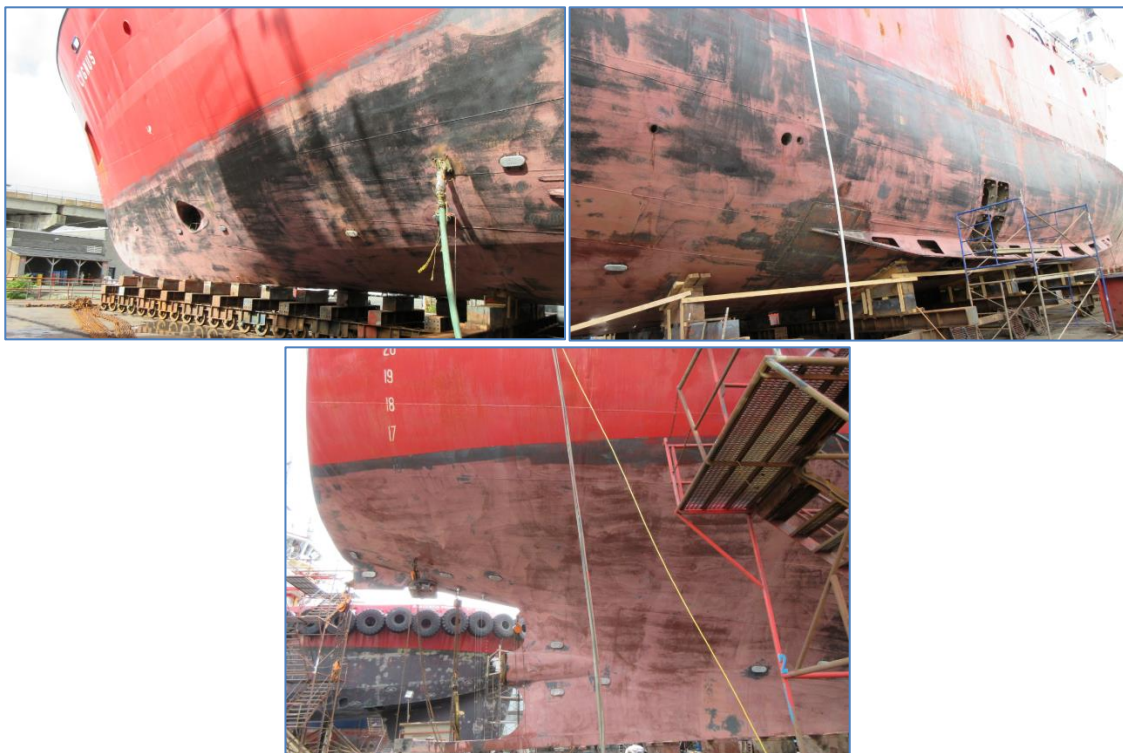


Fig.13: Images of Anti-fouling coating after biofouling was removed. The anti-fouling coating is deteriorated in large swatches across much of the hull.

Note that the anti-fouling paint is the black paint that can be observed in Fig.13. This image indicates the level of depletion of the anti-fouling paint after the biofouling was removed using a pressure

washer in dry dock. The anti-fouling paint adhesion was investigated by brushing it lightly by hand using a scouring pad. This resulted in the anti-fouling paint flaking off as a result of the brushing. It is possible that the May and September hull cleaning events enhanced this level of depletion.

The status of the anti-fouling paint was considered further by consulting with the Canadian Navy. A Canadian Navy biofouling Subject Matter Expert (SME) noted that the level of depletion of anti-fouling coating on the CCGS Cygnus was not typical given that the anti-coating was applied to the vessel only two years prior. The Canadian Navy SME indicated that this level of depletion was not seen on Navy vessels even after 5 years of use. They suggested to check on conditions during application and noted that application during high humidity levels could lead to faster depletion of coating. They also indicated that the type of coating used on the CCGS Cygnus was different than that used on Navy vessels and recommended that the CCG use an alternative coating.

The relatively high level of fouling present in September likely has an impact on the results presented in this report since there may have been a level of fouling present on the hull during post cleaning trials. This is particularly true for the post propeller cleaning trials which were not conducted until August 1, 2018. Unfortunately, there is no way to quantify the amount of fouling present during the post hull cleaning and post propeller cleaning trials. In general, if fouling was present during the post hull cleaning trials the analysis would indicate a lower level of power and fuel savings than the actual values. Also, if more fouling was present during post propeller cleaning trials than during post hull cleaning trials, the discrepancy between the measured savings potential and the actual savings potential would differ between trials and be larger for the post propeller cleaning trials. This could relate to the unexpected result of the post propeller trials found from the ITTC analysis methods.

10. Discussion and Recommendations

The measured results indicated an approximate 4% improvement in terms of required power to attain a given speed as a result of cleaning the hull and approximate 5% improvement as a result of cleaning the propeller, for speeds between 12.5 and 16 knots. However, there were variations in the environmental conditions and condition of the vessel between trials and these differences have an influence on vessel performance. The wind, wave and water temperature variations between trials were corrected based on ITTC guidelines. The wind correction was also made using two variations of the ITTC recommended wind resistance correction method for comparison. The discrepancy between vessel displacement during the different trials was not corrected for since there was no standard guideline available to correct for this when the displacement varied by more than 2%. It was estimated that the displacement between trials varied by approximately 8%. The hull condition also varied between trials in that there was likely some level of fouling present during both the post hull clean and post propeller clean trials. Therefore there is some uncertainty in level of fouling between the post hull and post propeller cleaning trials. Based on the data that was corrected for wind (NavCad correction method), waves and water temperature, there is an average of 5% savings in terms of power required to attain a given speed as a result of cleaning the hull, for speeds between 13.5 and 16 knots. The performance decreases after the propeller polishing in this same speed range based on this analysis. To correct for wind, wave and temperature variation a number of parameters (e.g. wind resistance coefficient, propeller pitch for each trial, hull underwater area) had to be estimated. As a result, there is uncertainty involved in the corrected power values.

In terms of fuel consumption, there appeared to be a measurement error during the post hull cleaning trials which led to lower fuel consumption rates for a given power setting. This could be a result of partially closed fuel valve(s) surrounding one of the main engines. Therefore, it was impossible to quantify fuel savings resulting from cleaning the hull directly from the measured data. The general fuel consumption rate versus shaft power regression equation was used to calculate the corrected fuel consumption rates for each trial using the corrected (NavCad wind, ITTC wave and sea temperature) power values. This resulted in a corrected fuel consumption rate versus speed through water plot for each set of sea trials. The results for each trial were very similar and there were no quantifiable differences in the three curves.

10.1 Recommendations to Reduce Uncertainty and Gain Result Clarity

There were a number of recommendations identified for conducting a similar study in the future which would lead to lower uncertainty in the data and more clarity in the results. These are summarized in point form below.

1. Conduct all tests in very low wind and wave conditions. In this project the baseline trials and post hull cleaning trials were conducted in similar conditions which were high in terms of the environmental condition limit. The post propeller cleaning trials were conducted in relatively mild conditions. The methods to correct for wind and wave conditions lead to uncertainty in the results since certain parameters need to be estimated. In mild conditions these corrections are much smaller and therefore less significant.
2. Conduct all tests at the same displacement. Variations in displacement lead to changes in vessel performance. In this project it was attempted to complete all trials at the same draft levels. However, since the Cygnus is an operational vessel and trials were completed weeks apart this was difficult to manage. As such, there was a variation in the draft (and displacement) and the effect of this on the results was not quantified. Trials at the same displacement would not have this source of variation and would lead to increased confidence in results.
3. Select vessel that has available propeller open water curves, wind tunnel test data and model resistance test data. This would reduce the number of parameters estimated in the data correction analysis and lead to lower uncertainty in the results.
4. Conduct tests closer together in time. The three tests involved in this test were completed between May – August of 2018. During this time there was some level of fouling that developed on the hull between trials and subsequent to the hull cleaning. This leads to a lower level of confidence in the results since there may have been some fouling present during both post hull and post propeller cleaning trials. If the trials had occurred closer together in time (e.g. days apart rather than months) this would limit the potential for fouling to develop on the hull or propeller between trials.
5. Conduct study on a vessel that has an off-season or longer alongside duration. The CCGS Cygnus is continuously in operation throughout the year and has a short, 2 day, layover period between operations. This gives limited time for the accumulation of biofouling and as such it was expected that the amount of fouling present initially on the Cygnus would be relatively low. The performance increase as a result of cleaning the hull and propeller would be larger for a vessel with more fouling in the baseline condition. A good candidate would be a vessel that does not operate for a portion of the year, during which time fouling would accumulate faster than during operations.

10.2 Comparisons to Similar Publicly Available Data

A brief literature search was completed to compare the results of this study to data available in the public domain. There were no directly comparable results identified in the literature in terms of comparable vessel size or initial level of fouling. However there were guidelines identified that provided insight as to what performance increases could be expected from cleaning the hull based on different initial levels of fouling (Schultz, 2007). These guidelines are based on model scale drag measurements and boundary layer similarity law analysis and were made for a mid-sized naval combatant at two speeds, 15 and 30 knots. Different fouling ratings (FR) as per the Naval Ships Technical Manual (2006) were used in this study. Table 8 summarizes the results of this study for a vessel speed of 15 knots in terms of increase in shaft power resulting from different levels of fouling. The fouled (baseline) condition of the CCGS Cygnus was mostly FR 20 with some areas having FR 30 (~15% of vessel). The corrected (for wind, wave and temperature) results indicate that the baseline trials required approximately 5 % more power than trials during which the hull was clean, for speeds greater than 13.5 knots. This is smaller than the 11% estimated increase in power for FR 10-20 as outlined in Table 8. However, the baseline condition was not a hydraulically smooth surface and was better described as a somewhat deteriorated coating. Therefore, it is reasonable to expect a lower power savings when comparing the two conditions.

Table 8: Expected performance changes as a result of hull fouling

NSTM Rating	Description	Increase in SHP
0	Hydraulically smooth surface	0%
0	Typical as applied antifouling coating	2%
10-20	Deteriorated coating or light slime	11%
30	Heavy slime	21%
40-60	Small calcareous fouling or weed	35%
70-80	Medium calcareous fouling	54%
90-100	Heavy calcareous fouling	86%

Giorgiutti et al. (2014) conducted a study to investigate the impact of fouling on a crude oil tanker. This study investigated the effects of fouling on the hull and propeller separately and involved several sea trials. The data from sea trials was analyzed using ITTC analysis guidelines and complimented with other recommended methods. The analysis involved corrections for wind, wave, sea temperature and displacement variation. Details on the displacement during each trial or how this was corrected for were not provided. In this study the level of fouling at baseline condition was much higher on both the hull and propeller than that which was present on the *Cygnus*. The fouling was not rated as per Naval Guidelines however it was indicated that there was severe hard, calcareous fouling that was difficult to remove covering the majority of the propeller and underwater hull surface. The savings resulting from cleaning the hull and propeller were approximately 45 % in terms of reduced power at cruising speed. This study included both propeller cleaning and polishing.

A Computational Fluid Dynamics (CFD) based study was presented by *Demirel et al. (2016)* in the *Journal of Applied Ocean Research*. This investigation predicted the effect of biofouling on resistance and power requirements of a container ship based on full scale simulations. These predictions indicated an increase in power by 18% for the ship fouled with light slime and an increase by 38% for the ship fouled with heavy slime. There were no sea trials used to compare or validate the CFD results. However, model test data was compared to the non-fouled predictions and they compared well.

In general, there is limited comparison data available in the public domain for this type of study, particularly data resulting from sea trials. The data that does exist can be compared generally but not directly since the hull forms and initial level of fouling vary. In addition, there are gaps in the methodologies applied for data analysis and trial corrections for the comparative data that is available in the literature.

11. Concluding Remarks

The primary goal of this study was to quantify the effects of cleaning the hull and propeller on the vessel performance in terms of speed and power, for the CCGS *Cygnus*. The corrected sea trials data indicated a reduction in power required to attain a given speed by an average of 5% between the speed ranges of 13.5-16 knots. However, these results were not corrected for variation in displacement across trials or the presence of slight fouling during the post cleaning trials. The results compare reasonably to estimations of power increase for a mid-sized Naval frigate for similar baseline and fouled conditions.

This study provided insight towards steps that could be taken to increase the value of future tests of a similar nature. These recommendations should be considered when planning future work to increase the level of confidence in results.

Acknowledgement

The authors would like to thank the Canadian Coast Guard for their support in coordinating sea trials, providing necessary vessel data and prompt response to questions during this work. Thanks to the Captain and crew of the CCGS Cygnus who executed the sea trials and were cooperative and supportive towards this research initiative.

References

GIORGIUTTI, Y.; REZENDE, F.; VAN, S.; MONTERIO, C.; PRETEROTE, G. (2014), *Impact of Fouling on Vessel's Energy Efficiency*, 25th National Congress of Waterway Transportation, Shipbuilding and Offshore, Rio de Janeiro

ITTC (2014), *Speed and Power Trials, Part 1: Preparation and Conduct*, Int. Towing Tank Conf., 7.5-04-01-01.1, Revision 1.1.

ITTC (2005), *Full Scale Measurements Speed and Power Trials Analysis of Speed/Power Trial Data*, Int. Towing Tank Conf., 7.5-04-01-01.2, Revision 00.

ISO (2015), *Ships and Marine Technology – Guidelines for the Assessment of Speed and Power Performance by Analysis of Speed Trial Data*, International Standard, ISO 15016, 2nd Ed.

ISO (2016), *Ships and Marine Technology – Measurement of Changes in Hull and Propeller Performance – Part 1: General Principles*, International Standard, ISO 19030-1

NAVAL SHIP'S TECHNICAL MANUAL (2006), *Waterborne Underwater Hull Cleaning of Navy Ships*, Chapter 081, S9086-CQ-STM-010, Revision 5, Published by Direction of Commander, Naval Sea Systems Command

ROYAL NAVY (2011), *Surface Ship Hull Fouling Management*, Maritime Acquisition Publication No 01-026, Issue 02

Information Sharing Concept in Ship Performance Management Systems

Wojciech Gorski, Enamor, Gdynia/Poland, wojciech.gorski@enamor.pl

Abstract

Modern Ship Performance Management Systems (SPMS) automatically collect large amount of diversified data and usually allow access also for users not physically present onboard. Typical scenario for this arrangement is ship crew access onboard and technical office onshore. In a most simple approach both users just have an access to the same dataset. However, providing access to the same data, does not ensure that SPMS efficiently supports vessel operation. Contrary it may easily create user confusion due to huge amount and diversity of data. Paper attempts to present means used to enhance user comprehension of ship data and collaboration between crew and owner office in a context of taking decisions towards ship performance enhancement. Variety of methods including data pre-processing and visualisation, transition of data towards information, information encapsulation, sharing and hierarchy are discussed based on Enamor's SeaPerformer SPMS.

1. Ship data digitalisation

Ship digitalisation is nowadays highly discussed topic. It is expected that process of digitalisation will reshape of maritime industry in coming years. Review of Maritime Transport provided by *UNCTAD (2018)* indicate that digitalisation process will be a key factor in transport optimisation. It however addresses also major threats connected with data safety and security which must be addressed. Report indicates also data sharing as the critical aspect since data transformation between systems is limiting factor for implementation of digital ship concept.

Digitalisation process has been already started by different initiatives described e.g. by *Schmode et al. (2018)* but yet have not converged into universal solution. The process, its tools and methods and data standards will develop and evolve however it is already visible two general approaches. First one is based on relatively low resources hardware onboard dedicated for data acquisition and transfer to cloud server. It has limited capability for instant data processing and visualisation thus is intended for decentralised systems where major processing is on remote server side and therefore rely on continuous data exchange. More traditional approach assumes high processing capabilities onboard which allows for data processing, visualisation and user interaction independent on cloud server. This paper presents SeaPerformer SPMS as an example of latter approach indicating its capabilities for ship digitalisation through support of user comprehension of data and collaboration between crew and owner office in a context of taking decisions towards ship performance enhancement.

2. Data sharing

Typical scenario of data sharing between ship and shore consists of single direction of data flow. Data collected onboard are send to onshore server. This scenario may however result in serious system limitations. It imposes that complete data set registered onboard must be send each time data are exchanged even in case some data are not important in daily operation. In case of data which changes seldom or high resolution data single direction data exchange results in increased data traffic and high demand for onshore server space. Bi-directional communication allows for data transfer optimisation. Some data may be excluded from data set periodically send onshore and kept onboard until they are needed. Such an approach may be efficiently used for data reflecting ship's system condition after failure. Until failure occurs these data do not provide useful information and may be retained onboard without impact SPMS performance. However, in case of failure these data contain critical information with respect to failure diagnostics and system recovery. Bi-directional communication allows onshore user to request specific subset of onboard data whenever needed. In most simple form onshore user may request onboard data based on situation description provided by ship crew. This simple approach requires crew to recognise failure, provide this information to onshore user (technical office, service

support) which in turn requests appropriate data set to be send. This scenario may be however automated. SPMS may evaluate specific signals (triggers) as indicators of abnormal situation and, whenever this situation is recognised, automatically request additional relevant data set. This approach has been implemented in Enamor’s SPMS system developed for one of the leading marine diesel engine developers. This version of system includes fast signal module which records each engine cylinder combustion pressure and other relevant information (valves positions) as a function of crankshaft angle. In order to maintain constant angular resolution of 0.1 degree irrespectively of engine rpm, cylinder signals are recorded at 10kHz frequency. Resulting data set exceeds few MB per hour of engine operation and is far too large taking into consideration onboard satellite communication restrictions. Therefore fast data set is excluded from data package send periodically to onshore server. High frequency data are kept only in onboard database for some time. Ship crew can use SPMS user interface to evaluate engine combustion signals and in case of need for assistance, select appropriate subset and send it onshore for consultancy. Moreover, SPMS allows remote engine monitoring. For this purpose set of standard engine key performance indicators (KPIs) are calculated based on high frequency cylinder signals for each engine stroke. These KPIs are send ashore and can be evaluated by competent personnel in order to detect abnormal situation. In case KPIs indicate situation which needs more detailed investigation relevant subset of high frequency data can be requested from the ship. Such request is automatically processed by onboard SPMS and appropriate data packed is send in return. Onboard SPMS can be also used for automated engine monitoring. Set of rules based on engine KPIs can be continuously monitored by the system and in defined conditions relevant subset of high frequency data is send ashore without onboard or shore personnel intervention.

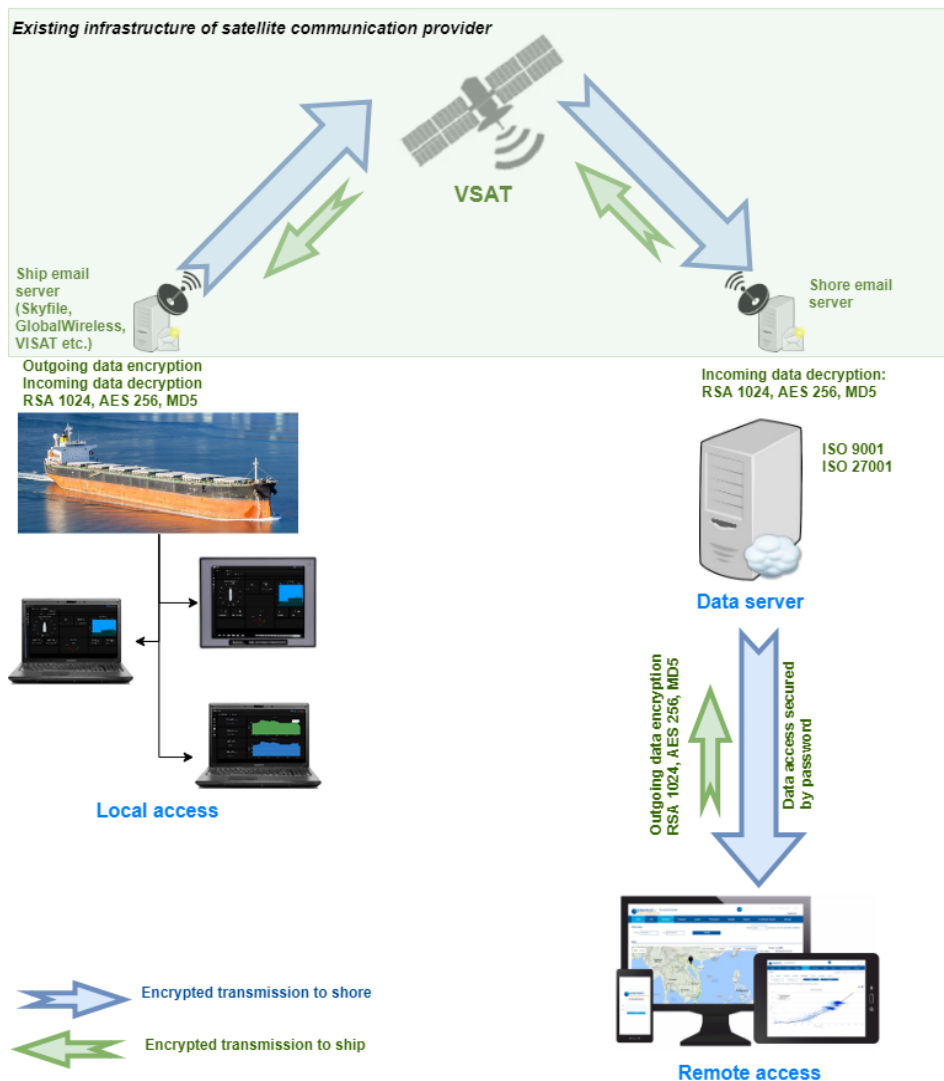


Fig.1: Scheme of data exchange implemented in SeaPerformer

Some of data exchange scenarios described in previous paragraph requires onshore user to interact with SeaPerformer SPMS onboard. Since typically vessels are not online due to limitations imposed by satellite communication systems or owner internal regulations, interaction with onboard system is realised with use of emails. General scheme of data exchange used in SeaPerformer is presented in Fig.1. SeaPerformer has been also furnished with remote diagnostic module (RDM) in order to allow safe channel of communication from shore to ship. RDM implements SMTP and POP3/IMAP client for receiving commands with data and sending responses. All the data exchanged with use of RDM are encrypted using combination RSA1024/RSA2048/AES/SHA256 encryption. Regardless the above the additional transport encryption is recommended between endpoints of email transfer. The onboard email clients support SSL/TLS when connecting to relevant server. This way data encrypted at source remains in that state until it reaches the destination. All commands sent to on-board system are encoded and signed. The on-board system checks the received message against the sender address, proper encoding, signature, the age, command syntax. Only verified commands are executed. The execution of commands requires an authorisation command to be executed first. RDM is therefore a great tool for secure remote diagnostic purposes. Onshore user can send onboard a command for SeaPerformer to prepare specific subset of data and send it back for further analyses. Although this feature is extremely useful, RDM can be also used for other purposes. Since, with use of RDM, remote user can get access to local files at authorised paths general operation system (OS) diagnostic can be handled. System or specific application log files can be downloaded from onboard computer and analysed onshore. Based on received information, maintenance commands can be executed remotely. This feature greatly simplifies OS maintenance minimising a need of IT expert's physical presence onboard. Last but not least RDM allows for remote update of SeaPerformer software. Encrypted and zipped update files can be uploaded onboard and update process can be completed remotely without involvement of ship crew.

3. Visualisation and contextualisation of data

Data visualisation comprise one of prime functionalities of SPMS. It allows user access to recorded data but what is even more important provides context which is required for data interpretation. Visualisation is also a significant tool supporting transition of data into information i.e. makes data understandable for user and helps him taking rational decisions. Taking above into consideration it is largely insufficient to provide user possibility to build graphs with arbitrary data. Usual time trend data plots although provide access to data, may not be very helpful in providing context and building data understanding. Furthermore, building user defined graphs is quite involving and requires sufficient level of experience. Therefore, SeaPerformer provides number of predefined graphs and views which incorporate data pre-processing (i.e. data cleaning and grouping), contextual selection of graphic elements types and blending of data elements. Although these graphs are predefined in order to minimise user effort it allows for certain degree of customisation, especially in case visualisation combines multiple data sources. Good example of this approach is a map view. It provides geographical context of vessel operation by default and therefore helps comprehension of data. It also allows for combination of different data in one consistent view i.e. providing bathymetry or weather data as the supplementary information to ship operational data. This feature is a powerful tool in building understanding of physical processes associated with ship operation. Although map view is very helpful in building context and blending multiple information it does not allow for direct presentation of data values as in case of typical X-Y plots. Therefore, appropriate data representation are used in map view. SeaPerformer map view combines colour coding (i.e. value representation by appropriate colour) for scalar data (i.e. ship speed through the water or engine power), arrow representation for vector data and text boxes for providing direct access to data values. Furthermore, map view can be enhanced with supplementary information such as bathymetry overview, navigation aids or extends of emission control areas (ECA). Such versatile visualisation can be easily overloaded with information and final effect can hinder understanding of presented information. Therefore, in order to facilitate handling of visualisation, map view elements are associated with layers which can be managed by user. This way visualisation can be easily adjusted for the purpose and needs of user.

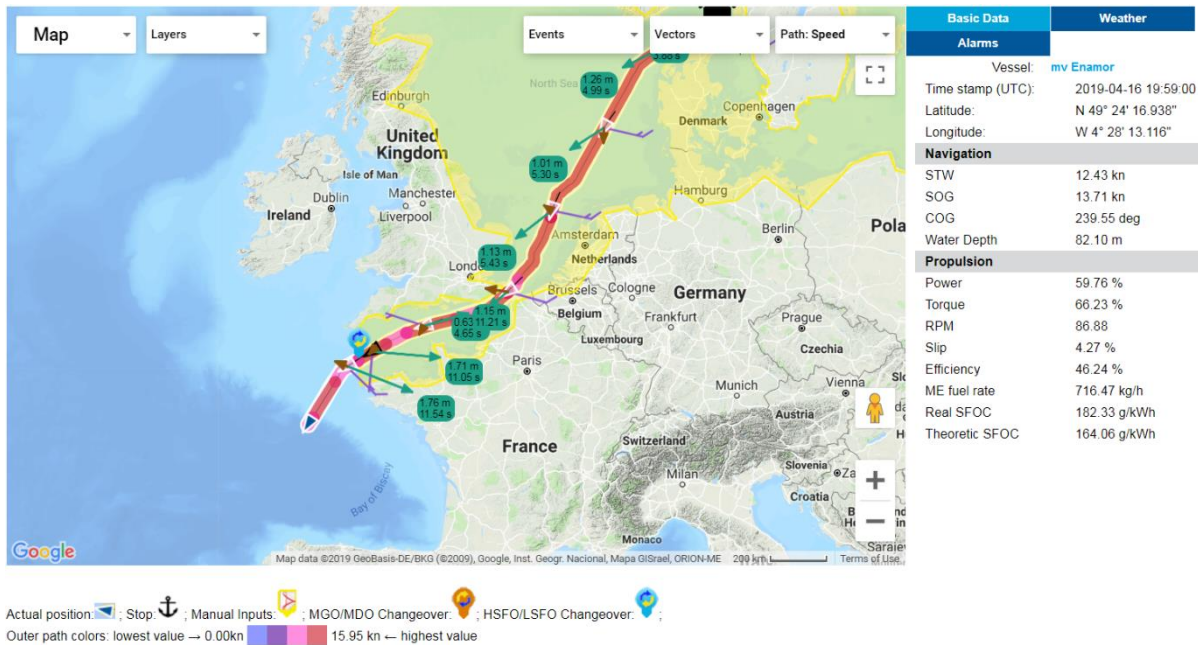


Fig.2: Different visualisation techniques used in map view

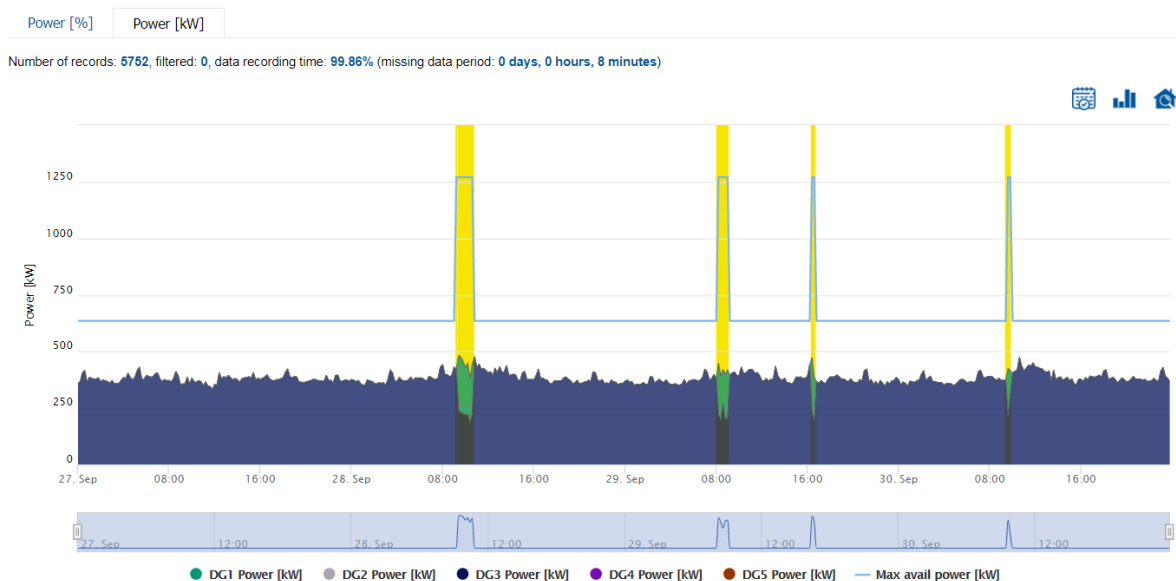


Fig.3: Time graph enhancements supporting data contextualisation

Sophisticated techniques can be also employed in more traditional visualisation such as time trend. This type of visualisation is probably the most common graph used in SPMS systems however in many cases does not sufficiently support user in understanding of presented data. An obvious advantage of time trend is visualisation of signal dynamics and providing easy access to data values either by use of axis and data grid or textual overlay (so called tool tips). Time trend graphs does not readily support visualisation of data which values are not numerical (i.e. binary data or system states) or which range is of different magnitude. Latter may be well handled by multiple Y-axis or re- scaling of data. Non-numerical data visualisation requires special techniques such as use of alternative graph background colour. Enhanced data comprehension can be also achieved by combination of different graph styles. An example of this approach in SeaPerformer is auxiliary engines load graph. This visualisation combines two principal graph styles; stack area graph for representation of individual genset load with colour differentiation of each unit, and line graph for indication of maximum output of gensets in operation. This type of graph is helpful in identification of concurrent use of many gensets resulting in low efficiency and excessive fuel consumption. Graph arrangement supports this task; colour layers

identify number of active gensets, stack area graph provide actual output of gensets in operation, line graph define total available output. Large gap between line graph and stack graph identify usage of too many gensets resulting in low efficiency. Inefficient use of gensets is identified onboard and communicated to the crew. In order to illustrate crew response to the warning, time of unnecessary concurrent use of gensets is visualised by colour overlay on a graph. Yellow overlay indicate time span when warning message is presented for the crew until corrective measures are taken (see Fig.3). In case reaction time is exceeded, overlay changes colour to red giving clear visual indication to supervising personnel.

4. Pre-processing

Data pre-processing is an indispensable feature of any SPMS if the system is intended to be capable of transforming data into information. Well known, and already numerous quoted in past editions of HullPIC conferences, term “garbage in, garbage out” emphatically highlights importance of this process. Handling of unverified data which may include errors, data gaps or data context misinterpretation will lead to false conclusions. While, to certain extent, data reliability problems can be overcome by experienced user who based on his past knowledge, abstract thinking and problem generalisation can detect, neglect or regenerate problematic dataset, automatic handling of improper data pose serious challenge. In SeaPerformer development of data pre-processing mechanisms is treated as key feature. Some of advances with this respect have been already presented in past edition of this conference by *Gorski (2017)*. These concerned data redundancy and regeneration. Both techniques address problems of data gaps or identified false readings. However, very often reliable identification of data failure became a challenging task. Onboard equipment used as data source seldom provide self-diagnostic features and does not deliver clear identification of malfunction (e.g. failure flag) which may be automatically interpreted by the SPMS. Except obvious case of data gap (i.e. system reads NULL signal from a data source) identification of corrupted signal is a difficult problem which requires implementation of advanced processing techniques usually taking into account context of analysed signal. In order to clearly explain these difficulties two practical examples are discussed in details. Both concerns vital signals for performance evaluation. First example concerns ship static draft which is important for determination of vessel operation condition and is crucial in evaluation of required engine power. Static draft fore and aft is used to determine actual ship trim (her longitudinal inclination with respect to water plane) which is essential for trim optimisation. Secondly rudder deflection signal is discussed. This signal is used for identification of ship manoeuvring and allowing appropriate engine power correction to reference conditions.

Static draft can be read directly from ships loading computer (LC) however interfacing LC is sometimes challenging. In case LC is not available static draft can be determined with use of draft sensors i.e. pressure sensors scaled according to static head of the water and corrected for sensors position with respect to ship bottom. Draft sensors readings shall be however treated with caution since they are vulnerable to dynamic changes of pressure due to water movement with respect to ship hull. Furthermore ship changes her position at speed with respect to water plane (dynamic trim and sinkage) which impacts draft sensor readings as well. Therefore static draft can be read with use of draft sensors only at ship rest (in port after loading and ballasting procedure is completed). Obtained value shall be retained in SPMS and used until next port call. This method can provide practical information unless major ballasting operation is performed. If re-ballasting is done during sea voyage use of this method e.g. for trim determination is misleading and additional data input such as trim inclinometer is required. As explained above determination of such basic parameters as ship static draft and trim may be quite complicated in practical operational conditions. It requires special approach which includes data sources redundancy and special processing. However, in order to reflect reality of ship operation it must be noted that draft signal reliability often pose a serious problem. Author experience in use of draft data collected on more than 200 vessels of various type and equipment reveals frequent problems with draft sensors. These sensors are prone to failure providing awkward results which, if not recognised, may lead to problems in performance analyses or trim optimisation. It is often observed that draft sensors after failure continue to provide data. Therefore, most common and simple detection of malfunction by recognition of lack of data may not be sufficient. However, since draft signal after sensor failure changes

its properties i.e. often exhibit lesser sensitivity and shift, failure detection based on data processing may be effectively used. For the purpose of draft sensor malfunction detection is based on parallel evaluation of four draft sensor signals (fore, aft, midship portside and starboard) and speed over ground signal. Detection algorithm works in two variants depending on ship speed. At higher speeds only signal lost or rapid shift uncorrelated with speed on any of single draft sensors is detected. At lower speeds above method is supplemented with calculation of hull trim, list and longitudinal deflection. Values obtained based on draft sensors are compared with typical operational ranges which allows for detection of possible failure. Algorithm automatically recognises port operations during which only signal continuity is verified.

Another signal which often poses difficulties in operation is rudder deflection. This signal is important since allows for detection of dynamic states during ship manoeuvres and thus enable proper signal filtering for performance analyses. Rudder deflection is usually taken from synchro transmitter/receiver as the analogue signal or, in modern equipment, already converted to digital NMEA format. Rudder deflection is often subject of errors, especially in case of analogue signal transmission. The most straightforward in processing is signal lost however often situation is more complicated. It has been observed that many cases rudder deflection transmitter continue to provide data but with significant error. Two types of erroneous signal patterns have been observed: signal stall and signal shift. Signal stall results in almost steady (sometime small oscillations can be observed) signal irrespectively of actual rudder deflection. Signal shift is characterised by appropriate reproduction of signal gradient but rudder neutral position is not preserved. It is important that SPMS is able to recognise not only rudder signal lost but also other errors. For this purpose, it should be able to continuously process data during acquisition process. SeaPerformer implements appropriate algorithms for detection of rudder signal stall and shift. Due to nature of these errors stall recognition algorithm works in shorter time window and offset in longer time window. Stall of rudder signal is recognised based on standard deviation. Small value of standard deviation indicates an error. Rudder signal offset error determination is based on 3% quantile calculation at extreme ends of signal distribution. Large value of quantile suggests problem with data source. Error determination based on statistical quantities proved to be efficient approach (see Fig.4) comparing to method based on signal comparison with expected range of signal variation since it copes also with signal having false analogue to digital scaling factors.

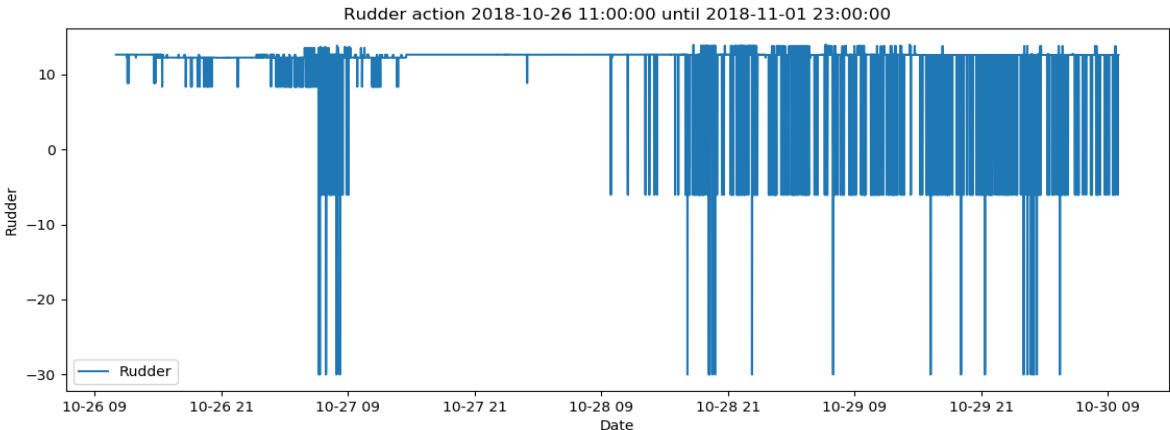


Fig. 4 – Erroneous rudder signal identified by signal processing module

As it has been highlighted in above examples, verification of signal quality and detection of possible data source malfunctions may involve special computational methods. It is usually not sufficient to relay on current value of signal or signal gradient. Due to scattered nature of signals registered onboard signal pre-processing is necessary. These methods include moving window averaging and statistical calculations (e.g. standard deviation and quantile calculations) on data subsets ranging from dozen of minutes up to couple of days. Data processing may apply to several thousands of records and therefore could be computationally demanding. It shall be noted that signal verification supposed to be realised in parallel to data acquisition and visualisation therefore it must be taken into account in SPMS hardware resources, mainly computing processor and memory.

5. Encapsulation

Data encapsulation, also known as data hiding, is a term used in programming and means mechanism whereby the implementation details are kept hidden from the user. In a context of SPMS it can be useful technique which simplifies user interaction and presentation of information. SeaPerformer system utilises encapsulation both in onboard and in web applications. System notifications can be taken as an example where this technique is employed. Onboard software processes multiple signals according to specific algorithms in real time. On this basis system detects situations which require ship crew action. However instead of presenting relevant signals system encapsulate them into warning symbol (bell icon as presented on Fig.5) and guidance information. This method allows to focus crew attention and minimises time to take necessary actions. Web application also uses encapsulation in case of system notifications but in different way comparing to onboard software. Instead of using bell symbol, warning information is encapsulated on ship track using colour. Yellow or red colours denote part of the voyage where unwanted situation occurred. This method allows for quick warning identification and at the same time provides larger context through map view.

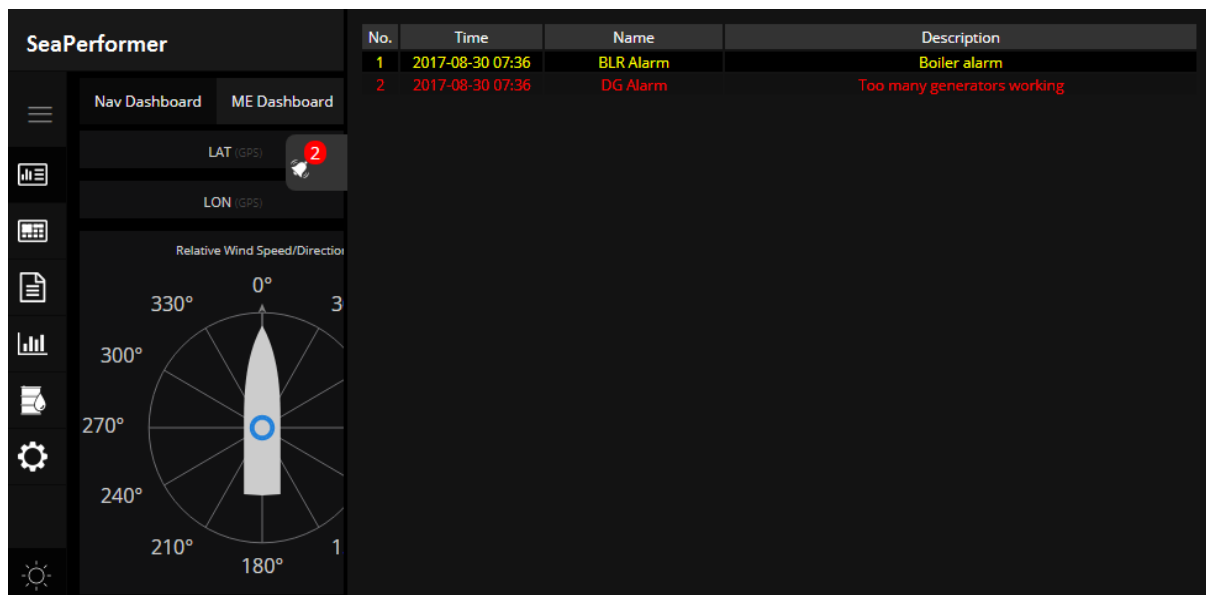


Fig.5: Information encapsulation in onboard application

6. Data hierarchy

Trim optimisation provides an interesting example of data hierarchy concept application. Ship hull trim is an important factor with respect to fuel consumption. Depending on hull form, selection of favourable trim setting may result in 3% to 8% savings in fuel consumption comparing to situation when trim is selected only with respect to stability and strength criteria. Due to complicated hydrodynamic phenomena of flow around hull geometry optimum trim vary with ship speed and draft and cannot be determined with use of simple methods. Traditionally hydrodynamic model tests performed in wide range of speed, draft and trim were employed for this purpose. For each combination of speed and draft, impact of trim on hull resistance or ship propulsive power was determined. Continuous interpolation of test results constitute a reference model upon which optimum trim can be determined during ship operation. Physical model tests can be nowadays substituted with methods of computational fluid dynamics resulting in lower costs and time of the reference model determination process. Another promising method for reference model elaboration is utilisation of operational data but this approach involves sophisticated data cleaning techniques and may be limited by range of parameters at which vessel is operated. Irrespectively of the reference model origin the method of optimum trim determination is the same. Initially vessel speed through the water, static draft and trim shall be determined. Local surrounding of operational parameters is searched for better solution (usually search is done for trim only while speed and draft is kept constant). If substantial improvement is recognised

trim change is recommended. It must be emphasised that trim optimisation process is highly dependent on proper recognition of actual operation parameters. In case speed, draft or trim is determined inaccurately it will influence a starting point of optimisation and thus also final result. Unfortunately, it is difficult to determine all of important parameters for the process. Problems of accurate determination of speed through the water has been already discussed e.g. by *Bos (2017)* but also in case of draft and trim their proper identification is sometime challenging. It should be noted that usually reference model for trim optimisation is based on static draft and trim while direct measurement of draft (and recalculation of trim) by draft sensors provides dynamic parameters. These values may differ substantially especially on higher speeds where dynamic trim and sinkage effects are pronounced. Furthermore, as already discussed in previous chapter, draft sensors are sensitive for dynamic pressure around the hull. These effects may falsify readings especially for bow sensors. In order to counteract mentioned problems SPMS may use multiple sources of data arranged in hierarchy of accuracy and reliability. SeaPerformer uses following sources for draft and trim determination:

- a) loading computer,
- b) draft sensor readings in port corrected for actual trim measured by ship inclinometer,
- c) direct draft sensor readings at speed corrected for actual trim as in b),
- d) direct draft sensor readings uncorrected for dynamic effects.

Static draft and trim shall be determined with use of loading computer. Accurate modelling of hull and internal compartments allows for determination of draft with error less than few cm. However, LCs are usually separated systems, difficult to interface with. Furthermore, even in case SPMS is connected to LC data exchange must be initiated by LC user which is often forgotten. For this purpose, in parallel to LC data SPMS reads and process data from draft sensors. SeaPerformer monitors draft readings during port operations and retains values at the completion of loading operations (final static draft at departure). Static draft may however change during voyage i.e. due to ballasting operations which may not be easily recognised since draft sensors are burdened by dynamic effects. In order to take account for these effects ship inclinometer is used. During ship voyage inclinometer measures dynamic trim. This may be however recalculated to static value based on reference model (it must contain both static and dynamic trim). In case actual dynamic trim is outside of reference model range and cannot be recalculated to static value, SPMS can use directly draft sensor readings as they were static ones. The latter is the less accurate method and shall be only used at low speeds where dynamic effects are not pronounced.

6. Conclusions

As indicated in the introductory note there are two general approaches differing in allocation of computational resources. Preceding paragraphs illustrate important features of SPMS which increase data comprehension and supports operational decisions resulting in improvements of ship performance. Irrespectively of the SPMS concept these features shall be incorporated as they are vital for achieving required functionality. Both concepts theoretically allow supporting data pre-processing and visualisation, transition of data towards information, information encapsulation, sharing and hierarchy. It must be however confronted with existing ship data transfer infrastructure. Nowadays majority of vessels do not support data streaming. Data are sent in packages and therefore data processing on cloud server is delayed by data exchange period. It is serious limitation especially in case of signal pre-processing with respect to possible data source malfunctions. Cloud server-side processing makes it necessary that results shall be send back onboard in case they require crew attention. This scenario therefore increases data transfer which is nowadays critical due to costs. Taking this into consideration solution which secures sufficient computing resources onboard reveal certain advantage until satellite communication enables data streaming on reasonable costs.

Ship Performance Management Systems can effectively support increase of vessel operation effectiveness thus enable cost savings and lower environmental impact. However, in order to take full advantage of the system it must incorporate features that enhance user comprehension of ship data and collaboration between crew and owner office. These important features include data pre-processing and visualisation, transition of data towards information, information encapsulation, sharing and hierarch

which were in details discussed in this paper. Available data transfer technology implies that solution allowing for local, onboard data processing pose advantage.

References

BOS, M. (2016), *How MetOcean Data Can Improve Accuracy and Reliability of Vessel Performance Estimates*, 1st HullPIC Conf., Pavone

GÓRSKI, W. (2017), *Automatic MRV Reporting with Use of Onboard Performance Management Systems*, 2nd HullPIC Conf., Ulrichshusen

SCHMODE, D.; HYMPENDAHL, O.; GUNDERMANN, D. (2018), *Hull Performance Prediction beyond ISO 19030*, 3rd HullPIC Conf., Redworth

UNCTAD, (2018), Review of Maritime Transport 2018, https://unctad.org/en/PublicationsLibrary/rmt2018_en.pdf

Application of Biotechnology in Antifouling Solutions for Hard Fouling Prevention

Philip Chaabane, Catherine Austin, Dan Isaksson, Oliver Weigenand, Cecilia Ohlauson,
I-Tech AB, Gothenburg/Sweden, philip.chaabane@i-tech.se

Abstract

This paper describes the development, subsequent application and success of using biotechnology in marine coatings for hard fouling prevention purposes. Existing self-polishing and controlled depletion polymer coating types that are suitable for the addition of 'Selektope®' are described. Current market uptake and in-service performance data for selected case studies are also presented. The paper also shares insight into I-Tech's research and development efforts to advance next generation antifouling materials that make use of Selektope®.

1. Introduction

Since the worldwide ban of the use of tri-butyl-tin (TBT) in antifouling coatings in 2002, suppliers of marine coatings have faced increasing pressure to offer antifouling products that deliver the same level of effectiveness as those that previously contained TBT for preventing the build-up of biofouling on ship wetted hard surfaces.

The banning of TBT use forced the marine coatings sector to reconstruct their formulations to accommodate different biocides, with copper designated as the favoured candidate, supplemented with booster biocides. Soon after, biocides faced new regulatory challenges in the shape of the EU Directive on Biocidal Products (98/8/EC). The effect of this was the number of certified biocides available for use in antifouling coatings reducing in number to just 12 active substances, including Selektope®.

Neither scheduling penalties, nor increased fuel costs were acceptable to a globalised industry reliant on just in time delivery. A solution had to be found and, for barnacle fouling, that solution was Selektope®.

Some two years earlier, in February 2000, biologists at the University of Gothenburg published a research paper on biofouling in Swedish waters. Researchers had been investigating how a range of substances that would prevent the settlement of hard fouling when dissolved in seawater could be used.

This research focused on the barnacle *Amphibalanus improvisus*, and its 'colonisation' of man-made surfaces at the larval stage. The goal of the research was to discover 'adrenoceptor active compounds' that manipulated the barnacle larvae's behaviour to inhibit invertebrate larvae from settling. *Dahlström et al. (2000)* found that larval-stage receptors were remarkably responsive to one substance in particular—medetomidine. This bioactive substance prevented barnacle larvae attempting to settle on a hard substrate.

Medetomidine was also distinguished by its reversible effects. Larvae that came into contact with the substance could still later metamorphose into juvenile barnacles with no apparent ill effect.

In collaboration with two Finnish universities, Swedish researchers discovered that medetomidine could bind to a specific group of receptors, the octopamine receptors. The receptors were cloned and the causality between the receptor and medetomidine was established. Further study led the researchers to link the binding to octopamine receptors to changes in the larval behaviour at a surface. This explained the high efficacy in preventing and deterring barnacle larvae in an antifouling paint without its being toxic to the barnacles.

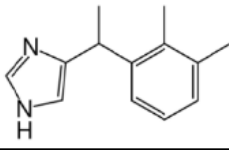
CAS-No.	86347-14-0
EINECS-no	Not listed
IUPAC Name	4-[1-(2,3-dimethylphenyl)ethyl]-1H-imidazole
Other common name	Medetomidine
Molecular formula	C ₁₃ H ₁₆ N ₂
Structural formula	
Molecular weight (g/mol)	200,28 g/mol

Fig.1: Medetomidine identity

In a counter-intuitive discovery, given its sedative effect on vertebrates, medetomidine was found to induce hyperactivity in the barnacle larvae to disrupt the settling process; similar to the effects to a small dose of adrenaline in humans.



Fig.2: Cyprid larvae stage of the barnacle



Fig.3: Adult stage of the barnacle

During initial panel testing, a further discovery was made. Remarkably, a polymer film containing medetomidine in a concentration equivalent to 0.02% by weight volume rejected 97% of the aggressive *Barnacle improvus* after two weeks, and 96% after four weeks. No other macro-fouling organisms were present at all. A further distinction pointed towards medetomidine's potential for "large scale synthesis": its "tendency to accumulate at the solid/liquid interface" across the full extent of a surface.

These significant research findings catalysed the development of the industry's first biotechnology approach to biofouling prevention. I-Tech AB commercialised the use of medetomidine in marine coatings, owning all IP and regulatory rights to the antifouling agent under the brand name Selektope®. I-Tech also controls the largest and most efficient source of medetomidine production.

In 2009, buoyed by the further confirmation of earlier research, I-Tech entered a new stage in the development of Selektope®, by initiating the registration of the marine antifouling agent for regulatory approvals. Few can doubt the dedication required to submit a new substance to the BPR's evaluation process; the dossier BPR (EU528/2012) consists of more than 20.000 pages 528 files and refers to 90 investigations regarding human and environmental safety. Even so, Selektope® was granted full approval in 2016 for use as a marine biocide under EU Biocide Product Regulation (EU) (528/2012).

Today, Selektope® has received approvals in all leading markets for new builds and dry-docking including China, South Korea and Japan. In the EU, Selektope® has been approved for all relevant use-types I. For Africa, South America and the rest of Asia, no registration is needed for the use of Selektope®. Following 15 years of development time and numerous regulatory hurdles, the first commercial antifouling coating product containing Selektope® was applied to the vertical sides of a ship in 2015 with the first commercial product containing Selektope® being officially launched into the market in 2016.

2. Increasing demand for advanced antifouling coatings

Ocean going vessels are increasingly at risk from negative commercial impacts associated with biofouling accumulation on the hull. Marine fouling is the biological process of single celled organisms, algae and hard-shelled organisms, predominantly barnacles, attaching to submerged surfaces and colonising at a rapid rate.

Any organisms anchored on the hull create increased drag (commonly referred to as added resistance) which significantly decreases hull performance. A biofouled vessel must burn more fuel to attain the same speed through water when in active service, resulting in higher fuel costs for the ship operator. A hull suffering from heavy fouling is also extremely impactful on maintenance costs. Costs associated with hull cleaning services are factored into a ship operator's operating expenditures (OPEX) but as global biofouling risk increases, hull cleaning is likely to be required more frequently, increasing maintenance costs. Repeated cleaning of the hull can also remove layers of the antifouling coating, reducing its service life.

Different types of biofouling require different hull cleaning practices. Soft fouling can be removed by diver cleaning with brushes or by Remote Operated Vehicle (ROV) cleaning technology. However, hard fouling presents a greater cost and risk for the ship operator. Encrusted colonies of barnacles or other hard-shelled organisms must be removed with methods such as scraping or blasting which are much more damaging to the antifouling coating.

Biofouling accumulation on vessels experiencing extended periods of static activity is also becoming an increasingly dominant issue on the agenda for many shipyards. Newly launched vessels remaining stationary for three or four months at shipyards located in biofouling hotspots, or longer in the case of LNG carriers, during the fitting out process are becoming so fouled that they perform badly during sea trials.

In addition, growing regulatory focus on the transportation of invasive aquatic species (IAS) by the international shipping fleet creates an increased risk of potential commercial impact. Some regional regulations are already in force that allow ports to refuse entry of heavily bio-fouled ships, resulting in greater financial costs for the operator. On an international level, IMO has recently shifted its focus on tackling IAS transfer via ballast water onto hull biofouling.

The afore-mentioned issues are driving the need for high performance, advanced antifouling technology in the maritime industry. Ship operators are increasingly demanding antifouling paints that are both well-suited to specific ship trading patterns, and varying activity levels in addition to protecting against both soft and hard fouling. When looking at the future trading potential, ship operators need to ensure that their ship is protected whether it be in constant active service, idle for long periods of time, or is at risk of fluctuating between the two.

This future-proofing approach to antifouling coating selection, without any certainty of future trade, is exerting great pressure on the coating suppliers, prospering great innovation and new approaches of fouling prevention technology using the active substance Selektope®. This is supported by increasing demand for antifouling coatings that contain the anti-barnacle active agent from ship owners and operators.

3. The use of Selektope® in self polishing coatings

Selektope® cannot be used in 'foul release' coatings with low surface energy based on siloxane elastomers and fluoropolymers, yet. Selektope® is a biocide that is currently suited for use only in coatings that are 'self-polishing' (SPCs) or 'Controlled Depletion Polymers' (CDPs) types. SPCs rely on the friction generated by the ship's motion through water causing tiny quantities of the base polymer paint to hydrolyse and to leach at a predetermined rate, while the active antifouling maintains its performance evenly through the paint's lifetime.

Selektope® is a biocide that has highly favourable antifouling properties at low concentrations (nano Molar). To obtain full protection against barnacle fouling, 0.1 - 0.3% w/w of Selektope® should be used in a wet paint formulation. Just 2 grams Selektope® is used per litre of paint, comparable to 500-700 grams of copper oxide used per litre of paint for barnacle prevention.

Selektope® binds to pigment and other particles in the paint system and is therefore continuously released in the same way as other active substances and components. This contributes to long-term performance as long as the paint remains on the hull. The paint formulation, which mainly comprises binding agents, biocides, pigment and filler material, is applied to the hull using a traditional spraying method. The compatibility between Selektope® and the paint matrix in the marine coatings industry, ensures as slow and steady release secures the antifouling effect over time.

However, how and when Selektope® is added during the formulation process is key to controlling the release rate of Selektope® from an antifouling paint. To prevent premature depletion of Selektope® the molecule should be able to interact with a carrier in the paint mixture. A carrier could be an inorganic particle such as zinc- or cuprous oxide. It could also be a metal ion such as Zn^{2+} or Cu^{2+} , or an acid group on a binder, for example the carboxylic acid on rosin.

I-Tech advises that Selektope® should be added early in the process, rather than adding it post formulation. I-Tech also advises that Selektope® should be added as a solution in a suitable solvent. Preferably the Selektope® solution and the carrier should be mixed first and then the rest of the components can be added. Selektope® will adhere to metal ions and metal oxide such as zinc oxide and cuprous oxide. This has been shown to be an effective way to control the release of Selektope® and prevent premature depletion.

Inorganic materials such as Al_2O_3 , SiO_2 , CuO , ZnO , TiO_2 and MgO can be used. Cuprous oxide, zinc oxide and iron oxide are commonly used. ZnO is advised as the best pigment particle for maximum Selektope® adsorption in xylene.

If Selektope® is added later in the paint formulation process the surface of the metal oxide pigment may already be occupied and Selektope® adsorption will not take place in an adequate or linear way with uneven distribution and weaker adhesions. This may cause Selektope® to leach out of the paint too quickly and result in premature depletion of Selektope® from the treated surface.

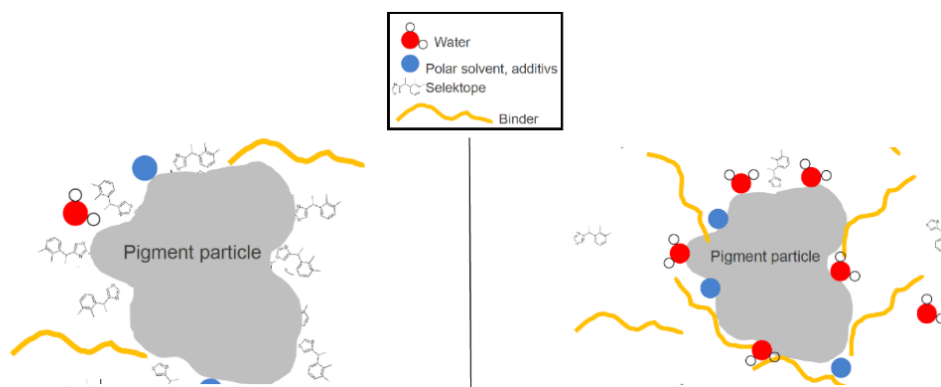


Fig.3. Selektope® added before the binder and other components - good adhesion will occur versus if Selektope® added at the end of the formulation process – weaker or no adhesion occurs potentially leading to premature depletion of Selektope®

Although most Selektope®-containing antifouling paint products on the market are combinations of copper oxides and Selektope®, Chugoku Marine Paints have launched a paint that is copper free. Therefore, the concentration of biocides in the paint has been reduced, while other qualities, such as prevention of soft fouling (e.g. slime and seaweed) have been notably improved.

4. Current market uptake and in-service performance data

Application data, as provided by paint manufacturers, suggest that to-date the total of ships coated with a Selektope®-containing antifouling totals over 300. There are 10 antifouling coating products available to the market that contain Selektope® (correct as of April 2019).

In this paper, a selection of case studies that demonstrate the hard fouling prevention effectiveness of Selektope®-containing antifouling coatings are presented.

4.1. CASE STUDY: 36-month medium range tanker trial

The vertical sides of the IMO II 2009-built chemical and products tanker *Team Calypso* were coated with a copper free Selektope®-based antifouling product with a service life of 60 months. At the 36-month position in its drydock interval *Team Calypso* had a hull completely free of barnacle fouling after spending more than 50% of its operating time spent in areas of high biofouling with up to 32°C water temperatures. The tanker had also encountered several extended idling periods of 25 days or more.



Fig.4: *Team Calypso* dive inspection report, Month 27



Fig.5: *Team Calypso* dive inspection report, Month 32



Fig.6: *Team Calypso* dive inspection report, Month 36

Independent, third party analysis of hydrodynamic data used to calculate the MR tanker hull’s added resistance also reinforced the underwater hull inspection findings at month 36. Data analysis confirms that the added resistance on the MR Tanker’s hull and propeller due to fouling was exceptionally low compared to that expected for a reference ship of similar age, size and trading patterns.

The independent data for *Team Calypso* at Month 36 is described in Fig.7.

Total added resistance	12 %
Hull added resistance	8 %
Propeller added resistance	4 %
Development rate of added resistance (normally 0.5% to 1.5%)	0.4 %
Excessive fuel consumption since last drydock at loaded condition	2.7 t/24h
Months since latest dry-docking	36
Months since latest hull cleaning	36
Months since latest propeller polish	6

Fig.7: *Team Calypso* added resistance data: Month 36

The performance of the Selektope®-containing SPC applied to *Team Calypso* was compared to two other sister ships in the fleet (ship A and ship B). Ship A coated with a foul release coating type and ship B coated with an SPC type. The added resistance data for each ship is presented in Fig.8.

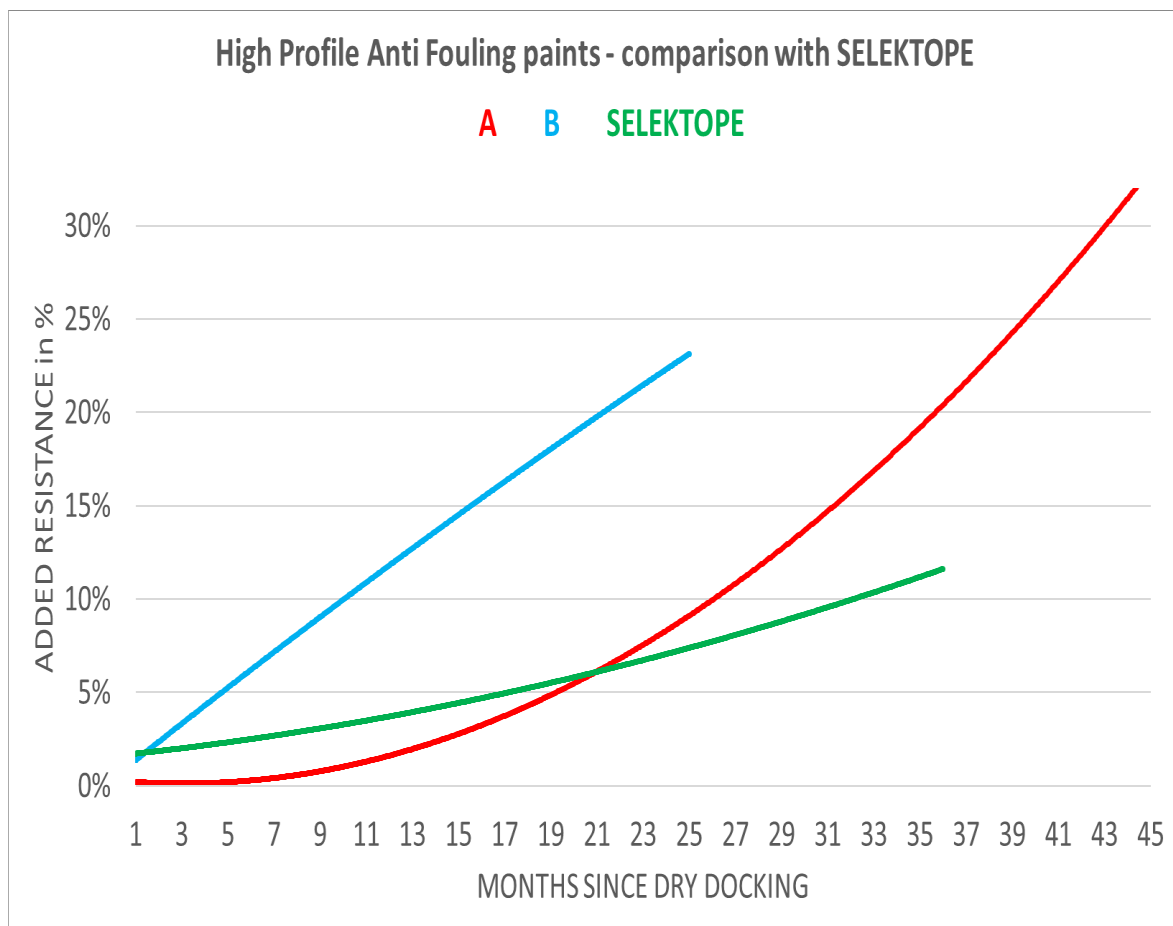


Fig.8: *Team Calypso* development of hull/propeller added resistance versus sister ships

The independent analysis of the tanker’s performance data coupled with underwater hull inspections provide yet more convincing long-term performance results for Selektope®-based coatings. These

results hold great importance as they confirm the superior efficacy of Selektope® for a vessel engaged in active service that encounters significant exposure to severe fouling conditions and undertakes periodic idling activity. This is proof that I-Tech's unique antifouling ingredient can offer ship operators using Selektope®-based antifouling coatings superior hard fouling prevention for any vessel regardless of its activity and trading patterns.

4.2. CASE STUDY: US Navy static panel tests

The Office of Naval Research Biofouling Program supports field testing at five sites located in Florida, California, Hawaii and Singapore. These sites are characterised by different environmental conditions, and different biofouling communities. Across the sites, however, any coating under evaluation will experience biofouling by the full suite of organisms likely to recruit on a ship hull.

The antifouling performance of a number of coating formulations have been examined during a test period of 12 months using coated test panels under static conditions at the five aforementioned test sites. Each coating formulation is a different product sourced from multiple paint manufacturers.

The first copper based SPC type containing Selektope® supports no macrofouling, with no barnacle growth, or slimes at most of the sites after 12-months static. Some panels at one of the Florida tests sites and at the Singapore site were covered with a layer of slime. At the 6-month point, panels at the California test site also had very little slime growth.

The second coating formulation, a copper-free SPC type containing Selektope®, after 12 months static at all test sites supported no macrofouling, with no barnacle growth. At one of the Florida tests sites, macrofouling, not barnacles, was present and some scattered amphipod tubes. Panels at the Singapore test site supported slightly heavier slime.

For the testing of third coating formulation, one set of panels were coated with a copper-based SPC and one set of panels were coated with a copper-based SPC type containing Selektope® at each test site location, after 12 months there was a clear difference in performance exhibited between the two sets of panels coated, with and without Selektope®. At the Florida test sites the set of panels with Selektope®-containing paint being free of barnacles, while scattered barnacles were present on the set of panels coated with paint not containing Selektope® and both sets of panels also supporting light to moderate slime and scattered amphipod tubes. At the Hawaii tests sites, both sets of panels were essentially clean, while those at the Singapore test site slime was slightly heavier. After 6 months, panels coated with paint containing Selektope® at the California test site remained barnacle free, whereas panels coated with paint not containing Selektope® supported barnacle growth.

This test provided the conclusion that the presence of Selektope® in antifouling coatings provides superior hard fouling prevention performance, even under static conditions of 12-month duration. This test also demonstrated that copper-free antifouling coatings containing Selektope® also offer superior colour retention to those copper-containing SPCs tested under the same conditions. This test will continue in 2019.

5. R&D projects

The challenges with cleaning submerged surfaces and equipment requires the development of new materials or combinations of materials that withstand cleaning and other kinds of mechanical wear. There is also submerged equipment that could benefit from having an antifouling coated surface that currently may only be coated with ordinary marine paint for corrosion protection. Fenders, buoys, nets, cables, measuring/monitoring devices and energy production devices can suffer from fouling, for example.

I-Tech, together with industry partners, has starting screening suitable materials either as coating or construction materials for submerged objects that are:

- Durable to withstanding cleaning / mechanical wear
- Slippery: to release fouling
- Permeable: to release biocides

Materials already available that can be mixed or tweaked to improve fouling resistance are:

- Polyurethanes
- Silicone epoxies

In this paper, research conducted by I-Tech in the areas of Polyurethanes and Silicone epoxies containing Selektope® is presented.

5.1. CASE STUDY: Polyurethanes with Selektope®

I-Tech has demonstrated that it is possible to protect submerged surfaces/object that are made out of polyurethane material. Test results have confirmed the prevention of barnacle settlement under static conditions over two seasons (summers).

This test provided the conclusion that the presence of Selektope® in polyurethane material successfully protects against barnacle fouling.

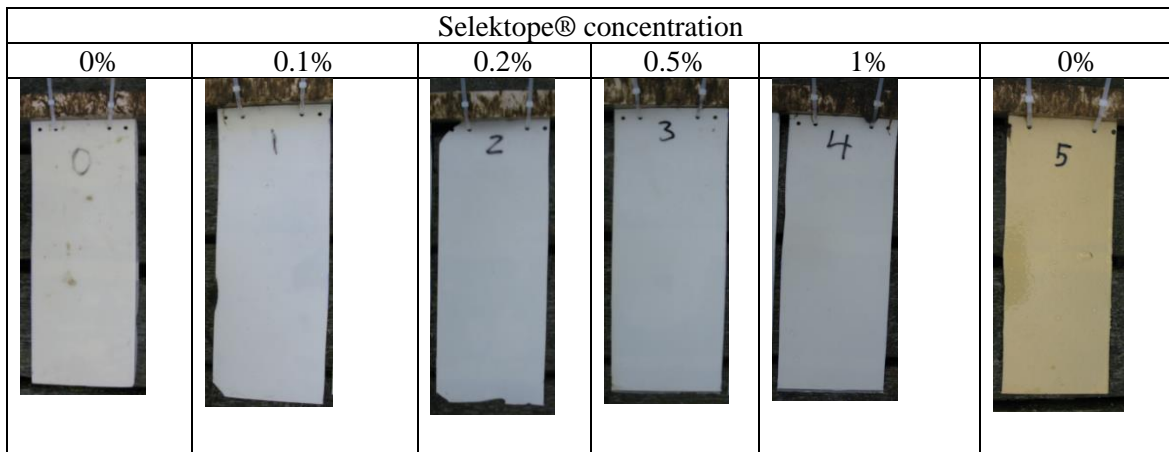


Fig.13: Reference polyurethane test panels

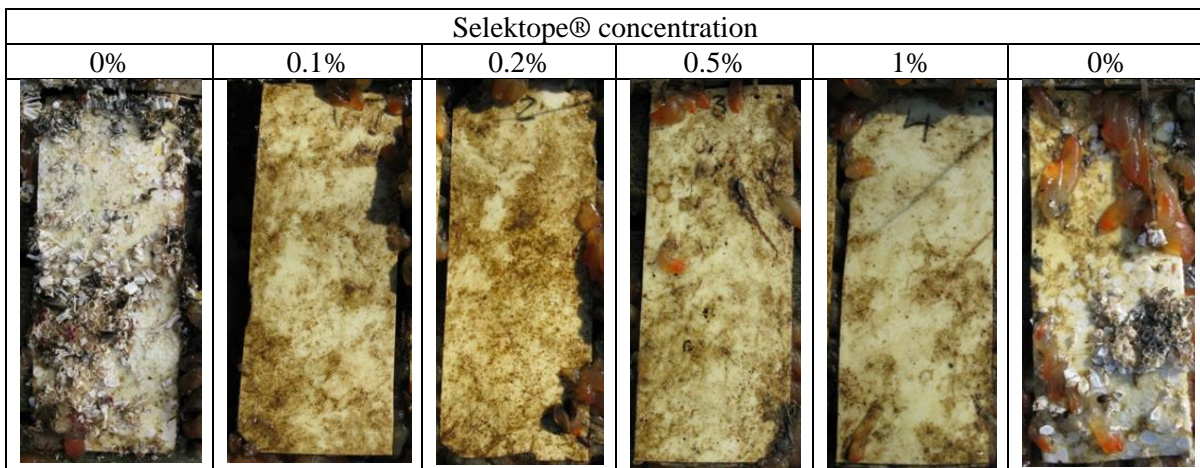


Fig.14: Polyurethane test results: May 2013 - September 2014



Fig.15: Three-panel polyurethane test conducted with only one formulation containing 0.37% Selektope® versus a reference panel with 0% Selektope® - October 2015 - November 2017

5.2. CASE STUDY: Silicon epoxy coatings

Whereas epoxy-silicone systems offer abrasion resistance and easy to clean properties, they still have limitations when exposed to sea water at static conditions. The addition of Selektope® enables highly innovative coating systems and, as such American paint specialist Wearlon®, part of Plastic Maritime Corp., trialled the inclusion of Selektope® in its Wearlon Super F-3M range to develop an abrasion-resistant coating with boosted antifouling properties. The trials concluded that the addition of Selektope® to Wearlon®'s epoxy-silicone coating resulted in significantly improved antifouling properties when exposed to raft tests in sea water. The coating is expected to be particularly effective in areas where high-wear strength is required such as around propellers, and for use on off shore equipment.

Wearlon®'s Super F-3M is a water-based silicone-epoxy coating whose silicone epoxies are blocked copolymerised and supplied through emulsion chemistry. The mol % of silicone to epoxy is varied and coupled with surfactant and filler selection to obtain properties that are unique for a variety of applications. Wearlon® Super F-3M is one of the most hydrophobic of all the Wearlon® coatings, having a low surface tension when in contact with water, resulting in drag reduction. Because of its excellent abrasion and corrosion resistance it is being used in a variety of marine applications including zebra mussel control.

Developing a coating that was inclusive of Selektope® has been key to producing a more impact-resistant, yet flexible and low abrasive epoxy silicone coating system that shows excellent antifouling performance.

The trialing of the Wearlon® epoxy-silicone product containing Selektope® was conducted at I-Tech's test facility on the west coast of Sweden over a period of 19 months. Test panels were coated with two layers of the test product by a roller. For the formulations that underwent panel testing, a concentration of 0.3% Selektope® w/w of the final wet paint mixture was used to ensure the steady release of the biocide.

A successful formulation was achieved through the addition of a 1-methoxy-2-propanol solution of Selektope® to component B of the two-component system of Super F-3M. Traditionally, when formulating rosin gum-based or acrylic-based antifouling paints, Selektope® is always best added to the paint as a solution. In order to add it to the formulation, it should be dissolved in an appropriate solvent before adding pigments, metal oxides (e.g. ZnO), fillers, binder and other additives.



Fig.16: Reference silicon epoxy-coated test panels submerged in April 2016 off the west coast of Sweden.



Fig.17: Month 18 results

At the 2-month inspection, all reference panels had plenty of barnacle fouling. Some of the test panels had a few barnacles attached except F-3M with 0.3% Selektope®. At 18 months, panels coated with F-3M with addition of 0.3% Selektope® had no fouling, whereas every other test panel was completely covered in barnacle fouling.

The trial of the Wearlon® Super F-3M range product with Selektope® included concluded that the addition of Selektope® to the Wearlon® epoxy-silicone coating resulted in significantly improved antifouling properties when exposed to raft tests in sea water. In the future, the partners are convinced that epoxy-silicone coating technology will achieve wider acceptance on ocean going vessels due to Selektope®-powered antifouling performance.

6. Conclusion

Selektope® is currently being used on over 300 vessels and I-Tech anticipate this number growing significantly in the near future. Independent data analysis of added resistance on the ship hull, dive inspections and static panel tests confirmed, and continue to confirm, the barnacle repellent power of this biotechnology when used in marine antifouling coatings. Further research efforts conducted by I-Tech confirm that it is possible to add Selektope® to a variety of materials not only to traditional marine paints. This can broaden the scope of use to other areas that are not coated today, but that would benefit from protection against barnacles. I-Tech intends to continue looking for new materials where Selektope® can be incorporated as well as enabling the use of the biotechnology in all currently used antifouling solutions on the market today and in the future.

Acknowledgement

We thank the University of Gothenburg, the United States Navy and Plastic Maritime Corporation.

References

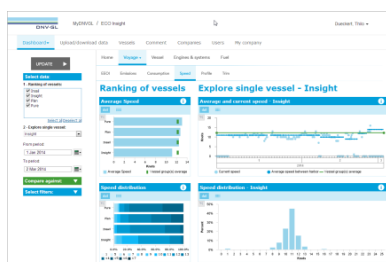
DAHLSTRÖM, M.; MÅRTENSSON, L.; JONSSON, P.; ARNEBRANT, T.; ELWING, H. (2000), *Surface active adrenoceptor compounds prevent the settlement of cyprid larvae of *Balanus improvisus**, *Biofouling* 16(2), pp.191-203

Index by Authors

Arango	143	Mathew	254
Ashida	38	Matsubara	21
Austin	301	McLaughlin	220
Becchi	76	Mieno	21
Bellusci	162	Mizutani	38
Bertelsen	114	Montazeri	211
Bertram	9	Montrose	272
Bonello	128	Murrant	272
Bretschneider	65	Mushiake	172
Castagna	254	Nielsen	229
Chabaane	301	Noh	86
Connelly	201	Östman	153
Daniel	254	Ohlauson	301
De Freitas	201	Paereli	261
Dietz	229	Pakkanen	38
Doran	97	Pallard	272
Eliasson	4	Pappas	201
Galeazzi	229	Park	193
Gangeskar	114	Patey	31
Gatin	13	Petersen	211
Giordamlis	56	Petoumenos	179
Gonzalez	143	Prytz	114
Gorski	292	Rahimi	254
Gundermann	220	Savio	153
Hansen	211	Schmode	162
Helsloot	50	Schrader	65
Holst	229	Shan	242
Holm	242	Shimada	21
Hympendahl	162	Shin	193
Igarashi	172	Sia	103
Ikonomakis	229	Silberschmidt	201
Inukai	172	Smith	128
Isaksson	301	Sogihara	21
Ishiguro	21	Spandonidis	56
Jasak	13	Stefanatos	179
Jeon	86	Sugimoto	21
Kauffeldt	179	Teo	103
Kawanami	172	Themelis	56
Kennedy	272	Väisänen	38
Khan	254	Van Ballegooijen	50
Ki	193	Vargas	242
Kluwe	65	Voosen	254
Koushan	153	Vukcevic	13
Lee	86,193	Wakabayashi	172
Levantis	261	Weigenand	301
Lim	103	Yonezawa	21,172
Manderbacka	38		
Marquardt	254		
Masuyama	21		

5th Hull Performance & Insight Conference (HullPIC)

Tullamore / Ireland, 23-25 March 2020



Topics: ISO 19030 and beyond / sensor technology / information fusion / big data / uncertainty analysis / hydrodynamic models / business models / cleaning technology / coating technology / ESDs

Organiser: Volker Bertram (Tutech Innovation)
Geir Axel Oftedahl (Jotun)

Advisory Committee:

Francesco Bellusci	Scorpio Group	Jeppe S. Juhl	BIMCO	Hideaki Saito	JSTRA
Johnny Eliasson	Chevron Shipping	Barry Kidd	Akzonobel	Daniel Schmode	DNV GL
Erik Hagestuen	Kyma	Andreas Krapp	Jotun	Ian Sellwood	BMT Smart
Liz Haslbeck	NSWC-CD	Tor Østerveld	ECOsubsea	Geoff Swain	FIT
Tsuyoshi Ishiguro	JMUC	Beom-Jin Park	KRISO	Diego M. Yebra	Hempel

Venue: The conference will be held at the Bridge House Hotel in Tullamore/Ireland

Format: Papers to the above topics are invited and will be selected by a selection committee. The proceedings will be made freely available to the general public.

Deadlines: anytime Optional "early warning" of interest to submit paper / participate
15.11.2019 First round of abstract selection (1/2 of available slots)
14.12.2019 Second round of abstract selection (remaining slots)
15.02.2020 Payment due for authors
28.02.2020 Final papers due

Fees: 700 € – early registration (by 15.02.2020)
800 € – late registration

Fees are subject to VAT (reverse charge mechanism in Europe)
Fees include proceedings, lunches, coffee breaks and conference dinner

Limited seating capacity

Sponsors: Jotun

Information: www.HullPIC.info
info@vb-conferences.com